MOLECULAR MECHANISMS UNDERLYING ASSEMBLY AND MAINTENANCE OF THE NEUROMUSCULAR JUNCTION

EDITED BY: Ruth Herbst, Hanns Lochmuller, Laure Strochlic and Inga Koneczny

PUBLISHED IN: Frontiers in Molecular Neuroscience and Frontiers in Human Neuroscience

frontiers Research Topics

Frontiers eBook Copyright Statement

The copyright in the text of individual articles in this eBook is the property of their respective authors or their respective institutions or funders. The copyright in graphics and images within each article may be subject to copyright of other parties. In both cases this is subject to a license granted to Frontiers.

The compilation of articles constituting this eBook is the property of Frontiers.

Each article within this eBook, and the eBook itself, are published under the most recent version of the Creative Commons CC-BY licence. The version current at the date of publication of this eBook is CC-BY 4.0. If the CC-BY licence is updated, the licence granted by Frontiers is automatically updated to the new version.

When exercising any right under the CC-BY licence, Frontiers must be attributed as the original publisher of the article or eBook, as applicable.

Authors have the responsibility of ensuring that any graphics or other materials which are the property of others may be included in the CC-BY licence, but this should be checked before relying on the CC-BY licence to reproduce those materials. Any copyright notices relating to those materials must be complied with.

Copyright and source acknowledgement notices may not be removed and must be displayed in any copy, derivative work or partial copy which includes the elements in question.

All copyright, and all rights therein, are protected by national and international copyright laws. The above represents a summary only. For further information please read Frontiers' Conditions for Website Use and Copyright Statement, and the applicable CC-BY licence.

ISSN 1664-8714
ISBN 978-2-88974-040-6
DOI 10.3389/978-2-88974-040-6

About Frontiers

Frontiers is more than just an open-access publisher of scholarly articles: it is a pioneering approach to the world of academia, radically improving the way scholarly research is managed. The grand vision of Frontiers is a world where all people have an equal opportunity to seek, share and generate knowledge. Frontiers provides immediate and permanent online open access to all its publications, but this alone is not enough to realize our grand goals.

Frontiers Journal Series

The Frontiers Journal Series is a multi-tier and interdisciplinary set of open-access, online journals, promising a paradigm shift from the current review, selection and dissemination processes in academic publishing. All Frontiers journals are driven by researchers for researchers; therefore, they constitute a service to the scholarly community. At the same time, the Frontiers Journal Series operates on a revolutionary invention, the tiered publishing system, initially addressing specific communities of scholars, and gradually climbing up to broader public understanding, thus serving the interests of the lay society, too.

Dedication to Quality

Each Frontiers article is a landmark of the highest quality, thanks to genuinely collaborative interactions between authors and review editors, who include some of the world's best academicians. Research must be certified by peers before entering a stream of knowledge that may eventually reach the public - and shape society; therefore, Frontiers only applies the most rigorous and unbiased reviews.
Frontiers revolutionizes research publishing by freely delivering the most outstanding research, evaluated with no bias from both the academic and social point of view. By applying the most advanced information technologies, Frontiers is catapulting scholarly publishing into a new generation.

What are Frontiers Research Topics?

Frontiers Research Topics are very popular trademarks of the Frontiers Journals Series: they are collections of at least ten articles, all centered on a particular subject. With their unique mix of varied contributions from Original Research to Review Articles, Frontiers Research Topics unify the most influential researchers, the latest key findings and historical advances in a hot research area! Find out more on how to host your own Frontiers Research Topic or contribute to one as an author by contacting the Frontiers Editorial Office: frontiersin.org/about/contact

MOLECULAR MECHANISMS UNDERLYING ASSEMBLY AND MAINTENANCE OF THE NEUROMUSCULAR JUNCTION

Topic Editors:
Ruth Herbst, Medical University of Vienna, Austria
Hanns Lochmuller, University of Ottawa, Canada
Laure Strochlic, Institut National de la Santé et de la Recherche Médicale (INSERM), France
Inga Koneczny, Medical University of Vienna, Austria

Citation: Herbst, R., Lochmuller, H., Strochlic, L., Koneczny, I., eds. (2022). Molecular Mechanisms Underlying Assembly and Maintenance of the Neuromuscular Junction. Lausanne: Frontiers Media SA.
doi: 10.3389/978-2-88974-040-6

Table of Contents

05 ***Editorial: Molecular Mechanisms Underlying Assembly and Maintenance of the Neuromuscular Junction***
Ruth Herbst, Inga Koneczny, Hanns Lochmüller and Laure Strochlic

08 ***The MX-Helix of Muscle nAChR Subunits Regulates Receptor Assembly and Surface Trafficking***
Jolene Chang Rudell, Lucia Soares Borges, Vladimir Yarov-Yarovoy and Michael Ferns

21 ***Myasthenia Gravis: From the Viewpoint of Pathogenicity Focusing on Acetylcholine Receptor Clustering, Trans-Synaptic Homeostasis and Synaptic Stability***
Masaharu Takamori

39 ***Arhgef5 Binds α-Dystrobrevin 1 and Regulates Neuromuscular Junction Integrity***
Krzysztof M. Bernadzki, Patrycja Daszczuk, Katarzyna O. Rojek, Marcin Pęziński, Marta Gawor, Bhola S. Pradhan, Teresa de Cicco, Monika Bijata, Krystian Bijata, Jakub Włodarczyk, Tomasz J. Prószyński and Paweł Niewiadomski

52 ***Wesley J. Thompson (1947–2019)***
Young il Lee and Mendell Rimer

60 ***Effects of ASC Application on Endplate Regeneration Upon Glycerol-Induced Muscle Damage***
Matteo Rigon, Sarah Janice Hörner, Tatjana Straka, Karen Bieback, Norbert Gretz, Mathias Hafner and Rüdiger Rudolf

73 ***Pathomechanisms and Clinical Implications of Myasthenic Syndromes Exacerbated and Induced by Medical Treatments***
Martin Krenn, Anna Grisold, Philipp Wohlfarth, Jakob Rath, Hakan Cetin, Inga Koneczny and Fritz Zimprich

90 ***The TOR Pathway at the Neuromuscular Junction: More Than a Metabolic Player?***
Perrine Castets, Daniel J. Ham and Markus A. Rüegg

109 ***Myasthenia Gravis With Antibodies Against Muscle Specific Kinase: An Update on Clinical Features, Pathophysiology and Treatment***
Michelangelo Cao, Inga Koneczny and Angela Vincent

122 ***The Structure, Function, and Physiology of the Fetal and Adult Acetylcholine Receptor in Muscle***
Hakan Cetin, David Beeson, Angela Vincent and Richard Webster

136 ***Gene Expression Profile at the Motor Endplate of the Neuromuscular Junction of Fast-Twitch Muscle***
Kun Huang, Jin Li, Mikako Ito, Jun-Ichi Takeda, Bisei Ohkawara, Tomoo Ogi, Akio Masuda and Kinji Ohno

146 ***Investigation of* MLH1, MGMT, CDKN2A, *and* RASSF1A *Gene Methylation in Thymomas From Patients With Myasthenia Gravis***
Fabio Coppedè, Roberta Ricciardi, Angela Lopomo, Andrea Stoccoro, Anna De Rosa, Melania Guida, Loredana Petrucci, Michelangelo Maestri, Marco Lucchi and Lucia Migliore

153 ***Lack of Desmin in Mice Causes Structural and Functional Disorders of Neuromuscular Junctions***
Nane Eiber, Franziska Fröb, Mirjam Schowalter, Christian Thiel, Christoph S. Clemen, Rolf Schröder and Said Hashemolhosseini

163 ***Impairment Mechanisms and Intervention Approaches for Aged Human Neuromuscular Junctions***
Yomna Badawi and Hiroshi Nishimune

179 ***The Neuromuscular Junction in Health and Disease: Molecular Mechanisms Governing Synaptic Formation and Homeostasis***
Pedro M. Rodríguez Cruz, Judith Cossins, David Beeson and Angela Vincent

201 ***Long Term Follow-Up on Pediatric Cases With Congenital Myasthenic Syndromes—A Retrospective Single Centre Cohort Study***
Adela Della Marina, Eva Wibbeler, Angela Abicht, Heike Kölbel, Hanns Lochmüller, Andreas Roos and Ulrike Schara

214 ***AChR β-Subunit mRNAs Are Stabilized by HuR in a Mouse Model of Congenital Myasthenic Syndrome With Acetylcholinesterase Deficiency***
Jennifer Karmouch, Perrine Delers, Fannie Semprez, Nouha Soyed, Julie Areias, Guy Bélanger, Aymeric Ravel-Chapuis, Alexandre Dobbertin, Bernard J. Jasmin and Claire Legay

227 ***Modulation of the Acetylcholine Receptor Clustering Pathway Improves Neuromuscular Junction Structure and Muscle Strength in a Mouse Model of Congenital Myasthenic Syndrome***
Sally Spendiff, Rachel Howarth, Grace McMacken, Tracey Davey, Kaitlyn Quinlan, Emily O'Connor, Clarke Slater, Stefan Hettwer, Armin Mäder, Andreas Roos, Rita Horvath and Hanns Lochmüller

frontiers in Molecular Neuroscience

EDITORIAL
published: 22 November 2021
doi: 10.3389/fnmol.2021.797832

Editorial: Molecular Mechanisms Underlying Assembly and Maintenance of the Neuromuscular Junction

Ruth Herbst[1]*, *Inga Koneczny*[2], *Hanns Lochmüller*[3,4,5] *and Laure Strochlic*[6]

[1] Center for Pathophysiology, Infectiology and Immunology, Medical University of Vienna, Vienna, Austria, [2] Division of Neuropathology and Neurochemistry, Department of Neurology, Medical University of Vienna, Vienna, Austria, [3] Children's Hospital of Eastern Ontario Research Institute, University of Ottawa, Ottawa, ON, Canada, [4] Division of Neurology, Department of Medicine, The Ottawa Hospital, University of Ottawa, Ottawa, ON, Canada, [5] Brain and Mind Research Institute, University of Ottawa, Ottawa, ON, Canada, [6] Sorbonne Université, Institut National de la Santé et de la Recherche Médicale, Institut de Myologie, Centre de Recherche en Myologie, Paris, France

Keywords: neuromuscular junction, skeletal muscle, motor neuron, neuromuscular disease, experimental disease models, muscle weakness, aging

OPEN ACCESS

Edited and reviewed by:
Jean-Marc Taymans, Institut National de la Santé et de la Recherche Médicale (INSERM), France

****Correspondence:***
Ruth Herbst
ruth.herbst@meduniwien.ac.at

Specialty section:
This article was submitted to Molecular Signalling and Pathways, a section of the journal Frontiers in Molecular Neuroscience

Received: *19 October 2021*
Accepted: *29 October 2021*
Published: *22 November 2021*

Citation:
Herbst R, Koneczny I, Lochmüller H and Strochlic L (2021) Editorial: Molecular Mechanisms Underlying Assembly and Maintenance of the Neuromuscular Junction. Front. Mol. Neurosci. 14:797832. doi: 10.3389/fnmol.2021.797832

Editorial on the Research Topic

Molecular Mechanisms Underlying Assembly and Maintenance of the Neuromuscular Junction

The Frontiers Research Topic "*Molecular mechanisms underlying assembly and maintenance of the neuromuscular junction*" highlights recent progress in the field of neuromuscular development and maintenance in health and disease. Every voluntary movement such as breathing, walking and eating relies on the appropriate function of the neuromuscular junction (NMJ), therefore much of our behavior, well-being, and productivity are governed by this specialized synapse. NMJ dysfunction occurs in many different diseases affecting the neuromuscular system, including motor neuron diseases, muscular dystrophies, autoimmune diseases, and congenital myasthenic syndromes (Li et al., 2018). Most of these disorders are difficult to treat and can be life threatening. Moreover, NMJ maintenance plays a key role in weakened muscle function during aging (Hunter et al., 2016). It is therefore of central importance to understand the mechanisms of NMJ development, maintenance, and function under healthy and pathological conditions to develop new therapeutic strategies for patients and an aging society. In this special issue, we combined comprehensive reviews of new emerging concepts together with original articles investigating the complex molecular mechanisms that govern the formation, maintenance, and integrity of the NMJ to its dysfunction in aging and diseases.

The NMJ is a complex structure, formed by a highly organized interplay between motoneuron, muscle endplate, and perisynaptic Schwann cells (Sanes and Lichtman, 2001; Li et al., 2018). Its development and functional maturation as well as physiological adaptation throughout life require a coordinated sequence of molecular mechanisms. Cruz et al. provide a comprehensive review about the complexity of NMJ development covering mechanisms involved in synapse formation and maintenance as well as in disease and aging. The muscle-type nicotinic acetylcholine receptor (AChR) is the key component at the post-synaptic muscle membrane that is activated upon presynaptic neurotransmitter release and controls muscle response. High concentration and localized AChR expression are prerequisites for efficient neurotransmission. Subunit composition changes during development and influences properties of the AChR. Cetin et al. summarize the structural and functional differences between the fetal and adult AChR isoforms and their distinct

roles during NMJ formation and function. The study by Rudell et al. characterized the MX-helix in the β and δ subunits of the AChR to show their role in receptor assembly and surface expression, thereby explaining the functional consequences of mutations found in congenital myasthenic syndromes. Synaptic nuclei closely associated with the post-synaptic membrane express specific genes and contribute to the development and function of the NMJ. Huang et al. used the RiboTag techniques to perform a large-scale gene expression profiling of transcripts present at NMJs in fast-twitch muscle. The authors found an enrichment of known and novel genes that are part of different networks such as diacylglycerol and phosphatidylinositol signaling or extracellular matrix components, thus expanding the group of molecular players involved in NMJ development.

NMJ maturation and maintenance are essential for precise and refined muscle contraction. The size of the NMJ increases, its morphology and molecular composition changes and high AChR density has to be maintained. The molecular mechanisms that regulate maturation and maintenance remain largely unresolved. Bernadzki et al. identified the guanine nucleotide factor Arhgef5 as binding partner of α-Dystrobrevin, which is part of the dystrophin-associated glycoprotein complex and important for NMJ maintenance. Mice lacking Arhgef5 expression in the muscle show a loss of NMJ structural integrity and a reduction of active RhoA and Cdc42 pointing to the importance of actin dynamics for NMJ maintenance. Eiber et al. found in a knock-out mouse model for the intermediate filament protein desmin that NMJs are structurally and functionally impaired. These findings support previous reports of patients with myasthenic syndrome in addition to the classical occurrence of myopathy and cardiomyopathy caused by mutation in desmin. NMJ perturbations have been critically linked to age-related loss of muscle mass and function. The mechanisms responsible for NMJ destabilization during aging remain elusive but the TOR (Target of Rapamycin) pathway has drawn attention due to its crucial role in proteostasis. Castets et al. discuss the recent insights on TOR and its role in NMJ stability and function. Badawi and Nishimune focus on age-dependent functional and morphological decline of human NMJs. Aging processes in mouse models of accelerated aging are compared to human phenotypes and potential intervention approaches to attenuate age-dependent NMJ dysfunction and sarcopenia are discussed.

Neuromuscular disorders are a large group of heterogeneous disorders that can affect the function of skeletal muscles, peripheral nerves or different components of the NMJ, resulting in skeletal muscle weakness, myoclonus, muscle stiffness, or myalgia. They are a diverse group of diseases with greatly varying parameters such as age of onset, affected muscle groups, pathogenic mechanisms, disease severity, co-morbidities, and treatment options. Unraveling the underlying molecular mechanisms of NMJ development and function is key to our understanding of pathogenic mechanisms and essential for the development of novel diagnostic/prognostic assays and therapies.

Three original reports highlight the importance of genetic defects in neuromuscular transmission disorders, so-called congenital myasthenic syndromes (CMS). Della Marina et al. report on 32 patients with defects in 8 different CMS-genes, who were followed for a median time of 12.8 years at a single clinical center in Germany. Karmouch et al. provide new insights into the signaling pathways that are regulated by ColQ-deficiency and highlight a role for HuR and p38 in mRNA stability in a mouse model of CMS. Finally, Spendiff et al. treated CMS model mice with a genetic defect in the *AGRN* gene using a small agrin compound, which restored post-synaptic structure and improved muscle strength through normalization of muscle fiber composition and the prevention of atrophy. Pathogenic autoantibodies against neuromuscular proteins interfere with NMJ structure and function in myasthenia gravis (MG). Takamori reviews the known intra- and extracellular autoantibodies in MG and how they affect AChR clustering, trans-synaptic homeostasis and synaptic stability, while Cao et al. provide an in-depth state-of the art of the clinical features, pathophysiology, and treatment of MG with autoantibodies against MuSK. A subgroup of MG with autoantibodies to the AChR is also strongly associated with the presence of thymoma (TAMG), which may play a role in the immunopathogenesis, as the thymus is essential to uphold central tolerance mechanisms and remove autoreactive T-cells that could initiate an immune reaction against NMJ proteins (Marx et al., 2013). Recent studies suggest that thymomas in TAMG may be of a distinct molecular subtype of thymic epithelial tumors, but little is known about the epigenetic modifications of thymomas in TAMG. Coppedè et al. investigated blood and thymoma tissues from 69 TAMG patients and studied the methylation pattern of tumor suppressor and DNA repair genes but did not observe any differences in the methylation between thymoma tissue and unaffected thymus tissue or any correlation between clinic, methylation and histopathology.

Treatment of neuromuscular disorders remains challenging and the development of stem cell-based therapies represents a promising alternative to current treatment options. Rigon et al. tested adipose-derived stromal cells for their potential to support NMJ and muscle regeneration. The authors find a short-term beneficial effect on NMJ regeneration but also observed late phase muscle necrosis and fibrosis induced by an inflammatory response. Myasthenic weakness may be exacerbated by a range of drugs that can interfere with NMJ function, pre- or post-synaptically, including antibiotics, cardiovascular drugs, volatile anesthetics, corticosteroids, lithium, magnesium and other drugs, and a range of drugs and treatments are under suspicion to precipitate *de novo* myasthenic syndromes, such as chloroquine, D-penicillamine, or immune checkpoint inhibitors. Krenn et al. provide an overview over drugs and treatments that influence or possibly induce myasthenic weakness, thereby increasing awareness of adverse treatment effects.

Within this special issue, articles discuss NMJ physiology and highlight some of the complex coordinated events critical for synaptic formation and homeostasis as well as the pathogenic mechanisms underlying NMJ dysfunction. We therefore believe that this special issue provides an excellent overview on current knowledge and future challenges in the field of the neuromuscular system.

DEDICATED TO WES THOMPSON

The research community lost Wesley J. Thompson, one of the pioneers of neuromuscular research in 2019. He contributed seminal work on the role of nerve activity and Schwann cells during NMJ development discussed in detail by Lee and Rimer. Wes was a passionate scientist, a great mentor and wonderful person. He is deeply missed and we would like to honor his loss by dedicating this special issue to our dear friend and colleague Wes Thompson.

AUTHOR CONTRIBUTIONS

All authors listed have made a substantial, direct, and intellectual contribution to the work and approved it for publication.

FUNDING

RH was supported by the Austrian Science Fund (FWF), projects P28485-B24 and P31199-B27. IK was funded by a Hertha Firnberg project grant by the Austrian Science Fund (FWF), project number T996-B30. HL receives support from the Canadian Institutes of Health Research (Foundation Grant FDN-167281), the Canadian Institutes of Health Research and Muscular Dystrophy Canada (Network Catalyst Grant for NMD4C), the Canada Foundation for Innovation (CFI-JELF 38412), and the Canada Research Chairs program (Canada Research Chair in Neuromuscular Genomics and Health, 950-232279). LS was supported by grants from AFM-Téléthon (grant ID 22691) and the Institut National de la Santé et de la Recherche Médicale (INSERM).

REFERENCES

Hunter, S. K., Pereira, H. M., and Keenan, K. G. (2016). The aging neuromuscular system and motor performance. *J. Appl. Physiol.* 121, 982–995. doi: 10.1152/japplphysiol.00475.2016

Li, L., Xiong, W. C., and Mei, L. (2018). Neuromuscular junction formation, aging, and disorders. *Annu. Rev. Physiol.* 80, 159–188. doi: 10.1146/annurev-physiol-022516-034255

Marx, A., Pfister, F., Schalke, B., Saruhan-Direskeneli, G., Melms, A., and Strobel, P. (2013). The different roles of the thymus in the pathogenesis of the various myasthenia gravis subtypes. *Autoimmun. Rev.* 12, 875–884. doi: 10.1016/j.autrev.2013.03.007

Sanes, J. R., and Lichtman, J. W. (2001). Induction, assembly, maturation and maintenance of a postsynaptic apparatus. *Nat. Rev. Neurosci.* 2, 791–805. doi: 10.1038/35097557

Conflict of Interest: The authors declare that the research was conducted in the absence of any commercial or financial relationships that could be construed as a potential conflict of interest.

Publisher's Note: All claims expressed in this article are solely those of the authors and do not necessarily represent those of their affiliated organizations, or those of the publisher, the editors and the reviewers. Any product that may be evaluated in this article, or claim that may be made by its manufacturer, is not guaranteed or endorsed by the publisher.

Copyright © 2021 Herbst, Koneczny, Lochmüller and Strochlic. This is an open-access article distributed under the terms of the Creative Commons Attribution License (CC BY). The use, distribution or reproduction in other forums is permitted, provided the original author(s) and the copyright owner(s) are credited and that the original publication in this journal is cited, in accordance with accepted academic practice. No use, distribution or reproduction is permitted which does not comply with these terms.

frontiers in Molecular Neuroscience

ORIGINAL RESEARCH
published: 24 March 2020
doi: 10.3389/fnmol.2020.00048

The MX-Helix of Muscle nAChR Subunits Regulates Receptor Assembly and Surface Trafficking

Jolene Chang Rudell[1†], Lucia Soares Borges[1], Vladimir Yarov-Yarovoy[1] and Michael Ferns[1,2]*

[1] Department of Physiology and Membrane Biology, University of California, Davis, Davis, CA, United States, [2] Department of Anesthesiology and Pain Medicine, University of California, Davis, Davis, CA, United States

Nicotinic acetylcholine receptors (AChRs) are pentameric channels that mediate fast transmission at the neuromuscular junction (NMJ) and defects in receptor expression underlie neuromuscular disorders such as myasthenia gravis and congenital myasthenic syndrome (CMS). Nicotinic receptor expression at the NMJ is tightly regulated and we previously identified novel Golgi-retention signals in the β and δ subunit cytoplasmic loops that regulate trafficking of the receptor to the cell surface. Here, we show that the Golgi retention motifs are localized in the MX-helix, a juxta-membrane alpha-helix present in the proximal cytoplasmic loop of receptor subunits, which was defined in recent crystal structures of cys-loop receptor family members. First, mutational analysis of CD4-MX-helix chimeric proteins showed that the Golgi retention signal was dependent on both the amphipathic nature of the MX-helix and on specific lysine residues (βK353 and δK351). Moreover, retention was associated with ubiquitination of the lysines, and βK353R and δK351R mutations reduced ubiquitination and increased surface expression of CD4-β and δ MX-helix chimeric proteins. Second, mutation of these lysines in intact β and δ subunits perturbed Golgi-based glycosylation and surface trafficking of the AChR. Notably, combined βK353R and δK351R mutations increased the amount of surface AChR with immature forms of glycosylation, consistent with decreased Golgi retention and processing. Third, we found that previously identified CMS mutations in the ε subunit MX-helix decreased receptor assembly and surface levels, as did an analogous mutation introduced into the β subunit MX-helix. Together, these findings indicate that the subunit MX-helix contributes to receptor assembly and is required for normal expression of the AChR and function of the NMJ. In addition, specific determinants in the β and δ subunit MX-helix contribute to quality control of AChR expression by intracellular retention and ubiquitination of unassembled subunits, and by facilitating the appropriate glycosylation of assembled surface AChR.

Keywords: nicotinic acetylcholine receptor, protein motif, trafficking, neuromuscular junction, congenital myasthenic syndrome

OPEN ACCESS

Edited by:
Ruth Herbst,
Medical University of Vienna, Austria

Reviewed by:
Mohammed Akaaboune,
University of Michigan, United States
Rüdiger Rudolf,
Mannheim University of Applied Sciences, Germany

****Correspondence:***
Michael Ferns
mjferns@ucdavis.edu

†Present address:
Jolene Chang Rudell,
Department of Ophthalmology,
University of California, San Diego,
La Jolla, CA, United States

Received: *24 January 2020*
Accepted: *06 March 2020*
Published: *24 March 2020*

Citation:
Rudell JC, Borges LS, Yarov-Yarovoy V and Ferns M (2020) The MX-Helix of Muscle nAChR Subunits Regulates Receptor Assembly and Surface Trafficking. Front. Mol. Neurosci. 13:48. doi: 10.3389/fnmol.2020.00048

INTRODUCTION

The muscle nicotinic acetylcholine receptor (AChR) is a ligand-gated ion channel belonging to the cys-loop superfamily of receptors that includes the neuronal ACh, $GABA_A$, glycine and $5HT_3$ receptors. The muscle AChR mediates fast transmission at the neuromuscular junction (NMJ) and is a pentamer composed of four subunits with the stoichiometry $\alpha_2\beta\varepsilon\delta$ (adult form). All of the receptor subunits are homologous and have a large extracellular N-terminal domain, 4 transmembrane domains and a large cytoplasmic loop between transmembrane domains 3 and 4 (Unwin, 2005; Sine, 2012). High resolution structures have recently been obtained for several members of the cys-loop family and reveal a conserved architecture of the channel and constituent subunits, as well as providing new insights into the structural basis of transmitter binding and channel gating (Unwin, 2005; Hassaine et al., 2014; Miller and Aricescu, 2014; Huang et al., 2015; Wu et al., 2015; Morales-Perez et al., 2016). One region that is only partially resolved in these structures, however, is the subunit large cytoplasmic loop domain, which contains critical determinants for trafficking and targeting of the receptor (Millar and Harkness, 2008; Albuquerque et al., 2009). This region begins with the short MX helix located just after TM3 and ends with the long MA helix that is continuous with TM4, but no structure is available for the intervening sequence (Wu et al., 2015).

Synaptic transmission at the NMJ is rapid and reliable due in part to the high density of AChRs in the postsynaptic membrane, and defects in AChR expression in genetic and autoimmune diseases impair transmission and result in myasthenia (Verschuuren et al., 2016; Engel, 2018). The expression of AChR at the NMJ is tightly regulated and depends on the appropriate assembly, trafficking and localization of receptors in the postsynaptic membrane (Millar and Harkness, 2008). This slow and complex process begins with the synthesis and assembly of receptor subunits in the ER. Assembled receptor is then exported from the endoplasmic reticulum (ER) and trafficked to the Golgi apparatus for further processing, which includes modification of N-linked oligosaccharides on the γ and δ subunit to more complex forms (Gu et al., 1989; St John, 2009). Finally, the mature AChR is sorted, trafficked to the plasma membrane, and localized in the postsynaptic membrane. Each step in this process is thought to be directed by specific molecular signals in the receptor subunits that function in distinct cellular compartments. Moreover, as the process is relatively inefficient with only 10–30% of the synthesized subunits being incorporated into surface nAChR (Merlie and Lindstrom, 1983; Wanamaker et al., 2003), quality control mechanisms play an important role in ensuring that only correctly assembled, functional channels are expressed on the cell surface (Fu et al., 2016).

The molecular basis for the initial steps in AChR biogenesis are relatively well understood, with several signals being defined on the receptor subunits that govern receptor assembly and ER quality control (Millar and Harkness, 2008; Colombo et al., 2013). For example, determinants in the subunit extracellular domains direct the ordered assembly of receptor subunits, helping ensure the correct stoichiometry of receptor. Other determinants in the subunit first transmembrane domain and major cytoplasmic loop permit the export of pentameric receptor from the ER, but retain unassembled or partially assembled subunits (Keller et al., 2001; Wang et al., 2002; Ren et al., 2005), where they are then ubiquitinated and degraded by the ER-associated degradation machinery (Christianson and Green, 2004). In contrast, little is known about the molecular signals that regulate subsequent steps in AChR trafficking. Golgi trafficking is likely regulated, as a genetic screen in *Caenorhabditis elegans* identified the Golgi-resident protein, unc-50, as being required for trafficking of one subtype of nAChR to the NMJ (Eimer et al., 2007). Moreover, it likely provides an additional quality control checkpoint, as mutations in the α subunit loop that allow ER export result in the unassembled subunit being retained in the Golgi by an unknown mechanism (Keller et al., 2001). To define the molecular determinants that regulate these later trafficking steps we performed an unbiased screen for post-ER trafficking signals in the AChR subunit major cytoplasmic loop. We identified novel motifs in the β and δ subunit loops that mediate Golgi retention, and mutation of this motif permits surface expression of unassembled subunit loops and increases surface levels of assembled AChR (Rudell et al., 2014). Here, we show that the Golgi retention signal is localized in the MX-alpha helix and is centered on key lysine residues. We find that the motif contributes to quality control both through ubiquitination and intracellular retention of unassembled subunits, and by facilitating the appropriate Golgi-based glycosylation of assembled receptor. In addition, we identify distinct determinants in the MX helix that contribute to receptor assembly, and CMS-linked mutations in this region impair subunit assembly and AChR expression. Thus, the MX-helix of receptor subunits contain important molecular signals that regulate the assembly, trafficking and expression of muscle AChR at the NMJ.

MATERIALS AND METHODS

Rosetta Molecular Modeling

Homology modeling of human AChR beta and delta subunits was performed using Rosetta structural modeling software (Rohl et al., 2004; Song et al., 2013; Bender et al., 2016; Alford et al., 2017) based Robetta server (Park et al., 2018) and x-ray structure of the human alpha4beta2 nicotinic receptor (Morales-Perez et al., 2016) as a template. Human AChR beta subunit was modeled based on human alpha4beta2 nicotinic receptor beta 2 subunit (PDB ID: 5KXI chain C) (Morales-Perez et al., 2016). Human AChR delta subunit was modeled based on human alpha4beta2 nicotinic receptor beta 2 subunit (PDB ID: 5KXI chain B) (Morales-Perez et al., 2016). 1,000 models were generated for each subunit and clustered (Bonneau et al., 2002) to identify top 5 models. We then superimposed a representative model from one of

the top human AChR beta subunit models onto human alpha4beta2 nicotinic receptor beta 2 subunit (PDB ID: 5KXI chain C) and a representative model from one of the top human AChR delta subunit models onto human alpha4beta2 nicotinic receptor beta 2 subunit (PDB ID: 5KXI chain B) in the complete structure of the human alpha4beta2 nicotinic receptor (Morales-Perez et al., 2016). All structural figures were generated using the UCSF Chimera package (Pettersen et al., 2004).

CD4-Subunit Loop Constructs

Chimeric constructs consisting of mouse CD4 extracellular and transmembrane domains fused with the major cytoplasmic loop of each mouse nAChR subunit were generated and described previously (Borges et al., 2008; Rudell et al., 2014). Mutations in the intracellular loops were introduced using the QuikChange Lightning site-directed mutagenesis kit (Agilent Tech.) and confirmed by sequencing.

Cell Culture and Transfection

HEK cells were maintained in growth media (DMEM supplemented with 10% fetal bovine serum, 2 mM L-glutamine and 200 U/ml penicillin-streptomycin) at 37°C and 5% CO_2. They were transfected at ∼70% confluence using calcium phosphate (for large 10 cm dishes) or Lipofectamine 3000 (Invitrogen).

C2 mouse muscle cells were maintained in growth media (DMEM supplemented with 20% fetal bovine serum, 0.5% chick embryo extract, 2 mM L-glutamine and 200 U/ml penicillin-streptomycin) at 37°C and 8% CO_2. Myoblasts were transfected at ∼60–70% confluence using Fugene (Roche) or Lipofectamine 3000 (Invitrogen). Upon reaching confluence the cells were incubated with fusion medium (DMEM supplemented with 5% horse serum and 2 mM L-glutamine) and allowed to differentiate into myotubes for 3–4 days prior to analysis (Borges et al., 2008).

Surface Expression of CD4 Chimeras and AChR

For on cell western assays, C2 muscle cells were grown on 8-well chamber slides and duplicate wells were transfected with each CD4-subunit loop chimera. After 3–4 days for expression the cells were fixed and one of the two wells was permeabilized with 0.5% Triton X-100. The slides were then incubated with anti-CD4 antibody to assay surface levels of CD4-chimera in non-permeabilized cells (first well), compared to total levels (surface + intracellular) of the same CD4-chimera in permeabilized cells (second well). Bound antibodies were detected using IRDye-conjugated anti-rat secondary antibodies and an Odyssey Imaging System (LiCor). Total signal intensity was measured for each well and the percentage of surface (non-permeabilized) versus total (permeabilized) expression calculated for each CD4-subunit loop chimera. Data was collected from 4–6 independent experiments for each construct.

To assay levels of surface AChR, HEK cells were grown on 6-well plates and transfected with mouse AChR subunits. After 1 d for expression, the cells were labeled with 10 nM I^{125}-labeled-α-BuTx (Perkin Elmer) for 45 min. Non-specific binding was determined by treating myotubes with 1 μM of cold α-BuTx for 30 min prior to incubation with I^{125}-α-BuTx. Cells were then washed three times with growth media to remove unbound I^{125}-α-BuTx, solubilized in 0.1N NaOH and the I^{125}-α-BuTx bound to surface AChR was measured with a Packard gamma counter. Background counts were subtracted from the experimental counts and values are reported as a percentage of the total surface counts for cells transfected with wild type AChR.

Isolation and Immunoblotting of CD4-Chimeras and AChR

To assay ubiquitination of CD4 subunit loop chimeras by western blotting, transfected C2 muscle cells were washed, scraped off and pelleted in ice cold PBS. They were then re-suspended in extraction buffer (0.5% Triton X-100, 25 mM Tris, 25 mM glycine, 150 mM NaCl, 5 mM EDTA, and protease inhibitors) and incubated for 10 min on ice, after which the insoluble proteins were pelleted by centrifugation at 13,000 rpm for 5 min. The CD4 chimeras were immunoprecipitated from the soluble fraction with monoclonal antibody GK1.5 (BD Biosciences-Pharmingen, San Jose, CA) chemically cross-linked to protein G-agarose (Invitrogen, Carlsbad, CA). The isolates were separated on 10% polyacrylamide gels and immunoblotted with anti-ubiquitin antibody P4D1 (Santa Cruz Biotech.). The bound antibodies were then detected using IRDye-conjugated secondary antibody, imaged with an Odyssey Imaging System, and band intensities quantified using ImageStudio (Li-Cor). Immunoblots were re-probed with rmCD4 antibody (R&D Systems) to confirm levels of the different CD4 subunit loop chimeras.

To assay AChR glycosylation, heterologous HEK cells were transfected with wild type or mutant AChR subunits. Epitope tagged (142) delta subunits were used to allow unambiguous identification of delta, and G1G2 delta variants had T78A and S145A mutations to eliminate the two N-linked glycosylation sites (Ramanathan and Hall, 1999). After 1 day for expression, the cells were incubated live with biotinylated α-bungarotoxin (α-BuTx) for 45 min to label surface AChR, and then washed, collected and extracted in buffer containing 0.5% Triton X-100, 25 mM Tris, 25 mM glycine, 150 mM NaCl, 5 mM EDTA and Halt protease inhibitor cocktail (ThermoScientific). First, biotin-α-BuTx-labeled surface receptor was isolated from the extracts using streptavidin-beads (Invitrogen). Then, unlabeled intracellular AChR was isolated from the remaining supernatant by re-incubation with biotin-α-BuTX and pulldown on streptavidin beads. The samples were separated on large format 10% polyacrylamide gels (14 × 14 cm) and immuno-blotted with anti-β (mAb148) and anti-δ (mAb142) subunit antibodies (Santa Cruz Biotech.). Bound antibodies were detected using IRDye-conjugated anti-rat secondary antibody, imaged with an Odyssey Imaging System, and band intensities quantified using ImageStudio (Li-Cor). In experiments to assay AChR assembly, unassembled β subunit was isolated from cell extracts after isolation of assembled

AChR, using mAb148 chemically cross-linked to protein G-agarose.

RESULTS

Molecular Structure and Determinants of MX-Helix Retention Motifs

In previous work we identified Golgi retention motifs in the β and δ subunit proximal cytoplasmic loops (Rudell et al., 2014). Interestingly, this region corresponds to the MX-helix, which is a juxta-membrane amphipathic α-helix defined in recent crystal structures of cys-loop receptor family members (Hassaine et al., 2014; Morales-Perez et al., 2016). As this region is not resolved in the lower resolution structures of the muscle AChR (Unwin, 2005), we used Rosetta software to model the MX-helices using the neuronal α4β2 AChR crystal structure (Morales-Perez et al., 2016). As shown in **Figures 1A–C**, the structure and position of the MX-helix is similar in all subunits, although differences exist in the distribution of charged residues. In the case of the β and δ subunits, the Golgi retention motifs consist of a short loop following TM3 and the laterally positioned MX-helix

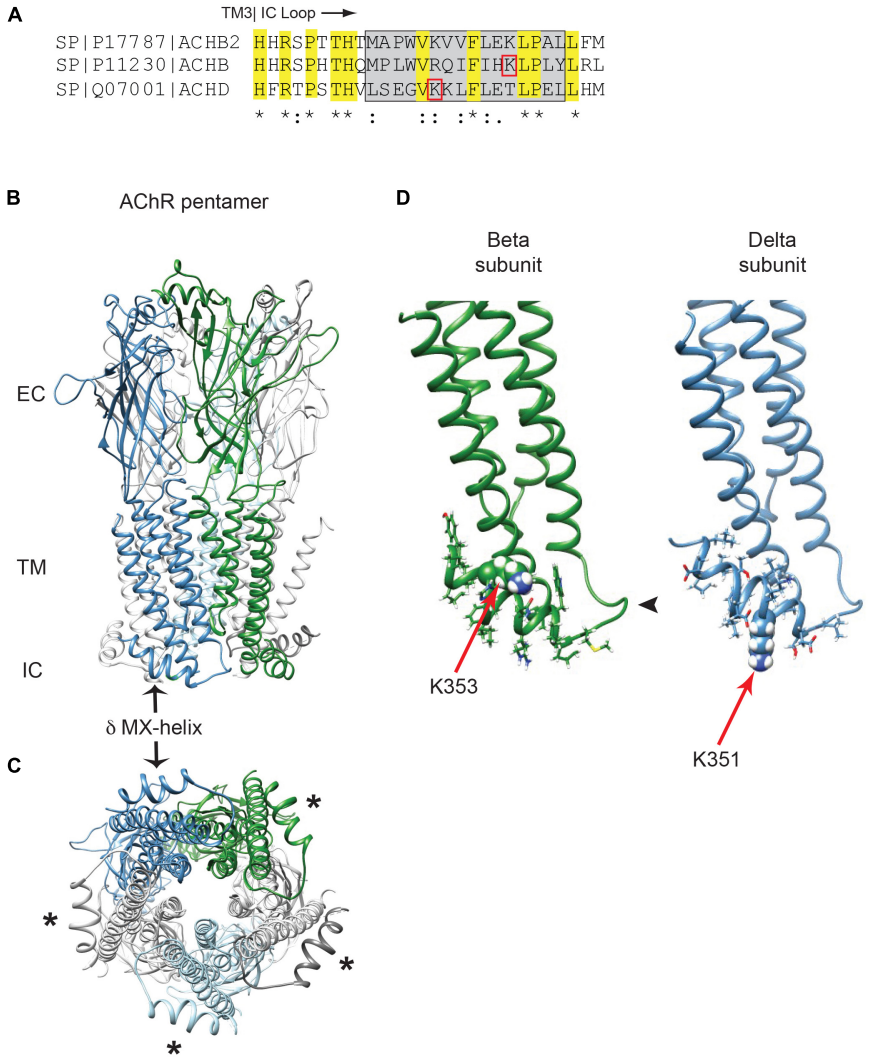

FIGURE 1 | Golgi retention motifs are localized in the MX-helix. **(A)** Sequence alignment of the neuronal beta 2 and muscle beta and delta subunits, depicting the initial portion of the large cytoplasmic (TM3-TM4) loop. The MX-helix region is shown by the gray box, and the Golgi retention signals in β and δ are both centered on lysine residues (βK353 and δK351; denoted by red boxes). Sequence identity and conservation are represented by * and : symbols. **(B)** General architecture of the nicotinic acetylcholine receptor, based on the α4β2 crystal structure, showing the extracellular (EC), transmembrane (TM), and intracellular (IC) domains. Alpha subunits are in light gray, beta subunit in green, delta subunit in blue and epsilon subunit in light blue. The arrow marks the δ subunit MX-alpha helix, which is positioned laterally just below the membrane. Note that the rest of the intracellular domain is missing from the structure. **(C)** View perpendicular to the membrane looking from the intracellular side. Asterisks mark the MX-helix in each subunit. **(D)** The muscle beta and delta subunits were modeled using Rosetta structural modeling software. The initial portion of the TM3-TM4 cytoplasmic segment consists of a short loop following TM3 (arrowhead) followed by the laterally positioned MX-helix (residues shown with sidechains). The MX-helix contains the critical determinants for the Golgi retention signal, which are centered around K353 in the beta subunit and K351 in the delta subunit (red arrows mark key lysine residues, which are shown in space filling representation).

(**Figure 1D**). The key sequence determinants for retention identified in our earlier study lie within the MX-helix and include an ordered sequence of hydrophobic and hydrophilic residues related to the partially amphipathic structure of the helix. Moreover, the critical lysine residues identified in the β and δ motifs (βK353 and δK351) are both surface-exposed in the model and potentially accessible, although the sidechains of βK353 are positioned close to the plasma membrane (**Figure 1D**). This MX helix structure provides a straightforward molecular basis for the functional effects described in our earlier mutational analysis (Rudell et al., 2014). For example, βK353L and δK351L mutations would locally alter the surface charge on the MX-helix, and other single amino-acid insertions or deletions that abolished retention (e.g., βQ348del, βL353ins, and δK354ins) would shift the rotational axis of the helix and also alter the relative position of the charged and hydrophobic residues. Together, this structural and functional analysis indicates that β and δ subunit trafficking motifs depend on the alpha-helical MX structure and its distribution of charged and hydrophobic residues.

Although all receptor subunits possess an MX-helix one feature of the β and δ subunits is the surface-exposed lysine residues (βK353 and δK351). To further probe their role in the retention signal, we compared the effects of mutating the lysine residues to either leucine or arginine. Substitution to leucine preserves the MX α-helical structure but replaces the positively charged lysine residue with a neutral amino acid, whereas substitution to arginine maintains the positively charged residue and thus the alignment of charged amino acids on the helix. For this, we expressed CD4-subunit loop chimeric proteins in C2 mouse muscle cells and used an on-cell western assay to quantify surface versus total expression for each chimera (**Supplementary Figure 1**). As shown in **Figure 2A**, the chimeras consist of the CD4 extracellular and transmembrane domains fused to the β or δ cytoplasmic loops, or to the minimal β or δ retention signals encompassing the MX-helix. As reported in our earlier study, a large fraction of CD4-β and δ loop chimeras were retained intracellularly, but mutating the key lysine residue in each motif to leucine (βK353L or δK351L) was sufficient to increase their surface expression several-fold (Rudell et al., 2014). Surprisingly, we found that lysine to arginine mutations also significantly increased their surface expression (**Figure 2B**), with surface levels approaching those of CD4-loop chimeras with K-L mutations. Indeed, β K353L and K353R mutations increased surface levels of CD4-β loop by 5.9 and 3.6-fold, and CD4-β333-369 by 3.2 and 2.5-fold, respectively. Similarly, δ K351L and K351R mutations increased surface levels of CD4-δ loop by 98 and 77-fold, and CD4-δ337-370 by 2.2 and 2.9-fold. These experiments indicate that the β and δ retention signals depend not only on the amphipathic nature of the MX-helix, but also on specific lysine residues (βK353 and δ K351).

Role of the MX-Helix Retention Motifs in Quality Control

Lysine residues are notable in that they are targets for several types of post-translational modification. The most common is ubiquitination, which plays an important role in the regulation of trafficking, degradation and quality control of many membrane proteins (Mukhopadhyay and Riezman, 2007; MacGurn et al., 2012; Foot et al., 2017). Consequently, we tested whether MX-helix lysine residues are ubiquitinated and if ubiquitination contributes to retention. For this, we expressed CD4-subunit loops in HEK cells as the low expression levels of some chimeras in muscle cells was prohibitive for biochemical experiments. The CD4-subunit loop chimeras were then immunoprecipitated from cell extracts using anti-CD4 antibody and immunoblotted with anti-ubiquitin antibody. Notably, we detected significant ubiquitination of CD4-β and δ loops but low or undetectable ubiquitination of CD4 or CD4-ε loops (**Figure 3A**). The ubiquitination of CD4-β and δ loops was evident as a higher molecular weight ladder beginning around 9 kD above the major CD4-β and δ bands detected with anti-CD4 antibody, consistent with the addition of one or more ubiquitin molecules. Thus, ubiquitination occurs on CD4-β and δ loops which are retained intracellularly, but not on CD4 and CD4-ε loop, which are trafficked efficiently to the cell surface.

To then define the determinants for ubiquitination, we expressed CD4-β and δ proximal loop fragments with mutations of βK353 and δK351 or of neighboring residues. We detected robust ubiquitination of CD4-β333-369, which was significantly reduced by mutation of K353 to either L or R (**Figure 3B**). Similarly, ubiquitination of CD4-δ337-370 was largely abolished by mutation of K351 to L or R and comparable to CD4 control (**Figures 3B,C**). In addition, we tested whether other mutations previously found to impair retention of CD4-β333-369 also reduced ubiquitination. Indeed, insertion of a leucine in the MX helix (L353ins) or substitution of L354 for lysine both greatly decreased ubiquitination, despite the presence of K353 or even an additional lysine. Finally, by immunoblotting with anti-CD4 antibody we confirmed that the differing levels of ubiquitination were unrelated to total expression of CD4-β333-369 and δ337-370, and also that only a small proportion of each occurred in the higher molecular weight, ubiquitinated form. Together, these findings suggest that ubiquitination occurs largely on βK353 and δK351 and is dependent on a specific recognition sequence that encompasses these lysines in the MX-helix. Ubiquitination correlates closely with intracellular retention of the CD4-β and δ loop chimeras, and likely regulates either their retention in the Golgi apparatus and/or their subsequent degradation. Thus, ubiquitination of the MX-helix motifs contributes to Golgi-based quality control of receptor trafficking.

Next, we tested whether the Golgi retention motifs also regulate trafficking and quality control of fully assembled AChR. For this, we focused on glycosylation of the AChR, which includes a key maturational step that occurs in the Golgi apparatus. Previous studies have shown all receptor subunits contain conserved N-linked glycosylation sites mostly with simple oligosaccharides added during receptor biosynthesis in the ER (Gehle et al., 1997). In the case of the gamma and delta subunits, however, the simple oligosaccharides at one of the glycosylation sites are modified to complex forms in the Golgi apparatus (Gu and Hall, 1988; Ramanathan and Hall, 1999), prior to receptor trafficking to the plasma membrane. First, to confirm the earlier studies, we sequentially isolated surface

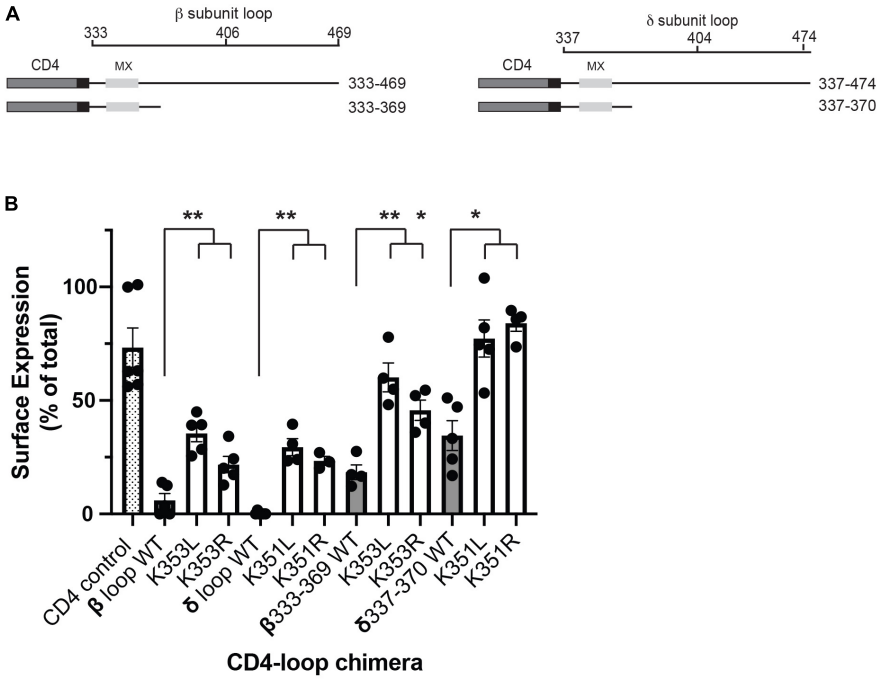

FIGURE 2 | Molecular determinants for retention include specific lysine residues. **(A)** Schematic showing the CD4-subunit cytoplasmic loop chimeras used to characterize the retention signal. These consist of CD4 extracellular and transmembrane domains fused to either the full β or δ subunit intracellular loops, or to proximal loop fragments encompassing the MX-helix. **(B)** C2 mouse muscle cells were transfected in duplicate with each CD4-subunit loop chimera, and the percentage of each protein that was expressed on the cell surface was measured in on-cell Western blot assays. The percentage of CD4-β and δ full loops and CD4-β333-369 and δ337-370 on the cell surface (gray bars) was much lower than for CD4 control (hatched bar). Surface expression of the CD4-β and δ chimeras was increased significantly, however, by substitution of βK353 or δK351 for either leucine or arginine (**$p < 0.01$;*$p < 0.05$; one way ANOVA with Tukey's multiple comparisons test; n = 4–6 experiments, error bars = SEM). The effect of K–L mutations tended to be slightly larger than K–R mutations, but this difference was not statistically significant.

and intracellular AChR from transfected HEK cells (see section "Methods"), and then immunoblotted for the β and δ subunits (**Figure 4A**). To unambiguously identify the δ subunit we utilized an antibody to a C-terminal epitope tag, as available antibodies recognize both the γ and δ subunits. We found that the wild type (WT) δ subunit in surface AChR runs at significantly higher molecular weight than δ in intracellular AChR (∼68 cf. 62 kD), confirming that its N-linked oligosaccharides are modified prior to trafficking to the plasma membrane. Indeed, quantification of these experiments shows that ∼90% of the delta subunit in surface AChR has mature glycosylation, compared to only 17% in intracellular receptor (**Figure 4B**). To confirm that the shift in molecular weight was due to changes in glycosylation we expressed AChR containing delta subunit with mutations of the glycosylation sites (δG1G2). As expected, deltaG1G2 was evident as a single band of lower molecular weight and present only in intracellular receptor (**Figure 4A**). Similarly, expression of an incomplete set of receptor subunits (α, β, and δ subunits) resulted in delta subunit with largely immature glycosylation and mostly in intracellular receptor. These findings confirm earlier studies and show that N-linked glycosylation of the delta subunit is required for efficient subunit assembly and surface expression of AChR.

We have shown previously that mutation of the retention motifs increases surface AChR by promoting Golgi to surface trafficking (Rudell et al., 2014). Consequently, we tested whether the β/δ retention motifs contribute to delta subunit glycosylation in the Golgi and if their mutation perturbs the selective expression of mature AChR on the cell surface. To do this, we expressed AChR in wild type form or with combined βK353L and δK351L mutations, and sequentially isolated surface and intracellular receptor and then immunoblotted for the β and δ subunits. We found that surface wild type and mutant AChR contained predominantly the high molecular form of the delta subunit with mature glycosylation. However, a significantly higher percentage of low molecular weight delta subunit was detected in βK353L/δK351L – AChR compared to wild type AChR (16% cf. 8%, **Figures 4C,D**). Thus, mutation of the retention motifs increases surface AChR with immature glycosylation by twofold, indicating that the motifs contribute to Golgi trafficking and quality control of assembled receptor.

Role of MX-Helix in AChR Assembly and Expression

The MX-helix is present in all receptor subunits and could regulate additional aspects of AChR assembly or trafficking that are critical for its expression and function at the NMJ. Consistent with this, two previously identified human mutations

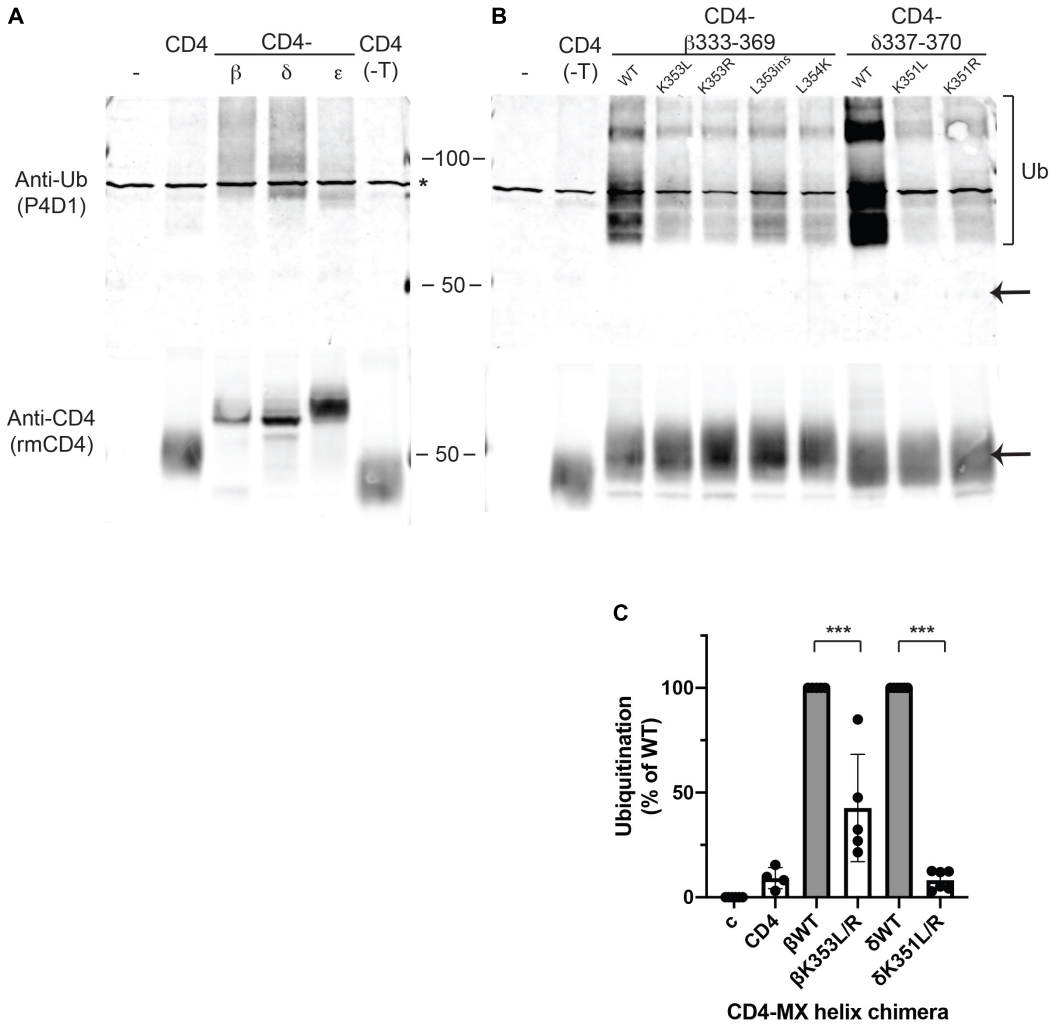

FIGURE 3 | Retention is associated with ubiquitination of MX-helix lysine residues. **(A,B)** CD4 subunit loop chimeras expressed in HEK cells were immunoprecipitated from cell extracts using anti-CD4 antibody cross-liked to agarose beads. The isolates were immunoblotted with monoclonal anti-ubiquitin antibody (P4D1), and then re-probed with polyclonal anti-CD4 antibody. We detected ubiquitination of both CD4-β and δ full loops **(A)** and CD4-β333-369 and δ337-370 MX-helix chimeras **(B)**. The ubiquitination was evident as a characteristic ladder of high molecular weight forms (bracket) beginning around 9 kD above the major band detected with anti-CD4 antibody (arrow). In contrast, little or no ubiquitination was evident for CD4 (control), CD4 with a deleted intracellular tail (CD4-T), or CD4-ε loop. Note that the asterisk marks a non-specific band present in non-transfected samples. **(B)** High levels of ubiquitination of CD4-β333-369 and δ337-370 were greatly reduced by mutation of βK353 or δK351 to either leucine (L) or arginine (R). Mutations adjacent to βK353 also reduced ubiquitination (βL353ins and βL354K). **(C)** Quantification of the immunoblots shows that ubiquitination of CD4-β333-369 was reduced 57% by K353L/R mutations, and ubiquitination of CD4-δ337-370 was reduced 92% by K351L/R mutations (***$p < 0.001$, one way ANOVA with Tukey's multiple comparison's test, $n = 4$–6 independent transfection experiments).

linked to congenital myasthenic syndrome (CMS) localize to the epsilon subunit MX-helix. The first is a homozygous missense mutation (CHRNE P351L; Croxen et al., 2001), which reduces assembly and surface expression of AChR in heterologous cells, and the second is a homozygous 27 base pair deletion (CHRNE 1046_1072del27 eliminating amino acids 349-357), whose functional effects are uncharacterized (Maselli et al., 2010). Interestingly, these mutations occur near the end of the MX helix (**Figure 5A**) and the structural model shows that these residues contribute to the cytoplasmic interface between the α and ε subunits (**Figure 5B**). Indeed, in the molecular structures of both the α4β2 and $5HT_3$ receptors, the end of each subunit MX-helix contacts the short loop following TM3 in the adjacent subunit (Hassaine et al., 2014; Morales-Perez et al., 2016). These findings suggest that the MX-helix could play a role in subunit assembly and AChR expression. To test this, we compared the effects of the CMS-linked mutations in both the epsilon and beta subunits. For this, wild type and mutant AChR subunits (α, β, ε, and δ) were expressed in heterologous HEK cells, and levels of surface receptor were measured by binding of I^{125}-labeled alpha-bungarotoxin. Compared to wild type AChR, we found that surface receptor

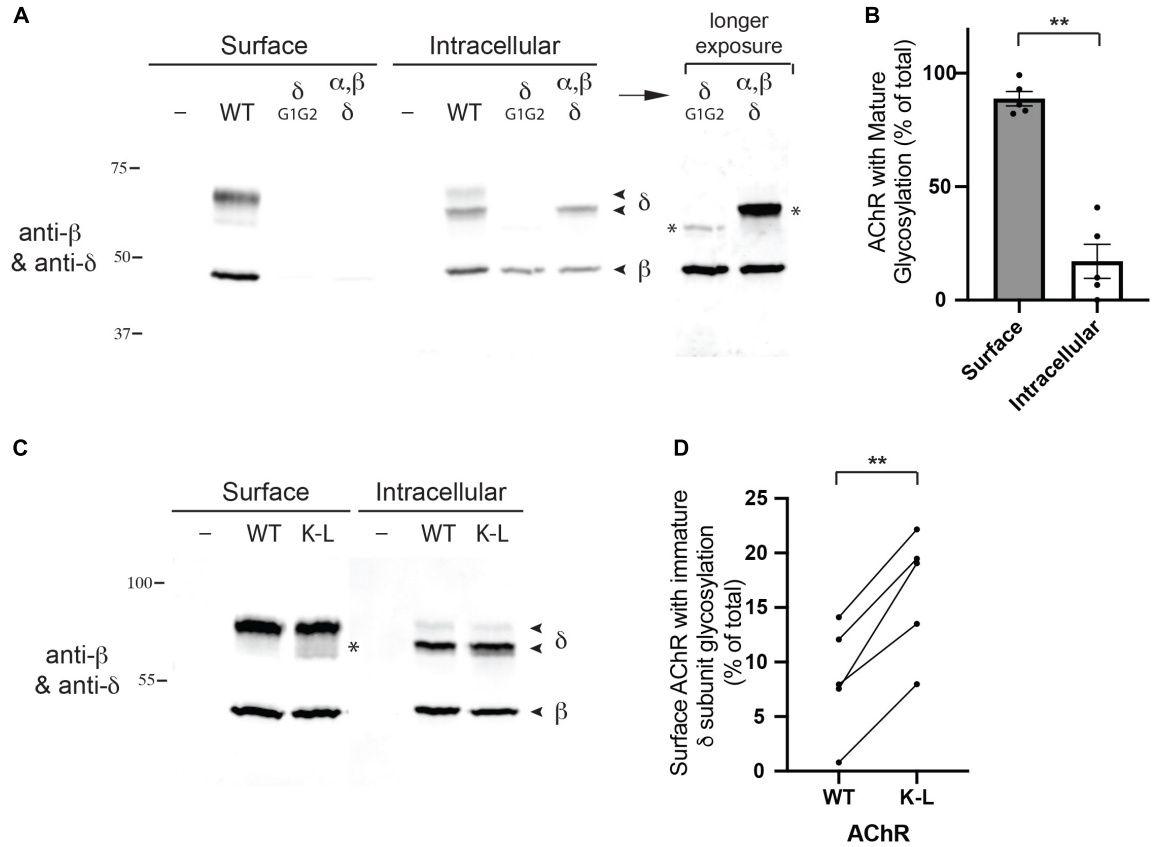

FIGURE 4 | Mutation of the Golgi retention motif increases surface AChR with immature glycosylation. **(A)** HEK cells were transfected with wild type AChR subunits (α, β, ε, and an epitope-tagged δ subunit), or with AChR containing δ subunit with mutated N-linked glycosylation sites. We then sequentially isolated surface and intracellular AChR and immunoblotted the isolates for the β and δ subunits. We found that surface AChR contained a higher molecular weight form of δ subunit compared to intracellular AChR (~68 cf. 62 kD), which has been shown to be due to modification of N-linked oligosaccharides during transit through the Golgi complex. Consistent with this, AChR containing δ with mutated glycosylation sites (δG1G2), or only α, β and δ subunits were largely retained in the intracellular receptor pool and contained only lower molecular weight forms of δ (marked by asterisks in longer exposure image). **(B)** Quantification shows that surface AChR contains largely high molecular weight δ subunit with mature glycosylation (89% of total). In contrast, intracellular AChR contains only 17% high molecular weight δ subunit, with the vast majority (83%) being low molecular weight δ subunit with immature glycosylation (**$p < 0.005$; paired t test; $n = 5$ experiments; error bars = SEM). **(C)** HEK cells were transfected with wild type AChR or AChR containing combined βK353L and δK351L mutations (K–L), and surface and intracellular AChR were sequentially isolated and immunoblotted with anti-β and δ subunit antibodies. Compared to wild type AChR, mutant AChR contained significantly more low molecular weight delta subunit with immature glycosylation (asterisk). **(D)** Quantification showing the percentage of WT and K–L surface AChR with immature δ subunit glycosylation, with each pair of data points representing a separate transfection experiment. Combined βK353L/δK351L mutations increased the amount of surface AChR with immature glycosylation by twofold, from 8 to 16% (**$p < 0.005$; paired *t*-test; $n = 5$ experiments).

levels were decreased 25% for εP351L-AChR and 55% for εdel349-357-AChR (**Figure 5C**). An analogous mutation in the β subunit (βP355L) decreased receptor levels by 50%, but a βP355A mutation had no discernable effect. In addition, we found that a targeted mutation of the preceding residue (βL354K) designed to misposition the MX-helix reduced surface receptor levels by 85%. In the case of CHRNE P351L, the decrease in surface receptor results primarily from impaired assembly of the mutant subunit (Croxen et al., 2001). To test whether this is also the case for βP355L we sequentially isolated assembled AChR and then unassembled beta subunit and immunoblotted to compare the amount of beta subunit in each pool (**Figure 5D**). Notably, βP355L subunit assembled into AChR much less efficiently than wild type β subunit (**Figure 5E**). Together, these findings show that CMS mutations in the epsilon subunit and analogous mutations in the beta subunit both reduce surface expression of the AChR, in large part by impairing subunit assembly. Thus, the MX-helix also contains shared determinants that contribute to subunit assembly and AChR expression.

DISCUSSION

AChR function at the NMJ depends on its appropriate assembly, processing and trafficking to the cell surface, with each step in receptor biogenesis being regulated by specific molecular determinants in the receptor subunits. Here, we identify important regulatory signals localized in the MX-helix, which is a juxta-membrane α-helix present in the proximal,

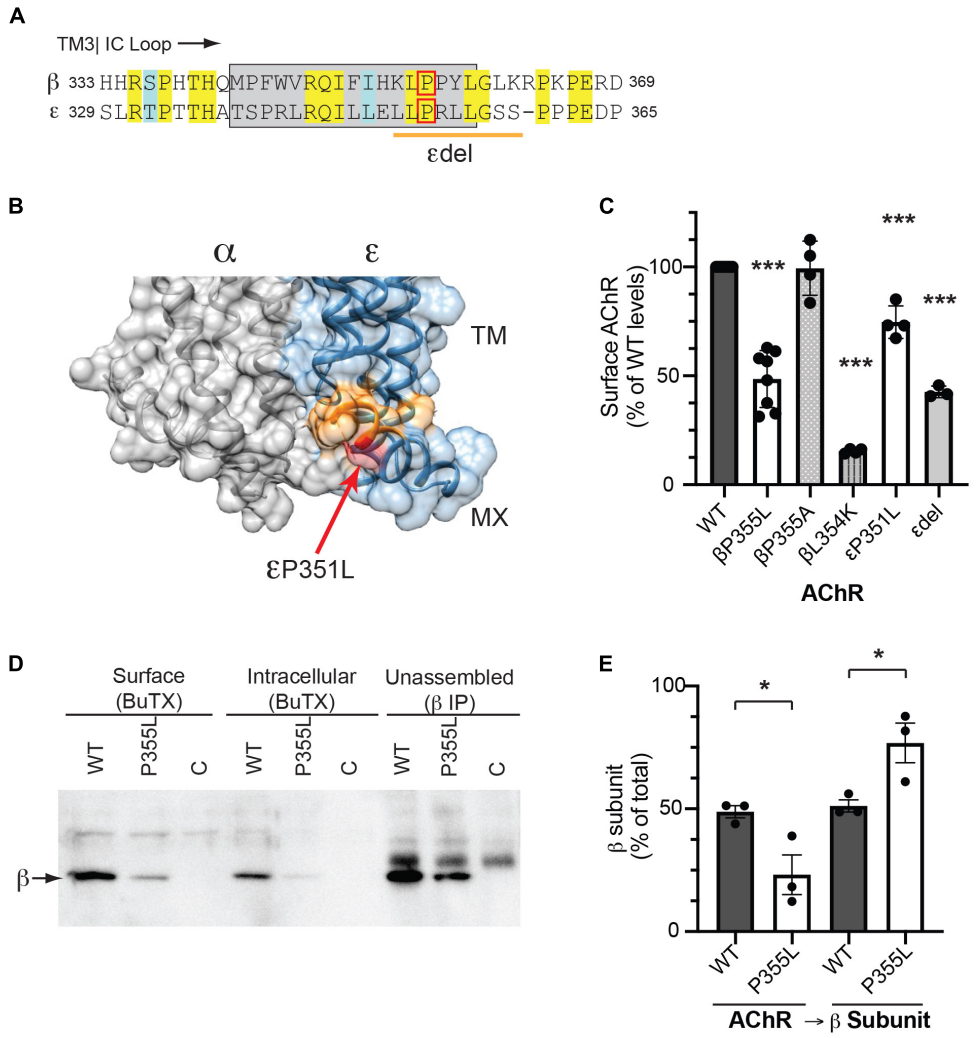

FIGURE 5 | CMS-linked mutations in the MX-helix impair AChR assembly and expression. **(A)** Sequence alignment showing the initial portion of the beta and epsilon cytoplasmic (TM3-TM4) loops, with the MX-helix shown by the gray box. The two CMS-linked mutations in the epsilon subunit are denoted by the red box (εP351L) and orange line (εdel349-357), respectively. The analogous proline in the β subunit MX-helix (βP355L) is indicated by the red box. **(B)** Molecular structure showing the cytoplasmic interface between the alpha and epsilon subunits. The end of the ε MX helix contacts the short loop connecting TM3 to the MX-helix of the α subunit. Residues deleted in the εdel mutation are shown in orange and the εP351L mutation is marked by the red arrow. **(C)** HEK cells were transfected with AChR in wild type form or with the indicated mutations in the MX-helix, and surface levels of AChR were measured by ^{125}I-alpha-BuTx binding. Compared to WT AChR, the CMS-linked mutations in epsilon (εP351L and εdel349-357) decreased surface levels of AChR by 25 and 57%, respectively. The corresponding βP355L mutation decreased surface AChR by 51% but βP355A mutation had no discernable effect. Beta L354K mutation, which is predicted to misposition the MX helix, decreased surface AChR by 85% (***$p < 0.0001$ as compared to WT; one way ANOVA with Dunnett's multiple comparison's test; n = 3–8 experiments). **(D)** HEK cells were transfected with wild type or βP355L-AChR. We then sequentially isolated surface AChR, intracellular AChR, and unassembled beta subunit, and immunoblotted with anti-beta subunit antibody to compare the levels in each pool. Significant amounts of wild type β subunit were detected in the pools of surface and intracellular AChR, as well as in the pool of unassembled subunit. In contrast, βP355L subunit was mostly detected in the unassembled subunit pool, indicating that it assembled less efficiently into AChR. **(E)** Quantification shows that a smaller percentage of P355L β subunit (23%) assembled into AChR compared to wild type β subunit (49%) (*$p < 0.05$, one way ANOVA with Sidak's multiple comparison's test, n = 3 experiments).

major cytoplasmic loop of all subunits. First, specific sequence determinants in the β and δ subunit MX-helices mediate Golgi retention and contribute to quality control of AChR expression by (i) retention of unassembled subunit loops, leading to their ubiquitination and degradation, and (ii) retention of assembled AChR, helping ensure appropriate glycosylation occurs in the Golgi prior to their surface trafficking. Second, shared determinants in a distinct region of the subunit MX-helices contribute to subunit assembly, as CMS and targeted mutations near the end of the MX-helix impair receptor assembly and surface expression.

Molecular Signals in MX Helix

The Golgi retention motifs that we previously identified in the β and δ subunits reside in the MX-helix, which was defined in crystal structures of both the α4β2 neuronal AChR

and the $5HT_3$ receptor (Hassaine et al., 2014; Morales-Perez et al., 2016). This juxta-membrane α-helix is present in all subunits and is positioned laterally in the proximal TM3-TM4 cytoplasmic loop, placing it in close proximity to the inner leaflet of the plasma membrane, and ending near the interface with the adjacent receptor subunit. Using the neuronal α4β2 structure we generated a molecular model of the muscle β and δ subunit motifs, whose structure readily accounts for the sequence requirements for Golgi retention identified in our earlier mutational analysis (Rudell et al., 2014). First, the requirement for an ordered array of charged and hydrophobic residues corresponds directly to the amphipathic nature of the helix, and explains why single amino-acid insertions, deletions, or substitutions of hydrophilic and hydrophobic residues all reduced intracellular retention. Second, the critical lysine residues in β and δ (βK353 and δK351) are both surface exposed with outward-facing sidechains, whereas lysine residues are absent at the equivalent positions in the other subunits (α, γ, and ε). The importance of βK353 and δK351 is further underscored by our finding that even substitution with another positively charged residue (arginine) significantly reduced Golgi retention. Together with our earlier findings, this suggests that the Golgi retention signal consists of a short, solvent-exposed face of the MX-helix encompassing the key lysine residue.

The MX-helix structure is conserved in all subunits of both the α4β2 AChR and $5HT_3$ receptors, however, consistent with additional functions in AChR assembly and function (Wu et al., 2015). Indeed, we found that CMS-linked mutations in epsilon (εP351L and εdel349-357) that reduce AChR assembly and levels are located at the end of the MX-helix, and our structural model shows that these residues contact the initial portion of the alpha subunit TM3-TM4 loop. An analogous P355L mutation in the β subunit MX-helix also impaired subunit receptor assembly and expression (**Figure 5**), whereas a P355A mutation had no detectable effect on either. The reason for this remains unclear, but potentially the longer sidechains of leucine could disrupt either the folding and/or inter-subunit interactions of the beta subunit. Notably, this proline residue is part of a highly conserved (L/I/V)P sequence pair, which is present in almost all muscle and neuronal AChR subunits and consequently could contribute generally to the cytoplasmic interface between subunits and their assembly. Moreover, we have shown previously that the LP residues are not required determinants for the β/δ Golgi retention signals (Rudell et al., 2014). Thus, these findings define additional molecular determinants in the MX-helix important for receptor assembly/expression, which map to the end of the MX-helix and are distinct from the Golgi retention signals.

Function and Mechanism of MX-Helix Signals

The retention signals specific to the β/δ subunit MX-helix regulate Golgi trafficking and we propose that they contribute to quality control of AChR expression in two ways. First, our findings suggest that the retention motifs help prevent surface expression of unassembled or incorrectly assembled receptor subunits that escape the ER quality control mechanisms. The presence of an additional quality control checkpoint at the Golgi complex has been documented in many systems (Arvan et al., 2002; MacGurn et al., 2012), and some studies have suggested such a checkpoint exists in AChR trafficking to the cell surface (Keller et al., 2001; Zhao et al., 2009; Rezvani et al., 2010; Crespi et al., 2018). The Golgi-resident protein that binds the β/δ motifs remains unknown, but is likely distinct from known proteins such as unc-50 or VILIP which both promote Golgi to surface trafficking of the receptor (Eimer et al., 2007; Zhao et al., 2009). It is also unlikely to be the sorting receptor Rer1p, which recognizes and retains unassembled α subunits (Valkova et al., 2011), rather than a motif specific to the β and δ subunits. The mechanism by which Golgi protein binding to the β/δ motifs discriminates between unassembled subunits and assembled receptor, and thereby provides quality control also remains unclear. One possibility is that the motifs are exposed in unassembled or incorrectly assembled subunits, leading to binding and retention, but are partially masked or regulated in correctly assembled receptor, permitting forward trafficking to the plasma membrane. Masking could occur through inter-subunit contacts or conformational changes that reduce the accessibility of the motif. For example, our molecular model suggests that appropriate assembly of the β subunit into pentameric receptor would position βK353 close to the inner leaflet of the plasma membrane (see **Figure 1**), which could potentially mask the β MX-helix retention motif.

Additional support for a quality control function comes from our finding that Golgi retention is associated with ubiquitination of the β/δ MX-helix motifs. Indeed, we observed robust and selective ubiquitination of CD4-β and δ MX-helices, which was largely abolished by mutation of the key lysine residues in each (βK353 and δK351). Thus, we propose that these lysines are the predominant sites of ubiquitination, and consistent with this, βK353 has been found to be ubiquitinated in proteomic studies (Hornbeck et al., 2015). As point mutations of neighboring residues also impaired ubiquitination, ubiquitination of βK353 or δK351 likely involves recognition of a specific amino-acid sequence by an E3 ubiquitin ligase. Potential candidates are the E3 ligases PDZRN3, MuRF1, NEDD4, and TRIM63, which have all been implicated in protein turnover at the NMJ (Lu et al., 2007; Liu et al., 2009; Rudolf et al., 2013; Khan et al., 2014). Golgi-based ubiquitination has previously been shown to sort mis-folded proteins into degradation pathways (MacGurn et al., 2012), and it seems likely that ubiquitination of the MX-helix motifs acts in a similar manner and targets unassembled or incorrectly assembled subunits for degradation via either the lysosomal or proteosomal pathways (Foot et al., 2017). One key question, however, is whether ubiquitination is the signal for retention, or a consequence of retention that marks the proteins for degradation. We tend to favor

the latter idea for several reasons: (i) in immunostaining experiments we detected significant accumulation of CD4-β/δ chimeras in the Golgi but no corresponding accumulation of ubiquitinated protein; (ii) in immunoblotting experiments, we found that only a small minority of CD4-β/δ chimeras is ubiquitinated (i.e., evident as higher molecular weight bands); and (iii) in immunostaining experiments we still observed some accumulation of CD4-βK353R MX-helix in the Golgi, despite little or no ubiquitination of this chimera. Thus, we propose that unassembled or incorrectly assembled subunits that escape the ER are retained in the Golgi through recognition of the β/δ motifs by a Golgi-resident protein and that this leads to their ubiquitination and degradation.

Second, our findings demonstrate that the β/δ motifs also contribute to quality control of assembled AChR by regulating its glycosylation in the Golgi complex. After receptor subunits are synthesized and assembled in the ER, the AChR is trafficked to the Golgi complex for further processing, which includes the modification of N-linked oligosaccharides on the γ and δ subunits to more complex forms. This process is normally highly efficient, as almost all surface receptor contains delta subunit with mature glycosylation. We found, however, that mutation of the β and δ subunit retention motifs (with combined βK353L/δK351L mutations) resulted in a significant 2-fold increase in the proportion of surface receptor with immature glycosylation. Thus, we propose that the β/δ motifs help retain the receptor in the Golgi to allow for modification of the oligosaccharides to complex forms. This is consistent with our earlier finding that mutation of the β/δ motifs increased surface levels of AChR (Rudell et al., 2014). Moreover, it implies that at least one of the retention motifs remains accessible in assembled AChR, although it may be regulated to permit Golgi to surface trafficking. These findings define a second form of quality control overseeing maturational steps in assembled AChR, and may have important functional consequences as N-linked glycosylation significantly affects AChR channel function and surface expression (Gehle et al., 1997; Ramanathan and Hall, 1999; Nishizaki, 2003; Dellisanti et al., 2007). Interestingly, a different form of Golgi-based quality control was recently demonstrated for the neuronal AChR, where receptors with α3β4α5 stoichiometry were found to be selectively recognized in the Golgi and recycled, whilst (α3)2(β4)3 receptors were trafficked to the cell surface (Crespi et al., 2018). Together with our current findings, this demonstrates that trafficking of assembled AChR is regulated at the Golgi complex and that this checkpoint governs additional aspects of AChR biogenesis and maturation.

Finally, in addition to regulating Golgi trafficking, we show that the MX-helix plays a role in receptor assembly. Two CMS-linked mutations in the epsilon subunit MX-helix (εP351L and εdel349-357) significantly reduced surface expression of the receptor, which is likely due to impaired α/ε heterodimer formation (Croxen et al., 2001). Similarly, we found that the corresponding mutation introduced into the beta subunit MX-helix (βP355L) also reduced AChR levels by inhibiting β subunit assembly, as did a βL354K mutation predicted to misposition the MX-helix. Notably, these mutations lie at the end of the MX-helix, which in the α4β2 crystal structure contacts the short loop following TM3 in the adjacent subunit. In addition, the end of the MX-helix may facilitate the correct folding of the following residues, which were not resolved in the crystal structure, but could also contribute to the interface between adjacent subunits. Consequently, these mutations likely directly disrupt subunit recognition and assembly, although we cannot discount the possibility that they perturb subunit folding and indirectly inhibit subunit assembly. These findings suggest, therefore, that shared determinants in the subunit MX-helices contribute to subunit assembly and are important for AChR surface expression.

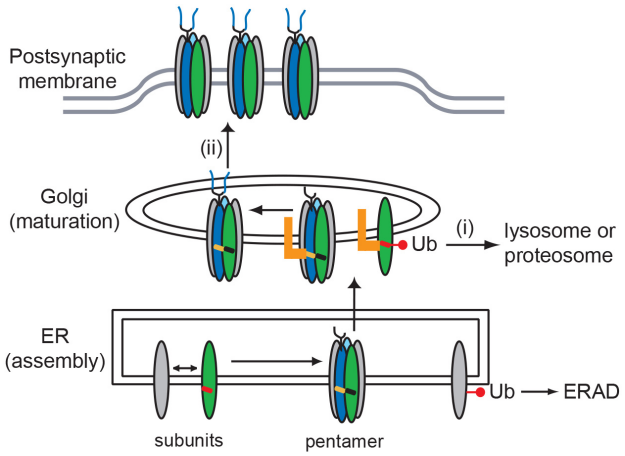

FIGURE 6 | Model for role of MX-helix in AChR assembly and trafficking. Our findings identify two molecular signals in the AChR subunit MX-helix that regulate receptor assembly and trafficking. First, shared determinants near the end of the MX-helix contribute to receptor assembly in the ER. Second, specific determinants in the β (green) and δ (blue) subunit MX-helix regulate Golgi trafficking and quality control by: (i) retention of incorrectly assembled subunits that escape endoplasmic reticulum associated protein degradation (ERAD), which leads to their ubiquitination and degradation; and (ii) transient retention of assembled AChR, which facilitates the modification of N-linked glycosylation (oligosaccharides depicted in blue). The molecular basis for the two forms of quality control could stem from the motifs being exposed in incorrectly assembled receptor (red MX-helix), but being masked or regulated in assembled receptor (black and orange MX-helices). The identity of the Golgi-resident protein that binds the motifs (orange L) remains unknown.

In summary, we define roles for the MX-helix in both AChR subunit assembly and Golgi trafficking and quality control. These functions are potentially linked as shown in our working model in **Figure 6**. We propose that incorrect or incomplete assembly of receptor subunits mispositions the MX-helix and exposes the retention signals, leading to their ubiquitination and sorting into degradative pathways. In contrast, correct assembly of receptor subunits positions the MX-helix so that the retention motifs are partially masked or regulated, and thereby allows forward

trafficking of the AChR. Together with earlier ER-based quality control mechanisms, this would ensure that only correctly assembled – fully functional – AChR is trafficked to the muscle plasma membrane and localized at the NMJ.

DATA AVAILABILITY STATEMENT

All datasets generated for this study are included in the article/**Supplementary Material**.

AUTHOR CONTRIBUTIONS

VY-Y performed the Rosetta structural modeling. JR and LB performed the experiments, analyzed the data, and edited the manuscript. MF performed the experiments, analyzed the data, and wrote the manuscript.

FUNDING

This work was supported in part by Muscular Dystrophy Association grant 134412 to MF and a University of California, Davis Physician Scientist Training Program award to JC.

ACKNOWLEDGMENTS

The authors thank Dr. Aldrin Gomes (University of California, Davis) for helpful discussions on protein ubiquitination.

SUPPLEMENTARY MATERIAL

The Supplementary Material for this article can be found online at: https://www.frontiersin.org/articles/10.3389/fnmol.2020.00048/full#supplementary-material

REFERENCES

Albuquerque, E. X., Pereira, E. F., Alkondon, M., and Rogers, S. W. (2009). Mammalian nicotinic acetylcholine receptors: from structure to function. *Physiol. Rev*. 89, 73–120. doi: 10.1152/physrev.00015.2008

Alford, R. F., Leaver-Fay, A., Jeliazkov, J. R., O'Meara, M. J., DiMaio, F. P., Park, H., et al. (2017). The rosetta all-atom energy function for macromolecular modeling and design. *J. Chem. Theory Comput*. 13, 3031–3048. doi: 10.1021/acs.jctc.7b00125

Arvan, P., Zhao, X., Ramos-Castaneda, J., and Chang, A. (2002). Secretory pathway quality control operating in Golgi, plasmalemmal, and endosomal systems. *Traffic* 3, 771–780. doi: 10.1034/j.1600-0854.2002.31102.x

Bender, B. J., Cisneros, A. III, Duran, A. M., Finn, J. A., Fu, D., Lokits, A. D., et al. (2016). Protocols for molecular modeling with rosetta3 and rosettascripts. *Biochemistry* 55, 4748–4763. doi: 10.1021/acs.biochem.6b00444

Bonneau, R., Strauss, C. E., Rohl, C. A., Chivian, D., Bradley, P., Malmstrom, L., et al. (2002). De novo prediction of three-dimensional structures for major protein families. *J. Mol. Biol*. 322, 65–78. doi: 10.1016/s0022-2836(02)00698-8

Borges, L. S., Yechikhov, S., Lee, Y. I., Rudell, J. B., Friese, M. B., Burden, S. J., et al. (2008). Identification of a motif in the acetylcholine receptor beta subunit whose phosphorylation regulates rapsyn association and postsynaptic receptor localization. *J. Neurosci*. 28, 11468–11476. doi: 10.1523/JNEUROSCI.2508-08.2008

Christianson, J. C., and Green, W. N. (2004). Regulation of nicotinic receptor expression by the ubiquitin-proteasome system. *EMBO J*. 23, 4156–4165. doi: 10.1038/sj.emboj.7600436

Colombo, S. F., Mazzo, F., Pistillo, F., and Gotti, C. (2013). Biogenesis, trafficking and up-regulation of nicotinic ACh receptors. *Biochem. Pharmacol*. 86, 1063–1073. doi: 10.1016/j.bcp.2013.06.023

Crespi, A., Plutino, S., Sciaccaluga, M., Righi, M., Borgese, N., Fucile, S., et al. (2018). The fifth subunit in alpha3beta4 nicotinic receptor is more than an accessory subunit. *FASEB J*. 32, 4190–4202. doi: 10.1096/fj.201701377R

Croxen, R., Young, C., Slater, C., Haslam, S., Brydson, M., Vincent, A., et al. (2001). End-plate gamma- and epsilon-subunit mRNA levels in AChR deficiency syndrome due to epsilon-subunit null mutations. *Brain* 124, 1362–1372. doi: 10.1093/brain/124.7.1362

Dellisanti, C. D., Yao, Y., Stroud, J. C., Wang, Z. Z., and Chen, L. (2007). Crystal structure of the extracellular domain of nAChR alpha1 bound to alpha-bungarotoxin at 1.94 A resolution. *Nat. Neurosci*. 10, 953–962. doi: 10.1038/nn1942

Eimer, S., Gottschalk, A., Hengartner, M., Horvitz, H. R., Richmond, J., Schafer, W. R., et al. (2007). Regulation of nicotinic receptor trafficking by the transmembrane Golgi protein UNC-50. *EMBO J*. 26, 4313–4323. doi: 10.1038/sj.emboj.7601858

Engel, A. G. (2018). Genetic basis and phenotypic features of congenital myasthenic syndromes. *Handb. Clin. Neurol*. 148, 565–589. doi: 10.1016/B978-0-444-64076-5.00037-5

Foot, N., Henshall, T., and Kumar, S. (2017). Ubiquitination and the regulation of membrane proteins. *Physiol. Rev*. 97, 253–281. doi: 10.1152/physrev.00012.2016

Fu, Y. L., Wang, Y. J., and Mu, T. W. (2016). Proteostasis maintenance of cys-loop receptors. *Adv. Protein Chem. Struct. Biol*. 103, 1–23. doi: 10.1016/bs.apcsb.2015.11.002

Gehle, V. M., Walcott, E. C., Nishizaki, T., and Sumikawa, K. (1997). N-glycosylation at the conserved sites ensures the expression of properly folded functional ACh receptors. *Brain Res. Mol. Brain Res*. 45, 219–229. doi: 10.1016/s0169-328x(96)00256-2

Gu, Y., and Hall, Z. W. (1988). Characterization of acetylcholine receptor subunits in developing and in denervated mammalian muscle. *J. Biol. Chem*. 263, 12878–12885.

Gu, Y., Ralston, E., Murphy-Erdosh, C., Black, R. A., and Hall, Z. W. (1989). Acetylcholine receptor in a C2 muscle cell variant is retained in the endoplasmic reticulum. *J. Cell Biol*. 109, 729–738. doi: 10.1083/jcb.109.2.729

Hassaine, G., Deluz, C., Grasso, L., Wyss, R., Tol, M. B., Hovius, R., et al. (2014). X-ray structure of the mouse serotonin 5-HT3 receptor. *Nature* 512, 276–281. doi: 10.1038/nature13552

Hornbeck, P. V., Zhang, B., Murray, B., Kornhauser, J. M., Latham, V., and Skrzypek, E. (2015). PhosphoSitePlus, 2014: mutations, PTMs and recalibrations. *Nucleic Acids Res*. 43, D512–D520. doi: 10.1093/nar/gku1267

Huang, X., Chen, H., Michelsen, K., Schneider, S., and Shaffer, P. L. (2015). Crystal structure of human glycine receptor-alpha3 bound to antagonist strychnine. *Nature* 526, 277–280. doi: 10.1038/nature14972

Keller, S. H., Lindstrom, J., Ellisman, M., and Taylor, P. (2001). Adjacent basic amino acid residues recognized by the COP I complex and ubiquitination govern endoplasmic reticulum to cell surface trafficking of the nicotinic acetylcholine receptor alpha-Subunit. *J. Biol. Chem*. 276, 18384–18391. doi: 10.1074/jbc.m100691200

Khan, M. M., Strack, S., Wild, F., Hanashima, A., Gasch, A., Brohm, K., et al. (2014). Role of autophagy, SQSTM1, SH3GLB1, and TRIM63 in the turnover of nicotinic acetylcholine receptors. *Autophagy* 10, 123–136. doi: 10.4161/auto.26841

Liu, Y., Oppenheim, R. W., Sugiura, Y., and Lin, W. (2009). Abnormal development of the neuromuscular junction in Nedd4-deficient mice. *Dev. Biol*. 330, 153–166. doi: 10.1016/j.ydbio.2009.03.023

Lu, Z., Je, H. S., Young, P., Gross, J., Lu, B., and Feng, G. (2007). Regulation of synaptic growth and maturation by a synapse-associated E3 ubiquitin ligase at the neuromuscular junction. *J. Cell Biol*. 177, 1077–1089. doi: 10.1083/jcb.200610060

MacGurn, J. A., Hsu, P. C., and Emr, S. D. (2012). Ubiquitin and membrane protein turnover: from cradle to grave. *Ann. Rev. Biochem*. 81, 231–259. doi: 10.1146/annurev-biochem-060210-093619

Maselli, R., Arredondo, J., Cagney, O., Mozaffar, T., Skinner, S., Yousif, S., et al. (2010). Congenital myasthenic syndrome associated with epidermolysis bullosa caused by homozygous mutations in PLEC1 and CHRNE. *Clin. Genet*. 80, 444–451. doi: 10.1111/j.1399-0004.2010.01602.x

Merlie, J. P., and Lindstrom, J. (1983). Assembly in vivo of mouse muscle acetylcholine receptor: identification of an alpha subunit species that may be an assembly intermediate. *Cell* 34, 747–757. doi: 10.1016/0092-8674(83)90531-7

Millar, N. S., and Harkness, P. C. (2008). Assembly and trafficking of nicotinic acetylcholine receptors (Review). *Mol. Membr. Biol*. 25, 279–292. doi: 10.1080/09687680802035675

Miller, P. S., and Aricescu, A. R. (2014). Crystal structure of a human GABAA receptor. *Nature* 512, 270–275. doi: 10.1038/nature13293

Morales-Perez, C. L., Noviello, C. M., and Hibbs, R. E. (2016). X-ray structure of the human alpha4beta2 nicotinic receptor. *Nature* 538, 411–415. doi: 10.1038/nature19785

Mukhopadhyay, D., and Riezman, H. (2007). Proteasome-independent functions of ubiquitin in endocytosis and signaling. *Science* 315, 201–205. doi: 10.1126/science.1127085

Nishizaki, T. (2003). N-glycosylation sites on the nicotinic ACh receptor subunits regulate receptor channel desensitization and conductance. *Brain Res. Mol. Brain Res*. 114, 172–176. doi: 10.1016/s0169-328x(03)00171-2

Park, H., Kim, D. E., Ovchinnikov, S., Baker, D., and DiMaio, F. (2018). Automatic structure prediction of oligomeric assemblies using Robetta in CASP12. *Proteins* 86(Suppl. 1), 283–291. doi: 10.1002/prot.25387

Pettersen, E. F., Goddard, T. D., Huang, C. C., Couch, G. S., Greenblatt, D. M., Meng, E. C., et al. (2004). UCSF Chimera–a visualization system for exploratory research and analysis. *J. Comput. Chem*. 25, 1605–1612. doi: 10.1002/jcc.20084

Ramanathan, V. K., and Hall, Z. W. (1999). Altered glycosylation sites of the delta subunit of the acetylcholine receptor (AChR) reduce alpha delta association and receptor assembly. *J. Biol. Chem*. 274, 20513–20520. doi: 10.1074/jbc.274.29.20513

Ren, X. Q., Cheng, S. B., Treuil, M. W., Mukherjee, J., Rao, J., Braunewell, K. H., et al. (2005). Structural determinants of alpha4beta2 nicotinic acetylcholine receptor trafficking. *J. Neurosci*. 25, 6676–6686. doi: 10.1523/jneurosci.1079-05.2005

Rezvani, K., Teng, Y., and De Biasi, M. (2010). The ubiquitin-proteasome system regulates the stability of neuronal nicotinic acetylcholine receptors. *J. Mol. Neurosci*. 40, 177–184. doi: 10.1007/s12031-009-9272-x

Rohl, C. A., Strauss, C. E., Misura, K. M., and Baker, D. (2004). Protein structure prediction using Rosetta. *Methods Enzymol*. 383, 66–93.

Rudell, J. C., Borges, L. S., Rudell, J. B., Beck, K. A., and Ferns, M. J. (2014). Determinants in the beta and delta subunit cytoplasmic loop regulate Golgi trafficking and surface expression of the muscle acetylcholine receptor. *J. Biol. Chem*. 289, 203–214. doi: 10.1074/jbc.M113.502328

Rudolf, R., Bogomolovas, J., Strack, S., Choi, K. R., Khan, M. M., Wagner, A., et al. (2013). Regulation of nicotinic acetylcholine receptor turnover by MuRF1 connects muscle activity to endo/lysosomal and atrophy pathways. *Age* 35, 1663–1674. doi: 10.1007/s11357-012-9468-9

Sine, S. M. (2012). End-plate acetylcholine receptor: structure, mechanism, pharmacology, and disease. *Physiol. Rev*. 92, 1189–1234. doi: 10.1152/physrev.00015.2011

Song, Y., DiMaio, F., Wang, R. Y., Kim, D., Miles, C., Brunette, T., et al. (2013). High-resolution comparative modeling with RosettaCM. *Structure* 21, 1735–1742. doi: 10.1016/j.str.2013.08.005

St John, P. A. (2009). Cellular trafficking of nicotinic acetylcholine receptors. *Acta Pharmacol. Sin*. 30, 656–662. doi: 10.1038/aps.2009.76

Unwin, N. (2005). Refined structure of the nicotinic acetylcholine receptor at 4A resolution. *J. Mol. Biol*. 346, 967–989. doi: 10.1016/j.jmb.2004.12.031

Valkova, C., Albrizio, M. I, Roder, V., Schwake, M., Betto, R., Rudolf, R., et al. (2011). Sorting receptor Rer1 controls surface expression of muscle acetylcholine receptors by ER retention of unassembled alpha-subunits. *Proc. Natl. Acad. Sci. U.S. A*. 108, 621–625. doi: 10.1073/pnas.1001624108

Verschuuren, J., Strijbos, E., and Vincent, A. (2016). Neuromuscular junction disorders. *Handb. Clin. Neurol*. 133, 447–466. doi: 10.1016/B978-0-444-63432-0.00024-4

Wanamaker, C. P., Christianson, J. C., and Green, W. N. (2003). Regulation of nicotinic acetylcholine receptor assembly. *Ann. N. Y. Acad. Sci*. 998, 66–80.

Wang, J. M., Zhang, L., Yao, Y., Viroonchatapan, N., Rothe, E., and Wang, Z. Z. (2002). A transmembrane motif governs the surface trafficking of nicotinic acetylcholine receptors. *Nat. Neurosci*. 5, 963–970. doi: 10.1038/nn918

Wu, Z. S., Cheng, H., Jiang, Y., Melcher, K., and Xu, H. E. (2015). Ion channels gated by acetylcholine and serotonin: structures, biology, and drug discovery. *Acta Pharmacol. Sin*. 36, 895–907. doi: 10.1038/aps.2015.66

Zhao, C. J., Noack, C., Brackmann, M., Gloveli, T., Maelicke, A., Heinemann, U., et al. (2009). Neuronal Ca2+ sensor VILIP-1 leads to the upregulation of functional alpha4beta2 nicotinic acetylcholine receptors in hippocampal neurons. *Mol. Cell. Neurosci*. 40, 280–292. doi: 10.1016/j.mcn.2008.11.001

Conflict of Interest: The authors declare that the research was conducted in the absence of any commercial or financial relationships that could be construed as a potential conflict of interest.

Copyright © 2020 Rudell, Borges, Yarov-Yarovoy and Ferns. This is an open-access article distributed under the terms of the Creative Commons Attribution License (CC BY). The use, distribution or reproduction in other forums is permitted, provided the original author(s) and the copyright owner(s) are credited and that the original publication in this journal is cited, in accordance with accepted academic practice. No use, distribution or reproduction is permitted which does not comply with these terms.

frontiers in Molecular Neuroscience

REVIEW
published: 29 May 2020
doi: 10.3389/fnmol.2020.00086

Myasthenia Gravis: From the Viewpoint of Pathogenicity Focusing on Acetylcholine Receptor Clustering, Trans-Synaptic Homeostasis and Synaptic Stability

*Masaharu Takamori**

Neurological Center, Kanazawa-Nishi Hospital, Kanazawa, Japan

Myasthenia gravis (MG) is a disease of the postsynaptic neuromuscular junction (NMJ) where nicotinic acetylcholine (ACh) receptors (AChRs) are targeted by autoantibodies. Search for other pathogenic antigens has detected the antibodies against muscle-specific tyrosine kinase (MuSK) and low-density lipoprotein-related protein 4 (Lrp4), both causing pre- and post-synaptic impairments. Agrin is also suspected as a fourth pathogen. In a complex NMJ organization centering on MuSK: (1) the Wnt non-canonical pathway through the Wnt-Lrp4-MuSK cysteine-rich domain (CRD)-Dishevelled (Dvl, scaffold protein) signaling acts to form AChR prepatterning with axonal guidance; (2) the neural agrin-Lrp4-MuSK (Ig1/2 domains) signaling acts to form rapsyn-anchored AChR clusters at the innervated stage of muscle; (3) adaptor protein Dok-7 acts on MuSK activation for AChR clustering from "inside" and also on cytoskeleton to stabilize AChR clusters by the downstream effector Sorbs1/2; (4) the trans-synaptic retrograde signaling contributes to the presynaptic organization *via*: (i) Wnt-MuSK CRD-Dvl-β catenin-Slit 2 pathway; (ii) Lrp4; and (iii) laminins. The presynaptic Ca^{2+} homeostasis conditioning ACh release is modified by autoreceptors such as M1-type muscarinic AChR and A2A adenosine receptors. The post-synaptic structure is stabilized by: (i) laminin-network including the muscle-derived agrin; (ii) the extracellular matrix proteins (including collagen Q/perlecan and biglycan which link to MuSK Ig1 domain and CRD); and (iii) the dystrophin-associated glycoprotein complex. The study on MuSK ectodomains (Ig1/2 domains and CRD) recognized by antibodies suggested that the MuSK antibodies were pathologically heterogeneous due to their binding to multiple functional domains. Focussing one of the matrix proteins, biglycan which functions in the manner similar to collagen Q, our antibody assay showed the negative result in MG patients. However, the synaptic stability may be impaired by antibodies against MuSK ectodomains because of the linkage of biglycan with MuSK Ig1 domain and CRD. The pathogenic diversity of MG is discussed based on NMJ signaling molecules.

Keywords: neuromuscular junction, myasthenia gravis, acetylcholine receptor, agrin, wnts, MuSK, Lrp4, matrix proteins

OPEN ACCESS

Edited by:
Hanns Lochmuller,
University of Ottawa, Canada

Reviewed by:
Lin Mei,
Case Western Reserve University, United States
Joern R. Steinert,
University of Leicester, United Kingdom

Correspondence:
Masaharu Takamori
m-takamori@vanilla.ocn.ne.jp

Received: *15 January 2020*
Accepted: *28 April 2020*
Published: *29 May 2020*

Citation:
Takamori M (2020) Myasthenia Gravis: From the Viewpoint of Pathogenicity Focusing on Acetylcholine Receptor Clustering, Trans-Synaptic Homeostasis and Synaptic Stability. Front. Mol. Neurosci. 13:86. doi: 10.3389/fnmol.2020.00086

INTRODUCTION

The neuromuscular junction (NMJ) functions as acetylcholine (ACh)-mediated synapse (Gray frame, **Figure 1**); its signal transmission depends on coordinated interaction between the pre-synaptic active zone (Südhof, 2012) and the post-synaptic nicotinic acetylcholine receptor (AChR; Kummer et al., 2006). In confirming the synaptic architecture, the trans-synaptic communications mediated by nerve-secreted or muscle membrane-bound proteins such as agrin (heparin sulfate proteoglycan) and Wnts (belonging to the Wingless-type integration site family of glycoproteins) play the pivotal roles *via* interactions with the muscle-specific tyrosine kinase (MuSK) and the low-density lipoprotein-related protein 4 (Lrp4; Wu et al., 2010; Shi et al., 2012; Takamori, 2013, 2017a). The review focusses on: (1) the AChR cluster formation by MuSK activation from inside (Dok-7 and Wnts) and outside (agrin and Wnts) of the muscle; (2) the synaptic compensatory mechanisms based on retrograde signals from muscle to nerve and presynaptic Ca^{2+} homeostasis by auto-receptors; and (3) the synaptic stabilization based on cytoskeletal dynamics by extracellular matrix proteins and dystrophin-associated glycoprotein complex. These have paved the way to search for the mechanisms underlying myasthenia gravis (MG) weakness (Burden et al., 2018; Sudres et al., 2018; Koneczny and Herbst, 2019). MG, an autoimmune NMJ disease characterized by fatigable weakness of voluntary muscles, are generally reviewed from the viewpoints of clinical subgroups and antibody characteristics (Vincent et al., 2018; Gilhus et al., 2019).

MYASTHENIA GRAVIS (MG) CAUSED BY ANTIBODIES TARGETING KEY MOLECULES IN NEUROMUSCULAR JUNCTION

Anti-AChR Antibodies

MG is the B cell-mediated, T cell-dependent autoimmune disease including thymic pathologies (Marx et al., 2013; Berrih-Aknin and Le Panse, 2014; Nemazee, 2017; Behin and Le Panse, 2018; Villegas et al., 2018; Yi et al., 2018; Koneczny and Herbst, 2019). In typical MG, most (∼85%) patients have AChR (Gray frame in **Figure 1**) antibodies (Y1 in **Figure 1**), the pathogenic mechanisms of which are classified into (1) removal of AChRs due to cross-linking and subsequent internalization (antigenic modulation; Drachman et al., 1978), (2) functional AChR block (Drachman et al., 1982; Takamori et al., 1988) and (3) activation of complement with the formation of membrane attack complexes that cause focal lysis. The main immunogenic region targeted by MG antibodies is the AChR α-subunit 67–76 (Tzartos et al., 1982, 1988). The AChR antibodies are predominantly IgG1 and IgG3 subtypes that bind the complement causing the post-synaptic disorder in NMJ (Sahashi et al., 1980; Vincent and Newsom-Davis, 1980; Tüzün and Christadoss, 2013; Cetin and Vincent, 2018; Howard, 2018); this mechanism is most pathogenic in patients with refractory MG, who have efficaciously been treated with C5 inhibitor (eculizumab and Zilucoplan; Muppidi et al., 2019; Howard et al., 2020). Experimentally, the investigational RNAi targeting C5 (Kusner et al., 2019) and the single-chain AChR antibody coupled to complement decay-accelerating factor (Kusner et al., 2014) are shown to be efficacious in the models of MG. Promising therapeutic strategies include the B cell-related therapies (Rituximab; Tandan et al., 2017; Beecher et al., 2019; Di Stefano et al., 2020; Huda, 2020; Litchman et al., 2020) and the neonatal Fc receptor antagonists (Efgartigimod and Rozanolixizumab; Ulrichts et al., 2018; Howard et al., 2019; Huijbers et al., 2019a; Zuercher et al., 2019; Gable and Guptill, 2020). Taking into consideration of the reduced suppressive activity of T regulatory cells (Treg) in MG (reflecting on elevated inflammatory cytokines in MG; Thiruppathi et al., 2012; Ha and Richman, 2015; Wen et al., 2016; Molin et al., 2017), the Treg-based therapy achieved with the use of IL-2/anti-IL-2 monoclonal antibody complexes could be useful for treating MG as shown by the experiment in experimental autoimmune MG (Liu et al., 2010; Danikowski et al., 2017). Thymic abnormalities (hyperplasia tending to be potential in MG patients before the age of 50) have long been paid attention as an underlying pathology of MG and the target for therapy. We have participated in the MGTX (enrollment at 18–65 years of age; the disease severity of America classification class II–IV) randomized trial of thymectomy (with alternative-day prednisone), resulting in the benefit in non-thymomatous MG patients (Wolfe et al., 2019).

Anti-striational Antigen Antibodies

The suggestive biomarkers for the presence of thymoma indicative for thymectomy are the antibodies against muscle striational antigens such as ryanodine receptor (a foot protein in the junctional gap between the dihydropyridine receptor containing T-tubules and the sarcoplasmic reticulum, functioning as Ca^{2+} release channel for E-C coupling) and titin (a protein to keep the thick filaments centered in the sarcomere, allowing optimum active force development; Mygland et al., 1992; Skeie et al., 2002; Somnier and Engel, 2002; Takamori et al., 2004; Romi et al., 2007; Romi, 2011; Choi Decroos et al., 2014; Stergiou et al., 2016). We electrophysiologically confirmed the muscular contractile (twitch and tetanus) weakness caused by anti-ryanodine receptor antibodies in the spontaneous thymoma rat (Buffalo/Mna strain suppled by Charles River Japan, Inc.; Iwasa et al., 1998).

Immune Checkpoint Inhibitors for Cancer Therapy and MG

The therapies by use of immune checkpoint inhibitors (anti-programmed cell death protein-1 (PD1), anti-programmed death ligand-1 (PD-L1) and anti-cytotoxic T lymphocyte associated-4) to manage various cancers are occasionally associated with immune-related adverse events (due to loss of Treg homeostasis; Danikowski et al., 2017; Dalakas, 2018; Kumar et al., 2018, 2019; Möhn et al., 2019; Dubey et al., 2020) including myasthenia gravis (Becquart et al., 2019; Johansen et al., 2019; Sato et al., 2019; Choi and Lee, 2020) Reportedly, PD-L1 mRNA is highly expressed in MG muscle cells (Iwasa et al., 2018); this

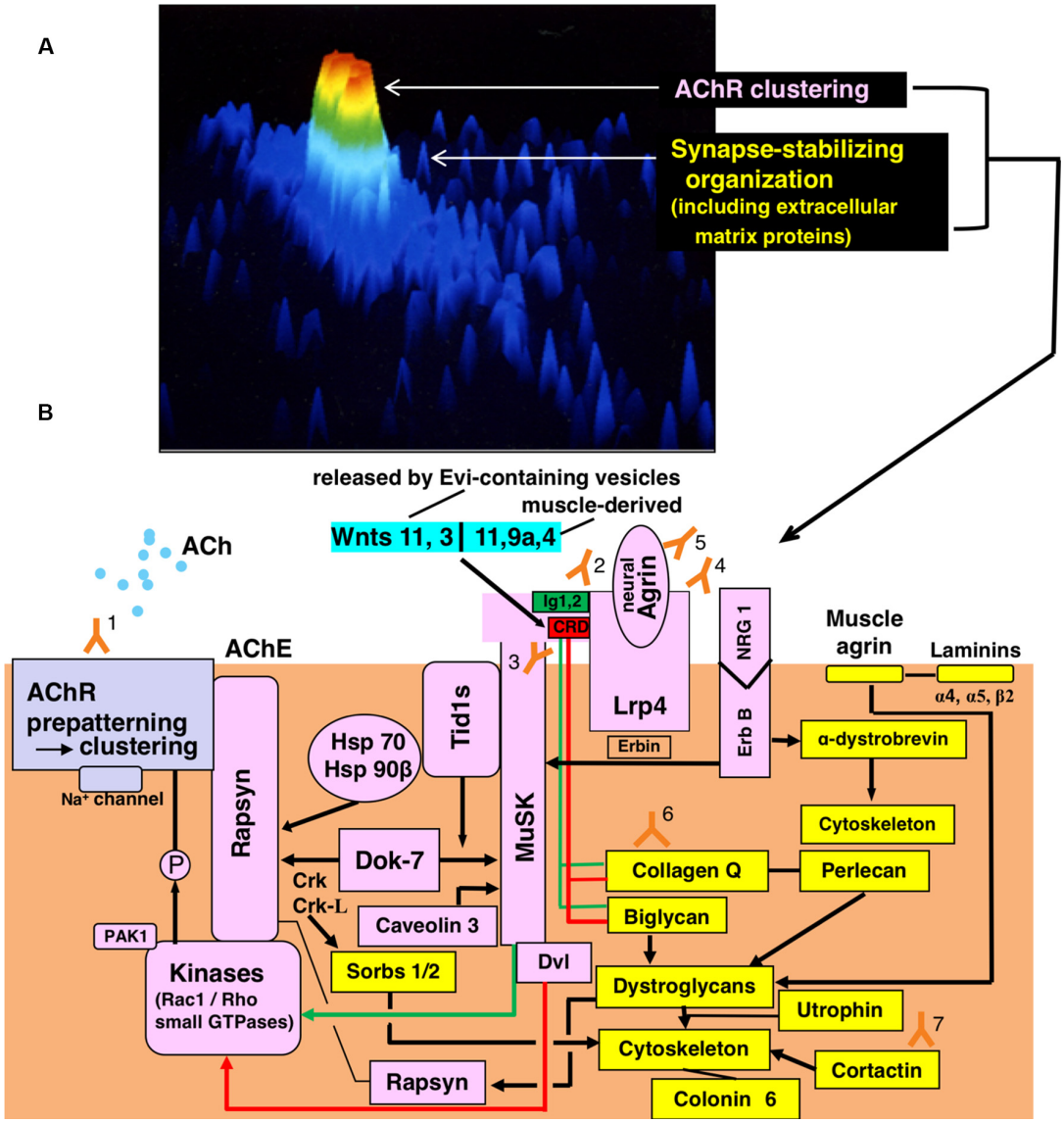

FIGURE 1 | Functional organization for synaptic transmission in neuromuscular junction (NMJ) and antibody-targets. **(A)** Presentation by staining of cultured rat myotube with fluorescence-labeled α-bungarotoxin and by the image analyzing using a laser cytometer, indicating acetylcholine receptor (AChR) cluster (red), a synaptic stabilizing organization including extracellular matrix proteins (gree and light blue). The image is constructed on ACAS 570 (Meridian Instruments Inc., Okemos, MI, USA) which provides a graded pseudocolor image on the computer display. **(B)** Schematic presentation of the post-synaptic structures. Y marks attached with numbers indicate the antibodies to recognize respective targets of the functional structures. Gray frame indicates the acetylcholine receptor (AChR) cluster formation. Pink frames indicate AChR clustering by way of two signaling pathways mediated *via* the muscle-specific tyrosine kinase (MuSK) 1/2 domains (green-limit in the pink MuSK ectodomain and green line with arrowhead) and MuSK cysteine-rich domain (CRD; red-limit in the pink MuSK ectodomain and red-line with arrowhead), the signals of which are mediated by Dishevelled (Dvl, adaptor protein). The low-density lipoprotein receptor-related protein 4 (Lrp4) is the receptor for agrin (partly for Wnts as described in the text). The small GTPases (shown in the pink frame of Kinases) effector PAK1 (p21-activated kinase 1) acts as a bridging molecule between the Wnt- and agrin-signaling pathways. From "inside" the muscle cell, MuSK is activated by Dok7 (downstream kinase); Dok7 recruits two adaptor protein, Crk and Crk-L (CT10 regulators of kinase) for rapsyn-anchored AChR cluster formation. The formed AChR clusters are anchored at the endplate membrane by rapsyn and immobilized by MuSK-linking heat-shock proteins (HSPs): tumorous imaginal disc 1 short form (Tid1s), HSP 70 and HSP 90β. Tid1s is required for the MuSK-Dok7 signaling during the MuSK activation. The interaction of neuregulin 1 (NRG 1) with ErbB receptor (receptor tyrosine kinase of epidermal growth factor receptor family) increases the MuSK tyrosine phosphorylation (*via* Erbin) and thereby modulates the MuSK-dependent AChR clustering. Caveolin 3 binds with the MuSK kinase domain and thereby driving AChR clustering. Yellow frames indicate the organizations for synaptic stability and maintenance. The synaptic stability of NMJ including AChR clusters (gray frame), MuSK (pink frame), Lrp4 (pink frame) and acetylcholinesterase (AChE) is modulated by extracellular matrix proteins (collagen Q, perlecan, biglycan, laminin-network including muscle agrin and laminins and dystroglycan) worked in cooperation with the cytoskeleton. The interaction of NRG 1 (neuregulin 1) with ErbB receptor (pink frames) contributes to the cytoskeletal organization through α-dystrobrevin phosphorylation on one hand (yellow frame) and the MuSK activation *via* Erbin on the other hand (pink frame). The downstream effector of Dok7-recruited Crk-L (Sorbs1/2) acts on the cytoskeleton for synaptic stability. Collagen Q-Perlecan and Biglycan act on Dystroglycans in cooperation with cytoskeleton for synaptic stability on one hand

(*Continued*)

FIGURE 1 | Continued
(yellow frame) and implicate in AChR cluster formation *via* their interaction with pink-MuSK ectodomains (Ig1 shown by green limit with a green line and CRD shown by red limit with red line) on the other hand. The former is cooperated by linking to dystrophin/utrophin-associated protein complex; the latter is cooperated by linking with rapsyn to firmly anchor AChR clusters at the post-synaptic membrane. Cortactin (yellow frame) has the function of phosphorylation-dependent signaling downstream from Agrin/Lrp4/MuSK (pink frame) in promoting actin polymerization and also stabilizing AChR clusters at the postsynaptic membrane. Coronin 6 is the actin-binding protein contributive to synaptic stability. Targets recognized by antibodies: Y1, Acetylcholine receptor (AChR); Y2, Muscle-specific tyrosine kinase (MuSK) 1/2 domains; Y3, MuSK cysteine-rich domain (CRD); Y4, Low-density lipoprotein receptor-related protein 4 (Lrp4); Y5, neural Agrin; Y6, Collagen Q; Y7, Cortactin.

may suggest the participation of the local immune-mediated damage in MG muscle by the checkpoint inhibitor effect which leads to abnormal T-regulatory (Treg) cell function and altered Treg/Th17 cell axis (Dalakas, 2018). Also, PD-1 and PD-L1 are expressed in thymic epithelial tumors, suggesting a poor prognostic factor in thymomas (Bagir et al., 2018; Song et al., 2019).

Anti-MuSK Antibodies

MuSK (Pink frame, **Figure 1**), a member of the receptor tyrosine kinase superfamily, is composed of four ligand-binding ectodomains (linking with neural agrin <Pink frame, **Figure 1**> *via* first and second immunoglobulin-like domains, Ig1/2 <green -limit in pink- MuSK, **Figure 1**>, and with Wnts <Blue frames, **Figure 1**> *via* cysteine-rich domain (CRD), <red- limit in pink-MuSK, **Figure 1**>, through Lrp4 <Pink frame, **Figure 1**>), a single transmembrane-spanning domain and an intracellular kinase domain; this receptor tyrosine kinase acts as the key organizer to form AChR clusters in the post-synaptic membrane of NMJ (Ghazanfari et al., 2011; Burden et al., 2013; Takamori, 2013; Zong and Jin, 2013; Koneczny et al., 2014; Herbst, 2019; green and red lines *via* Dishevelled (Dvl, Pink frame, **Figure 1**). Mesdec2 plays a key role in cell-surface expression of Lrp4 and postsynaptic specialization (Hoshi et al., 2013).

Hoch and colleagues (Hoch et al., 2001) detected the antibodies against MuSK (as discussed later, two types of antibodies are determined: Y2 targeting the Ig1/2 domains and Y3 targeting CRD in **Figure 1**) in the serum samples of MG patients without AChR antibodies. In general, the patients show predominant involvement in the facial, pharyngeal, tongue (often with muscle atrophy), neck, and shoulder, but extraocular muscles are rarely involved at onset in contrast to AChR antibody-positive MG; they are occasionally seized with a respiratory crisis. The patients respond to immunosuppressant therapy (Evoli et al., 2008, 2018; Pasnoor et al., 2010; Guptill et al., 2011; Evoli and Padura, 2013; Koneczny et al., 2014; Morren and Li, 2018; Li et al., 2019). The B-cell depletion therapy (Rituximab) provides more benefit to MuSK-MG patients than AChR-MG patients (Evoli et al., 2008, 2018; Díaz-Manera et al., 2012; Evoli and Padura, 2013; Tandan et al., 2017; Morren and Li, 2018; Beecher et al., 2019; Di Stefano et al., 2020; Huda, 2020; Litchman et al., 2020). In the experimental model of MuSK MG, the fetal Fc receptor antibodies (Gable and Guptill, 2020), antigen-specific immunoadsorption (Skriapa et al., 2014; Lazaridis et al., 2020) and the inhibition of tyrosine phosphatase inhibitor (SHP2; Huda et al., 2020) alleviate the MuSK antibody-induced AChR cluster deformation. One must be cautious that the hypersensitivity and worsening of symptoms to cholinesterase inhibitors tend to occur (Punga et al., 2006; Evoli and Padura, 2013). In general, thymic abnormalities are not detected and thus no apparent clinical benefit of thymectomy is obtained (Leite et al., 2005; Evoli et al., 2008; Evoli and Padura, 2013; Nakata et al., 2013; Clifford et al., 2019).

Immunologically, MuSK antibodies are mainly IgG4 subclass (Koneczny, 2018) and known to cause MG by inhibiting binding between MuSK and Lrp4 independently of complement activation (Huijbers et al., 2013), but IgG1-3 MuSK antibodies can disperse preformed agrin-independent AChR clusters (Koneczny et al., 2013).

Anti-Lrp4 Antibodies

Lrp4 (Pink frame, **Figure 1**) which plays a pivotal role in mediating agrin (*via* green-limit, MuSK Ig1/2, **Figure 1**)—and Wnt (*via* red-limit, MuSK CRD, **Figure 1**)—signalings for AChR clustering at the postsynaptic membrane and also serves the retrograde signaling from muscle to nerve (Barik et al., 2014a; Guarino et al., 2020). The molecular structure of Lrp4 consists of a large extracellular domain that contains eight low-density lipoprotein receptor domains class A (LDLa), EGF-like domains and four β-propeller domains; its N-terminal region (including the last few LDLa repeats and the first β-propeller domain) interacts with agrin (Zhang et al., 2011; Zong et al., 2012); in its third β-propeller domain, the edge part mediates the MuSK signaling and the central part mediates the Wnt signaling (Ohkawara et al., 2014). Autoantibodies (complement-activating IgG1 and IgG2; Y4 in **Figure 1**) are detected in a proportion of MG with or without antibodies to AChR and MuSK (Higuchi et al., 2011; Pevzner et al., 2011; Cossins et al., 2012; Zhang et al., 2012b; Shen et al., 2013; Zouvelou et al., 2013; Zisimopoulou et al., 2014; Marino et al., 2015; Li et al., 2017; Rivner et al., 2018; Yan et al., 2018b; Aoki et al., 2020). The severity of disease in most patients is mild to moderate, but some patients have severe symptoms causing the myasthenic crisis. Most patients respond to anti-acetylcholinesterases, steroids, and immunosuppressant medications. Thymic pathology is usually not present but underlies in some patients including thymomas (Zisimopoulou et al., 2014; Marino et al., 2015; Aoki et al., 2020). The active immunization of mice with Lrp4 was proved to induce myasthenia gravis; the pathogenicity of Lrp4 antibodies was confirmed by the study in animal models that showed both pre- and post-synaptic impairments and active complements (Mori et al., 2012, 2017; Shen et al., 2013; Ulusoy et al., 2017).

Anti-agrin Antibodies

Agrin, a proteoglycan expressed in both motor neuron (Pink frame, **Figure 1**) and skeletal muscle (Yellow frame, **Figure 1**), is essential to form NMJ formation (Burden et al., 2018). The neural agrin-dependent pathways include the two muscle-bound transmembrane co-receptors Lrp4 and MuSK (Pink frames,

Figure 1). In the functional structure of Agrin (Hoch et al., 1994; Gesemann et al., 1995; Burgess et al., 1999; Bezakova and Ruegg, 2003; Stetefeld et al., 2004; Scotton et al., 2006; Zong et al., 2012; Tezuka et al., 2014; Zhang et al., 2015), the N-terminus is required for agrin-immobilization at the NMJ; the C-terminus segment contains two of the three laminin-like G domains (G2 and G3). G2 is essential for binding of muscle agrin (Yellow frame, **Figure 1**) to α-dystroglycan which contributes, *via* β-dystroglycan, to the stabilization of the post-synaptic apparatus at the NMJ through the organization of the intracellular cytoskeleton of muscle (Yellow frames with black linking lines, **Figure 1**; muscle agrin: this is >5,000 less active compared with neural agrin as far as AChR aggregation is concerned). G3 consists of four amino acid insertion at the A/y splicing site and 8, 11 or 19 amino acid insertion at the B/z splicing site (neural agrin: Pink frame, **Figure 1**) and is essential for the AChR clustering activity of agrin through Lrp4-MuSK signaling (green and red lines *via* pink-framed Dvl).

Anti-agrin antibodies (Y5 in **Figure 1**) have been detected in some of MG patients with or without antibodies against AChR, MuSK, and Lrp4 (Gasperi et al., 2014; Zhang et al., 2014; Cordts et al., 2017; Yan et al., 2018b). Induction of anti-agrin antibodies was proved to cause MG in mice by an impairment of agrin-Lrp4 interaction (Yan et al., 2018a). We must be cautious of the antigen used for agrin-antibody assay because of the above-mentioned difference of functional structure between neural agrin and muscle agrin.

The myasthenic weakness in anti-agrin antibody-positive patients is mild to severe but tends to be moderate to the treatment, suggesting that the early detection of anti-agrin antibodies could help disease management (Cordts et al., 2017). It is worthy of note as a therapeutic device in future that a fragment of neural agrin (NT-1654) has the potential to counteract the symptoms of the diseased NMJ in the sarcopenia-like phenotype in neurotrypsin-overexpressing mice (Hettwer et al., 2014; Rudolf et al., 2014). The engineered agrin was reported to attenuate the severity of experimental autoimmune myasthenia gravis (Li Z. et al., 2018). The active form of vitamin D (1.25D) upregulates the agrin-induced AChR clustering in association with the upregulated expression of rapsyn in C2C12 myotubes (Arakawa and Wagatsuma, 2020); this pharmacologic effect could apply to a group of MG, the antibodies of which are maleficient more to rapsyn-clustered AChR than non-clustered AChR (Cetin et al., 2020).

Matrix metalloproteinases (MMPs) are membrane-anchored extracellular proteinases capable of degrading a variety of proteins including agrin; the function of agrin is regulated by the site-specific cleavage by MMPs (Patel et al., 2012; Chan et al., 2020). Additionally shown was that MMP-3 removes agrin from synaptic basal lamina (Werle and VanSaun, 2003). Reportedly, the MMP-3 level is high in the serum samples from a proportion of MG patients (Helgeland et al., 2011; Romi et al., 2012), suggesting that the NMJ might be affected by the pathogenic mechanisms as the result of the dysfunction of agrin that is brought about non-immunologically by high MMP-3 level in addition to the immune response to agrin (Luckman et al., 2011; Chan et al., 2020).

AGRIN/WNT-LRP4-MUSK SIGNALINGS IN NEUROMUSCULAR JUNCTION

Agrin/Dok7 Signaling *via* Lrp4/MuSK Contributes to AChR Clustering

In the ligand-binding ectodomains of MuSK, the first and second immunoglobulin-like domains (Ig1 and Ig2: Ig1/2; green limit in the pink-MuSK frame, **Figure 1**) mediate the agrin-Lrp4 signaling (Stiegler et al., 2006) *via* binding of the Ig1 domain (green limit in the pink-MuSK frame, **Figure 1**) with Lrp4 to form a tetrameric complex (Zhang et al., 2011; Zong et al., 2012). The MuSK (Pink frame, **Figure 1**) is stimulated from "inside" the muscle cell by an adaptor protein Dok7 (Pink frame, **Figure 1**) which forms a dimeric unit to dimerize and activate MuSK (Pink frame, **Figure 1**; Okada et al., 2006; Bergamin et al., 2010) and also recruits two adaptor proteins, CT10 regulators of the kinase (Crk and Crk-L) contributive to rapsyn (Pink frame, **Figure 1**)—anchored AChR cluster formation (Gray frame, **Figure 1**; Hallock et al., 2010). The results from the experiments to modify the Dok7 functions are such as follows: in muscles lacking Dok7, agrin failed to stimulate MuSK tyrosine phosphorylation (Inoue et al., 2009); silencing of Dok7 in rat muscle increases susceptibility to passive transfer MG (Gomez et al., 2016); overexpression of Dok7 in rat muscle enhances neuromuscular transmission with structural alterations of NMJ (Eguchi et al., 2020).

From "outside" the muscle cell, MuSK is stimulated by neural agrin (Pink frame, **Figure 1**) *via* Lrp4 (Pink frame, **Figure 1**) which is the agrin receptor and also activates MuSK without agrin (Weatherbee et al., 2006; Kim et al., 2008; Zhang et al., 2008, 2011, 2012a; Barik et al., 2014b; Stamatakou and Salinas, 2014).

Rapsyn and Tid1s Stabilize AChR Clusters at the Membrane

The AChR clusters formed by the agrin-Lrp4-MuSK signaling are anchored at the end-plate membrane by rapsyn (Pink frame, **Figure 1**; Lee et al., 2009; Zuber and Unwin, 2013; Xing et al., 2020) which is immobilized by the short-form of tumorous imaginal discs-1 (Tid1s: MuSK- and Dok7-binding protein belongs to a family of heat-shock protein 40, HSP40) in cooperation with HSP70 and HSP90β (Pink frames, Figure) and thereby maintains AChR clusters (Gray frame, **Figure 1**) at the end-plate membrane (Linnoila et al., 2008; Luo et al., 2008; Zong and Jin, 2013). Tid1s (Pink frame, **Figure 1**) is also contributive to the MuSK-Dok7 signaling during the activation of MuSK (Linnoila et al., 2008). The RING domain of rapsyn contains E3 ligase activity to induce AChR clustering and NMJ formation, possibly by regulation of AChR neddylation (Li et al., 2016).

Wnt-Mediating Signal *via* MuSK Contributes to AChR Cluster Prepatterning

In addition to the above-mentioned role as the mediator in agrin-Lrp4-MuSK signaling, MuSK acts as the mediator for Wnts (Blue frames, **Figure 1**) which belong to a family of secreted glycoproteins and released from motor neurons or derived from

muscle (Wu et al., 2010; Gordon et al., 2012; Koles and Budnik, 2012; Zhang et al., 2012a; Barik et al., 2014b; Stamatakou and Salinas, 2014). Of 19 different Wnt molecules existing in mice and humans (Wu et al., 2010), Wnt 11 (Jing et al., 2009; Wu et al., 2010; Zhang et al., 2012a) and Wnt 3 (Henriquez et al., 2008) are released from the motor neurons; the neuron-released Wnts are transferred across the synapse by exosome-like Evi-containing vesicles (Koles et al., 2012). Wnt 11 (Wu et al., 2010; Zhang et al., 2012a), Wnt 9a (Zhang et al., 2012a), and Wnt4 (Strochlic et al., 2012; Zhang et al., 2012a) are derived from muscles. The binding of the Ig4 domain (CRD) of MuSK (red-limit in pink MuSK, **Figure 1**) with Wnts contributes to AChR clustering through the non-canonical pathway mediated by the Dishevelled protein (Dvl; Pink frame, **Figure 1**), leading to the formation of AChR microclusters at the early non-innervated stage, termed as the AChR prepatterning (Kummer et al., 2006) which forms the clusters at the central part of the muscle and guides the incoming axon (Gray frame, **Figure 1**; Luo et al., 2002; Jing et al., 2009; Stiegler et al., 2009; Wu et al., 2010; Gordon et al., 2012; Koles and Budnik, 2012; Barik et al., 2014b; Burden et al., 2018; Guarino et al., 2020). The motoneuron-derived Wnt7a and Wnt7b serve nerve terminal development (Shen et al., 2018).

In the clustering of AChR, Wnt 11 and Wnt 9a require Lrp4 but not agrin (Zhang et al., 2012a); Wnt 4 requires neither agrin nor Lrp4 (Strochlic et al., 2012). Wnt 3 promotes the agrin-Lrp4-MuSK (Ig1/2 domains)-mediated clustering of AChR (Henriquez et al., 2008; Wnts 11, 9a, 4 and 3: Blue frames in **Figure 1**). In contrast to the neuron-released Wnt 3, the muscle-derived Wnt 3a reduces the agrin-mediated AChR clustering *via* the canonical Dvl pathway to β-catenin causing the reduced rapsyn expression (Wang et al., 2008); this negative regulation maintains balance with the positive regulator (neuron-released Wnt 3) and thereby helps to sculpt the mature synaptic architecture (Henriquez and Salinas, 2012; Koles and Budnik, 2012).

Linking to the intracellular kinase domain of MuSK, the small GTPases (Rac1 and Rho) effector p21-activated kinase 1 (PAK1; Pink frame, **Figure 1**) acts as a bridging molecule between the Wnt- and agrin-signaling pathways required for AChR clustering (Luo et al., 2002; Wu et al., 2010; Koles and Budnik, 2012). Wnt activates Rac1 in a more efficient usage than agrin which preferentially increases Rho activity (Henriquez and Salinas, 2012).

In the innervated stage of muscle when the agrin-Lrp4-MuSK (Ig1/2 domains) signaling plays a principal role in AChR cluster formation, the cyclin-dependent kinase 5 (Cdk5) concentrated at the postsynaptic NMJ is activated and required for ACh-induced removal of prepatterning AChR clusters which are not stabilized by agrin; this is mediated through two molecular mechanisms (the upregulation of calpain activity and the interaction of Cdk5 with nestin; Lin et al., 2005; Chen et al., 2007; Mohseni et al., 2011; Yang et al., 2011; Shi et al., 2012).

Neuregulin 1-ErbB Signaling to MuSK Activation

The ErbB receptors (receptor tyrosine kinase of EGF, epidermal growth factor, receptor family) for neuregulin 1 (NRG 1; Pink frames, **Figure 1**) link to the MuSK through the adaptor protein, Erbin (Simeone et al., 2010), suggesting that this signaling cascade increases the tyrosine phosphorylation of MuSK and thereby modulates MuSK-dependent AChR clustering (Ngo et al., 2012). Anti-ErbB antibodies were not detected in the sera of MG patients; however, the thymic expression of ErbB receptors was reduced in these patients (Vrolix et al., 2011).

A Variety of Immunogenicity of MuSK

By immunoblotting against recombinant proteins (expressed in HEK 293F cells) of MuSK ectodomains, we showed that the MuSK Ig1/2 antibodies (Y2 in **Figure 1**) were positive in the serum samples from 33 of 43 AChR antibody-negative MG patients; 10 of them (30%) were additionally positive for MuSK CRD antibodies (Y3 in **Figure 1**), suggesting an impairment of both the agrin-Lrp4-MuSK (Ig1/2 domains) signaling pathway (the green line from the green limit in pink-MuSK to Kinases *via* Dvl, **Figure 1**) and Wnt-Lrp4-MuSK(CRD) signaling pathway (the red line from the red limit in pink-MuSK to Kinases *via* Dvl, **Figure 1**) in the neuromuscular transmission; however, none was positive for anti-MuSK CRD alone in our study (Takamori et al., 2013). Reportedly, the experiments by the inhibition assay in the presence of unlabelled competitive proteins (McConville et al., 2004) and the immunoprecipitation assay using MuSK Ig1 domain and CRD (Otsuka et al., 2015) suggested the co-existence of antibodies against MuSK Ig1/2 domains and MuSK CRD in MuSK antibody-positive MG. The longitudinal epitope mapping study in 53 MuSK antibody-positive MG patients by the European group showed that 22.6% of the patients were positive for MuSK CRD antibodies, although they emphasized the MuSK Ig 1 domain as the main immunogenic region (Huijbers et al., 2016). It seems likely that the MuSK antibodies have pathological heterogeneity based on their binding to functionally different domains.

To determine the functional significance of MuSK CRD in neuromuscular transmission, Messéant and associates showed that the CRD deletion of MuSK in mice caused exuberant axonal growth bypassing AChR clusters and decreased synaptic vesicle density (presynaptic impairment), and a drastic deficit in AChR clustering (postsynaptic impairment; Messéant et al., 2015). They also suggested an implication of MuSK CRD in the Wnt-canonical signaling by demonstrating that this pre- and post-synaptic impairments were rescued by lithium chloride which acts as an inhibitor of the glycogen synthese kinase-3β (Gsk3β) and an activator of the Wnt/β-catenin signaling (Messéant et al., 2015). This study was followed by the demonstration that MuSK ΔCRD is malfunctioning since $MuSK^{\Delta CRD/-}$ embryos present defective pre- and post-synaptic differentiation (Boëx et al., 2018). In addition to the above-mentioned Wnt-canonical signaling pathway, they proposed the β catenin-dependent and vangl 2 (coimmunoprecipitated with Wnts 4 and 11 in muscle)-dependent Wnt non-canonical signaling pathway (Messéant et al., 2017). The experiment in mice suggested that the NMJ pre- and post-synaptic organizations by β-catenin-dependent or Wnt-dependent

signaling is regulated by Yes-associated protein (Yap) in the muscle (Zhao et al., 2017). Reportedly, the inhibition of the MuSK-Dvl signaling pathway (Wu et al., 2010; Koles and Budnik, 2012) decreased not only the amplitude of spontaneous synaptic currents but also their frequency (Luo et al., 2002), suggesting a defect in ACh-release upregulation to compensate for the post-synaptic dysfunction (Takamori et al., 1984; Plomp et al., 1995; Plomp, 2017; Takamori, 2019). This, in turn, may reflect an impairment in the retrograde Wnt-MuSK (CRD)-Dvl-Gsk3β inhibition-β catenin-slit 2 signaling at the nerve terminal (Luo et al., 2002; Salinas, 2005; Li et al., 2008; Budnik and Salinas, 2011; Koles and Budnik, 2012; Wu et al., 2012a, 2015; Barik et al., 2014b). Postsynaptically shown in the experiment is that β catenin regulates agrin-induced AChR clustering through interaction with rapsyn in a manner dependent on α catenin-associated cytoskeleton (Zhang et al., 2007). These can help explain the reports showing both pre- and post-synaptic defects in MuSK antibody-positive MG patients (Niks et al., 2010) and animal models (Cole et al., 2008; Klooster et al., 2012; Mori et al., 2012; Richman et al., 2012; Viegas et al., 2012). In the study of congenital myasthenic syndrome due to MuSK mutation, the changes in the presynaptic morphology were assumed to reflect a disturbance in muscle-derived retrograde signals resulting from the impairment of agrin- and Dok7-induced MuSK phosphorylation (Maselli et al., 2010; Ben Ammar et al., 2013).

We noted the debate by Remédio and associates who proposed that dependently on species, the prepatterning of AChR clusters is influenced by an additional presence of Kringle domain in the MuSK extracellular region (Remédio et al., 2016; Burden et al., 2018); this is likely to augue against the participation of MuSK CRD in signaling variety in MuSK antibody-positive MG patients. In this regard, Legay and Mei (2017) suggested that the controversial result may reflect the genotype-phenotype relationships because opposite phenotypes can be found depending on the genetic background (Sittig et al., 2016).

In the MuSK antibody-positive MG patients, the recent research reported that the monovalent MuSK antibodies abolished agrin-induced MuSK phosphorylation and AChR clustering, while the divalent monospecific MuSK antibodies had the opposing effect which leads to partially induced AChR clustering; this is independent of agrin (Huijbers et al., 2019b). It is also noticeable that Takata and his associates generated human MuSK monoclonal autoantibodies (2 IgG4 and 1 IgG3 subclasses obtained using isolation of MuSK autoantibody-expressing B cells from MuSK antibody-positive MG patients) and showed that these antibodies inhibited AChR clustering, but enhanced MuSK phosphorylation; they suggested an alternative mechanism for inhibiting AChR clustering (Takata et al., 2019).

Bone-Morphogenic Proteins (BMPs) and MuSK Activation

The BMPs, which are secreted ligands belonging to the transforming growth factor β (TGFβ) superfamily of signaling proteins, have been focused in highlighting insight into the possibility that BMPs work in vertebrate organisms as diffusible signals to ensure proper communication between motor neurons and skeletal muscles (Osses and Henriquez, 2015). In a variety of function and localization of BMPs, it is an interest to note the reports that the Wnt-MuSK Ig3 domain interaction acts as a BMP co-receptor which shapes BMP transcriptional output and cholinergic signaling to communicate motor neurons and skeletal muscles in the vertebrate (Henríquez et al., 2011; Yilmaz et al., 2016). The BMP-4 has been confirmed to be expressed in the skeletal muscle and localized in close vicinity to postsynaptic densities at the NMJ (Chou et al., 2013). Further work may provide a clue to the understanding of BMPs-mediated pathology in MuSK antibody-positive MG patients.

SYNAPTIC RETROGRADE SIGNALINGS FROM MUSCLE TO NERVE

Wnt-MuSK, Lrp4, and Laminins

As previously discussed in a variety of immunogenicity of MuSK, the interaction of Wnt with MuSK CRD leading to Dvl-GSK3β inhibition-β catenin-Slit 2 signaling (Luo et al., 2002; Salinas, 2005; Li et al., 2008; Budnik and Salinas, 2011; Koles and Budnik, 2012; Wu et al., 2012a; Barik et al., 2014b; Messéant et al., 2015) and the muscle Lrp4 (extracellular eight low-density lipoproteins repeats; Wu et al., 2012b; Yumoto et al., 2012) contribute to the retrograde signaling and thereby modulate the pre-synaptic differentiation including synaptic vesicles and active zone in the nerve terminal. Additional retrograde signaling in the synapse is mediated by the muscle-derived laminins α4, α5, and β2 which contribute to the presynaptic organization acting for ACh release; this includes the action of laminin β2 which tethers P/Q- and N-types voltage-gated Ca^{2+} channels (VGCCs) to the active zone proteins (Nishimune et al., 2008; Carson et al., 2010; Chen et al., 2011; Nishimune, 2012; Samuel et al., 2012; Yamada and Sekiguchi, 2015; Zhang et al., 2015; Rogers and Nishimune, 2017).

Presynaptic Ca^{2+} Homeostasis and Autoreceptors

From the standpoint of clinical electrophysiology, the AChR antibody-positive MG and animal models showed that the compensatory ACh release upregulation cannot be sustained at the high frequency of nerve stimulation (Plomp et al., 2015). This may reflect the impairment of the presynaptic Ca^{2+} homeostasis for ACh release (Takamori, 2012) to compensate for postsynaptic dysfunction. The presynaptic Ca^{2+} homeostasis is promoted by the activation of G protein-coupled receptors such as M1-type muscarinic AChR (M1 mAChR) and A2A adenosine receptor along with the interaction of brain-derived neurotrophic factor (BDNF) with receptor tyrosine kinase B (TrkB); these biological mechanisms lead to P/Q-type VGCC activation by the signaling mediated by phospholipase C (PLC)-phosphatidylinositol 4,5-bisphosphate (PIP2)-diacylglycerol (DAG)-protein kinase C (PKC; Amaral and Pozzo-Miller, 2012; Santafé et al., 2015; Nadal et al., 2016; Hurtado et al., 2017; Simö et al., 2018; Tomàs et al., 2018). Also, PLC-generated DAG regulates the presynaptic

vesicle priming protein (Munc13-1) to recruit ACh-containing vesicles for the immediately releasable pool (Bauer et al., 2007). Taking these into consideration, the presynaptic impairments to compensate postsynaptic dysfunction could, at least in part, be compatible with the result of our immunological study that the M1 mAChR antibodies were positive in 7 (28%) of our 25 post-synaptic nicotinic AChR antibody-positive MG patients (Takamori et al., 2007; Takamori, 2019); additionally, the anti-M1 mAChR antibodies were often (76%) positive in our 25 patients with Lambert-Eaton myasthenic syndrome (an autoimmune presynaptic disease caused by antibodies against mainly P/Q-type VGCC and partly synaptotagmin 1; Takamori et al., 2007; Takamori, 2008a). Of note, the M1 mAChR is physiologically associated with the non-voltage-gated Ca^{2+}-dominant influx channel (Transient receptor potential canonical; Kim and Saffen, 2005), the antibodies against which were positive in 7 (28%) of our 25 MG patients (Takamori, 2008b). An alternative theory postulated is that the impaired compensatory mechanism could be referred to the reduction in homeostatic small reserve pool of synaptic vesicles that depends on presynaptic adenosine A2A receptor operating Ca^{2+} influx *via* L-type VGCC (Oliverira et al., 2004; Ma et al., 2015; Wang et al., 2016). In a long-tetanic load in muscle, the complex compensatory mechanisms including the presynaptic autoreceptors and Ca^{2+} influx channel(s) may underlie to compensatory postsynaptic dysfunction.

THERAPEUTIC OPTION OF β_2-ADRENOCEPTOR AGONISTS IN MYASTHENIAS

Besides the biological signal (compensatory presynaptic Ca^{2+} homeostasis) triggered by G protein-coupled receptor, it is worthy to note that BDNF in the synapse is activated by β_2-adrenoceptor agonists and thereby contributes to the maintenance of the structural and functional integrity of motor end-plate; this signaling pathway may include the cyclic adenosine monophosphate (cAMP)/protein kinase A/cAMP-responsive element-binding protein; Bartus et al., 2015). The therapeutic pre- and post-synaptic benefits of β_2-adrenoceptor agonists (salbutamol and ephedrine) have been reported in MuSK MG animal model (Ghazanfari et al., 2014), autoimmune MG patients (Rodríquez Cruz et al., 2015b; Lipka et al., 2017; Vanhaesebrouck et al., 2019) and various types of congenital myasthenic syndromes (Engel et al., 2015; Beeson, 2016) including the patients with mutations in MuSK (Gallenmller et al., 2014; Rodríquez Cruz et al., 2020; Vanhaesebrouck and Beeson, 2019), Lrp4 (Selcen et al., 2015; Beeson, 2016), Dok7 (Lashley et al., 2010; Liewluck et al., 2011; Burke et al., 2013; Lorenzoni et al., 2013), agrin (Nicole et al., 2014; Beeson, 2016; Vanhaesebrouck and Beeson, 2019), collagen Q (McMacken et al., 2019) and collagen XIII (Beeson, 2016; Rodríguez Cruz et al., 2018, 2019; Dusl et al., 2019). In pharmacotherapeutic options, the β_2-agonist stimulation could be chosen as a novel therapeutic strategy in autoimmune and genetic myasthenias.

CANDIDATES AS THE MOLECULES IMPLICATING IN PATHOGENICITIES OF MYASTHENIAS

The studies including clinical researches may suggest the following molecules as candidates to implicate in the pathogenic mechanisms of myasthenic diseases: (1) caveolin 3 (Pink frame, **Figure 1**; MuSK kinase domain-binding protein which participates in agrin-induced phosphorylation and activation of MuSK, thereby driving AChR clustering; Hezel et al., 2010; Iwasa et al., 2016); (2) doublecortin (expressed in motor neurons and skeletal muscles to orderly form the pre- and post-synaptic morphology; Bourgeois et al., 2015); (3) R-spondin 2 (expressed in motor neurons and reactive with leucine-rich repeat-containing G-protein-coupled receptor which is expressed in skeletal muscles and enriched in the NMJ so as to regulate Wnt-mediated AChR clustering and also acting on an effect for synaptic vesicle recycling and number of active zones in the nerve terminal; Vieira et al., 2015; Nakashima et al., 2016); (4) amyloid precursor protein (APP)/APP-like protein (contributive to AChR clustering *via* the Lrp4-MuSK signal in cooperation with agrin-mediated signal and also to the presynaptic differentiation of the NMJ, and additionally contributive to the density of ACh-containing synaptic vesicles which is modulated by glia cell-derived neurotrophic factor, GDNF, expressed in muscle cells; Akaaboune et al., 2000; Wang et al., 2009; Caldwell et al., 2013; Choi et al., 2013; Stanga et al., 2016), and (5) α-neurexins (contributive to neurotransmission and differentiation of the synapse by functioning as the trans-synaptic complex with postsynaptic proteins such as neuroligins (Sons et al., 2006; Reissner et al., 2013; Plomp, 2017).

SYNAPTIC STABILITY AND MAINTENANCE BY EXTRACELLULAR MATRIX AND DYSTROPHIN-ASSOCIATED GLYCOPROTEIN COMPLEX

To be precisely opposed to the nerve terminal including the active zone artitecture (Nishimune, 2012; Südhof, 2012; Harris and Littleton, 2015; Körber and Kuner, 2016), the postsynaptic structure is stabilized by the extracellular matrix proteins (including synaptic collagens such as Q, IV and XIII, perlecan, biglycan, laminins, muscle agrin, nidogens and α-dystroglycan; Yellow frames, **Figure 1**), dystrophin-associated glycoprotein complex (including β-dystroglycan which links to rapsyn and utrophin; Yellow frames, **Figure 1**), cortactin (Yellow frame, **Figure 1**; cortactin-directing antibodies: Y7 in **Figure 1**; acting as not only a synaptic kinase substrate but also a regulator of actin polymerization), coronin 6 (Yellow frame, **Figure 1**; actin-binding protein which plays a role in synaptic stability), α-dystrobrevin (Yellow frame, **Figure 1**; contributive to cytoskeletal organization due to its phosphorylation by neuregulin 1(NRG 1)-ErbB receptor interaction: Pink frames in **Figure 1**) and Sorbs 1/2 (Yellow frame, **Figure 1**; contributive to synaptic stabilization by its interaction with Dok7-recruited Crk-L Nishimune et al., 2008; Madhavan et al., 2009; Hallock

et al., 2010, 2015; Pilgram et al., 2010; Schmidt et al., 2011; Singhal and Martin, 2011; Yurchenco, 2011; Amenta et al., 2012; Maselli et al., 2012; Nastase et al., 2012; Shi et al., 2012; Hochenester and Yurchenco, 2013; Karmouch et al., 2013; Chen et al., 2014; Constantin, 2014; Takamori, 2017a,b; Belhasan and Akaaboune, 2020). The following is the synaptic partners organizing molecules that regulate synaptic stability.

Collagen Q (Col Q) and Perlecan

Collagen Q (Yellow frame, **Figure 1**) is one of the muscle basal lamina proteins (junctional collagens; Singhal and Martin, 2011). Its N-terminus interacts with acetylcholinesterase (AChE); the two heparin-binding sites of its central collagenic domain mediate the interaction with perlecan (Yellow frame, **Figure 1**) which binds α-dystroglycan (Yellow frame, **Figure 1**) for linking the extracellular matrix to the cytoskeleton (Yellow frame, **Figure 1**). Its C-terminus binds the Ig1 domain (green limit) and CRD (red limit) in MuSK (Pink frame, **Figure 1**); these links make ColQ (*via* green and red lines, **Figure 1**) to modulate the action of the other ligands of the MuSK/Lrp4 complex for NMJ formation (Karmouch et al., 2013). The ColQ anchors AChE in the synaptic basal lamina, and thereby the association between Col Q and MuSK conforms Col Q/AChE to the synaptic localization (Cartaud et al., 2004). The MuSK antibodies were found to block the Col Q-MuSK interaction (Kawakami et al., 2011). Reportedly, the Col Q and MuSK antibodies competitively suppress agrin/Lrp4/MuSK signaling (Otsuka et al., 2015). Col Q antibodies (Y6 in **Figure 1**) were detected in some MG patients positive for MuSK and AChR antibodies (Cossins et al., 2012; Zoltowska Katarzyna et al., 2015). These findings are compatible with the electrophysiological finding characterized by slow miniature end-plate potential kinetics and hypersensitivity to AChE inhibitors in MuSK antibody-positive MG (Shin et al., 2014) and its animal model (Mori et al., 2012).

Collagen XIII

Collagen XIII is encoded as an extracellular matrix protein and is known to be crucial for the formation and function of pre- and post-synaptic organization of the NMJ, including the synaptic integrity through binding to the Col Q tail of AChE, AChR clustering, synaptic vesicle accumulation and axonal neurofilament (Latvanlehto et al., 2010; Logan et al., 2015; Härönen et al., 2017, 2019; Beeson et al., 2018; Heikkinen et al., 2019; Rodríquez Cruz et al., 2019). Autoantibodies to the collagen XIII have recently been reported in MG (Tu et al., 2018), suggesting the test as to if the Collagen XIII could be a pathogenic antigen in MG patients.

Biglycan

Biglycan (Yellow frame, **Figure 1**) is one of the proteoglycans and is enriched in the postsynaptic membrane and is a ubiquitous structural component of the extracellular matrix, and also acts as signaling molecules (Amenta et al., 2012; Nastase et al., 2012). The glycosaminoglycan-binding form of biglycan mediates its binding to extracellular α-dystroglycan (Yellow frame, **Figure 1**); the transmembrane β-dystroglycan (Yellow frame, **Figure 1**) binds to rapsyn (Pink frame, **Figure 1**) for firmly anchoring AChR clusters at the postsynaptic membrane (from Yellow frame to Pink frame, being connected by a black line, **Figure 1**) and also binding to the dystrophin/utrophin (Yellow frame, **Figure 1**)—associated protein complex contributive to the organization of cytoskeleton (Yellow frame, **Figure 1**) for synaptic stability. The non-glycosylated form of biglycan (lacking glycosaminoglycan side chain) directly interacts with two extracellular domains of MuSK: one (green line) is the agrin/Lrp4-mediating Ig1 domain of MuSK (green limit in pink-MuSK, **Figure 1**; Weatherbee et al., 2006; Kim et al., 2008; Zhang et al., 2008, 2011; Zong et al., 2012; Zong and Jin, 2013) and the other (red line) is the Wnt-mediating MuSK CRD (red limit in pink-MuSK, **Figure 1**; Jing et al., 2009; Koles and Budnik, 2012; Strochlic et al., 2012; Zhang et al., 2012a). The evidence that the two sites of MuSK ectodomain bind biglycan suggest possible participation of this matrix protein in reinforcing a functional bridge between the agrin-signaling (*via* Ig1 domain) and Wnt-signaling (*via* CRD; Barik et al., 2014b). Since biglycan becomes incapable of linking to MuSK by mutations of Ig1 domain and CRD (Amenta et al., 2012), the interaction between MuSK and biglycan (non-glycanated form) is potentially blocked by MuSK antibodies in the manner similar to the block of the MuSK-Col Q linkage by MuSK antibodies (Kawakami et al., 2011). In the serum samples from MG patients that we previously studied for the detection of antibodies recognizing MuSK Ig1/2 domains and CRD (Takamori et al., 2013), we tested if they harbor antibodies that directly recognize biglycan, but obtained the negative result (Takamori, 2017b). However, the MuSK antibodies may impair the synaptic stability by the disturbed MuSK-biglycan linkage. In addition to the immunological participation, biglycan stimulates multifunctional proinflammatory signaling linking the innate to adaptive immune systems when it is in a soluble form; this is based on that biglycan is capable of clustering several types of pathogen recognition receptors and orchestrating their signalings (Bavelova et al., 2009; Moreth et al., 2012; Nastase et al., 2012; Frey et al., 2013). In MG, biglycan produced in thymic myoid cells is known to play in generation and maintenance of the hyperplastic change of MG thymus (Tomoyasu et al., 1998; Takamori, 2017b).

Cortactin

Cortactin (Yellow frame, **Figure 1**) is a protein that is a tyrosine kinase substrate and regulates actin polymerization, and is co-enriched at AChR clusters; its tyrosine phosphorylation is enhanced by agrin, suggesting a novel function of phosphorylation-dependent cortactin signaling downstream from agrin/MuSK in promoting actin polymerization (through actin-related proteins 2/3 complex activation) and stabilizing AChR cluster at the postsynaptic membrane (Madhavan et al., 2009). Cortactin antibodies (Y7 in **Figure 1**) were detected in some of the MG patients (Gallardo et al., 2014; Cortés-Vicente et al., 2016; Illa et al., 2018), and also found in a patient with Lambert-Eaton myasthenic syndrome (a presynaptic autoimmune disease; Gallardo et al., 2014); this may reflect the fact that cortactin expresses in the presynaptic side (Peng et al., 1997) and acts as the Wnt signaling-dependent presynaptic effector molecule (Alicea et al., 2017).

CONCLUSION AND PERSPECTIVE

We emphasize: (1) the AChR cluster formation based on the Wnts-Lrp4-MuSK (CRD)-Dvl signaling (pre-innervated stage) which converges upon the agrin-Lrp4-MuSK (Ig1/2 domains) pathway (innervated stage); (2) the retrograde signaling (from muscle to the nerve) for presynaptic differentiation *via* MuSK CRD, Lrp4 and Laminins; (3) presynaptic Ca^{2+} homeostasis by autoreceptors; and (4) the synaptic stability based on the laminin-network including the extracellular matrix and the cytoskeleton. The insight into the NMJ structural mechanisms discussed in this review will foster further immunological approaches to search for new antigenic targets (Li L. et al., 2018; Koneczny and Herbst, 2019) and to enhance antibody detection (Vincent et al., 2012, 2018; Rodríguez Cruz et al., 2015a; Huda et al., 2017; Lazaridis and Tzartos, 2020) in MG, and may thereby help to view clinical profiles in MG subtypes (Verschuuren et al., 2013; Gilhus et al., 2019) and to provide potential therapeutic approaches (Losen et al., 2005; Ghazanfari et al., 2014; Gomez et al., 2014; Dalakas, 2015, 2019; Behin and Le Panse, 2018; Ito and Ohno, 2018; Morren and Li, 2020).

AUTHOR CONTRIBUTIONS

The author confirms being the sole contributor of this work and has approved it for publication.

REFERENCES

Akaaboune, M., Allinguant, B., Farza, H., Roy, K., Magoul, R., Fiszman, M., et al. (2000). Developmental regulation of amyloid precursor protein at the neuromuscular junction in mouse skeletal muscle. *Mol. Cell Neurosci.* 15, 355–367. doi: 10.1006/mcne.2000.0834

Alicea, D., Perez, M., Maodonado, C., Dominicci-Cotto, C., and Marie, B. (2017). Cortactin is a regulator of activity-dependent synaptic plasticity controlled by Wingless. *J. Neurosci.* 37, 2203–2215. doi: 10.1523/JNEUROSCI.1375-16.2017

Amaral, M. D., and Pozzo-Miller, L. (2012). Intracellular Ca^{2+} stores and Ca^{2+} influx are both required for BDNF to rapidly increase quantal vesicular transmitter release. *Neural Plast.* 2012:203536. doi: 10.1155/2012/203536

Amenta, A. R., Creely, H. E., Mercado, M. L. T., Hagiwara, H., McKechnie, B. A., Lechner, B. E., et al. (2012). Biglycan is an extracellular MuSK binding protein important for synaptic stability. *J. Neurosci.* 32, 2324–2334. doi: 10.1523/JNEUROSCI.4610-11.2012

Aoki, S., Nagashima, K., Furuta, M., Makioka, K., Fujita, Y., Saito, K., et al. (2020). A case of anti-Lrp4 antibody-associated myasthenia gravis with a rare complication of thymoma successfully treated by thymectomy. *Intern. Med.* 59, 1219–1222. doi: 10.2169/internalmedicine.3828-19

Arakawa, M., and Wagatsuma, A. (2020). $1\alpha, 25(OH)_2D_3$ regulates agrin-induced acetylcholine receptor clustering through upregulation of rapsyn expression in C_2C1_2 myotubes. *Biochem. Biophys. Res. Commun.* 525, 80–86. doi: 10.1016/j.bbrc.2020.02.027

Bagir, E. K., Acikalin, A., Gumurdulu, D., and Paydas, S. (2018). PD-1 and PD-L1 expression in thymic epithelial tumours and non-neoplastic thymus. *J. Clin. Pathol.* 71, 637–641. doi: 10.1136/jclinpath-2017-204788

Barik, A., Lu, Y., Sathyamurthy, A., Bowman, A., Shen, C., Li, L., et al. (2014a). LRP4 is critical for neuromuscular junction maintenance. *J. Neurosci.* 34, 13892–13905. doi: 10.1523/JNEUROSCI.1733-14.2014

Barik, A., Zhang, B., Sohal, G. S., Xiong, W. C., and Mei, L. (2014b). Crosstalk between agrin and Wnt signaling in development of vertebrate neuromuscular junction. *Dev. Neurobiol.* 74, 828–838. doi: 10.1002/dneu.22190

Bartus, R. T., Bétourné, A., Basile, A., Peterson, B. L., Glass, J., and Boulis, N. M. (2015). β-adrenoceptor agonists as novel, safe and potentially effective therapies for amyotrophic lateral sclerosis (ALS). *Neurobiol. Dis.* 85, 11–24. doi: 10.1016/j.nbd.2015.10.006

Bauer, C. S., Woolley, R. J., Teschemacher, A. G., and Seward, E. P. (2007). Potentiation of exocytosis by phospholipase C-coupled G-protein-coupled receptors requires the priming protein Munc13–1. *J. Neurosci.* 27, 212–219. doi: 10.1523/JNEUROSCI.4201-06.2007

Bavelova, A., Moreth, K., Tsalastra-Grreul, W., Zeng-Brouwers, J., Eickelberg, O., Young, M. F., et al. (2009). Biglycan, a danger signal that activates the NLRP3 inflammasome *via* Toll-like and P2X receptors. *J. Biol. Chem.* 284, 24035–24048. doi: 10.1074/jbc.m109.014266

Becquart, O., Lacotte, J., Malissart, P., Nadal, J., Lesage, C., Guillot, B., et al. (2019). Myasthenia gravis induced by immune checkpoint inhibitors. *J. Immunother.* 42, 309–312. doi: 10.1097/CJI.0000000000000278

Beecher, S., Putko, B. N., Wagner, A. N., and Siddiqi, Z. A. (2019). Therapeutic directed against B-cells and downstream effects in generalized autoimmune myasthenia gravis: current status. *Drugs* 79, 353–364. doi: 10.1007/s40265-019-1065-0

Beeson, D. (2016). Congenital myasthenic syndromes: recent advances. *Curr. Opin. Neurol.* 29, 565–571. doi: 10.1097/WCO.0000000000000370

Beeson, D., Cossins, J., Rodriquez Cruz, P. M., Maxwell, S., Liu, W. W., and Palace, J. (2018). Myasthenic syndromes due to defects in COL13A1 and in the N-linked glycosylation pathway. *Ann. N Y Acad. Sci.* 1413, 163–169. doi: 10.1111/nyas.13576

Behin, A., and Le Panse, R. (2018). New pathway and therapeutic targets in autoimmune myasthenia gravis. *J. Neuromuscul. Dis.* 5, 265–277. doi: 10.3233/jnd-170294

Belhasan, D. C., and Akaaboune, M. (2020). The role of the dystrophin glycoprotein complex on the neuromuscular system. *Neurosci. Lett.* 722:134833. doi: 10.1016/j.neulet.2020.134833

Ben Ammar, A., Soltanzadeh, P., Bauché, S., Richard, P., Goillot, E., Herbst, R., et al. (2013). A mutation causes MuSK reduced sensitivity to agrin and congenital myasthenia. *PLoS One* 8:e53826. doi: 10.1371/journal.pone.0053826

Bergamin, E., Hallock, P. T., Burden, S. J., and Hubbard, S. R. (2010). The cytoplasmic adaptor protein Dok7 activates the receptor tyrosine kinase MuSK *via* dimerization. *Mol. Cell* 39, 100–109. doi: 10.1016/j.molcel.2010.06.007

Berrih-Aknin, S., and Le Panse, R. (2014). Myasthenia gravis: a complrehensive review of immune dysregulation and etiological mechanisms. *J. Autoimmun.* 52, 90–100. doi: 10.1016/j.jaut.2013.12.011

Bezakova, G., and Ruegg, M. A. (2003). New insight into the roles of agrin. *Nat. Rev. Mol. Cell Biol.* 4, 295–308. doi: 10.1038/nrm1074

Boëx, M., Messéant, J., Bauché, S., Fontaine, B., Legay, C., and Strochlic, L. (2018). Regulation of mammalian neuromuscular junction formation and maintenance by Wnt signaling. *Curr. Opin. Physiol.* 4, 88–95. doi: 10.1016/j.cophys.2018.07.002

Bourgeois, F., Messéant, J., Kordeli, E., Petit, J. M., Delers, P., Bahi-Buisson, N., et al. (2015). A critical and previously unsuspected role for doublecortin at the neuromuscular junction in mouse and human. *Neuromuscul. Disord.* 25, 461–473. doi: 10.1016/j.nmd.2015.01.012

Budnik, V., and Salinas, P. C. (2011). Wnt signaling during synaptic development and plasticity. *Curr. Opin. Neurobiol.* 21, 151–159. doi: 10.1016/j.conb.2010.12.002

Burden, S. J., Huijbers, M. G., and Remedio, L. (2018). Fundamental molecules and mechanisms for forming and maintaining neuromuscular synapses. *Int. J. Mol. Sci.* 19:E490. doi: 10.3390/ijms19020490

Burden, S. J., Yomoto, N., and Zhang, W. (2013). The role of MuSK in synapse formation and neuromuscular disease. *Cold Spring Harb. Perspect. Biol.* 5:e009167. doi: 10.1101/cshperspect.a009167

Burgess, R. W., Nguyen, Q. T., Son, Y. J., Lichtman, J. W., and Sanes, J. R. (1999). Alternatively spliced isoforms of nerve- and muscle-derived agrin: their roles at the neuromuscular junction. *Neuron* 23, 33–44. doi: 10.1016/s0896-6273(00)80751-5

Burke, G., Hiscock, A., Klein, A., Niks, E. H., Main, M., Manzur, A. Y., et al. (2013). Sulbutamol benefits children with congenital myasthenic syndrome due to DOk7 mutations. *Neuromuscul. Disord.* 23, 170–175. doi: 10.1016/j.nmd.2012.11.004

Caldwell, J. H., Klevanski, M., Saar, M., and Müller, U. C. (2013). Roles of the amyloid precursor protein family in the peripheral nervous system. *Mech. Dev.* 130, 433–446. doi: 10.1016/j.mod.2012.11.001

Carson, S. S., Valdez, G., and Sanes, J. R. (2010). Presynaptic calcium channels and α3-integrins are complexed with synaptic cleft laminins, cytoskeletal elements and active zone components. *J. Neurochem.* 115, 654–666. doi: 10.1111/j.1471-4159.2010.06965.x

Cartaud, A., Strochlic, L., Guerra, M., Blanchard, B., Lambergeon, M., Krejci, E., et al. (2004). MuSK is required for anchoring acetylcholinesterase at the neuromuscular junction. *J. Cell Biol.* 165, 505–515. doi: 10.1083/jcb.200307164

Cetin, H., and Vincent, A. (2018). Pathogenic mechanisms and clinical correlations in autoimmune myasthenic syndromes. *Semin. Neurol.* 38, 344–354. doi: 10.1055/s-0038-1660500

Cetin, H., Webster, R., Liu, W. W., Nagaishi, A., Koneczny, I., Zimprich, F., et al. (2020). Myasthenia gravis AChR antibodies inhibit function of rapsyn-cluster AChRs. *J. Neurol. Neurosurg. Psychiatry* 91, 526–532. doi: 10.1136/jnnp-2019-322640

Chen, J., Billings, S. E., and Nishimune, H. (2011). Calcium channels link the muscle-derived synapse organizer laminin β2 to Bassoon and CAST/Erc2 to organize presynaptic active zones. *J. Neurosci.* 31, 512–525. doi: 10.1523/JNEUROSCI.3771-10.2011

Chen, Y., Ip, F. C. F., Shi, L., Zhang, Z., Tang, H., Ng, Y. P., et al. (2014). Coronin 6 regulates acetylcholine receptor clustering through modulating receptor anchorage to actin cytoskeleton. *J. Neurosci.* 34, 2413–2421. doi: 10.1523/JNEUROSCI.3226-13.2014

Chen, F., Qian, L., Yang, Z. H., Huang, Y., Ngo, S. T., Ruan, N. J., et al. (2007). Rapsyn interaction with calpain stabilizes AChR clusters at the neuromuscular junction. *Neuron* 55, 247–260. doi: 10.1016/j.neuron.2007.06.031

Choi Decroos, E., Hobson-Webb, L. D., Juel, V. C., Massey, J. M., and Sanders, D. B. (2014). Do acetylcholine receptor and striated muscle antibodies predict the presence of thymoma in patients with myasthenia gravis? *Muscle Nerve* 49, 30–34. doi: 10.1002/mus.23882

Choi, J., and Lee, S. Y. (2020). Clinical characteristics and treatment of immune-related adverse events of immune checkpoint inhibitors. *Immune Netw.* 20:e9. doi: 10.4110/in.2020.20.e9

Choi, H. Y., Liu, Y., Tennert, C., Sugiura, Y., Karakatsani, A., Kröger, S., et al. (2013). APP interacts with Lrp4 and agrin to coordinate the development of the neuromuscular junction in mice. *Elife* 2:e00220. doi: 10.7554/eLife.00220

Chou, H. J., Lai, D. M., Huang, C. W., McLennan, I. S., Wang, H. D., and Wang, P. Y. (2013). BMP4 is a peripherally-derived factor for motor neurons and attenuates glutamate-induced excitotoxicity *in vitro*. *PLoS One* 8:e58441. doi: 10.1371/journal.pone.0058441

Chan, Z., Oentaryo, M. J., and Lee, C. W. (2020). MMP-mediated modulation of ECM environment during axonal growth and NMJ development. *Neurosci. Lett.* 724:134822. doi: 10.1016/j.neulet.2020.134822

Clifford, K. M., Hobson-Webb, L. D., Benatar, M., Burns, T. M., Barnett, C., Silvestri, N. J., et al. (2019). Thymectomy may not be associated with clinical improvement in MuSK myasthenia gravis. *Muscle Nerve* 59, 404–410. doi: 10.1002/mus.26404

Cole, R. N., Reddel, S. W., Gervásio, O. L., and Phillips, W. D. (2008). Anti-MuSK patient antibodies disrupt the mouse neuromuscular junction. *Ann. Neurol.* 63, 782–789. doi: 10.1002/ana.21371

Constantin, B. (2014). Dystrophin complex functions as a scaffold for signaling proteins. *Biochim. Biophys. Acta* 1838, 635–642. doi: 10.1016/j.bbamem.2013.08.023

Cordts, I., Bodart, N., Hartmann, K., Karagiorgou, K., Tzartos, J. S., Mei, L., et al. (2017). Screening for lipoprotein receptor-protein 4-, agrin- and titin-antibodies and exploring the autoimmune spectrum in myasthenia gravis. *J. Neurol.* 264, 1193–1203. doi: 10.1007/s00415-017-8514-z

Cortés-Vicente, E., Gallardo, E., Martínez, M. Á., Díaz-Manera, J., Querol, L., Rojas-García, R., et al. (2016). Clinical characteristics of patients with double-seronegative myasthenia gravis and antibodies to cortactin. *JAMA Neurol.* 73, 1099–1104. doi: 10.1001/jamaneurol.2016.2032

Cossins, J., Belaya, K., Zoltowska, K., Koneczny, I., Maxwell, S., Jacobson, L., et al. (2012). The search for new antigenic targets in myasthenia gravis. *Ann. N Y Acad. Sci.* 1275, 123–128. doi: 10.1111/j.1749-6632.2012.06833.x

Dalakas, M. C. (2015). Future perspectives in target-specific immunotherapies of myasthenia gravis. *Ther. Adv. Neurol. Disord.* 8, 316–327. doi: 10.1177/1756285615605700

Dalakas, M. C. (2018). Neurological complications of immune checkpoint inhibitors: what happens when you 'take the brakes off' the immune system. *Ther. Adv. Neurol. Disord.* 11:1756286418799864. doi: 10.1177/1756286418799864

Dalakas, M. C. (2019). Immunotherapy in myasthenia gravis in the era of biologics. *Nat. Rev. Neurol* 15, 113–124. doi: 10.1038/s41582-018-0110-z

Danikowski, K. M., Jayaraman, S., and Prabhaakar, B. S. (2017). Regulatory T cells in multiple sclerosis and myasthenia gravis. *J. Neuroinflammation* 14:117. doi: 10.1186/s12974-017-0892-8

Di Stefano, V., Lupica, A., Rispoli, M. G., Di Muzio, A., Brighina, F., and Rodolico, C. (2020). Rituximab in AChR subtype of myasthenia gravis: systematic review. *J. Neurol. Neurosurg. Psychiatry* 91, 392–395. doi: 10.1136/jnnp-2019-322606

Díaz-Manera, J., Martínez-Hernández, E., Querol, L., Klooster, R., Rojas-García, R., Suárez-Calvet, X., et al. (2012). Long-lasting treatment effect of rituximab in MuSK myasthenia. *Neurology* 78, 189–193. doi: 10.1212/WNL.0b013e3182407982

Drachman, D. B., Adams, R. N., Josifek, L. F., and Self, S. G. (1982). Functional activities of antibodies to acetylcholine receptors and clinical severity of myasthenia gravis. *N. Engl. J. Med.* 307, 769–775. doi: 10.1056/NEJM19820.9233071.301

Drachman, D. B., Angus, C. W., Adams, R. N., Michelson, J. D., and Hoffamn, G. J. (1978). Myasthenic antibodies cross-link acetylcholine receptors to accelerate degradation. *N. Engl. J. Med.* 298, 1116–1122. doi: 10.1056/nejm197805182982004

Dubey, D., David, W. S., Reynolds, K. L., Chute, D. F., Chement, N. F., Cohen, J. V., et al. (2020). Severe neurological toxicity in immune checkpoint inhibitors: growing spectrum. *Ann. Neurol.* 87, 659–669. doi: 10.1002/ana.25708

Dusl, M., Moreno, T., Munell, F., Macaya, A., Gratacòs, M., Abicht, A., et al. (2019). Congenital myasthenic syndrome caused by novel COL13A1 mutations. *J. Neurol.* 266, 1107–1112. doi: 10.1007/s00415-019-09239-7

Eguchi, T., Tezuka, T., Fukudome, T., Watanabe, Y., Sagara, H., and Yamanashi, Y. (2020). Overespression of Dok-7 in skeletal muscle enhances neuromuscular transmission with structural alterations of neuromuscular junctions: Implications in robustness of neuromuscular transmission. *Biochem. Biophys. Res. Commun.* 523, 214–219. doi: 10.1016/j.bbrc.2019.12.011

Engel, A. G., Shen, X. M., Selcen, D., and Sine, S. M. (2015). Congenital myasthenic syndromes: pathogenesis, diagnosis, and treatment. *Lancet Neurol.* 144, 420–434. doi: 10.1016/S1474-4422(14)70201-7

Evoli, A., Alboini, P. E., Damato, V., Iorio, R., Provenzano, C., Bartoccioni, E., et al. (2018). Myasthenia gravis with antibodies to MuSK: an update. *Ann. N Y Acad. Sci.* 1412, 82–89. doi: 10.1111/nyas.13518

Evoli, A., Bianchi, M. R., Riso, R., Minicuci, G. M., Batocchi, A. P., Servidei, S., et al. (2008). Response to therapy in myasthenia gravis with anti-MuSK antibodies. *Ann. N Y Acad. Sci.* 1132, 76–83. doi: 10.1196/annals.1405.012

Evoli, A., and Padura, J. (2013). Dianosis and therapy of myasthenia gravis with antibodies to muscle-specific kinase. *Autoimmun. Rev.* 12, 931–935. doi: 10.1016/j.autrev.2013.03.004

Frey, H., Schroeder, N., Manon-Jensen, T., Iozzo, R. V., and Schaefer, L. (2013). Biological interplay between proteoglycans and their innate immune receptors in inflammation. *FEBS J.* 280, 2165–2179. doi: 10.1111/febs.12145

Gable, K. L., and Guptill, J. T. (2020). Antagonism of the neonatal Fc receptor as an emerging treatment for myasthenia gravis. *Front. Immunol.* 10:3052. doi: 10.3389/fimmu.2019.03052

Gallardo, E., Martinez-Hernández, E., Titulaer, M. J., Huijbers, M. G., Martinez, M. A., Ramos, A., et al. (2014). Cortactin autoantibodies in myasthenia gravis. *Autoimmun. Rev.* 13, 1003–1007. doi: 10.1016/j.autrev.2014.08.039

Gallenmller, C., Mller-Felber, W., Dusl, M., Strucka, R., Guergueltcheva, V., Blaschek, A., et al. (2014). Salbutamol-responsive limb-girdle congenital myasthenic syndome due to a novel missense mutation and heteroallelic

deletion in MuSK. *Neuromuscul. Disord.* 24, 31–35. doi: 10.1016/j.nmd.2013.08.002

Gasperi, C., Melms, A., Schoser, B., Zhang, Y., Meltoranta, J., Risson, V., et al. (2014). Anti-agrin autoantibodies in myasthenia gravis. *Neurology* 82, 1976–1983. doi: 10.1212/WNL.0000000000000478

Gesemann, M., Denzer, A. J., and Ruegg, M. A. (1995). Acetylcholine receptor-aggregating activity of agrin isoforms and mapping of the active state. *J. Cell Biol.* 128, 625–636. doi: 10.1083/jcb.128.4.625

Ghazanfari, N., Fernandez, K. J., Murata, Y., Morsch, M., Ngo, S. T., Reddel, S. W., et al. (2011). Muscle specific kinase: organizer of synaptic membrane domains. *Int. J. Biochem. Cell Biol.* 43, 295–298. doi: 10.1016/j.biocel.2010.10.008

Ghazanfari, N., Morsch, M., Tse, N., Reddel, S. W., and Phillips, W. D. (2014). Effects of the β2-adrenoceptor agonist, alubuterol, in a mouse model of anti-MuSK myasthenia gravis. *PLoS One* 9:e87840. doi: 10.1371/journal.pone.0087840

Gilhus, N. E., Tzartos, S., Evoli, A., Palace, J., Burns, T. M., and Verschuuren, J. J. G. M. (2019). Myasthenia gravis. *Nat. Rev. Dis. Primers* 5:30. doi: 10.1038/s41572-019-0079-y

Gomez, A. M., Stevens, J. A., Mané-Damas, M., Molenaar, P., Duimel, H., Verheyen, F., et al. (2016). Silencing of Dok-7 in adult rat muscle increases susceptibility to passive transfer myasthenia gravis. *Am. J. Pathol.* 186, 2559–2568. doi: 10.1016/j.ajpath.2016.05.025

Gomez, A. M., Willcox, N., Vrolix, K., Hummel, J., Nogales-Gadea, G., Saxena, A., et al. (2014). Proteasome inhibition with bortezomid depletes plasma cells and specific autoantibody production in primary thymic cell cultures from early-onset myasthenia gravis patients. *J. Immunol.* 193, 1055–1063. doi: 10.4049/jimmunol.1301555

Gordon, L. R., Gribble, K. D., Syrett, C. M., and Granato, M. (2012). Initiation of synapse formation by Wnt-induced MuSK endocytosis. *Development* 139, 1023–1033. doi: 10.1242/dev.071555

Guarino, S. R., Canciani, A., and Ferneris, F. (2020). Dissecting the extracellular complexity of neuromuscular junction organizers. *Front. Mol. Biosci.* 6:156. doi: 10.3389/fmolb.2019.00156

Guptill, J. T., Sanders, D. B., and Evoli, A. (2011). Anti-MuSK antibody myasthenia gravis: clinical findings and response to treatment in two large cohorts. *Muscle Nerve* 44, 36–40. doi: 10.1002/mus.22006

Ha, J. C., and Richman, D. P. (2015). Myasthenia gravis and related disorders: pathology and molecular pathogenesis. *Biochem. Biophys. Acta* 1852, 651–657. doi: 10.1016/j.bbadis.2014.11.022

Hallock, P. T., Chin, S., Blais, S., Neubert, T. A., and Glass, D. J. (2015). Sorbs1 and -2 interact with CrkL and are required for acetylcholine receptor cluster formation. *Mol. Cell. Biol.* 36, 262–270. doi: 10.1128/mcb.00775-15

Hallock, P. T., Xu, C. F., Park, T. J., Neubert, T. A., Curran, T., and Burden, S. J. (2010). Dok-7 regulates neuromuscular synapse formation by recruiting Crk and Crk-L. *Genes Dev.* 24, 2451–2461. doi: 10.1101/gad.1977710

Harris, K. P., and Littleton, J. T. (2015). Transmission, development, and plasticity of synapses. *Genetics* 201, 345–375. doi: 10.1534/genetics.115.176529

Heikkinen, A., Härönen, H., Norman, O., and Pihlajaniemi, T. (2019). Collagen XIII and other ECM components in the assembly and disease of the neuromuscular junction. *Anat. Rec.* doi: 10.1002/ar.24092 [Epub ahead of print].

Helgeland, G., Petzold, A., Luckman, S. P., Gilhus, N. E., Plant, G. T., and Romi, F. R. (2011). Matrix metalloproteinases in myasthenia gravis. *Eur. Neurol.* 65, 53–58. doi: 10.1159/000322737

Henríquez, J. P., Krull, C. E., and Osses, N. (2011). The Wnt and BMP families of signaling morphogens at the vertebrate neuromuscular junction. *Int. J. Mol. Sci.* 12, 8924–8946. doi: 10.3390/ijms12128924

Henriquez, J. P., and Salinas, P. C. (2012). Dual roles for Wnt signaling during the formation of the vertebrate neuromuscular junction. *Acta Physiol.* 204, 128–136. doi: 10.1111/j.1748-1716.2011.02295.x

Henriquez, J. P., Webb, A., Bence, M., Bildose, H., Sahores, M., Hughes, S. M., et al. (2008). Wnt signaling promotes AChR aggregation at the neuromuscular synapse in collaboration with agrin. *Proc. Natl. Acad. Sci. U S A* 105, 18812–18817. doi: 10.1073/pnas.0806300105

Herbst, R. (2019). MuSK function during health and disease. *Neurosci. Lett.* 716:134676. doi: 10.1016/j.neulet.2019.134676

Hettwer, S., Lin, S., Kucsera, S., Haubitz, M., Oliveri, F., Fariello, R. G., et al. (2014). Injection of soluble fragment of neural agrin (N-1654) considerably improves the muscle pathology caused by the disassembly of the neuromuscular junction. *PLoS One* 9:e88739. doi: 10.1371/journal.pone.0088739

Hezel, M., de Groat, W. C., and Galbiati, F. (2010). Caveolin-3 promotes nicotinic acetylcholine receptor clustering and regulates neuromuscular junction activity. *Mol. Biol. Cell* 21, 302–310. doi: 10.1091/mbc.e09-05-0381

Higuchi, O., Hamuro, J., Motomura, M., and Yamanashi, Y. (2011). Autoantibodies to low-density lipoprotein receptor-related protein 4 in myasthenia gravis. *Ann. Neurol.* 69, 418–422. doi: 10.1002/ana.22312

Hoch, W., Campanelli, J. T., Harrison, S., and Scheller, R. H. (1994). Structural domains of agrin required for clustering of nicotinic acetylcholine receptors. *EMBO J.* 13, 2814–2821. doi: 10.1002/j.1460-2075.1994.tb06575.x

Hoch, W., McConville, J., Helmes, S., Newsom-Davis, J., Melms, A., and Vincent, A. (2001). Auto-antibodies to the receptor tyrosine kinase MuSK in patients with myasthenia gravis without acetylcholine receptor antibodies. *Nat. Med.* 7, 365–368. doi: 10.1038/85520

Hochenester, E., and Yurchenco, P. D. (2013). Laminins in basement membrane assembly. *Cell Adh. Migr.* 7, 56–63. doi: 10.4161/cam.21831

Hoshi, T., Tezuka, T., Yokoyama, K., Iemura, S., Natsume, T., and Yamanashi, Y. (2013). Mesdc2 plays a key role in cell-surface expression of Lrp4 and postsynaptic specialization in myotubes. *FEBS Lett.* 587, 3749–3754. doi: 10.1016/j.febslet.2013.10.001

Howard, J. F. Jr. (2018). Myasthenia gravis: the role of complement at the neuromuscular junction. *Ann. N Y Acad. Sci.* 1412, 113–128. doi: 10.1111/nyas.13522

Howard, J. F. Jr., Bril, V., Burns, T. M., Mantegazza, R., Bilinska, M., Szczudlik, A., et al. (2019). Randomized phase 2 study of FcRn antagonist efgartigimod in generalized myasthenia gravis. *Neurology* 92, e2661–e2673. doi: 10.1212/wnl.0000000000007600

Howard, J. F. Jr., Nowak, R. J., Wolfe, G. I., Freimer, M. L., Vu, T. H., Hinton, J. L., et al. (2020). Clinical effects of the self-administered subcutaneous complement inhibitor Zilucoplan in patients with moderate to severe generalized myasthenia gravis: results of a phase 2 randomized double-blind, placebo-controlled, multicenter clinical trial. *JAMA Neurol.* doi: 10.1001/jamaneurol.2019.5125 [Epub ahead of print].

Härönen, H., Zainul, Z., Naumenko, N., Sormunen, R., Miinalainen, I., Shakirzyanova, A., et al. (2019). Correct expression and localization of collagen XIII are crucial for the normal formation and function of the neuromuscular system. *Eur. J. Neurosci.* 49, 1491–1511. doi: 10.1111/ejn.14346

Härönen, H., Zainul, Z., Tu, H., Naumenko, N., Sormunen, R., Miinalainen, I., et al. (2017). Collagen XIII secures pre- and postsynaptic integrity of the neuromuscular synapse. *Hum. Mol. Genet.* 26, 2076–2090. doi: 10.1093/hmg/ddx101

Huda, R. (2020). New approaches to targeting B cells for myasthenia gravis. *Front. Immunol.* 11:240. doi: 10.3389/fimmu.2020.00240

Huda, S., Cao, M., De Rosa, A., Woodhall, M., Rodriquez Cruz, P. M., Cossins, J., et al. (2020). SHP2 inhibitor protects AChRs from effects of myasthenia gravis MuSK antibody. *Neurol. Neuroimmunol. Neuroinflamm.* 7:e645. doi: 10.1212/nxi.0000000000000645

Huda, S., Waters, P., Woodhall, M., Leite, M. I., Jacobson, L., De Rosa, A., et al. (2017). IgG-specific cell-based assay detected potentially pathogenic MuSK-abs in seronegative MG. *Neurol. Neuroimmunol. Neuroinflamm.* 4:e357. doi: 10.1212/nxi.0000000000000357

Huijbers, M. G., Plomp, J. J., van Es, I. E., Fillié-Grijpma, Y. E., Kamar-Al Majidi, S., Ulrichts, P., et al. (2019a). Efgartigimod improves muscle weakness in a mouse model for muscle-specific kinase myasthenia gravis. *Exp. Neurol.* 317, 133–143. doi: 10.1016/j.expneurol.2019.03.001

Huijbers, M. G., Vergoossen, D. L., Fillié-Grijpma, Y. E., van Es, I. E., Koning, M. T., Slot, L. M., et al. (2019b). MuSK myasthenia gravis monoclonal antibodies: valency dictates pathogenicity. *Neurol. Neuroimmunol. Neuroinflamm.* 6:e547. doi: 10.1212/nxi.0000000000000547

Huijbers, M. G., Vink, A. F., Niks, E. H., Westhuis, R. H., van Zwet, E. W., de Meel, R. H., et al. (2016). Longitudinal epitope mapping in MuSK myasthenia gravis: implications for disease severity. *J. Neuroimmunol.* 291, 82–88. doi: 10.1016/j.jneuroim.2015.12.016

Huijbers, M. G., Zhang, W., Klooster, R., Niks, E. H., Friese, M. B., Staasheijm, K. R., et al. (2013). MuSK IgG4 autoantibodies cause myasthenia

gravis by inhibiting binding between MuSK and Lrp4. *Proc. Natl. Acad. Sci. U S A* 110, 20783–20788. doi: 10.1073/pnas.1313944110

Hurtado, E., Cilleros, V., Nadal, L., Simö, A., Obis, T., Gracia, N., et al. (2017). Muscle contraction regulates BDNF/TrkB signaling to modulate synaptic function through presynaptic cPKCα and cPKCβI. *Front. Mol. Neurosci.* 10:147. doi: 10.3389/fnmol.2017.00147

Illa, I., Cortés-Vicente, E., Martinez, M. Á., and Gallardo, E. (2018). Dioagnostic utility of cortactin antibodies in myasthenia gravis. *Ann. N Y Acad. Sci.* 1412, 90–94. doi: 10.1111/nyas.13502

Inoue, A., Setoguchi, K., Matsubara, Y., Okada, K., Sato, N., Iwakura, Y., et al. (2009). Dok-7 activates the muscle receptor kinase MuSK and shapes synaptic formation. *Sci. Signal.* 2:ra7. doi: 10.1126/scisignal.2000113

Ito, M., and Ohno, K. (2018). Protein-anchoring therapy to target extracellular matrix proteins to their physiological destinations. *Matrix Biol.* 68–69, 628–636. doi: 10.1016/j.matbio.2018.02.014

Iwasa, K., Furukawa, Y., Yoshikawa, H., and Yamada, M. (2016). Caveolin-3 is aberrantly expressed in skeletal muscle cells in myasthenia gravis. *J. Neuroimmunol.* 301, 30–34. doi: 10.1016/j.jneuroim.2016.10.011

Iwasa, K., Komai, K., and Takamori, M. (1998). Spontaneous thymoma rat as a model for myasthenic weakness caused by anti-ryanodine receptor antibodies. *Muscle Nerve* 21, 1655–1660. doi: 10.1002/(sici)1097-4598(199812)21:12<1655::aid-mus5>3.0.co;2-f

Iwasa, K., Yoshikawa, H., Furukawa, Y., and Yamada, M. (2018). Programmed cell death ligand 1 expression is upregulated in the skeletal muscle of patients with myasthenia gravis. *J. Neuroimmunol.* 325, 74–78. doi: 10.1016/j.jneuroim.2018.09.012

Jing, L., Lefebvre, J. L., Gordon, L. R., and Granato, M. (2009). Wnt signals organize synaptic prepattern and axon guidance through the Zebrafish unplugged/MuSK receptor. *Neuron* 61, 721–733. doi: 10.1016/j.neuron.2008.12.025

Johansen, A., Christensen, S. J., Scheie, D., Højgaard, J. L. S., and Kondziella, D. (2019). Neuromuscular adverse events associated with anti-PD-1 monoclonal antibodies: systemic review. *Neuerology* 92, 663–674. doi: 10.1212/wnl.0000000000007235

Karmouch, J., Dobbertin, A., Sigoillot, S., and Legay, C. (2013). Developmental consequences of the ColQ/MuSK interactions. *Chem. Biol. Interact.* 203, 287–291. doi: 10.1016/j.cbi.2012.10.006

Kawakami, Y., Ito, M., Hirayama, M., Sahashi, K., Ohkawara, B., Masuda, A., et al. (2011). Anti-MuSK autoantibodies block binding of collagen Q to MuSK. *Neurology* 77, 1819–1826. doi: 10.1212/WNL.0b013e318237f660

Kim, Y., and Saffen, D. (2005). Activation of M1 muscarinic acetylcholine receptors stimulates the formation of multiprotein complex centered on TRPC6 channels. *J. Biol. Chem.* 280, 32035–32047. doi: 10.1074/jbc.m500429200

Kim, N., Stiegler, A. L., Cameron, T. O., Hallock, P. T., Gomez, A. M., Huang, J. H., et al. (2008). Lrp4 is a receptor for agrin and forms a complex with MuSK. *Cell* 135, 334–342. doi: 10.1016/j.cell.2008.10.002

Klooster, R., Plomp, J. J., Huijbers, M. G., Niks, E. H., Straasheijm, K. R., Detmers, F. J., et al. (2012). Muscle-specific kinase myasthenia gravis IgG4 autoantibodies cause severe neuromuscular junction dysfunction in mice. *Brain* 135, 1081–1101. doi: 10.1093/brain/aws025

Koles, K., and Budnik, V. (2012). Wnt signaling in neuromuscular junction development. *Cold Spring Harb. Perspect. Biol.* 4:a008045. doi: 10.1101/cshperspect.a008045

Koles, K., Nunnari, J., Korkut, C., Barria, R., Brewer, C., Li, Y., et al. (2012). Mechanism of evenness interrupted (Evi)-exosome release at synaptic boutons. *J. Biol. Chem.* 287, 16820–16834. doi: 10.1074/jbc.m112.342667

Koneczny, I. (2018). A new classification systemfor IgG4 autoantibodies. *Front. Immunol.* 9:97. doi: 10.3389/fimmu.2018.00097

Koneczny, I., Cossins, J., and Vincent, A. (2014). The role of muscle-specific tyrosine kinase (MuSK) and mystery of MuSK myasthenia gravis. *J. Anat.* 224, 29–35. doi: 10.1111/joa.12034

Koneczny, I., Cossins, J., Waters, P., Beeson, D., and Vincent, A. (2013). MuSK myasthenia gravis IgG4 disrupts the interaction of Lrp4 with MuSK but both IgG4 and IgG1–3 can disperse preformed agrin-independent AChR clusters. *PLoS One* 8:e80695. doi: 10.1371/journal.pone.0080695

Koneczny, I., and Herbst, R. (2019). Myasthenia gravis: pathogenic effects of autoantibodies on neuromuscular architecture. *Cells* 8, 671–705. doi: 10.3390/cells8070671

Körber, C., and Kuner, T. (2016). Molecular machines regulating the release probability of synaptic vesicles at the active zone. *Front. Synaptic Neurosci.* 8:5. doi: 10.3389/fnsyn.2016.00005

Kumar, P., Bhattacharya, P., and Prabhakar, B. S. (2018). A comprehensive review on the role of co-signalling receptors and Treg homeostasis in autoimmunity and tumor immunity. *J. Autoimmun.* 95, 77–99. doi: 10.1016/j.jaut.2018.08.007

Kumar, P., Saini, S., and Prabhakar, B. S. (2019). Cancer immunotherapy with ckeck point inhibitor can cause autoimmune adverse events due to loss of Treg. *Semin. Cancer Biol.* doi: 10.1016/j.semcancer.2019.01.006 [Epub ahead of print].

Kummer, T. T., Misgeld, T., and Sanes, J. R. (2006). Assembly of the postsynaptic membrane at the neuromuscular junction: paradigm lost. *Curr. Opin. Neurobiol.* 16, 74–82. doi: 10.1016/j.conb.2005.12.003

Kusner, L. L., Satija, N., Cheng, G., and Kaminski, H. J. (2014). Targeting therapy to the neuromuscular junction: proof of concept. *Muscle Nerve* 49, 749–756. doi: 10.1002/mus.24057

Kusner, L. L., Yucius, K., Sengupta, M., Sprague, A. G., Desai, D., Nguyen, T., et al. (2019). Investigational RNAi therapeutic targeting C5 is efficacious in pre-clinical models of myasthenia gravis. *Mol. Ther. Methods Clin. Dev.* 13, 484–492. doi: 10.1016/j.omtm.2019.04.009

Lashley, D., Palace, J., Jayawant, S., Robb, S., and Beeson, D. (2010). Ephedrine treatment in congenital myasthenic syndrome due to mutations in Dok7. *Neurology* 74, 1517–1523. doi: 10.1212/wnl.0b013e3181dd43bf

Latvanlehto, A., Fox, M. A., Sormunen, R., Tu, H., Oikarainen, T., Koski, A., et al. (2010). Muscle-derived collagen XIII regulates maturation of the skeletal neuromuscular junction. *J. Neurosci.* 30, 12230–12241. doi: 10.1523/JNEUROSCI.5518-09.2010

Lazaridis, K., Baltatzidour, V., Tektonidis, N., and Tzartos, S. J. (2020). Antigen-specific immunoadsorption of MuSK autoantibodies as a treatment of MuSK-induced experimental autoimmune myasthenia gravis. *J. Neuroimmunol.* 339:577136. doi: 10.1016/j.jneuroim.2019.577136

Lazaridis, K., and Tzartos, S. J. (2020). Antibody specificities in myasthenia gravis; implications for improved diagnostics and therapeutics. *Front. Immunol.* 11:212. doi: 10.3389/fimmu.2020.00212

Lee, Y., Rudell, J., and Ferns, M. (2009). Rapsyn interacts with the muscle acetylcholine receptor *via* α-helical domains in the α, β, and ε subunit intracellular loops. *Neuroscience* 163, 222–232. doi: 10.1016/j.neuroscience.2009.05.057

Legay, C., and Mei, L. (2017). Moving forward with the neuromuscular junction. *J. Neurochem.* 142, 59–63. doi: 10.1111/jnc.14028

Leite, M. I., Ströbel, P., Jones, M., Micklem, K., Moritz, R., Gold, R., et al. (2005). Fewer thymic changes in MuSK antibody-positive than in MuSK antibody-negative MG. *Ann. Neurol.* 57, 444–448. doi: 10.1002/ana.20386

Li, L., Cao, Y., Wu, H., Ye, X., Zhu, Z., Xing, G., et al. (2016). Enzymatic activity of the scaffold protein rapsyn for synapse formation. *Neuron* 92, 1007–1019. doi: 10.1016/j.neuron.2016.10.023

Li, X. M., Dong, X. P., Luo, S. W., Zhang, B., Lee, D. H., Ting, A. K., et al. (2008). Retrograde regulation of motoneuron differentiation by muscle-β-catenin. *Nat. Neurosci.* 11, 262–268. doi: 10.1038/nn2053

Li, Y., Guptill, J. T., Russo, M. A., Massey, J. M., Jud, V. C., Hobson-Webb, L. D., et al. (2019). Tacrolimus inhibits Th1 and Th12 responses in MuSK-antibody positive myasthenia gravis patients. *Exp. Neurol.* 312, 43–50. doi: 10.1016/j.expneurol.2018.11.006

Li, Z., Li, M., Wood, K., Hettwer, S., Muley, S. A., Shi, F. D., et al. (2018). Engineered agrin attenuates the severity of experimental autoimmune myasthenia gravis. *Muscle Nerve* 57, 814–820. doi: 10.1002/mus.26025

Li, L., Xiong, W. C., and Mei, L. (2018). Neuromuscular junction formation, aging, and disorders. *Annu. Rev. Physiol.* 80, 159–188. doi: 10.1146/annurev-physiol-022516-034255

Li, Y., Zhang, Y., Cai, G., He, D., Dai, Q., Xu, Z., et al. (2017). Anti-Lrp4 autoantibodies in chinese patients with myasthenia gravis. *Muscle Nerve* 56, 938–942. doi: 10.1002/mus.25591

Liewluck, T., Selecen, D., and Engel, A. G. (2011). Beneficial effects of Albuterol in congenital endplate acetylcholinesterase deficiency and DOK-7 myasthenia. *Muscle Nerve* 44, 789–794. doi: 10.1002/mus.22176

Lin, W., Dominguez, B., Yang, J., Aryal, P., Brandon, E. P., Gage, F. H., et al. (2005). Neurotransmitter acetylcholine negatively regulates neuromuscular synapse formation by a Cdk5-dependent mechanism. *Neuron* 46, 569–579. doi: 10.1016/j.neuron.2005.04.002

Linnoila, J., Wang, Y., Yao, Y., and Wang, Z. Z. (2008). A mammalian homolog of Drosophila tumorous imaginal discs, Tid1, mediates agrin signaling at the neuromuscular junction. *Neuron* 60, 625–641. doi: 10.1016/j.neuron.2008.09.025

Lipka, A. F., Vrinten, C., van Zwet, E. W., Schirmmel, K. J., Cornel, M. C., Kuijpers, M. R., et al. (2017). Ephedrine treatment for autoimmune myasthenia gravis. *Neuromuscul. Disord.* 27, 259–265. doi: 10.1016/j.nmd.2016.11.009

Litchman, T., Roy, B., Kumar, A., Sharma, A., Nike, V., and Nowak, R. J. (2020). Differential response to rituximab in anti-AChR and anti-MuSK positive myasthenia gravis patients: a single-center retrospective study. *J. Neurol. Sci.* 411:116690. doi: 10.1016/j.jns.2020.116690

Liu, R., Zhou, Q., La Cava, A., Campagnolo, D. I., Van Kaer, L., and Shi, F. D. (2010). Expansion of regulatory T cells *via* IL-2/anti-IL-2 mAb complexes suppresses experimental myasthenia. *Eur. J. Immunol.* 40, 1577–1589. doi: 10.1002/eji.200939792

Logan, C. V., Cossins, J., Rodríguez Cruz, P. M., Parry, D. A., Maxwell, S., Martínez-Martínez, P., et al. (2015). Congenital myasthenic syndrome type 19 is caused by mutations in COL13A1, encoding the atypical non-fibrillar collagen type XIII α1 chain. *Am. J. Hum. Genet.* 97, 878–885. doi: 10.1016/j.ajhg.2015.10.017

Lorenzoni, P. J., Scola, R. H., Kay, C. S. K., Filla, L., Miranda, A. P. P., Pinherio, J. M. R., et al. (2013). Salbutamol therapy in congenital myasthenic syndrome due to DOK7 mutation. *J. Neurol. Sci.* 331, 155–157. doi: 10.1016/j.jns.2013.05.017

Losen, M., Stassen, M. H., Martínez-Martínez, P., Machiels, B. M., Duimel, P., Frederik, P., et al. (2005). Increased expression of rapsyn in muscle prevents acetylcholine receptor loss in experimental autoimmune myasthenia gravis. *Brain* 128, 2327–2337. doi: 10.1093/brain/awh612

Luckman, S. P., Gilhus, N. E., and Romi, F. (2011). Matrix metalloproteinase-3 in myasthenia gravis compared to other neurological disorders and healthy controls. *Autoimmune Dis.* 2011, 151258–151261. doi: 10.4061/2011/151258

Luo, Z. G., Wang, Q., Zhou, J. Z., Wang, J., Luo, Z., Liu, M., et al. (2002). Regulation of AChR clustering by Dishevelled interacting with MuSK and PAK1. *Neuron* 35, 489–505. doi: 10.1016/s0896-6273(02)00783-3

Luo, S., Zhang, B., Dong, X. P., Tao, Y., Ting, A., Zhou, Z., et al. (2008). HSP90 β regulates rapsyn turnover and subsequent AChR cluster formation and maintenance. *Neuron* 60, 97–110. doi: 10.1016/j.neuron.2008.08.013

Ma, J., Kelly, L., Ingram, J., Price, T. J., Meriney, S. D., and Dittrich, M. (2015). New insights into short-term synaptic facilitation at the frog neuromuscular junction. *J. Neurophysiol.* 113, 71–87. doi: 10.1152/jn.00198.2014

Madhavan, R., Gong, Z. L., Ma, J. J., Chan, A. W. S., and Peng, H. B. (2009). The function of cortactin in the clustering of acetylcholine receptors at the vertebrate neuromuscular junction. *PLoS One* 4:e8478. doi: 10.1371/journal.pone.0008478

Marino, M., Scuderi, F., Samengo, D., Saltelli, G., Maiuri, M. T., Shen, C., et al. (2015). Flow cytofluorimetric analysis of anti-Lrp4 (LDL receptor-related protein 4) autoantibodies in Italian patients with myasthenia gravis. *PLoS One* 10:e0135378. doi: 10.1371/journal.pone.0135378

Marx, A., Pfister, F., Schalke, B., Saruhan-Direskeneli, G., Melms, A., and Strobel, P. (2013). The different roles of the thymus in the pathogenesis of the various myasthenia gravis subtypes. *Autoimmun. Rev.* 12, 875–884. doi: 10.1016/j.autrev.2013.03.007

Maselli, R. A., Arredondo, J., Cagney, O., Ng, J. J., Anderson, J. A., Williams, C., et al. (2010). Mutations in MUSK causing congenital myasthenic syndrome impair MuSK-Dok-7 interaction. *Hum. Mol. Genet.* 19, 2370–2379. doi: 10.1093/hmg/ddq110

Maselli, R. A., Arredondo, J., Ferns, M. J., and Wollmann, R. L. (2012). Synaptic basal lamina-associated congenital myasthenic syndrome. *Ann. N Y Acad. Sci.* 1275, 36–48. doi: 10.1111/j.1749-6632.2012.06807.x

McConville, J., Farrugia, M. E., Beeson, D., Kishore, U., Metcalfe, R., Newsom-Davis, J., et al. (2004). Detection and characterization of MuSK antibodies in seronegative myasthenia gravis. *Ann. Neurol.* 55, 580–584. doi: 10.1002/ana.20061

McMacken, G. M., Spendiff, S., Whittaker, R. G., O'Connor, E., Howarth, B. M., Boczonadi, V., et al. (2019). Salbutamol modifies the neuromuscular junction in a mouse model of ColQ myasthenic syndrome. *Hum. Mol. Genet.* 28, 2339–2351. doi: 10.1093/hmg/ddz059

Messéant, J., Dobbertin, A., Girard, E., Delers, P., Manuel, M., Mangione, F., et al. (2015). MuSK Frizzled-like domain is critical for mammalian neuromuscular junction formation and maintenance. *J. Neurosci.* 35, 4926–4941. doi: 10.1523/JNEUROSCI.3381-14.2015

Messéant, J., Ezan, J., Delers, P., Glebov, K., Marchiol, C., Lager, F., et al. (2017). Wnt proteins contribute to neuromuscular junction formation through distinct signaling pathways. *Development* 144, 1712–1724. doi: 10.1242/dev.146167

Möhn, N., Beutel, G., Gutzmer, R., Ivanyi, P., Satzger, I., and Skripu, T. (2019). Neurological immune related adverse events associated with Nivolumab, Ipilimumab, and pembrolizumab therapy-review of the literature and future outlook. *J. Clin. Med.* 8:E1777. doi: 10.3390/jcm8111777

Mohseni, P., Sung, H. K., Murphy, A. J., Laliberte, C. L., Pallari, H. M., Henkelman, M., et al. (2011). Nestin is not essential for development of the CNS but required for dispersion of acetylcholine receptor clusters at the area of neuromuscular junctions. *J. Neurosci.* 31, 11547–11552. doi: 10.1523/JNEUROSCI.4396-10.2011

Molin, C. J., Westerberg, E., and Pung, A. R. (2017). Profile of upregulated inflammatory proteins in sera of myasthenia gravis patients. *Sci. Rep.* 7:39716. doi: 10.1038/srep39716

Moreth, K., Iozzo, R. V., and Schaefer, L. (2012). Small leucine-rich proteoglycans orchestrate receptor crosstalk during inflammation. *Cell Cycle* 11, 2084–2901. doi: 10.1038/srep39716

Mori, S., Kubo, S., Akiyoshi, T., Yamada, S., Miyazaki, T., Hotta, H., et al. (2012). Antibodies against muscle-specific kinase impair both presynaptic and postsynaptic functions in a murine model of myasthenia gravis. *Am. J. Pathol.* 180, 798–810. doi: 10.1016/j.ajpath.2011.10.031

Mori, S., Motohashi, N., Takashima, R., Kishi, M., Nishimune, H., and Shigemoto, K. (2017). Immunization of mice with Lrp4 induces myasthenia similar to MuSK-associated myasthenia gravis. *Exp. Neurol.* 297, 158–167. doi: 10.1016/j.expneurol.2017.08.006

Morren, J., and Li, Y. (2018). Myasthenia gravis with musk-specific tyrosine kinase antibodies: a narrative review. *Muscle Nerve* 58, 344–358. doi: 10.1002/mus.26107

Morren, J., and Li, Y. (2020). Maintenance immunosuppression in myasthenia gravis, an update. *J. Neurol. Sci.* 410:116648. doi: 10.1016/j.jns.2019.116648

Muppidi, S., Utsugisawa, K., Benatar, M., Murai, H., Barohn, R. J., Illa, I., et al. (2019). Long-term safety and efficacy of eculizumab in generalized myasthenia gravis. *Muscle Nerve* 60, 14–24. doi: 10.1002/mus.26447

Mygland, A., Tysnes, O. B., Matre, R., Volpe, P., Aarli, J. A., and Gilhus, N. E. (1992). Ryanodine receptor autoantibodies in myasthenia gravis patients with a thymoma. *Ann. Neurol.* 32, 589–591. doi: 10.1002/ana.410320419

Nadal, L., Garcia, N., Hurtado, E., Simó, A., Tomàs, M., Lanuza, M. A., et al. (2016). Presynaptic muscarinic acetylcholine autoreceptors (M1, M2 and M4 subtypes), adenosine receptors (A1 and A2A) and tropomyosin-related kinase B receptor (TrkB) modulate the developmental synapse elimination process at the neuromuscular junction. *Mol. Brain* 9:67. doi: 10.1186/s13041-016-0248-9

Nakashima, H., Ohkawara, B., Ishigaki, S., Fukudome, T., Ito, K., Tsushima, M., et al. (2016). R-spondin 2 promotes acetylcholine receptor clustering at the neuromuscular junction *via* Lgr 5. *Sci. Rep.* 6:28512. doi: 10.1038/srep28512

Nakata, R., Motomura, M., Masuda, T., Shiraishi, H., Tokuda, M., Fukuda, T., et al. (2013). Thymus histology and concomitant autoimmune diseases in Japanese patients with muscle-specific receptor tyrosine kinase-antibody-positive myasthenia gravis. *Eur. J. Neurol.* 20, 1272–1276. doi: 10.1111/ene.12169

Nastase, M. V., Young, M. F., and Schaefer, L. (2012). Biglycan: a multivalent proteoglycan providing structure and signals. *J. Histochem. Cytochem.* 60, 963–975. doi: 10.1369/0022155412456380

Nemazee, D. (2017). Mechanisms of central tolerance for B cells. *Nat. Rev. Immunol.* 17, 281–294. doi: 10.1038/nri.2017.19

Ngo, S. T., Cole, R. N., Sunn, N., Phillips, W. D., and Noakes, P. G. (2012). Neuregulin-1 potentiates agrin-induced acetylcholine receptor clustering

through muscle-specific kinase phosphorylation. *J. Cell Sci.* 125, 1531–1543. doi: 10.1242/jcs.095109

Nicole, S., Chaouch, A., Torbergsen, T., Bauché, S., de Bruyckere, E., Fontenille, M. J., et al. (2014). Agrin mutations lead to a congenital myasthenic syndrome with distal muscle weakness and atrophy. *Brain* 137, 2429–2443. doi: 10.1093/brain/awu160

Niks, E. H., Kuks, J. B., Wokke, J. H., Veldman, H., Bakker, E., Verschuuren, J. J., et al. (2010). Pre- and postsynaptic neuromuscular junction abnormalities in musk myasthenia. *Muscle Nerve* 42, 283–288. doi: 10.1002/mus.21642

Nishimune, H. (2012). Molecular mechanism of active zone organization at vertebrate neuromuscular junctions. *Mol. Neurobiol.* 45, 1–16. doi: 10.1007/s12035-011-8216-y

Nishimune, H., Valdez, G., Jarad, G., Moulson, C. L., Müller, J. H., Miner, J. H., et al. (2008). Laminins promote postsynaptic maturation by an autocrine mechanism at the neuromuscular junction. *J. Cell Biol.* 182, 1201–1215. doi: 10.1083/jcb.200805095

Ohkawara, B., Cabrera-Serrano, M., Nakata, T., Milone, M., Asai, N., Ito, K., et al. (2014). Lrp4 third β-propeller domain mutations cause novel congenital myasthenia by compromising agrin-mediated MuSK signaling in a position-specific manner. *Hum. Mol. Genet.* 23, 1856–1868. doi: 10.1093/hmg/ddt578

Okada, K., Inoue, A., Okada, M., Murata, Y., Kakuta, S., Jigami, T., et al. (2006). The muscle protein Dok-7 is essential for neuromuscular synaptogenesis. *Science* 312, 1802–1805. doi: 10.1126/science.1127142

Oliverira, L., Timóteo, M. A., and Correira-de-Sá, P. (2004). Tetanic depression is overcome by tonic adenosine A_{2A} receptor facilitation of L-type Ca^{2+} influx into rat motor nerve terminals. *J. Physiol.* 560, 157–168. doi: 10.1113/jphysiol.2004.067595

Osses, N., and Henriquez, J. P. (2015). Bone morphogenetic protein signaling in vertebrate motor neurons and neuromuscular communication. *Front. Cell. Neurosci.* 8:453. doi: 10.3389/fncel.2014.00453

Otsuka, K., Ito, M., Ohkawara, B., Masuda, A., Kawakami, Y., Sahashi, K., et al. (2015). Collagen Q and anti-MuSK autoantibody competitively suppress agrin/Lrp4/MuSK signaling. *Sci. Rep.* 5:13928. doi: 10.1038/srep13928

Pasnoor, M., Wolfe, G. I., Nations, S., Trivedi, J., Barohn, R. J., Herbelin, L., et al. (2010). Clinical findings in MuSK-antibody positive myasthenia gravis: a US experience. *Muscle Nerve* 41, 370–374. doi: 10.1002/mus.21533

Patel, T. R., Butler, G., McFarlane, A., Xie, I., Overall, C. M., and Stetefeld, J. (2012). Site specific cleavage mediated by MMPs regulates function of agrin. *PLoS One* 7:e43669. doi: 10.1371/journal.pone.0043669

Peng, H. B., Xie, H., and Dai, Z. (1997). Association of cortactin with developing neuromuscular specializations. *J. Neurocytol.* 26, 637–650. doi: 10.1023/a:1018545827369

Pevzner, A., Schoser, B., Peters, K., Cosma, N. C., Karakatsani, A., Schalke, B., et al. (2011). Anti-LRP4 autoantibodies in AChR- and MuSK-antibody-negative myasthenia gravis. *J. Neurol.* 259, 427–435. doi: 10.1007/s00415-011-6194-7

Pilgram, G. S. K., Potikanond, S., Baines, R. A., Fradkin, L. G., and Noordermeer, J. N. (2010). The roles of the dystrophin-associated glycoprotein complex at the synapse. *Mol. Neurobiol.* 41, 1–21. doi: 10.1007/s12035-009-8089-5

Plomp, J. J. (2017). Trans-synaptic homeostasis at the myasthenic neuromuscular junction. *Front. Biosci.* 22, 1033–1051. doi: 10.2741/4532

Plomp, J. J., Morsch, M., Phillips, W. D., and Verschuuren, J. J. (2015). Electrophysiological analysis of neuromuscular synaptic function in myasthenia gravis patients and animal models. *Exp. Neurol.* 270, 41–54. doi: 10.1016/j.expneurol.2015.01.007

Plomp, J. J., Van Kempen, G. T., De Baets, M. B., Graus, Y. M., Kuks, J. B., and Molenaar, P. C. (1995). Acetylcholine release in myasthenia gravis: regulation at single end-plate level. *Ann. Neurol.* 37, 627–636. doi: 10.1002/ana.410370513

Punga, A. R., Flink, R., Askmark, H., and Stalberg, E. V. (2006). Cholinergic neuromuscular hypersensitivity in patients with myasthenia gravis seropositive for MuSK antibody. *Muscle Nerve* 34, 111–115. doi: 10.1002/mus.20515

Reissner, C., Runkel, F., and Missler, M. (2013). Neurexins. *Genome Biol.* 14:213. doi: 10.1186/gb-2013-14-9-213

Remédio, L., Gribble, K. D., Lee, J. K., Kim, N., Hallock, P. T., Delestrée, N., et al. (2016). Diverging roles for Lrp4 and Wnt signaling in neuromuscular synapse development during evolution. *Genes Dev.* 30, 1058–1069. doi: 10.1101/gad.279745.116

Richman, D. P., Nishi, K., Ferns, M. J., Schnier, J., Pytel, P., Maselli, R. A., et al. (2012). Animal models of antimuscle-specific kinase myasthenia. *Ann. N Y Acad. Sci.* 1274, 140–147. doi: 10.1111/j.1749-6632.2012.06782.x

Rivner, M. H., Pasnoor, M., Dimachkie, M. M., Barohn, R. J., and Mei, L. (2018). Muscle-specific tyrosine kinase and myasthenia gravis owing to other antibodies. *Neurol. Clin.* 36, 293–310. doi: 10.1016/j.ncl.2018.01.004

Rodríguez Cruz, P. M., Al-Hajjar, M., Huda, S., Jacobson, L., Woodhall, M., Jayawant, S., et al. (2015a). Clinical features and diagnostic usefulness of antibodies to clustered acetylcholine receptors in the diagnosis of seronegative myasthenia gravis. *JAMA Neurol.* 72, 642–649. doi: 10.1001/jamaneurol.2015.0203

Rodríquez Cruz, P. M., Palace, J., Ramjattan, H., Jayawand, S., Eoff, S. A., and Beeson, D. (2015b). Salbutamol and ephedrine in the treatment of severe AChR deficiency syndromes. *Neurology* 85, 1043–1047. doi: 10.1212/wnl.0000000000001952

Rodríquez Cruz, P. M., Cossin, J., Estephan, E. P., Munell, F., Selby, K., Hirano, M., et al. (2019). The clinical spectrum of the congenital myasthenic syndrome resulting from COL13A mutations. *Brain* 142, 1547–1560. doi: 10.1093/brain/awz107

Rodríquez Cruz, P. M., Cossins, J., Cheung, J., Maxwell, S., Jayawant, S., Herbst, R., et al. (2020). Congenital myasthenic syndrome due to mutations in MuSK suggests that the level of MuSK phosphorylation is crucial for govering synaptic structure. *Hum. Mutat.* 41, 619–631. doi: 10.1002/humu.23949

Rodríguez Cruz, P. M., Palace, J., and Beeson, D. (2018). The neuromuscular junction and wide heterogeneity of congenital myasthenic syndromes. *Int. J. Mol. Sci.* 19:1677. doi: 10.3390/ijms19061677

Rogers, R. S., and Nishimune, H. (2017). The role of laminins in the organization and function of neuromuscular junctions. *Matrix Biol.* 57, 86–105. doi: 10.1016/j.matbio.2016.08.008

Romi, F. (2011). Thymoma in myasthenia gravis: from diagnosis to treatment. *Autoimmune Dis.* 2011:474512. doi: 10.4061/2011/474512

Romi, F., Aarli, J. A., and Gilhus, N. E. (2007). Myasthenia gravis patients with ryanodine receptor antibodies have distinctive clinical features. *Eur. J. Neurol.* 14, 617–620. doi: 10.1111/j.1468-1331.2007.01785.x

Romi, F., Helgeland, G., and Gilhus, N. E. (2012). Serum levels of matrix metalloproteinases: implications in clinical neurology. *Eur. Neurol.* 67, 121–128. doi: 10.1159/000334862

Rudolf, R., Khan, M. M., Labeit, S., and Deschenes, M. R. (2014). Degeneration of neuromuscular junction in age and dystrophy. *Front. Aging Neursci.* 6:99. doi: 10.3389/fnagi.2014.00099

Sahashi, K., Engel, A. G., Lambert, E. H., and Howard, F. M. Jr. (1980). Ultrastructural localization of the terminal and lytic ninth complement (C9) at the motor end-plate in myasthenia gravis. *J. Neuropathol. Exp. Neurol.* 39, 160–172. doi: 10.1097/00005072-198003000-00005

Salinas, P. C. (2005). Retrograde signalling at the synapse: a role for Wnt proteins. *Biochem. Soc. Trans.* 33, 1295–1298. doi: 10.1042/bst20051295

Samuel, M. A., Valdez, G., Tapia, J. C., Lichtman, J. W., and Sanes, J. R. (2012). Agrin and synaptic laminin are required to maintain adult neuromuscular junctions. *PLoS One* 7:e46663. doi: 10.1371/journal.pone.0046663

Santafé, M. M., Priego, M., Obis, T., Garcia, N., Tomàs, M., Lanuza, M. A., et al. (2015). Adenosine receptors and muscarinic receptors cooperate in acetylcholine release modulation in the neuromuscular synapse. *Eur. J. Neurosci.* 42, 1775–1787. doi: 10.1111/ejn.12922

Sato, K., Mano, T., Iwata, A., and Toda, T. (2019). Neurological and related adverse events in immune checkpoint inhibitors: a pharmacovigilance study from the Japanese adverse drug event report database. *J. Neurooncol.* 145, 1–9. doi: 10.1007/s11060-019-03273-1

Schmidt, N., Akaaboune, M., Gajendran, N., Martinez-Pena y Valenzuela, I., Wakefield, S., Thurnheer, R., et al. (2011). Neuregulin/ErbB regulate neuromuscular junction development by phosphorylation of α-dystrobrevin. *J. Cell Biol.* 195, 1171–1184. doi: 10.1083/jcb.201107083

Scotton, P., Bleckmann, D., Stebler, M., Sciandra, F., Brancaccio, A., Meier, T., et al. (2006). Activation of muscle-specific receptor tyrosine kinase and binding to dystroglycan are regulated by alternative mRNA splicing of agrin. *J. Biol. Chem.* 281, 36835–36845. doi: 10.1074/jbc.m607887200

Selcen, D., Ohkawara, B., Shen, X. M., McEvoy, K., Ohno, K., and Engel, A. G. (2015). Impaired synaptic development, maintenance, and neuromuscular transmission in Lrp4-related myasthenia. *JAMA Neurol.* 72, 889–896. doi: 10.1001/jamaneurol.2015.0853

Shen, C., Li, L., Zhao, K., Bai, L., Wang, A., Shu, X., et al. (2018). Motoneuron Wnts regulate neuromuscular junction development. *Elife* 7:e34625. doi: 10.7554/elife.34625

Shen, C., Lu, Y., Zhang, B., Figueiredo, D., Bean, J., Jung, J., et al. (2013). Antibodies against low-density lipoprotein receptor-related protein 4 induce myasthenia gravis. *J. Clin. Investig.* 123, 5190–5202. doi: 10.1172/JCI66039

Shi, L., Fu, A. K., and Ip, N. Y. (2012). Molecular mechanisms underlying maturation and maintenance of the vertebrate neuromuscular junction. *Trends Neurosci.* 35, 441–453. doi: 10.1016/j.tins.2012.04.005

Shin, H. Y., Park, H. J., Lee, H. E., Choi, Y. C., and Kim, S. M. (2014). Clinical and electrophysiologic responses to acetylcholinesterase inhibitors in MuSK-antibody-positive myasthenia gravis: Evidence for cholinergic neuromuscular hypersensitivity. *J. Clin. Neurol.* 10, 119–124. doi: 10.3988/jcn.2014.10.2.119

Simeone, L., Straubinger, M., Khan, M. A., Nalleweg, N., Cheusova, T., and Hashemolhosseini, S. (2010). Identification of Erbin interlinking MuSK and ErbB2 and its impact on acetylcholine receptor aggregation at the neuromuscular junction. *J. Neurosci.* 30, 6620–6634. doi: 10.1523/jneurosci.5778-09.2010

Simö, A., Just-Borràs, L., Cilleros-Mañé, V., Hurtado, E., Nadal, L., Tomàs, M., et al. (2018). BDNF-TrkB signaling coupled to nPKCε and cPKCβI modulate the phosphorylation of the exocytotic protein Munc18–1 during synaptic activity at the neuromuscular junction. *Front. Mol. Neurosci.* 11:207. doi: 10.3389/fnmol.2018.00207

Singhal, N., and Martin, P. T. (2011). Role of extracellular matrix proteins and their receptors in the development of the vertebrate neuromuscular junction. *Dev. Neurobiol.* 71, 982–1005. doi: 10.1002/dneu.20953

Sittig, L. J., Carbonetto, P., Engel, K. A., Krauss, K. S., Barrios-Camacho, C. M., and Palmer, A. A. (2016). Genetic background limits generalizability genotype-phenotype relationships. *Neuron* 91, 1253–1259. doi: 10.1016/j.neuron.2016.08.013

Skeie, G. O., Mygland, A., Treves, S., Gilhus, N. E., Aarli, J. A., and Zorzato, F. (2002). Ryanodine receptor antibodies in myasthenia gravis: epitope mapping and effect on calcium release *in vitro*. *Muscle Nerve* 27, 81–89. doi: 10.1002/mus.10294

Skriapa, L., Zisimopoulou, P., Trakas, N., Grapas, E., and Tzartos, S. J. (2014). Expression of extracellular domains of muscle specific kinase (MuSK) and use as immunoadsorbents for the development of an antigen-specific therapy. *J. Neuroimmunol.* 276, 150–158. doi: 10.1016/j.jneuroim.2014.09.013

Somnier, F. E., and Engel, P. J. (2002). The occurrence of anti-titin antibodies and thymomas: a population survey of MG 1970–1999. *Neurology* 59, 92–98. doi: 10.1212/wnl.59.1.92

Song, J. S., Kim, D., Kwon, J. H., Kim, H. R., Choi, C. M., and Jang, S. J. (2019). Clinicopathologic significance and immunogenomic analysis of programmed death-ligand 1 (PD-L1) and programmed death 1 (PD-1) expression in thymic epithelial tumors. *Front. Oncol.* 9:1055. doi: 10.3389/fonc.2019.01055

Sons, M. S., Busche, N., Strenzke, N., Moser, T., Ernsberger, U., Mooren, F. C., et al. (2006). α-Neurexions are required for efficient transmitter release and synaptic homeostasis at the mouse neuromuscular junction. *Neuroscience* 138, 433–446. doi: 10.1016/j.neuroscience.2005.11.040

Stamatakou, E., and Salinas, P. C. (2014). Postsynaptic assembly: a role for Wnt signaling. *Dev. Neurobiol.* 74, 818–827. doi: 10.1002/dneu.22138

Stanga, S., Zanou, N., Audouard, E. T., Tasiaux, B., Contino, S., Vandermeulen, G., et al. (2016). APTT-dependent glial cell line-derived neurotrophic gactor gene expression drives neuromuscular junction. *FASEB J.* 30, 1696–1711. doi: 10.1096/fj.15-278739

Stergiou, C., Lazaridis, K., Zouvelou, V., Tzartos, J., Mantegazza, R., Antozzi, C., et al. (2016). Titin antibodies in "seronegative" myasthenia gravis-A new role for an old antigen. *J. Neuroimmunol.* 292, 108–115. doi: 10.1016/j.jneuroim.2016.01.018

Stetefeld, J., Alexandrescu, A. T., Maciejewski, M. W., Jenny, M., Rathgeb-szabo, K., Schulthess, T., et al. (2004). Modulation of agrin function by alternative splicing and Ca^{2+} binding. *Structure* 12, 503–515. doi: 10.1016/j.str.2004.02.001

Stiegler, A. L., Burden, S. J., and Hubbard, S. R. (2006). Crystal structure of the agrin-responsive immunoglobulin-like domains 1 and 2 of the receptor tyrosine kinase MuSK. *J. Mol. Biol.* 364, 424–433. doi: 10.1016/j.jmb.2006.09.019

Stiegler, A. L., Burden, S. J., and Hubbard, S. R. (2009). Crystal structure of the Frizzled-like cycteine-rich domain of the receptor tyrosine kinase MuSK. *J. Mol. Biol.* 393, 1–9. doi: 10.1016/j.jmb.2009.07.091

Strochlic, L., Falk, J., Goillot, E., Sigoillot, S., Bourgeois, F., Delers, P., et al. (2012). Wnt4 participates in the formation of vertebrate neuromuscular junction. *PLoS One* 7:e29976. doi: 10.1371/journal.pone.0029976

Südhof, T. C. (2012). The presynaptic active zone. *Neuron* 75, 11–25. doi: 10.1016/j.neuron.2012.06.012

Sudres, M., Verdier, J., Truffault, F., Le Panse, R., and Berrih-Aknin, S. (2018). Pathophyusiological mechanisms of autoimmunity. *Ann. N Y Acad. Sci.* 1413, 59–68. doi: 10.1111/nyas.13560

Takamori, M. (2008a). Lambert-Eaton myasthenic syndrome: search for alternative autoimmune targets and possible compensatory mechanisms based on presynaptic calcium homeostasis. *J. Neuroimmunol.* 201–202, 145–152. doi: 10.1016/j.jneuroim.2008.04.040

Takamori, M. (2008b). Autoantibodies against TRPC3 and ryanodine receptor in myasthenia gravis. *J. Neuroimmunol.* 200, 142–144. doi: 10.1016/j.jneuroim.2008.06.001

Takamori, M. (2012). Structure of the neuromuscular junction: function and cooperative mechanisms in the synapse. *Ann. N Y Acad. Sci.* 1274, 14–23. doi: 10.1111/j.1749-6632.2012.06784.x

Takamori, M. (2013). Structural and pathogenic mechanisms centered on muscle-specific tyrosine kinase in autoimmune neuromuscular junction disorders. *Curr. Immunol. Rev.* 9, 207–213. doi: 10.2174/1573395510666140318003732

Takamori, M. (2017a). Synaptic homeostasis and its immunological disturbance in neuromuscular junction disorders. *Int. J. Mol. Sci.* 18:E896. doi: 10.3390/ijms18040896

Takamori, M. (2017b). Pathogenic participation of MuSK-biglycan linkage contributive to synaptic stability and signaling in myasthenia gravis. *J. Autoimmun. Disord.* 3, 41–48. doi: 10.21767/2471-8513

Takamori, M. (2019). Synaptic compensatory mechanism and its impairment in autoimmune myasthenic diseases. *J. Immunol. Sci.* 3, 6–13. doi: 10.29245/2578-3009/2019/3.1173

Takamori, M., Motomura, M., Fukudome, T., and Yoshikawa, H. (2007). Autoantibodies against M1 muscarinic acetylcholine receptor in myasthenic disorders. *Eur. J. Neurol.* 14, 1230–1235. doi: 10.1111/j.1468-1331.2007.01931.x

Takamori, M., Motomura, M., Kawaguchi, N., Nemoto, Y., Hattori, T., Yoshikawa, H., et al. (2004). Anti-ryanodine receptor antibodies and FK506 in myasthenia gravis. *Neurology* 62, 1894–1896. doi: 10.1212/01.wnl.0000125254.99397.68

Takamori, M., Nakamura, T., and Motomura, M. (2013). Antibodies against Wnt receptor of muscle-specific tyrosine kinase in myasthenia gravis. *J. Neuroimmunol.* 254, 183–186. doi: 10.1016/j.jneuroim.2012.09.001

Takamori, M., Okumura, S., Nagata, M., and Yoshikawa, H. (1988). Myasthenogenic significance of synthetic α-subunit peptide 183–200 of Torpedo californica and human acetylcholine receptor. *J. Neurol. Sci.* 85, 121–129. doi: 10.1016/0022-510x(88)90150-5

Takamori, M., Sakato, S., and Okumura, S. (1984). Presynaptic function modified by acetylcholine-receptor interaction in experimental autoimmune myasthenia gravis. *J. Neurol. Sci.* 66, 245–253. doi: 10.1016/0022-510x(84)90013-3

Takata, K., Stathopoulos, P., Cao, M., Mané-Damas, M., Fichtner, M. L., Benotti, E. S., et al. (2019). Characterization of pathogenic monoclonal autoantibodies derived from muscle-specific kinase myasthenia gravis patients. *JCI Insight* 4:e127167. doi: 10.1172/jci.insight.127167

Tandan, R., Hehir, M. K. II., Waheed, W., and Howard, D. B. (2017). Rituximab treatment of myasthenia gravis: a systematic review. *Muscle Nerve* 56, 185–196. doi: 10.1002/mus.25597

Tezuka, T., Inoue, A., Hoshi, T., Wheatherbee, S. D., Burgees, R. W., Ueta, R., et al. (2014). The MuSK activator agrin has a separate role essential for postnatal

maintenance of neuromuscular synapses. *Proc. Natl. Acad. Sci. U S A* 111, 16556–16561. doi: 10.1073/pnas.1408409111

Thiruppathi, M., Rowin, J., Ganesh, B., Sheng, J. R., Prabbakar, B. S., and Meriggioli, M. N. (2012). Impaired regulatory function in circulating $CD4^{+}CD25^{high}CD127^{low/-}$ T cells in patients with myasthenia gravis. *Clin. Immunol.* 145, 209–223. doi: 10.1016/j.clim.2012.09.012

Tomàs, J., Gracia, N., Lanuza, M. A., Santafé, M. M., Tomàs, M., Nodal, L., et al. (2018). Adenosine receptors in developing and adult mouse neuromuscular junctions and functional links with other metabotrophic receptor pathways. *Front. Pharmacol.* 9:397. doi: 10.3389/fphar.2018.00397

Tomoyasu, H., Kikuchi, A., and Kamo, I. (1998). Identification of haemopoietic biglycan in hyperplastic thymus associated with myasthenia gravis. *J. Neuroimmunol.* 89, 59–63. doi: 10.1016/s0165-5728(98)00092-7

Tu, H., Pirskanen-Matell, R., Heikkinen, A., Oikarainen, T., Risteli, J., and Pihlajaniemi, T. (2018). Autoimmune antibodies to collagen XIII in myasthenia gravis patients. *Muscle Nerve* 57, 506–510. doi: 10.1002/mus.25969

Tüzün, E., and Christadoss, P. (2013). Complement associated pathogenic mechanisms in myasthenia gravis. *Autoimmun. Res.* 12, 904–911. doi: 10.1016/j.autrev.2013.03.003

Tzartos, S. J., Kokla, A., Walgrave, S. L., and Conti-Tronconi, B. M. (1988). Localization of the main immunogenic region of human muscle acetylcholine receptor to residues 67–76 of the α subunit. *Proc. Natl. Acad. Sci. U S A* 85, 2899–2903. doi: 10.1073/pnas.85.9.2899

Tzartos, S. J., Seybold, M. E., and Lindstrom, J. M. (1982). Specificities of antibodies to acetylcholine receptors in sera from myasthenia gravis patients measured by monoclonal antibodies. *Proc. Natl. Acad. Sci. U S A* 79, 188–192. doi: 10.1073/pnas.79.1.188

Ulrichts, P., Guglietta, A., Dreier, T., van Bragt, T., Hanssens, V., Hofman, E., et al. (2018). Neonatal Fc receptor antagonist Efgartigimod safely and sustainably reduces IgGs in humans. *J. Clin. Invest.* 128, 4372–4386. doi: 10.1172/JCI97911

Ulusoy, C., Cavus, F., Yilmaz, V., and Tuzűn, E. (2017). Immunization with recombinantly expressed LRP4 induces experimental autoimmune myasthenia gravis in C57BL/6 mice. *Immunol. Invest.* 46, 490–499. doi: 10.1080/08820139.2017.1299754

Vanhaesebrouck, A. E., and Beeson, D. (2019). The congenital myasthenic syndromes: expanding genetic and phenotypic spectrums and refining treatment strategies. *Curr. Opin. Neurol.* 32, 696–703. doi: 10.1097/wco.0000000000000736

Vanhaesebrouck, A. E., Webster, R., Maxwell, S., Rodriquez Cruz, P. M., Cossins, J., Wickens, J., et al. (2019). β2-Adrenergic receptor agonists ameliorate the adverse effect of long-term pyridostigmine on neuromuscular junction structure. *Brain* 142, 3713–3727. doi: 10.1093/brain/awz322

Verschuuren, J. J. G. M., Huijbers, M. G., Plomp, J. J., Niks, E. H., Molenaar, P. C., Martinez-Martinez, P., et al. (2013). Pathophysiology of myasthenia gravis with antibodies to the acetylcholine receptor, muscle-specific kinase and low-density lipoprotein receptor-related protein 4. *Autoimmun. Rev.* 12, 918–923. doi: 10.1016/j.autrev.2013.03.001

Viegas, S., Jacobson, L., Waters, P., Cossins, J., Jacob, S., Leite, M. I., et al. (2012). Passive and active immunization models of MuSK-ab positive myasthenia: electrophysiological evidence for pre and postsynaptic defects. *Exp. Neurol.* 234, 506–512. doi: 10.1016/j.expneurol.2012.01.025

Vieira, G. C., Chockalingam, S., Melegh, Z., Greenhough, A., Malik, S., Szemes, M., et al. (2015). LGR5 regulates pro-survival MEK/ERK and proliferative Wnt/β-catenin signaling in neuroblastoma. *Oncotarget* 6, 40053–40067. doi: 10.18632/oncotarget.5548

Villegas, J. A., Van Wassenhove, J., Le Panse, R., Berrih-Aknin, S., and Dragin, N. (2018). An imbalance between regulatory T cells and T helper 17 cells in acetylcholine receptor-positive myasthenia gravis pateints. *Ann. N Y Acad. Sci.* 1413, 154–162. doi: 10.1111/nyas.13591

Vincent, A., Huda, S., Cao, M., Cetin, H., Koneczny, I., Rodriguez Cruz, P. M., et al. (2018). Serological and experimental studies in different forms of myasthenia gravis. *Ann. N Y Acad. Sci.* 1413, 143–153. doi: 10.1111/nyas.13592

Vincent, A., and Newsom-Davis, J. (1980). Anti-acetylcholine receptor antibodies. *J. Neurol. Neurosurg. Psychiatry* 43, 590–600. doi: 10.1136/jnnp.43.7.590

Vincent, A., Waters, P., Leite, M. I., Jacobson, L., Koneczny, I., Cossins, J., et al. (2012). Antibodies identified by cell-based assays in myasthenia gravis and associated diseases. *Ann. N Y Acad. Sci.* 1274, 92–98. doi: 10.1111/j.1749-6632.2012.06789.x

Vrolix, K., Niks, E. H., Le Panse, R., van Ostaijen-Ten Dam, M. M., Murin, A. H., Jol-van der Zijde, C. M., et al. (2011). Reduced thymic expression of ErbB receptors without auto-antibodies against synaptic ErbB in myasthenia gravis. *J. Neuroimmunol.* 232, 158–165. doi: 10.1016/j.jneuroim.2010.10.024

Wang, J., Ruan, N. J., Qian, L., Lei, W. L., Chen, F., and Luo, Z. G. (2008). Wnt/β-catenin signaling suppresses rapsyn expression and inhibits acetylcholine receptor clustering at the neuromuscular junction. *J. Biol. Chem.* 283, 21668–21675. doi: 10.1074/jbc.m709939200

Wang, X., Pinter, M. J., and Rich, M. M. (2016). Reversible recruitment of a homeostatic reserve pool of synaptic vesicles underlies rapid homeostatic plasticity of quantal content. *J. Neurosci.* 36, 828–836. doi: 10.1523/jneurosci.3786-15.2016

Wang, Z., Wang, B., Yang, L., Guo, Q., Aithmitti, N., Songyang, Z., et al. (2009). Presynaptic and postsynaptic interaction of the amyloid precursor protein promotes peripheral and central synaptogenesis. *J. Neurosci.* 29, 10788–10801. doi: 10.1523/jneurosci.2132-09.2009

Weatherbee, S. D., Anderson, K. V., and Niswander, L. A. (2006). LDL-receptor-related protein 4 is critical for formation of the neuromuscular junction. *Development* 133, 4993–5000. doi: 10.1242/dev.02696

Wen, Y., Yang, B., Lu, J., Zhang, J., Yang, H., and Li, J. (2016). Imbalance of circulating $CD^{+}CXCR5^{+}FOXP3^{+}$ Tfr-like cells and $CD^{+}CXCR5^{+}FOXP3^{-}$ Tfh-like cells in myasthenia gravis. *Neurosci. Lett.* 630, 176–182. doi: 10.1016/j.neulet.2016.07.049

Werle, M. J., and VanSaun, M. (2003). Activity dependent removal of agrin from synaptic basal lamina by matrix metalloproteinase 3. *J. Neurocytol.* 32, 905–915. doi: 10.1023/b:neur.0000020631.69804.f5

Wolfe, G. I., Kaminski, H. J., Aban, I. B., Minisman, G., Kuo, H. C., Marx, A., et al. (2019). Long-term effect of thymectomy plus prednisone versus prednisone alone in patients with non-thymomatous myasthenia gravis: 2-year extension of MGTX randmised trial. *Lancet Neurol.* 18, 259–268. doi: 10.1016/S1474-4422(18)30392-2

Wu, H., Barik, A., Lu, Y., Shen, C., Bowman, A., Li, L., et al. (2015). Slit2 as a β-catenin/Ctnnb1-dependent retrograde signal for presynaptic differentiation. *Elife* 4:e07266. doi: 10.7554/elife.07266

Wu, H., Lu, Y., Barik, A., Joseph, A., Taketo, M. M., Xiong, W. C., et al. (2012a). β-catenin gain of function in muscles impairs neuromuscular junction formation. *Development* 139, 2392–2404. doi: 10.1242/dev.080705

Wu, H., Lu, Y., Shen, C., Patel, N., Gan, L., Xiong, W. C., et al. (2012b). Distict roles of muscle and motoneuron Lrp4 in neuromuscular junction formation. *Neuron* 75, 94–107. doi: 10.1016/j.neuron.2012.04.033

Wu, H., Xiong, W. C., and Mei, L. (2010). To bild a synapse: signaling pathways in neuromuscular junction assembly. *Development* 137, 1017–1033. doi: 10.1242/dev.038711

Xing, G., Xiong, W. C., and Mei, L. (2020). Rapsyn as a signaling and scaffolding molecule in NMJ formation and maintenance. *Neurosci. Lett.* 135013. doi: 10.1016/j.neulet.2020.135013

Yamada, M., and Sekiguchi, K. (2015). Molecular basis of laminin-integrin interactions. *Curr. Top. Membr.* 76, 197–229. doi: 10.1016/bs.ctm.2015.07.002

Yan, M., Liu, Z., Fei, E., Chen, W., Lai, X., Luo, B., et al. (2018a). Induction of anti-agrin antibodies causes myasthenia gravis in mice. *Neuroscience* 373, 113–121. doi: 10.1016/j.neuroscience.2018.01.015

Yan, M., Xin, G. L., Xiong, W. C., and Mei, L. (2018b). Agrin and Lrp4 antibodies as new biomarkers of myasthenia gravis. *Ann. N Y Acad. Sci.* 1413, 126–135. doi: 10.1111/nyas.13573

Yang, J., Dominguez, B., de Winter, F., Gould, T. W., Eriksson, J. E., and Lee, K. F. (2011). Nestin negatively regulates postsynaptic differentiation of the neuromuscular synapse. *Nat. Neurosci.* 14, 324–330. doi: 10.1038/nn.2747

Yi, J. S., Guptill, J. T., Stathopoulos, P., Nowak, R. J., and O'Connor, K. C. (2018). B cells in the pathophysiology of myasthenia gravis. *Muscle Nerve* 57, 172–184. doi: 10.1002/mus.25973

Yilmaz, A., Kattamuri, C., Ozdeslik, R. N., Schmiedel, C., Mentzer, S., Schorl, C., et al. (2016). MuSK is a BMP co-receptor that shapes BMP responses and calcium signaling in muscle cells. *Sci. Signal.* 9:ra87. doi: 10.1126/scisignal.aaf0890

Yumoto, N., Kim, N., and Burden, S. J. (2012). Lrp4 is a retrograde signal for presynaptic differentiation at neuromuscular synapses. *Nature* 489, 438–442. doi: 10.1038/nature11348

Yurchenco, P. D. (2011). Basement membranes: Cell scaffoldings and signaling platforms. *Cold Spring Harb. Perspect. Biol.* 3:e004911. doi: 10.1101/cshperspect.a004911

Zhang, W., Coldefy, A. S., Hubbard, S. R., and Burden, S. J. (2011). Agrin binds to the N-terminal region of Lrp4 protein and stimulates association between Lrp4 and the first immunoglobulin-like domain in muscle-specific kinase (MuSK). *J. Biol. Chem.* 286, 40624–40630. doi: 10.1074/jbc.m111.279307

Zhang, B., Liang, C., Bates, R., Yin, Y., Xiong, W. C., and Mei, L. (2012a). Wnt proteins regulate acetylcholine receptor clustering in muscle cells. *Mol. Brain* 5:7. doi: 10.1186/1756-6606-5-7

Zhang, B., Tzartos, J. S., Belimezi, M., Ragheb, S., Bealmear, B., Lewis, R. A., et al. (2012b). Autoantibodies to lipoprotein-related protein 4 in patients with double-seronegative myasthenia gravis. *Arch. Neurol.* 69, 445–451. doi: 10.1001/archneurol.2011.2393

Zhang, B., Luo, S., Dong, X. P., Zhang, X., Liu, C., Luo, Z., et al. (2007). β-catenin regulates acetylcholine receptor clustering in muscle cells through interaction with rapsyn. *J. Neurosci.* 27, 3968–3973. doi: 10.1523/JNEUROSCI.4691-06.2007

Zhang, B., Luo, S., Wang, Q., Suzuki, T., Xiong, W. C., and Mei, L. (2008). Lrp4 serves as a coreceptor of agrin. *Neuron* 60, 285–297. doi: 10.1016/j.neuron.2008.10.006

Zhang, B., Shen, C., Bealmear, B., Ragheb, S., Xiong, W. C., Lewis, R. A., et al. (2014). Autoantibodies to agrin in myasthenia gravis patients. *PLoS One* 9:e91816. doi: 10.1371/journal.pone.0091816

Zhang, B. G., Quigley, A. F., Bourke, J. L., Nowell, C. J., Myers, D. E., Choong, P. F., et al. (2015). Combination of agrin and laminin increase acetylcholine receptor clustering and enhance functional neuromuscular junction formation *in vitro*. *Dev. Neurobiol.* 76, 551–565. doi: 10.1002/dneu.22331

Zhao, K., Shen, C., Lu, Y., Huang, Z., Li, L., Rand, C. D., et al. (2017). Muscle Yap is a regulator of neuromuscular junction formation and regeneration. *J. Neurosci.* 37, 3465–3477. doi: 10.1523/NEUROSCI.2934-16.2017

Zisimopoulou, P., Evangelakou, P., Tzartos, J., Lazaridis, K., Zouvelou, V., Mantegazza, R., et al. (2014). A comprehensive analysis of the epidemiology and clinical characteristics of anti-Lrp4 in myasthenia gravis. *J. Autoimmun.* 52, 139–145. doi: 10.1016/j.jaut.2013.12.004

Zoltowska Katarzyna, M., Belaya, K., Leite, M., Patrick, W., Vincent, A., and Beeson, D. (2015). Collagen Q-a potential target for autoantibodies in myasthenia gravis. *J. Neurol. Sci.* 348, 241–244. doi: 10.1016/j.jns.2014.12.015

Zong, Y., and Jin, R. (2013). Structural mechanisms of the agrin-Lrp4-MuSK signaling pathway in neuromuscular junction differentiation. *Cell. Mol. Life Sci.* 70, 3077–3088. doi: 10.1007/s00018-012-1209-9

Zong, Y., Zhang, B., Gu, S., Lee, K., Zhou, J., Yao, G., et al. (2012). Structural basis of agrin-Lrp4-MuSK signaling. *Genes Dev.* 26, 247–258. doi: 10.1101/gad.180885.111

Zouvelou, V., Zisimopoulou, P., Rentzos, M., Karandreas, N., Evangelakou, P., Stramboulis, E., et al. (2013). Double seronegative myasthenia gravis with anti-LRP4 antibodies. *Neuromuscul. Disord.* 23, 568–570. doi: 10.1016/j.nmd.2013.03.013

Zuber, B., and Unwin, N. (2013). Structure and superorganization of acetylcholine receptor-rapsyn complexes. *Proc. Natl. Acad. Sci. U S A* 110, 10622–10627. doi: 10.1073/pnas.1301277110

Zuercher, A. W., Spring, R., Baz Morelli, A., Rowe, T., and Kasemann, F. (2019). Next-generation Fc receptor-targeting biologics for autoimmune diseases. *Autoimmun. Rev.* 18:102366. doi: 10.1016/j.autrev.2019.102366

Conflict of Interest: The author declares that the research was conducted in the absence of any commercial or financial relationships that could be construed as a potential conflict of interest.

Copyright © 2020 Takamori. This is an open-access article distributed under the terms of the Creative Commons Attribution License (CC BY). The use, distribution or reproduction in other forums is permitted, provided the original author(s) and the copyright owner(s) are credited and that the original publication in this journal is cited, in accordance with accepted academic practice. No use, distribution or reproduction is permitted which does not comply with these terms.

frontiers in Molecular Neuroscience

ORIGINAL RESEARCH
published: 10 June 2020
doi: 10.3389/fnmol.2020.00104

Arhgef5 Binds α-Dystrobrevin 1 and Regulates Neuromuscular Junction Integrity

Krzysztof M. Bernadzki[1], Patrycja Daszczuk[1], Katarzyna O. Rojek[1,2], Marcin Pęziński[1], Marta Gawor[1], Bhola S. Pradhan[1], Teresa de Cicco[1], Monika Bijata[3], Krystian Bijata[3], Jakub Włodarczyk[3], Tomasz J. Prószyński[1,4] and Paweł Niewiadomski[1,5]**

[1] Laboratory of Synaptogenesis, Nencki Institute of Experimental Biology, Warsaw, Poland, [2] Institute of Physical Chemistry, Polish Academy of Sciences, Warsaw, Poland, [3] Laboratory of Cell Biophysics, Nencki Institute of Experimental Biology, Warsaw, Poland, [4] Łukasiewicz Research Network – PORT Polish Center for Technology Development, Wrocław, Poland, [5] Laboratory of Molecular and Cellular Signaling, Centre of New Technologies, University of Warsaw, Warsaw, Poland

The neuromuscular junctions (NMJs) connect muscle fibers with motor neurons and enable the coordinated contraction of skeletal muscles. The dystrophin-associated glycoprotein complex (DGC) is an essential component of the postsynaptic machinery of the NMJ and is important for the maintenance of NMJ structural integrity. To identify novel proteins that are important for NMJ organization, we performed a mass spectrometry-based screen for interactors of α-dystrobrevin 1 (aDB1), one of the components of the DGC. The guanidine nucleotide exchange factor (GEF) Arhgef5 was found to be one of the aDB1 binding partners that is recruited to Tyr-713 in a phospho-dependent manner. We show here that Arhgef5 localizes to the NMJ and that its genetic depletion in the muscle causes the fragmentation of the synapses in conditional knockout mice. Arhgef5 loss *in vivo* is associated with a reduction in the levels of active GTP-bound RhoA and Cdc42 GTPases, highlighting the importance of actin dynamics regulation for the maintenance of NMJ integrity.

Keywords: neuromuscular junction, dystrophin-glycoprotein complex, Arhgef5, Rho GEFs, Rho-family GTPases, muscle development, neuromuscular disease

OPEN ACCESS

Edited by:
Laure Strochlic, Institut National de la Santé et de la Recherche Médicale (INSERM), France

Reviewed by:
Mohammed Akaaboune, The University of Michigan, United States
Rüdiger Rudolf, Mannheim University of Applied Sciences, Germany
Claire Legay, Université Paris Descartes, France

****Correspondence:***
Tomasz J. Prószyński
tomasz.proszynski@port.org.pl
Paweł Niewiadomski
p.niewiadomski@cent.uw.edu.pl

Received: *27 February 2020*
Accepted: *13 May 2020*
Published: *10 June 2020*

Citation:
Bernadzki KM, Daszczuk P, Rojek KO, Pęziński M, Gawor M, Pradhan BS, de Cicco T, Bijata M, Bijata K, Włodarczyk J, Prószyński TJ and Niewiadomski P (2020) Arhgef5 Binds α-Dystrobrevin 1 and Regulates Neuromuscular Junction Integrity. Front. Mol. Neurosci. 13:104. doi: 10.3389/fnmol.2020.00104

INTRODUCTION

The neuromuscular junction (NMJ) is an essential interface between the central nervous system and a skeletal muscle fiber. It consists of the presynaptic axonal terminals, terminal Schwann cells that play a role in its maintenance and regeneration, and the postsynaptic machinery localized on the surface of the myofiber. The postsynaptic part of the NMJ is composed of an intricate array of protein complexes that facilitate high concentration of neurotransmitter receptors for acetylcholine (AChR) and allows for generation of muscle action potential. The postsynaptic machinery is linked to the extracellular matrix through membrane-embedded receptors. Many components of the postsynaptic apparatus provide a platform for the recruitment of the intracellular signal transduction machinery. Others anchor the NMJ to the cytoskeletal scaffold, and particularly to the F-actin network.

During postnatal development, the postsynaptic part of the NMJ is transformed from a simple plaque-like form into an elaborate, branched structure that resembles a pretzel. The molecular basis underlying this transformation is poorly understood. Studies on *in vitro* models (cultured

muscle cells) suggested that the remodeling of the postsynaptic machinery is accomplished through actin-based organelles known as podosomes (Proszynski et al., 2009; Proszynski and Sanes, 2013; Bernadzki et al., 2014), which create gaps between AChR-rich areas. In cultured myotubes, the inhibition of podosome formation leads to altered distribution of AChR receptors in postsynaptic clusters (Proszynski et al., 2009). However, the function of podosomes in NMJ development *in vivo* has not been elucidated.

Apart from podosomes, the actin cytoskeleton is important for the formation and maintenance of postsynaptic AChR assemblies. AChR are anchored to F-actin (Mitsui et al., 2000) and actin dynamics drives AChR trafficking and clustering (Dai et al., 2000; Lee et al., 2009). Specifically, the regulation of actin cytoskeleton by Rho family GTPases appears to be involved in postsynaptic AChR clustering (Luo et al., 2002; Weston et al., 2003; Shi et al., 2010). The mechanisms of recruitment and regulation of Rho GTPases at the NMJ are poorly understood.

The dystrophin-glycoprotein complex (DGC) is a major muscle receptor for extracellular laminins and an important component of the postsynaptic NMJ machinery (Ervasti and Campbell, 1991; Nishimune et al., 2008; Gawor and Prószyński, 2018). The core of the DGC complex consist of dystrophin, syntrophin, α-dystroglycan, β-dystroglycan, the sarcoglycan complex, sarcospan, and α-dystrobrevin (Nakamori and Takahashi, 2011; Aittaleb et al., 2017; Belhasan and Akaaboune, 2020). The dysfunction of the DGC core components leads to myopathies in humans, including Duchenne muscular dystrophy, a disease characterized by progressive damage and impaired regeneration of skeletal muscles (Campbell, 1995). DGC core components can recruit additional, peripherally associated proteins. For instance the cytoplasmic protein α-dystrobrevin 1 (aDB1) is believed to be an adaptor for recruitment of various signaling molecules (Oh et al., 2012; Gingras et al., 2016; Gawor and Prószyński, 2018). The loss of aDB1 in mice results in abnormal NMJ morphology and impaired maturation of the postsynaptic apparatus (Grady et al., 2003, 2000, 1999). In humans, aDB1 mutations cause congenital heart disease with left ventricular non-compaction (Ichida et al., 2001). The function of aDB1 is dependent at least in part on its phosphorylation by tyrosine kinases (Grady et al., 2003; Schmidt et al., 2011; Gingras et al., 2016). To identify the mechanisms of the regulation of NMJ maturation by aDB1, we have previously searched for proteins that interact with aDB1 in a phosphorylation-dependent manner using a protein pull-down assay followed by mass spectrometry (Gingras et al., 2016). One of the proteins that we thus identified as an aDB1 interactor was Arhgef5. Arhgef5 is a guanidine nucleotide exchange factor (GEF) for the small GTPases from the Rho family and is involved in the regulation of actin dynamics (Xie et al., 2005). Interestingly, Arhgef5, which also interacts with another aDB1-binding protein α-catulin (Lyssand et al., 2010; Gingras et al., 2016) was shown to be pivotal for the Src-dependent formation of podosomes (Kuroiwa et al., 2011). We therefore hypothesized that Arhgef5 may cooperate with aDB1 and α-catulin to regulate the maturation and stability of the NMJ postsynaptic machinery by altering the dynamics of the actin cytoskeleton via Rho-family GTPases. Here, we show that Arhgef5 localizes at the NMJ *in vivo* and concentrates at the postsynaptic machinery. Loss of Arhgef5 in mouse skeletal muscles results in NMJ defects characterized by increased fragmentation of the postsynaptic apparatus, an effect that may be attributed to the abnormal function of the GTPases RhoA and Cdc42.

RESULTS

Arhgef5 Binds to Phosphorylated aDB1s

Arhgef5 was originally identified in our unbiased mass spectrometry-based screen for interaction partners of the phosphorylated form of aDB1. Arhgef5 was one of the top proteins from myotube extracts that specifically bind the aDB1-derived phosphopeptide TQPEDGN**pY**ENESVRQ (Y713-P; corresponding to phosphorylated tyrosine 713 of aDB1) but not to its unphosphorylated control peptide TQPEDGN**Y**ENESVRQ (Y713) (**Figure 1A**). Arhgef5 has a typical domain structure of Rho GEFs: it contains a Dbl homology (DH), a pleckstrin homology (PH), and a Src homology 3 (SH3) domain (**Figure 1B**). Additionally, it contains an N-terminal domain that has several proline-rich motifs (Kuroiwa et al., 2011). In humans, in addition to the full-length protein, a shorter isoform called TIM lacking the N-terminal domain is expressed, but this isoform has not been identified in mice. Using western blot, we confirmed that the C-terminal domain of Arhgef5 binds the Y713-P, but not the Y713 peptide (**Figure 1C**). We also independently showed that full-length Arhgef5 binds to full-length aDB1, as evidenced by co-immunoprecipitation of overexpressed proteins (**Figures 1D,E**).

Arhgef5 Localizes to AChR-Rich Domains of the Neuromuscular Junction

α-dystrobrevin 1 and its phosphorylated form pY713-aDB1 concentrate in AChR-rich regions at the NMJ postsynaptic machinery (Grady et al., 2003; Gingras et al., 2016). We thus expected that Arhgef5 localizes in the same regions. Indeed, endogenous Arhgef5 colocalizes with AChR on the tibialis anterior (TA) muscle cross-sections (**Figure 2A**). To confirm independently that Arhgef5 is a novel synaptic protein, we electroporated muscles with plasmids expressing GFP-tagged Arhgef5 constructs. Both the longer and the shorter C-terminal isoform of Arhgef5 were enriched at the muscle postsynaptic machinery (**Figures 2B,C**). In contrast, overexpressed GFP (used as a control) did not concentrate at the NMJ (**Figure 2D**).

Arhgef5 Loss Does Not Block AChR Cluster Formation in Cultured Myotubes

Arhgef5 is an important regulator of podosome formation in MDCK and NIH/3T3 cells (Kuroiwa et al., 2011). Podosomes contribute to the formation of complex pretzel-like structures of the postsynaptic machinery in cultured myotubes (Proszynski et al., 2009), and aDB1-depleted myotubes fail to form complex AChR clusters (Pawlikowski and Maimone, 2009; Gingras et al., 2016). Accordingly, we predicted that inhibition of Arhgef5

A

Protein symbol	MS/MS Spectra detected		Coverage (%)
	peptide 713	peptide 713-P	
Grb2	0	57	48.8
Arhgef5	0	23	30.8

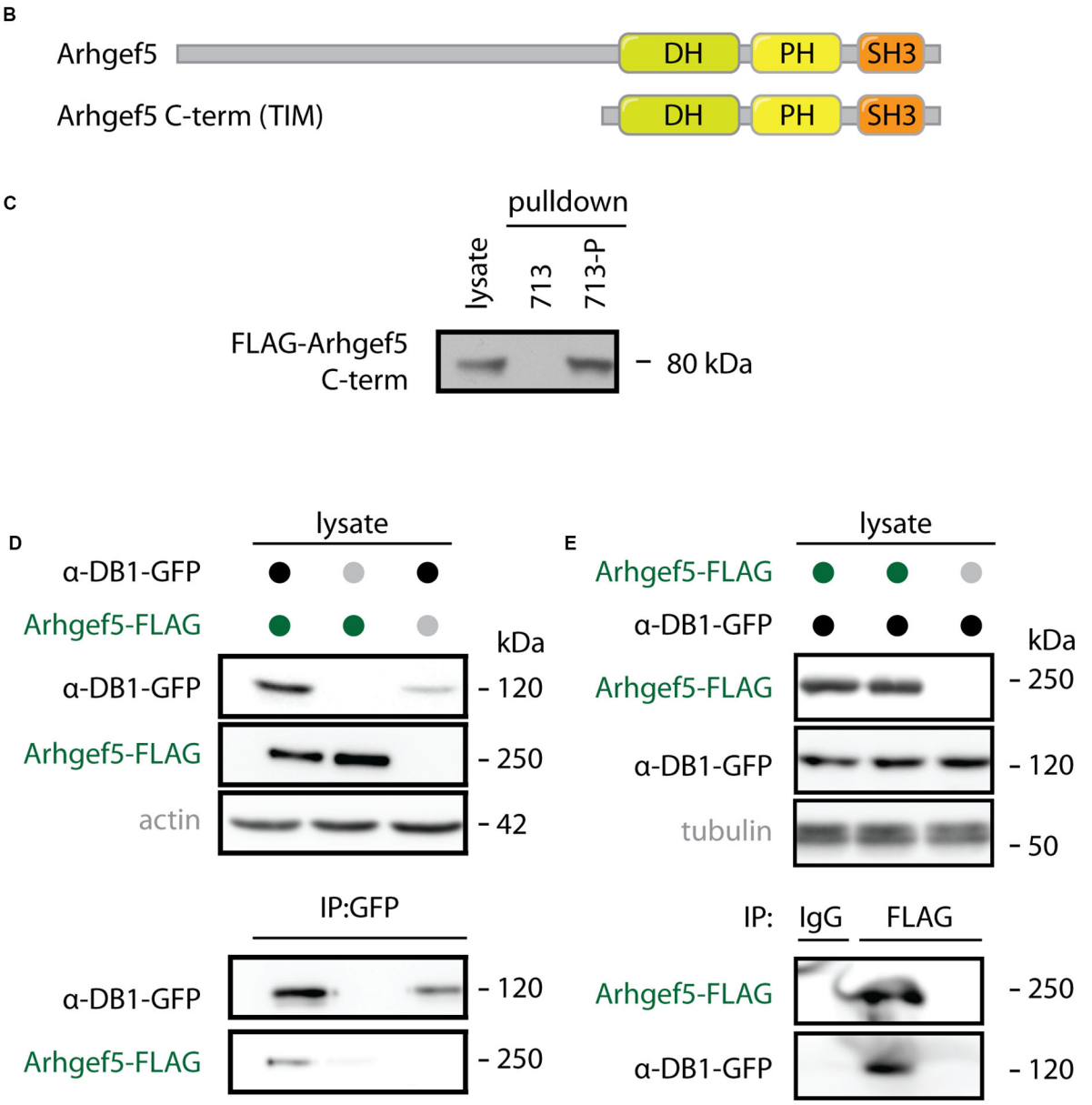

FIGURE 1 | Arhgef5 binds to aDB1. **(A)** Lysates from C2C12 cells were incubated with beads coupled to either the unphosphorylated (713) or the phosphorylated (713-P) variant of aDB1 peptide containing the Y713 residue. Eluates from the beads were analyzed using mass spectrometry. Number of peptides from Grb2 and Arhgef5 identified in each eluate and percent peptide coverage of the full-length protein are shown. Data shown is a reanalysis of supplementary information from Gingras et al. (2016). **(B)** Domain architecture of Arhgef5 and its shorter C-terminal isoform TIM (only detected in humans). **(C)** FLAG-Arhgef5 C-terminal isoform was expressed in HEK293T cells and lysates were incubated with beads coupled to peptide 713 or 713-P. Eluates from the beads were analyzed by immunoblot. **(D,E)** FLAG-tagged Arhgef5 and GFP-tagged aDB1 were coexpressed in HEK293T cells, as indicated. **(D)** GFP-aDB1 was immunoprecipitated from the lysates using anti-GFP-coupled beads and eluates were analyzed by immunoblot. **(E)** FLAG-Arhgef5 was immunoprecipitated from the lysates using anti-FLAG- or rabbit IgG-coupled beads and eluates were analyzed by immunoblot.

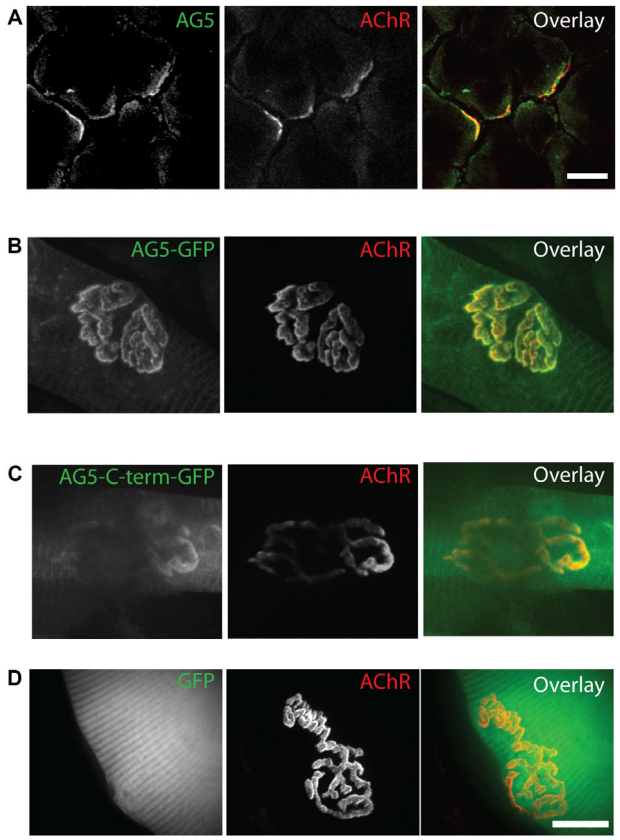

FIGURE 2 | Arhgef5 localizes to AChR-rich regions of the NMJ. **(A)** Cryostat sections of TA muscle were analyzed by immunofluorescence. AChRs were detected using fluorescently labeled BTX. **(B–D)** TA muscle of P30 mice were electroporated with GFP-tagged Arhgef5 **(B)** or Arhgef5-C-term **(C)** or with GFP alone **(D)**. After 14 days, the muscle was fixed and stained with fluorescently labeled BTX. Single fibers were isolated and imaged. Scale bars are 20 μm.

function would impair complex cluster formation by blocking podosomes. To test this hypothesis, we knocked down the expression of Arhgef5 in C2C12 cells using siRNAs. Out of four siRNAs tested, three efficiently reduced Arhgef5 mRNA and protein levels (**Figures 3A,B**). Surprisingly, we found that Arhgef5 knock-down did not block either the appearance of pretzel-like postsynaptic machinery clusters in C2C12 cells cultured on laminin, or the formation of synaptic podosomes visualized by F-actin stained with phalloidin (**Figures 3C–E**). Moreover, Arhgef5 knock-down had no effect on the formation of simple AChR clusters that appear in C2C12 cells stimulated with agrin (**Figures 3F,G**).

Generation of Mice With Muscle-Specific Arhgef5 Knockdown

The lack of a clear effect of *Arhgef5* knock-down on the postsynaptic machinery *in vitro* does not preclude the importance of Arhgef5 for NMJ formation or maintenance *in vivo*. We wanted to determine if depletion of Arhgef5 in mouse muscles would, like that of aDB1, cause abnormal NMJ morphology. To that end, we crossed *Arhgef5* flox/flox ($AG5^{fl/fl}$) conditional knockout mice with mice expressing Cre under the control of the human skeletal actin (HAS or Acta) promoter, which is specifically activated in differentiated skeletal muscle fibers. We found that exon 3 of *Arhgef5* was excised in $AG5^{fl/fl}$;Acta-Cre (**Figures 4A,B**), as evaluated by genotyping PCR reaction. We additionally measured the level of *Arhgef5* mRNA in muscles of $AG5^{fl/fl}$;Acta-Cre and $AG5^{fl/fl}$ mice. The expression of *Arhgef5* mRNA containing exon 3 in $AG5^{fl/fl}$;Acta-Cre muscles was reduced compared to $AG5^{fl/fl}$ mouse muscles, in which Cre was not expressed (**Figure 4C**). The expression went down over time from around postnatal day 50 (P50) to P500 with more apparent decline in older animals. The lack of complete elimination of *Arhgef5* expression in the muscles of $AG5^{fl/fl}$;Acta-Cre mice could be attributed either to incomplete excision of all Arhgef5 alleles in the multinuclear myotubes or to contamination of samples with non-muscle cells, such as blood vessels, connective tissue, fibroblasts, and neurons. The decline of *Arhgef5* mRNA with age could also suggest that muscle fibers are supplemented with *Arhgef5* mRNA coming from muscle satellite cells, which are less numerous in older animals and in which the Acta promoter driving Cre expression is inactive. Because we could still detect residual *Arhgef5* in $AG5^{fl/fl}$;Acta-Cre muscles, we refer to the genotype of these mice as muscle-specific *Arhgef5* knockdown rather than knockout.

Neuromuscular Junctions Are Abnormally Fragmented in Arhgef5 Knockdown Muscles

To determine if the muscle-specific knockdown of Arhgef5 affects NMJ formation and maintenance, we isolated TA muscles from $AG5^{fl/fl}$; Acta-Cre and $AG5^{fl/fl}$ (control) mice and imaged their NMJs using α-bungarotoxin staining to visualize postsynaptic AChRs. In both types of mice NMJs formed normally with well aligned postsynaptic specialization (AChR), presynaptic elements (neurofilament and synaptophysin), and synaptic extracellular matrix marker (acetylcholinesterase stained with fasciculin II) (**Figure 4D**).

Because the DGC is involved in the stability of the NMJ, we speculated that loss of Arhgef5 might result in more excessive fragmentation of NMJs. Indeed, when we scored NMJs according to the degree of fragmentation (**Figure 5A**), NMJs from $AG5^{fl/fl}$;Acta-Cre showed more profound disintegration than control mice (**Figure 5B**). The effect of NMJ fragmentation was increased with age of animals and correlated with the decline in Arhgef5 mRNA (**Figure 5C**). This suggests that loss of Arhgef5 in muscles results in poorer NMJ stability.

To check if the increased NMJ fragmentation in mutant mice was associated with decreased total area of AChR-rich regions at each postsynaptic cluster, we performed unsupervised measurements of the total area of the NMJ, the area containing AChR receptors (α-bungarotoxin-positive) and the area of perforations between AChR-rich branches of the NMJ. Neither of these parameters was changed in $AG5^{fl/fl}$;Acta-Cre mice compared to controls (**Figures 5D,E**).

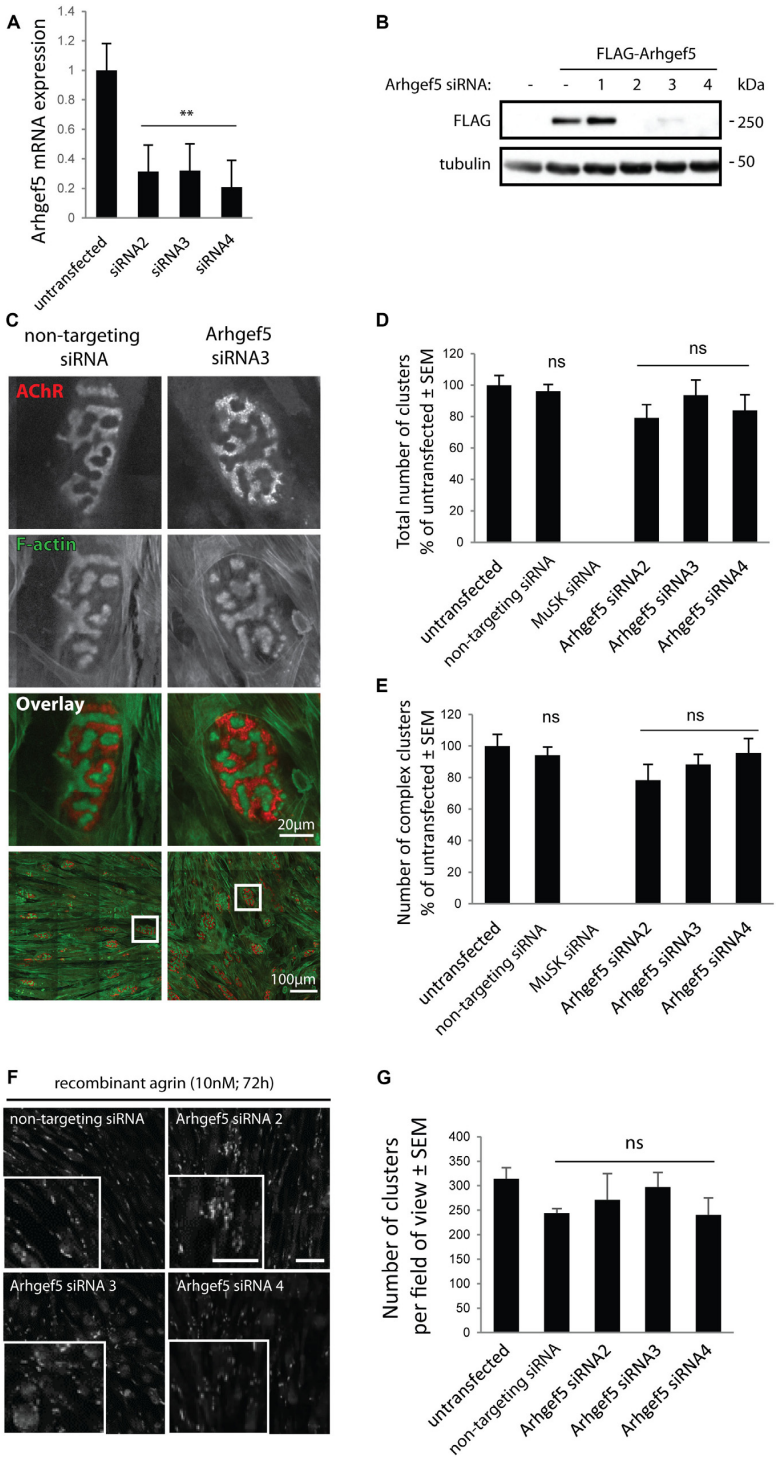

FIGURE 3 | Arhgef5 is not required for AChR cluster formation in cultured myotubes. **(A)** C2C12 myotubes were transfected with control siRNA or three different siRNAs targeting Arhgef5. Arhgef5 mRNA levels were measured by RT-qPCR in the transfected cells. **(B)** HEK293T cells were transfected with FLAG-Arhgef5 and either control siRNA or four different siRNAs against Arhgef5 (siRNA 1, 2, 3, 4). FLAG-Arhgef5 levels were measured by Western blot. **(C–E)** C2C12 cells were transfected with negative control (non-targeting) siRNA, Arhgef5 siRNA, or MuSK siRNA as positive control. Cells were stained with fluorescently labeled BTX to visualize AChR and actistain to visualize F-actin. No differences in total cluster number or complex pretzel-like cluster formation was observed upon Arhgef5 knockdown. As expected, knockdown of MuSK fully abrogates AChR cluster formation. Scale bar is 20 µm or 100 µm, as indicated. **(F,G)** C2C12 were transfected as in **(C)** and treated with soluble agrin for 72 h. Cells were fixed and stained with fluorescently labeled BTX to visualize AChR. Arhgef5 knockdown does not affect the abundance of AChR cluster in cells stimulated with agrin. Scale bars are 100 µm. See **Supplementary Figure S1** for an image of sparse AChR clusters that form in the absence of agrin or laminin. $^{**}p < 0.01$.

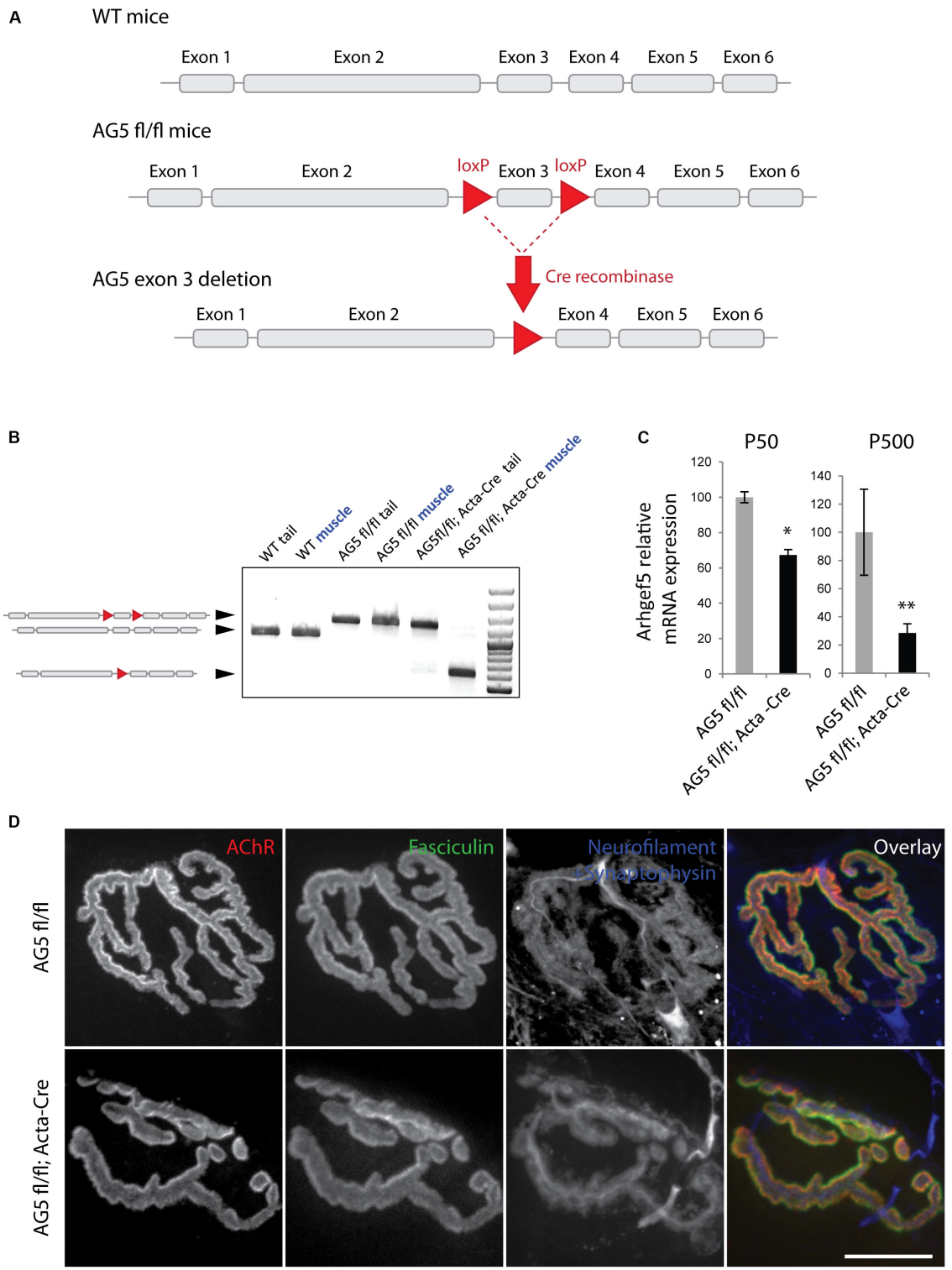

FIGURE 4 | Generation of muscle-specific Arhgef5 KO mice. **(A)** Strategy for the generation of conditional Arhgef5 knockouts. Mice with loxP sites flanking the third exon of *Arhgef5* were crossed with Cre-recombinase expressing mice to produce knockout. **(B)** Genotyping shows successful recombination in the muscles but not tail tipss of AG5$^{fl/fl}$; Acta-Cre mice. **(C)** Quantification of *Arhgef5* mRNA expression in AG5$^{fl/fl}$ and AG5$^{fl/fl}$; Acta-Cre mice at 50 and 500 days of age. Results are mean ± SEM of three mice from each genotype. **(D)** Proper alignment of pre- and post-synaptic elements in AG5$^{fl/fl}$; Acta-Cre muscles. Single fibers of tibialis anterior muscles isolated from AG5$^{fl/fl}$ and AG5$^{fl/fl}$; Acta-Cre mice were stained with BTX (to visualize AChR), fasciculin II (to visualize the synaptic cleft marker acetylcholinesterase), and anti-neurofilament + anti-synaptophysin antibodies (to visualize the presynaptic nerve terminal). Scale bar is 20 μm. *$p < 0.05$, **$p < 0.01$.

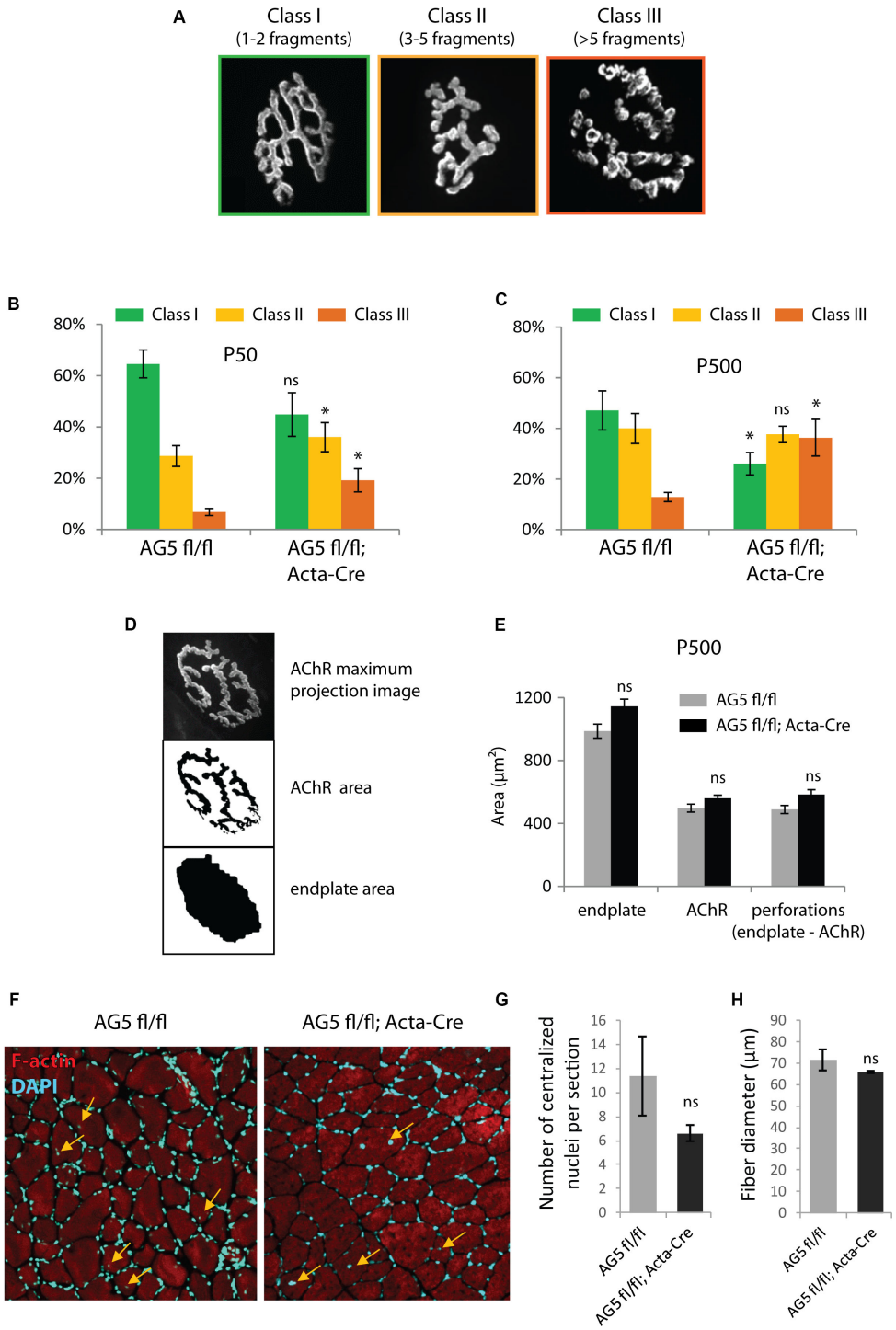

FIGURE 5 | Muscle-specific loss of Arhgef5 results in progressive loss of NMJ integrity **(A)**. Classification of NMJs according to their fragmentation. Representative examples of NMJs from each class are shown **(B,C)**. Relative percentages of NMJs belonging to each of the three classes in tibialis anterior muscles of AG5$^{fl/fl}$ and AG5$^{fl/fl}$; Acta-Cre mice at 50 and 500 days of age. Results are mean ± SEM of three mice from each genotype. At least 30 synapses were counted for each mouse. Arhgef5 muscle-specific knocdown causes increased fragmentation of NMJs at both ages **(D)**. Visualization of the automated quantification of endplate and AChR areas of NMJs. The algorithm takes a maximum projection fluorescence image (top panel) and performs the segmentation of the image to calculate the AChR area (middle panel) or the total area of the endplate (bottom panel). Perforations area is calculated as the difference between endplate area and AChR area. **(E)** Neither the total endplate area nor the AChR area nor the perforations area were significantly different in tibialis anterior muscles of 500-day old AG5$^{fl/fl}$; Acta-Cre mice compared to AG5$^{fl/fl}$. Results are mean ± SEM. **(F)** Representative cross-sections of TA muscle of AG5$^{fl/fl}$ and AG5$^{fl/fl}$; Acta-Cre mice. F-actin was stained with Actistain and nuclei were stained with DAPI. Centralized nuclei are indicated with arrows. **(G)** Quantification of centralized nuclei per TA muscle cross-section for $n = 3$ mice per genotype. Results are mean ± SEM. **(H)** Quantification of fiber diameters in TA muscle cross-sections (samples as in **G**). Results are mean ± SEM. $^{*}p < 0.05$.

We also wanted to make sure that the fragmentation of the postsynaptic machinery in AG5$^{fl/fl}$;Acta-Cre mice is not a downstream consequence of increased degeneration and regeneration of muscle fibers. To that end, we measured the number of centralized nuclei per cross-section in TA muscles of AG5$^{fl/fl}$;Acta-Cre mice and AG5$^{fl/fl}$ controls. We did not observe increased numbers of centralized nuclei or abnormal fiber size in AG5$^{fl/fl}$;Acta-Cre muscles, suggesting that the synaptic defects are not due to increased degeneration and regeneration of muscle fibers (**Figures 5F–H** and **Supplementary Figure S2**, **Supplementary Movies S1–S3**).

Levels of Active Cdc42 and RhoA Are Reduced in Arhgef5 Knockdown Muscles

Arhgef5 is a guanidine exchange factor involved in the regulation of small GTPases from the Rho family. It activates these GTPases by inducing the exchange of GDP to GTP (Wang et al., 2009; Kuroiwa et al., 2011). Therefore, we reasoned that in Arhgef5-knockdown muscles activated GTP-bound Rho-family GTPases should be less abundant. Indeed, GTP-bound RhoA and Cdc42 were reduced in muscles from AG5$^{fl/fl}$;Acta-Cre compared to control mice (**Figure 6**), suggesting that Arhgef5 is required for the maintenance of high levels of active RhoA and Cdc42, as previously shown in other cell types (Kuroiwa et al., 2011).

MATERIALS AND METHODS

Plasmids

For co-IP Arhgef5 C-terminally tagged with a triple FLAG tag was cloned into pSBbi-Puro. GFP-aDB1 was engineered by cloning aDB1 cDNA into the pEGFP-C1 plasmid (Clontech) (Grady et al., 2003). For electroporation, full-length Arhgef5 or Arghef5 C-term were cloned into pCDNA3.1(+)/Puro in frame with the C-terminal GFP tag.

Antibodies and Staining Reagents

The following antibodies were used for immunofluorescence: mouse anti-neurofilament (clone 2H3, Developmental Studies Hybridoma Bank), guinea pig anti-synaptophysin (Synaptic Systems). The following antibodies were used for western blot: rabbit anti-α tubulin (ab18251; Abcam), rabbit anti-GFP (GTX113617; Genetex), mouse anti-GFP (12A6; Developmental Studies Hybridoma Bank), mouse anti-GFP (9F9.F9; Novus Biologicals) mouse anti-FLAG (clone M2, F3165; Sigma), mouse anti-FLAG (635691; Clontech), mouse anti-β-actin (A1978; Sigma), mouse anti-α tubulin (T6199; Sigma). For visualization of AChR we used fluorescently labeled α-bungarotoxin (B35451 or B13422; Thermo), and for visualizing the synaptic cleft, we used fasciculin II, which binds to acetylcholinesterase (F-225; Alomone Labs, labeled with FluoReporter FITC kit from Thermo).

Western Blot

SDS-PAGE was performed on hand-cast polyacrylamide gels. Transfer was performed using *Trans*-Blot Turbo (Bio-Rad) onto nitrocellulose membranes (0.2 μm pore size; PALL). For detection, we used HRP-coupled secondary antibodies (Jackson) and Clarity Western ECL substrate (Bio-Rad). ECL images were collected on photographic film (CL-XPosure, Thermo) and digitized using a film scanner (Epson) or were digitally acquired on the Amersham 680RGB instrument.

Peptide Pulldown

Pulldown of Arhgef5 using synthetic peptides was performed as in Gingras et al. (2016). Briefly, synthetic peptides (phospho-Y713: DEST–Biotin–Ahx–TQPEDGNpYENESVRQ-NH2, Y713: DEST–Biotin–Ahx–TQPEDGNYENESVRQ-NH2) were purchased from Lifetein. The peptides were bound to Streptavidin-coupled Dynabeads M-280 (Life Technologies). Recombinant Arhgef5-GST (C-terminal; Proteintech) was resuspended in bead binding buffer [20 mM Hepes, 150 mM NaCl, 0.5 mM EDTA, 10% Glycerol, 0.05% Nonidet P-40, 1 mM DTT, EDTA-free Mini protease inhibitor cocktail (Roche), pH 7.9] and incubated with the beads overnight at 4°C. The beads were washed 2x in bead binding buffer, and the proteins were eluted in 2x Laemmli sample buffer with 50 mM DTT for 10 min at 95°C.

Co-immunoprecipitation

HEK 293T cells were transfected with plasmids encoding α-dystrobrevin 1-GFP, Arhgef5-FLAG, or both for 24 h. Cells were lysed in lysis buffer: 50 mM Tris, 150 mM NaCl, 0.1% Nonidet P-40, 50 mM NaH2PO4, 1 mM sodium pervanadate, 10 mM NaF, 1x SigmaFAST EDTA-free protease inhibitors (Sigma), 2 μM bortezomib and incubated with Dynabeads-protein G (Life Technologies) precoated with rabbit anti-GFP (GTX113617; Genetex) for 1 h at 4°C or with rabbit-anti-FLAG (PA1984B; Thermo) or rabbit IgG isotype control (Sigma) overnight at 4°C. Beads were washed 3x with lysis buffer and protein was eluted using 2x Laemmli sample buffer for 30 min at 65°C.

Animals

All animals used in the study were on the C57/Bl6 genetic background. Acta-Cre mice (Jax #: 006149; B6.Cg-Tg[ACTA1-cre]79Jme/J) were purchased from The Jackson Laboratory (Stock No: 006149) (Miniou et al., 1999). Arhgef5 conditional knockout mouse line (C57BL/6N-Arhgef5 < tm1c(NCOM)Mfgc > /Tcp) was generated at the Mammalian Functional Genomics Centre, University of Manitoba and provided through The Canadian Mouse Mutant Repository at The Hospital for Sick Children (Toronto, ON, Canada) (Bradley et al., 2012). The original allele was created under the North American Conditional Mouse Mutagenesis (NorCOMM) Project. Animals were kept at the Nencki Institute Animal House on a 12 h light/dark cycle with food and water *ad libitum*. All experiments were conducted in accordance with the animal experimentation permit from the local ethics committee.

Genotyping

Genomic DNA was isolated from mouse tail tips or TA muscles using Chelex 100 (Sigma). A small piece of tissue was added into

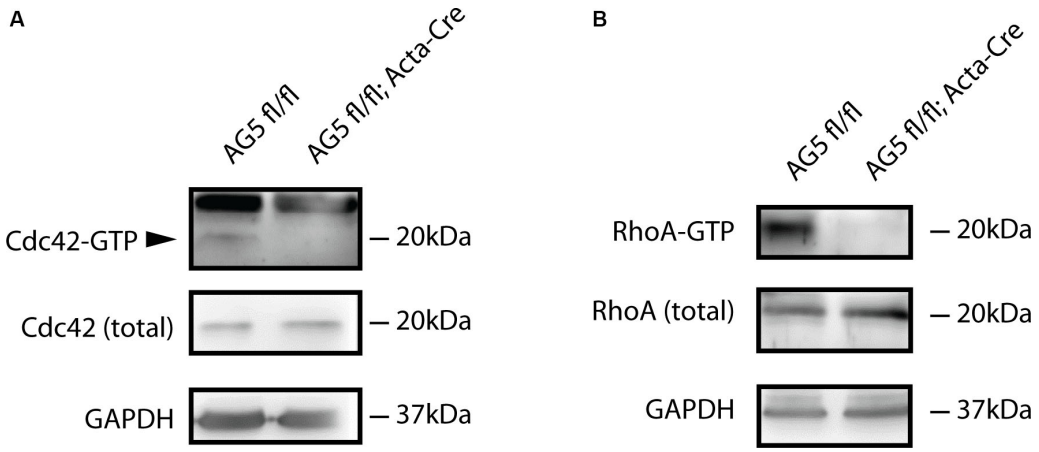

FIGURE 6 | Active forms of Cdc42 and RhoA are reduced by muscle-specific Arhgef5 knockdown. **(A,B)** Active GTP-bound forms of Cdc42 **(A)** and RhoA **(B)** were precipitated from TA homogenates (upper panels) and Cdc42 and RhoA proteins were detected by Western blot from precipitates and tissue lysates (total). GAPDH was used as a loading control.

200 μl of 10% Chelex solution, incubated at 95°C for 20 min, and centrifuged at 12 000 *g* at RT for 10 min. The supernatant was collected and used for the PCR reactions as a template. PCR was performed using 2 × PCR Master Mix (Thermo) using the following primers: CACCTACATCAGCTCAGAAAGTCAT (forward), CAACAGGTGACTCTGACACAGCA (reverse).

RNA Isolation and qRT-PCR

RNA was isolated using TRIsure reagent (Bioline), and cDNA was synthesized using a High-Capacity cDNA Reverse Transcription Kit (Thermo) according to the manufacturer's instructions. qRT-PCR was performed using the Step One Plus Real-Time PCR system (Thermo) and SYBR Green PCR Master Mix (Thermo). The instrument's default programs were used for data acquisition, and the results were analyzed using the comparative Ct method for relative quantification. The housekeeping gene glyceraldehyde-3-phosphate dehydrogenase (*Gapdh*) was used to standardize the samples. The following primers were used: *Gapdh* (GGCCTTCCGTGTTCCTAC and TGTCATCATACTTGGCAGGTT) and *Arhgef5* (CCAA CAAGCAAAAGGGCTGG and TCTTCTCCCGGAAAACAA CAGA).

Electroporation of TA Muscle

Mice were anesthetized using intraperitoneal injection of ketamine (90 mg/kg) and xylazine (4.5 mg/kg). Five to 10 min after the addition of anesthetics, the leg was shaved using hair removal cream. 25 μl of ∼1 mg/mL solution of DNA were injected into the TA muscle with a Hamilton syringe followed by electroporation of the whole leg 10 × with 20 ms pulses at 1 Hz by BTX ECM 830 square wave electroporator. Electrodes were wetted with PBS to enable ion flow and the voltage was ∼175 V/cm. Postoperative analgesia was achieved by subcutaneous injection of 1–5 mg/kg of butorphanol and local anesthesia using 2% lidocaine gel. Mice were sacrificed by pentobarbital injection 14 days after the procedure.

Fresh-Frozen Tissue Sections Immunofluorescence

Tibialis anterior muscle was frozen in cold isopentane and sectioned on a cryostat. Slides were stained with an anti-Arhgef5 antibody and α -bungarotoxin.

Fixed Muscle Fiber Immunostaining and Imaging

Immediately after sacrificing the animal, the skin of the leg was surgically removed and fascia from the TA muscle was taken off. The whole leg was severed and incubated in fresh 4% PFA for 1 h at room temperature. The leg was washed 3 × 5 min in PBS and stored in PBS containing 0.02% sodium azide at 4°C. Fixed muscles were teased into single fibers using fine forceps. Non-specific staining was blocked with 2% bovine serum albumin (BSA) and 2% goat serum in PBS supplemented with 0.5% Triton-X100. The fibers were incubated with primary antibodies overnight in the same buffer. Fibers were washed 3 × 5 min in PBS followed by incubation with secondary antibodies and fluorescently labeled bungarotoxin in 2% BSA and 2% goat serum in PBS containing 0.1% Triton-X100 for 1 h at room temperature. Cells were washed 3 × 5 min in PBS and mounted in fluoromount with DAPI, covered with coverslips, and sealed with nail polish. Image acquisition was performed at the Confocal Microscopy Facility at the Nencki Institute, using the Zeiss spinning disk confocal microscope or the Leica TCS SP8 scanning confocal microscope. Images were analyzed using ImageJ/Fiji software.

NMJ Phenotype Quantification

Tibialis anterior muscles were fixed in 4% PFA and stained with fluorescently labeled bungarotoxin. Teased fibers from the muscle were mounted on slides and imaged using the Zeiss spinning disk confocal microscope. To ensure reliable measurements, only NMJs that were placed directly facing and parallel to the coverslip were used for downstream analyses.

NMJs (30–50 per animal) were manually assigned to one of three populations based on the number of discrete fragments they were composed of: class I contained 1-2 fragments, class II contained 3-5 fragments and class III contained 6 fragments or more. For morphometric analysis, we used the "NMJ-morph" ImageJ plugin (Jones et al., 2016).

Quantification of Centralized Nuclei

Tibialis anterior muscles were dissected, embedded in OCT and snap-frozen in isopentane cooled by liquid nitrogen and stored at −80°C at least overnight. Transverse 20 μm-thick sections were generated by using Leica Cryostat CM1950, collected on slides, dried at room temperature for 1 h and stored at −20°C. For immunohistochemistry, sections were fixed with 4% PFA for 10 min at room temperature and then treated with blocking solution for 1 h [0.2% BSA, 0.5% Triton X-100, 2% normal goat serum (NGS) in phosphate-buffered saline (PBS)]. Sections were counterstained with AlexaFluor-555-conjugated phalloidin (A34055, Thermo Scientific) at 1:500 dilution in blocking solution for 1 h at room temperature. Afterward, slides were washed for 5 min in PBS. Coverslips were applied over the slides and mounted with mounting media containing 1:1000 dilution of DAPI (A4099, AppliChem). Immunofluorescence microscopy was performed using a spinning disk confocal microscope (Zeiss).

Cell Culture

C2C12 myoblasts were cultured as described previously (Pęziński et al., 2019). Briefly, myoblasts were cultured on 0.2% gelatin-coated plates in Dulbecco's Modified Eagle Medium (DMEM) supplemented with 20% fetal bovine serum (FBS), 4.5 g/L glucose, L-glutamine, penicillin, streptomycin, and fungizone. For myotube fusion, cells were trypsinized and plated on Permanox slides (VWR) in eight-well Flexiperm chambers (Sarstedt). The slides were coated with 111-laminin (Sigma). To induce myotube differentiation, the media were replaced with DMEM with 2% horse serum. For experiments involving agrin, slides were coated with 0.2% gelatin instead of laminin, and myotubes were stimulated with 10 nM recombinant rat Z'-spliced agrin (R&D Systems) for 72 h. The cells were fixed in 4% paraformaldehyde (PFA) and permeabilized with 0.5% Triton X-100 for 30 min. The myotubes were stained using Alexa Fluor 555-coupled bugarotoxin (BTX) (B35451, Life Technologies) and Acti-Stain 488 (PHDG1, Cytoskeleton). Cells were imaged on the Zeiss spinning disk confocal microscope at the Nencki Institute Microscopy Core Facility. Images were processed using ImageJ/Fiji and analyzed in R.

Arhgef5 Knock Down

Arhgef5 silencing in differentiated C2C12 myotubes was performed with Lipofectamine RNAiMAX (Life Technologies). The following siRNAs were used at 20 nM: siRNA1 (#2430, Sigma-Aldrich), siRNA2 (#30088, Sigma-Aldrich), siRNA3 (#6911, Sigma-Aldrich), siRNA4 (#4390771, ID: s79541, Ambion), and non-targeting control siRNA (#12935300, Invitrogen). The cells were fixed 2 days later and examined by confocal microscopy.

RhoA/Cdc42 Activity Assay

Experiments were carried out as described previously with minor modifications (Bijata et al., 2015; Schill et al., 2020). Briefly, for biochemical determination of RhoA/Cdc42 activity TA muscles were homogenized in lysis buffer [25 mM HEPES (pH 7.5), 150 mM NaCl, 1% Nonidet P-40, 10 mM MgCl2, 1 mM ethylenediaminetetraacetic acid (EDTA), and 2% glycerol] and centrifuged at 14000 × *g* for 10 min at 4°C. The extracts were incubated with GST-PAK-PBD fusion protein that had been conjugated with glutathione beads (for Cdc42; Cell BioLabs) at 4°C overnight or an anti-active RhoA monoclonal antibody and protein A/G Agarose beads (for RhoA, Neweast Biosciences) for 1 h at 4°C and then washed three times with lysis buffer. Active RhoA/Cdc42 was analyzed by SDS-PAGE and subsequently immunoblotted with RhoA-specific antibody (Neweast Biosciences, 1:500) and Cdc42-specific antibody (11A11, Cell Signaling, 1:500).

Statistics

Statistical analyses were performed using GraphPad Prism 7, Microsoft Excel, and R. Quantitative data are presented as the mean ± SEM or SD. Two-tailed unpaired *t*-test or ANOVA with Bonferroni's *post hoc* test were used to test for statistical significance, as appropriate. $P > 0.05$ was labeled as ns-not significant, $p < 0.05$ as *, $p < 0.01$ as **, $p < 0.001$ as ***, and $p < 0.0001$ as ****. Values of $p < 0.05$ were considered statistically significant.

DISCUSSION

The DGC is essential for the maturation and maintenance of the NMJ. The dysfunctions of its components often lead to myopathies, such as Duchenne muscular dystrophy or limb-girdle muscular dystrophy (Mercuri et al., 2019). One of the DGC components is aDB1, whose deletion in mice results in lower density, decreased stability and abnormal distribution of AChR at the NMJ (Grady et al., 2003, 2000; Pawlikowski and Maimone, 2009). It has been recently proposed that aDB1 serves as a scaffold for the binding of signaling molecules, including Liprin-α1 (Bernadzki et al., 2017), Grb2, α-catulin (Lyssand et al., 2010; Gingras et al., 2016), and the Rho GEF Arhgef2. Here, we showed that phospho-aDB1-binding protein Arhgef5 accumulates at the NMJ and is required for the maintenance of NMJ integrity *in vivo*. Arhgef5 was of particular interest to us, because it had previously found to bind another aDB1 interactor α-catulin in HEK293 cells (Lyssand et al., 2010), and because it is known to be essential for the formation of Src-induced podosomes in fibroblasts (Kuroiwa et al., 2011). We therefore hypothesized that Arhgef5 promotes the remodeling of NMJ postsynaptic machinery through actin dynamics and synaptic podosomes in muscle cells. However, the knockdown of Arhgef5 failed to affect the formation of synaptic podosomes in cultured myotubes and had no obvious effect on the formation of AChR clusters. The most parsimonious explanation for that result is that C2C12 cells, unlike fibroblasts, do not rely on Arhgef5 to activate Rho family GTPases and induce podosomes. Two potential candidates for such a function

in C2C12 cells are RhoGEFs ephexin1 and Arhgef2. We have previously shown that Arhgef2 also associates with phospho-aDB1, suggesting that it could be compensating for the loss of Arhgef5 in C2C12 cells (Gingras et al., 2016). Ephexin1 had been shown to affect the maturation of postsynaptic clusters in C2C12 cells (Shi et al., 2010) and NMJ *in vivo*, but whether it does so in collaboration with the DGC or through the regulation of actin-rich podosomes remains unknown.

In contrast to the apparent lack of effect of Arhgef5 loss in cultured myotubes, the knockdown of Arhgef5 in muscle fibers *in vivo* leads to synaptic abnormalities. NMJs in muscle-specific Arhgef5 KO mice are more fragmented, implying that Arhgef5 is important for NMJ stability once the postsynaptic maturation is accomplished. This phenotype does not mimic the abnormalities observed in aDB1 KO mice, whose NMJs lack a clear demarcation between AChR-rich and AChR-poor areas, resulting in a "fuzzy" appearance (Grady et al., 2000; Wang et al., 2018). Since aDB1 recruits many signaling proteins, it is plausible that the synaptic defects in the absence of aDB1 and Arhgef5 differ. On the other hand, Arhgef5 becomes depleted in conditional KO muscles only later in life (**Figure 4C**), so it is possible that the observed differences between the phenotypes of aDB1 KO and Arhgef5 muscle-specific knockdown mice are due at least in part to the different timing of the loss of function of their respective genes. Therefore, it is difficult to speculate about the lack of Arhgef5 function in synaptic development.

The knockout of another RhoGEF ephexin1 has also been shown to cause fragmentation of the NMJ postsynaptic machinery (Shi et al., 2010). However, the mechanisms of action of ephexin1 and Arhgef5 appear to be different. Whereas ephexin1 plays a pivotal role in the early development of NMJs and the creation of complex postsynaptic pretzels *in vivo*, loss of Arhgef5 in the muscle does not induce early developmental aberrations of the NMJ (data not shown). It is only later in development that the effects of Arhgef5 knockdown become more pronounced. This could explain why depletion of Arhgef5 has no effect on the short-lived AChR clusters in C2C12 cells. However, as discussed above, Arhgef5 only becomes strongly depleted in adult conditional KO mice, so it is plausible that an earlier loss of function of Arhgef5 might result in a different phenotype more reminiscent of ephexin1 KO mice.

How might Arhgef5 affect the stability of NMJs *in vivo*? Our data indicate that the mechanism might involve the regulation of cytoskeleton dynamics via small Rho-family GTPases. We showed that the active GTP-bound forms of RhoA and Cdc42 are reduced in the muscles of conditional AG5 KO mice. Reduced RhoA activity was shown to be the main causal factor in the abnormal NMJ phenotype of epehexin1 KO mice (Shi et al., 2010). Moreover, RhoA is essential for the fusion of microclusters of AChR into larger clusters in muscle cells (Weston et al., 2003), which might explain the loss of integrity of NMJs in AG5 conditional KO mice. RhoA may also help anchor the NMJ to the cytoskeleton by promoting the expression and membrane localization of utrophin, a DGC component known to bind actin filaments via its N-terminal tail (Galkin et al., 2002; Bonet-Kerrache et al., 2005). Cdc42 is also important in the formation of AChR clusters in mammalian muscle cells (Weston et al., 2000) and for the proper formation of the NMJ postsynaptic machinery in Drosophila (Rodal et al., 2008). In conclusion, it appears that Rho GEFs and their target small GTPases are important players in the formation, maturation, and maintenance of the postsynaptic structures of the NMJ. Going forward, it will be important to decipher the respective roles of the different GEFs at various time points of NMJ development, and their potential involvement in muscular dystrophies in humans.

DATA AVAILABILITY STATEMENT

All datasets generated for this study are included in the article/**Supplementary Material**.

ETHICS STATEMENT

The animal study was reviewed and approved by the 1st Local Ethics Committee for Animal Experiments in Warsaw.

AUTHOR CONTRIBUTIONS

TP and PN devised the study and edited the manuscript. KB, PD, KR, MP, MG, BP, TC, MB, KB, TP, and PN designed and performed the experiments and analyzed the data. JW, TP, and PN supervised the study. PN, KB, PD, KR, MG, TC, and MB wrote sections of the first draft of the manuscript.

FUNDING

This work was funded by the NCN OPUS grant 2014/13/B/NZ3/00909 from the National Science Centre (Poland).

ACKNOWLEDGMENTS

We would like to thank Adrian Kobiela for his technical contributions.

SUPPLEMENTARY MATERIAL

The Supplementary Material for this article can be found online at: https://www.frontiersin.org/articles/10.3389/fnmol.2020.00104/full#supplementary-material

FIGURE S1 | Image of spontaneous clusters of AChR that form in C2C12 myotubes in the absence of agrin and laminin. AChR was labeled with fluorescently labeled BTX.

FIGURE S2 | Images of fragmented synapses corresponding to X-Z cross-sections shown in Supplementary Movies S1–S3. AChRs were stained with fluorescently labeled BTX (green). Nuclei were stained with DAPI (magenta). Maximum projection images through the fibers are shown.

MOVIES S1–S3 | X-Z slices through TA muscle fibers with fragmented NMJs in AG5$^{fl/fl}$; Acta-Cre mice. We did not see any evidence of increased abundance of centralized nuclei in these fibers. AChRs were stained with fluorescently labeled BTX (green). Nuclei were stained with DAPI (magenta).

REFERENCES

Aittaleb, M., Martinez-Pena, Y., Valenzuela, I., and Akaaboune, M. (2017). Spatial distribution and molecular dynamics of dystrophin glycoprotein components at the neuromuscular junction in vivo. *J. Cell. Sci.* 130, 1752–1759. doi: 10.1242/jcs.198358

Belhasan, D. C., and Akaaboune, M. (2020). The role of the dystrophin glycoprotein complex on the neuromuscular system. *Neurosci. Lett.* 722:134833. doi: 10.1016/j.neulet.2020.134833

Bernadzki, K. M., Gawor, M., Pęziński, M., Mazurek, P., Niewiadomski, P., Rędowicz, M. J., et al. (2017). Liprin-α-1 is a novel component of the murine neuromuscular junction and is involved in the organization of the postsynaptic machinery. *Sci. Rep.* 7, 1–12. doi: 10.1038/s41598-017-09590-7

Bernadzki, K. M., Rojek, K. O., and Prószyński, T. J. (2014). Podosomes in muscle cells and their role in the remodeling of neuromuscular postsynaptic machinery. *Eur. J. Cell Biol.* 93, 478–485. doi: 10.1016/j.ejcb.2014.06.002

Bijata, M., Wlodarczyk, J., and Figiel, I. (2015). Dystroglycan controls dendritic morphogenesis of hippocampal neurons in vitro. *Front. Cell. Neurosci.* 9:199. doi: 10.3389/fncel.2015.00199

Bonet-Kerrache, A., Fortier, M., Comunale, F., and Gauthier-Rouvière, C. (2005). The GTPase RhoA increases utrophin expression and stability, as well as its localization at the plasma membrane. *Biochem. J.* 391, 261–268. doi: 10.1042/BJ20050024

Bradley, A., Anastassiadis, K., Ayadi, A., Battey, J. F., Bell, C., Birling, M.-C., et al. (2012). The mammalian gene function resource: the International Knockout Mouse Consortium. *Mamm. Genome* 23, 580–586. doi: 10.1007/s00335-012-9422-2

Campbell, K. P. (1995). Three muscular dystrophies: loss of cytoskeleton-extracellular matrix linkage. *Cell* 80, 675–679. doi: 10.1016/0092-8674(95)90344-5

Dai, Z., Luo, X., Xie, H., and Peng, H. B. (2000). The actin-driven movement and formation of acetylcholine receptor clusters. *J. Cell Biol.* 150, 1321–1334.

Ervasti, J. M., and Campbell, K. P. (1991). Membrane organization of the dystrophin-glycoprotein complex. *Cell* 66, 1121–1131. doi: 10.1016/0092-8674(91)90035-w

Galkin, V. E., Orlova, A., VanLoock, M. S., Rybakova, I. N., Ervasti, J. M., and Egelman, E. H. (2002). The utrophin actin-binding domain binds F-actin in two different modes: implications for the spectrin superfamily of proteins. *J. Cell Biol.* 157, 243–251. doi: 10.1083/jcb.200111097

Gawor, M., and Prószyński, T. J. (2018). The molecular cross talk of the dystrophin-glycoprotein complex. *Ann. N. Y. Acad. Sci.* 1412, 62–72. doi: 10.1111/nyas.13500

Gingras, J., Gawor, M., Bernadzki, K. M., Grady, R. M., Hallock, P., Glass, D. J., et al. (2016). α-Dystrobrevin-1 recruits Grb2 and α-catulin to organize neurotransmitter receptors at the neuromuscular junction. *J. Cell Sci.* 129, 898–911. doi: 10.1242/jcs.181180

Grady, R. M., Akaaboune, M., Cohen, A. L., Maimone, M. M., Lichtman, J. W., and Sanes, J. R. (2003). Tyrosine-phosphorylated and nonphosphorylated isoforms of alpha-dystrobrevin: roles in skeletal muscle and its neuromuscular and myotendinous junctions. *J. Cell Biol.* 160, 741–752. doi: 10.1083/jcb.200209045

Grady, R. M., Grange, R. W., Lau, K. S., Maimone, M. M., Nichol, M. C., Stull, J. T., et al. (1999). Role for alpha-dystrobrevin in the pathogenesis of dystrophin-dependent muscular dystrophies. *Nat. Cell Biol.* 1, 215–220. doi: 10.1038/12034

Grady, R. M., Zhou, H., Cunningham, J. M., Henry, M. D., Campbell, K. P., and Sanes, J. R. (2000). Maturation and maintenance of the neuromuscular synapse: genetic evidence for roles of the dystrophin–glycoprotein complex. *Neuron* 25, 279–293.

Ichida, F., Tsubata, S., Bowles, K. R., Haneda, N., Uese, K., Miyawaki, T., et al. (2001). Novel gene mutations in patients with left ventricular noncompaction or Barth syndrome. *Circulation* 103, 1256–1263.

Jones, R. A., Reich, C. D., Dissanayake, K. N., Kristmundsdottir, F., Findlater, G. S., Ribchester, R. R., et al. (2016). NMJ-morph reveals principal components of synaptic morphology influencing structure-function relationships at the neuromuscular junction. *Open Biol.* 6:160240. doi: 10.1098/rsob.160240

Kuroiwa, M., Oneyama, C., Nada, S., and Okada, M. (2011). The guanine nucleotide exchange factor Arhgef5 plays crucial roles in Src-induced podosome formation. *J. Cell. Sci.* 124, 1726–1738. doi: 10.1242/jcs.080291

Lee, C. W., Han, J., Bamburg, J. R., Han, L., Lynn, R., and Zheng, J. Q. (2009). Regulation of Acetylcholine Receptor Clustering by ADF/Cofilin-Directed Vesicular Trafficking. *Nat. Neurosci.* 12, 848–856. doi: 10.1038/nn.2322

Luo, Z. G., Wang, Q., Zhou, J. Z., Wang, J., Luo, Z., Liu, M., et al. (2002). Regulation of AChR Clustering by Dishevelled Interacting with MuSK and PAK1. *Neuron* 35, 489–505. doi: 10.1016/S0896-6273(02)00783-3

Lyssand, J. S., Whiting, J. L., Lee, K.-S., Kastl, R., Wacker, J. L., Bruchas, M. R., et al. (2010). α-Dystrobrevin-1 recruits α-catulin to the α1D-adrenergic receptor/dystrophin-associated protein complex signalosome. *PNAS* 107, 21854–21859. doi: 10.1073/pnas.1010819107

Mercuri, E., Bönnemann, C. G., and Muntoni, F. (2019). Muscular dystrophies. *Lancet* 394, 2025–2038. doi: 10.1016/S0140-6736(19)32910-1

Miniou, P., Tiziano, D., Frugier, T., Roblot, N., Le Meur, M., and Melki, J. (1999). Gene targeting restricted to mouse striated muscle lineage. *Nucleic Acids Res.* 27:e27. doi: 10.1093/nar/27.19.e27

Mitsui, T., Kawajiri, M., Kunishige, M., Endo, T., Akaike, M., Aki, K., et al. (2000). Functional association between nicotinic acetylcholine receptor and sarcomeric proteins via actin and desmin filaments. *J. Cell. Biochem.* 77, 584–595.

Nakamori, M., and Takahashi, M. P. (2011). The role of α-dystrobrevin in striated muscle. *Int. J. Mol. Sci.* 12, 1660–1671. doi: 10.3390/ijms12031660

Nishimune, H., Valdez, G., Jarad, G., Moulson, C. L., Müller, U., Miner, J. H., et al. (2008). Laminins promote postsynaptic maturation by an autocrine mechanism at the neuromuscular junction. *J. Cell Biol.* 182, 1201–1215. doi: 10.1083/jcb.200805095

Oh, H. J., Abraham, L. S., van Hengel, J., Stove, C., Proszynski, T. J., Gevaert, K., et al. (2012). Interaction of α-catulin with dystrobrevin contributes to integrity of dystrophin complex in muscle. *J. Biol. Chem.* 287, 21717–21728. doi: 10.1074/jbc.M112.369496

Pawlikowski, B. T., and Maimone, M. M. (2009). Formation of complex AChR aggregates in vitro requires alpha-dystrobrevin. *Dev. Neurobiol.* 69, 326–338. doi: 10.1002/dneu.20703

Pęziński, M., Daszczuk, P., Pradhan, B. S., Lochmüller, H., and Prószyński, T. J. (2019). An improved method for culturing myotubes on laminins for the robust clustering of postsynaptic machinery. *bioRxiv* [Preprint]. doi: 10.1101/664268

Proszynski, T. J., Gingras, J., Valdez, G., Krzewski, K., and Sanes, J. R. (2009). Podosomes are present in a postsynaptic apparatus and participate in its maturation. *Proc. Natl. Acad. Sci. U.S.A.* 106, 18373–18378. doi: 10.1073/pnas.0910391106

Proszynski, T. J., and Sanes, J. R. (2013). Amotl2 interacts with LL5β, localizes to podosomes and regulates postsynaptic differentiation in muscle. *J. Cell. Sci.* 126, 2225–2235. doi: 10.1242/jcs.121327

Rodal, A. A., Motola-Barnes, R. N., and Littleton, J. T. (2008). Nervous Wreck and Cdc42 cooperate to regulate endocytic actin assembly during synaptic growth. *J. Neurosci.* 28, 8316–8325. doi: 10.1523/JNEUROSCI.2304-08.2008

Schill, Y., Bijata, M., Kopach, O., Cherkas, V., Abdel-Galil, D., Böhm, K., et al. (2020). Serotonin 5-HT 4 receptor boosts functional maturation of dendritic spines via RhoA-dependent control of F-actin. *Commun. Biol.* 3, 1–16. doi: 10.1038/s42003-020-0791-x

Schmidt, N., Akaaboune, M., Gajendran, N., Martinez-Pena y Valenzuela, I., Wakefield, S., Thurnheer, R., et al. (2011). Neuregulin/ErbB regulate neuromuscular junction development by phosphorylation of α-dystrobrevin. *J. Cell Biol.* 195, 1171–1184. doi: 10.1083/jcb.201107083

Shi, L., Butt, B., Ip, F. C. F., Dai, Y., Jiang, L., Yung, W.-H., et al. (2010). Ephexin1 is required for structural maturation and neurotransmission at the neuromuscular junction. *Neuron* 65, 204–216. doi: 10.1016/j.neuron.2010.01.012

Wang, D., Kelly, B. B., Albrecht, D. E., Adams, M. E., Froehner, S. C., and Feng, G. (2018). Complete Deletion of All α-Dystrobrevin Isoforms does not reveal new neuromuscular junction phenotype. *Gene Expr.* 14, 47–57.

Wang, Z., Kumamoto, Y., Wang, P., Gan, X., Lehmann, D., Smrcka, A. V., et al. (2009). Regulation of immature dendritic cell migration by RhoA guanine nucleotide exchange factor Arhgef5. *J. Biol. Chem.* 284, 28599–28606. doi: 10.1074/jbc.M109.047282

Weston, C., Gordon, C., Teressa, G., Hod, E., Ren, X.-D., and Prives, J. (2003). Cooperative Regulation by Rac and Rho of Agrin-induced Acetylcholine Receptor Clustering in Muscle Cells. *J. Biol. Chem.* 278, 6450–6455. doi: 10.1074/jbc.M210249200

Weston, C., Yee, B., Hod, E., and Prives, J. (2000). Agrin-Induced acetylcholine receptor clustering is mediated by the small guanosine Triphosphatases Rac and Cdc42. *J. Cell Biol.* 150, 205–212. doi: 10.1083/jcb.150.1.205

Xie, X., Chang, S. W., Tatsumoto, T., Chan, A. M. L., and Miki, T. (2005). TIM, a Dbl-related protein, regulates cell shape and cytoskeletal organization in a Rho-dependent manner. *Cell. Signal.* 17, 461–471. doi: 10.1016/j.cellsig.2004.09.012

Conflict of Interest: The authors declare that the research was conducted in the absence of any commercial or financial relationships that could be construed as a potential conflict of interest.

Copyright © 2020 Bernadzki, Daszczuk, Rojek, Pęziński, Gawor, Pradhan, de Cicco, Bijata, Bijata, Włodarczyk, Prószyński and Niewiadomski. This is an open-access article distributed under the terms of the Creative Commons Attribution License (CC BY). The use, distribution or reproduction in other forums is permitted, provided the original author(s) and the copyright owner(s) are credited and that the original publication in this journal is cited, in accordance with accepted academic practice. No use, distribution or reproduction is permitted which does not comply with these terms.

frontiers in Molecular Neuroscience

OPINION
published: 12 June 2020
doi: 10.3389/fnmol.2020.00091

Wesley J. Thompson (1947–2019)

Young il Lee[1]* *and Mendell Rimer*[2]*

[1] Department of Biology, Texas A&M University, College Station, TX, United States, [2] Department of Neuroscience and Experimental Therapeutics, Texas A&M University Health Science Center, Bryan, TX, United States

Keywords: Wesley J. Thompson, neuromuscular junction (NMJ), synapse elimination, schwann cell, activity-dependent synaptic plasticity, nestin, neuregulin1, muscle fiber development

Wesley Jay (Wes) Thompson, known for his seminal contributions to the studies of neuromuscular synapses and glial cells, passed away on March 26, 2019, at the age of 71. Surviving family, friends, trainees, colleagues, and others who hold Wes in fond memory gathered at the campus of Texas A&M University in College Station, TX, for a memorial service in his honor some weeks later. All of the speakers recounted with fondness their interactions with Wes that exemplified the impact his approaches to life and work had on the lives of many others. Most who knew Wes would agree that he never liked to talk about himself much except in performing self-deprecating humor and voicing his displeasure with the current political climate. Wes abhorred any public recognition of his accomplishments (or good deeds) and only begrudgingly tolerated those accompanied by research funds. We are certain Wes would have protested the production of this article that pays him tribute. There are aspects of his life, however, that were readily apparent to those who have spent any meaningful amount of time with Wes—his generosity, drive and integrity as a scientist, affinity for history and simpler things in life such as his vegetable garden and backyard barbeque with friends that brought him joy, and love for his daughter. Jeff Lichtman, a fellow towering contemporary figure in the study of neuromuscular synapses, once called Wes "a gem of a human being," a much-deserved compliment that sweetly sums up the warm character of the man we all knew.

Wes was born on December 10, 1947, in Alice, TX, to Jay and Harriett Thompson from whom Wes inherited many of his endearing traits: rough-around-the-edges Texan charm, a desire/willingness to fix any mechanical instruments (often with mixed results) from his inventor/oilman father, and a deep belief in the value of education from his mother, a school teacher. The family relocated to Crawford, TX, where Wes spent a large part of his childhood. In 1966, Wes graduated from Crawford High School, and in 1970, earned a Bachelor of Science degree with High Honors from North Texas State University (since renamed the University of North Texas), a short 2-h drive away. Perhaps as a preview of what lay ahead in his long and respected scientific career punctuated with honors, a survey of his high school and college yearbooks (**Figure 1**) provides hints that fellow students had already recognized Wes's academic accomplishments and potential. As his career progressed, clearly, Wes did not fall victim to enemies of promise. In addition to receiving several postdoctoral fellowships, he was named a Searle Scholar in 1981 (Searle Scholars Program, Chicago Community Trust) and received a National Institutes of Health (NIH) Research Career Development Award in 1984 and a Javits Neuroscience Investigator award in 2001. He maintained a research program that was continuously funded by the NIH until his death. As a testament to his long-standing dedication to educate undergraduate students, Wes was also recognized with a University of Texas at Austin Teaching Excellence Award in 2000.

THE JOURNEY WEST

After submitting his thesis for a Master of Arts degree at North Texas State University in December 1971, Wes headed west to pursue graduate studies at the University of California, Berkeley. Early 70s Berkeley, CA, was probably as foreign a place as could be imagined for a young man from

OPEN ACCESS

Edited by:
Ruth Herbst,
Medical University of Vienna, Austria

Reviewed by:
Alberto Cangiano,
University of Verona, Italy
Noreen Reist,
Colorado State University,
United States

***Correspondence:**
Young il Lee
ylee@bio.tamu.edu
Mendell Rimer
rimer@tamu.edu

Received: *26 March 2020*
Accepted: *30 April 2020*
Published: *12 June 2020*

Citation:
Lee Y and Rimer M (2020) Wesley J. Thompson (1947–2019). Front. Mol. Neurosci. 13:91. doi: 10.3389/fnmol.2020.00091

central Texas. At Berkeley, Wes joined the lab of Gunther Stent, a disciple of the "phage group" led by Caltech's Max Delbrück, whose research on the genetic structure and replication of bacterial viruses (bacteriophages) helped launch the modern field of Molecular Biology. By the time Wes joined his lab, Gunther Stent had famously declared Molecular Biology near dead as a field and had moved on to Neurobiology using the medicinal leech, *Hirudo medicinalis*, as a model organism for investigating the neurobiological basis of behavior. With its relatively simple and accessible nervous system, the leech offered an excellent experimental model to characterize and understand the neuronal circuits that underlie rhythmic movements such as swimming or crawling (Kristan et al., 2005). While the rest of the Stent group was focused on finding the neuronal circuitry that produced swimming in the leech, for his doctoral thesis, Wes tackled the regulation of heartbeat. The leech heartbeat consists of neuronally driven, pulsing contractions of muscular lateral, longitudinal vessels, known as the heart tubes, which drive blood flow through a closed circulatory system (Kristan et al., 2005). Wes carried out pioneering work that first described the innervation circuit of the heart tubes by excitatory motor neurons (HE cells) (Thompson and Stent, 1976a). Most importantly, Wes discovered the ensemble of inhibitory heart interneurons (HN cells) that constitute the oscillator circuit driving the bursting firing pattern of the HE cells, which generates the heartbeat (Thompson and Stent, 1976b,c). Wes characterized the mechanism of the oscillation as the reciprocal inhibition between HN cells, how the oscillatory pattern was imposed on the HE cells, and how the hearts on the two sides of the leech were coordinated. This work provided the basis for later, elegant studies by Ron Calabrese et al. that have advanced in great detail the understanding of the neuronal circuitry controlling this behavior (Calabrese et al., 2016). The leech heartbeat system, the heartbeat circuitry in the lobster, and the control of the stomatogastric systems of lobsters and crabs are among the very few completely characterized oscillator circuits in all of neuroscience. Bill Kristan, then a postdoctoral fellow in the Stent lab, who became an eminent figure in leech biology and the neurobiology of behavior, has observed that Wes's thesis work "required a huge amount of very careful experiments along with great insight at many stages of the project. I could tell when he was being most productive because he would take minimal time to satisfy creature needs like eating and drinking. His lunches and dinners during these times consisted almost entirely of candy bars and cokes!" Stent and co-disciples, affectionately known as Stent's "neurobiological minions" (Weisblat and Thompson, 2008), influenced Wes's intellectual and practical approach to science for the rest of his career. Kristan, in particular, played an important mentoring role during Wes's time in the Stent lab, and they remained close friends and colleagues throughout Wes's life.

FIGURE 1 | (**Top left**) Wes at North Texas State University (1966–1970). As a senior, when he was recognized for outstanding work in his major field of study—Biology. Source: The Yucca, Yearbook of North Texas State University, 1970, Fort Worth, TX; University of North Texas Libraries, UNT Digital Library (https://digital.library.unt.edu), crediting UNT Libraries Special Collections. (**Bottom**) Wes, in his customary presentation stance, at the 2010 biennial "Molecular and Cell Biology of the Neuromuscular System" meeting, organized by Hans Brenner, Stephan Kröger, and Markus Rüegg, Guarda, Switzerland. Photograph kindly provided by Dr. Shuo Lin, University of Basel, Switzerland. (**Top right**) Wes at a dinner during the 2012 Guarda meeting. From an original photograph kindly provided by Dr. Noreen Reist, Colorado State University, USA.

TO OSLO, NORWAY

One of us once asked Wes what compelled him to move all the way to Oslo, Norway, to join the laboratory of Jan Jansen for a postdoc. His sheepish answer, delivered with his characteristic half-smile, was that Stent had already decided for him and he "didn't have a say in the matter." Wes's work with Jansen in the late 70s was foundational to the study of activity-dependent plasticity, and laid the foundation for Wes's work for the rest of his career. When Wes arrived at the University of Oslo, experiments had just been completed that described a dramatic and puzzling change from innervation of individual rat muscle fibers by several different motor neurons at birth to innervation by a single motor neuron some 2 weeks later (Brown et al., 1976). The process was named "synapse elimination." At the Oslo institute, Wes overlapped with Terje Lømo, a pioneer in studying activity-dependent plasticity in the nervous system. Influenced by ideas and works by Stent and Lømo, Wes was well aware of the important role neural activity played in the developing nervous system, particularly in the maturation of muscle fibers and their synaptic innervation. He thus spent his time in the Jansen lab, and much of his independent career, studying how activity shaped developmental synapse elimination using rodent neuromuscular junctions (NMJs) as a model system. Wes, Damien Kuffler, and Jan Jansen were the first to demonstrate in a heroic series of *in*

vivo experiments that blocking action potential conduction along nerves delayed or prevented synapse elimination in postnatal rats (Thompson et al., 1979). Perhaps the most important and impactful insight Wes and his work in Jansen's lab provided was that synapse elimination was a reflection of an active, competitive process among motor neurons innervating the same NMJ, rather than a passive, random process. Wes demonstrated this by surgically reducing the number of motor axons innervating a muscle shortly after birth, which led to a dramatic increase in the number of muscle fibers innervated by each of the spared motor neurons (Thompson and Jansen, 1977). The concept that developmental synapse elimination was competitive has been foundational to neuroscience and was further fleshed out in later studies by Lichtman and colleagues among others (Walsh and Lichtman, 2003; Schafer et al., 2012).

By reducing the number of motor neurons innervating skeletal muscles to understand the drivers of synapse elimination, Wes had also become interested in the process of sprouting, how the spared motor neurons expand their innervation of muscle fibers transiently denervated subsequent to injury. Wes found there was a limit to how much individual remaining motor neurons could expand their innervation. In the jargon of the field, he discovered that there was an upper limit to motor unit size which was about five times the typical number of muscle fibers innervated by a single motor neuron (Thompson and Jansen, 1977). Wes's findings also set a lower limit on how many motor neurons could be lost before muscle function was compromised. This work continues to have important implications for understanding neuromuscular diseases and injury, and the impact of these on muscle function, themes to which Wes and his lab would return later in his career.

RETURN TO TEXAS

Despite the lack of a prominent Texas drawl, Wes remained a Texan through and through. He longed to return to his home state as an independent scientist. Returning to the United States, Wes did a second postdoc in the laboratory of Dale Purves at Washington University in St. Louis. While in the Purves lab, Wes studied the reestablishment of synaptic connections after nerve injury in sympathetic ganglia as a model system (Purves and Thompson, 1979; Purves et al., 1981).

While in St. Louis, Wes would befriend Jeff Lichtman, who was a graduate student in the Purves lab at the time and would himself become a leader in the study of the role of activity as a modulator of synapse elimination. The two would spend the next three decades working on this topic, Wes at the University of Texas, later at Texas A&M University, and Jeff at Washington University and later at Harvard. These pioneering scientists produced many of the landmark studies that extend our understanding of the role of activity in shaping neural circuitry during development and plasticity in the reestablishment of innervation following nerve or muscle injury.

Wes's statement of his research interests, provided by the Searle Scholar Program, which recognized him as an exceptional young faculty, exemplifies Wes's style of communication—clear, to the point, and exceedingly modest. It reads: "Formation and Maintenance of Synaptic Connections: I am interested in the formation and maintenance of synaptic connections in the developing nervous system. In particular, I am investigating the remodeling [sic] of neuromuscular synapses which occurs in mammalian muscles during late fetal and early postnatal stages. I wish to understand how the different kinds of motor neurons and muscle fibers achieve their final differentiation and how the motor neurons come to selectively innervate the appropriate muscle fibers. In the course of this work, my lab has generated antibodies which recognize a novel component of the NMJ. An additional objective is to determine the identity of this component and its role in the differentiation of this synapse."

THE UNIVERSITY OF TEXAS YEARS

After about a year in the Purves lab, in 1979, Wes established his own research lab at the University of Texas in Austin, where his work continued to advance our understanding of how activity influences developmental synapse elimination using NMJs as a model system. By this time, it was well-recognized, from Wes's work and that of others, that the absolute levels of activity profoundly impacted the time course of neuromuscular synapse elimination. In his seminal 1983 *Nature* paper, Wes elegantly demonstrated that the activity patterns with which muscle fibers were stimulated shaped the time course of synapse elimination in developing muscles (Thompson, 1983). This was a key observation that suggested that pre- and postsynaptic activities were crucial drivers of competition. Additionally, his report lent support to the hypothesis that competitive synapse elimination occurred *via* a Hebbian mechanism: coordinate pre- and postsynaptic activity strengthened synapses, while dis-coordinate activity weakened synapses, perhaps, thus driving their loss. This hypothesis was tested in various ways over the years that followed, by Wes, his colleagues, and other labs, ultimately leading to the demonstration that the relative timing of action potentials impacts profoundly synaptic strength and synapse loss at neuromuscular (Personius and Balice-Gordon, 2001; Buffelli et al., 2002) and other synapses (e.g., Lorenzetto et al., 2009; Zhang et al., 2011).

Prior to Wes's work, programmed motor neuron cell death and muscle fiber addition during development had been proposed to drive neuromuscular synapse elimination (Harris, 1981; Nurcombe et al., 1981; Bennett et al., 1983). It had been argued that because motor neuron death preceded the removal of distal terminal axonal branches, downstream loss of their synapse with muscle fibers would inevitably occur. Similarly, because muscle fibers increase in number during early postnatal life, the hypothesis was posited that the postnatal emergence of new fibers would result in the shifting of synapses from multiple innervated fibers to new, as yet uninnervated fibers. Such change in synapse distribution could be mischaracterized as synapse elimination. Wes observed alterations to neither the number of motor units (the functional readout of the number of innervating motor neuron) nor the number of muscle fibers within a target muscle during the postnatal period of

synapse elimination (Balice-Gordon and Thompson, 1988b). He further showed that the tension generated by individual motor units decreased during this period, consistent with previous work (Brown et al., 1976). Wes's findings showed that each motor neuron reduced the number of muscle fibers it innervated as a consequence of synapse elimination, ruling out a change in motor neuron or muscle fiber number as factors in this process.

Despite the heterogeneity of muscle fiber types (e.g., defined by myosin heavy chain expression and/or contractile speed), each mature motor unit contains only a single muscle fiber type innervated by a motor neuron, whose firing pattern is functionally matched to the muscle fiber's contractile properties. Wes and others had demonstrated that motor unit fiber type homogeneity is present prior to the completion of synapse elimination (Thompson et al., 1984; Gordon and Van Essen, 1985; Balice-Gordon and Thompson, 1988b). To this day, it remains unclear how a homogeneous group of muscle fibers comes to reside within each mature motor unit. Despite variation in levels and pattern of activity, the contractile property of a given muscle—and even more remarkably, the distribution of fiber types within a muscle—shows limited variability among individuals of a species. Wes's demonstrations of the profound influence neuromuscular activity pattern has on muscle fiber contractile properties, in addition to the timing of neuromuscular synapse elimination (Thompson, 1983), raised an obvious question: What is the extent of muscle fiber autonomy in fiber type differentiation? To address this question, Wes needed antibodies that would differentiate muscle fiber types, which at the time were not available. He went about generating monoclonal antibodies—a substantial undertaking in the 1980s, and he even attended a Cold Spring Harbor Laboratory course on how to do so. While at Cold Spring Harbor Laboratory, Wes met Laura Silberstein, then a postdoc with Helen Blau, who would share with him the necessary antibody reagents to facilitate his experiments. Because innervation of adult muscles by foreign nerves (or direct stimulations that mimic such foreign innervation) resulted in dramatic changes in muscle fiber types (Buller et al., 1960; Lømo et al., 1974; Thompson, 1983), it had been assumed that developmental muscle fiber type differentiation was also innervation- and activity-dependent. Instead, Wes showed that muscle fiber type differentiation, and the pattern of fiber type distribution within developing muscles, occurred normally even in the absence of innervation (Condon et al., 1990). He also showed that while some muscles eventually degenerated if permanently denervated during development, in agreement with previous studies (e.g., Harris, 1981), secondary myogenesis occurred with normal timing in muscles that persisted. These findings, thus, illustrated a surprisingly significant degree of autonomy in the generation and differentiation of muscle fibers. In addition, as muscle fiber types can differentiate independently of the nervous system, motor axons are paired with fiber types of appropriate contractile properties within predestined "compartments" of developing muscles (Balice-Gordon and Thompson, 1988a).

A fortuitous by-product of Wes's efforts to generate muscle fiber type-specific monoclonal antibodies was the generation of clones that would take his career on a picturesque, and highly productive, detour: Wes himself, on a number of occasions, commented that although he was trained as an electrophysiologist, he had become more of a morphologist. As it turned out, some of the antibodies Wes generated recognized the intermediate filament nestin, a protein localized postsynaptically at NMJs (Astrow et al., 1992). Upon denervation induced by nerve injury, however, nestin expression is suppressed in postsynaptic muscle fibers. Instead, its expression is turned on in the reactive Schwann cells (SCs) that form the bands of Büngner within the nerve segment distal to the injury site as well as in the SCs that localize to junctions, called terminal SCs (Astrow et al., 1994; Kang et al., 2007). These SCs exhibited elaborate process extensions, called sprouts (Reynolds and Woolf, 1992), similar in pattern to the axonal sprouts extended by regrowing motor axons. In a series of elegant papers in the mid-1990s, Wes and his colleagues discovered novel aspects of cell–cell interactions among motor axons and SCs that were essential for the establishment and maintenance of muscle innervation as well as reinnervation after injury. Wes demonstrated that terminal SCs and their processes both stimulated and guided regenerating motor axons back to denervated postsynaptic sites on muscle fibers in adult rodents (Son and Thompson, 1995a,b). Wes further showed that reinnervation of neonatal muscles is poor because of the dependence of regenerating motor axons on terminal SC processes: he found that denervation of neonatal muscles rapidly led to apoptotic death of terminal SCs and that denervation-induced SC apoptosis was prevented by injection of recombinant soluble neuregulin 1 (Trachtenberg and Thompson, 1996). Thus, this work demonstrated that neonatal SCs require neuregulin 1-dependent trophic support from motor axons, unlike the SCs in adult animals. The essential role of neuregulin 1 from motor axons in SC development *in vivo* suggested by this study was later confirmed and extended by mouse genetic experiments (Woldeyesus et al., 1999; Wolpowitz et al., 2000; Yang et al., 2001).

Desiring a more detailed understanding of the terminal SC sprouting response, Wes undertook the generation of transgenic mouse lines in which SCs expressed green fluorescent protein (GFP) (Zuo et al., 2004). Bred to another transgenic mouse, whose motor axons were labeled with a spectrally distinct (cyan) fluorescent protein (Feng et al., 2000), mice with fluorescent SCs allowed repeated vital imaging of motor axons and terminal SCs at NMJs in normal muscles, during denervation and subsequent reinnervation. This work led to the demonstration that SC sprouts actually preceded and led the outgrowth of motor axons during reinnervation. Wes further showed that the coverage of denervated synaptic sites by remaining terminal SCs significantly influences which sites are reinnervated (Kang et al., 2003, 2019). The creation of mouse lines with fluorescent SCs also led to other unanticipated, but nonetheless exciting and impactful observations. The transgene used to fluorescently label SCs (*S100-eGFP*) is also expressed in other cell types, including in central nervous system astrocytes and microglia. It thus became possible to isolate nearly-pure populations of astrocytes from the brains of these transgenic mice for transcriptomic analysis, a feat first accomplished by the late Ben Barres (Cahoy et al., 2008). The astrocyte expression database made possible by the "off-label" use of Wes's fluorescent glial mice has become an invaluable resource

for countless neuroscientists all over the world. His trainees collectively delight in this inadvertent legacy of a neuroscientist who spent his career studying the peripheral nervous system and was determined to steer clear of the brain when conducting his work.

Wes's interest in NMJs extended to a quest to understand the mechanisms that underlie its morphological changes in aging and with diseases. The morphology of mature mammalian neuromuscular synapses is largely stable following the period of synapse elimination, with growth occurring by intercalary expansion as the muscle fibers grow. Several groups had observed that NMJs undergo conspicuous morphological changes as rodents age, becoming "fragmented" or "moth-eaten" in appearance, distinct from NMJs of young adult rodents (Balice-Gordon, 1997; Valdez et al., 2010; Li et al., 2011). It was believed that such dramatic change arose from incremental accumulation of small losses and additions of synaptic contacts at individual synapses, as mechanisms that ensure the stability of NMJs gradually waned with advancing age. However, following repeated *in vivo* imaging of NMJs from aged mice (Li et al., 2011), Wes found that junctional morphology is stable even in advanced age, with a large majority of junctions showing no changes to their morphology. He further found that a small fraction of junctions abruptly undergoes stochastic, wholesale morphologic changes, with the fraction of junctions that appear "fragmented" accumulating with age. He made the surprising observation that age-related morphologic changes in NMJs are instigated by the injury and subsequent regeneration of the innervated segment of muscle fibers. This was further corroborated by Wes's work that showed that similar rapid synaptic morphological changes occur in muscles from rodent models of Duchenne muscular dystrophy, as well as after deliberate muscle injury (Lyons and Slater, 1991; Li and Thompson, 2011; Haddix et al., 2018). Wes and his colleagues also studied mouse models of a severe form of the hereditary motor neuron disease spinal muscular atrophy (SMA). SMA results from low levels of the ubiquitously expressed protein survival of motor neuron (SMN). His group was among the first to demonstrate that, at least in these mice, SMA was not exclusively a motor neuron-autonomous disease, as specific muscles in SMA mice showed profound defects in neuromuscular development, even in the absence of any presynaptic deficits (Lee et al., 2011). With the recent approval of interventions that raise SMN levels in patient's motor neurons with ensuing remarkable clinical gains (Sumner and Crawford, 2018), Wes's work underscores the importance of continuing to study muscle function over time, to understand the contribution of postsynaptic muscle fibers to disease pathophysiology.

THE TEXAS A&M YEARS

In 2013, Jack McMahan, then head of the Biology Department at Texas A&M University, managed to convince Wes to move his lab "down the street" to College Station, TX, and join his department. And so, Wes became a Texas "Aggie" after more than 30 years as a fervent supporter of his beloved Texas "Longhorns." For those in the know about Texas, Texans, and their traditions, this was a significant switch of allegiances for a born-and-bred Texan.

Wes's contributions while at A&M were as impactful as those earlier in his career. He used *in vivo* imaging of transiently denervated endplates to demonstrate that the degree to which reinnervation recapitulates the original synaptic morphology is inversely correlated with the duration of denervation. Wes noted that terminal SCs gradually retract their processes from endplate regions with prolonged denervation (Kang et al., 2014). The topology of the remaining terminal SCs and their processes was found to determine the branching pattern of returning motor axon terminals and the redistribution of postsynaptic acetylcholine receptors, thus providing a mechanistic explanation for the junction remodeling observed following nerve injury. Neuregulin 1, in addition to its role as a nerve-derived trophic factor for neonatal SCs, can induce responses in these cells *in vivo* that mimic responses to denervation and/or modify the morphology of NMJs (Trachtenberg and Thompson, 1997; Hayworth et al., 2006; Lee et al., 2016). Based on these findings, Wes believed it was a distinct possibility that neuregulin 1 signaling and SCs play important roles in neuromuscular synapse elimination. Indeed, genetic modulation of motor neuron-derived membrane-bound neuregulin 1 expression, which normally peaks during the first two postnatal weeks, shifts the time course of synapse elimination (Lee et al., 2016). An ultrastructural examination of early postnatal NMJs revealed two key features of terminal SCs that had previously gone unnoticed and unappreciated: the intercalation of their processes into the synaptic cleft and the phagocytic engulfment of motor axon terminals in contact with developing muscle fibers by these cells (Smith et al., 2013). These neuregulin 1-driven terminal SC responses are not observed at normal junctions beyond the period of synapse elimination (Lee et al., 2017). Collectively, Wes's work suggests a model in which terminal SCs randomly remove presynaptic motor nerve terminals, leading to the rapid reoccupation of the transiently abandoned postsynaptic receptor site by a nearby, competing motor nerve terminal. This hypothesis provides additional cellular and mechanistic context for the activity-dependence of synapse elimination. It further demonstrates that peripheral glia are active mediators of neuromuscular synapse elimination, as is the case with astrocytes and microglia during activity-dependent synapse elimination in the central nervous system (Neniskyte and Gross, 2017; Wilton et al., 2019).

EMBRACING THE "THE PEANUT GALLERY"

Wes was passionate about science and committed to understanding how the nervous system develops and functions. His contributions have had a lasting impact in the fields of developmental and cellular neuroscience, providing fundamentally new insights into neuromuscular synapses in development and disease and revealing surprising facets of SC biology. Because of his efforts, we now have a better understanding of cellular and physiological mechanisms that

promote developmental synapse elimination, the autonomy of muscle fiber development, the molecular nature of SC–motor neuron trophic interdependence, and the SC behaviors that promote efficacious reinnervation of target muscle fibers and any accompanying morphological changes to the synapse. Wes was creative: he never limited his approach to a particular experimental model or technique, instead inventing and/or adopting tools and techniques along the way that were essential to asking the right question. Success did not alter Wes's humility or generosity, two values which were core to his personality and for which he was much loved by all who knew him. Despite his many accomplishments and accolades, Wes always felt that he was privileged to be making a living as a research scientist. Perhaps because of the ever-increasing difficulty with which one might secure research funding, Wes would occasionally say, while worrying about grant proposals, that he could "go be a farmer." Considering his affinity for growing things (in particular his love for and skill growing plumeria in his Texas garden), there is more than a grain of truth in those words. Yet, his passion for neuroscience—with his insightful, ask-the-right-question approach—was infectious. To the end of his life, Wes shared his love for a good research question—and the answer—with all who had the privilege of knowing him. Despite his penchant for playfully dismissing the lighthearted criticisms levied by his trainees and friends as noise from "the peanut gallery," Wes encouraged others to speak with candor—especially about science. Equally generous with his time and advice as he was passionate about science, Wes remained a lifelong mentor, advocate, and friend to his many students and postdocs. Wes tirelessly encouraged and nurtured the careers of his trainees, as well as those of junior faculty members he had mentored at his own and other institutions. Many of his trainees and mentees have gone on to productive careers as scientists, and some became attorneys, educators, and physicians. Wes also selflessly and tirelessly served the larger neuroscience community for many years as a reviewer on NIH study sections and as an instructor for the renowned summer Neurobiology course at the Marine Biological Laboratory in Woods Hall, MA. All of us are deeply indebted to Wes for his mentorship, advice about science and life, encouragement, generosity, and most of all, for his friendship. We mourned his passing and remain grateful for the gifts Wes gave us and the foundation for future research that his life's work has provided to us and to the field.

We end this piece with a touching note of condolences from Bill Kristan, "Wes was a wonderful scientist—smart, creative, great experimentalist—and an even better person. He was gentle and humble, always concerned about others more than himself. He was a thoroughly dependable and enjoyable friend. The world has too few like him; we will miss him greatly."

AUTHOR CONTRIBUTIONS

All authors listed have made a substantial, direct and intellectual contribution to the work, and approved it for publication.

ACKNOWLEDGMENTS

We thank Terje Lømo, Young-Jin Son, and especially Rita Balice-Gordon and Bill Kristan for reading and improving an initial version of this manuscript with their sample and informative suggestions and for sharing with us their recollections and thoughts on Wes's life and work.

REFERENCES

Astrow, S. H., Son, Y. J., and Thompson, W. J. (1994). Differential neural regulation of a neuromuscular junction-associated antigen in muscle fibers and schwann cells. *J. Neurobiol.* 25, 937–952. doi: 10.1002/neu.480250804

Astrow, S. H., Sutton, L. A., and Thompson, W. J. (1992). Developmental and neural regulation of a subsarcolemmal component of the rat neuromuscular junction. *J. Neurosci.* 12, 1602–1615. doi: 10.1523/JNEUROSCI.12-05-01602.1992

Balice-Gordon, R. J. (1997). Age-related changes in neuromuscular innervation. *Muscle Nerve Suppl.* 5, S83–87. doi: 10.1002/(SICI)1097-4598(1997)5+<83::AID-MUS20>3.0.CO;2-Z

Balice-Gordon, R. J., and Thompson, W. J. (1988a). The organization and development of compartmentalized innervation in rat extensor digitorum longus muscle. *J. Physiol.* 398, 211–231. doi: 10.1113/jphysiol.1988.sp017039

Balice-Gordon, R. J., and Thompson, W. J. (1988b). Synaptic rearrangements and alterations in motor unit properties in neonatal rat extensor digitorum longus muscle. *J. Physiol.* 398, 191–210. doi: 10.1113/jphysiol.1988.sp017038

Bennett, M. R., Mcgrath, P. A., Davey, D. F., and Hutchinson, I. (1983). Death of motorneurons during the postnatal loss of polyneuronal innervation of rat muscles. *J. Comp. Neurol.* 218, 351–363. doi: 10.1002/cne.902180311

Brown, M. C., Jansen, J. K., and Van Essen, D. (1976). Polyneuronal innervation of skeletal muscle in new-born rats and its elimination during maturation. *J. Physiol.* 261, 387–422. doi: 10.1113/jphysiol.1976.sp011565

Buffelli, M., Busetto, G., Cangiano, L., and Cangiano, A. (2002). Perinatal switch from synchronous to asynchronous activity of motoneurons: link with synapse elimination. *Proc. Natl. Acad. Sci. U. S. A.* 99, 13200–13205. doi: 10.1073/pnas.202471199

Buller, A. J., Eccles, J. C., and Eccles, R. M. (1960). Interactions between motoneurones and muscles in respect of the characteristic speeds of their responses. *J. Physiol.* 150, 417–439. doi: 10.1113/jphysiol.1960.sp006395

Cahoy, J. D., Emery, B., Kaushal, A., Foo, L. C., Zamanian, J. L., Christopherson, K. S., et al. (2008). A transcriptome database for astrocytes, neurons, and oligodendrocytes: a new resource for understanding brain development and function. *J. Neurosci.* 28, 264–278. doi: 10.1523/JNEUROSCI.4178-07.2008

Calabrese, R. L., Norris, B. J., and Wenning, A. (2016). The neural control of heartbeat in invertebrates. *Curr. Opin. Neurobiol.* 41, 68–77. doi: 10.1016/j.conb.2016.08.004

Condon, K., Silberstein, L., Blau, H. M., and Thompson, W. J. (1990). Differentiation of fiber types in aneural musculature of the prenatal rat hindlimb. *Dev. Biol.* 138, 275–295. doi: 10.1016/0012-1606(90)90197-Q

Feng, G., Mellor, R. H., Bernstein, M., Keller-Peck, C., Nguyen, Q. T., Wallace, M., et al. (2000). Imaging neuronal subsets in transgenic mice expressing multiple spectral variants of GFP. *Neuron* 28, 41–51. doi: 10.1016/S0896-6273(00)00084-2

Gordon, H., and Van Essen, D. C. (1985). Specific innervation of muscle fiber types in a developmentally polyinnervated muscle. *Dev. Biol.* 111, 42–50. doi: 10.1016/0012-1606(85)90433-6

Haddix, S. G., Lee, Y. I., Kornegay, J. N., and Thompson, W. J. (2018). Cycles of myofiber degeneration and regeneration lead to remodeling of the neuromuscular junction in two mammalian models of Duchenne muscular dystrophy. *PLoS ONE* 13:e0205926. doi: 10.1371/journal.pone.0205926

Harris, A. J. (1981). Embryonic growth and innervation of rat skeletal muscles. I. Neural regulation of muscle fibre numbers. *Philos. Trans. R Soc. Lond. B Biol. Sci.* 293, 257–277. doi: 10.1098/rstb.1981.0076

Hayworth, C. R., Moody, S. E., Chodosh, L. A., Krieg, P., Rimer, M., and Thompson, W. J. (2006). Induction of neuregulin signaling in mouse schwann cells in vivo mimics responses to denervation. *J. Neurosci.* 26, 6873–6884. doi: 10.1523/JNEUROSCI.1086-06.2006

Kang, H., Tian, L., Mikesh, M., Lichtman, J. W., and Thompson, W. J. (2014). Terminal schwann cells participate in neuromuscular synapse remodeling during reinnervation following nerve injury. *J. Neurosci.* 34, 6323–6333. doi: 10.1523/JNEUROSCI.4673-13.2014

Kang, H., Tian, L., Son, Y. J., Zuo, Y., Procaccino, D., Love, F., et al. (2007). Regulation of the intermediate filament protein nestin at rodent neuromuscular junctions by innervation and activity. *J. Neurosci.* 27, 5948–5957. doi: 10.1523/JNEUROSCI.0621-07.2007

Kang, H., Tian, L., and Thompson, W. (2003). Terminal schwann cells guide the reinnervation of muscle after nerve injury. *J. Neurocytol.* 32, 975–985. doi: 10.1023/B:NEUR.0000020636.27222.2d

Kang, H., Tian, L., and Thompson, W. J. (2019). Schwann cell guidance of nerve growth between synaptic sites explains changes in the pattern of muscle innervation and remodeling of synaptic sites following peripheral nerve injuries. *J. Comp. Neurol.* 527, 1388–1400. doi: 10.1002/cne.24625

Kristan, W. B. Jr., Calabrese, R. L., and Friesen, W. O. (2005). Neuronal control of leech behavior. *Prog. Neurobiol.* 76, 279–327. doi: 10.1016/j.pneurobio.2005.09.004

Lee, Y., Mikesh, M., Smith, I., Rimer, M., and Thompson, W. (2011). Muscles in a mouse model of spinal muscular atrophy show profound defects in neuromuscular development even in the absence of failure in neuromuscular transmission or loss of motor neurons. *Dev. Biol.* 356, 432–444. doi: 10.1016/j.ydbio.2011.05.667

Lee, Y. I., Li, Y., Mikesh, M., Smith, I., Nave, K. A., Schwab, M. H., et al. (2016). Neuregulin1 displayed on motor axons regulates terminal schwann cell-mediated synapse elimination at developing neuromuscular junctions. *Proc. Natl. Acad. Sci. U. S. A.* 113, E479–487. doi: 10.1073/pnas.1519156113

Lee, Y. I., Thompson, W. J., and Harlow, M. L. (2017). Schwann cells participate in synapse elimination at the developing neuromuscular junction. *Curr. Opin. Neurobiol.* 47, 176–181. doi: 10.1016/j.conb.2017.10.010

Li, Y., Lee, Y., and Thompson, W. J. (2011). Changes in aging mouse neuromuscular junctions are explained by degeneration and regeneration of muscle fiber segments at the synapse. *J. Neurosci.* 31, 14910–14919. doi: 10.1523/JNEUROSCI.3590-11.2011

Li, Y., and Thompson, W. J. (2011). Nerve terminal growth remodels neuromuscular synapses in mice following regeneration of the postsynaptic muscle fiber. *J. Neurosci.* 31, 13191–13203. doi: 10.1523/JNEUROSCI.2953-11.2011

Lømo, T., Westgaard, R. H., and Dahl, H. A. (1974). Contractile properties of muscle: control by pattern of muscle activity in the rat. *Proc. R Soc. Lond. B Biol. Sci.* 187, 99–103. doi: 10.1098/rspb.1974.0064

Lorenzetto, E., Caselli, L., Feng, G., Yuan, W., Nerbonne, J. M., Sanes, J. R., et al. (2009). Genetic perturbation of postsynaptic activity regulates synapse elimination in developing cerebellum. *Proc. Natl. Acad. Sci. U. S. A.* 106, 16475–16480. doi: 10.1073/pnas.0907298106

Lyons, P. R., and Slater, C. R. (1991). Structure and function of the neuromuscular junction in young adult mdx mice. *J. Neurocytol.* 20, 969–981. doi: 10.1007/BF01187915

Neniskyte, U., and Gross, C. T. (2017). Errant gardeners: glial-cell-dependent synaptic pruning and neurodevelopmental disorders. *Nat. Rev. Neurosci.* 18, 658–670. doi: 10.1038/nrn.2017.110

Nurcombe, V., Ncgrath, P. A., and Bennett, M. R. (1981). Postnatal death of motor neurons during the development of the brachial spinal cord of the rat. *Neurosci. Lett.* 27, 249–254. doi: 10.1016/0304-3940(81)90438-9

Personius, K. E., and Balice-Gordon, R. J. (2001). Loss of correlated motor neuron activity during synaptic competition at developing neuromuscular synapses. *Neuron* 31, 395–408. doi: 10.1016/S0896-6273(01)00369-5

Purves, D., and Thompson, W. (1979). The effects of post-ganglionic axotomy on selective synaptic connexions in the superior cervical ganglion of the guinea-pig. *J. Physiol.* 297, 95–110. doi: 10.1113/jphysiol.1979.sp013029

Purves, D., Thompson, W., and Yip, J. W. (1981). Re-innervation of ganglia transplanted to the neck from different levels of the guinea-pig sympathetic chain. *J. Physiol.* 313, 49–63. doi: 10.1113/jphysiol.1981.sp013650

Reynolds, M. L., and Woolf, C. J. (1992). Terminal Schwann cells elaborate extensive processes following denervation of the motor endplate. *J. Neurocytol.* 21, 50–66. doi: 10.1007/BF01206897

Schafer, D. P., Lehrman, E. K., Kautzman, A. G., Koyama, R., Mardinly, A. R., Yamasaki, R., et al. (2012). Microglia sculpt postnatal neural circuits in an activity and complement-dependent manner. *Neuron* 74, 691–705. doi: 10.1016/j.neuron.2012.03.026

Smith, I. W., Mikesh, M., Lee, Y., and Thompson, W. J. (2013). Terminal schwann cells participate in the competition underlying neuromuscular synapse elimination. *J. Neurosci.* 33, 17724–17736. doi: 10.1523/JNEUROSCI.3339-13.2013

Son, Y. J., and Thompson, W. J. (1995a). Nerve sprouting in muscle is induced and guided by processes extended by schwann cells. *Neuron* 14, 133–141. doi: 10.1016/0896-6273(95)90247-3

Son, Y. J., and Thompson, W. J. (1995b). Schwann cell processes guide regeneration of peripheral axons. *Neuron* 14, 125–132. doi: 10.1016/0896-6273(95)90246-5

Sumner, C. J., and Crawford, T. O. (2018). Two breakthrough gene-targeted treatments for spinal muscular atrophy: challenges remain. *J. Clin. Invest.* 128, 3219–3227. doi: 10.1172/JCI121658

Thompson, W. (1983). Synapse elimination in neonatal rat muscle is sensitive to pattern of muscle use. *Nature* 302, 614–616. doi: 10.1038/302614a0

Thompson, W., and Jansen, J. K. (1977). The extent of sprouting of remaining motor units in partly denervated immature and adult rat soleus muscle. *Neuroscience* 2, 523–535. doi: 10.1016/0306-4522(77)90049-5

Thompson, W., Kuffler, D. P., and Jansen, J. K. (1979). The effect of prolonged, reversible block of nerve impulses on the elimination of polyneuronal innervation of new-born rat skeletal muscle fibers. *Neuroscience* 4, 271–281. doi: 10.1016/0306-4522(79)90088-5

Thompson, W. J., and Stent, G. S. (1976a). Neuronal control of heartbeat in the medicinal leech. *I. Generation of the vascular constriction rythm by heart motor neurons. J. Comp. Physiol.* 111, 261–279. doi: 10.1007/BF00606468

Thompson, W. J., and Stent, G. S. (1976b). Neuronal control of heartbeat in the medicinal leech. *II. Intersegmental coordination of heart motor neuron activity by heart interneurons. J. Comp. Physiol.* 111, 281–307. doi: 10.1007/BF00606469

Thompson, W. J., and Stent, G. S. (1976c). Neuronal control of heartbeat in the medicinal leech. *III. Synaptic relations of heart interneurons. J. Comp. Physiol.* 111, 309–333. doi: 10.1007/BF00606470

Thompson, W. J., Sutton, L. A., and Riley, D. A. (1984). Fibre type composition of single motor units during synapse elimination in neonatal rat soleus muscle. *Nature* 309, 709–711. doi: 10.1038/309709a0

Trachtenberg, J. T., and Thompson, W. J. (1996). Schwann cell apoptosis at developing neuromuscular junctions is regulated by glial growth factor. *Nature* 379, 174–177. doi: 10.1038/379174a0

Trachtenberg, J. T., and Thompson, W. J. (1997). Nerve terminal withdrawal from rat neuromuscular junctions induced by neuregulin and schwann cells. *J. Neurosci.* 17, 6243–6255. doi: 10.1523/JNEUROSCI.17-16-06243.1997

Valdez, G., Tapia, J. C., Kang, H., Clemenson, G. D. Jr., Gage, F. H., Lichtman, J. W., et al. (2010). Attenuation of age-related changes in mouse neuromuscular synapses by caloric restriction and exercise. *Proc. Natl. Acad. Sci. U.S.A.* 107, 14863–14868. doi: 10.1073/pnas.1002220107

Walsh, M. K., and Lichtman, J. W. (2003). *In vivo* time-lapse imaging of synaptic takeover associated with naturally occurring synapse elimination. *Neuron* 37, 67–73. doi: 10.1016/S0896-6273(02)01142-X

Weisblat, D., and Thompson, W. (2008). Gunther stent. *Curr. Biol.* 18, R585–R587. doi: 10.1016/j.cub.2008.06.056

Wilton, D. K., Dissing-Olesen, L., and Stevens, B. (2019). Neuron-glia signaling in synapse elimination. *Annu. Rev. Neurosci.* 42, 107–127. doi: 10.1146/annurev-neuro-070918-050306

Woldeyesus, M. T., Britsch, S., Riethmacher, D., Xu, L., Sonnenberg-Riethmacher, E., Abou-Rebyeh, F., et al. (1999). Peripheral nervous system defects in erbB2 mutants following genetic rescue of heart development. *Genes. Dev.* 13, 2538–2548. doi: 10.1101/gad.13.19.2538

Wolpowitz, D., Mason, T. B., Dietrich, P., Mendelsohn, M., Talmage, D. A., and Role, L. W. (2000). Cysteine-rich domain isoforms of the neuregulin-1 gene are required for maintenance of peripheral synapses. *Neuron* 25, 79–91. doi: 10.1016/S0896-6273(00)80873-9

Yang, X., Arber, S., William, C., Li, L., Tanabe, Y., Jessell, T. M., et al. (2001). Patterning of muscle acetylcholine receptor gene expression in the absence of motor innervation. *Neuron* 30, 399–410. doi: 10.1016/S0896-6273(01)00287-2

Zhang, J., Ackman, J. B., Xu, H. P., and Crair, M. C. (2011). Visual map development depends on the temporal pattern of binocular activity in mice. *Nat. Neurosci.* 15, 298–307. doi: 10.1038/nn.3007

Zuo, Y., Lubischer, J. L., Kang, H., Tian, L., Mikesh, M., Marks, A., et al. (2004). Fluorescent proteins expressed in mouse transgenic lines mark subsets of glia, neurons, macrophages, and dendritic cells for vital examination. *J. Neurosci.* 24, 10999–11009. doi: 10.1523/JNEUROSCI.3934-04.2004

Conflict of Interest: The authors declare that the research was conducted in the absence of any commercial or financial relationships that could be construed as a potential conflict of interest.

Copyright © 2020 Lee and Rimer. This is an open-access article distributed under the terms of the Creative Commons Attribution License (CC BY). The use, distribution or reproduction in other forums is permitted, provided the original author(s) and the copyright owner(s) are credited and that the original publication in this journal is cited, in accordance with accepted academic practice. No use, distribution or reproduction is permitted which does not comply with these terms.

frontiers in Molecular Neuroscience

ORIGINAL RESEARCH
published: 23 June 2020
doi: 10.3389/fnmol.2020.00107

Effects of ASC Application on Endplate Regeneration Upon Glycerol-Induced Muscle Damage

*Matteo Rigon[1], Sarah Janice Hörner[1], Tatjana Straka[1], Karen Bieback[2], Norbert Gretz[3,4], Mathias Hafner[1,4] and Rüdiger Rudolf[1,4,5]**

[1] Institute of Molecular and Cell Biology, Mannheim University of Applied Sciences, Mannheim, Germany, [2] Institute of Transfusion Medicine and Immunology, Medical Faculty Mannheim, Heidelberg University, Mannheim, Germany, [3] Medical Research Center, Medical Faculty Mannheim, Heidelberg University, Mannheim, Germany, [4] Institute of Medical Technology, Medical Faculty Mannheim, Mannheim University of Applied Sciences, Mannheim, Germany, [5] Interdisciplinary Center for Neurosciences, Heidelberg University, Heidelberg, Germany

Amongst other approaches, adipose-derived stromal cells (ASCs) have recently been tested with respect to their regenerative capacity for treatment of neuromuscular disorders. While beneficial effects of ASCs on muscle recovery were observed previously, their impact on regeneration of neuromuscular junctions (NMJs) is unclear. Here, we used a murine glycerol damage model to study disruption and regeneration of NMJs and to evaluate the effects of systemic application of ASCs on muscle and NMJ recovery. In mice that were not treated with ASCs, a differential response of NMJ pre- and post-synapses to glycerol-induced damage was observed. While post-synapses were still present in regions that were necrotic and lacking actin and dystrophin, pre-synapses disappeared soon in those affected areas. Partial regeneration of NMJs occurred within 11 days after damage. ASC treatment slightly enhanced NMJ recovery and reduced the loss of presynaptic sites, but also led to a late phase of muscle necrosis and fibrosis. In summary, the results suggest a differential sensitivity of NMJ pre- and post-synapses to glycerol-induced muscle damage and that the use of ASC for the treatment of neuromuscular disorders needs further careful evaluation.

Keywords: glycerol, skeletal muscle, NMJ, ASC, regeneration

OPEN ACCESS

Edited by:
Hanns Lochmuller,
University of Ottawa, Canada

Reviewed by:
Claire Legay,
Université Paris Descartes, France
Mohammed Akaaboune,
University of Michigan, United States

Correspondence:
Rüdiger Rudolf
r.rudolf@hs-mannheim.de

Received: *25 January 2020*
Accepted: *20 May 2020*
Published: *23 June 2020*

Citation:
Rigon M, Hörner SJ, Straka T, Bieback K, Gretz N, Hafner M and Rudolf R (2020) Effects of ASC Application on Endplate Regeneration Upon Glycerol-Induced Muscle Damage. Front. Mol. Neurosci. 13:107. doi: 10.3389/fnmol.2020.00107

INTRODUCTION

Despite decades of research and numerous trials, the treatment options for most neuromuscular disorders are still disappointing. While the number of drugs approved or in clinical trials has strongly risen in the past decade (Cowling and Thielemans, 2020) the development of stem-cell based therapies is another important line of activity in this context. The hope is, that stem cells might enable direct tissue regeneration *in vivo* (Gois et al., 2019). At present, different stem cell sources are being tested, including autologous or heterologous muscle-derived stem

cells, mesangioblasts, muscle-derived progenitors, interstitial cells, and mesenchymal stromal/stem cells (Gois et al., 2019). The latter group includes adipose-derived stromal cells (ASCs), that are interesting as a source of stem cells, because besides being immune-privileged they are readily accessible from lipoaspirates and can be easily isolated and expanded in vitro (Kern et al., 2006; Torres-Torrillas et al., 2019). It remains open whether their local or systemic application might be more beneficial for the treatment of neuromuscular disorders. While local injection might come with a higher potential for targeted cell integration, it is difficult to achieve for diseases where different organs or large parts of the body are affected, as it is true for most neuromuscular disorders (Gois et al., 2019). On the other hand, while systemic application might have a drawback in the entrapment of most injected cells in organs such as lungs and liver (Gois et al., 2019) recent studies suggest that a principal function of stem cell therapies relies in their modulatory activities on cellular signaling rather than direct cell engraftment (Gorecka et al., 2018; Boldyreva et al., 2019; Mitchell et al., 2019; Torres-Torrillas et al., 2019). Although in different animal models and clinical applications beneficial effects of stem cell grafts on recovery of muscle tissue were reported (Forcales, 2015; Torres-Torrillas et al., 2019), little emphasis has been put on their impact at the level of the neuromuscular junction (NMJ).

In order to study skeletal muscle recovery mechanisms, several muscle damage models have been developed (Arnold et al., 2007; McCarthy et al., 2011; Czerwinska et al., 2012; Iwata et al., 2013; Tiryakioglu et al., 2015; Hardy et al., 2016; Mahdy, 2018). Those models differ in the injury mechanism and in the type of harm caused, affecting the degrees of degeneration and regeneration capabilities of the muscle. Among those, glycerol was reported to cause a damage by osmotic shock, affecting not only myofibers but also other muscle elements, including the basal lamina (Kawai et al., 1990; Pisani et al., 2010; Mahdy et al., 2015). This leads to an impaired regeneration with ectopic infiltration of adipocytes and fibrosis (Lluís et al., 2001; Mahdy et al., 2015, 2016; Hardy et al., 2016) and deprives the regenerating muscle cells of the interaction with extra-cellular matrix (ECM) elements that can enhance tissue recovery (Murphy et al., 2011; Iwata et al., 2013; Webster et al., 2015). Although characterized by a severe initial destruction, muscles treated with intra-muscular glycerol injection are able to recover anyway (Arsic et al., 2004; Mahdy et al., 2015, 2016). This suggested that glycerol injection might be a model well suited for the study of muscle regeneration. Accordingly, to investigate de- and regeneration of NMJs in the absence and presence of systemic ASC administration, a glycerol-induced muscle damage model was chosen. Upon toxin- or chemical-induced injury, muscle necrosis and fibrosis take place. Necrotic muscle cells, due to their compromised plasma membrane, allow the uptake of serum proteins, including immunoglobulins, into the cytosol (Iwata et al., 2013; Judson et al., 2013; Proto et al., 2015; Arecco et al., 2016; Rodrigues et al., 2016), rendering immunofluorescence against immunoglobulin G (mIgG) useful to identify necrotic areas. Necrotic leakage and linked degradative processes can also lead to the loss of dominant cytosolic skeletal muscle proteins, such as f-actin (Huang and Gopalakrishnakone, 1996) and dystrophin (Biral et al., 2000). Muscle fibrosis is characterized by deposition of collagen type I (Gibertini et al., 2014), one of the major components of ECM (Huebner et al., 2008; Serrano and Muñoz-Cánoves, 2010; Gillies and Lieber, 2011; Feng et al., 2019). Following muscle degeneration, muscle recovery involves detection of regenerating myofibers, which are characterized by the expression of embryonic myosin heavy chain (eMHC, also known as myosin 3) (Schiaffino et al., 1986; Murphy et al., 2011; Judson et al., 2013; McDonald et al., 2015; Kastenschmidt et al., 2019) and by nuclei in central position (in the following, referred to as center-nucleated fibers, CNFs) (Judson et al., 2013; McDonald et al., 2015; Arecco et al., 2016; Kastenschmidt et al., 2019). In order to monitor NMJ degradation and recovery, markers for pre- and post-synapses were analyzed. While vesicular acetylcholine transporter (VAChT) is localized to small synaptic vesicles at the endplate terminal (Maeda et al., 2004; Sugita et al., 2016), acetylcholine receptor (AChR) is highly enriched at the postsynaptic membrane of NMJs (Fambrough et al., 1979).

The present study aimed at developing and characterizing a reliable glycerol-based de/regeneration model and to apply this for the analysis of potential effects of ASCs on regeneration of muscle and NMJs. Using the glycerol damage paradigm, we obtained differential profiles for pre- and postsynaptic destruction and recovery. While post-synapses appeared to remain relatively stable even upon heavy muscle fiber damage and loss of internal structures, presynaptic contacts were severely affected upon glycerol injection and needed to recover over a couple of days. Treatment with ASCs led to a slightly reduced loss of post-synapses and improvement of pre- to postsynapse match upon glycerol treatment, but these intermediate effects were reverted during a second phase of inflammation.

MATERIALS AND METHODS

Glycerol and Stem Cell Injection

All animal experiments were conducted in accordance with the German Animal Protection Law and approved by the local authority (Regierungspräsidium Nordbaden, Karlsruhe/Germany in agreement with EU guideline 2010/63/EU; license G-139/18). In order to induce muscle damage, 20 μl of a 50% glycerol solution diluted in physiological saline were injected into the tibialis anterior (TA) muscle of anesthetized 2 months old C57BL6 female mice. The decision to use female arose from two observations: first, females are experimentally easier to handle, since animals should preferentially be kept in groups for social interactions, but males under these circumstances often bite each other and this can lead to damage of muscles that is not due to the experimental protocol. Second, females seem to possess a slightly better regenerative capability (Deasy et al., 2007; Kitajima and Ono, 2016). The same volume of saline solution was injected contralaterally as a sham. The animals were then euthanized by cervical dislocation after 18 h or 3, 5, 8, or 11 days following the procedure and the

muscles were dissected. Where ASCs were applied, one million cells diluted in 100 μl of sterile PBS where injected via tail vein directly after glycerol treatment. In this case, animals were euthanized by cervical dislocation and dissected 3, 5, and 11 days after the injection. At least three animals for each timepoint and condition (glycerol and ASC with glycerol) were analyzed.

Human Adipose-Derived Mesenchymal Stem Cells

Adipose-derived stromal cells were isolated from adult adipose tissue obtained from lipoaspirates of healthy donors, after obtained informed consent (Mannheim Ethics Commission II vote numbers 2010-262 N-MA, 2009-210 N-MA, 49/05 and 48/05), as described before (Bieback et al., 2012). Briefly, the lipoaspirate was washed with sterile PBS to remove cellular debris and red blood cells and digested with 0.15% w/v collagenase type I (Sigma-Aldrich, Munich, Germany), for 45 min at 37°C. After washing, the pellet was resuspended in medium (DMEM low glucose, 10% human AB serum, 100 U/ml penicillin, 0.1 mg/ml streptomycin and 4 mM L-glutamine), plated and incubated overnight at 37°C, 5% CO_2. After 1 day, the non-adherent and red blood cells were removed. Expanded cells were characterized regarding their proliferation capacity, immune phenotype, and adipo- and osteogenic differentiation potential, as described previously (Bieback et al., 2012). Before injection, ASCs were seeded at 750 ASC/cm^2 and expanded. On injection days, ASCs were trypsinized for 5 min at 37°C and washed once with medium. The ASC pellet was then resuspended in sterile PBS at a concentration of 1×10^7 cells/ml shortly before the injection.

Immunofluorescence Analysis

Freshly after dissection, TA muscles were covered with a thin layer of Frozen Section Compound (Leica) and frozen on liquid nitrogen. Transverse cryosections of 15–20 μm thickness were cut using a Leica CM1950 cryostat, carefully positioned on glass microscope slides (Thermo Fisher Scientific) and then immunostained for epitope detection. Cryosections were permeabilized with 0.1% TritonX-100/PBS for 10 min at room temperature and, after three washing steps in PBS (5 min each), incubated with 2% BSA/PBS for 2 h to avoid unspecific binding of primary antibodies. The sections were then incubated overnight at +4°C with primary antibodies diluted in 2% BSA/PBS. After three washing steps in 2% BSA/PBS, sections were incubated with the secondary antibodies/dyes/toxins in 2% BSA/PBS for 3 h at room temperature and in the darkness. Antibodies, dyes, and dilution rates are listed in **Table 1**. Subsequently, after 15 min incubation with DAPI (Sigma) in 2 % BSA/PBS and three more washing steps with PBS, glass slides were left to briefly dry and then mounted in Mowiol. The samples were then analyzed at the confocal microscope the day after. Images were taken using a Leica TCS SP8 microscope equipped with 405, 488, 555, and 633 nm lasers, and Leica HC PLAN APO 20×/0.75 IMM CORR CS2 objective and at z-steps of 3 μm. For every sample, three to five entire cryosections from the central portion of the muscle at an intersection interval of roughly 200 μm were visualized. Staining of ASCs used a slightly modified protocol as follows. Cells on Eppendorf 8 chamber cell imaging slides were briefly fixed with 2% PFA/PBS and then permeabilized with 0.1% TritonX-100/PBS for 5 min at room temperature and, after three washing steps in PBS (5 min each), incubated with 2% BSA/PBS for 1 h. Subsequently, cells were incubated overnight at 4°C with primary antibody diluted in 2% BSA/PBS. After three washing steps in 2% BSA/PBS, cells were incubated with the secondary antibody and DAPI diluted in 2% BSA/PBS for 45 min and in the darkness. After three more washing steps with PBS and one with ddH_2O, the slides were mounted in Mowiol and analyzed using the same microscope and objective used for the muscle

TABLE 1 | List of used antibodies and dyes.

	Company	Catalog number	Lot number	Dilution rate
Primary antibody				
Anti-Dystrophin antibody	Invitrogen	PA 1-21011	TK2665551J	1:200
Anti-Myosin 3 antibody	Biorbyt	orb385438	RBQ34	1:100
Anti-VAChT antibody	Synaptic Systems	139 103	2-44	1:500
Anti-Collagen type I antibody	Rockland	600-401-103-0.1	40681	1:500
Recombinant anti-Ku80 antibody (EPR3468)	Abcam	GR3216586-3	ab80592	1:300
Secondary antibody/marked toxins/dyes				
Donkey anti-Rabbit IgG (H + L) Highly Cross-Adsorbed Secondary Antibody, Alexa Fluor 488	Thermo Fisher Scientific	A-21206	176375	1:500
Donkey anti-Rabbit IgG (H + L) Highly Cross-Adsorbed Secondary Antibody, Alexa Fluor 488	Thermo Fisher Scientific	A-21206	176375	1:500
Goat anti-Rabbit IgG (H + L) Cross-Adsorbed ReadyProbes Secondary Antibody, Alexa Fluor 594	Thermo Fisher Scientific	R37117	1875978	1:500
F(ab')2-Goat anti-Rabbit IgG (H+L) Cross-Adsorbed Secondary Antibody, Alexa Fluor 647	Thermo Fisher Scientific	A-21246	55002A	1:500
Goat anti-Mouse IgG (H + L) Highly Cross-Adsorbed Secondary Antibody, Alexa Fluor 555	Thermo Fisher Scientific	A-21424	1802436	1:500
Goat anti-Mouse IgG (H + L) Cross-Adsorbed Secondary Antibody, Alexa Fluor 488	Thermo Fisher Scientific	A-11001	1834337	1:500
α-Bungarotoxin, Alexa Fluor 488 conjugate	Thermo Fisher Scientific	B13422	1750294	1:500
α-Bungarotoxin, Alexa Fluor 555 conjugate	Thermo Fisher Scientific	B35451	1880574	1:500
Alexa Fluor 555 Phalloidin	Thermo Fisher Scientific	A34055	1780358	1:500
DAPI	Sigma-Aldrich	D9542	28114320	1:1000

cryosections. Antibodies, dyes, and dilution rates are listed in **Table 1**.

Semi-Automated Quantification

Confocal images obtained from muscles cryosections were processed and analyzed using ImageJ (FIJI version). From maximum projections of the images, areas which showed the presence of mIgG, collagen I, or actin were manually thresholded, areas selected and measured. The entire area of the cryosection was contoured by hand using the background signal. The areas where dystrophin-outlined cells were present were obtained from maximum projected confocal images to which a median filter was applied and then thresholded. Subsequently the "analyze particles" function of ImageJ was used (selecting 20 μm as lowest value and including holes). The image obtained was then measured. Muscle fibers, CNFs, and eMHC+ fibers were counted manually. For each sample, a minimum of three cryosections was processed and analyzed. NMJs, identified by AChR and VAChT expression together with their shape and/or position with respect to muscle fibers, were analyzed and quantified manually. Where indicated, the areas positive for AChR and/or VAChT (per endplate) were thresholded, segmented and measured. Numbers of analyzed synapses are given in **Supplementary Table S1**. Signals for pre- and post-synapses obtained from three different cryosections per sample were analyzed. For the Ku80 detection, DAPI signals corresponding to cell nuclei were thresholded and segmented. A selection created from those signals was then used to hand-segment the Ku80+ signals, selecting those areas where it was colocalizing within cell nuclei.

Statistical Analysis and Figure Compilation

For statistical analysis, data were first screened for normality and homoscedasticity using Kolmogorov–Smirnov test and F-test. Mean and SD/SEM were calculated. Then, significance was assessed with Student's *t*-test or Welch test. Data compilation was done in Microsoft Excel for Mac, plots were made using either Microsoft Excel for Mac or Graph Pad Prism. Figures were prepared in Adobe Photoshop and then compiled in Adobe Illustrator.

RESULTS

Glycerol Injection Leads to Robust Muscle Necrosis With Fast Regeneration

To understand the effects of glycerol injection on muscle integrity and regeneration, a panel of markers for muscle necrosis, function, and regeneration was analyzed. Therefore, TA muscles were injected with 20 μl of either saline (control) or glycerol and then muscles were harvested after 18 h and 3, 5, 8, and 11 days. Sliced muscles were co-stained with DAPI for nuclei and antibodies against mouse IgG, collagen I, dystrophin, or eMHC to assess the status of necrosis, fibrosis, muscle fiber integrity, and regeneration. Co-staining with phalloidin served to visualize the presence of f-actin. Confocal images of these sections revealed a massive muscle damage already after 18 h of glycerol injection (**Supplementary Figure S1**). As shown in **Figure 1** and **Supplementary Figure S2**, after 3 days of injury due to glycerol injection involved large parts of muscles and was characterized by passage of immunoglobulins through sarcolemma, enhanced accumulation of collagen I, and loss of the functional markers, dystrophin and f-actin. Subsequently, these signs of muscle damage progressively decreased and were followed by a wave of eMHC expression, principally between days 5 and 8 after glycerol injection. On day 11 after glycerol treatment, muscles had largely reassumed their normal appearance lacking degeneration and regeneration markers and showing regular distribution of dystrophin and f-actin. Also, numbers of muscle fibers, that were significantly decreased on day 3 post glycerol injection, were comparable to saline-treated muscles at day 11 (**Figure 1C**). Cross-sectional areas of remaining fibers did not vary between the different experimental groups (**Supplementary Table S2**). The only clear sign of ongoing muscle regeneration at 11 days post injection was the presence of CNFs that rose from less than 1% in control conditions to around 40% on days 5 and 8 after glycerol injection and decreased to roughly 25% on day 11. In summary, the glycerol injection paradigm displayed a simple, regular, and controlled sequence of muscle damage and regeneration. In the following, we used this model to address NMJ degeneration and regeneration.

Glycerol Injection Induces a Transient Loss of Pre-synapses

To visualize the effect of glycerol injection on NMJs, TA muscles injected with either glycerol or saline (control) were taken at days 3, 5, 8, and 11 after injection. Slices were stained against postsynaptic nicotinic AChR and presynaptic VAChT with fluorescent α-bungarotoxin (αBGT) and anti-VAChT antibody, respectively. Confocal microscopy analysis of these samples revealed that while AChR+ sites were present at all timepoints, many of these were negative for VAChT at 3, 5, and 8 days post glycerol injection (**Figure 2A**). Quantitative analysis confirmed that in glycerol-treated muscles, the number of AChR+ sites per sample was slightly but not significantly reduced (**Figure 2B**) compared to saline-treated controls. The size of synaptic regions was unaltered (**Supplementary Table S3**). The only exception was at 11 days post injection, where a higher amount of post-synapses was detected in the control samples than at the other timepoints. With respect to VAChT- and AChR-double positive synapses, glycerol-treated muscles showed significantly lower values between days 3 and 8 post injection as compared to saline samples (**Figure 2C**). These data suggest that glycerol, although affecting both pre- and postsynaptic sites, had a more detrimental impact on the presynaptic component.

Kinetics of Glycerol-Induced Muscle Damage and Regeneration Are Altered by ASCs

The second goal of this study was to address the effect of ASCs on muscle and NMJ regeneration. Thus, directly after intra-muscular application of either saline or glycerol,

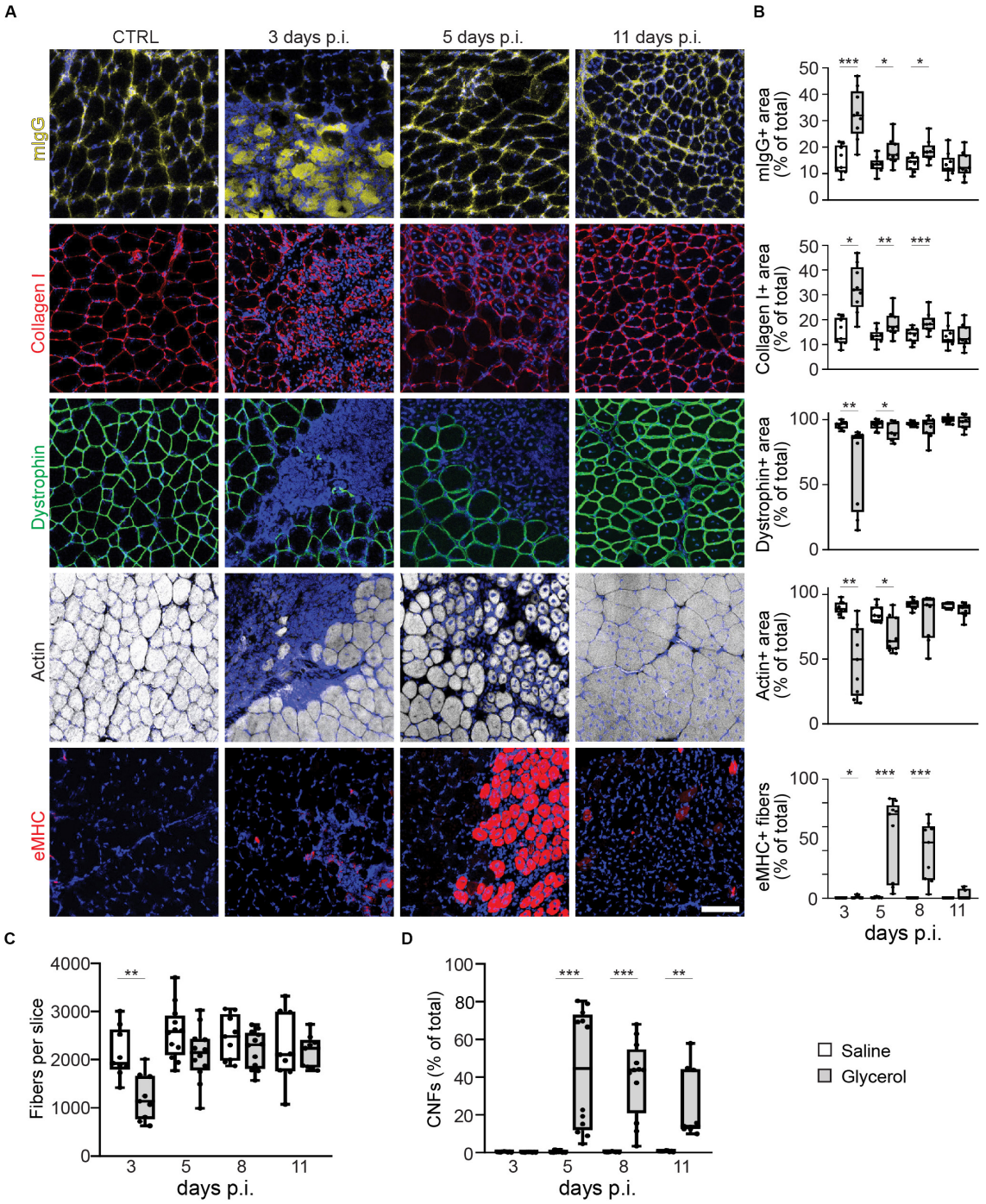

FIGURE 1 | Glycerol-induced muscle damage leads to early necrosis, loss of dystrophin and actin, transient eMHC appearance, and prolonged presence of center-nucleated fibers. TA muscles were injected with 20 μl of either saline or glycerol and then harvested and snap frozen after3, 5, 8, or 11 days post-injection (days p.i.). Upon cryosectioning, muscle slices were stained with DAPI and either antibodies against mouse IgG (mIgG), collagen I, dystrophin, or embryonic myosin heavy chain (eMHC), or with phalloidin-TRITC to label actin. Sections were analyzed by confocal microscopy. **(A)** Representative optical sections of fluorescence signals as indicated, nuclear DAPI staining always shown in blue, mIgG in yellow, collagen I and eMHC in red, dystrophin in green, actin in gray. CTRL, saline-injected muscles at 3 days p.i., the other panels depict glycerol-injected muscles at3, 5, and 11 days p.i., as indicated. Scalebar, 100 μm. **(B)** Quantitative analysis of section areas positive for fluorescence signals of either mIgG, collagen I, dystrophin, or actin, or number of eMHC-positive fibers, as a function of days p.i. Box–Whisker plots show all individual data points as dots, the extensions of upper and lower quartiles in the boxes, the medians as horizontal lines in the boxes, and maxima and minima as whiskers. $^{*}p \leq 0.05$, $^{**}p \leq 0.01$, $^{***}p \leq 0.001$. **(C,D)** Quantitative analysis of fibers per muscle slice **(C)** or CNFs (% of fiber number, **D**) as a function of days p.i. Box–Whisker plots show all individual data points as dots, the extensions of upper and lower quartiles in the boxes, the medians as horizontal lines in the boxes, and maxima and minima as whiskers. $^{**}p \leq 0.01$, $^{***}p \leq 0.001$.

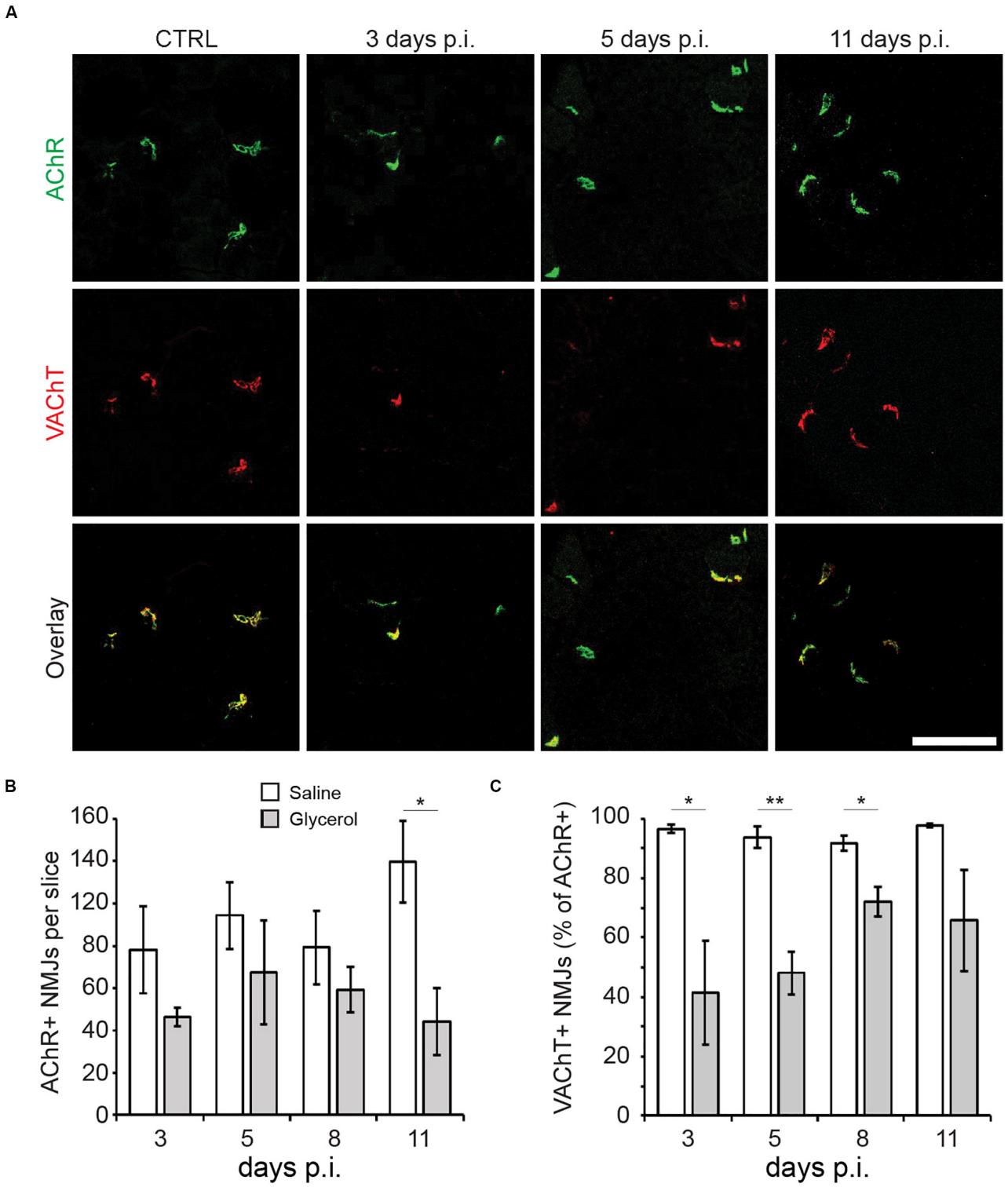

FIGURE 2 | Glycerol injection primarily affects pre-synapses. TA muscles were injected with 20 μl of either saline or glycerol and then harvested and snap frozen after 3, 5, 8, or 11 days (days p.i.). Upon cryosectioning, muscle slices were stained with αBGT (for AChR detection) and antibodies against VAChT to label post- and presynaptic portions of NMJs, respectively. Sections were analyzed by confocal microscopy. **(A)** Representative optical sections of fluorescence signals as indicated, αBGT in green, VAChT in red, yellow in overlay images indicates colocalization of both signals. CTRL, saline-injected muscles at 3 days p.i., the other panels depict glycerol-injected muscles at 3, 5, and 11 days p.i., as indicated. Scalebar, 100 μm. **(B,C)** Quantitative analysis of αBGT+ postsynaptic sites per slice **(B)** and VAChT+ NMJs (% of αBGT+ structures, **C**) as a function of days p.i. Shown is mean ± SEM (n = 3 muscles). $^{*}p \leq 0.05$, $^{**}p \leq 0.01$.

ASCs were administered systemically via the tail vein. Then, microscopic analysis was performed to evaluate the consequences of ASC treatment on muscle de- and regeneration. Therefore, muscles were harvested at days 3, 5, and 11 post injection and then sliced. Sections were stained for nuclei and mouse IgG, collagen I, dystrophin, eMHC, or f-actin. While fiber numbers, dystrophin and f-actin results were similar to the samples not treated with ASCs, the data for mIgG, collagen I, eMHC, and CNFs showed interesting differences (**Figure 3** and **Supplementary Figure S3**). Indeed, mIgG and collagen I signals came up at 11 days post glycerol injection and the staining of eMHC showed a basal expression of this regeneration marker in saline-treated muscles. Finally, in glycerol plus ASC-treated animals the number of CNFs continued to increase over time to around 71.4 ± 15.8% (mean ± SEM, n = 3 muscles) at day 11 post injection, while it remained low in corresponding saline controls (0.6 ± 0.7%, mean ± SEM, n = 3 muscles). In summary, these results suggested that ASC application induced a late-phase inflammatory response and basal regenerative processes.

ASC Transiently Mitigate Loss of Pre-synapses in the Glycerol Model

Finally, the effects of ASC treatment on NMJs were quantified. Therefore, muscle slices from animals treated with glycerol plus ASCs or saline plus ASCs were labeled for AChR and VAChT and then analyzed with confocal microscopy (**Figure 4A**). Counting of AChR+ sites did not reveal any significant differences between glycerol and saline injected muscles (**Figure 4B**) although at day 3 a trend toward lower numbers of postsynaptic sites in glycerol samples was visible. Quantitative analysis of AChR and VAChT double positive NMJs showed a good recovery at days 3 and 5 post injection. Indeed, while the fractions of double-positive NMJs in mice not treated with ASCs were low at these timepoints (day 3: 41.4 ± 17.3%; day 5: 48.1 ± 7.2%; mean ± SEM, n = 3 muscles), they reached 65.1% ± 10.3% and 83.4 ± 1.3% (mean ± SEM, n = 3 muscles) upon ASC injection. However, in ASC-treated mice, the numbers dropped at day 11 to a value of 57.3 ± 3.7% (mean ± SEM, n = 3 muscles) (**Figure 4C**), instead of a further recovery as observed in ASC-untreated animals (day 11: 65.8 ± 16.9%; mean ± SEM, n = 3 muscles). Thus, although ASC treatment showed some beneficial effect on NMJ recovery at early timepoints, this effect did not persist.

DISCUSSION

Stem cells have become a widely studied option to treat neuromuscular disorders. However, while their effects on the sarcomeric part of muscles have been investigated regularly, little is known on their regenerative capacity with respect to NMJs. In this study, a glycerol-based muscle damage model was employed to address three biological questions: (i) If a low dose of glycerol could trigger a degeneration – regeneration process, (ii) how this affected NMJs, and (iii) if and how a systemic treatment with ASCs could modulate muscle and synapse recovery.

Low-Dose Application of Glycerol to Study Skeletal Muscle Degeneration-Regeneration

Most studies based on glycerol damage applied quantities of 50–100 μl of glycerol per mouse TA muscle (Lluís et al., 2001; Mahdy et al., 2015; Mahdy, 2018). This protocol was also used to induce massive rhabdomyolysis, in particular for the investigation of acute kidney disease (Korrapati et al., 2012; Huang et al., 2018; Reis et al., 2019). However, since we were more interested in the effects of ASCs on muscle and NMJ regeneration, a milder protocol was sought. One group reported that a dose of 25 μl of glycerol is able to cause a limited damage in mouse TA muscles including adipocyte infiltration, fibrosis, and necrosis (Arsic et al., 2004). In the present work, 20 μl per TA muscle were injected and this led to a consistent profile of local muscle degeneration and regeneration (**Figure 5A**). Regularly, necrosis was evident at 3 days post injection with loss of plasma membrane integrity, dystrophin, and f-actin/contractile apparatus in the affected area. Thereafter, the regeneration marker, eMHC, appeared between days 5 and 8 post injection, and at day 11, all parameters returned to normal except a persisting presence of CNFs. Thus, this paradigm appeared apt for investigating effects of ASC injection on NMJ regeneration.

Effects of Glycerol on NMJ Degeneration-Regeneration

An analysis of post- and pre-synapses in the presence and absence of glycerol showed that the two synaptic compartments responded differently to the treatment: while a small but insignificant loss of post-synapses was detected over the entire experimental period, the pre-synapse marker VAChT was missing in around 60% of postsynaptic regions at 3 days post glycerol injection and then steadily recovered at the later timepoints (**Figure 5A**). A more in-depth analysis showed that the distribution of VAChT and AChR signal colocalization was similar between glycerol and saline injected muscles except for one trait: in the presence of glycerol, much more completely VAChT-negative synapses were found (**Supplementary Figure S4**), suggesting that the loss and reestablishment of presynaptic signals was not gradual but occurred in a rather digital manner. However, presynaptic regeneration in all synapses was not obtained within 11 days post injection. It is unclear, why pre- and postsynapse showed a differential susceptibility to glycerol. One possible hypothesis is that the presynaptic terminal as such was more prone to glycerol-induced damage than the postsynaptic part. Another possibility could be due to the focal glycerol-induced damage: it could be that at these sites it led to damage of nerve bundles upstream of undamaged muscle regions. If these damaged bundles were innervating a muscle region unaffected by glycerol, this could, by axon degeneration, affect the presynaptic elements also in apparently unaffected muscle regions. Interestingly, post-synapses were often found also in the most heavily damaged areas in muscle fibers that were infiltrated by mIgG and had lost their dystrophin and f-actin expression. Conversely, VAChT-positive NMJs were hardly detected in these areas. We have

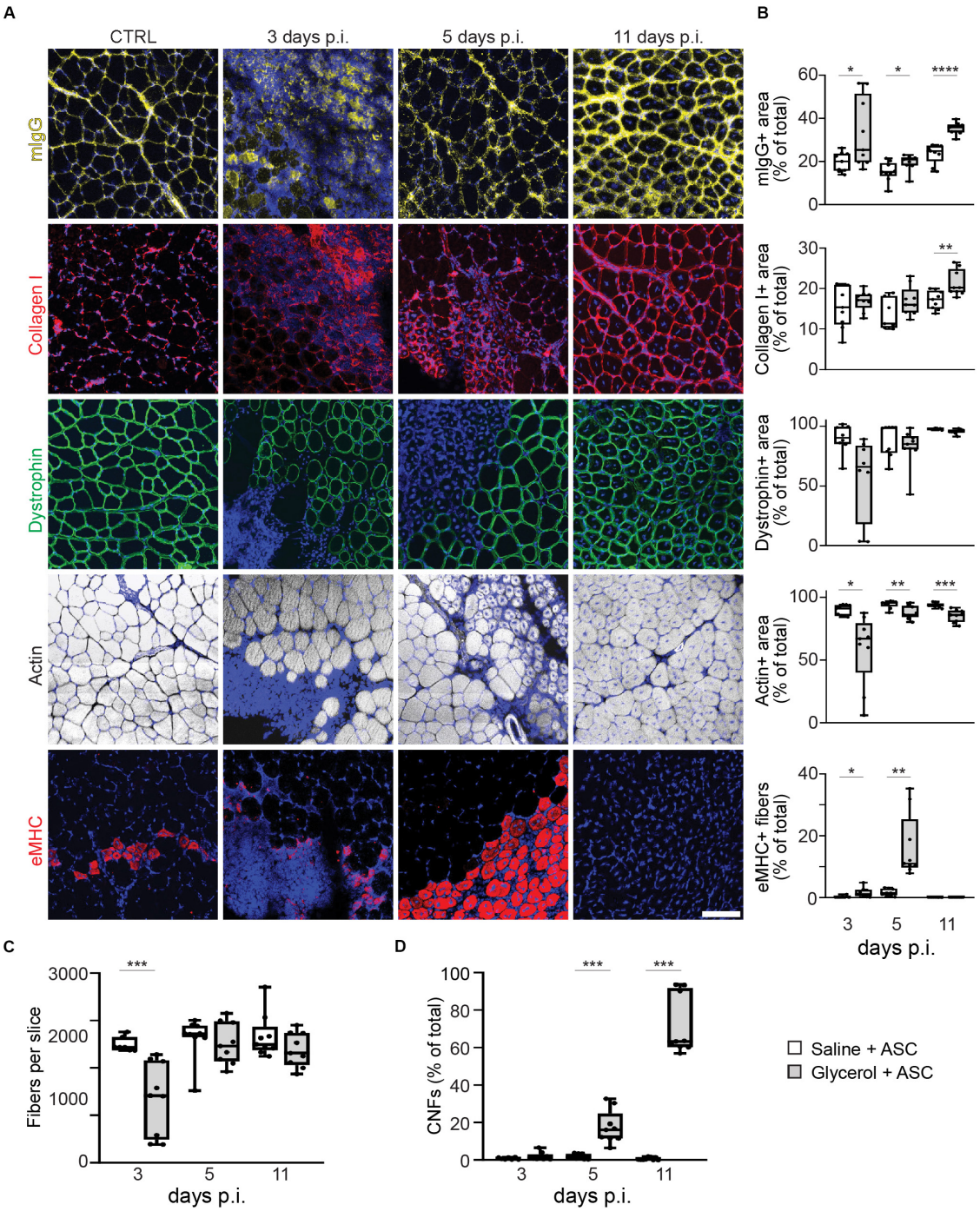

FIGURE 3 | Systemic injection of ASCs induces a late phase of IgG infiltration, enhanced basal eMHC expression, and increase in center-nucleated fibers. Simultaneous to tail-vein injection of ASCs, TA muscles were injected with 20 μl of either saline or glycerol and then harvested and snap frozen after 3, 5, or 11 days (days p.i.). Upon cryosectioning, muscle slices were stained with DAPI and either antibodies against mouse IgG (mIgG), collagen I, dystrophin, or embryonic myosin heavy chain (eMHC), or with phalloidin-TRITC to label actin. Sections were analyzed by confocal microscopy. **(A)** Representative optical sections of fluorescence signals as indicated, nuclear DAPI staining always shown in blue, mIgG in yellow, collagen I and eMHC in red, dystrophin in green, actin in gray. CTRL, saline-injected muscles at 3 days p.i., the other panels depict glycerol-injected muscles at 3, 5, and 11 days p.i., as indicated. Scalebar, 100 μm. **(B)** Quantitative analysis of section areas positive for fluorescence signals of either mIgG, collagen I, dystrophin, or actin, or number of eMHC-positive fibers, as a function of days p.i. Box–Whisker plots show all individual data points as dots, the extensions of upper and lower quartiles in the boxes, the medians as horizontal lines in the boxes, and maxima and minima as whiskers. $^{*}p \leq 0.05$, $^{**}p \leq 0.01$, $^{***}p \leq 0.001$, $^{****}p \leq 0.0001$. **(C,D)** Quantitative analysis of fibers per muscle slice **(C)** or center-nucleated fibers (% of fiber number) as a function of days p.i. Box–Whisker plots show all individual data points as dots, the extensions of upper and lower quartiles in the boxes, the medians as horizontal lines in the boxes, and maxima and minima as whiskers. $^{***}p \leq 0.001$.

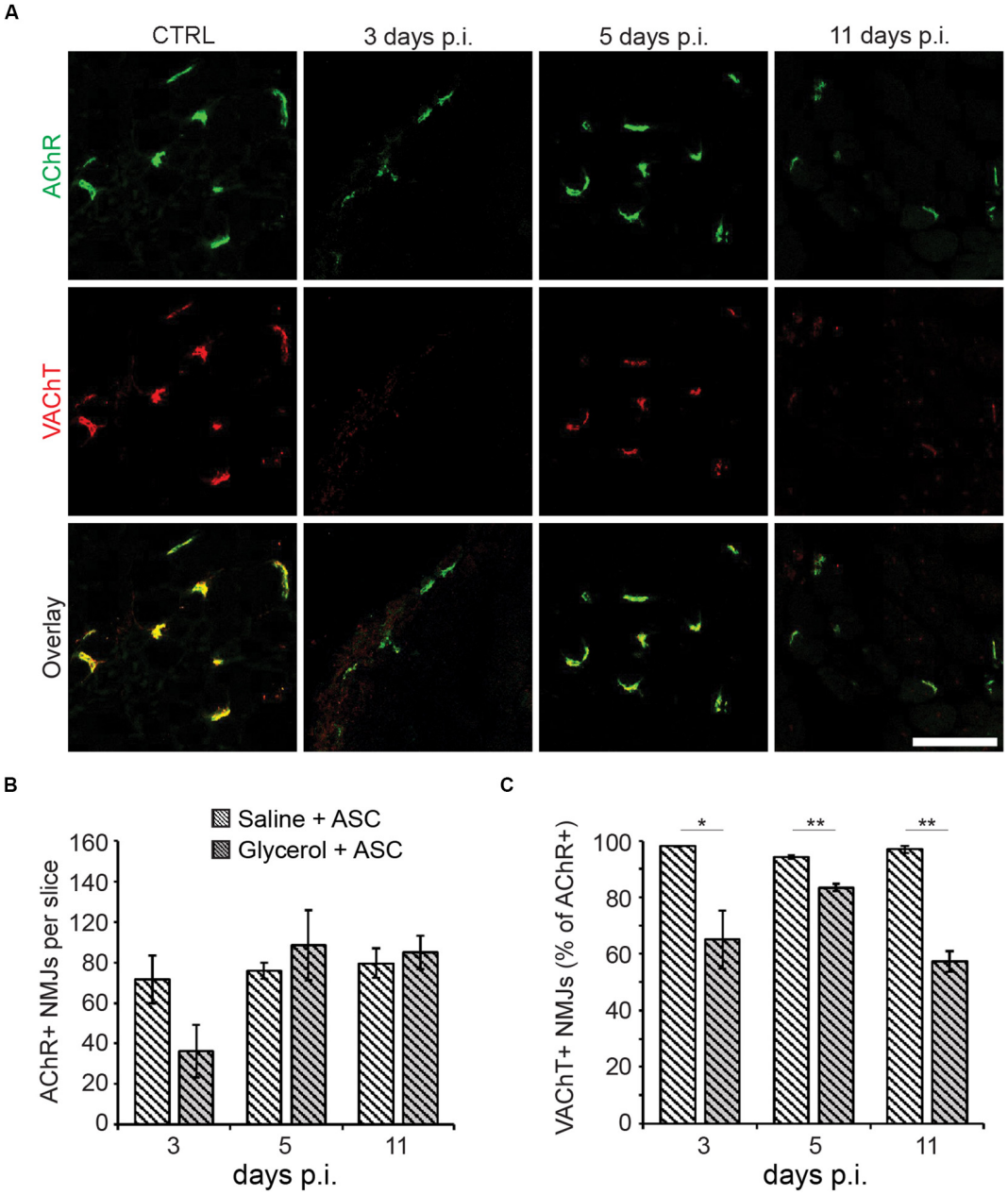

FIGURE 4 | ASCs enhance early recovery of presynaptic VAChT enrichment, but this effect is transient. Simultaneous to tail-vein injection of ASCs, TA muscles were injected with 20 μl of either saline or glycerol and then harvested and snap frozen after 3, 5, or 11 days (days p.i.). Upon cryosectioning, muscle slices were stained with αBGT (for AChR detection) and antibodies against VAChT to label post- and presynaptic portions of NMJs, respectively. Sections were analyzed by confocal microscopy. **(A)** Representative optical sections of fluorescence signals as indicated, αBGT in green, VAChT in red, yellow in overlay images indicates colocalization of both signals. CTRL, saline-injected muscles at 3 days p.i., the other panels depict glycerol-injected muscles at 3, 5, and 11 days p.i., as indicated. Scalebar, 100 μm. **(B,C)** Quantitative analysis of αBGT+ postsynaptic sites per slice **(B)** and of VAChT+ NMJs (% of αBGT+ structures, **C**) as a function of days p.i. Shown is mean ± SEM (n = 3 muscles). $^{*}p \leq 0.05$, $^{**}p \leq 0.01$.

no formal proof that these same postsynaptic sites were later on reinnervated, but at least the rather constant amounts of postsynaptic sites obtained throughout the experiment argue against a massive phase of ectopic synapse formation. Depending on the type of damage model, different parts of a skeletal muscle can be affected. For example, treatments like mechanical, thermal, or ischemic injury induce a degeneration of cytoplasm and plasma membrane, but will leave the extracellular matrix largely intact (McMahan et al., 1980; Slater and Schiaffino, 2008; Anderson et al., 2017). Conversely, studies using glycerol showed that this kind of treatment leads to an extensive damage of the extracellular matrix (Hardy et al., 2016; Mahdy, 2018). Previously,

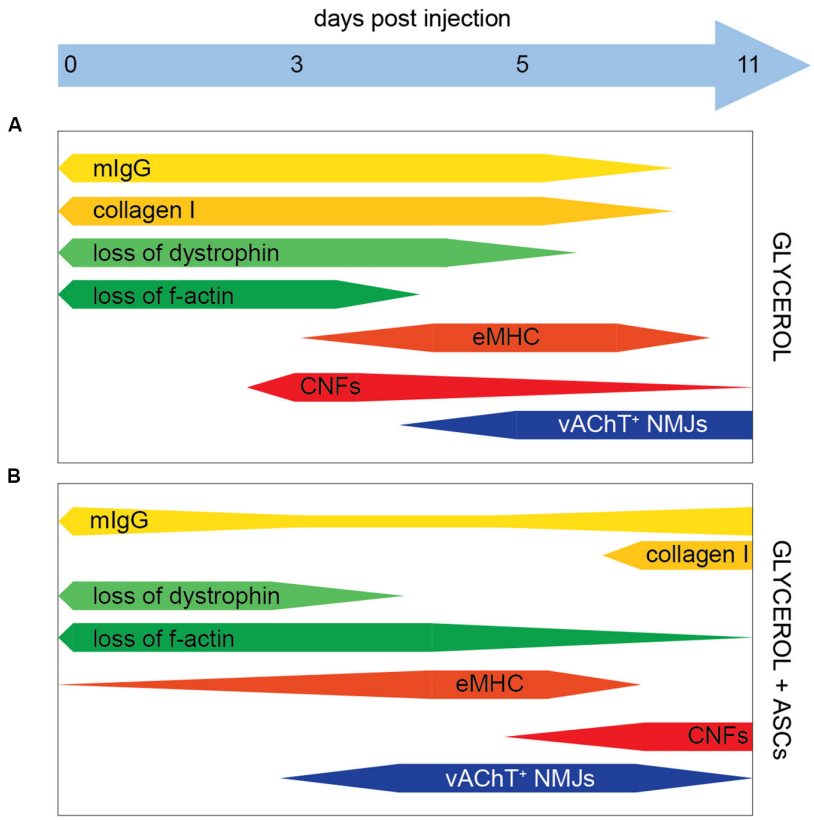

FIGURE 5 | Schematic summary of glycerol and ASC effects. Bars indicate the presence of markers as indicated, the relative amount is shown by the bar width. **(A,B)** In the presence of Glycerol and Glycerol + ASC, respectively.

it was described that an intact extracellular matrix is important for postsynaptic preservation and that it can efficiently guide motor axons to original synaptic sites (McMahan et al., 1980). Instead, the present study suggests that the loss of extracellular matrix is not sufficient to disperse postsynaptic assembly of AChR, but it might result in an impaired synapse recovery and pre-postsynaptic matching (Warren et al., 2007; Vilmont et al., 2016; Rogers and Nishimune, 2017). Nonetheless, a partial recovery of pre-postsynaptic matching was found here to start around day 5 post glycerol injection (**Figure 5A**). Compared to previous reports using either tourniquet (Tu et al., 2017) or nerve injury (Zainul et al., 2018), recovery was apparently faster here. In both previous studies, presynaptic recovery took weeks to complete. One might speculate that the nerve damage was only local in the case of glycerol injection, while it was global in the other models, which could potentially explain the different time courses observed. Thus, having achieved a robust series of degeneration and regeneration processes, we continued in investigating effects of ASC injection on NMJ regeneration.

Effects of ASCs on De/Regeneration of Muscle and NMJs

Adipose-derived stromal cells were previously found to be interesting for clinical application due to their differentiation capacity, their beneficial effects on other cell types involved in tissue regeneration, and their immunomodulatory properties. In the present work, systemic ASC injection plus local glycerol application led to two major differences in the muscle degeneration – regeneration profiles as compared to glycerol injection alone: First, the reduced amounts of mIgG and collagen I as well as the early detection of eMHC and presynapse regeneration jointly indicated a slightly less severe damage at day 3 post glycerol injection. Second, however, the increasing amounts of mIgG, fibrosis, and CNFs at day 11 post glycerol suggested a secondary damage or differing regeneration phase. The latter effect of ASC application might be due to a mobilization of immune and stem cells into the muscle, causing a stronger regeneration phase. Initially, ASC may dampen the initial degeneration and inflammation by reducing the degree of necrosis and consequently the intensity of neutrophil-induced inflammation. In the following, they may impact the repair and regeneration phase for instance by an IL-6 dependent mechanism, as direct injection of mesenchymal stem/stromal cells was found to increase muscle regeneration via promoting the switch from M1 to M2 macrophages, hence, stimulating muscle stem cell activity (Arnold et al., 2007; Saclier et al., 2013; Mahdy, 2018). Finally, they may affect the remodeling of the regenerating muscle and the maturation of muscle cells, perhaps by a direct effect of ASCs migrating to affected muscles

as reported previously (Vieira et al., 2012). Thus, ASCs could directly act on muscle recovery and enhance muscle regeneration (Rodriguez et al., 2005; Rybalko et al., 2017). By immunostaining of human nuclear marker Ku80 (Koike et al., 1999; Allard et al., 2014), we addressed settlement of systemically applied ASCs in muscles (**Supplementary Figure S5**). This did not reveal any clear sign of substantial integration of ASCs in glycerol-treated muscle tissue, rather suggesting that paracrine factors released by ASCs were involved in the observed modulation of degeneration – regeneration processes and immune responses. Recent findings on the effects of ASC secretome injection upon ischemic muscle damage favor this as a principal therapeutic mechanism (Mitchell et al., 2019; Figliolini et al., 2020). Here, ASC-derived exosomes promoted vascular growth and tissue regeneration. With respect to NMJs, two principal differences between mice treated with or without ASC were noted. First, upon application of saline, a rise in the number of postsynaptic sites per muscle slice was observed at day 11 p.i. in the absence (**Figure 2B**) but not in the presence of ASCs (**Figure 4B**). At present, the reason for this discrepancy is unclear. Likely, this was not due to general effects of ASC treatment on muscle integrity, since all other measured parameters, i.e. presence of mIgG, collagen I, dystrophin, actin, eMHC, fiber number, and CNFs, were unchanged. This suggests, that the observed difference was due to either, experimental variability or a specific effect of the ASCs on NMJ regeneration that needs further investigation. Second, upon injection of glycerol, ASC administration led to a fast recovery of post-synapse numbers within 5 days post injection and by trend also to a higher and faster presynapse recovery than in the absence of ASCs. The latter aspect, though, was reverted, likely due to the late-phase degenerative response, as indicated by enhanced levels of mIgG and collagen I on day 11 p.i. (**Figure 5**).

CONCLUSION

In conclusion, although our data suggest a partially positive effect of ASCs on the recovery of NMJs in the early regenerative phase, a secondary degenerative or aberrant regenerative period reverted these benefits at a later stage. Due to the manifold effects of ASCs on various phases of de- and regeneration, which were likely involving muscle and neuronal cells, endothelial cells, but also all kind of immune cells, future studies need to further explore the mechanisms involved and work around late degenerative processes.

DATA AVAILABILITY STATEMENT

The raw data supporting the conclusions of this article will be made available by the authors, without undue reservation, to any qualified researcher.

ETHICS STATEMENT

The animal study was reviewed and approved by the Regierungspräsidium Karlsruhe.

AUTHOR CONTRIBUTIONS

NG and RR contributed to conception and design of the study. MR, SH, and TS performed the experiments and statistical analysis. MR and RR wrote the first draft of the manuscript. KB and MH contributed to resources and materials. All authors contributed to manuscript revision and, read and approved the submitted version.

FUNDING

This work was supported by the Cooperative Research Training Group: Tissue Analytics for Stem Cell based Diagnostics and Therapy (TASCDT). This work was funded by the German Federal Ministry of Education and Research (BMBF) as part of the Innovation Partnership M^2Aind, project M^2OGA (03FH8I02IA) within the framework Starke Fachhochschulen–Impuls für die Region (FH-Impuls).

ACKNOWLEDGMENTS

We are grateful to Viktoria Skude for technical assistance and to Adriana Torres Crigna and Daniela Nardozi for the precious insights and help regarding the use of ASCs.

SUPPLEMENTARY MATERIAL

The Supplementary Material for this article can be found online at: https://www.frontiersin.org/articles/10.3389/fnmol.2020.00107/full#supplementary-material

REFERENCES

Allard, J., Li, K., Lopez, X., Blanchard, S., Barbot, P., Rorive, S., et al. (2014). Immunohistochemical toolkit for tracking and quantifying xenotransplanted human stem cells. *Regenerat. Med.* 9, 437–452. doi: 10.2217/rme.14.26. Immunohistochemical

Anderson, J., Mai-khoi, Q., Daneshvar, T., Suzuki, J., Dort, W., Mizunoya, K., et al. (2017). The role of semaphorin3A in myogenic regeneration and the formation of functional neuromuscular junctions on new fibres. *Biol. Rev.* 92, 1389–1405. doi: 10.1111/brv.12286

Arecco, N., Clarke, F. K., Jones, D. M., Simpson, D., Mason, R. J., Beynon, M., et al. (2016). Elastase levels and activity are increased in dystrophic muscle and impair myoblast cell survival, proliferation and differentiation. *Sci. Rep.* 6, 1–20. doi: 10.1038/srep24708

Arnold, L., Henry, F., Poron, Y., Baba-Amer, Y., Van Rooijen, N., Plonquet, R., et al. (2007). Inflammatory monocytes recruited after skeletal muscle injury switch into antiinflammatory macrophages to support myogenesis. *J. Exp. Med.* 204, 1057–1069. doi: 10.1084/jem.20070075

Arsic, N., Zacchigna, L., Zentilin, G., Ramirez-Correa, L., Salvi, G., Sinagra, U., et al. (2004). Vascular endothelial growth factor stimulates skeletal muscle regeneration in vivo. *Mol. Ther.* 10, 844–854. doi: 10.1016/j.ymthe.2004.08.007

Bieback, K., Hecker, T., Schlechter, T., Hofmann, N., Brousos, T., Redmer, D., et al. (2012). Replicative aging and differentiation potential of human adipose tissue-derived mesenchymal stromal cells expanded in pooled human or fetal bovine serum. *Cytotherapy* 14, 570–583. doi: 10.3109/14653249.2011.652809

Biral, D., Jakubiec-Puka, I., Ciechomska, M., Sandri, K., Rossini, S., Carraro, U., et al. (2000). Loss of dystrophin and some dystrophin-associated proteins with concomitant signs of apoptosis in rat leg muscle overworked in extension. *Acta Neuropathol.* 100, 618–626. doi: 10.1007/s004010000231

Boldyreva, M. A., Shevchenko, Y., Molokotina, P., Makarevich, I., Beloglazova, E., Zubkova, K., et al. (2019). Transplantation of adipose stromal cell sheet producing hepatocyte growth factor induces pleiotropic effect in ischemic skeletal muscle. *Int. J. Mol.Sci.* 20:3088. doi: 10.3390/ijms20123088

Cowling, B. S., and Thielemans, L. (2020). Translational medicine in neuromuscular disorders: from academia to industry. *Dis. Models Mech.* 13, 1–6. doi: 10.1242/dmm.041434

Czerwinska, A. M., Streminska, M., Ciemerych, M., and Grabowska, I. (2012). Mouse gastrocnemius muscle regeneration after mechanical or cardiotoxin injury. *Folia Histochem. Cytobiol.* 50, 144–153. doi: 10.5603/FHC.2012.0021

Deasy, B. M., Lu, J., Tebbets, J., Feduska, R., Schugar, J., Pollett, B., et al. (2007). A role for cell sex in stem cell-mediated skeletal muscle regeneration: female cells have higher muscle regeneration efficiency. *J. Cell Biol.* 177, 73–86. doi: 10.1083/jcb.200612094

Fambrough, D. M., Devreotes, P., Gardner, J. M., and Card, D. (1979). The life history of acetylcholine receptors. *Prog. Brain Res.* 49, 325–334. doi: 10.1016/S0079-6123(08)64644-0

Feng, F., Deng, J., Luo, L., and Huang, Q. (2019). Role of the notch signaling pathway in fibrosis of denervated skeletal muscle. *Curr. Med. Sci.* 39, 419–425. doi: 10.1007/s11596-019-2053-z

Figliolini, F., Ranghino, C., Grange, M., Cedrino, M., Tapparo, C., Cavallari, A., et al. (2020). Extracellular vesicles from adipose stem cells prevent muscle damage and inflammation in a mouse model of hind limb ischemia: role of neuregulin-1. *Arterioscler. Thromb. Vasc. Biol.* 40, 239–254. doi: 10.1161/ATVBAHA.119.313506

Forcales, S. V. (2015). Potential of adipose-derived stem cells in muscular regenerative therapies. *Front. Aging Neurosci.* 7:123. doi: 10.3389/fnagi.2015.00123

Gibertini, S., Zanotti, S., Savadori, M., Curcio, S., Saredi, F., Salerno, F., et al. (2014). Fibrosis and inflammation are greater in muscles of beta-sarcoglycan-null mouse than mdx mouse. *Cell Tissue Res.* 356, 427–443. doi: 10.1007/s00441-014-1854-4

Gillies, A. R., and Lieber, R. L. (2011). Structure and function of the skeletal muscle extracellular matrix. *Muscle Nerve* 44, 318–331. doi: 10.1002/mus.22094. Structure

Gois, B., Samuel, D., Horita, I., da Fonseca, M., Alves, L., Nagaraju, K., et al. (2019). A Promising future for stem-cell-based therapies in muscular dystrophies-in vitro and in vivo treatments to boost cellular engraftment. *Int. J. Mol. Sci.* 20, 5433. doi: 10.3390/ijms20215433

Gorecka, A., Salemi, D., Haralampieva, F., Moalli, D., Stroka, D., Candinas, D., et al. (2018). Autologous transplantation of adipose-derived stem cells improves functional recovery of skeletal muscle without direct participation in new myofiber formation. *Stem Cell Res. Ther.* 9, 1–12. doi: 10.1186/s13287-018-0922-1

Hardy, D., Besnard, M., Latil, G., Jouvion, D., Briand, C., Thépenier, G., et al. (2016). Comparative study of injury models for studying muscle regeneration in mice. *PLoS One* 11:e0147198. doi: 10.1371/journal.pone.0147198

Huang, M. Z., and Gopalakrishnakone, P. (1996). Pathological changes induced by an acidic phospholipase A2 from ophiophagus hannah venom on heart and skeletal muscle of mice after systemic injection. *Toxicon* 34, 201–211. doi: 10.1016/0041-0101(95)00128-X

Huang, R., Shi, M., Guo, F., Feng, Y., Feng, Y., and Liu, J. (2018). Pharmacological inhibition of fatty protects against rhabdomyolysis-induced acute kidney injury. *Front. Pharmacol.* 9:917. doi: 10.3389/fphar.2018.00917

Huebner, K. D., Jassal, D., Halevy, O., Pines, M., and Anderson, J. (2008). Functional resolution of fibrosis in mdx mouse dystrophic heart and skeletal muscle by halofuginone. *Am. J. Physiol. Heart Circ. Physiol.* 294, 1550–1561. doi: 10.1152/ajpheart.01253.2007

Iwata, Y., Suzuki, O., and Wakabayashi, S. (2013). Decreased surface sialic acid content is a sensitive indicator of muscle damage. *Muscle Nerve* 47, 372–378. doi: 10.1002/mus.23632

Judson, R. N., Gray, C., Walker, A., Carroll, C., Itzstein, A., Lionikas, P., et al. (2013). Constitutive expression of yes-associated protein (Yap) in adult skeletal muscle fibres induces muscle atrophy and myopathy. *PLoS One* 8:e0059622. doi: 10.1371/journal.pone.0059622

Kastenschmidt, J. M., Ellefsen, L., Mannaa, J., Giebel, R., Yahia, R., Ayer, P., et al. (2019). QuantiMus: a machine learning-based approach for high precision analysis of skeletal muscle morphology. *Front. Physiol.* 10:1116. doi: 10.3389/fphys.2019.01416

Kawai, H., Nishino, K., Kusaka, T., Naruo, Y., Tamaki, Y., and Iwasa, M. (1990). Experimental glycerol myopathy: a histological study. *Acta Neuropathol.* 80, 192–197. doi: 10.1007/BF00308923

Kern, S., Eichler, J., Stoeve, H., Klüter, Z., and Bieback, K. (2006). Comparative analysis of mesenchymal stem cells from bone marrow, umbilical cord blood, or adipose tissue. *Stem Cells* 24, 1294–1301. doi: 10.1634/stemcells.2005-0342

Kitajima, Y., and Ono, Y. (2016). Estrogens maintain skeletal muscle and satellite cell functions. *J. Endocrinol.* 229, 267–275. doi: 10.1530/JOE-15-0476

Koike, M., Awaji, M., Kataoka, G., Tsujimoto, T., Kartasova, Y. T., and Koike, A. (1999). Differential subcellular localization of DNA-dependent protein kinase components ku and dna-pkcs during mitosis. *J. Cell Sci.* 112, 4031–4039.

Korrapati, M. C., Brooke, E., Shaner, R., and Schnellmann, R. G. (2012). Recovery from glycerol-induced acute kidney injury is accelerated by suramin. *J. Pharmacol. Exp. Ther.* 341, 126–136. doi: 10.1124/jpet.111.190249

Lluís, F., Roma, M., Suelves, M., Parra, G., Aniorte, E., Gallardo, I., et al. (2001). Urokinase-dependent plasminogen activation is required for efficient skeletal muscle regeneration in vivo. *Blood* 97, 1703–1711. doi: 10.1182/blood.V97.6.1703

Maeda, M., Ohba, S., Nakagomi, Y., Suzuki, S., Kiryu-Seo, K., Namikawa, K., et al. (2004). Vesicular acetylcholine transporter can be a morphological marker for the reinnervation to muscle of regenerating motor axons. *Neurosci. Res.* 48, 305–314. doi: 10.1016/j.neures.2003.11.008

Mahdy, M. A., Warita, A., and Hosaka, Y. (2016). Early ultrastructural events of skeletal muscle damage following cardiotoxin-induced injury and glycerol-induced injury. *Micron* 91, 29–40. doi: 10.1016/j.micron.2016.09.009

Mahdy, M. A. A. (2018). Glycerol-induced injury as a new model of muscle regeneration. *Cell Tissue Res* 374, 233–241. doi: 10.1007/s00441-018-2846-6

Mahdy, M. A. A., Hsiao, A., Lei, Y., Wakamatsu, J., Hosaka, Y., and Nishimura, T. (2015). Comparative study of muscle regeneration following cardiotoxin and glycerol injury. *Ann. Anat.* 202, 18–27. doi: 10.1016/j.aanat.2015.07.002

McCarthy, J., Mula, J., Miyazaki, M., Erfani, R., Garrison, M., Farooqui, A., et al. (2011). Effective fiber hypertrophy in satellite cell-depleted skeletal Muscle. *Development* 138, 3657–3666. doi: 10.1242/dev.068858

McDonald, A. A., Sadie, L., Kunz, S., Ralles, S., and McLoon, L. (2015). Disease course in Mdx:Utrophin+/- mice: comparison of three mouse models of duchenne muscular dystrophy. *Physiol. Rep.* 3, 1–22. doi: 10.14814/phy2.12391

McMahan, U. J., Edgington, D., and Kuffler, D. P. (1980). Factors that influence regeneration of the neuromuscular junction. *J. Exp. Biol.* 89, 31–42.

Mitchell, R., Mellows, B., Sheard, J., Antonioli, M., Kretz, O., and Chambers, D. (2019). Secretome of adipose-derived mesenchymal stem cells promotes skeletal muscle regeneration through synergistic action of extracellular vesicle cargo and soluble proteins. *Stem Cell Res. Ther.* 10, 1–19. doi: 10.1186/s13287-019-1213-1

Murphy, M. M., Lawson, J., Mathew, S., David, A., Hutcheson, A., and Kardon, G. (2011). Satellite cells, connective tissue fibroblasts and their interactions are crucial for muscle regeneration. *Development* 138, 3625–3637. doi: 10.1242/dev.064162

Pisani, D. F., Cynthia, D. K., Bottema, C., Butori, C., Dani, C., and Claude, A. (2010). Mouse model of skeletal muscle adiposity: a glycerol treatment approach. *Biochem. Biophys. Res. Commun.* 396, 767–773. doi: 10.1016/j.bbrc.2010.05.021

Proto, J. D., Tang, A., Lu, W. C. W., Chen, E., Stahl, M., Poddar, S. A., et al. (2015). NF-KB inhibition reveals a novel role for HGF during skeletal muscle repair. *Cell Death Dis.* 6:e1730. doi: 10.1038/cddis.2015.66

Reis, N. G., Della, C., Francescat, L., De Almeida, F., Giovanini, R., Silva Costa, R. M., et al. (2019). Protective effect of calcitriol on rhabdomyolysis-induced acute kidney injury in rats. *Sci. Rep.* 9:7090. doi: 10.1038/s41598-019-43564-1

Rodrigues, M., Echigoya, Y., Maruyama, R., Rowel, Q., Fukada, I., and Yokota, T. (2016). Impaired regenerative capacity and lower revertant fibre expansion in dystrophin-deficient mdx muscles on DBA/2 background. *Sci. Rep.* 6:38371. doi: 10.1038/srep38371

Rodriguez, A. M., Pisani, C., Dechesne, C., Turc-Carel, J., Kurzenne, Y., Wdziekonski, B., et al. (2005). Transplantation of a multipotent cell population from human adipose tissue induces dystrophin expression in the immunocompetent mdx mouse. *J. Exp. Med.* 201, 1397–1405. doi: 10.1084/jem.20042224

Rogers, R. S., and Nishimune, H. (2017). The role of laminins in the organization and function of neuromuscular junctions. *Matrix Biol.* 5, 86–105. doi: 10.1016/j.matbio.2016.08.008

Rybalko, V., Hsieh, L., Ricles, M., Chung, E., Farrar, R., and Suggs, L. (2017). Therapeutic potential of adipose-derived stem cells and macrophages for ischemic skeletal muscle repair. *Regenerat. Med.* 12, 153–167. doi: 10.2217/rme-2016-0094

Saclier, M., Yacoub-Youssef, A., Mackey, L., Arnold, H., Ardjoune, M., Magnan, M., et al. (2013). Differentially activated macrophages orchestrate myogenic precursor cell fate during human skeletal muscle regeneration. *Stem Cells* 31, 384–396. doi: 10.1002/stem.1288

Schiaffino, S., Gorza, S., Sartore, L., Saggin, L., and Carli, M. (1986). Embryonic myosin heavy chain as a differentiation marker of developing human skeletal muscle and rhabdomyosarcoma. a monoclonal antibody study. *Exp. Cell Res.* 163, 211–220. doi: 10.1016/0014-4827(86)90574-4

Serrano, A. L., and Muñoz-Cánoves, P. (2010). Regulation and dysregulation of fibrosis in skeletal muscle. *Exp. Cell Res.* 316, 3050–3058. doi: 10.1016/j.yexcr.2010.05.035

Slater, C. R., and Schiaffino, S. (2008). "Innervation of regenerating muscle," in *Skeletal Muscle Repair and Regeneration*, Vol. 3, eds S. Schiaffino and T. Partridge (Dordrecht: Springer), 303–334. doi: 10.1007/978-1-4020-6768-6_14

Sugita, S., Leland, L., Wood, S., Vaughan, M., Gomes, M., Camargo, L., et al. (2016). VAChT overexpression increases acetylcholine at the synaptic cleft and accelerates aging of neuromuscular junctions. *Skeletal Muscle* 6, 1–17. doi: 10.1186/s13395-016-0105-7

Tiryakioglu, O., Erkoc, B., Tunerir, O., Uysal, H., Altin, T., and Aydin, S. (2015). The effect of iloprost and N-Acetylcysteine on skeletal muscle injury in an acute aortic ischemia-reperfusion model: an experimental study. *BioMed Res. Int.* 2015:453748. doi: 10.1155/2015/453748

Torres-Torrillas, M., Rubio, M., Damia, E., Cuervo, B., Romero, A., Peláez, P., et al. (2019). Adipose-derived mesenchymal stem cells: a promising tool in the treatment of musculoskeletal diseases. *Int. J. Mol. Sci.* 20:3105. doi: 10.3390/ijms20123105

Tu, H., Zhang, D., Corrick, R. M., Muelleman, R. L., Wadman, M., and Li, Y. (2017). Morphological regeneration and functional recovery of neuromuscular junctions after tourniquet-induced injuries in mouse hindlimb. *Front. Physiol.* 8:207. doi: 10.3389/fphys.2017.00207

Vieira, N. M., Valadares, E., Zucconi, M., Secco, C. R., Bueno Junior, V., Brandalise, A., et al. (2012). Human adipose-derived mesenchymal stromal cells injected systemically into grmd dogs without immunosuppression are able to reach the host muscle and express human dystrophin. *Cell Transplant.* 21, 1407–1417. doi: 10.3727/096368911X

Vilmont, V., Cadot, B., Vezin, E., Le Grand, F., and Gomes, E. R. (2016). Dynein disruption perturbs post-synaptic components and contributes to impaired MuSK clustering at the NMJ: implication in ALS. *Sci. Rep.* 6, 1–13. doi: 10.1038/srep27804

Warren, G. L., Summan, M., Gao, X., Chapman, R., Hulderman, T., and Simeonova, P. (2007). Mechanisms of skeletal muscle injury and repair revealed by gene expression studies in mouse models. *J. Physiol.* 582, 825–841. doi: 10.1113/jphysiol.2007.132373

Webster, M. T., Manor, U., Lippincott-Schwartz, J., and Fan, C. M. (2015). Intravital imaging reveals ghost fibers as architectural units guiding myogenic progenitors during regeneration. *Cell Stem Cell* 18, 243–252. doi: 10.1016/j.stem.2015.11.005

Zainul, Z., Heikkinen, A., Koivisto, H., Rautalahti, I., Kallio, M., Lin, S., et al. (2018). Collagen XIII is required for neuromuscular synapse regeneration and functional recovery after peripheral nerve injury. *J. Neurosci.* 38, 4243–4258. doi: 10.1523/JNEUROSCI.3119-17.2018

Conflict of Interest: The authors declare that the research was conducted in the absence of any commercial or financial relationships that could be construed as a potential conflict of interest.

Copyright © 2020 Rigon, Hörner, Straka, Bieback, Gretz, Hafner and Rudolf. This is an open-access article distributed under the terms of the Creative Commons Attribution License (CC BY). The use, distribution or reproduction in other forums is permitted, provided the original author(s) and the copyright owner(s) are credited and that the original publication in this journal is cited, in accordance with accepted academic practice. No use, distribution or reproduction is permitted which does not comply with these terms.

frontiers in Molecular Neuroscience

REVIEW
published: 14 August 2020
doi: 10.3389/fnmol.2020.00156

Pathomechanisms and Clinical Implications of Myasthenic Syndromes Exacerbated and Induced by Medical Treatments

*Martin Krenn[1], Anna Grisold[1], Philipp Wohlfarth[2], Jakob Rath[1], Hakan Cetin[1], Inga Koneczny[1,3] and Fritz Zimprich[1]**

[1] Department of Neurology, Medical University of Vienna, Vienna, Austria, [2] Division of Blood and Marrow Transplantation, Department of Medicine I, Medical University of Vienna, Vienna, Austria, [3] Division of Neuropathology and Neurochemistry, Department of Neurology, Medical University of Vienna, Vienna, Austria

Myasthenic syndromes are typically characterized by muscle weakness and increased fatigability due to an impaired transmission at the neuromuscular junction (NMJ). Most cases are caused by acquired autoimmune conditions such as myasthenia gravis (MG), typically with antibodies against the acetylcholine receptor (AChR). Different drugs are among the major factors that may complicate pre-existing autoimmune myasthenic conditions by further impairing transmission at the NMJ. Some clinical observations are substantiated by experimental data, indicating that presynaptic, postsynaptic or more complex pathomechanisms at the NMJ may be involved, depending on the individual compound. Most robust data exist for the risks associated with some antibiotics (e.g., aminoglycosides, ketolides, fluoroquinolones) and cardiovascular medications (e.g., class Ia antiarrhythmics, beta blockers). Apart from primarily autoimmune-mediated disorders of the NMJ, *de novo* myasthenic manifestations may also be triggered by medical treatments that induce an autoimmune reaction. Most notably, there is growing evidence that the immune checkpoint inhibitors (ICI), a modern class of drugs to treat various malignancies, represent a relevant risk factor to develop severe and progressive medication-induced myasthenia via an immune-mediated mechanism. From a clinical perspective, it is of utmost importance for the treating physicians to be aware of such adverse treatment effects and their consequences. In this article, we aim to summarize existing evidence regarding the key molecular and immunological mechanisms as well as the clinical implications of medication-aggravated and medication-induced myasthenic syndromes.

Keywords: drug-related myasthenia, neuromuscular transmission, neuromuscular junction, drug-induced myasthenia, immune checkpoint inhibitors

OPEN ACCESS

Edited by:
Robert W. Burgess, Jackson Laboratory, United States

Reviewed by:
William Donald Phillips, The University of Sydney, Australia
James N. Sleigh, University College London, United Kingdom

***Correspondence:**
Fritz Zimprich
friedrich.zimprich@meduniwien.ac.at

Received: *31 May 2020*
Accepted: *28 July 2020*
Published: *14 August 2020*

Citation:
Krenn M, Grisold A, Wohlfarth P, Rath J, Cetin H, Koneczny I and Zimprich F (2020) Pathomechanisms and Clinical Implications of Myasthenic Syndromes Exacerbated and Induced by Medical Treatments. Front. Mol. Neurosci. 13:156. doi: 10.3389/fnmol.2020.00156

INTRODUCTION

Myasthenia gravis (MG) is the prototype disorder of the neuromuscular junction (NMJ) typically characterized by an autoimmune-mediated muscle weakness and premature fatigue. In more than 80% of patient sera, antibodies directed against the nicotinic acetylcholine receptor (AChR) can be detected (Cetin and Vincent, 2018; Koneczny and Herbst, 2019). Other conditions affecting

neuromuscular transmission include Lambert-Eaton myasthenic syndrome (LEMS) (Titulaer et al., 2011), a range of congenital myasthenic syndromes (CMS) due to variants in > 30 different genes (e.g., *CHRNE*, *RAPSN*, *DOK7*, etc.) (Vanhaesebrouck and Beeson, 2019) and botulism (Guidon, 2019), all of which may be caused by various presynaptic, postsynaptic or combined mechanisms at the NMJ. In addition, drugs or medical treatments may also compromise neuromuscular transmission, the physiology of which will be introduced before outlining the mechanisms underlying the exacerbation of myasthenic syndromes by medical treatments.

Upon arrival of an action potential at the nerve terminal, presynaptic voltage-gated calcium channels (VGCC) open and give rise to an increase of the intracellular Ca^{2+} concentration. This triggers the fusion of presynaptic vesicles containing acetylcholine (ACh) with the cell membrane, releasing their content into the synaptic cleft. In humans, around 50 presynaptic vesicles are released upon each nerve action potential (i.e., quantal content). AChRs are densely concentrated at the postsynaptic muscle membrane by rapsyn, an intracellular 43 kDa receptor-associated protein of the synapse (Maimone and Merlie, 1993), and bind up to two ACh molecules and become permeable to cations with a net inflow of sodium. The activation of AChRs by the release of the quantal content leads to the endplate potential (EPP) at the postsynapse, a locally restricted depolarization of the muscle membrane. Occasional spontaneous release of a single vesicle gives rise to the much smaller (quantal) miniature endplate potential (MEPP). The EPP usually exceeds the threshold potential of −50 mV required for the activation of voltage-gated sodium channels (VGSC) at the depths of the postsynaptic folds, which triggers an action potential in the muscle fiber. The summation of all muscle fiber action potentials generated by the stimulation of a motor axon results in the compound muscle action potential. A safety factor defines the excess local depolarization of the muscle membrane that exceeds the threshold potential required for VGSC activation, ensuring that each nerve action potential is translated into a muscle action potential under physiological conditions. Different factors including the release of a substantially high number of presynaptic vesicles together with high AChR and VGSC densities at the postsynaptic membrane contribute to the safety factor that is around 2 in humans (Elmqvist et al., 1964; Wood and Slater, 2001). There is a non-linear relationship between the quantal content and the EPP. As the membrane potential approaches the reversal potential of the AChR (around 0 mV) during the EPP, the driving force for the cationic inward current through AChRs also decreases, so that with an increasing quantal content more quanta have to be released to cause a further unit increase in EPP amplitude (Slater, 2008).

Some medications, for instance various antibiotics or cardiovascular drugs (beta blockers, calcium channel blockers), that directly impair neuromuscular transmission due to different pre- or postsynaptic or combined mechanisms, usually cause transient worsening of symptoms in patients with a previously diagnosed myasthenic condition (**Figure 1**). It can be hypothesized that most of such drug-related adverse events that are caused by interference with the NMJ only last for a short period of time, mainly depending on the half-life of the drug and patient-related factors (gender, age, renal function, etc.) influencing its elimination. One of the few studies systematically addressing this issue reported that 19% of all recorded MG exacerbations were due to pharmaceutical interventions (Gummi et al., 2019). Withdrawal of myasthenia-aggravating drugs should be effective in these cases, and once an acute aggravation has been managed successfully, the clinical baseline may again be reached without further intervention.

In contrast to these directly NMJ-related mechanisms, a small number of drugs (e.g., D-penicillamine, immune checkpoint inhibitors) or treatments (e.g., allogeneic stem cell transplantation) may lead to *de novo* myasthenic syndromes (**Figure 2**). This is primarily explained by setting in train a previously unknown autoimmune process that subsequently affects neuromuscular transmission, similar to classical autoimmune myasthenia (Penn et al., 1998). In such cases, simply stopping the causative treatment may not be sufficient to reverse the symptoms right away, as enduring auto-reactive immune responses have been initiated. Based on this pathophysiological concept, it can be presumed that immunomodulatory treatments may be more effective in treating medication-induced myasthenic syndromes caused by immune-related mechanisms.

In this review article, we aim to summarize the well-characterized molecular mechanisms of various medical treatments related to worsening of myasthenia (summarized in **Table 1**) or the development of *de novo* myasthenic symptoms (summarized in **Table 2**). Since evidence is scanty for many classes of medication, we will also descriptively mention drugs/treatments with as yet unknown mechanisms but a potential clinical relevance.

A broad range of drugs have been reported to worsen neuromuscular weakness in patients with pre-existing NMJ disorders. The most commonly observed clinical effect is a transient aggravation of symptoms and a relatively prompt recovery upon drug withdrawal. However, for the same drugs also unmasking of a previously unknown myasthenic condition has been hypothesized, but this phenomenon is apparently difficult to prove based on case description. Generally speaking, these drugs usually directly interfere with NMJ function due to different pre- or postsynaptic and combined pathomechanisms.

PRESYNAPTIC NEUROMUSCULAR JUNCTION EFFECTS

The Botulinum Toxin Effect

One of the best-characterized and long-known mechanisms is the one caused by botulinum toxin A (BoNT-A), a toxin produced by *Clostridium botulinum*. BoNT-A is routinely used for the medical treatment of various (focal) neurological disorders (e.g., dystonia, spasticity). The main mode of action is the blockade of ACh release at the presynaptic nerve terminal. More specifically, BoNT-A causes proteolytic cleavage of SNAP-25, which is part of the soluble N-ethylmaleimide-sensitive-factor attachment receptor (SNARE) complex and crucially involved

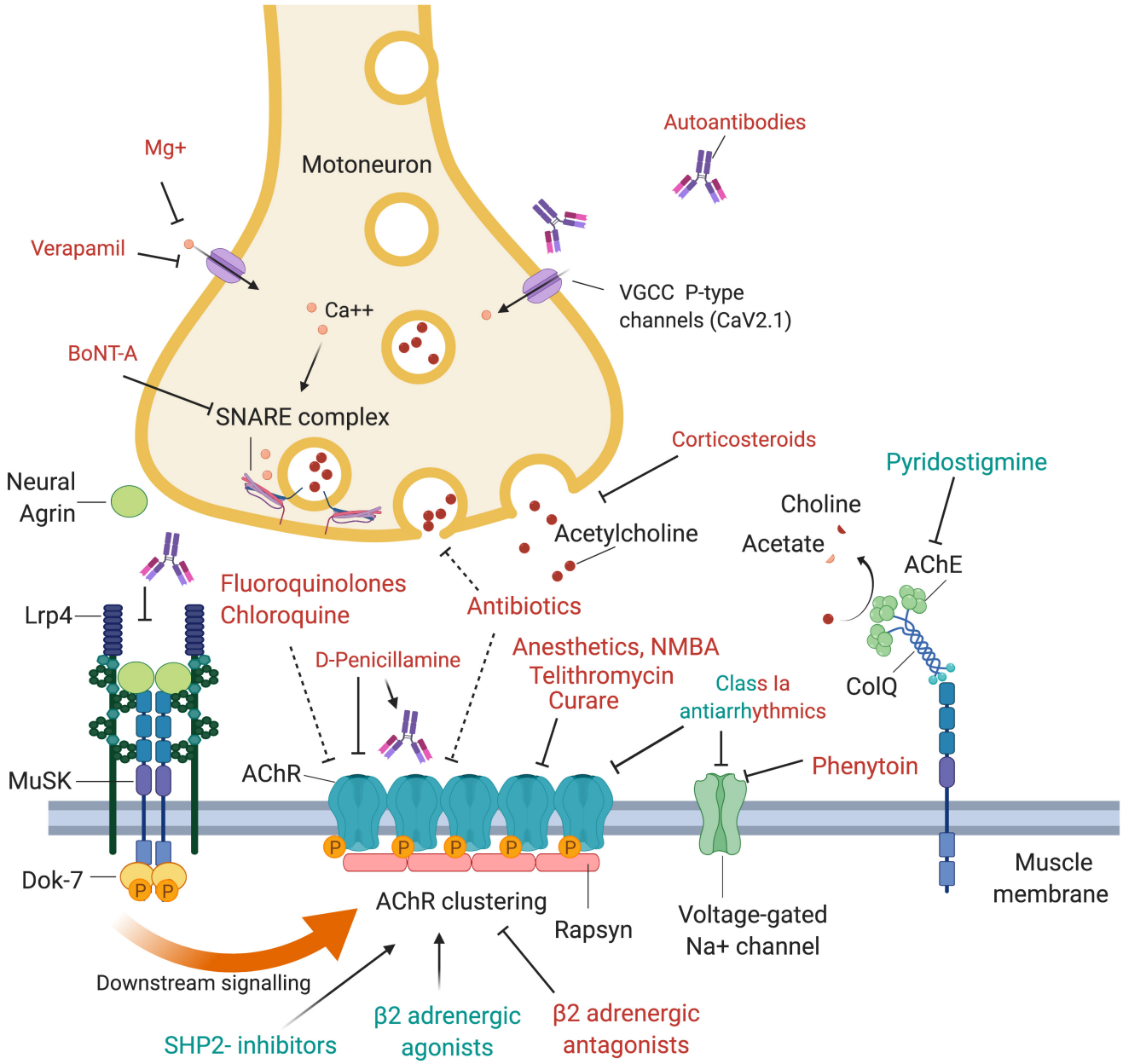

FIGURE 1 | Drugs and antibodies that affect the function of the neuromuscular junction. Upon arrival of an action potential, presynaptic P-type VGCC (voltage-gated calcium channels) open and calcium enters the motoneuron terminal. This may be negatively affected by autoantibodies that block the VGCC, Mg^{+} or Verapamil. Calcium stimulates Ca^{2+} mediated exocytosis of neurotransmitters via the SNARE complex, which is negatively affected by BoNT-A which induces cleavage of one of its components, SNAP-25. Release of acetylcholine may also be reduced by corticosteroids or antibiotics. At the postsynaptic side, AChRs are densely aggregated, which is regulated via the agrin-Lrp4-MuSK-Dok-7 signaling pathway. Neural agrin is released by the motoneuron and binds to its co-receptor, Lrp4, located in the muscle membrane. Lrp4 and agrin bind as a dimer of dimers to the muscle-specific kinase (MuSK), a receptor tyrosine kinase that then phosphorylates itself, leading to the attachment of the adapter protein Dok-7. This binding leads to a full activation of MuSK and phosphorylation of downstream molecules, cumulating in the phosphorylation and dense aggregation of AChRs. The interaction between MuSK and Lrp4 can be blocked by autoantibodies, leading to interrupted signal transduction and reduced AChR clustering. The AChR clustering can be strengthened by SHP2-inhibitors and β2-adrenergic agonists, and de-stabilized by β2-adrenergic antagonists. Binding of acetylcholine to the AChR leads to opening of the channel, influx of cations, depolarization of the membrane and opening of voltage-gated Na + channels, which amplifies the depolarization. A range of drugs was shown to block the AChR, including fluoroquinolones, chloroquine, antibiotics, anesthetics, NMBA, telithromycin, curare and class Ia antiarrhythmics. Quinidine, a class Ia antiarrhythmic drug, may also be beneficial in the context of slow channel CMS with a pathological prolonged open state of the AChR. Voltage-gated Na^{+} channels are inhibited by phenytoin and class Ia antiarrhythmics. Acetylcholine is recycled in the synaptic cleft by the acetylcholinesterase (AChE), which hydrolyses acetylcholine to choline and acetate. AChE is arranged in tetramers attached to collagen q like tail (ColQ), which in turn is anchored to the synapse via binding to MuSK. AChE is inhibited by pyridostigmine, leading to prolonged presence of acetylcholine in the synaptic cleft, and is used as first line symptomatic treatment in myasthenia gravis.

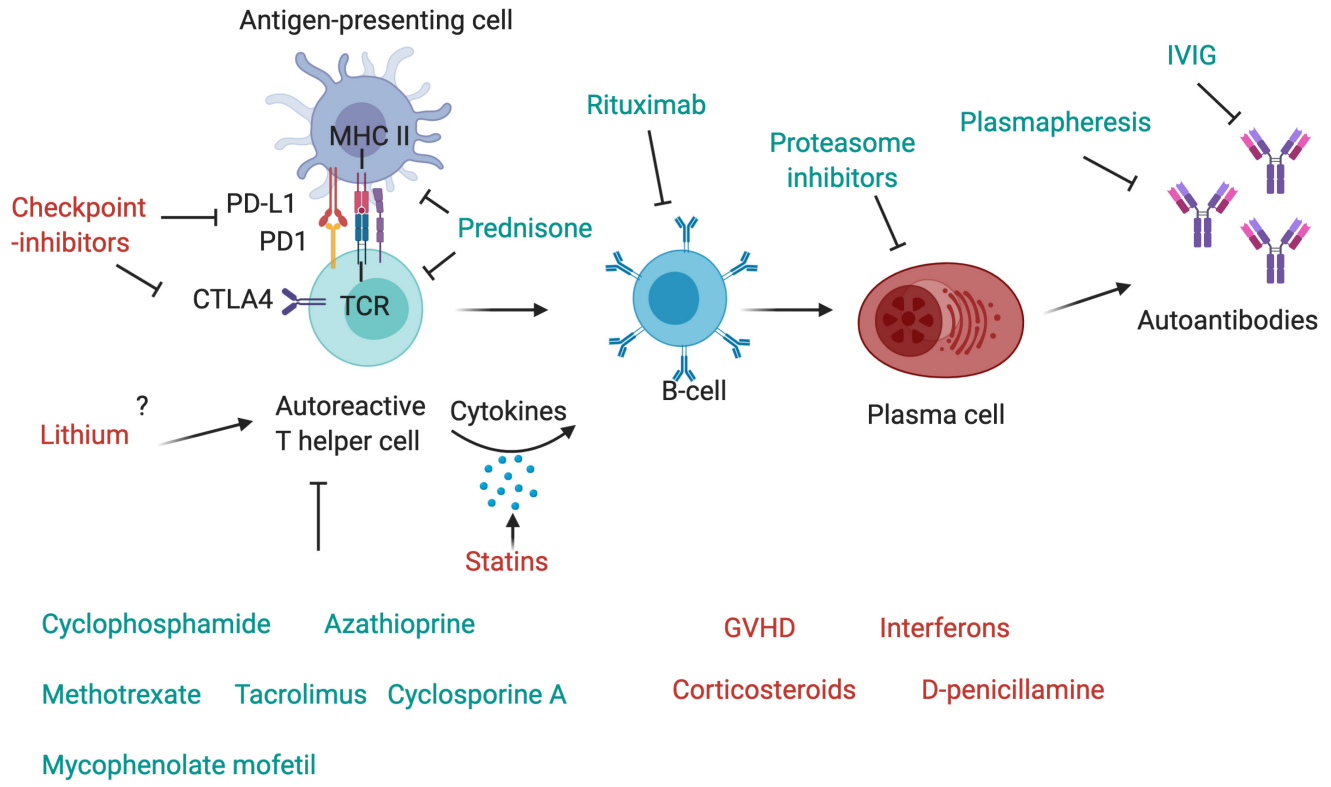

FIGURE 2 | Drugs affecting components of the immune system. The T-cell receptor (TCR) of autoreactive T-helper cells recognizes antigen peptides that are presented by the MHC II complex on antigen-presenting cells. The binding of programmed cell death protein 1 (PD-1) to its ligand, PD-L1, expressed, respectively, on antigen-presenting cell and T-cell, inhibits immune activation and is an important immune checkpoint to guard against autoimmunity. CTLA4 is another checkpoint that is expressed on regulatory T-cells and upregulated on conventional T cells after activation and turns off T-cell activation when it interacts with its ligands, CD80 or CD86, on antigen-presenting cells. Checkpoint inhibitors are used as therapy to stimulate an attack on tumor cells, but they may also activate autoreactive T-cells and induce autoimmunity. Corticosteroids such as Prednisone inhibit antigen processing and presenting in antigen-presenting cells and block T-cell activation in the nucleus. T-cells are further targeted by other immunosuppressant drugs, such as cyclophosphamide, azathioprine, methotrexate, mycophenolate mofetil, cyclosporin A or tacrolimus. T helper cells activate autoreactive B-cells via MHC II-antigen-TCR interaction and the secretion of pro-inflammatory cytokines, these may be increased by statins. B-cells can be depleted by the use of Rituximab, a therapeutic monoclonal antibody against CD20, which is beneficial in many antibody-mediated autoimmune diseases. Plasma cells, which produce autoantibodies, may be targeted by proteasome inhibitors, and autoantibodies can be depleted by plasmapheresis. IVIg are also a therapeutic drug in autoimmune diseases that ameliorate antibody-mediated effects, although their exact mechanism of action is unknown.

in neurotransmitter release through Ca^{2+}-mediated exocytosis (Dolly and Aoki, 2006).

Although transient and usually mild, typical side effects include neuromuscular symptoms through local (to the injection site) but also distant effects at the NMJ, including dysphagia, ptosis, diplopia and limb weakness (Dashtipour and Pedouim, 2016). Interestingly, single-fiber electromyography demonstrated changes in neuromuscular transmission in muscles distant from the injection site (Garner et al., 1993). In keeping with these observations, myasthenic disorders may significantly worsen due to BoNT-A (Watts et al., 2015). As a result, pre-existing disorders of the NMJ represent a relative contraindication for the injection of BoNT-A, hence requiring a cautious risk-benefit assessment by the treating clinicians beforehand.

In addition to the known NMJ-related side effects, anecdotal evidence suggests an association between BoNT-A injections and an initial manifestation of a myasthenic condition. To the best of our knowledge, eight cases have so far reported a first manifestation of MG following BoNT-A injection, with the majority of described patients showing predominantly ocular symptoms with a latency between 1 day and 6 weeks after injection (Timmermans et al., 2019). Moreover, one publication reported that LEMS first presented after BoNT-A injection (Erbguth et al., 1993). Given the known directly NMJ-related mechanism, it can be assumed that previously subtle conditions may have been unmasked by further impairing neuromuscular transmission.

Electrolyte-Related Neuromuscular Junction Effects

An electrolyte-related impairment of NMJ function may be caused by electrolyte imbalances, most typically by an excess of magnesium. Magnesium competitively blocks the entry of calcium into the presynaptic nerve terminal – a process that is crucial for the release of ACh into the synaptic cleft. The

TABLE 1 | Selection of clinically relevant classes of drugs associated with exacerbations of pre-existing myasthenic syndromes.

Class of drugs	Main mode of action	Myasthenia-related pathomechanism(s)	Clinical features	Evidence supporting myasthenia-related effects	Additional information	References
Aminoglycoside antibiotics	Inhibition of protein synthesis	Pre-, postsynaptic, and combined (depending on compound)	Dose-dependent muscle weakness partially reversible by AChEI and calcium	Case reports, *in vitro* data, electrophysiological investigations	Neomycin most toxic, tobramycin least toxic	Pittinger and Adamson, 1972; Singh et al., 1978a,b; Caputy et al., 1981; Kaeser, 1984
Fluoroquinolone antibiotics	Gyrase inhibition	Postsynaptic blockade of AChRs	Rapid clinical worsening of known MG or unmasking MG	Large number of case-based evidence; chemical similarity to quinine, quinidine and chloroquine, which cause neuromuscular blockade	Levofloxacin, ofloxacin and ciprofloxacin cause severe exacerbations (FDA warning)	Moore et al., 1988; Mumford and Ginsberg, 1990; Azevedo et al., 1993; Roquer et al., 1996; De Sarro and De Sarro, 2001; Gunduz et al., 2006
Macrolide/ ketolide antibiotics (telithromycin)	Interference with protein synthesis via ribosomal 50S subunit	Postsynaptic blockade of AChRs	Symptom aggravation within 2 h after first telithromycin administration	Case series with 10 patients, *in vitro* data (whole-cell patch-clamp)	Telithromycin withdrawn from market	May and Calvert, 1990; Cadisch et al., 1996; Nieman et al., 2003; Jennett et al., 2006; Perrot et al., 2006; Liu and Somps, 2010
Class Ia antiarrhythmics (procainamide, quinidine)	Blockade of sodium channels	Pre- and postsynaptic blockade	Procainamide – rapid and severe deterioration of weakness in MG; Quinidine – potential to unmask MG	Microelectrode and patch clamp recordings, animal models (rodent)	Quinidine used as a treatment in (slow channel) CMS	Lee et al., 1983; Oh et al., 1986; Godley et al., 1990; Yeh et al., 1992; Miller et al., 1993
Class IV antiarrhythmics (verapamil)	Blockade of voltage-dependent Ca^{++} channels	Presynaptic reduction of released ACh (but also postsynaptic effects?)	Clinical worsening of LEMS and MG	Single case-based observations, *in vitro* data, electrophysiological investigations	–	Krendel and Hopkins, 1986; Ribera and Nastuk, 1989; Swash and Ingram, 1992; Jonkers et al., 1996; Protti et al., 1996
Beta-adrenergic blockers	Selective or non-selective blockade of beta-adrenergic receptors	Destabilizing effect on AChR clusters	Worsening of previously diagnosed as well as newly diagnosed MG	Retrospective chart review study, experimental data on inverse effects of beta agonists (for CMS)	2.7-fold increased risk of developing an MG aggravation	Harry et al., 1974; Verkijk, 1985; Leys et al., 1987; Confavreux et al., 1990; Clausen et al., 2018; Gummi et al., 2019
Botulinum toxin A	Presynaptic blockade of ACh release	Presynaptic blockade of ACh release	Local and distant neuromuscular effects (flaccid weakness), mimicking or unmasking /aggravating MG, including dysphagia, ptosis, diplopia, limb weakness (latency: 1 day and 6 weeks)	Case reports, single-fiber electromyography (impaired neuromuscular transmission distant from injection site)	Unmasking of LEMS reported in 1 case; BoNT-A should be considered contraindicated in NMJ-related disorders	Erbguth et al., 1993; Garner et al., 1993; Watts et al., 2015; Dashtipour and Pedouim, 2016; Timmermans et al., 2019
Corticosteroids	Complex metabolic, anti-inflammatory, immunosuppressive, anti-proliferative effects	Altered depolarization of nerve cells, reduction of ACh release, changes in choline transport, depletion of potassium	Initial exacerbation, 8.6% severe, requiring mechanical ventilation or intubation	Case reports, observational study, experimental models	Gradually increasing steroid dose may avoid initial exacerbations	Seybold and Drachman, 1974; Wilson et al., 1974; Abramsky et al., 1975; Dengler et al., 1979; Kim et al., 1979; Pascuzzi et al., 1984; Kanai et al., 2019
Magnesium	Electrolyte with multiple metabolic functions, involved in hormone receptor binding, muscle contraction, neural activity, transmitter release, cardiac excitability	Reduced AChR release due to competitive block of calcium entry into the presynaptic nerve terminal; Possibly additional mild postsynaptic effect	Reminiscent of LEMS, ocular muscles tend to be spared	Electrophysiological investigations of nerve and muscle tissue	Parenteral use should be avoided in MG patients	del Castillo and Engbaek, 1954; Lipsitz, 1971; Gutmann and Takamori, 1973; Cohen et al., 1976; Swift, 1979; Pritchard, 1979; Krendel, 1990; Singh et al., 2015

(Continued)

TABLE 1 | Continued

Class of drugs	Main mode of action	Myasthenia-related pathomechanism(s)	Clinical features	Evidence supporting myasthenia-related effects	Additional information	References
Lithium	Unknown	Enhancing T-cell activity; reducing AChRs at NMJ	Aggravations of MG and unmasking of autoimmune myasthenia	Case reports, functional evidence derived from studies in rodents	Clinically used as a mood stabilizer	Neil et al., 1976; Mizuno et al., 1982; Lipton, 1987; Pestronk and Drachman, 1987; Ronzière et al., 2000
Phenytoin	Blockade of voltage-gated sodium channels	Pre- and postsynaptic effects	In some published cases immediate amelioration of symptoms after PHT discontinuation	Few case reports, *in vitro* studies	Weak evidence also for other AEDs (CBZ, GBP)	Norris et al., 1964; Brumlik and Jacobs, 1974; Yaari et al., 1977
Neuromuscular blocking agents	Competitively blocking the binding of ACh to its receptors (non-depolarizing) or depolarizing the muscle fiber	Postsynaptic blockade	Prolonged NMJ blockade in MG and LEMS, with severe disease and higher doses of pyridostigmine correlating with increased sensitivity	Case reports	Sugammadex, has the potential to reverse the neuromuscular blockade of NMBAs	Nilsson and Meretoja, 1990; Schaller and Lewald, 2016
Volatile (inhalation) anesthetics	Inhibition of nicotinic AChR	Changing kinetics of postsynaptic conductance at synapses	Increased sensitivity of MG patients regarding neuromuscular side effects	Case-based observations, experimental data	Thorough pre- and postsurgical management of patients with NMJ disorders	Gage and Hamill, 1976; Nitahara et al., 2007

Ach, Acetylcholine; AChEI, Acetylcholine esterase inhibitors; AChR, Acetylcholine receptor; AED, anti-epileptic drug; BoNT-A, Botulinum toxin A; CBZ, Carbamazepine; CMS, Congenital myasthenic syndrome; FDA, Food and Drug Administration; GBP, Gabapentin; LEMS, Lambert-Eaton myasthenic syndrome; MG, Myasthenia gravis; NMBA, Neuromuscular blocking agent; NMJ, neuromuscular junction; PHT, phenytoin.

subsequent magnesium-induced reduction of ACh release eventually impairs neuromuscular transmission (Krendel, 1990). Accordingly, the pathophysiological mechanisms of hypermagnesemia resemble LEMS, in which Abs are directed against the presynaptic VGCC. Investigations of nerve and muscle tissue showed that endplate potential amplitudes evoked by nerve stimulation were reduced in the presence of magnesium, which could be reversed by adding calcium. This finding corroborates a presynaptic mechanism as the key mode of action. A slight decrease in sensitivity of the motor endplate to ACh was also observed, potentially suggesting a mild additional postsynaptic effect (del Castillo and Engbaek, 1954).

In concordance with the mainly presynaptic mode of action, the clinical picture also resembles LEMS rather than classical MG (Swift, 1979). Nonetheless, also patients with known disorders of the postsynaptic membrane (i.e., MG) appear to react particularly sensitive to magnesium. Hence, individuals with MG and LEMS may develop increased weakness already at slightly elevated serum levels (Gutmann and Takamori, 1973; Cohen et al., 1976).

An excess of magnesium may especially be relevant in patients with concomitant renal failure and the use of magnesium-containing drugs such as laxatives, antacids or enemas (Krendel, 1990). Moreover, hypermagnesemia is a pharmacologically intended state in women with (pre)eclampsia (Pritchard, 1979), and the application of high parental doses may result in myasthenic crises in these patients (Lipsitz, 1971; Singh et al., 2015). Clinical symptoms have been reported to correlate well with magnesium serum levels (Fishman, 1965). In patients with no previous history of neuromuscular disease but myasthenic symptoms due to iatrogenic magnesium application, magnesium withdrawal and the intravenous use of calcium can be efficient. Hemodialysis may remain reserved for severe cases (Alfrey et al., 1970). In contrast, low oral doses of magnesium are usually not considered as a clinically relevant problem.

Calcium-Dependent Presynaptic Effects

As mentioned above, the influx of calcium through VGCC, induced by a motor axonal action potential, represents one of the key functional events of neuromuscular transmission in the presynaptic nerve terminal. Yet, the exact influences of calcium channel blocking agents (which are mainly used for cardiovascular indications) on neuromuscular activity are not fully understood, but some functional data and clinical reports suggest a clinically relevant impairment of neuromuscular function.

From an experimental point of view, a presynaptic reduction of released ACh but also postsynaptic effects have been observed for the calcium channel blocker verapamil (Ribera and Nastuk, 1989). When studying the effects of different calcium channel blockers on transmitter release at the neuromuscular junction, it was found that P-type calcium channel blockers inhibited nerve-evoked action potentials and subsequent synaptic transmission, while transmitter release remained unaffected by selective L-type and N-type channel blocking agents (Protti et al., 1996). These findings underscore that P-type channels

TABLE 2 | Drugs and medical treatments with best evidence for an association with the development of *de novo* myasthenic syndromes.

Class of drugs/type of treatment	Main mode of action	Myasthenia-related pathomechanism(s)	Clinical features	Evidence supporting myasthenia-related effects	Additional information	References
D-penicillamine	Pyridoxine antagonist and chelating drug	Production of AChR Abs due to a newly developed immune response directed against the drug (and mild unspecific presynaptic effects)	Mostly mild ocular symptoms 2–12 months after initiation, usually responding well to pyridostigmine, remission often within 1 year after discontinuation	Large number of case reports, experimental immunological data	Used for the treatment of Wilson's disease, MG phenotype observed in up to 7%	Vincent et al., 1978; Aldrich et al., 1979; Albers et al., 1981; Kuncl et al., 1986; Drosos et al., 1993; Andonopoulos et al., 1994; Adelman et al., 1995; Penn et al., 1998
Chloroquine	Anti-malarial drug that prevents biocrystallization of heme	Postsynaptic blockade of AChRs and additional immune-modulatory properties	Reminiscent of classical autoimmune MG	Case reports, electrophysiological investigations	Recently suggested as a COVID-19 drug, study reporting ineffectiveness has been retracted	Robberecht et al., 1989; Varan et al., 2015; Mehra et al., 2020
Interferon	Multiple effects including inhibition of protein synthesis, inactivation of viral RNA, phagocytic and cytotoxic mechanisms (leading to anti-viral, anti-tumor, anti-angiogenic activity)	Primarily humoral immune response, comparable to that in human MG	AChR-positive MG, often additional myopathic findings in EMG	Case reports for both inducing and aggravating myasthenia, transgenic mice studies, histological-immunological work-up	Most reported cases occurred when IFN was used for hepatitis C (additional pathogenic role of viral infection?)	Conlon et al., 1990; Batocchi et al., 1995; Gu et al., 1995; Borgia et al., 2001; Wolfe et al., 2007; Congeni and Kirkpatrick, 2013; Baik et al., 2016; Saleem, 2016
Allogeneic hematopoietic stem cell transplantation	Transfer of the donor hematopoietic and immune system to the host to treat (hematological malignancies)	Combined cellular (T- and B-cells) and humoral alloreactivity as a manifestation of chronic GVHD	Develops 3–12 months after HSCT, often supported by AChR Abs	Large-scale observational data	Rare occurrence with incidence < 1%	Bolger et al., 1986; Lefvert and Björkholm, 1987; Maffini et al., 2017; Tsutsumi et al., 2019
Immune checkpoint inhibitors	Inhibition of checkpoint molecules CTLA4, PD-1, PD-L1	Induction of autoimmune activity due to interference with immunological homeostasis, reduced T-cell tolerance, increase of inflammatory cytokines	Very severe and progressive clinical course, often accompanied by respiratory failure, overall mortality 20–30%; AChR Abs in 66%; overlap syndromes with myositis/myocarditis	Large-scale pharmacovigilance studies, numerous case reports/series	Incidence approximately 0.5%; Most commonly due to PD-1 or PD-L1 inhibition	Johnson et al., 2015, 2019; Montes et al., 2018; Sato et al., 2019; Safa et al., 2019; Xing et al., 2020
Statins	HMG-CoA reductase inhibitors	Increase of Th2 interleukins, depletion of coenzyme Q10	Predominantly affecting oculo-bulbar muscles with symptom onset between 1 week and 4 months after initiating treatment	Case series	Both aggravating and developing myasthenia has been described	Parmar et al., 2002; Cartwright et al., 2004; Purvin et al., 2006; Oh et al., 2008; Khalid et al., 2016

Ach, Acetylcholine; AChR, Acetylcholine receptor; COVID-19, coronavirus disease 2019; CTLA4, cytotoxic T-lymphocyte-associated protein 4; EMG, Electromyography; GVHD, Graft-versus-host disease; HSCT, Hematopoietic stem cell transplantation; HMG-CoA reductase, 3-hydroxy-3-methyl-glutaryl-coenzyme A reductase; IFN, Interferon; MG, Myasthenia gravis; PD-1, Programmed cell death protein 1; PD-L1, Programmed cell death 1 ligand 1; Th2, T helper type 2.

($Ca_V2.1$) are the primary mediators of transmitter release at motor nerve terminals.

In addition, case-based observations of paraneoplastic LEMS and autoimmune MG showed clinical worsening following a treatment with verapamil, a class IV antiarrhythmic drug that blocks voltage-dependent calcium channels (Krendel and Hopkins, 1986; Swash and Ingram, 1992). The effect of verapamil on neuromuscular transmission was addressed by Jonkers et al., who studied the influence of intravenous verapamil on repetitive nerve stimulation and clinical function in 10 patients with MG. However, no reproducible effects on neuromuscular transmission were found in this study, that was mainly limited by its small sample size (Jonkers et al., 1996).

POSTSYNAPTIC NEUROMUSCULAR JUNCTION EFFECTS

Blockade of Acetylcholine Receptors (Curare-Like Effects)

The plant-derived toxin curare is a historical example for neuromuscular blockade, acting by a competitive inhibition of the nicotinic AChR at the postsynaptic membrane. Functionally similar (curare-like) mechanisms have also been proposed for various drugs.

A broad range of antibiotics have already been associated with clinical worsening in patients with MG. This is particularly relevant, since many patients with MG are under immunosuppressive treatment, partly suffering from recurrent respiratory symptoms and requiring antimicrobial treatment. Yet, the exact mechanisms underlying neuromuscular blockade are diverse and often poorly understood.

First, Telithromycin, a relatively new ketolide antibiotic, is known to induce myasthenia or lead to severe symptom exacerbations including fatal respiratory failure and death (Nieman et al., 2003; Jennett et al., 2006). *In vitro* studies substantiated these observations by showing that telithromycin inhibits nicotinic AChRs and blocks neuromuscular transmission (Liu and Somps, 2010). A case series comprising 10 affected individuals highlights the potential to aggravate and unmask MG, also reporting that most patients develop symptoms within 2 h after the first administration of telithromycin, which is in line with the aforementioned mechanism (Perrot et al., 2006). The drug has already been withdrawn from the market due to its severe side effects.

There is a long list of anecdotal reports indicating (sometimes severe) symptom deterioration following the administration of fluoroquinolones, i.e., gyrase inhibitors, which led to a "black box" warning by the FDA, for their use in patients with MG (De Sarro and De Sarro, 2001). Notably, the fluoroquinolones, particularly levofloxacin, ofloxacin and ciprofloxacin, may cause acute and severe exacerbations of myasthenic symptoms (Moore et al., 1988; Mumford and Ginsberg, 1990; Azevedo et al., 1993; Roquer et al., 1996; Gunduz et al., 2006). From a biochemical perspective, these adverse effects may in part be explained by the structural similarities to quinine and chloroquine, which have been shown to cause a neuromuscular blockade (Sieb et al., 1996).

Chloroquine is used for the treatment of malaria, but also for some rheumatological diseases. Moreover, the pandemic COVID-19 caused by the virus infection with SARS-CoV-2 has recently brought widespread attention to this drug, as it has initially been suggested as a potentially promising anti-viral treatment for this indication (Touret and de Lamballerie, 2020). A subsequent multi-national analysis showing an increased mortality rate and no beneficial effects was later retracted by the journal (Mehra et al., 2020). In general, clinical, electrophysiological and serological characteristics of chloroquine-related myasthenia are strikingly reminiscent of acquired autoimmune MG. In view of the complete recovery 2 weeks after treatment cessation (compatible with the long half-life of chloroquine) and the absence of anti-AChR Abs, it has been hypothesized that chloroquine-induced MG may be caused by a direct postsynaptic mechanism (Robberecht et al., 1989). However, in contrast to most classical antimicrobial drugs, chloroquine seems to have the ability to induce (partly anti-AChR-positive) MG, usually recovering after drug withdrawal (Varan et al., 2015). It is worthy of note, that chloroquine has immune-modulatory properties that may play an additional role in such cases.

Primarily postsynaptic effects at the NMJ have also been ascribed to class Ia antiarrhythmics, which interfere with sodium channels. Intracellular microelectrode recordings in rats provided evidence for both pre- and postsynaptic effects of procainamide, with postsynaptic blockade representing the dominant mode of action (Lee et al., 1983). One study by Yeh et al. (1992) demonstrated a perturbed AChR-dependent contractile muscle function in a rat model of experimental MG caused by procainamide. Clinically, procainamide may lead to a rapid and severe deterioration of weakness in MG patients (Godley et al., 1990). Moreover, also the primary induction of myasthenic symptoms including bulbar features has been reported occasionally in the literature (Oh et al., 1986; Miller et al., 1993). Though immunological properties have been ascribed to this drug, the rapid clinical manifestation of neuromuscular symptoms rather supports a directly NMJ-related mechanism.

Drug-induced side effects that might be related to alterations of the membrane potential of the NMJ are most obvious for the neuromuscular blocking agents (NMBAs), which are used in anesthesiology. In fact, both depolarizing and non-depolarizing NMBAs may interfere with the muscle membrane potential. Relatively small doses of non-depolarizing agents can cause a profound and prolonged NMJ blockade in individuals with MG and LEMS, with more severe disease and higher doses of pyridostigmine correlating with an increased sensitivity toward non-depolarizing NMBAs (Nilsson and Meretoja, 1990). A comparably novel drug, sugammadex, has the potential to reverse the neuromuscular blockade of NMBAs within minutes by 1:1 binding of rocuronium or vecuronium (Schaller and Lewald, 2016). Given most reports published to date, it can be considered as a safe option to restore neuromuscular transmission for this vulnerable

patients population, if the use of NMBAs is necessary (Cata et al., 2019).

It is a commonly observed phenomenon that patients with NMJ disorders are specifically prone to prolonged weakness after surgery with various types of anesthesia. Patients with MG pose a major challenge for anesthesiologists, and the post-surgical risk of respiratory problems is a matter of concern. Yet, surgery is often necessary in MG, especially because thymectomy is a standard treatment of seropositive patients with AChR Abs (Wolfe et al., 2016). A careful selection of anesthetic drugs must be made to avoid complications. Elective surgery should ideally be performed in a stable phase of myasthenic disease, and the clinical situation should be optimized beforehand (Jamal and Herb, 2009).

may result in a superimposed impairment of neuromuscular transmission when used together with NMBAs, volatile (inhalation) anesthetics may interfere with neuromuscular transmission in a more direct way, that is mainly through the inhibition of nicotinic AChR. Experimental data indicate that they change the kinetics of postsynaptic conductance at synapses (Gage and Hamill, 1976). Myasthenic patients display an increased sensitivity to the relaxant effects of these drugs (e.g., sevoflurane) (Nitahara et al., 2007). Regarding anesthesia, a thorough pre- and post-operative evaluation, the continuation of pyridostigmine and a careful monitoring should be helpful to safely manage patients with MG. In addition, it is important to use neuromuscular monitoring (i.e., train-of-four monitoring) during surgery to ensure optimal recovery before terminating anesthesia (Blichfeldt-Lauridsen and Hansen, 2012).

Effects of Beta-Adrenergic Blockade

Beta-adrenergic blocking agents are under the suspicion of adversely affecting neuromuscular strength in MG patients (Verkijk, 1985). *In vitro* studies of nerve-muscle preparations revealed that various beta-adrenergic blockers may lead to a dose-dependent reduction of neuromuscular transmission in rats with propranolol having the most pronounced effect on neuromuscular transmission (Harry et al., 1974). Adrenergic beta-2 receptor agonists are increasingly used in the treatment of CMS, and it has been shown that they directly interfere with proteins located at the NMJ, exerting a stabilizing effect on AChR clusters (Clausen et al., 2018). This strongly suggests a reverse effect at the NMJ as the mechanism underlying beta blocker-related worsening of myasthenic symptoms. It is also worthy of note that the stabilization of AChR clusters using an SRC homology 2 domain-containing phosphotyrosine phosphatase 2 (SHP2) inhibitor has recently been found in early cell culture studies to be a promising mechanisms against MuSK-MG (Huda et al., 2020).

A retrospective chart review study showed that the odds of developing a transient aggravation of MG is increased 2.7-fold under beta-adrenergic antagonists in general, which represents a statistically significant signal (Gummi et al., 2019). A small-scale systematic trial studying the neuromuscular effects of an intravenously applied beta blocker (propranolol) in 10 patients could not prove an acute and significant deterioration of neuromuscular transmission in MG using repetitive nerve stimulation and clinical tests, but the work was clearly limited by the small number of participants (Jonkers et al., 1996). Several case reports indicated that latent myasthenia may be unmasked by beta blocker treatment (Leys et al., 1987; Confavreux et al., 1990).

Apart from cardiovascular indications, beta-adrenergic antagonists are used for the local treatment of open angle glaucoma to depress intraocular pressure. Although applied as eye drops, there may be systemic adverse events including increased neuromuscular weakness in rare cases. Both worsening of previously diagnosed as well as newly diagnosed MG have been described for the non-selective beta blocker timolol (Coppeto, 1984; Verkijk, 1985) and for the beta1-selective blocker betaxolol (Khella and Kozart, 1997).

PRESUMED (COMBINED) PRE- AND POSTSYNAPTIC EFFECTS

In many classes of drugs, the functional evidence for the pathomechanisms underlying neuromuscular blockade is scanty at best. Often, both pre- and postsynaptic mechanisms are presumed, mostly on the basis of electrophysiological studies. Hence, for many of these medications, the exact mechanism remains unknown.

Various reports have been published for aminoglycoside antibiotics to cause a clinically relevant neuromuscular blockade. Functional data indicate that aminoglycoside antibiotics may impair neuromuscular transmission through both presynaptic (via inhibition of prejunctional ACh release) and postsynaptic (via depression of post-junctional sensitivity) molecular mechanisms, which are overall still poorly appreciated (Pittinger and Adamson, 1972). The resulting effects appear to be (partly) reversible by calcium gluconate, AChE inhibitors and aminopyridines (Singh et al., 1978a,b). One study evaluated neuromuscular toxicity of several aminoglycosides including amikacin, gentamicin, kanamycin, neomycin, netilmicin, streptomycin and tobramycin, with neomycin being classified as the most toxic and tobramycin as the least toxic of all investigated aminoglycosides (Caputy et al., 1981). Interestingly, gentamicin, neomycin, streptomycin, tobramycin, and kanamycin have also been implicated in clinical weakness occurring in otherwise healthy (non-myasthenic) individuals (Kaeser, 1984).

Neuromuscular blockade due to antibiotics is certainly not confined to aminoglycosides. The monobasic amino acid antibiotics lincomycin and clindamycin structurally differ from classical aminoglycosides, but may cause a neuromuscular blockade which can be reversed by calcium and aminopyridines (Booij et al., 1978). Electrophysiological studies showed that both drugs cause the blockade via different modes of action. Lincomycin displayed predominantly nerve-terminal depressant properties, while clindamycin showed stimulatory presynaptic effects (Rubbo et al., 1977). However, real-life data confirming the clinical relevance of these *in vitro* effects are still lacking.

Polymyxin B and colistin, which are used as a last-resort for resistant Gram-negative bacteria, show neuromuscular toxicity,

mainly in patients with renal failure or in combination with other NMJ-blocking drugs, perhaps potentiating their effects (Pittinger and Adamson, 1972). Again, the presumed mechanisms of action are a reduced release of ACh and, to a certain degree, the concomitant postsynaptic blockade of AChR receptors (Wright and Collier, 1976; Viswanath and Jenkins, 1978; Durant and Lambert, 1981).

Aside from antimicrobial drugs, the class Ia antiarrhythmic drug quinidine (and its stereoisomer quinine) have been observed to transiently worsen neuromuscular weakness in patients with MG (Weisman, 1949). Somewhat paradoxically at first sight, while deteriorating MG, quinidine represents an effective therapeutic option in (slow channel) CMS (Lee et al., 2018). In such cases with a pathologically prolonged open state of the AChR channel due to monogenic mutations, an open-channel blocker can be of clinical benefit (Peyer et al., 2013). The adverse effects causing neuromuscular blockade are localized in the presynaptic membrane, impairing ACh release, but also (to a lesser extent) in the postsynaptic membrane with curare-like effects, as demonstrated by microelectrode and patch-clamp investigations (Sieb et al., 1996).

One anti-epileptic drug (AED) that has been associated with myasthenic symptoms a long time ago is phenytoin (PHT), a blocker of voltage-gated sodium channels. *In vitro* studies demonstrated both presynaptic and postsynaptic effects on neuromuscular transmission (Yaari et al., 1977). Aside from functional data, few reports with an MG-like presentation have been published in the literature, often ameliorating after PHT discontinuation, potentially pointing toward an actual drug-associated effect (Norris et al., 1964; Brumlik and Jacobs, 1974).

IMMUNOLOGICAL MECHANISMS IN DRUG-RELATED MYASTHENIA

As opposed to the delineated NMJ-related drug effects, some medical treatments are known or presumed to set in motion a *de novo* immunological process, thus initiating new-onset autoimmune phenomena that may clinically resemble acquired conditions such as MG. This pathophysiological concept is in line with new-onset diseases in previously healthy individuals rather than a transient aggravation of a pre-existing disorder. However, also previous autoimmunological conditions may be more likely to flare up as a consequence of immune-modulatory treatments.

D-Penicillamine

Occurring in up to 7% of patients taking D-penicillamine (D-P), myasthenia represents a relatively common adverse event (Andonopoulos et al., 1994). Clinical, electrophysiological and serological features do not seem to differ remarkably from classical MG. Most patients present with mild, predominantly ocular symptoms occurring 2–12 months after D-P initiation and usually responding to pyridostigmine (Drosos et al., 1993). However, marked respiratory symptoms have also been reported (Adelman et al., 1995). In many cases, D-P-related MG remits within 1 year following drug discontinuation (Albers et al., 1981). The prolonged latency of symptom onset and remissions and the gradual decline of Ab levels after withdrawal are in keeping with the mechanism of a drug-induced immunological effect (Vincent et al., 1978).

Basic research also supports that the production of AChR Abs plays an essential role and that D-P-induced MG may arise due to a newly developed immune-mediated response that is directed against the compound itself (Penn et al., 1998). Studies of D-P reacting with purified AChR demonstrated a covalent attachment to two receptor subunits (alpha and gamma). Moreover, D-P appears to impact the equilibrium of ACh binding properties of both purified receptor and receptor-rich membrane fragments (Bever et al., 1982). The detailed characterization of a patient with D-P-induced myasthenia indicated pathophysiological overlaps with idiopathic MG, including the production of anti-AChR Abs, as well as subsequent degradation and quantitative reduction of junctional AChRs (Kuncl et al., 1986). Electrophysiological changes in rats indicated also mild and unspecific presynaptic effects of D-P at high concentrations (Aldrich et al., 1979). Of note, the lower incidence of D-P-induced myasthenia in patients with Wilson's disease compared to those with rheumatoid arthritis may suggest a general immunogenetic susceptibility to autoimmune disorders as an additional role (Komal Kumar et al., 2004).

Interferon

Similar to D-P, patients under interferon (IFN) treatment may develop autoimmune-mediated disorders for the first time (Conlon et al., 1990). Among others, generalized, partly severe manifestations of MG were either triggered or aggravated by IFN alpha (Borgia et al., 2001; Wolfe et al., 2007; Congeni and Kirkpatrick, 2013; Baik et al., 2016; Saleem, 2016).

Studies in transgenic mice confirmed that the presence of IFN gamma in the NMJ results in generalized flaccid weakness and disrupted neuromuscular transmission that could successfully be reversed by AChE inhibitors (AChEi) such as pyridostigmine. The histological work-up identified mononuclear cells and Ab deposition at motor end plates. Immunoprecipitation found a novel target antigen which was recognized by sera from investigated mice but also from human MG patients. These data associate IFN with a humoral immune response, comparable to that in human MG pathogenesis (Gu et al., 1995).

Clinically, reported cases are often accompanied by the presence of AChR Abs and sometimes by additional myopathic findings on electromyography (Batocchi et al., 1995). MG was found to occur under a treatment with IFN beta for multiple sclerosis in three unrelated cases, in all of which it manifested within the first year after initiation (Blake and Murphy, 1997; Dionisiotis et al., 2004). Despite the lack of systematic data, the pathophysiological rationale as well as the time span from drug initiation to symptom onset support immune-related rather than NMJ-related effects.

Statins

Statins, the most commonly used class of lipid-lowering drugs, also show a variety of immunomodulatory properties such as increasing the serum levels of multiple Th2 interleukins (Youssef et al., 2002). Well-fitting, studies in animals and humans indicate

that Th2 cytokines may generally be crucial in the development of MG (Milani et al., 2003). Therefore, these changes may be responsible for inducing *de novo* MG (Gale and Danesh-Meyer, 2014). Another pathomechanism potentially underlying statin-induced myasthenia is the depletion of coenzyme Q_{10}, which may result in mitochondrial dysfunction (Evans and Rees, 2002; Vaklavas et al., 2009). This is particularly relevant, as presynaptic endings and the postsynaptic junction have a high density of mitochondria.

In contrast to new-onset MG, non-inflammatory myopathy is a well-known side effect of statins, potentially explaining the case reports that suggest an aggravation of pre-existing MG (Parmar et al., 2002; Cartwright et al., 2004; Purvin et al., 2006). A small case series reported worsening of symptoms in 6 patients with MG receiving statins (11% of the small analyzed cohort), predominantly affecting oculo-bulbar muscles with symptom onset between 1 week and 4 months after initiating treatment (Oh et al., 2008). This latency appears too long for a mechanism directly related to NMJ function. Some reported patients had no previous history of myasthenic symptoms, indicating that statins may have the potential to trigger or unmask myasthenia in previously healthy individuals (Purvin et al., 2006; Khalid et al., 2016).

Immune-Checkpoint Inhibitors

Immune checkpoint inhibitors (ICIs) are an emerging type of cancer immunotherapy that target intrinsic down-regulators of immunity, more specifically the checkpoint molecules CTLA-4, PD-1, and PD-L1 (Postow et al., 2018). These proteins may allow the proliferation of malignant cells by evading T-cell-mediated anti-tumor activity, and their blockade in turn enables T-cells to recognize and attack the tumor (Fife and Bluestone, 2008).

The checkpoint molecules, expressed on the surface of T-cells, play a crucial role in the regulation of immunological homeostasis, maintenance of self-tolerance and prevention of autoimmunity (Postow et al., 2015). Interference with immunological homeostasis and a reduction of T-cell tolerance are also postulated as crucial mechanisms in immune-related adverse events (Postow et al., 2018). ICIs may elevate the levels of pre-existing auto-Abs, but can also increase the levels of inflammatory cytokines, which may promote the activation of auto-reactive T cells (Kimbara et al., 2018). Additionally, the similarity between normal tissue antigens and tumor antigens may lead to a cross-reactivity, further favoring a self-directed immune response (Michot et al., 2016). Given these effects, activated T-cells may subsequently attack healthy tissue including structures of the NMJ, resulting in adverse reactions with clinical and serological features reminiscent of autoimmune diseases (Choi and Lee, 2020).

The clinical spectrum of immune-related adverse events includes a wide range of neurological complications affecting both the central and the peripheral nervous system (Bruna et al., 2020; Haugh et al., 2020). Together with peripheral neuropathies and myositis, MG is a characteristic side effect involving the peripheral nervous system, occurring in approximately 0.5% of cases receiving ICI treatment (Johnson et al., 2019). The median time period from drug administration to the clinical onset of MG was 28 days (Sato et al., 2019). ICI-triggered MG is an often severe and progressive complication with potentially life-threatening consequences and a mortality rate of up to 30% (Johnson et al., 2019; Safa et al., 2019). In the vast majority of reported cases with ICI-related MG, the underlying treatment was a pharmacological inhibition of PD-1 or its ligand PD-L1, most commonly with the drug nivolumab. Less commonly, cases under ipilimumab (targeting CTLA-4) have been described, and combination treatments seem to be particularly hazardous (Johnson et al., 2015; Montes et al., 2018).

In the single-center study by Safa et al., most patients (63%) developed moderate to severe disease (MGFA class III to V), with ptosis (75%), dyspnea (62%), generalized weakness (55%), dysphagia (48%), and double vision (42%) being the most commonly reported symptoms. Of note, almost half of the patients in this study rapidly developed respiratory failure requiring mechanical ventilation. Characteristic laboratory features were positive AChR Abs in 66%, anti-striated Abs in 67% and elevated CK levels in 84% (Safa et al., 2019). To the best of our knowledge, auto-Abs against the muscle-specific kinase (MuSK) have so far only been reported in one single case under nivolumab (occurring together with AChR Abs) (Mitsune et al., 2018).

ICI-induced MG may further be complicated by overlap manifestations comprising myositis or myocarditis with potentially fatal consequences (Xing et al., 2020). Overall, when compared to classic acquired MG, the clinical course of ICI-related disease clearly appears to be remarkably more aggressive with a tendency toward fast disease progression and myasthenic crises. Altogether, no significant clinical differences were found between patients with new-onset MG or an acute flare-up of pre-existing disease due to ICI (Safa et al., 2019).

Steroids are often used as first-line treatment approach, followed by immune-modulatory agents in refractory cases (Choi and Lee, 2020). However, the data presented by Safa et al. support the early use of intravenous immunoglobulins (IVIg) and plasma exchange (PLEX), leading to improved outcomes compared to steroids alone (Safa et al., 2019). The response to a symptomatic treatment with cholinesterase inhibitors seems to be variable (Johansen et al., 2019). As it is still not entirely clear whether ICI-induced MG is a monophasic disease, the decision regarding a possible withdrawal of ICIs remains a dilemma and should especially be discussed in life-threatening cases (Shi et al., 2020).

Allogeneic Hematopoietic Stem Cell Transplantation

Allogeneic HSCT is a standard treatment for a variety of hematological malignancies involving the transfer of a donor's hematopoietic and immune system to a host. Graft-versus-host disease (GVHD) is one of the major complications of the procedure and summarizes host end-organ damage due to alloreactivity of the donor's immune system. T-cell infiltration and epithelial damage to the skin, gut and liver are the hallmarks of acute GVHD, usually occurring within the first 100 days after HSCT (Zeiser and Blazar, 2018). Chronic GVHD

typically develops 3–12 months after HSCT and resembles a spectrum of autoimmune-related diseases through combined pathomechanisms of cellular (T- and B-cells) and humoral alloreactivity (Zeiser and Blazar, 2017).

Myasthenia-like manifestations have been described as rare immune-mediated complications after HSCT in case reports with an estimated incidence under 1%. The time of disease onset ranged between 3 and 100 months after HSCT, and a clear association with a prior diagnosis of chronic GVHD could be noted (Tsutsumi et al., 2019). In this context, MG has also been described during the taper of immunosuppressive medication used for the treatment of GVHD (Bolger et al., 1986). The detection of serum AChR Abs strongly supports the diagnosis of MG in the presence of classic symptoms after HSCT, but these auto-Abs can also be detected in up to 40% of HSCT recipients without apparent neurological symptoms (Lefvert and Björkholm, 1987). In a review of 27 post-HSCT cases with MG, treatment mainly consisted of prednisone in combination with a calcineurin inhibitor, azathioprine, IVIg and the anti-CD20 antibody rituximab. These treatments led to a sustained improvement in the majority of cases and only three deaths have been reported (Maffini et al., 2017).

Importantly, MG has to be distinguished from other causes of muscle weakness related to HSCT, including steroid myopathy, wasting syndrome or other immune-mediated neurological disorders. As such, myositis or Guillain-Barré-like syndromes are more frequently observed as chronic GVHD than MG (Maffini et al., 2017; Balaguer-Rosello et al., 2019).

MISCELLANEOUS AND UNKNOWN MECHANISMS

A certain range of drugs have been associated with myasthenic side effects, but details regarding the underlying mechanisms are lacking in the literature. Hence, it can only be assumed based on pharmacological properties and the time course of neuromuscular manifestations, whether the effects relate to NMJ function or the immune system. Since the present article focuses on the underlying mechanisms of medication-associated myasthenia, such treatments with poorly characterized or unknown mechanisms will only be mentioned briefly, focusing on clinical aspects.

Some Antibiotics

The aminopenicillin antibiotics ampicillin and amoxicillin, have anecdotally been associated with myasthenic weakness. Most recently, a series of six cases indicated symptom onset within few days after drug application, subsequently leading to clinical worsening, followed by symptom recovery after pyridostigmine and IVIg (Vacchiano et al., 2020). Moreover, ampicillin increased the degree of decrement in rabbits with experimental autoimmune myasthenia gravis but had no negative effects in normal rabbits (Argov et al., 1986).

Further, the macrolide antibiotics, which inhibit protein synthesis by binding to ribosomal structures, are broadly available for a wide range of infectious diseases. Occasional anecdotal reports have described a mild to moderate symptom aggravation by some macrolides (e.g., azithromycin, erythromycin) in myasthenic patients (May and Calvert, 1990; Cadisch et al., 1996). Albeit evidence is weak and no clear recommendations exist, patients with MG should be monitored closely under a treatment with these antibiotics.

Corticosteroids

Corticosteroids require specific attention with regard to MG, since they are frequently used as a standard treatment. In experimental models, complex influences on the NMJ due to corticosteroids have been shown, including altered depolarization of nerve terminals, a reduction of ACh release, altered MEPPs, changes in choline transport and depletion of potassium (Wilson et al., 1974; Dengler et al., 1979; Kim et al., 1979). Yet, it is not far to seek that immunological mechanisms may also be involved in this phenomenon. Notably, one study found that an early clinical deterioration under corticosteroids was accompanied by a transient increase in lymphocyte response *in vitro*, stressing a role of cell-mediated immunological mechanisms (Abramsky et al., 1975).

Almost 50% of MG patients with high-dose steroid treatment experience an initial exacerbation of neuromuscular symptoms, of which 8.6% are severe, requiring mechanical ventilation or intubation (Pascuzzi et al., 1984). This potentially life-threatening complication can be avoided by gradually increasing the dosage, starting with 25 mg every other day (Seybold and Drachman, 1974). Apart from high initial dosages, thymoma, early-onset disease and upper limb weakness have been associated with steroid-induced worsening of myasthenia (Kanai et al., 2019).

Hormonal Disturbances

Autoimmune thyroid disorders such as Grave's disease and Hashimoto thyroiditis are more prevalent in individuals with MG (Song et al., 2019). A causal relation has been proposed, as symptoms were reported to fluctuate depending on thyroid hormone levels. However, systematic data corroborating this relationship are still lacking (Maclean and Wilson, 1954; Mallikarjuna et al., 2019).

It is also a frequently observed phenomenon that some female patients with autoimmune MG experience fluctuating weakness with the menstrual cycle and pregnancy, suggesting some modifying effects of female sex hormones. There is some evidence that a higher rate of remissions during menstruation may be due to reduced activity of acetylcholinesterase (Vijayan et al., 1977). While robust clinical data are missing to draw any definite conclusions, experimental data show conflicting results regarding the effect of sex hormones. First, one group used a rat model with experimental MG to analyze whether MG aggravation may be induced by changes in female sex hormones in rodents with and without ovariectomy. No electrophysiological and serological (AChR Abs) changes were observed after hormonal replacement, indicating no major influence on the susceptibility and severity of MG (Leker et al., 2000). By contrast, another work using an animal model showed that a temporary exposure to beta-17-estradiol

enhances the production of anti-AChR Abs and significantly increases the severity of EAMG in mice, providing evidence that estrogen aggravates experimental MG (Delpy et al., 2005). Clinically, the notion that female sex hormones *per se* increase the susceptibility to autoimmune MG is supported by case descriptions (Brittain and Lange, 1995).

Lithium

Lithium salts such as lithium carbonate, which are used as mood-stabilizing drugs, have been reported to either aggravate weakness in MG or unmask an autoimmune myasthenic syndrome (Neil et al., 1976; Lipton, 1987; Ronzière et al., 2000). The drugs have been shown to carry an inherent potential to foster T-lymphocytes activity, which is in favor of an immune-mediated mechanism as the main actor (Mizuno et al., 1982). However, lithium also appears to selectively reduce AChR synthesis and its insertion into the cell membrane (Pestronk and Drachman, 1987). It remains open to speculation, if these effects occur secondarily to an immunological mechanism.

Iodinated Contrast Agents

Iodinated contrast agents (ICAs), which are commonly used for computed tomography (CT) scans, have for a long time been regarded as potential triggers of myasthenic symptoms. ICAs are subdivided into high- and low-osmolality compounds, and those with a high degree of osmolality (i.e., >1500 mOsm/L) are not in clinical use any more. Instead, low-osmolality agents (290–860 mOsm/L) are now routinely used due to their better tolerability (Pasternak and Williamson, 2012).

Several case reports and small case series as well as experimental data in rabbits suggested worsening of pre-existing MG related to the use of high-osmolality agents (Chagnac et al., 1985; Anzola et al., 1986; Bonmarchand et al., 1987; Eliashiv et al., 1990; Rocha and Bacheschi, 1994). Aside from anecdotal evidence, there has been one systematic trial in 136 patients retrospectively investigating acute events within 24 h after receiving high-osmolality agents, showing that 7 patients (5.1%) experienced an exacerbation of myasthenic weakness, whereas in the majority of cases, alternative explanations other than ICA were also conceivable (Frank et al., 1987).

With regard to the nowadays more commonly used low-osmolality ICAs, there are only a few publications to date. One study focusing on adverse reactions occurring just after ICA application reported a rate below 1%, hence suggesting no significant immediate risk due to neuromuscular blockade for MG patients (Mehrizi and Pascuzzi, 2014). By contrast, another retrospective work with an extended observation period found significantly more MG-related exacerbations within the first day after the contrast-enhanced scans, mainly respiratory manifestations, while there was no significant difference between the contrast and the non-contrast group thereafter (up to 45 days after the radiological investigation) (Somashekar et al., 2013). Most recently, one study retrospectively investigated acute and delayed aggravations of myasthenic symptoms in 72 patients with MG and found an increased rate (12.3%) of delayed exacerbations of MG after the application of low-osmolality ICAs, again stressing the high likelihood of alternative causes (unrelated to MG) for symptom exacerbation in the majority of cases (Rath et al., 2017).

Based upon the existing evidence, ICA administration should not be considered contraindicated in individuals with MG, as long as the patients are monitored regarding immediate and delayed adverse reactions. However, published results are somewhat contradictory, and large prospective studies are required for clarification.

CONCLUSION

Our comprehensive review of the existing literature underscores that medication-related aggravations of myasthenic syndromes due to various molecular mechanisms represent a clinically relevant problem. The evidence for specific classes of drugs or treatments is often scanty and merely based on single case descriptions. First, one must be extremely cautious not to overinterpret anecdotal observations or suggestive (but unspecific) functional data, and risks and benefits need to be weighed carefully. Likewise, it is extremely important that appropriate treatments are not withheld because of anecdotal evidence only.

Apart from drug-related aggravations, our article also highlights a probably still underappreciated phenomenon, that is the induction of *de novo* myasthenia due to drugs with immune-modulatory properties. We specifically stress the emerging group of ICIs as a relatively novel etiology of drug-induced MG, which is particularly characterized by a rapidly progressive and potentially lethal clinical course.

Taken all together, it is obvious that more systematic data are required to estimate the associated risks of specific medical treatments more precisely. However, the thorough knowledge of cases already reported in the literature and the underlying molecular mechanisms may relevantly increase awareness of treating clinicians, so that patients can be monitored carefully, if potentially hazardous drugs have to be used.

AUTHOR CONTRIBUTIONS

MK drafted the manuscript. AG provided specific expertise for the chapter on ICIs. PW provided expertise regarding allogeneic HSCT. JR critically revised the article and provided specific input with regard to iodinated contrast agents. HC critically revised the manuscript and provided specific input regarding beta blocker-related mechanisms. IK designed the two figures with Biorender and critically revised the manuscript. FZ proposed and supervised the manuscript. All authors contributed to the article and approved the submitted version.

FUNDING

IK was funded by the Hertha Firnberg Fellowship (project no. T996-B30) from the Austrian Science Fund (FWF).

REFERENCES

Abramsky, O., Aharonov, A., Teitelbaum, D., and Fuchs, S. (1975). Myasthenia gravis and acetylcholine receptor. Effect of steroids in clinical course and cellular immune response to acetylcholine receptor. *Arch. Neurol.* 32, 684–687. doi: 10.1001/archneur.1975.00490520054008

Adelman, H. M., Winters, P. R., Mahan, C. S., and Wallach, P. M. (1995). D-penicillamine-induced myasthenia gravis: diagnosis obscured by coexisting chronic obstructive pulmonary disease. *Am. J. Med. Sci.* 309, 191–193. doi: 10.1097/00000441-199504000-00001

Albers, J. W., Beals, C. A., and Levine, S. P. (1981). Neuromuscular transmission in rheumatoid arthritis, with and without penicillamine treatment. *Neurology* 31, 1562–1564. doi: 10.1212/wnl.31.12.1562

Aldrich, M. S., Kim, Y. I., and Sanders, D. B. (1979). Effects of D-penicillamine on neuromuscular transmission in rats. *Muscle Nerve* 2, 180–185. doi: 10.1002/mus.880020305

Alfrey, A. C., Terman, D. S., Brettschneider, L., Simpson, K. M., and Ogden, D. A. (1970). Hypermagnesemia after renal homotransplantation. *Ann. Intern. Med.* 73, 367–371. doi: 10.7326/0003-4819-73-3-367

Andonopoulos, A. P., Terzis, E., Tsibri, E., Papasteriades, C. A., and Papapetropoulos, T. (1994). D-penicillamine induced myasthenia gravis in rheumatoid arthritis: an unpredictable common occurrence? *Clin. Rheumatol.* 13, 586–588. doi: 10.1007/bf02242998

Anzola, G. P., Capra, R., Magoni, M., and Vignolo, L. A. (1986). Myasthenic crisis during intravenous iodinated contrast medium injection. *Ital. J. Neurol. Sci.* 7, 273. doi: 10.1007/bf02230893

Argov, Z., Brenner, T., and Abramsky, O. (1986). Ampicillin may aggravate clinical and experimental myasthenia gravis. *Arch. Neurol.* 43, 255–256. doi: 10.1001/archneur.1986.00520030045010

Azevedo, E., Ribeiro, J. A., Polónia, J., and Pontes, C. (1993). Probable exacerbation of myasthenia gravis by ofloxacin. *J. Neurol.* 240, 508–508. doi: 10.1007/bf00874123

Baik, S. J., Kim, T. H., Kim, H. I., and Rhie, J. Y. (2016). Myasthenia crisis induced by pegylated-interferon in patient with chronic hepatitis c: a case report. *Medicine (Baltimore)* 95:e3782. doi: 10.1097/MD.0000000000003782

Balaguer-Rosello, A., Bataller, L., Piñana, J. L., Montoro, J., Lorenzo, I., Villalba, A., et al. (2019). Noninfectious neurologic complications after allogeneic hematopoietic stem cell transplantation. *Biol. Blood Marrow Transplant.* 25, 1818–1824. doi: 10.1016/j.bbmt.2019.05.024

Batocchi, A. P., Evoli, A., Servidei, S., Palmisani, M. T., Apollo, F., and Tonali, P. (1995). Myasthenia gravis during interferon alfa therapy. *Neurology* 45, 382–383. doi: 10.1212/wnl.45.2.382

Bever, C. T., Chang, H. W., Penn, A. S., Jaffe, I. A., and Bock, E. (1982). Penicillamine-induced myasthenia gravis: effects of penicillamine on acetylcholine receptor. *Neurology* 32, 1077–1082. doi: 10.1212/wnl.32.10.1077

Blake, G., and Murphy, S. (1997). Onset of myasthenia gravis in a patient with multiple sclerosis during interferon-1b treatment. *Neurology* 49, 1747–1748. doi: 10.1212/wnl.49.6.1747-a

Blichfeldt-Lauridsen, L., and Hansen, B. D. (2012). Anesthesia and myasthenia gravis. *Acta Anaesthesiol. Scand.* 56, 17–22. doi: 10.1111/j.1399-6576.2011.02558.x

Bolger, G. B., Sullivan, K. M., Spence, A. M., Appelbaum, F. R., Johnston, R., Sanders, J. E., et al. (1986). Myasthenia gravis after allogeneic bone marrow transplantation: relationship to chronic graft-versus-host disease. *Neurology* 36, 1087–1091. doi: 10.1212/wnl.36.8.1087

Bonmarchand, G., Weiss, P., Clavier, E., Lerebours-Pigeonniere, G., Massari, P., and Leroy, J. (1987). Myasthenic crisis following the injection of an iodinated contrast medium. *Intensive Care Med.* 13:365.

Booij, L. H., Miller, R. D., and Crul, J. F. (1978). Neostigmine and 4-aminopyridine antagonism of lincomycin-pancuronium neuromuscular blockade in man. *Anesth. Analg.* 57, 316–321. doi: 10.1213/00000539-197805000-00007

Borgia, G., Reynaud, L., Gentile, I., Cerini, R., Ciampi, R., Russo, M. D., et al. (2001). Myasthenia gravis during low-dose IFN-alpha therapy for chronic hepatitis C. *J. Interferon Cytokine Res.* 21, 469–470. doi: 10.1089/10799900152434321

Brittain, J., and Lange, L. S. (1995). Myasthenia gravis and levonorgestrel implant. *Lancet* 346:1556. doi: 10.1016/s0140-6736(95)92084-6

Brumlik, J., and Jacobs, R. S. (1974). Myasthenia gravis associated with diphenylhydantoin therapy for epilepsy. *Can. J. Neurol. Sci.* 1, 127–129. doi: 10.1017/s0317167100019697

Bruna, J., Argyriou, A. A., Anastopoulou, G. G., Alemany, M., Nadal, E., Kalofonou, F., et al. (2020). Incidence and characteristics of neurotoxicity in immune checkpoint inhibitors with focus on neuromuscular events: experience beyond the clinical trials. *J. Peripher. Nerv. Syst.* 25, 171–177. doi: 10.1111/jns.12371

Cadisch, R., Streit, E., and Hartmann, K. (1996). [Exacerbation of pseudoparalytic myasthenia gravis following azithromycin (Zithromax)]. *Schweiz Med. Wochenschr* 126, 308–310.

Caputy, A. J., Kim, Y. I., and Sanders, D. B. (1981). The neuromuscular blocking effects of therapeutic concentrations of various antibiotics on normal rat skeletal muscle: a quantitative comparison. *J. Pharmacol. Exp. Ther.* 217, 369–378.

Cartwright, M. S., Jeffery, D. R., Nuss, G. R., and Donofrio, P. D. (2004). Statin-associated exacerbation of myasthenia gravis. *Neurology* 63, 2188–2188. doi: 10.1212/01.wnl.0000145708.03876.c3

Cata, J. P., Lasala, J. D., Williams, W., and Mena, G. E. (2019). Myasthenia gravis and thymoma surgery: a clinical update for the cardiothoracic anesthesiologist. *J. Cardiothorac. Vasc. Anesth.* 33, 2537–2545. doi: 10.1053/j.jvca.2018.07.036

Cetin, H., and Vincent, A. (2018). Pathogenic mechanisms and clinical correlations in autoimmune myasthenic syndromes. *Semin. Neurol.* 38, 344–354. doi: 10.1055/s-0038-1660500

Chagnac, Y., Hadani, M., and Goldhammer, Y. (1985). Myasthenic crisis after intravenous administration of iodinated contrast agent. *Neurology* 35, 1219–1220. doi: 10.1212/wnl.35.8.1219

Choi, J., and Lee, S. Y. (2020). Clinical characteristics and treatment of immune-related adverse events of immune checkpoint inhibitors. *Immune Netw.* 20:e9. doi: 10.4110/in.2020.20.e9

Clausen, L., Cossins, J., and Beeson, D. (2018). Beta-2 adrenergic receptor agonists enhance AChR clustering in C2C12 myotubes: implications for therapy of myasthenic disorders. *J. Neuromuscul. Dis.* 5, 231–240. doi: 10.3233/JND-170293

Cohen, B. A., London, R. S., and Goldstein, P. J. (1976). Myasthenia gravis and preeclampsia. *Obstet. Gynecol.* 48, 35S–37S.

Confavreux, C., Charles, N., and Aimard, G. (1990). Fulminant myasthenia gravis soon after initiation of acebutolol therapy. *Eur. Neurol.* 30, 279–281. doi: 10.1159/000117380

Congeni, J. P., and Kirkpatrick, R. B. (2013). Pegylated interferon induced myasthenia crisis–a case report. *J. Clin. Neuromuscul. Dis.* 14, 123–125. doi: 10.1097/CND.0b013e318285257f

Conlon, K. C., Urba, W. J., Smith, J. W., Steis, R. G., Longo, D. L., and Clark, J. W. (1990). Exacerbation of symptoms of autoimmune disease in patients receiving alpha-interferon therapy. *Cancer* 65, 2237–2242. doi: 10.1002/1097-0142(19900515)65:10<2237::aid-cncr2820651013<3.0.co;2-5

Coppeto, J. R. (1984). Timolol-associated myasthenia gravis. *Am. J. Ophthalmol.* 98, 244–245. doi: 10.1016/0002-9394(87)90366-7

Dashtipour, K., and Pedouim, F. (2016). Botulinum toxin: preparations for clinical use, immunogenicity, side effects, and safety profile. *Semin. Neurol.* 36, 29–33. doi: 10.1055/s-0035-1571213

De Sarro, A., and De Sarro, G. (2001). Adverse reactions to fluoroquinolones. an overview on mechanistic aspects. *Curr. Med. Chem.* 8, 371–384. doi: 10.2174/0929867013373435

del Castillo, J., and Engbaek, L. (1954). The nature of the neuromuscular block produced by magnesium. *J. Physiol. (Lond.)* 124, 370–384. doi: 10.1113/jphysiol.1954.sp005114

Delpy, L., Douin-Echinard, V., Garidou, L., Bruand, C., Saoudi, A., and Guéry, J.-C. (2005). Estrogen enhances susceptibility to experimental autoimmune myasthenia gravis by promoting type 1-polarized immune responses. *J. Immunol.* 175, 5050–5057. doi: 10.4049/jimmunol.175.8.5050

Dengler, R., Rüdel, R., Warelas, J., and Birnberger, K. L. (1979). Corticosteroids and neuromuscular transmission: electrophysiological investigation of the effects of prednisolone on normal and anticholinesterase-treated neuromuscular junction. *Pflugers Arch.* 380, 145–151. doi: 10.1007/bf00582150

Dionisiotis, J., Zoukos, Y., and Thomaides, T. (2004). Development of myasthenia gravis in two patients with multiple sclerosis following interferon beta treatment. *J. Neurol. Neurosurg. Psychiatry* 75, 1079–1079. doi: 10.1136/jnnp.2003.028233

Dolly, J. O., and Aoki, K. R. (2006). The structure and mode of action of different botulinum toxins. *Eur. J. Neurol.* 13(Suppl. 4), 1–9. doi: 10.1111/j.1468-1331.2006.01648.x

Drosos, A. A., Christou, L., Galanopoulou, V., Tzioufas, A. G., and Tsiakou, E. K. (1993). D-penicillamine induced myasthenia gravis: clinical, serological and genetic findings. *Clin. Exp. Rheumatol.* 11, 387–391.

Durant, N. N., and Lambert, J. J. (1981). The action of polymyxin B at the frog neuromuscular junction. *Br. J. Pharmacol.* 72, 41–47. doi: 10.1111/j.1476-5381.1981.tb09102.x

Eliashiv, S., Wirguin, I., Brenner, T., and Argov, Z. (1990). Aggravation of human and experimental myasthenia gravis by contrast media. *Neurology* 40, 1623–1625. doi: 10.1212/wnl.40.10.1623

Elmqvist, D., Hofmann, W. W., Kugelberg, J., and Quastel, D. M. (1964). An electrophysiological investigation of neuromuscular transmission in myasthenia gravis. *J. Physiol.* 174, 417–434. doi: 10.1113/jphysiol.1964.sp007495

Erbguth, F., Claus, D., Engelhardt, A., and Dressler, D. (1993). Systemic effect of local botulinum toxin injections unmasks subclinical Lambert-Eaton myasthenic syndrome. *J. Neurol. Neurosurg. Psychiatry* 56, 1235–1236. doi: 10.1136/jnnp.56.11.1235

Evans, M., and Rees, A. (2002). Effects of HMG-CoA reductase inhibitors on skeletal muscle: are all statins the same? *Drug Saf.* 25, 649–663. doi: 10.2165/00002018-200225090-00004

Fife, B. T., and Bluestone, J. A. (2008). Control of peripheral T-cell tolerance and autoimmunity via the CTLA-4 and PD-1 pathways. *Immunol. Rev.* 224, 166–182. doi: 10.1111/j.1600-065X.2008.00662.x

Fishman, R. A. (1965). Neurological aspects of magnesium metabolism. *Arch. Neurol.* 12, 562–569. doi: 10.1001/archneur.1965.00460300010002

Frank, J. H., Cooper, G. W., Black, W. C., and Phillips, L. H. (1987). Iodinated contrast agents in myasthenia gravis. *Neurology* 37, 1400–1402. doi: 10.1212/wnl.37.8.1400

Gage, P. W., and Hamill, O. P. (1976). Effects of several inhalation anaesthetics on the kinetics of postsynaptic conductance changes in mouse diaphragm. *Br. J. Pharmacol.* 57, 263–272. doi: 10.1111/j.1476-5381.1976.tb07476.x

Gale, J., and Danesh-Meyer, H. V. (2014). Statins can induce myasthenia gravis. *J. Clin. Neurosci.* 21, 195–197. doi: 10.1016/j.jocn.2013.11.009

Garner, C. G., Straube, A., Witt, T. N., Gasser, T., and Oertel, W. H. (1993). Time course of distant effects of local injections of botulinum toxin. *Mov. Disord.* 8, 33–37. doi: 10.1002/mds.870080106

Godley, P. J., Morton, T. A., Karboski, J. A., and Tami, J. A. (1990). Procainamide-induced myasthenic crisis. *Ther. Drug Monit.* 12, 411–414. doi: 10.1097/00007691-199007000-00019

Gu, D., Wogensen, L., Calcutt, N. A., Xia, C., Zhu, S., Merlie, J. P., et al. (1995). Myasthenia gravis-like syndrome induced by expression of interferon gamma in the neuromuscular junction. *J. Exp. Med.* 181, 547–557. doi: 10.1084/jem.181.2.547

Guidon, A. C. (2019). Lambert-eaton myasthenic syndrome, botulism, and immune checkpoint inhibitor-related myasthenia gravis. *Continuum (Minneap Minn)* 25, 1785–1806. doi: 10.1212/CON.0000000000000807

Gummi, R. R., Kukulka, N. A., Deroche, C. B., and Govindarajan, R. (2019). Factors associated with acute exacerbations of myasthenia gravis. *Muscle Nerve* 60, 693–699. doi: 10.1002/mus.26689

Gunduz, A., Turedi, S., Kalkan, A., and Nuhoglu, I. (2006). Levofloxacin induced myasthenia crisis. *Emerg. Med. J.* 23, 662–662. doi: 10.1136/emj.2006.038091

Gutmann, L., and Takamori, M. (1973). Effect of Mg++ on neuromuscular transmission in the Eaton-Lambert syndrome. *Neurology* 23, 977–980. doi: 10.1212/wnl.23.9.977

Harry, J. D., Linden, R. J., and Snow, H. M. (1974). The effects of three beta-adrenoceptor blocking drugs on isolated preparations of skeletal and cardiac muscle. *Br. J. Pharmacol.* 52, 275–281. doi: 10.1111/j.1476-5381.1974.tb09710.x

Haugh, A. M., Probasco, J. C., and Johnson, D. B. (2020). Neurologic complications of immune checkpoint inhibitors. *Expert Opin. Drug Saf.* 18, 1–10. doi: 10.1080/14740338.2020.1738382

Huda, S., Cao, M., De Rosa, A., Woodhall, M., Rodríguez Cruz, P. M., Cossins, J., et al. (2020). SHP2 inhibitor protects AChRs from effects of myasthenia gravis MuSK antibody. *Neurol. Neuroimmunol. Neuroinflamm.* 7:e645. doi: 10.1212/NXI.0000000000000645

Jamal, B. T., and Herb, K. (2009). Perioperative management of patients with myasthenia gravis: prevention, recognition, and treatment. *Oral Surg. Oral Med. Oral Pathol. Oral Radiol. Endod.* 107, 612–615. doi: 10.1016/j.tripleo.2009.01.015

Jennett, A. M., Bali, D., Jasti, P., Shah, B., and Browning, L. A. (2006). Telithromycin and myasthenic crisis. *Clin. Infect. Dis.* 43, 1621–1622. doi: 10.1086/509646

Johansen, A., Christensen, S. J., Scheie, D., Højgaard, J. L. S., and Kondziella, D. (2019). Neuromuscular adverse events associated with anti-PD-1 monoclonal antibodies: systematic review. *Neurology* 92, 663–674. doi: 10.1212/WNL.0000000000007235

Johnson, D. B., Manouchehri, A., Haugh, A. M., Quach, H. T., Balko, J. M., Lebrun-Vignes, B., et al. (2019). Neurologic toxicity associated with immune checkpoint inhibitors: a pharmacovigilance study. *J. Immunother. Cancer* 7:134. doi: 10.1186/s40425-019-0617-x

Johnson, D. B., Saranga-Perry, V., Lavin, P. J. M., Burnette, W. B., Clark, S. W., Uskavitch, D. R., et al. (2015). Myasthenia gravis induced by ipilimumab in patients with metastatic melanoma. *J. Clin. Oncol.* 33, e122–e124. doi: 10.1200/JCO.2013.51.1683

Jonkers, I., Swerup, C., Pirskanen, R., Bjelak, S., and Matell, G. (1996). Acute effects of intravenous injection of beta-adrenoreceptor- and calcium channel at antagonists and agonists in myasthenia gravis. *Muscle Nerve* 19, 959–965. doi: 10.1002/(SICI)1097-4598(199608)19:8<959::AID-MUS4<3.0.CO;2-7

Kaeser, H. E. (1984). Drug-induced myasthenic syndromes. *Acta Neurol. Scand. Suppl.* 100, 39–47.

Kanai, T., Uzawa, A., Kawaguchi, N., Oda, F., Ozawa, Y., Himuro, K., et al. (2019). Predictive score for oral corticosteroid-induced initial worsening of seropositive generalized myasthenia gravis. *J. Neurol. Sci.* 396, 8–11. doi: 10.1016/j.jns.2018.10.018

Khalid, R., Ibad, A., and Thompson, P. D. (2016). Statins and myasthenia gravis. *Muscle Nerve* 54, 509–509. doi: 10.1002/mus.25155

Khella, S. L., and Kozart, D. (1997). Unmasking and exacerbation of myasthenia gravis by ophthalmic solutions: betoxolol, tobramycin, and dexamethasone. A case report. *Muscle Nerve* 20, 631–631. doi: 10.1002/mus.880200501

Kim, Y. I., Goldner, M. M., and Sanders, D. B. (1979). Short-term effects of prednisolone on neuromuscular transmission in normal rats and those with experimental autoimmune myasthenia gravis. *J. Neurol. Sci.* 41, 223–234. doi: 10.1016/0022-510x(79)90041-8

Kimbara, S., Fujiwara, Y., Iwama, S., Ohashi, K., Kuchiba, A., Arima, H., et al. (2018). Association of antithyroglobulin antibodies with the development of thyroid dysfunction induced by nivolumab. *Cancer Sci.* 109, 3583–3590. doi: 10.1111/cas.13800

Komal Kumar, R. N., Patil, S. A., Taly, A. B., Nirmala, M., Sinha, S., and Arunodaya, G. R. (2004). Effect of D-penicillamine on neuromuscular junction in patients with Wilson disease. *Neurology* 63, 935–936. doi: 10.1212/01.wnl.0000137021.90567.37

Koneczny, I., and Herbst, R. (2019). Myasthenia gravis: pathogenic effects of autoantibodies on neuromuscular architecture. *Cells* 8:671. doi: 10.3390/cells8070671

Krendel, D. A. (1990). Hypermagnesemia and neuromuscular transmission. *Semin. Neurol.* 10, 42–45. doi: 10.1055/s-2008-1041252

Krendel, D. A., and Hopkins, L. C. (1986). Adverse effect of verapamil in a patient with the Lambert-Eaton syndrome. *Muscle Nerve* 9, 519–522. doi: 10.1002/mus.880090607

Kuncl, R. W., Pestronk, A., Drachman, D. B., and Rechthand, E. (1986). The pathophysiology of penicillamine-induced myasthenia gravis. *Ann. Neurol.* 20, 740–744. doi: 10.1002/ana.410200617

Lee, D. C., Kim, Y. I., Liu, H. H., and Johns, T. R. (1983). Presynaptic and postsynaptic actions of procainamide on neuromuscular transmission. *Muscle Nerve* 6, 442–447. doi: 10.1002/mus.880060608

Lee, M., Beeson, D., and Palace, J. (2018). Therapeutic strategies for congenital myasthenic syndromes. *Ann. N.Y. Acad. Sci.* 1412, 129–136. doi: 10.1111/nyas.13538

Lefvert, A. K., and Björkholm, M. (1987). Antibodies against the acetylcholine receptor in hematologic disorders: implications for the development of myasthenia gravis after bone marrow grafting. *N. Engl. J. Med.* 317, 170–171. doi: 10.1056/NEJM198707163170315

Leker, R. R., Karni, A., Brenner, T., Weidenfeld, J., and Abramsky, O. (2000). Effects of sex hormones on experimental autoimmune myasthenia gravis. *Eur. J. Neurol.* 7, 203–206. doi: 10.1046/j.1468-1331.2000.00042.x

Leys, D., Pasquier, F., Vermersch, P., Gosset, D., Michiels, H., Kassiotis, P., et al. (1987). Possible revelation of latent myasthenia gravis by labetalol chlorhydrate. *Acta Clin. Belg.* 42, 475–476. doi: 10.1080/22953337.1987.11719269

Lipsitz, P. J. (1971). The clinical and biochemical effects of excess magnesium in the newborn. *Pediatrics* 47, 501–509.

Lipton, I. D. (1987). Myasthenia gravis unmasked by lithium carbonate. *J. Clin. Psychopharmacol.* 7:57. doi: 10.1097/00004714-198702000-00030

Liu, C.-N., and Somps, C. J. (2010). Telithromycin blocks neuromuscular transmission and inhibits nAChR currents in vitro. *Toxicol. Lett.* 194, 66–69. doi: 10.1016/j.toxlet.2010.02.005

Maclean, B., and Wilson, J. A. (1954). See-saw relationship between hyperthyroidism and myasthenia gravis. *Lancet* 266, 950–953. doi: 10.1016/s0140-6736(54)91566-4

Maffini, E., Festuccia, M., Brunello, L., Boccadoro, M., Giaccone, L., and Bruno, B. (2017). Neurologic complications after allogeneic hematopoietic stem cell transplantation. *Biol. Blood Marrow Transplant.* 23, 388–397. doi: 10.1016/j.bbmt.2016.12.632

Maimone, M. M., and Merlie, J. P. (1993). Interaction of the 43 kd postsynaptic protein with all subunits of the muscle nicotinic acetylcholine receptor. *Neuron* 11, 53–66. doi: 10.1016/0896-6273(93)90270-2

Mallikarjuna, S. K., Velayutham, S. S., Sowmini, P. R., Jeyaraj, M. K., and Arunan, S. (2019). See-saw relationship and its reversal after immunotherapy in a case of Graves' disease with coexisting myasthenia gravis. *J. Neurosci. Rural Pract.* 10, 136–138. doi: 10.4103/jnrp.jnrp_150_18

May, E. F., and Calvert, P. C. (1990). Aggravation of myasthenia gravis by erythromycin. *Ann. Neurol.* 28, 577–579. doi: 10.1002/ana.410280417

Mehra, M. R., Desai, S. S., Ruschitzka, F., and Patel, A. N. (2020). Hydroxychloroquine or chloroquine with or without a macrolide for treatment of COVID-19: a multinational registry analysis. *Lancet* 395:1820. doi: 10.1016/S0140-6736(20)31180-6

Mehrizi, M., and Pascuzzi, R. M. (2014). Complications of radiologic contrast in patients with myasthenia gravis. *Muscle Nerve* 50, 443–444. doi: 10.1002/mus.24254

Michot, J. M., Bigenwald, C., Champiat, S., Collins, M., Carbonnel, F., Postel-Vinay, S., et al. (2016). Immune-related adverse events with immune checkpoint blockade: a comprehensive review. *Eur. J. Cancer* 54, 139–148. doi: 10.1016/j.ejca.2015.11.016

Milani, M., Ostlie, N., Wang, W., and Conti-Fine, B. M. (2003). T cells and cytokines in the pathogenesis of acquired myasthenia gravis. *Ann. N.Y. Acad. Sci.* 998, 284–307. doi: 10.1196/annals.1254.032

Miller, C. D., Oleshansky, M. A., Gibson, K. F., and Cantilena, L. R. (1993). Procainamide-induced myasthenia-like weakness and dysphagia. *Ther. Drug Monit.* 15, 251–254. doi: 10.1097/00007691-199306000-00013

Mitsune, A., Yanagisawa, S., Fukuhara, T., Miyauchi, E., Morita, M., Ono, M., et al. (2018). Relapsed myasthenia gravis after nivolumab treatment. *Intern. Med.* 57, 1893–1897. doi: 10.2169/internalmedicine.9153-17

Mizuno, Y., Dosch, H. M., and Gelfand, E. W. (1982). Carbamycholine modulation of E-rosette formation: identification of nicotinic acetylcholine receptors on a subpopulation of human T lymphocytes. *J. Clin. Immunol.* 2, 303–308. doi: 10.1007/bf00915071

Montes, V., Sousa, S., Pita, F., Guerreiro, R., and Carmona, C. (2018). Myasthenia gravis induced by Ipilimumab in a patient with metastatic melanoma. *Front. Neurol.* 9:150. doi: 10.3389/fneur.2018.00150

Moore, B., Safani, M., and Keesey, J. (1988). Possible exacerbation of myasthenia gravis by ciprofloxacin. *Lancet* 1:882. doi: 10.1016/s0140-6736(88)91627-3

Mumford, C. J., and Ginsberg, L. (1990). Ciprofloxacin and myasthenia gravis. *BMJ* 301, 818–818. doi: 10.1136/bmj.301.6755.818-a

Neil, J. F., Himmelhoch, J. M., and Licata, S. M. (1976). Emergence of myasthenia gravis during treatment with lithium carbonate. *Arch. Gen. Psychiatry* 33, 1090–1092. doi: 10.1001/archpsyc.1976.01770090080007

Nieman, R. B., Sharma, K., Edelberg, H., and Caffe, S. E. (2003). Telithromycin and myasthenia gravis. *Clin. Infect. Dis.* 37, 1579–1579. doi: 10.1086/379617

Nilsson, E., and Meretoja, O. A. (1990). Vecuronium dose-response and maintenance requirements in patients with myasthenia gravis. *Anesthesiology* 73, 28–32. doi: 10.1097/00000542-199007000-00005

Nitahara, K., Sugi, Y., Higa, K., Shono, S., and Hamada, T. (2007). Neuromuscular effects of sevoflurane in myasthenia gravis patients. *Br. J. Anaesth.* 98, 337–341. doi: 10.1093/bja/ael368

Norris, F. H., Colella, J., and Mcfarlin, D. (1964). Effect of diphenylhydantoin on neuromuscular synapse. *Neurology* 14, 869–876. doi: 10.1212/wnl.14.9.869

Oh, S. J., Dhall, R., Young, A., Morgan, M. B., Lu, L., and Claussen, G. C. (2008). Statins may aggravate myasthenia gravis. *Muscle Nerve* 38, 1101–1107. doi: 10.1002/mus.21074

Oh, S. J., Elmore, R. S., Sarala, P. K., and Kuba, T. (1986). Procainamide-induced myasthenia-like syndrome. *Muscle Nerve* 9, 670–672.

Parmar, B., Francis, P. J., and Ragge, N. K. (2002). Statins, fibrates, and ocular myasthenia. *Lancet* 360:717. doi: 10.1016/S0140-6736(02)09846-X

Pascuzzi, R. M., Coslett, H. B., and Johns, T. R. (1984). Long-term corticosteroid treatment of myasthenia gravis: report of 116 patients. *Ann. Neurol.* 15, 291–298. doi: 10.1002/ana.410150316

Pasternak, J. J., and Williamson, E. E. (2012). Clinical pharmacology, uses, and adverse reactions of iodinated contrast agents: a primer for the non-radiologist. *Mayo Clin. Proc.* 87, 390–402. doi: 10.1016/j.mayocp.2012.01.012

Penn, A. S., Low, B. W., Jaffe, I. A., Luo, L., and Jacques, J. J. (1998). Drug-induced autoimmune myasthenia gravis. *Ann. N.Y. Acad. Sci.* 841, 433–449. doi: 10.1111/j.1749-6632.1998.tb10961.x

Perrot, X., Bernard, N., Vial, C., Antoine, J. C., Laurent, H., Vial, T., et al. (2006). Myasthenia gravis exacerbation or unmasking associated with telithromycin treatment. *Neurology* 67, 2256–2258. doi: 10.1212/01.wnl.0000247741.72466.8c

Pestronk, A., and Drachman, D. B. (1987). Mechanism of action of lithium on acetylcholine receptor metabolism in skeletal muscle. *Brain Res.* 412, 302–310. doi: 10.1016/0006-8993(87)91137-1

Peyer, A.-K., Abicht, A., Heinimann, K., Sinnreich, M., and Fischer, D. (2013). Quinine sulfate as a therapeutic option in a patient with slow channel congenital myasthenic syndrome. *Neuromuscul. Disord.* 23, 571–574. doi: 10.1016/j.nmd.2013.04.001

Pittinger, C., and Adamson, R. (1972). Antibiotic blockade of neuromuscular function. *Annu. Rev. Pharmacol.* 12, 169–184. doi: 10.1146/annurev.pa.12.040172.001125

Postow, M. A., Callahan, M. K., and Wolchok, J. D. (2015). Immune checkpoint blockade in cancer therapy. *J. Clin. Oncol.* 33, 1974–1982. doi: 10.1200/JCO.2014.59.4358

Postow, M. A., Sidlow, R., and Hellmann, M. D. (2018). Immune-related adverse events associated with immune checkpoint blockade. *N. Engl. J. Med.* 378, 158–168. doi: 10.1056/NEJMra1703481

Pritchard, J. A. (1979). The use of magnesium sulfate in preeclampsia-eclampsia. *J. Reprod. Med.* 23, 107–114.

Protti, D. A., Reisin, R., Mackinley, T. A., and Uchitel, O. D. (1996). Calcium channel blockers and transmitter release at the normal human neuromuscular junction. *Neurology* 46, 1391–1396. doi: 10.1212/wnl.46.5.1391

Purvin, V., Kawasaki, A., Smith, K. H., and Kesler, A. (2006). Statin-associated myasthenia gravis: report of 4 cases and review of the literature. *Medicine (Baltimore)* 85, 82–85. doi: 10.1097/01.md.0000209337.59874.aa

Rath, J., Mauritz, M., Zulehner, G., Hilger, E., Cetin, H., Kasprian, G., et al. (2017). Iodinated contrast agents in patients with myasthenia gravis: a retrospective cohort study. *J. Neurol.* 264, 1209–1217. doi: 10.1007/s00415-017-8518-8

Ribera, A. B., and Nastuk, W. L. (1989). The actions of verapamil at the neuromuscular junction. *Comp. Biochem. Physiol. C Comp. Pharmacol. Toxicol.* 93, 137–141. doi: 10.1016/0742-8413(89)90023-6

Robberecht, W., Bednarik, J., Bourgeois, P., van Hees, J., and Carton, H. (1989). Myasthenic syndrome caused by direct effect of chloroquine on neuromuscular junction. *Arch. Neurol.* 46, 464–468. doi: 10.1001/archneur.1989.00520400124033

Rocha, M. S., and Bacheschi, L. A. (1994). Exacerbation of myasthenia gravis by contrast media. *AJR Am. J. Roentgenol.* 162, 997. doi: 10.2214/ajr.162.4.8141034

Ronzière, T., Auzou, P., Ozsancak, C., Magnier, P., Sénant, J., and Hannequin, D. (2000). [Myasthenic syndrome induced by lithium]. *Presse Med.* 29, 1043–1044.

Roquer, J., Cano, A., Seoane, J. L., and Pou Serradell, A. (1996). Myasthenia gravis and ciprofloxacin. *Acta Neurol. Scand.* 94, 419–420. doi: 10.1111/j.1600-0404.1996.tb00055.x

Rubbo, J. T., Gergis, S. D., and Sokoll, M. D. (1977). Comparative neuromuscular effects of lincomycin and clindamycin. *Anesth. Analg.* 56, 329–332. doi: 10.1213/00000539-197705000-00001

Safa, H., Johnson, D. H., Trinh, V. A., Rodgers, T. E., Lin, H., Suarez-Almazor, M. E., et al. (2019). Immune checkpoint inhibitor related myasthenia gravis:

single center experience and systematic review of the literature. *J. Immunother. Cancer* 7:319. doi: 10.1186/s40425-019-0774-y

Saleem, A. (2016). Unmasking of myasthenia gravis during pegylated Alfa 2 a interferon and ribavirin therapy for chronic hepatitis C. *J. Pak. Med. Assoc.* 66, 618–620.

Sato, K., Mano, T., Iwata, A., and Toda, T. (2019). Neurological and related adverse events in immune checkpoint inhibitors: a pharmacovigilance study from the Japanese adverse drug event report database. *J. Neurooncol.* 145, 1–9. doi: 10.1007/s11060-019-03273-1

Schaller, S. J., and Lewald, H. (2016). Clinical pharmacology and efficacy of sugammadex in the reversal of neuromuscular blockade. *Expert Opin. Drug Metab. Toxicol.* 12, 1097–1108. doi: 10.1080/17425255.2016.1215426

Seybold, M. E., and Drachman, D. B. (1974). Gradually increasing doses of prednisone in myasthenia gravis. Reducing the hazards of treatment. *N. Engl. J. Med.* 290, 81–84. doi: 10.1056/NEJM197401102900204

Shi, J., Niu, J., Shen, D., Liu, M., Tan, Y., Li, Y., et al. (2020). Clinical diagnosis and treatment recommendations for immune checkpoint inhibitor-related adverse reactions in the nervous system. *Thorac. Cancer* 11, 481–487. doi: 10.1111/1759-7714.13266

Sieb, J. P., Milone, M., and Engel, A. G. (1996). Effects of the quinoline derivatives quinine, quinidine, and chloroquine on neuromuscular transmission. *Brain Res.* 712, 179–189. doi: 10.1016/0006-8993(95)01349-0

Singh, P., Idowu, O., Malik, I., and Nates, J. L. (2015). Acute respiratory failure induced by magnesium replacement in a 62-year-old woman with myasthenia gravis. *Tex Heart Inst. J.* 42, 495–497. doi: 10.14503/THIJ-14-4584

Singh, Y. N., Harvey, A. L., and Marshall, I. G. (1978a). Antibiotic-induced paralysis of the mouse phrenic nerve-hemidiaphragm preparation, and reversibility by calcium and by neostigmine. *Anesthesiology* 48, 418–424. doi: 10.1097/00000542-197806000-00008

Singh, Y. N., Marshall, I. G., and Harvey, A. L. (1978b). Reversal of antibiotic-induced muscle paralysis by 3,4-diaminopyridine. *J. Pharm. Pharmacol.* 30, 249–250. doi: 10.1111/j.2042-7158.1978.tb13216.x

Slater, C. R. (2008). Reliability of neuromuscular transmission and how it is maintained. *Handb. Clin. Neurol.* 91, 27–101. doi: 10.1016/S0072-9752(07)01502-3

Somashekar, D. K., Davenport, M. S., Cohan, R. H., Dillman, J. R., and Ellis, J. H. (2013). Effect of intravenous low-osmolality iodinated contrast media on patients with myasthenia gravis. *Radiology* 267, 727–734. doi: 10.1148/radiol.12121508

Song, R.-H., Yao, Q.-M., Wang, B., Li, Q., Jia, X., and Zhang, J.-A. (2019). Thyroid disorders in patients with myasthenia gravis: a systematic review and meta-analysis. *Autoimmun. Rev.* 18:102368. doi: 10.1016/j.autrev.2019.102368

Swash, M., and Ingram, D. A. (1992). Adverse effect of verapamil in myasthenia gravis. *Muscle Nerve* 15, 396–398. doi: 10.1002/mus.880150321

Swift, T. R. (1979). Weakness from magnesium-containing cathartics: electrophysiologic studies. *Muscle Nerve* 2, 295–298. doi: 10.1002/mus.880020409

Timmermans, G., Depierreux, F., Wang, F., Hansen, I., and Maquet, P. (2019). Cosmetic injection of botulinum toxin unmasking subclinical myasthenia gravis: a case report and literature review. *Case Rep. Neurol.* 11, 244–251. doi: 10.1159/000502350

Titulaer, M. J., Lang, B., and Verschuuren, J. J. (2011). Lambert-Eaton myasthenic syndrome: from clinical characteristics to therapeutic strategies. *Lancet Neurol.* 10, 1098–1107. doi: 10.1016/S1474-4422(11)70245-9

Touret, F., and de Lamballerie, X. (2020). Of chloroquine and COVID-19. *Antiviral Res.* 177:104762. doi: 10.1016/j.antiviral.2020.104762

Tsutsumi, Y., Kamiishi, T., Kikuchi, R., Ito, S., Matsuoka, S., and Teshima, T. (2019). Myasthenia gravis after allogeneic bone marrow transplantation: a case report and literature review. *Hematol. Oncol. Stem Cell Ther.* 12, 110–114. doi: 10.1016/j.hemonc.2017.04.001

Vacchiano, V., Solli, P., Bartolomei, I., Lai, G., Liguori, R., and Salvi, F. (2020). Exacerbation of myasthenia gravis after amoxicillin therapy: a case series. *Neurol. Sci.* 41, 2255–2257. doi: 10.1007/s10072-020-04387-5

Vaklavas, C., Chatzizisis, Y. S., Ziakas, A., Zamboulis, C., and Giannoglou, G. D. (2009). Molecular basis of statin-associated myopathy. *Atherosclerosis* 202, 18–28. doi: 10.1016/j.atherosclerosis.2008.05.021

Vanhaesebrouck, A. E., and Beeson, D. (2019). The congenital myasthenic syndromes: expanding genetic and phenotypic spectrums and refining treatment strategies. *Curr. Opin. Neurol.* 32, 696–703. doi: 10.1097/WCO.0000000000000736

Varan, O., Kucuk, H., and Tufan, A. (2015). Myasthenia gravis due to hydroxychloroquine. *Reumatismo* 67:849. doi: 10.4081/reumatismo.2015.849

Verkijk, A. (1985). Worsening of myasthenia gravis with timolol maleate eyedrops. *Ann. Neurol.* 17, 211–212. doi: 10.1002/ana.410170222

Vijayan, N., Vijayan, V. K., and Dreyfus, P. M. (1977). Acetylcholinesterase activity and menstrual remissions in myasthenia gravis. *J. Neurol. Neurosurg. Psychiatry* 40, 1060–1065. doi: 10.1136/jnnp.40.11.1060

Vincent, A., Newsom-Davis, J., and Martin, V. (1978). Anti-acetylcholine receptor antibodies in D-penicillamine-associated myasthenia gravis. *Lancet* 1:1254. doi: 10.1016/s0140-6736(78)92481-9

Viswanath, D. V., and Jenkins, H. J. (1978). Neuromuscular block of the polymyxin group of antibiotics. *J. Pharm. Sci.* 67, 1275–1280. doi: 10.1002/jps.2600670922

Watts, J., Brew, B., and Tisch, S. (2015). Myasthenia gravis exacerbation with low dose ocular botulinum toxin for epiphoria. *J. Clin. Neurosci.* 22, 1979–1981. doi: 10.1016/j.jocn.2015.05.032

Weisman, S. J. (1949). Masked myasthenia gravis. *J. Am. Med. Assoc.* 141, 917–918. doi: 10.1001/jama.1949.62910130001008

Wilson, R. W., Ward, M. D., and Johns, T. R. (1974). Corticosteroids: a direct effect at the neuromuscular junction. *Neurology* 24, 1091–1095. doi: 10.1212/wnl.24.11.1091

Wolfe, C. M., Tafuri, N., and Hatfield, K. (2007). Exacerbation of myasthenia gravis during imiquimod treatment. *J. Drugs Dermatol.* 6, 745–746.

Wolfe, G. I., Kaminski, H. J., and Cutter, G. R. (2016). Randomized trial of thymectomy in myasthenia gravis. *N. Engl. J. Med.* 375, 2006–2007. doi: 10.1056/NEJMc1611704

Wood, S. J., and Slater, C. R. (2001). Safety factor at the neuromuscular junction. *Prog. Neurobiol.* 64, 393–429. doi: 10.1016/s0301-0082(00)00055-1

Wright, J. M., and Collier, B. (1976). The site of the neuromuscular block produced by polymyxin B and rolitetracycline. *Can. J. Physiol. Pharmacol.* 54, 926–936. doi: 10.1139/y76-129

Xing, Q., Zhang, Z.-W., Lin, Q.-H., Shen, L.-H., Wang, P.-M., Zhang, S., et al. (2020). Myositis-myasthenia gravis overlap syndrome complicated with myasthenia crisis and myocarditis associated with anti-programmed cell death-1 (sintilimab) therapy for lung adenocarcinoma. *Ann. Transl. Med.* 8:250. doi: 10.21037/atm.2020.01.79

Yaari, Y., Pincus, J. H., and Argov, Z. (1977). Depression of synaptic transmission by diphenylhydantoin. *Ann. Neurol.* 1, 334–338. doi: 10.1002/ana.410010405

Yeh, T. M., Tami, J. A., and Krolick, K. A. (1992). Exacerbated muscle dysfunction by procainamide in rats with experimental myasthenia gravis. *Drug Chem. Toxicol.* 15, 53–65. doi: 10.3109/01480549209035172

Youssef, S., Stüve, O., Patarroyo, J. C., Ruiz, P. J., Radosevich, J. L., Hur, E. M., et al. (2002). The HMG-CoA reductase inhibitor, atorvastatin, promotes a Th2 bias and reverses paralysis in central nervous system autoimmune disease. *Nature* 420, 78–84. doi: 10.1038/nature01158

Zeiser, R., and Blazar, B. R. (2017). Pathophysiology of chronic graft-versus-host disease and therapeutic targets. *N. Engl. J. Med.* 377, 2565–2579. doi: 10.1056/NEJMra1703472

Zeiser, R., and Blazar, B. R. (2018). Acute graft-versus-host disease. *N. Engl. J. Med.* 378, 586–586. doi: 10.1056/NEJMc1716969

Conflict of Interest: The authors declare that the research was conducted in the absence of any commercial or financial relationships that could be construed as a potential conflict of interest.

Copyright © 2020 Krenn, Grisold, Wohlfarth, Rath, Cetin, Koneczny and Zimprich. This is an open-access article distributed under the terms of the Creative Commons Attribution License (CC BY). The use, distribution or reproduction in other forums is permitted, provided the original author(s) and the copyright owner(s) are credited and that the original publication in this journal is cited, in accordance with accepted academic practice. No use, distribution or reproduction is permitted which does not comply with these terms.

frontiers in Molecular Neuroscience

REVIEW
published: 28 August 2020
doi: 10.3389/fnmol.2020.00162

The TOR Pathway at the Neuromuscular Junction: More Than a Metabolic Player?

Perrine Castets[1], Daniel J. Ham[2] and Markus A. Rüegg[2]**

[1] Department of Cell Physiology and Metabolism, Faculty of Medicine, University of Geneva, Geneva, Switzerland,
[2] Biozentrum, University of Basel, Basel, Switzerland

The neuromuscular junction (NMJ) is the chemical synapse connecting motor neurons and skeletal muscle fibers. NMJs allow all voluntary movements, and ensure vital functions like breathing. Changes in the structure and function of NMJs are hallmarks of numerous pathological conditions that affect muscle function including sarcopenia, the age-related loss of muscle mass and function. However, the molecular mechanisms leading to the morphological and functional perturbations in the pre- and post-synaptic compartments of the NMJ remain poorly understood. Here, we discuss the role of the metabolic pathway associated to the kinase TOR (*Target of Rapamycin*) in the development, maintenance and alterations of the NMJ. This is of particular interest as the TOR pathway has been implicated in aging, but its role at the NMJ is still ill-defined. We highlight the respective functions of the two TOR-associated complexes, TORC1 and TORC2, and discuss the role of localized protein synthesis and autophagy regulation in motor neuron terminals and sub-synaptic regions of muscle fibers and their possible effects on NMJ maintenance.

Keywords: NMJ, TOR, mTORC1, mTORC2, autophagy, aging, sarcopenia, ALS

OPEN ACCESS

Edited by:
Ruth Herbst,
Medical University of Vienna, Austria

Reviewed by:
Michael R. Deschenes,
College of William & Mary,
United States
Rüdiger Rudolf,
Mannheim University of Applied Sciences, Germany

****Correspondence:***
Perrine Castets
perrine.castets@unige.ch
Markus A. Rüegg
markus-a.ruegg@unibas.ch

Received: *31 May 2020*
Accepted: *05 August 2020*
Published: *28 August 2020*

Citation:
Castets P, Ham DJ and Rüegg MA (2020) The TOR Pathway at the Neuromuscular Junction: More Than a Metabolic Player? Front. Mol. Neurosci. 13:162. doi: 10.3389/fnmol.2020.00162

INTRODUCTION

Preserving muscle mass and function during aging has emerged as a major public health priority. As populations continue to age in many countries, the societal and personal burden stemming from the natural loss of muscle integrity and thereby life quality of the elderly is growing. The age-related loss of muscle mass (atrophy) and force (weakness), referred to as sarcopenia, is a major contributor to frailty, morbidity and mortality (for a review, see Cruz-Jentoft et al., 2019). Moreover, as frailty and disability increase, reduced activity or even disuse accelerate and aggravate the loss of muscle mass, resulting in a vicious cycle leading to a precipitous decline of the individual (Rezus et al., 2020). The situation is even more dramatic when the geriatric syndrome associates with other pathologic conditions, such as obesity. It is estimated that more than 200 million individuals worldwide will be afflicted by sarcopenia by 2050, with dramatic socioeconomic and clinical implications (Janssen et al., 2004; Cruz-Jentoft et al., 2010; Dhillon and Hasni, 2017). A well-described feature of sarcopenia is the structural changes of neuromuscular junctions (NMJs) (for a review, see Ham and Rüegg, 2018 and Rudolf et al., 2014). NMJs are the synapses connecting motor neurons to muscle fibers. Deterioration of muscle innervation during aging has been documented in several species, and treatments that slow sarcopenia also preserve NMJ integrity

(Valdez et al., 2010). Such observations led to the idea that NMJ perturbations are crucial determinants of the initiation and progression of sarcopenia, although the mechanisms responsible for age-dependent NMJ destabilization remain elusive.

Neuromuscular junctions are highly specialized chemical synapses, designed to transmit action potentials from pre-synaptic motor neurons to post-synaptic muscle fibers, thereby initiating muscle contraction. The formation and maintenance of NMJs require a complex interplay between nerves, muscle fibers and terminal Schwann cells (for a review, see Tintignac et al., 2015). In muscle fibers, post-synaptic proteins specifically accumulate at the sarcolemma immediately beneath the contact point between nerve and muscle, ultimately leading to motor endplate formation (**Figure 1**). In adult, innervated muscle, transcription of synaptic genes, encoding post-synaptic proteins, is confined to sub-synaptic (also called fundamental) myonuclei and repressed in all non-synaptic myonuclei. Previous work has uncovered several epigenetic and transcriptional effectors that ensure the tight constraint of synaptic gene expression to fundamental myonuclei. Similarly, various factors have been implicated in regulating synaptic protein dynamics (e.g., acetylcholine receptor clustering and internalization) at the motor endplate (for a review, see Li et al., 2018). A complex network of effectors and compartments is crucial for NMJ maintenance and, hence, NMJ destabilization as a consequence of a disease or aging can be initiated by pre-synaptic motor neurons, terminal Schwann cells or muscle fibers (Li et al., 2018, 2019; Martineau et al., 2018).

One of the underlying drivers of the aging process is a change in proteostasis, the balance between protein synthesis and protein degradation (Tan et al., 2019). Alterations in proteostasis have also been implicated in neurodegenerative diseases, such as Amyotrophic Lateral Sclerosis (ALS) (Ferri and Coccurello, 2017). TOR (*Target Of Rapamycin*) is at the heart of one of the key signaling pathways responsible for proteostasis. TOR activity is essential for muscle development and growth, however, overactive TOR signaling is also implicated in aging and sarcopenia (Tang et al., 2019; Ham et al., in press) and suppressing TOR by pharmacological or nutritional means remains a primary target of anti-aging interventions. While TOR is well known for its role in metabolism and aging, its role in NMJ development and maintenance is less well described. Given the broad medical interest in TOR activity manipulation and the essential role of the NMJ in maintaining skeletal muscle function and thereby mobility, it is important to establish the impact and importance of TOR activity on the NMJ. In this review, we discuss the role of TOR on NMJ stability and function in different species and compartments, and examine the proposed underlying mechanisms linking TOR to NMJ maintenance.

THE TOR SIGNALING NETWORK

TOR and TOR-Associated Proteins

Target of Rapamycin is a serine/threonine kinase, fortuitously identified in yeast mutants based on their resistance to the antifungal and immunosuppressive drug rapamycin (Heitman et al., 1991; Loewith et al., 2002). Since its identification in yeast, homologs of TOR have been identified in all eukaryotes. In the following, we will limit the discussion to **(m)TOR,** referring to mammals (mTOR for *mammalian* or *mechanistic TOR*) or flies (TOR), as most reports regarding NMJ physiology have been obtained in human, rodents and *Drosophila*. Although mammals and flies possess only one *(m)TOR* gene, the (m)TOR protein assembles into two distinct multi-protein complexes, (m)TORC1 and (m)TORC2 (Soulard et al., 2009; Gonzalez and Hall, 2017; Kim and Guan, 2019). Raptor (*Regulatory associated-protein of mTOR*) and PRAS40 (*40kDa Proline-Rich Akt Substrate*) specifically complement (m)TORC1, while (m)TORC2 comprises Rictor (*Rapamycin-insensitive companion of mTOR*), mSin1 (*mammalian stress-activated protein kinase-interacting protein 1*) and Protor1/2 (*Protein observed with rictor*) (**Figure 2A**). Although originally considered mTORC1 specific, several reports now show that

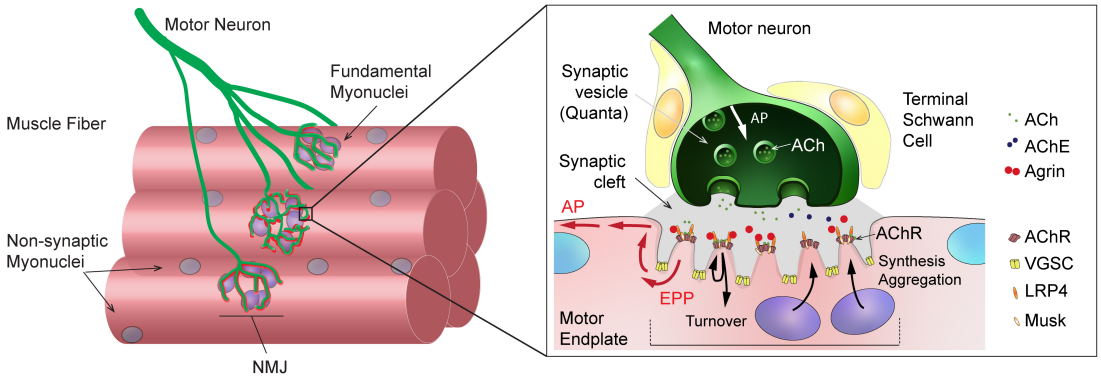

FIGURE 1 | General organization and function of mammalian neuromuscular junction (NMJ). **Left:** Scheme showing a motor axon, which branches and forms NMJs to innervate skeletal muscle fibers. Sub-synaptic (or fundamental) nuclei are seen underneath the NMJ. **Right:** Enlarged view of NMJ, showing capping Schwann cells in close contact with the muscle and axon, the junctional folds and the accumulation of synaptic proteins at the post-synaptic muscle membrane, and the liberation of synaptic vesicles at the pre-synaptic membrane upon action potential arrival. ACh, acetylcholine; AChE, acetylcholinesterase; AChR, acetylcholine receptor; AP, action potential; EPP, endplate potential; LRP4, LDL Receptor Related Protein 4; VGSC, voltage-gated sodium channel.

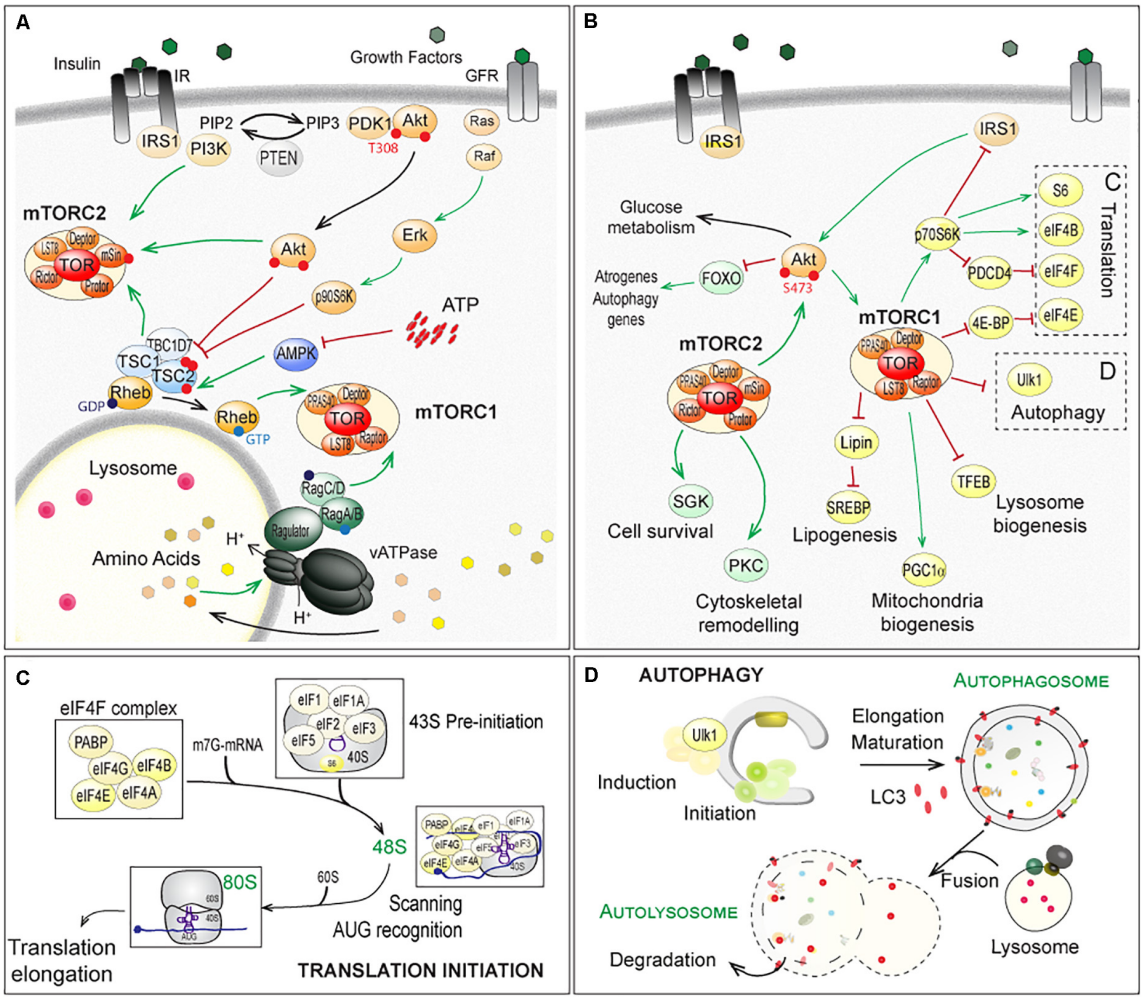

FIGURE 2 | Regulation of (m)TOR pathways and downstream factors and processes in fly and mammals. **(A)** Up-stream mechanisms regulating the (m)TOR-associated complex (m)TORC1 and (m)TORC2. Extracellular stimuli, nutrients and energy contribute to the regulation of mTORC1, at the lysosome. Growth factors, such as insulin, activate PKB/Akt, *via* the recruitment of IRS1 and PI3K and the formation of PIP3 (*Phosphatidylinositide-3,4,5-triPhosphate*). Active PKB/Akt destabilizes the complex formed by TSC1, TSC2 and TBC1D7, which releases Rheb and in turn activates (m)TORC1. Similarly, ERKs (*Extracellular signal-Regulated Kinases*) and p90S6K (*p90 ribosomal S6 Kinase*, also known as *MAPK-activated protein kinase-1*) phosphorylate TSC2 and activate (m)TORC1, in response to growth factors (Ma et al., 2005; Roux et al., 2007). Amino acids activate the vacuolar proton pomp v-ATPase, which acidifies lysosome and promotes GTP or GDP loading on Rag proteins. Interaction of Raptor with GTP-bound RagA/B and GDP-bound RagC/D leads to the activation of (m)TORC1 after its recruitment at the lysosomal membrane (Kim et al., 2008; Sancak et al., 2010; Zoncu et al., 2011; Bar-Peled et al., 2012). AMPK (*AMP-activated Kinase*) inhibits (m)TORC1 by phosphorylating Raptor (Gwinn et al., 2008) and TSC2 (Inoki et al., 2006), in response to a lowering of cellular energy (*i.e.* AMP/ATP levels). PI3K, PKB/Akt and TSC1/TSC2 complex activate mTORC2. **(B–D)** Downstream effectors of (m)TORC1 and (m)TORC2, with special focus on translation initiation **(C)** and autophagy **(D)**, both mainly controlled by (m)TORC1. Note that mTORC1 indirectly inhibits PKB/Akt and mTORC2, *via* p70S6K and the degradation of IRS1. In contrast, mTORC2 promotes mTORC1, by activating PKB/Akt. Red lines indicate inhibition; Green arrows represent activation. TFEB, Transcription factor EB; SREBP, Sterol regulatory element-binding proteins; PGC1α, Peroxisome proliferator-activated receptor gamma coactivator 1-alpha. The other abbreviations are included in the text.

long-term exposure to rapamycin also dampens mTORC2 activity (Lamming et al., 2012).

Regulation and Subcellular Localization of (m)TOR Complexes

(m)TORC1 is a central sensor of extra- and intra-cellular stimuli, including growth factors, amino acids and energy (for a detailed review, see Gonzalez et al., 2020). Growth factors, such as IGF-1 (*Insulin-like Growth Factor 1*), activate PKB/Akt (*Protein Kinase B/Akt*), *via* the recruitment of IRS1 (*Insulin Receptor Substrate 1*) and PI3K (*PhosphoInositide-3-Kinases*) (**Figure 2A**). Active PKB/Akt phosphorylates TSC2 (*Tuberosis Sclerosis Complex 2*), and thereby destabilizes the complex formed by TSC1, TSC2 and TBC1D7 (*TBC1 Domain family member 7*) (Inoki et al., 2002; Manning et al., 2002; Potter et al., 2002). This releases the small, lysosomal GTP-binding protein Rheb (*Ras Homolog Enriched in Brain*), which in turn activates (m)TORC1 (Inoki et al., 2003a,b; Tee et al., 2003; Long et al., 2005). Levels of free amino acids regulate (m)TORC1 activation, *via* the family of Rag GTPases

(*small Guanosine TriPhosphatases*) and Ragulator (Kim et al., 2008; Sancak et al., 2010; Zoncu et al., 2011; Bar-Peled et al., 2012; **Figure 2A**).

Signaling up- and downstream of mTORC2 is less well described. PKB/Akt is known to activate mTORC2 by phosphorylating mSin1 (Zinzalla et al., 2011; Yang et al., 2015) and in turn, (m)TORC2 phosphorylates and activates PKB/Akt by phosphorylating Ser473 (Jacinto et al., 2006). Paradoxically, the TSC1/TSC2 complex, while inhibiting mTORC1, activates mTORC2 independently from Rheb (Yang et al., 2006; Huang et al., 2008, 2009; **Figure 2A**). By controlling p70S6K (*p70 ribosomal S6 Kinase*, or S6K), which targets the degradation of IRS1, mTORC1 indirectly inhibits PKB/Akt and mTORC2 (Haruta et al., 2000; Manning et al., 2005). By inducing PKB/Akt, mTORC2 promotes mTORC1. These intricate regulations and feedbacks make it difficult to identify the primary cause for the deregulation of (m)TOR targets.

(m)TOR Targets Accumulate at the NMJ

(m)TORC1 promotes cell growth, by activating anabolic processes (*e.g.* protein or lipid synthesis) and by inihibiting catabolic processes, such as autophagy (**Figures 2A–D**). The main direct targets of (m)TORC1, 4E-BP1 (*eIF4E-Binding Protein 1*) and S6Ks are involved in the regulation of cap-dependent translation (**Figure 2B**). (m)TORC1-dependent activation of S6Ks triggers phosphorylation of several targets, including the S6 ribosomal protein, while (m)TORC1-dependent phosphorylation of 4E-BP1 releases inhibition of the translation factor eIF4E (*eukaryotic translation Initiation Factor 4E*). The best characterized targets of mTORC2 include SGK1 (*Serum and Glucocorticoid-regulated Kinase 1*), PKCs (*Protein Kinases C*) and PKB/Akt, which mediate the effects of mTORC2 on cell survival and cell migration (**Figure 2B**).

While (m)TOR itself has not been localized to NMJs, several (m)TORC1 targets including eIF4E in *Drosophila* larvae (Sigrist et al., 2000) and phosphorylated forms of S6 in mice (Tang et al., 2014; Castets et al., 2019) are enriched at NMJs. mTORC1 activity is also strongly regulated by innervation status, with experimental denervation potently stimulating mTORC1 activity in fast-type mouse skeletal muscle (Quy et al., 2013; Tang et al., 2014; Castets et al., 2019). Transient activation of mTORC1 has also been observed under other muscle wasting (catabolic) conditions that reduce neural stimulation, such as hindlimb suspension, where mTORC1 activity peaks after 6 h and returns to basal levels after 12 h (Chibalin et al., 2018). These observations point to (m)TOR as an early sensor of lost innervation in skeletal muscle. Activation of mTORC1 in situations of muscle wasting seems paradoxical as mTORC1 is also activated during muscle growth. However, as free amino acids are both necessary and sufficient to activate mTORC1, it is conceivable that this counter-intuitive increase in mTORC1 activity during catabolic conditions results from the release of amino acids by muscle protein breakdown. While future work is still required to determine whether mTORC1 is helpful or harmful during muscle atrophy (Quy et al., 2013; Tang et al., 2014; Castets et al., 2019), the enrichment of TOR targets at the NMJ and the marked increase in TOR activity following lost innervation points to a prominent role of TOR in NMJ physiology.

CONSEQUENCES OF (M)TOR DEREGULATION ON NMJ DEVELOPMENT AND MAINTENANCE: LESSONS FROM ANIMAL MODELS

The importance of the (m)TOR pathway in the central nervous system is highlighted by the Tuberous Sclerosis syndrome caused by mutations in the *TSC1* or *TSC2* genes, which result in benign tumors associated with neurological anomalies. Mutations of *TSC1/2* alter brain development and synaptic function (for a review, see Polchi et al., 2018). There is also evidence that changes in TSC-TOR signaling affect the peripheral nervous system, in particular the development and function of NMJs. Modern techniques have allowed extensive characterization of the consequences of specific manipulations of the (m)TOR pathway in both pre- and post-synaptic compartments on the structure and the function of NMJs.

NMJ Development and Maintenance in *Drosophila* With TOR Deregulation

Drosophila NMJs, especially at the third larval stage, are a commonly used model system to study the role of specific genes in synapse development and plasticity. One major difference to vertebrate NMJs is that they are glutamatergic synapses, which has been used to argue that they are more suitable as a model for synapses of the central nervous system. Moreover, the synaptic cleft of *Drosophila* NMJs is not filled with basal lamina, a highly structured assembly of extracellular matrix proteins. However, thanks to the availability of genetic tools, the accessibility and stereotyped organization of NMJs, and gene homology with vertebrates, studies in *Drosophila* have led to important insights for the NMJ field. In *Drosophila*, the motor neuron establishes a chain of 20-50 synaptic boutons with muscle fibers. Each synaptic bouton contains around ten active zones in the pre-synaptic compartment, each of them often being referred to as a "synapse" (**Figure 3A**). This characteristic allows the effect of gene mutations on the strength of the connection between motor neuron and muscle to be assessed by simply counting the number of synaptic boutons (for a review, see Collins and DiAntonio, 2007). An overview of *Drosophila* TOR-pathway mutants and their phenotypes is provided in **Table 1**.

While altered post-synaptic TOR signaling has little effect on the size and function of NMJs in *Drosophila*, activation of TOR, *via* the PI3K/TSC/Rheb branch, in motor neurons leads to overgrown NMJs (Martin-Pena et al., 2006; Knox et al., 2007; Natarajan et al., 2013). Inversely, inhibition of TOR, *via* overexpression of *Tsc1/2* or depletion of Rheb reduce NMJ size (Knox et al., 2007), thereby highlighting the essential role of pre-synaptic PI3K/TSC/Rheb/TOR signaling in NMJ development and growth. However, conclusions resulting from experiments focusing on TOR-associated complexes or on downstream targets that potentially mediate these NMJ phenotypes are controversial.

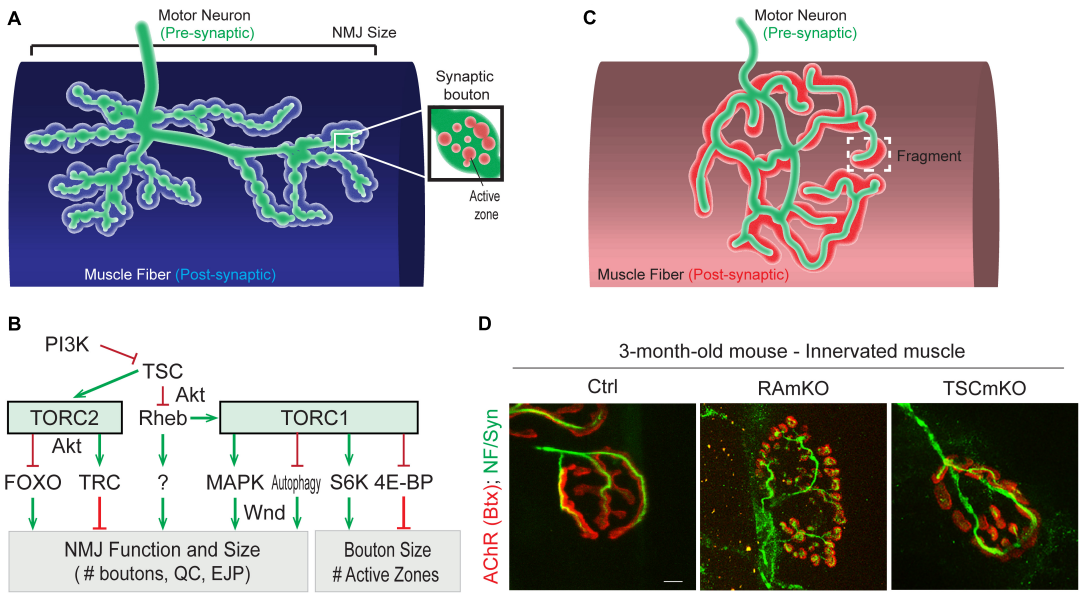

FIGURE 3 | Role of (m)TORC1 signaling in NMJ maintenance. **(A)** NMJ organization in *Drosophila,* showing the synaptic boutons spreading on the muscle fiber. **(B)** TORC1 and TORC2 signaling regulate the size of the NMJ (number of synaptic boutons), via the MAPK pathway, the autophagy process, FOXOs and the kinase Trc. TORC1 also controls the size of the synaptic boutons, via S6K and 4E-BP1. **(C,D)** Typical pretzel-shape structure of rodent NMJ (up), with the pre-synaptic compartment (motor axon) shown in green and the post-synaptic region in red. Deregulation of mTORC1 in muscle leads to NMJ alterations, with an increased fragmentation of the motor endplate (D). Motor axon is stained with Neurofilament and Synaptotagmin (green); AChRs at the muscle membrane are labeled with fluorescent bungarotoxin (red). Scale bar, 10 μm.

Especially, deletion of raptor decreases NMJ size in some cases (Wong et al., 2015), but not in others (Natarajan et al., 2013). On the other hand, most reports conclude that TORC1/S6K promotes growth of synaptic boutons (Cheng et al., 2011; Natarajan et al., 2013), but does not affect their number (Knox et al., 2007; Shen and Ganetzky, 2009; Cheng et al., 2011; Natarajan et al., 2013; Wong et al., 2015). S6K also contributes to the number of active zones at the NMJ (Cheng et al., 2011). Hence, the TORC1/S6K axis regulates structural and functional properties of NMJs in *Drosophila*, but may not mediate the effect on NMJ size (i.e., synaptic bouton number) ascribed to PI3K/TSC/Rheb signaling. A recent study instead indicated that the lysosome-Rag/TORC1 branch promotes NMJ growth *via* the MAPK (*Mitogen-activated protein kinases)*/JNK (*c-Jun N-terminal kinases*) pathway (Wong et al., 2015). Hence, TORC1 in the pre-synaptic compartment would both control the number and the size of synaptic boutons, by regulating MAPK and S6K signaling, respectively (**Figure 3B**).

Besides the effects of TORC1 activity, several pieces of evidence point to a role of TORC2 in mediating the effects of PI3K/TSC on NMJ growth. TSC activates TORC2, and inhibition of TORC2 by deleting rictor, triggers NMJ overgrowth (Natarajan et al., 2013). The negative effect of TSC/TORC2 on NMJ size could involve the activation of two kinases, PKB/Akt and Trc (*Serine/threonine-protein kinase tricorner*), and the consequent inhibition of FOXO (*Forkhead Box O*) signaling (Nechipurenko and Broihier, 2012) and WASP proteins, respectively (Natarajan et al., 2015; **Figure 3B**). Such an inhibitory effect of TORC2/Akt on NMJ size may explain why only high doses of rapamycin (i.e., sufficient to inhibit mTORC2) induce an increase in NMJ size in *Drosophila* larvae (Knox et al., 2007; Shen and Ganetzky, 2009; Wong et al., 2015). However, the role of PKB/Akt remains unclear as PKB/Akt activation also triggers NMJ overgrowth (Natarajan et al., 2013). Further investigation of the role of PKB/Akt in controlling NMJ size are hence required to understand these discrepancies. Similarly, the primary effect of Rheb on synapse size is independent of both TORC1 (Knox et al., 2007) and TORC2 (Natarajan et al., 2013), indicating the existence of alternative downstream effectors.

Consequences of Suppressing mTOR Signaling on NMJ Development and Maintenance in Mouse

In rodents, NMJs typically display a pretzel-like organization, marked by dense synaptic protein aggregation, including acetylcholine receptors (AChR), in post-synaptic regions (**Figure 3C**). Fragmentation of the endplate structure into several clusters (detected by staining AChRs with α-bungarotoxin), as well as partial or complete loss of innervation of the endplate region, are common readouts of NMJ health. **Table 2** provides an overview of mouse mTORC1 pathway mutants and their corresponding NMJ defects.

Elimination of mTORC1 Signaling in Muscle

Recent insights into the importance of mTOR in NMJ maintenance come from inducible, muscle-specific mTOR deficient (mTORmKO) mice, where 1 month of mTOR deletion

TABLE 1 | Modulation of the TOR pathway in *Drosophila* larvae and its effects on NMJ.

Genetic change	Pre/Post	Morphological changes	Electrophysiology	References
Pi3k overexpression	MN	Overgrowth	Increased mEPP frequency and amplitude	Martin-Pena et al., 2006; Knox et al., 2007
Pi3k DN	MN	Reduced size		Martin-Pena et al., 2006
Akt1 mutant	Larvae	Overgrowth		Natarajan et al., 2013
	Larvae	Reduced size		Martin-Pena et al., 2006
Akt overexpression	MN	Overgrowth		Martin-Pena et al., 2006
Rheb overexpression	MN	Overgrowth	Increased QC and EPP	Knox et al., 2007; Natarajan et al., 2013
	Muscle	Normal growth		Knox et al., 2007
Rheb mutants	Larvae MN	Reduced size	Reduced mEPP frequency, EPP amplitude and QC	Knox et al., 2007
Tsc1 mutants	Larvae	Overgrowth		Natarajan et al., 2013
Tsc2 mutants	Larvae	Overgrowth Increased bouton size	Unchanged EPP and mEPP	Natarajan et al., 2013
Tsc2 RNAi	MN	Overgrowth		Natarajan et al., 2013
	Muscle	Slight overgrowth		Natarajan et al., 2013
Tsc1/2 overexpression	MN	Reduced size		Knox et al., 2007
Rictor mutant	Larvae	Overgrowth		Natarajan et al., 2013
Raptor RNAi	MN	Normal growth Decreased boutons size		Natarajan et al., 2013
		Reduced size		Wong et al., 2015
S6K active form	MN	Overgrowth		Howlett et al., 2008
		Normal growth		Shen and Ganetzky, 2009
S6k DN	MN	Normal growth		Shen and Ganetzky, 2009; Wong et al., 2015
S6k null mutation	MN	Normal growth Decreased bouton size and AZ number	Decreased EPP amplitude, QC, and mEPP frequency	Knox et al., 2007; Cheng et al., 2011
Foxo overexpression	MN	Overgrowth		Nechipurenko and Broihier, 2012
		Normal growth		Howlett et al., 2008
Trc mutants	Larvae	Overgrowth		Natarajan et al., 2015
RagA/C mutants	Larvae	Reduced size		Wong et al., 2015

Overgrowth/Reduced size refer to NMJ size, i.e., increased vs. reduced number of synaptic boutons per muscle area. DN, dominant negative. MN, Motoneuron. AZ, Active Zones. QC, Quantal Content (number of synaptic vesicles released upon neuron impulse). EPP, excitatory post-synaptic potential (induced upon neuron stimulation). mEPP, miniature EPP, corresponding to the post-synaptic response to spontaneous release of a single synaptic vesicle.

leads to denervated fibers (around 5%) and rapamycin further exacerbates denervation (Zhang et al., 2019; Baraldo et al., 2020). Unfortunately, NMJ phenotypes have not been investigated in the constitutive, severely myopathic mTORmKO mice or mTORmKOKI mice, in which a kinase-dead version of mTOR is expressed in muscle fibers of mTORKO mice and exacerbates the myopathy (Risson et al., 2009; Zhang et al., 2019). Evidence for mTORC1 mediating the effect of mTOR on NMJs came from mTORC1-specific mouse models.

Conditional depletion of Raptor in muscle precursor cells (RAmyfKO mice) during development results in abnormal development of NMJs with aberrant innervation in the diaphragm at embryonic day 17.5 (E17.5) and a severe phenotype with perinatal lethality related to respiratory failure (Rion et al., 2019a). However, it remains unknown if the impaired innervation observed in this mouse model arises directly from a lack of mTORC1 signaling at the NMJ, or from an overall defect in muscle development. Mouse models with mTORC1 depletion in muscle fibers, triggered by constitutive or inducible Raptor depletion, have also been widely analyzed. The first report in 2008 established that RAmKO (*Raptor muscle-specific KO*) mice develop an early, severe myopathy that results in early death at the age of 5-7 months (Bentzinger et al., 2008). There were no gross alterations of NMJs in diaphragm from 3-month-old RAmKO mice, although clusters of AChRs were also found in extra-synaptic regions of muscle fibers, indicative of denervation (Bentzinger et al., 2008). Examination of NMJs in hindlimb muscle from 3-month-old RAmKO mice also revealed an increased fragmentation of NMJs (Castets and Rüegg, unpublished observation) (**Figures 3C,D**). Although only a small fraction of fibers (1 to 4%) have centralized myonuclei, we cannot rule out that the NMJ phenotype results from muscle fiber degeneration/regeneration events. Similar changes in NMJs have been described in *mdx* mice, a mouse model for Duchenne muscular dystrophy, where degeneration/regeneration is a prominent feature (Haddix et al., 2018). Generation of inducible,

TABLE 2 | Modulation of TOR pathway in mouse and its effects on NMJ.

Model	Effect on signaling pathway	Defect/Loss of innervation	Changes in post-synaptic compartment	Response to nerve injury	References
Inducible mTOR k.o. mTOR depletion	↓ mTORC1/2 (*HSA* promoter)	4% denervated fibers			Baraldo et al., 2020
RAmyfKO Raptor depletion	↓ mTORC1 (*Myf5* promoter)	Abnormal innervation of the diaphragm muscle			Rion et al., 2019a
RAmKO Raptor depletion	↓ mTORC1 (*HSA* promoter)		Extra-synaptic clusters Endplate fragmentation		Bentzinger et al., 2008
Inducible Raptor k.o. Raptor depletion	↓ mTORC1 (*HSA* promoter)	5% denervated fibers (7M) Pre-synaptic changes (7M)	Endplate fragmentation		Baraldo et al., 2020
RImyfKO Rictor depletion	↓ mTORC2 (*Myf5* promoter)	Not observed	Not observed		Rion et al., 2019b
RImKO Rictor depletion	↓ mTORC1 (*HSA* promoter)	Not observed	Not observed		Bentzinger et al., 2008
TSCmKO TSC1 depletion	↑ mTORC1 (*HSA* promoter)	Altered transmission (9M)	Fragmentation (3M) ↓ AChR density (9M)	Endplate degeneration	Castets et al., 2019; Ham et al., in press

HSA, Human Skeletal Actin; M, month.

muscle-specific Raptor-KO mice offer an opportunity to detect NMJ dysfunction before myopathic onset (Baraldo et al., 2020; Ham et al., 2020). Baraldo et al., reported that one-month Raptor depletion increases the proportion of denervated fibers, which further increases when mice are treated with rapamycin (the idea here being that rapamycin inhibits some residual mTORC1 activity, but non-muscle effects of rapamycin-induced mTORC1 suppression could also contribute). However, even 5 months post-depletion, there was no change in muscle mass, fiber size distribution and *ex vivo* muscle force, suggesting a minor contribution of the muscle denervation to the overall health (Ham et al., 2020). At 7 months post-deletion, the proportion of denervated fibers and the fragmentation of the motor endplate were increased; alterations in the motor neurons were also detected (Baraldo et al., 2020). These results suggest that mTORC1 depletion in muscle fibers affects both post- and pre-synaptic compartments. However, as inducible raptor KO mice also display centro-nucleated fibers at this late stage, one still cannot rule out an influence of muscle degeneration on NMJ alterations. Hence, although mouse models generated in the last decade point to a role of mTORC1 in the development and maintenance of NMJs, its local effect at the NMJ, independent from its function in myofibers, requires further investigations.

Depletion of mTORC2 in Muscle

mTORC2 suppression *via* Rictor depletion in muscle precursors (RImyfKO) or muscle fibers (RImKO) show little phenotype (Bentzinger et al., 2008; Kumar et al., 2008; Rion et al., 2019a). Further investigations on NMJ organization and function in these models are required to confirm or oppose a role of mTORC2 in NMJ development and/or maintenance.

Effects of mTOR Activation in Mouse Muscle on NMJ Maintenance

So far, the consequence of mTORC1 or mTORC2 activation in motor neurons on NMJs has not been studied. Similarly, there is no report assessing the effect of mTORC2 activation in muscle fibers on NMJs in rodents. In contrast, mouse models with constant activation of mTORC1 have been obtained by deleting *Tsc1* specifically in skeletal muscle (TSCmKO mice). TSCmKO mice develop a late-onset myopathy, associated with a progressive accumulation of aggregates, vacuoles and abnormal organelles in muscle fibers, related to autophagy blockade (Castets et al., 2013). At 3 months of age, TSCmKO mice display increased fragmentation of the motor endplate (**Figure 3D**), with no sign of fiber degeneration, suggesting that constant activation of mTORC1 in muscle is deleterious for NMJ maintenance. Consistently, fragmentation of the motor endplate is exacerbated in 9-month-old TSCmKO mice, together with a reduction in post-synaptic AChR density and impaired transmission properties (Ham et al., in press). Interestingly, nerve sprouting and quantal content are increased at this age, reflecting changes in the pre-synaptic compartment. As in aging (see below), these changes may compensate for the lower AChR density. Increased transmission fatigue and reduction in nerve-induced muscle force confirm the functional impairment of NMJs in TSCmKO mice (Ham et al., in press). Of note, nerve injury dramatically exacerbates the defects observed in TSCmKO muscle, with rapid motor endplate degeneration. In parallel to loss of the original post-synaptic structures, abnormal, enlarged extra-synaptic clusters accumulate throughout muscle fibers (Castets et al., 2019). It remains unclear how these clusters form in non-synaptic regions in spite of failed up-regulation of synaptic genes in response to nerve injury. Whether these clusters represent nascent clusters or derive from degenerating motor endplates remains to be explored. These studies point to a major role of mTORC1 in the maintenance of the NMJ, especially upon challenging conditions, such as nerve injury. NMJ destabilization in response to mTORC1 activation may involve local changes in protein synthesis, autophagy and/or gene expression, as discussed below.

Together, genetic manipulations in *Drosophila* and mouse models highlight the importance of tightly coordinated TOR signaling within both pre- and post-synaptic compartments

for NMJ development and maintenance, however, specific aspects of our knowledge is lacking in each organism. While experiments point to a primary role of pre-synaptic TOR signaling in *Drosophila* larvae, studies in adult flies are lacking. In contrast, post-synaptic deregulation of mTORC1 disturbs the NMJ in mice, but these observations cannot yet be untangled from muscle degeneration/regeneration ongoing in some of the mouse models.

TOR-DEPENDENT MECHANISMS INVOLVED IN NMJ MAINTENANCE

(m)TOR and Local Translation in Pre- and Post-synaptic Regions

Translation Regulation in Brief

Protein synthesis involves translation initiation, elongation, termination and ribosome recycling. Translation is mainly regulated at the initiation stage by numerous initiation factors (IFs – eIFs for eukaryotic). In cap-dependent translation, initiation requires the interaction of the 5' capped region (m7GpppN) of mRNAs with the cap-binding complex eIF4F, which includes eIF4E and its partners eIF4G and eIF4A. The ternary structure formed allows binding of the pre-initiation complex containing the 40S ribosomal unit, methionine transfer RNA and eIF1/1A/2/3/5 (**Figure 2C**). Upon scanning and identification of the AUG initiation codon, the release of eIFs promotes formation of the 80S structure, by recruitment of the 60S subunit, which ensures peptide elongation (for a review, see Sonenberg and Hinnebusch, 2009).

(m)TORC1 promotes protein synthesis by regulating S6K and 4E-BP1 (**Figures 2B,C**). (m)TORC1 phosphorylates and thereby activates S6K at Thr389, which in turn phosphorylates eIF4B, PDCD4 (*ProgrammeD Cell Death protein 4*) and S6 proteins. Phosphorylation of eIF4B increases its interaction with eIF4A in the cap-binding complex, eIF3 in the preinitiation complex (Holz et al., 2005) and the elongation factor eEF2K (Wang et al., 2001). Phosphorylation of PDCD4 releases its inhibitory activity onto eIF4A and thereby promotes formation of the cap-binding eIF4F complex (Yang et al., 2003; Dorrello et al., 2006). *Via* S6, S6K promotes the translation of mRNA with oligopyrimidine tracts (5'TOP), which encode proteins of the translation machinery (Jefferies et al., 1994; Terada et al., 1994). In parallel, 4E-BP1 is a key repressor of translation initiation, by trapping the rate-limiting factor eIF4E of the cap-binding complex. Phosphorylation of 4E-BP1 by mTORC1 allows the dissociation of eIF4E, which binds to eIF4G and initiates cap-dependent translation (Heesom and Denton, 1999; Marcotrigiano et al., 1999). Interaction of eIF4E with PABP (*Poly(A)-Binding Protein*) also facilitates translation (re)-initiation by binding the 3' end of mRNAs and ensuring the formation of loop structures.

Role of Local Translation in Motor Neurons

Several reports point to the role of local protein synthesis in long-term synaptic plasticity in the central nervous system for learning and memory (for a review, see Santini et al., 2014). Results obtained in both invertebrates and vertebrates suggest similar roles of local translation in the regulation of NMJ function. In crayfish, long-term facilitation occurs at NMJs of opener muscles from the leg in response to high frequency stimulation and requires local active translation (Beaumont et al., 2001). In *Drosophila* larvae, activation of PI3K in the motor neuron, upon glutamate release, would ensure the maintenance of neuronal activity, by promoting TOR/translation-dependent synaptic growth and, by limiting glutamate liberation *via* Akt-dependent inhibition of FOXO (Howlett et al., 2008). In rodents, studies on Spinal Muscular Atrophy (SMA) led to the identification of CTRP3 (*C1QTNF3, C1q/Tumor Necrosis Factor-related protein 3*), which is secreted by muscle and promotes protein synthesis locally in motor neurons, *via* the activation of mTOR (**Figure 4A**). In SMA, reduced levels of CTRP3 would limit protein synthesis and thereby, contribute to motor neuron degeneration (Rehorst et al., 2019).

Role of Local Translation in Muscle Sub-Synaptic Compartment

Early studies unveiled the accumulation of free ribosomes and endoplasmic reticulum in the sub-synaptic region of muscle fibers (Padykula and Gauthier, 1970). Moreover, free ribosomes accumulate underneath the sarcolemma shortly after denervation (Gauthier and Dunn, 1973; Gauthier and Schaeffer, 1974), which correlates with the synthesis of new AChRs and hypersensitivity of denervated muscle to acetylcholine (**Figure 4A**). In *Drosophila* larvae, aggregates containing eIF4E and PABP, together with polysomes, are observed in sub-synaptic regions of NMJs, consistent with local translation activity (Sigrist et al., 2000). It is noteworthy that there were no similar aggregates detected in the pre-synaptic regions. In mice, local inhibition of protein synthesis in the sub-synaptic region leads to rapid withdrawal of the motor axon and to the elimination of the NMJ (McCann et al., 2007). Consistent with a role of protein synthesis in the regulation of neuronal viability, depletion of the translation elongation factor eEF1A2 leads to motor axon degeneration, *via* a dying back process, in *Wst* mutant mice (Murray et al., 2008). In contrast, loss of eEF1A2 limits neuronal degeneration induced by nerve injury, suggesting that local translation at the NMJ differentially regulates dying back and Wallerian degenerative processes.

Beyond its role in NMJ maintenance, evidence has emerged for a role of translation in supporting NMJ plasticity. High neuronal activity triggers an increase in translation, especially of synaptic components, in sub-synaptic regions of *Drosophila* larval muscle, and thereby allows for pre- and post-synaptic remodeling (Sigrist et al., 2000; Menon et al., 2004). Interestingly, translation-mediated retrograde signaling from the post-synaptic compartment has been reported to control pre-synaptic activity in *Drosophila* larval muscle. Penney et al., first established that TOR-dependent translation in the post-synaptic region mediates the compensatory increase in neurotransmitter release in response to reduced post-synaptic activity (Petersen et al., 1997; Frank et al., 2006; Penney et al., 2012). TOR activation likely allows local translation of specific targets at the motor endplate, which act on the pre-synaptic compartment to adapt neuronal activity. It remains to be established how TOR becomes activated

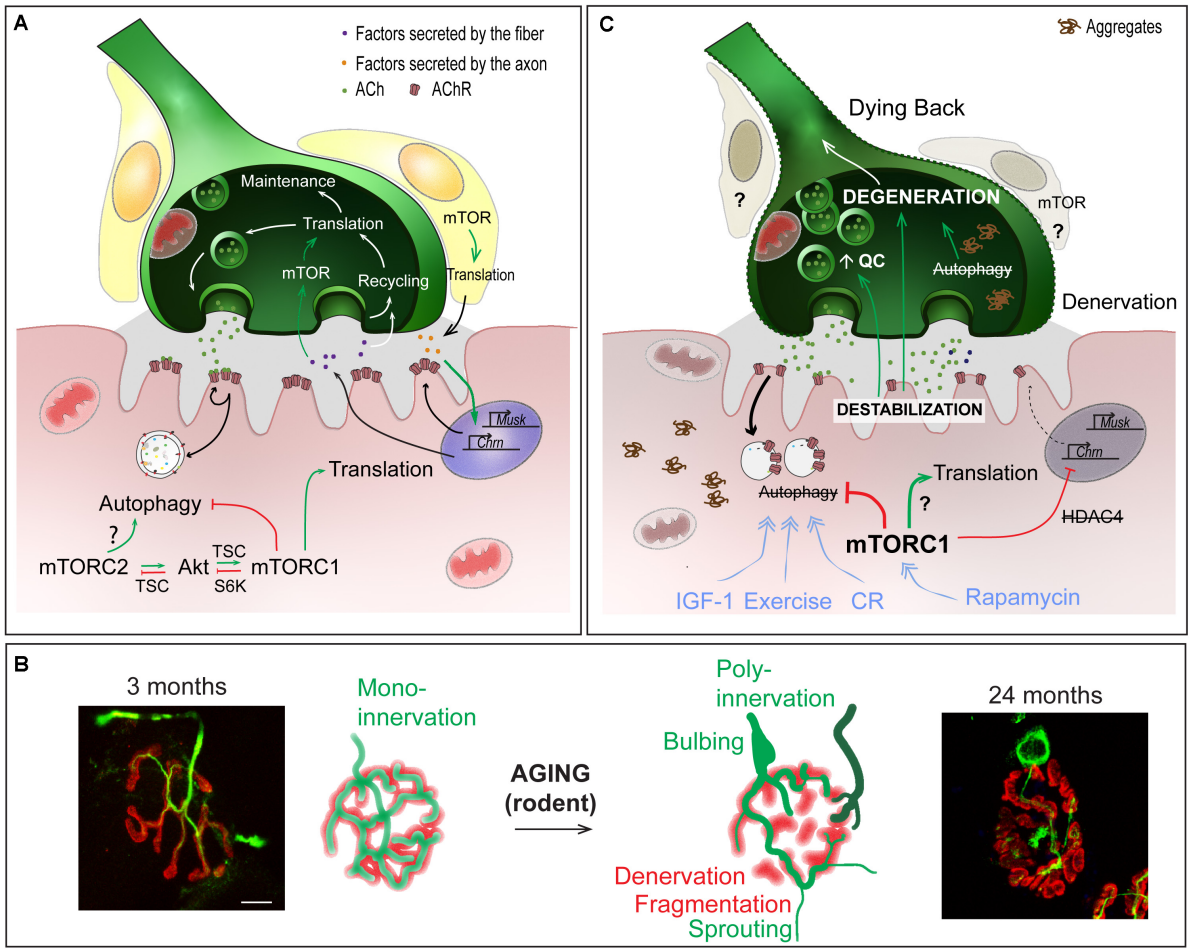

FIGURE 4 | Role of mTOR-dependent processes in NMJ alteration upon aging. **(A)** Importance of protein synthesis and autophagy in the pre- and post-synaptic compartments of NMJs. **(B)** Age-dependent changes in NMJ morphology, showing post-synaptic changes (*e.g.* fragmentation, denervation) and compensatory changes in the pre-synaptic region (*e.g.,* sprouting, poly-innervation). Scale bar, 10 μm. **(C)** Pathomechanisms involved in NMJ deterioration in aged muscle, and associated with (m)TOR deregulation. Primary destabilization of the post-synaptic compartment likely involves autophagy blockade and defective turnover in synaptic proteins. Changes in neural transmission, including increase in quantal content (QC) may be an attempt to compensate for post-synaptic decline and may in turn further aggravate NMJ deterioration. Decline of the post-synaptic compartment and retrograde feedback from muscle onto motor neuron may lead to the degeneration of the motor axon (dying back process). Exercise, IGF1, rapamycin and caloric restriction (CR) may limit age-related NMJ deterioration by modulating autophagy and/or (m)TOR-associated complexes. Red lines indicate inhibition; Green arrows represent activation; blue arrows show the beneficial effect of treatments.

in the sub-synaptic muscle region and whether specific sub-synaptic transcripts are targeted for TOR-mediated translation. Whether adaptive or compensatory changes at NMJs in mammals involve similar local regulation of mTOR-dependent translation in the sub-synaptic muscle region also needs exploring.

(m)TOR and the Regulation of Autophagy at the NMJ

Autophagy Regulation in Brief

Autophagy is an evolutionarily conserved homeostatic process that is induced under stressful or unfavorable conditions (Lum et al., 2005) but also ensures basal turnover of long-lived proteins and organelles. Autophagy proceeds through the formation of double membrane vesicles, called autophagosomes, that engulf large parts of cytoplasm and organelles to degrade them after fusion with lysosomes (Tanida, 2011; **Figure 2D**). In most cells, inhibition of (m)TORC1 is sufficient to induce autophagic flux, even in the presence of nutrients (Jung et al., 2010). The inhibitory effect of mTORC1 on autophagy is primarily mediated through regulation of the Ulk1/Atg13/FIP200 complex involved in autophagy induction (Chan, 2009; Hosokawa et al., 2009). mTORC1 directly phosphorylates Ulk1 and Atg13 and inhibits their activation by AMPK (Egan et al., 2011; Kim et al., 2011).

In skeletal muscle, a tight regulation of autophagy is essential to maintain homeostasis. Conditions like starvation, where mTORC1 activity is suppressed, strongly induce autophagy, which contributes to muscle atrophy (Mizushima et al., 2004). Genetic mutations or drugs that either induce or impair autophagic flux cause muscle atrophy and are associated with

muscle degeneration or aggregate and vacuole accumulation, respectively (Wang et al., 2005; Masiero et al., 2009). Early studies suggested that autophagy in skeletal muscle was controlled by FOXO transcription factors independent of mTORC1 (Mordier et al., 2000; Mammucari et al., 2007; Zhao et al., 2007; Sandri, 2010; Yamazaki et al., 2010; Sanchez et al., 2012). However, in TSCmKO muscle (in which mTORC1 is always active), autophagic flux is blocked at the initiation step, because of the inhibitory phosphorylation of Ulk1. This occurs despite activation of FOXOs and high autophagy-related gene expression (Castets et al., 2013; Castets and Ruegg, 2013). Inversely, mTORC1 inactivation by raptor depletion increases autophagy induction, while reduced expression of FOXO-dependent autophagy genes may dampen degradation steps (Castets et al., 2013; Baraldo et al., 2020). Therefore, mTORC1 deregulation in muscle fibers strongly perturbs autophagy with deleterious consequences. In RImKO mice (*i.e.,* mTORC2 inactivation), changes in PKB/Akt phosphorylation (Ser473) do not affect the mTORC1 pathway and there are no signs of autophagy defects (Bentzinger et al., 2008; Castets et al., 2013), suggesting that mTORC2 is not involved in autophagy regulation in rodent muscle.

Importance of the Autophagic Flux in Pre- and Post-synaptic Compartments of NMJ

In *Drosophila* larvae, overexpression or knockdown of autophagy genes using specific neuronal drivers alters autophagy in motor neurons. An increase in autophagic flux promotes NMJ growth (Shen and Ganetzky, 2009). This is achieved by degrading specific factors, such as the E3 ubiquitin ligase Hiw, which, in turn, preserves factors involved in NMJ growth, such as Wnd (Shen and Ganetzky, 2009). Thus, the positive effects of rapamycin on NMJs reported in *Drosophila* may involve autophagy induction mediated by TORC1 inhibition (Knox et al., 2007; Shen and Ganetzky, 2009; Wong et al., 2015). Autophagy also contributes to the recycling of synaptic components, especially upon high frequency stimulation. Autophagy blockade in neurons hence leads to neurodegeneration associated with the accumulation of protein aggregates and inclusions (Hara et al., 2006; Komatsu et al., 2006, 2007; Soukup et al., 2016; Vanhauwaert et al., 2017).

At the motor endplate, the accumulation of synaptic proteins relies on their tightly regulated turnover, defined by the balance between synthesis and degradation. AChRs are degraded *via* selective autophagy, which involves the E3 ubiquitin ligase MuRF1 (TRIM63), the cargo protein p62, as well as endophilin B1, a SH3-domain protein involved in endocytosis (Rudolf et al., 2013; Khan et al., 2014). Upon denervation, high rates of autophagy-dependent AChR degradation, coupled with a marked up-regulation of AChR synthesis, lead to major increases in AChR turnover (Akaaboune et al., 1999; Bruneau and Akaaboune, 2006; Strack et al., 2011, 2015; **Figure 4A**). A recent study suggested that blocking autophagy may protect motor endplates, by limiting AChR degradation. Indeed, CGRP (α-*Calcitonin Gene-Related Peptide*) treatment induces mTORC1-dependent blockade of autophagy and limits endplate degeneration in denervated muscle (Machado et al., 2019). In contrast, several reports point to the need of functional autophagic flux for NMJ maintenance. In particular, muscle-specific deletion of *Atg7* blocks autophagy in muscle and causes spontaneous fiber denervation and increased fragmentation of motor endplates (Carnio et al., 2014). Consistent with autophagy blockade, AChRs accumulate in endocytic vesicles underneath the motor endplate (Khan et al., 2014). More surprisingly, AChR turnover is increased in Atg7-deficient muscle (Carnio et al., 2014), which suggests that their internalization and/or the incorporation of new receptors are augmented (Yampolsky et al., 2010; Strack et al., 2015). Whether this occurs in response to their abnormal accumulation in endocytic vesicles remains to be determined. As in Atg7-deficient muscle, endplate fragmentation in TSCmKO mice may arise from autophagy impairment, although AChR turnover is unchanged (Castets et al., 2019). Limited autophagy flux may also contribute to NMJ destabilization in muscle-specific, inducible Raptor-KO mice, as autophagy restoration with a Tat-Beclin1 peptide is sufficient to reduce fiber denervation (Baraldo et al., 2020). Further evaluation of AChR dynamics in Raptor-KO muscle may help confirm the role of autophagy in the observed motor endplate changes and rule out the possibility that Tat-Beclin1-mediated NMJ improvements arise from amelioration of the overall muscle phenotype. Together, these data support the notion that autophagy flux must be tightly regulated to maintain NMJ stability. It remains to be investigated as to how autophagy blockade leads to NMJ destabilization and whether/how it involves an abnormal increase in synaptic protein turnover. Moreover, whether specific blockade of autophagy (*e.g.,* in Atg7-deficient muscle) can preserve motor endplate stability in response to nerve injury and functionally support re-innervation capacity needs to be explored.

Role of mTORC1 in the Transcriptional Regulation of Synaptic Genes

Constant mTORC1 activation in TSCmKO muscle precipitates denervation-induced motor endplate degeneration (Castets et al., 2019). In mutant mice, AChRs do not accumulate in endocytic vesicles, suggesting that the denervation-induced defect is not related to autophagy blockade. Instead, the failure of TSCmKO mice to stimulate AChR turnover upon denervation points to insufficient synthesis of new receptors, consistent with the defective up-regulation of the expression of genes encoding AChR subunits in TSCmKO denervated muscle (Castets et al., 2019). Interestingly, mTORC1-mediated dampening of PKB/Akt mediates the suppression of denervation-induced synaptic gene transcription through defective nuclear import (and hence activity) of HDAC4 (*Histone DeACetylase 4)* (Castets et al., 2019). HDAC4 contributes to denervation-induced synaptic gene expression by releasing HDAC9- and DACH2-dependent inhibition of the myogenic marker myogenin (Cohen et al., 2007, 2009; Tang et al., 2009; Moresi et al., 2010). Thus, the lack of incorporation of newly formed receptors at the post-synaptic plasma membrane is probably the reason for the destabilization of motor endplates in TSCmKO muscle upon denervation. It is unlikely that this contributes to endplate fragmentation in TSCmKO innervated muscle, as basal

expression of synaptic genes is similar to that in controls. Hence, by controlling transcription and translation of synaptic genes, as well as autophagy-mediated degradation of synaptic proteins, PI3K/Akt/mTORC1 signaling is important for both stability and remodeling capacity of the motor endplate after injury.

Role of mTOR in Schwann Cells

Several reports indicate a role of mTORC1 signaling in Schwann cell (SC)-mediated axon myelination in the peripheral nervous system (for a review, see Figlia et al., 2018). The role of SC mTOR activity in the development and maintenance of NMJs remains more elusive. In mice deficient for the PI3P-phosphatase PTEN (Phosphatase and TENsin homolog) and the GAP protein NF1 (Neurofibromin 1) in SCs, increased activity of Akt/mTORC1 delays the development of NMJs, with persistent immature AChR clusters, poly-innervation and reduced expression of synaptic genes at late embryonic stages (Li et al., 2019). Further investigations on the underlying mechanisms, especially on whether this implies changes in translation and/or autophagy in SCs and defective secretion of specific factors, such as agrin, by SCs, will be of interest.

Together, these data highlight that local changes in transcription, translation and autophagic degradation of synaptic components in pre- and post-synaptic compartments, as well as in SCs, are essential to maintain and orchestrate NMJ structure and function. Tight spatial and temporal control of TOR activity is required to facilitate these processes, but to fully understand the pathological effects of their perturbations in aging and disease, the intricate interplay between these cellular processes and TOR remains to be fully explored.

MTOR AS A NEW THERAPEUTIC TARGET TO STABILIZE NMJS

mTORC1 signaling is deregulated in numerous pathologies, including cancer, where developing therapeutic inhibitors of the pathway is of major importance. Emerging evidence indicates that imbalanced mTORC1 signaling contributes to muscle atrophy in various neuromuscular diseases, as well as in aging. As muscle dysfunction severely affects the quality of life of patients and increases the risk of morbidity and mortality, efforts to counteract muscle deterioration is of major public health importance. Growing evidence suggests that manipulating mTOR in contexts such as aging may help to restore or preserve muscle homeostasis, in particular by its effect on NMJs.

Role in Neurodegenerative Diseases – Amyotrophic Lateral Sclerosis

Neurodegenerative diseases are severe disorders affecting motor neurons, and consequently muscle. In the last decade, similarities in the pathomechanisms responsible for age-dependent nerve/muscle alterations and those responsible for neurodegenerative pathologies have emerged. In this section, we focus on the potential role of mTOR signaling in the pathology of Amyotrophic Lateral Sclerosis (ALS).

Amyotrophic Lateral Sclerosis is a fatal neurodegenerative disorder, caused by loss of motor neurons. Although most ALS cases are sporadic, genetic mutations in different genes, including *SOD1, FUS, C9ORF72*, or *UBQL2* are responsible for familial forms. Early reports suggested that the primary cause of ALS is the death of motor neurons. However, recent studies suggest that the primary pathologic events actually occur at NMJs or even in the muscle fibers themselves. A dying back process, starting from motor neuron terminals, would then cause retrograde degeneration of axons and neuron soma. In fly and rodent models of ALS, NMJ alterations and defective synaptic transmission precede the distal degeneration of motor neurons (Fischer et al., 2004; Rocha et al., 2013; Shahidullah et al., 2013; Tremblay et al., 2017; Chand et al., 2018; Martineau et al., 2018). Dynamic axonal sprouting and re-innervation have also been reported (Fischer et al., 2004; Martineau et al., 2018). Importantly, the expression of diseased forms of SOD1 (Superoxide Dismutase) in muscle leads to muscle atrophy, alters neuromuscular transmission and/or triggers the degeneration of motor neurons (Dobrowolny et al., 2008; Wong and Martin, 2010). Hence, it is possible that ALS primarily involves deleterious events in muscle fibers, which secondarily cause degeneration of the motor neuron, and in turn denervation of the muscle fibers.

Autophagy impairment plays a central role in ALS, causing protein aggregation in motor neurons and contributing to their death (Zhang et al., 2011). Consistent with autophagy blockade, Saxena et al. (2013) showed that mTORC1 activity increases in motor neurons in an ALS mouse model. However, mTORC1 activity seems to attenuate neuron degeneration since rapamycin precipitates the disease in mouse models of ALS (Zhang et al., 2011; Saxena et al., 2013). mTOR-dependent neuroprotection is associated with up-regulation of the transcriptional regulator, Btg2, which may promote neuroprotective pathways in motor neurons (Saxena et al., 2013). In contrast to rapamycin, treatment with trehalose is sufficient to increase lifespan of $SOD1^{G93A}$ mice and limit motor neuron degeneration. Although there was no clear evidence of changes in autophagic flux, authors suggest that trehalose acts independently of mTORC1, by improving autophagy in late degradation stages (Zhang et al., 2014). One could hypothesize that reducing mTOR activation in motor neurons aggravates ALS, as it promotes autophagy induction in a context where the degradation steps are blocked. In contrast, drugs targeting later stages of autophagy may eventually prove beneficial. In parallel, it remains unclear whether autophagy is altered in muscle fibers, especially in sub-synaptic regions, and whether this contributes to primary NMJ destabilization. Heightened AChR turnover, related to high autophagy flux, has been suggested to contribute to endplate deterioration in SOD^{G93A} mice. However, these changes were ascribed to PKC deregulation rather than mTORC1 (Dobrowolny et al., 2018). Still, local IGF-1 expression in muscle of ALS mice reduces motor neuron degeneration and NMJ deterioration (Dobrowolny et al., 2005). This effect may involve a combination of mTORC1-dependent anabolic processes and mTORC1-independent increases in autophagy within motor neurons. Interestingly, a recent report unveiled down-regulation of AChR expression in sub-synaptic myonuclei

mediated by the ALS-associated mutant FUS protein (Picchiarelli et al., 2019). Therefore, defective synaptic gene regulation in muscle may contribute to the primary events triggering NMJ destabilization in ALS. Further investigations focusing on the potent effects of mTOR on synaptic gene deregulation in sub-synaptic muscle regions and the capacity of mTOR-targeting strategies to counteract these effects will be of major interest.

Role of mTOR in Sarcopenia and Effects of mTOR Targeting Strategies

Preserving muscle quality in aging has become in the last years a worldwide public health issue with major clinical, social and economic impacts. Both mTORC1 and the NMJ are strongly implicated in the progression of age-related muscle loss, or sarcopenia. In the following, we focus on the potential role of mTOR signaling in age-related NMJ deterioration and on strategies targeting mTOR to limit these defects.

Defects in NMJs in Sarcopenia

One hallmark of sarcopenia is deterioration of NMJs and muscle fiber innervation. The sequence of events leading to NMJ deterioration remains debated, particularly in regards to whether changes in the motor axon or muscle fiber initiate these events. Regardless of the primary cause, NMJ dysfunction is thought to play a central role in the age-related loss of muscle function. Evidence is, however, lacking regarding its role in initiating this deterioration. Multiple morphological and functional changes occur in aging NMJs (**Figures 4B,C**). Denervated muscle fibers become more prevalent in muscle from both aged humans and rodents (Deschenes et al., 2010; Valdez et al., 2010; Chai et al., 2011; Chung et al., 2017; Sheth et al., 2018). Together with denervation, motor endplate area shrinks and post-synaptic AChR clusters become fragmented with age (Banker et al., 1983; Valdez et al., 2010; Cheng et al., 2013). However, growing evidence refutes a direct role of motor endplate fragmentation on NMJ function or sarcopenic progression (Willadt et al., 2016; Jones et al., 2017). Similarly, abnormal pre-synaptic patterns, such as poly-innervation and sprouting (Arizono et al., 1984; Oda, 1984; Wokke et al., 1990; Valdez et al., 2010; Cheng et al., 2013) are now thought to be compensatory processes aimed at re-establishing innervation of fibers left denervated following motor unit loss, rather than detrimental factors. Nevertheless, fragmentation, poly-innervation and sprouting are all indicative of either synaptic remodeling or instability. In fact, defects in sprouting may actually be responsible for exacerbating muscle fiber denervation and loss of muscle function at high age (Arizono et al., 1984). Several, sometimes contradictory, reports point to changes in the motor neuron terminal organization and in neurotransmission (Gutmann et al., 1971; Banker et al., 1983; Smith, 1984; Chen et al., 2012; Mahoney et al., 2014). These pre-synaptic changes may actually well be the attempts to compensate for post-synaptic decline (Courtney and Steinbach, 1981; Arizono et al., 1984; Khosa et al., 2019), and may arise from retrograde feedback from muscle onto the motor neuron (Ouanounou et al., 2016). Hence, destabilization of the post-synaptic compartment is likely a primary event in the progressive loss of integrity of NMJs and muscle, and may in particular lead to the degeneration of the motor neuron in a dying back process (Chai et al., 2011; Chung et al., 2017; Sheth et al., 2018).

Changes in mTORC1 Signaling With Age and Role in Sarcopenia-Associated NMJ Defects

Muscle atrophy is usually associated with an imbalance between protein synthesis and protein degradation. First reports on the metabolic capacity of sarcopenic muscles suggested that anabolic pathways, such as Akt/mTORC1, are less active in muscle from aged individuals, as compared to young ones. Indeed, sarcopenic muscle shows impaired or delayed response to anabolic stimuli, such as amino acids, IGF-1 injection, exercise or electric stimulation ["anabolic resistance" – (Guillet et al., 2004; Parkington et al., 2004; Cuthbertson et al., 2005; Funai et al., 2006; Kumar et al., 2009; Fry et al., 2011; Burd et al., 2013; Barclay et al., 2019)]. However, several studies also point to higher basal mTORC1 activation in aged or sarcopenic rodent muscle (Barns et al., 2014; Baar et al., 2016; White et al., 2016; Joseph et al., 2019; Tang et al., 2019; Ham et al., in press) and in humans (Markofski et al., 2015), which may mediate the blunted response to nutrition and exercise. The up-stream factors leading to mTORC1 activation with aging remain elusive. In fact, lower levels of IGF-1 in the circulation (Lamberts et al., 1997; Leger et al., 2008; Hofmann et al., 2015) together with local changes associated with inflammation are thought to contribute to age-related muscle decline (Owino et al., 2001; Hameed et al., 2002; Barbieri et al., 2003). Indeed, increasing muscle IGF-1 levels effectively counteracts age-related muscle atrophy and NMJ alterations in mice (Barton-Davis et al., 1998; Messi and Delbono, 2003; Payne et al., 2007; Ascenzi et al., 2019). Interestingly, only mild age-related changes in PKB/Akt activation have been reported (Clavel et al., 2006; Leger et al., 2008; White et al., 2016). The apparent discrepancy between low IGF-1 signaling and high mTORC1 activation in aged muscle suggests an independent contribution of IGF-1 and mTORC1 signaling in sarcopenia. As nerve injury strongly activates mTORC1, it is plausible that denervation in sarcopenic muscle precedes and contributes to activation of mTORC1, which may, in turn, further disrupt NMJs.

In line with heightened mTORC1 activity, evidence that autophagy impairment contributes to muscle aging is also emerging (**Figure 4C**). In *Drosophila*, decreased autophagic flux precipitates abnormal protein aggregate accumulation, while improving autophagic flux slows age-related muscle deterioration (Demontis and Perrimon, 2010). Signs of dampened autophagic flux have also been observed in aging rodent and human muscle, including abnormal organelle and protein aggregate accumulation and reduced autophagy marker expression (Drummond et al., 2008; Wohlgemuth et al., 2010; Kim et al., 2013; Sakuma et al., 2016; Sebastian et al., 2016; White et al., 2016). In Atg7-deficient muscle, autophagy blockade accelerates the appearance of age-related NMJ alterations (Carnio et al., 2014). Interestingly, reduced IGF-1 levels may actually contribute to sarcopenia, by limiting autophagic flux *via* mTORC2 and PKC (Renna et al., 2013; Ascenzi et al., 2019). As previously mentioned, autophagy in motor neuron terminals is also important to sustain protein turnover associated with synaptic vesicle cycling. Therefore, defective autophagy in motor neurons

may progressively impinge normal axonal trafficking and synaptic function with age, ultimately leading to motor neuron death and muscle fiber denervation. Several other factors, including reactive oxygen species, mitochondrial defects, satellite cell dysfunction and low grade inflammation, also contribute to NMJ destabilization and may also be influenced by high mTOR signaling in aging muscle (for a review, see Ham and Rüegg, 2018).

Strategies Targeting mTOR to Slow-Down NMJ Alterations Upon Aging

Based on the low anabolic response to amino acids in sarcopenic muscle and low protein intake in some elderly populations, amino acid supplementation and/or improved dietary habits are frequently recommended as strategies to limit sarcopenia (Drummond et al., 2008; Robinson et al., 2012). In contrast, long-term caloric restriction slows muscle aging and preserves both pre- and post-synaptic structures of the NMJ (Valdez et al., 2010). Caloric restriction may restore autophagic flux in sarcopenic muscle by suppressing mTORC1 (Valdez et al., 2010; Wohlgemuth et al., 2010). Similarly, exercise, which may reduce anabolic resistance and release autophagy inhibition in sarcopenic muscle (He et al., 2012; Kim et al., 2013; Luo et al., 2013; Lenhare et al., 2017), reduces both pre-synaptic changes (*e.g.,* reduction in quantal content) and post-synaptic muscle abnormalities with aging (Fahim, 1997; Valdez et al., 2010; Cheng et al., 2013). As discussed above, treatment with IGF-1 or analogous drugs is also sufficient to counteract age-related muscle loss and NMJ deterioration. As in ALS, this may involve mTORC1-dependent anabolic processes, mTORC2-dependent autophagy induction, and improved satellite cell function (Barton-Davis et al., 1998; Chakravarthy et al., 2000; Messi and Delbono, 2003; Payne et al., 2007; Ascenzi et al., 2019; Pennuto et al., 2020). Although IGF-1 treatment seems promising, the risk of cancer, associated with its anti-apoptotic effect, still raises concerns. Surprisingly, inhibition of mTORC1 by rapamycin or rapalogs is also sufficient to reverse age-associated muscle alterations. In particular, rapamycin/rapalogs limit NMJ alterations and restore autophagic flux (Joseph et al., 2019; Tang et al., 2019; Ham et al., in press). Although consistent with the overall beneficial impact of rapamycin on organismal aging, further investigation focusing on the distinct effects of these drugs on different muscles and on the consequences of inhibiting mTORC1 signaling pathway on muscle mass and function will be essential. Together, these data suggest that NMJ destabilization in both ALS and sarcopenia primarily involves post-synaptic changes, followed by adaptive changes in the pre- and post-synaptic compartments, which precede motor neuron degeneration. The role of local mTORC1 activity in initiating and/or accentuating these changes remains to be established. With it, efforts to identify the mechanisms triggering changes in TOR signaling and solutions to maintain the delicate balance between protein synthesis and degradation at the NMJ are essential.

CONCLUSION

Growing evidence points to a prominent role of TOR signaling in the formation and maintenance of the NMJ. While most *Drosophila* studies have implied an important function of TOR signaling in the pre-synaptic compartment, work in mice has demonstrated the importance of tightly controlled mTOR signaling in the post-synaptic compartment. The different focus on pre- and post-synaptic compartments between species may result from several factors, including the distinct nature of the chemical synapses (*i.e.,* glutamatergic *vs.* cholinergic), different NMJ organization and developmental mechanisms, stage of developmental analysis (*i.e.,* developing vs. adult), and/or technical limitations relating to modulating factors specifically in pre- and post- synaptic compartments. Interestingly, in *Drosophila*, evidence suggests that TORC1 and TORC2 play in concert to regulate NMJ development and plasticity. In contrast, mTORC1 in rodents is predominantly involved in the formation and maintenance of the NMJ. Perturbations in mTORC1 activity likely contribute or even initiate NMJ destabilization in pathological conditions, by altering the finely tuned balance between synthesis (transcription and translation) and degradation (*via* autophagy and proteasome) of synaptic components. However, future investigations should aim to delineate the effects of TOR deregulation on muscle homeostasis from those on NMJ maintenance, by characterizing the consequences of local changes in TOR activity at the endplate or in the terminal branch of the motor neuron. Similarly, efforts to identify the primary mechanisms leading to TOR deregulation in pathological conditions involving NMJ/muscle affection, such as sarcopenia or ALS, need to be made. Further understanding of the complex mechanisms involving (m)TOR signaling in NMJ physiology will uncover essential insights for the design of therapeutic strategies to counteract or limit the loss of NMJ integrity and muscle function in aging and neurodegenerative disorders.

AUTHOR CONTRIBUTIONS

PC wrote and edited the manuscript. DH and MR edited the manuscript. All authors contributed to the article and approved the submitted version.

FUNDING

PC is funded by the Swiss National Science Foundation (Eccellenza PCEFP3_181102). MR received support from the Cantons of Basel-Stadt and Basel-Landschaft, and grants from the Swiss National Science Foundation.

REFERENCES

Akaaboune, M., Culican, S. M., Turney, S. G., and Lichtman, J. W. (1999). Rapid and reversible effects of activity on acetylcholine receptor density at the neuromuscular junction in vivo. *Science* 286, 503–507. doi: 10.1126/science.286.5439.503

Arizono, N., Koreto, O., Iwai, Y., Hidaka, T., and Takeoka, O. (1984). Morphometric analysis of human neuromuscular junction in different ages. *Acta Pathol. Jpn.* 34, 1243–1249. doi: 10.1111/j.1440-1827.1984.tb00551.x

Ascenzi, F., Barberi, L., Dobrowolny, G., Villa Nova Bacurau, A., Nicoletti, C., Rizzuto, E., et al. (2019). Effects of IGF-1 isoforms on muscle growth and sarcopenia. *Aging Cell* 18:e12954. doi: 10.1111/acel.12954

Baar, E. L., Carbajal, K. A., Ong, I. M., and Lamming, D. W. (2016). Sex- and tissue-specific changes in mTOR signaling with age in C57BL/6J mice. *Aging Cell* 15, 155–166. doi: 10.1111/acel.12425

Banker, B. Q., Kelly, S. S., and Robbins, N. (1983). Neuromuscular transmission and correlative morphology in young and old mice. *J. Physiol.* 339, 355–377. doi: 10.1113/jphysiol.1983.sp014721

Baraldo, M., Geremia, A., Pirazzini, M., Nogara, L., Solagna, F., Turk, C., et al. (2020). Skeletal muscle mTORC1 regulates neuromuscular junction stability. *J. Cachexia Sarcopenia Muscle* 11, 208–225. doi: 10.1002/jcsm.12496

Barbieri, M., Ferrucci, L., Ragno, E., Corsi, A., Bandinelli, S., Bonafe, M., et al. (2003). Chronic inflammation and the effect of IGF-I on muscle strength and power in older persons. *Am. J. Physiol. Endocrinol. Metab.* 284, E481–E487.

Barclay, R. D., Burd, N. A., Tyler, C., Tillin, N. A., and Mackenzie, R. W. (2019). The role of the IGF-1 signaling cascade in muscle protein synthesis and anabolic resistance in aging skeletal muscle. *Front. Nutr.* 6:146. doi: 10.3389/fnut.2019.00146

Barns, M., Gondro, C., Tellam, R. L., Radley-Crabb, H. G., Grounds, M. D., and Shavlakadze, T. (2014). Molecular analyses provide insight into mechanisms underlying sarcopenia and myofibre denervation in old skeletal muscles of mice. *Int. J. Biochem. Cell Biol.* 53, 174–185. doi: 10.1016/j.biocel.2014.04.025

Bar-Peled, L., Schweitzer, L. D., Zoncu, R., and Sabatini, D. M. (2012). Ragulator is a GEF for the rag GTPases that signal amino acid levels to mTORC1. *Cell* 150, 1196–1208. doi: 10.1016/j.cell.2012.07.032

Barton-Davis, E. R., Shoturma, D. I., Musaro, A., Rosenthal, N., and Sweeney, H. L. (1998). Viral mediated expression of insulin-like growth factor I blocks the aging-related loss of skeletal muscle function. *Proc. Natl. Acad. Sci. U.S.A.* 95, 15603–15607. doi: 10.1073/pnas.95.26.15603

Beaumont, V., Zhong, N., Fletcher, R., Froemke, R. C., and Zucker, R. S. (2001). Phosphorylation and local presynaptic protein synthesis in calcium- and calcineurin-dependent induction of crayfish long-term facilitation. *Neuron* 32, 489–501. doi: 10.1016/s0896-6273(01)00483-4

Bentzinger, C. F., Romanino, K., Cloëtta, D., Lin, S., Mascarenhas, J. B., Oliveri, F., et al. (2008). Skeletal muscle-specific ablation of raptor, but not of rictor, causes metabolic changes and results in muscle dystrophy. *Cell Metab.* 8, 411–424. doi: 10.1016/j.cmet.2008.10.002

Bruneau, E. G., and Akaaboune, M. (2006). The dynamics of recycled acetylcholine receptors at the neuromuscular junction in vivo. *Development* 133, 4485–4493. doi: 10.1242/dev.02619

Burd, N. A., Gorissen, S. H., and van Loon, L. J. (2013). Anabolic resistance of muscle protein synthesis with aging. *Exerc. Sport Sci. Rev.* 41, 169–173. doi: 10.1097/jes.0b013e318292f3d5

Carnio, S., LoVerso, F., Baraibar, M. A., Longa, E., Khan, M. M., Maffei, M., et al. (2014). Autophagy impairment in muscle induces neuromuscular junction degeneration and precocious aging. *Cell Rep.* 8, 1509–1521. doi: 10.1016/j.celrep.2014.07.061

Castets, P., Lin, S., Rion, N., Di Fulvio, S., Romanino, K., Guridi, M., et al. (2013). Sustained activation of mTORC1 in skeletal muscle inhibits constitutive and starvation-induced autophagy and causes a severe, late-onset myopathy. *Cell Metab.* 17, 731–744. doi: 10.1016/j.cmet.2013.03.015

Castets, P., Rion, N., Theodore, M., Falcetta, D., Lin, S., Reischl, M., et al. (2019). mTORC1 and PKB/Akt control the muscle response to denervation by regulating autophagy and HDAC4. *Nat. Commun.* 10:3187.

Castets, P., and Ruegg, M. A. (2013). MTORC1 determines autophagy through ULK1 regulation in skeletal muscle. *Autophagy* 9, 1435–1437. doi: 10.4161/auto.25722

Chai, R. J., Vukovic, J., Dunlop, S., Grounds, M. D., and Shavlakadze, T. (2011). Striking denervation of neuromuscular junctions without lumbar motoneuron loss in geriatric mouse muscle. *PLoS One* 6:e28090. doi: 10.1371/journal.pone.0028090

Chakravarthy, M. V., Davis, B. S., and Booth, F. W. (2000). IGF-I restores satellite cell proliferative potential in immobilized old skeletal muscle. *J. Appl. Physiol.* 89, 1365–1379. doi: 10.1152/jappl.2000.89.4.1365

Chan, E. Y. (2009). mTORC1 phosphorylates the ULK1-mAtg13-FIP200 autophagy regulatory complex. *Sci. Signal.* 2:e51.

Chand, K. K., Lee, K. M., Lee, J. D., Qiu, H., Willis, E. F., Lavidis, N. A., et al. (2018). Defects in synaptic transmission at the neuromuscular junction precede motor deficits in a TDP-43(Q331K) transgenic mouse model of amyotrophic lateral sclerosis. *FASEB J.* 32, 2676–2689. doi: 10.1096/fj.201700835r

Chen, J., Mizushige, T., and Nishimune, H. (2012). Active zone density is conserved during synaptic growth but impaired in aged mice. *J. Comp. Neurol.* 520, 434–452. doi: 10.1002/cne.22764

Cheng, A., Morsch, M., Murata, Y., Ghazanfari, N., Reddel, S. W., and Phillips, W. D. (2013). Sequence of age-associated changes to the mouse neuromuscular junction and the protective effects of voluntary exercise. *PLoS One* 8:e67970. doi: 10.1371/journal.pone.0067970

Cheng, L., Locke, C., and Davis, G. W. (2011). S6 kinase localizes to the presynaptic active zone and functions with PDK1 to control synapse development. *J. Cell Biol.* 194, 921–935. doi: 10.1083/jcb.201101042

Chibalin, A. V., Benziane, B., Zakyrjanova, G. F., Kravtsova, V. V., and Krivoi, I. I. (2018). Early endplate remodeling and skeletal muscle signaling events following rat hindlimb suspension. *J. Cell Physiol.* 233, 6329–6336. doi: 10.1002/jcp.26594

Chung, T., Park, J. S., Kim, S., Montes, N., Walston, J., and Hoke, A. (2017). Evidence for dying-back axonal degeneration in age-associated skeletal muscle decline. *Muscle Nerve* 55, 894–901. doi: 10.1002/mus.25267

Clavel, S., Coldefy, A. S., Kurkdjian, E., Salles, J., Margaritis, I., and Derijard, B. (2006). Atrophy-related ubiquitin ligases, atrogin-1 and MuRF1 are up-regulated in aged rat Tibialis Anterior muscle. *Mech. Ageing Dev.* 127, 794–801. doi: 10.1016/j.mad.2006.07.005

Cohen, T. J., Barrientos, T., Hartman, Z. C., Garvey, S. M., Cox, G. A., and Yao, T. P. (2009). The deacetylase HDAC4 controls myocyte enhancing factor-2-dependent structural gene expression in response to neural activity. *FASEB J.* 23, 99–106. doi: 10.1096/fj.08-115931

Cohen, T. J., Waddell, D. S., Barrientos, T., Lu, Z., Feng, G., Cox, G. A., et al. (2007). The histone deacetylase HDAC4 connects neural activity to muscle transcriptional reprogramming. *J. Biol. Chem.* 282, 33752–33759. doi: 10.1074/jbc.m706268200

Collins, C. A., and DiAntonio, A. (2007). Synaptic development: insights from *Drosophila*. *Curr. Opin. Neurobiol.* 17, 35–42. doi: 10.1016/j.conb.2007.01.001

Courtney, J., and Steinbach, J. H. (1981). Age changes in neuromuscular junction morphology and acetylcholine receptor distribution on rat skeletal muscle fibres. *J. Physiol.* 320, 435–447. doi: 10.1113/jphysiol.1981.sp013960

Cruz-Jentoft, A. J., Baeyens, J. P., Bauer, J. M., Boirie, Y., Cederholm, T., Landi, F., et al. (2010). Sarcopenia: european consensus on definition and diagnosis: report of the european working group on sarcopenia in older people. *Age Ageing* 39, 412–423. doi: 10.1093/ageing/afq034

Cruz-Jentoft, A. J., Bahat, G., Bauer, J., Boirie, Y., Bruyere, O., Cederholm, T., et al. (2019). Sarcopenia: revised European consensus on definition and diagnosis. *Age Ageing* 48:601. doi: 10.1093/ageing/afz046

Cuthbertson, D., Smith, K., Babraj, J., Leese, G., Waddell, T., Atherton, P., et al. (2005). Anabolic signaling deficits underlie amino acid resistance of wasting, aging muscle. *FASEB J.* 19, 422–424.

Demontis, F., and Perrimon, N. (2010). FOXO/4E-BP signaling in *Drosophila* muscles regulates organism-wide proteostasis during aging. *Cell* 143, 813–825. doi: 10.1016/j.cell.2010.10.007

Deschenes, M. R., Roby, M. A., Eason, M. K., and Harris, M. B. (2010). Remodeling of the neuromuscular junction precedes sarcopenia related alterations in myofibers. *Exp. Gerontol.* 45, 389–393. doi: 10.1016/j.exger.2010.03.007

Dhillon, R. J., and Hasni, S. (2017). Pathogenesis and management of sarcopenia. *Clin. Geriatr. Med.* 33, 17–26. doi: 10.1016/j.cger.2016.08.002

Dobrowolny, G., Aucello, M., Rizzuto, E., Beccafico, S., Mammucari, C., Boncompagni, S., et al. (2008). Skeletal muscle is a primary target of SOD1G93A-mediated toxicity. *Cell Metab.* 8, 425–436. doi: 10.1016/j.cmet.2008.09.002

Dobrowolny, G., Giacinti, C., Pelosi, L., Nicoletti, C., Winn, N., Barberi, L., et al. (2005). Muscle expression of a local Igf-1 isoform protects motor neurons in an ALS mouse model. *J. Cell Biol.* 168, 193–199. doi: 10.1083/jcb.200407021

Dobrowolny, G., Martini, M., Scicchitano, B. M., Romanello, V., Boncompagni, S., Nicoletti, C., et al. (2018). Muscle Expression of SOD1(G93A) triggers the dismantlement of neuromuscular junction via PKC-Theta. *Antioxid Redox Signal.* 28, 1105–1119. doi: 10.1089/ars.2017.7054

Dorrello, N. V., Peschiaroli, A., Guardavaccaro, D., Colburn, N. H., Sherman, N. E., and Pagano, M. (2006). S6K1- and betaTRCP-mediated degradation of PDCD4 promotes protein translation and cell growth. *Science* 314, 467–471. doi: 10.1126/science.1130276

Drummond, M. J., Dreyer, H. C., Pennings, B., Fry, C. S., Dhanani, S., Dillon, E. L., et al. (2008). Skeletal muscle protein anabolic response to resistance exercise and essential amino acids is delayed with aging. *J. Appl. Physiol.* 104, 1452–1461. doi: 10.1152/japplphysiol.00021.2008

Egan, D., Kim, J., Shaw, R. J., and Guan, K. L. (2011). The autophagy initiating kinase ULK1 is regulated via opposing phosphorylation by AMPK and mTOR. *Autophagy* 7, 643–644. doi: 10.4161/auto.7.6.15123

Fahim, M. A. (1997). Endurance exercise modulates neuromuscular junction of C57BL/6NNia aging mice. *J. Appl. Physiol.* 83, 59–66. doi: 10.1152/jappl.1997.83.1.59

Ferri, A., and Coccurello, R. (2017). What is Hyper in the ALS hypermetabolism? *Mediators Inflamm* 2017:7821672.

Figlia, G., Gerber, D., and Suter, U. (2018). Myelination and mTOR. *Glia* 66, 693–707.

Fischer, L. R., Culver, D. G., Tennant, P., Davis, A. A., Wang, M., Castellano-Sanchez, A., et al. (2004). Amyotrophic lateral sclerosis is a distal axonopathy: evidence in mice and man. *Exp. Neurol.* 185, 232–240. doi: 10.1016/j.expneurol.2003.10.004

Frank, C. A., Kennedy, M. J., Goold, C. P., Marek, K. W., and Davis, G. W. (2006). Mechanisms underlying the rapid induction and sustained expression of synaptic homeostasis. *Neuron* 52, 663–677. doi: 10.1016/j.neuron.2006.09.029

Fry, C. S., Drummond, M. J., Glynn, E. L., Dickinson, J. M., Gundermann, D. M., Timmerman, K. L., et al. (2011). Aging impairs contraction-induced human skeletal muscle mTORC1 signaling and protein synthesis. *Skeletal Muscle* 1:11. doi: 10.1186/2044-5040-1-11

Funai, K., Parkington, J. D., Carambula, S., and Fielding, R. A. (2006). Age-associated decrease in contraction-induced activation of downstream targets of Akt/mTor signaling in skeletal muscle. *Am. J. Physiol. Regul. Integr. Comp. Physiol.* 290, R1080–R1086.

Gauthier, G. F., and Dunn, R. A. (1973). Ultrastructural and cytochemical features of mammalian skeletal muscle fibres following denervation. *J. Cell Sci.* 12, 525–547.

Gauthier, G. F., and Schaeffer, S. F. (1974). Ultrastructural and cytochemical manifestations of protein synthesis in the peripheral sarcoplasm of denervated and newborn skeletal muscle fibres. *J. Cell Sci.* 14, 113–137.

Gonzalez, A., and Hall, M. N. (2017). Nutrient sensing and TOR signaling in yeast and mammals. *EMBO J.* 36, 397–408. doi: 10.15252/embj.201696010

Gonzalez, A., Hall, M. N., Lin, S. C., and Hardie, D. G. (2020). AMPK and TOR: the yin and yang of cellular nutrient sensing and growth control. *Cell Metab.* 31, 472–492. doi: 10.1016/j.cmet.2020.01.015

Guillet, C., Prod'homme, M., Balage, M., Gachon, P., Giraudet, C., Morin, L., et al. (2004). Impaired anabolic response of muscle protein synthesis is associated with S6K1 dysregulation in elderly humans. *FASEB J.* 18, 1586–1587. doi: 10.1096/fj.03-1341fje

Gutmann, E., Hanzlikova, V., and Vysokocil, F. (1971). Age changes in cross striated muscle of the rat. *J. Physiol.* 216, 331–343. doi: 10.1113/jphysiol.1971.sp009528

Gwinn, D. M., Shackelford, D. B., Egan, D. F., Mihaylova, M. M., Mery, A., Vasquez, D. S., et al. (2008). AMPK phosphorylation of raptor mediates a metabolic checkpoint. *Mol. Cell* 30, 214–226. doi: 10.1016/j.molcel.2008.03.003

Haddix, S. G., Lee, Y. I., Kornegay, J. N., and Thompson, W. J. (2018). Cycles of myofiber degeneration and regeneration lead to remodeling of the neuromuscular junction in two mammalian models of Duchenne muscular dystrophy. *PLoS One* 13:e0205926. doi: 10.1371/journal.pone.0205926

Ham, A. S., Chojnowska, K., Tintignac, L. A., Lin, S., Schmidt, A., Ham, D. J., et al. (2020). mTORC1 signalling is not essential for the maintenance of muscle mass and function in adult sedentary mice. *J. Cachexia Sarcopenia Muscle* 11, 259–273. doi: 10.1002/jcsm.12505

Ham, D. J., Börsch, A., Lin, S., Thürkauf, M., Weihrauch, M., Reinhard, J. R., et al. (in press). The neuromuscular junction is a focal point of mTORC1 signaling in sarcopenia. *Nat. Commun.*

Ham, D. J., and Rüegg, M. A. (2018). Causes and consequences of age-related changes at the neuromuscular junction. *Curr. Opin. Physiol.* 04, 32–39. doi: 10.1016/j.cophys.2018.04.007

Hameed, M., Harridge, S. D., and Goldspink, G. (2002). Sarcopenia and hypertrophy: a role for insulin-like growth factor-1 in aged muscle? *Exerc. Sport Sci. Rev.* 30, 15–19. doi: 10.1097/00003677-200201000-00004

Hara, T., Nakamura, K., Matsui, M., Yamamoto, A., Nakahara, Y., Suzuki-Migishima, R., et al. (2006). Suppression of basal autophagy in neural cells causes neurodegenerative disease in mice. *Nature* 441, 885–889. doi: 10.1038/nature04724

Haruta, T., Uno, T., Kawahara, J., Takano, A., Egawa, K., Sharma, P. M., et al. (2000). A rapamycin-sensitive pathway down-regulates insulin signaling via phosphorylation and proteasomal degradation of insulin receptor substrate-1. *Mol. Endocrinol.* 14, 783–794. doi: 10.1210/mend.14.6.0446

He, C., Bassik, M. C., Moresi, V., Sun, K., Wei, Y., Zou, Z., et al. (2012). Exercise-induced BCL2-regulated autophagy is required for muscle glucose homeostasis. *Nature* 481, 511–515. doi: 10.1038/nature10758

Heesom, K. J., and Denton, R. M. (1999). Dissociation of the eukaryotic initiation factor-4E/4E-BP1 complex involves phosphorylation of 4E-BP1 by an mTOR-associated kinase. *FEBS Lett.* 457, 489–493. doi: 10.1016/s0014-5793(99)01094-7

Heitman, J., Movva, N. R., and Hall, M. N. (1991). Targets for cell cycle arrest by the immunosuppressant rapamycin in yeast. *Science* 253, 905–909. doi: 10.1126/science.1715094

Hofmann, M., Halper, B., Oesen, S., Franzke, B., Stuparits, P., Tschan, H., et al. (2015). Serum concentrations of insulin-like growth factor-1, members of the TGF-beta superfamily and follistatin do not reflect different stages of dynapenia and sarcopenia in elderly women. *Exp. Gerontol.* 64, 35–45. doi: 10.1016/j.exger.2015.02.008

Holz, M. K., Ballif, B. A., Gygi, S. P., and Blenis, J. (2005). mTOR and S6K1 mediate assembly of the translation preinitiation complex through dynamic protein interchange and ordered phosphorylation events. *Cell* 123, 569–580. doi: 10.1016/j.cell.2005.10.024

Hosokawa, N., Hara, T., Kaizuka, T., Kishi, C., Takamura, A., Miura, Y., et al. (2009). Nutrient-dependent mTORC1 association with the ULK1-Atg13-FIP200 complex required for autophagy. *Mol. Biol. Cell* 20, 1981–1991. doi: 10.1091/mbc.e08-12-1248

Howlett, E., Lin, C. C., Lavery, W., and Stern, M. (2008). A PI3-kinase-mediated negative feedback regulates neuronal excitability. *PLoS Genet.* 4:e1000277. doi: 10.1371/journal.pgen.1000277

Huang, J., Dibble, C. C., Matsuzaki, M., and Manning, B. D. (2008). The TSC1-TSC2 complex is required for proper activation of mTOR complex 2. *Mol. Cell Biol.* 28, 4104–4115. doi: 10.1128/mcb.00289-08

Huang, J., Wu, S., Wu, C. L., and Manning, B. D. (2009). Signaling events downstream of mammalian target of rapamycin complex 2 are attenuated in cells and tumors deficient for the tuberous sclerosis complex tumor suppressors. *Cancer Res.* 69, 6107–6114. doi: 10.1158/0008-5472.can-09-0975

Inoki, K., Li, Y., Xu, T., and Guan, K. L. (2003a). Rheb GTPase is a direct target of TSC2 GAP activity and regulates mTOR signaling. *Genes Dev.* 17, 1829–1834. doi: 10.1101/gad.1110003

Inoki, K., Zhu, T., and Guan, K. L. (2003b). TSC2 mediates cellular energy response to control cell growth and survival. *Cell* 115, 577–590. doi: 10.1016/s0092-8674(03)00929-2

Inoki, K., Li, Y., Zhu, T., Wu, J., and Guan, K. L. (2002). TSC2 is phosphorylated and inhibited by Akt and suppresses mTOR signalling. *Nat. Cell Biol.* 4, 648–657. doi: 10.1038/ncb839

Inoki, K., Ouyang, H., Zhu, T., Lindvall, C., Wang, Y., Zhang, X., et al. (2006). TSC2 integrates Wnt and energy signals via a coordinated phosphorylation by AMPK and GSK3 to regulate cell growth. *Cell* 126, 955–968. doi: 10.1016/j.cell.2006.06.055

Jacinto, E., Facchinetti, V., Liu, D., Soto, N., Wei, S., Jung, S. Y., et al. (2006). SIN1/MIP1 maintains rictor-mTOR complex integrity and regulates Akt phosphorylation and substrate specificity. *Cell* 127, 125–137. doi: 10.1016/j.cell.2006.08.033

Janssen, I., Shepard, D. S., Katzmarzyk, P. T., and Roubenoff, R. (2004). The healthcare costs of sarcopenia in the United States. *J. Am. Geriatr. Soc.* 52, 80–85. doi: 10.1111/j.1532-5415.2004.52014.x

Jefferies, H. B., Reinhard, C., Kozma, S. C., and Thomas, G. (1994). Rapamycin selectively represses translation of the polypyrimidine tract mRNA family. *Proc. Natl. Acad. Sci. U.S.A.* 91, 4441–4445. doi: 10.1073/pnas.91.10.4441

Jones, R. A., Harrison, C., Eaton, S. L., Llavero Hurtado, M., Graham, L. C., Alkhammash, L., et al. (2017). Cellular and molecular anatomy of the human neuromuscular junction. *Cell Rep.* 21, 2348–2356.

Joseph, G. A., Wang, S. X., Jacobs, C. E., Zhou, W., Kimble, G. C., Tse, H. W., et al. (2019). Partial inhibition of mTORC1 in aged rats counteracts the decline in muscle mass and reverses molecular signaling associated with sarcopenia. *Mol. Cell Biol.* 39:e00141-19. doi: 10.1128/MCB.00141-19

Jung, C. H., Ro, S. H., Cao, J., Otto, N. M., and Kim, D. H. (2010). mTOR regulation of autophagy. *FEBS Lett.* 584, 1287–1295.

Khan, M. M., Strack, S., Wild, F., Hanashima, A., Gasch, A., Brohm, K., et al. (2014). Role of autophagy, SQSTM1, SH3GLB1, and TRIM63 in the turnover of nicotinic acetylcholine receptors. *Autophagy* 10, 123–136. doi: 10.4161/auto.26841

Khosa, S., Trikamji, B., Khosa, G. S., Khanli, H. M., and Mishra, S. K. (2019). An overview of neuromuscular junction aging findings in human and animal studies. *Curr. Aging Sci.* 12, 28–34. doi: 10.2174/1874609812666190603165746

Kim, E., Goraksha-Hicks, P., Li, L., Neufeld, T. P., and Guan, K. L. (2008). Regulation of TORC1 by Rag GTPases in nutrient response. *Nat. Cell Biol.* 10, 935–945. doi: 10.1038/ncb1753

Kim, J., and Guan, K. L. (2019). mTOR as a central hub of nutrient signalling and cell growth. *Nat. Cell Biol.* 21, 63–71. doi: 10.1038/s41556-018-0205-1

Kim, J., Kundu, M., Viollet, B., and Guan, K. L. (2011). AMPK and mTOR regulate autophagy through direct phosphorylation of Ulk1. *Nat. Cell Biol.* 13, 132–141. doi: 10.1038/ncb2152

Kim, Y. A., Kim, Y. S., Oh, S. L., Kim, H. J., and Song, W. (2013). Autophagic response to exercise training in skeletal muscle with age. *J. Physiol. Biochem.* 69, 697–705. doi: 10.1007/s13105-013-0246-7

Knox, S., Ge, H., Dimitroff, B. D., Ren, Y., Howe, K. A., Arsham, A. M., et al. (2007). Mechanisms of TSC-mediated control of synapse assembly and axon guidance. *PLoS One* 2:e375. doi: 10.1371/journal.pone.0000375

Komatsu, M., Waguri, S., Chiba, T., Murata, S., Iwata, J., Tanida, I., et al. (2006). Loss of autophagy in the central nervous system causes neurodegeneration in mice. *Nature* 441, 880–884. doi: 10.1038/nature04723

Komatsu, M., Wang, Q. J., Holstein, G. R., Friedrich, V. L. Jr., Iwata, J., Kominami, E., et al. (2007). Essential role for autophagy protein Atg7 in the maintenance of axonal homeostasis and the prevention of axonal degeneration. *Proc. Natl. Acad. Sci .U.S.A.* 104, 14489–14494. doi: 10.1073/pnas.0701311104

Kumar, A., Harris, T. E., Keller, S. R., Choi, K. M., Magnuson, M. A., Lawrence, J. C. Jr., et al. (2008). Muscle-specific deletion of rictor impairs insulin-stimulated glucose transport and enhances Basal glycogen synthase activity. *Mol. Cell Biol.* 28, 61–70. doi: 10.1128/mcb.01405-07

Kumar, V., Selby, A., Rankin, D., Patel, R., Atherton, P., Hildebrandt, W., et al. (2009). Age-related differences in the dose-response relationship of muscle protein synthesis to resistance exercise in young and old men. *J. Physiol.* 587, 211–217. doi: 10.1113/jphysiol.2008.164483

Lamberts, S. W., van den Beld, A. W., and van der Lely, A. J. (1997). The endocrinology of aging. *Science* 278, 419–424.

Lamming, D. W., Ye, L., Katajisto, P., Goncalves, M. D., Saitoh, M., Stevens, D. M., et al. (2012). Rapamycin-induced insulin resistance is mediated by mTORC2 loss and uncoupled from longevity. *Science* 335, 1638–1643. doi: 10.1126/science.1215135

Leger, B., Derave, W., De Bock, K., Hespel, P., and Russell, A. P. (2008). Human sarcopenia reveals an increase in SOCS-3 and myostatin and a reduced efficiency of Akt phosphorylation. *Rejuvenation Res.* 11, 163–175.

Lenhare, L., Crisol, B. M., Silva, V. R. R., Katashima, C. K., Cordeiro, A. V., Pereira, K. D., et al. (2017). Physical exercise increases Sestrin 2 protein levels and induces autophagy in the skeletal muscle of old mice. *Exp. Gerontol.* 97, 17–21. doi: 10.1016/j.exger.2017.07.009

Li, L., Xiong, W. C., and Mei, L. (2018). Neuromuscular junction formation. Aging, and disorders. *Annu. Rev. Physiol.* 80, 159–188.

Li, X. X., Zhang, S. J., Chiu, A. P., Lo, L. H., To, J. C., Cui, H. N., et al. (2019). Conditional inactivation of Nf1 and pten in schwann cells results in abnormal neuromuscular junction maturation. *G3* 9, 297–303. doi: 10.1534/g3.118.200795

Loewith, R., Jacinto, E., Wullschleger, S., Lorberg, A., Crespo, J. L., Bonenfant, D., et al. (2002). Two TOR complexes, only one of which is rapamycin sensitive, have distinct roles in cell growth control. *Mol. Cell* 10, 457–468. doi: 10.1016/s1097-2765(02)00636-6

Long, X., Lin, Y., Ortiz-Vega, S., Yonezawa, K., and Avruch, J. (2005). Rheb binds and regulates the mTOR kinase. *Curr. Biol.* 15, 702–713. doi: 10.1016/j.cub.2005.02.053

Lum, J. J., DeBerardinis, R. J., and Thompson, C. B. (2005). Autophagy in metazoans: cell survival in the land of plenty. *Nat. Rev. Mol. Cell Biol.* 6, 439–448. doi: 10.1038/nrm1660

Luo, L., Lu, A. M., Wang, Y., Hong, A., Chen, Y., Hu, J., et al. (2013). Chronic resistance training activates autophagy and reduces apoptosis of muscle cells by modulating IGF-1 and its receptors, Akt/mTOR and Akt/FOXO3a signaling in aged rats. *Exp. Gerontol.* 48, 427–436. doi: 10.1016/j.exger.2013.02.009

Ma, L., Chen, Z., Erdjument-Bromage, H., Tempst, P., and Pandolfi, P. P. (2005). Phosphorylation and functional inactivation of TSC2 by Erk implications for tuberous sclerosis and cancer pathogenesis. *Cell* 121, 179–193. doi: 10.1016/j.cell.2005.02.031

Machado, J., Silveira, W. A., Goncalves, D. A., Schavinski, A. Z., Khan, M. M., Zanon, N. M., et al. (2019). alpha-Calcitonin gene-related peptide inhibits autophagy and calpain systems and maintains the stability of neuromuscular junction in denervated muscles. *Mol. Metab.* 28, 91–106. doi: 10.1016/j.molmet.2019.06.024

Mahoney, R. E., Rawson, J. M., and Eaton, B. A. (2014). An age-dependent change in the set point of synaptic homeostasis. *J. Neurosci.* 34, 2111–2119. doi: 10.1523/jneurosci.3556-13.2014

Mammucari, C., Milan, G., Romanello, V., Masiero, E., Rudolf, R., Del Piccolo, P., et al. (2007). FoxO3 controls autophagy in skeletal muscle in vivo. *Cell Metab.* 6, 458–471. doi: 10.1016/j.cmet.2007.11.001

Manning, B. D., Logsdon, M. N., Lipovsky, A. I., Abbott, D., Kwiatkowski, D. J., and Cantley, L. C. (2005). Feedback inhibition of Akt signaling limits the growth of tumors lacking Tsc2. *Genes Dev.* 19, 1773–1778. doi: 10.1101/gad.1314605

Manning, B. D., Tee, A. R., Logsdon, M. N., Blenis, J., and Cantley, L. C. (2002). Identification of the tuberous sclerosis complex-2 tumor suppressor gene product tuberin as a target of the phosphoinositide 3-kinase/akt pathway. *Mol. Cell* 10, 151–162. doi: 10.1016/s1097-2765(02)00568-3

Marcotrigiano, J., Gingras, A. C., Sonenberg, N., and Burley, S. K. (1999). Cap-dependent translation initiation in eukaryotes is regulated by a molecular mimic of eIF4G. *Mol. Cell* 3, 707–716. doi: 10.1016/s1097-2765(01)80003-4

Markofski, M. M., Dickinson, J. M., Drummond, M. J., Fry, C. S., Fujita, S., Gundermann, D. M., et al. (2015). Effect of age on basal muscle protein synthesis and mTORC1 signaling in a large cohort of young and older men and women. *Exp. Gerontol* 65, 1–7. doi: 10.1016/j.exger.2015.02.015

Martineau, E., Di Polo, A., Vande Velde, C., and Robitaille, R. (2018). Dynamic neuromuscular remodeling precedes motor-unit loss in a mouse model of ALS. *eLife* 7:e41973. doi: 10.7554/eLife.41973

Martin-Pena, A., Acebes, A., Rodriguez, J. R., Sorribes, A., de Polavieja, G. G., Fernandez-Funez, P., et al. (2006). Age-independent synaptogenesis by phosphoinositide 3 kinase. *J. Neurosci.* 26, 10199–10208. doi: 10.1523/jneurosci.1223-06.2006

Masiero, E., Agatea, L., Mammucari, C., Blaauw, B., Loro, E., Komatsu, M., et al. (2009). Autophagy is required to maintain muscle mass. *Cell Metab.* 10, 507–515. doi: 10.1016/j.cmet.2009.10.008

McCann, C. M., Nguyen, Q. T., Santo Neto, H., and Lichtman, J. W. (2007). Rapid synapse elimination after postsynaptic protein synthesis inhibition in vivo. *J. Neurosci.* 27, 6064–6067. doi: 10.1523/jneurosci.0627-07.2007

Menon, K. P., Sanyal, S., Habara, Y., Sanchez, R., Wharton, R. P., Ramaswami, M., et al. (2004). The translational repressor Pumilio regulates presynaptic morphology and controls postsynaptic accumulation of translation factor eIF-4E. *Neuron* 44, 663–676. doi: 10.1016/j.neuron.2004.10.028

Messi, M. L., and Delbono, O. (2003). Target-derived trophic effect on skeletal muscle innervation in senescent mice. *J. Neurosci.* 23, 1351–1359. doi: 10.1523/jneurosci.23-04-01351.2003

Mizushima, N., Yamamoto, A., Matsui, M., Yoshimori, T., and Ohsumi, Y. (2004). In vivo analysis of autophagy in response to nutrient starvation using transgenic mice expressing a fluorescent autophagosome marker. *Mol. Biol. Cell* 15, 1101–1111. doi: 10.1091/mbc.e03-09-0704

Mordier, S., Deval, C., Bechet, D., Tassa, A., and Ferrara, M. (2000). Leucine limitation induces autophagy and activation of lysosome-dependent proteolysis in C2C12 myotubes through a mammalian target of rapamycin-independent signaling pathway. *J. Biol. Chem.* 275, 29900–29906. doi: 10.1074/jbc.m003633200

Moresi, V., Williams, A. H., Meadows, E., Flynn, J. M., Potthoff, M. J., McAnally, J., et al. (2010). Myogenin and class II HDACs control neurogenic muscle atrophy by inducing E3 ubiquitin ligases. *Cell* 143, 35–45. doi: 10.1016/j.cell.2010.09.004

Murray, L. M., Thomson, D., Conklin, A., Wishart, T. M., and Gillingwater, T. H. (2008). Loss of translation elongation factor (eEF1A2) expression in vivo differentiates between Wallerian degeneration and dying-back neuronal pathology. *J. Anat.* 213, 633–645. doi: 10.1111/j.1469-7580.2008.01007.x

Natarajan, R., Barber, K., Buckley, A., Cho, P., Egbejimi, A., and Wairkar, Y. P. (2015). Tricornered kinase regulates synapse development by regulating the levels of wiskott-aldrich syndrome protein. *PLoS One* 10:e0138188. doi: 10.1371/journal.pone.0138188

Natarajan, R., Trivedi-Vyas, D., and Wairkar, Y. P. (2013). Tuberous sclerosis complex regulates *Drosophila* neuromuscular junction growth via the TORC2/Akt pathway. *Hum. Mol. Genet.* 22, 2010–2023. doi: 10.1093/hmg/ddt053

Nechipurenko, I. V., and Broihier, H. T. (2012). FoxO limits microtubule stability and is itself negatively regulated by microtubule disruption. *J. Cell Biol.* 196, 345–362. doi: 10.1083/jcb.201105154

Oda, K. (1984). Age changes of motor innervation and acetylcholine receptor distribution on human skeletal muscle fibres. *J. Neurol. Sci.* 66, 327–338. doi: 10.1016/0022-510x(84)90021-2

Ouanounou, G., Baux, G., and Bal, T. (2016). A novel synaptic plasticity rule explains homeostasis of neuromuscular transmission. *eLife* 5:e12190. doi: 10.7554/eLife.12190

Owino, V., Yang, S. Y., and Goldspink, G. (2001). Age-related loss of skeletal muscle function and the inability to express the autocrine form of insulin-like growth factor-1 (MGF) in response to mechanical overload. *FEBS Lett.* 505, 259–263. doi: 10.1016/s0014-5793(01)02825-3

Padykula, H. A., and Gauthier, G. F. (1970). The ultrastructure of the neuromuscular junctions of mammalian red, white, and intermediate skeletal muscle fibers. *J. Cell Biol.* 46, 27–41. doi: 10.1083/jcb.46.1.27

Parkington, J. D., LeBrasseur, N. K., Siebert, A. P., and Fielding, R. A. (2004). Contraction-mediated mTOR, p70S6k, and ERK1/2 phosphorylation in aged skeletal muscle. *J. Appl. Physiol.* 97, 243–248. doi: 10.1152/japplphysiol.01383.2003

Payne, A. M., Messi, M. L., Zheng, Z., and Delbono, O. (2007). Motor neuron targeting of IGF-1 attenuates age-related external Ca2+-dependent skeletal muscle contraction in senescent mice. *Exp. Gerontol.* 42, 309–319. doi: 10.1016/j.exger.2006.11.003

Penney, J., Tsurudome, K., Liao, E. H., Elazzouzi, F., Livingstone, M., Gonzalez, M., et al. (2012). TOR is required for the retrograde regulation of synaptic homeostasis at the *Drosophila* neuromuscular junction. *Neuron* 74, 166–178. doi: 10.1016/j.neuron.2012.01.030

Pennuto, M., Pandey, U. B., and Polanco, M. J. (2020). Insulin-like growth factor 1 signaling in motor neuron and polyglutamine diseases: from molecular pathogenesis to therapeutic perspectives. *Front. Neuroendocrinol.* 57:100821. doi: 10.1016/j.yfrne.2020.100821

Petersen, S. A., Fetter, R. D., Noordermeer, J. N., Goodman, C. S., and DiAntonio, A. (1997). Genetic analysis of glutamate receptors in *Drosophila* reveals a retrograde signal regulating presynaptic transmitter release. *Neuron* 19, 1237–1248. doi: 10.1016/s0896-6273(00)80415-8

Picchiarelli, G., Demestre, M., Zuko, A., Been, M., Higelin, J., Dieterle, S., et al. (2019). FUS-mediated regulation of acetylcholine receptor transcription at neuromuscular junctions is compromised in amyotrophic lateral sclerosis. *Nat. Neurosci.* 22, 1793–1805. doi: 10.1038/s41593-019-0498-9

Polchi, A., Magini, A., Meo, D. D., Tancini, B., and Emiliani, C. (2018). mTOR signaling and neural stem cells: the tuberous sclerosis complex model. *Int. J. Mol. Sci.* 19:1474. doi: 10.3390/ijms19051474

Potter, C. J., Pedraza, L. G., and Xu, T. (2002). Akt regulates growth by directly phosphorylating Tsc2. *Nat. Cell Biol.* 4, 658–665. doi: 10.1038/ncb840

Quy, P. N., Kuma, A., Pierre, P., and Mizushima, N. (2013). Proteasome-dependent activation of mammalian target of rapamycin complex 1 (mTORC1) is essential for autophagy suppression and muscle remodeling following denervation. *J. Biol. Chem.* 288, 1125–1134. doi: 10.1074/jbc.m112.399949

Rehorst, W. A., Thelen, M. P., Nolte, H., Turk, C., Cirak, S., Peterson, J. M., et al. (2019). Muscle regulates mTOR dependent axonal local translation in motor neurons via CTRP3 secretion: implications for a neuromuscular disorder, spinal muscular atrophy. *Acta Neuropathol. Commun.* 7:154.

Renna, M., Bento, C. F., Fleming, A., Menzies, F. M., Siddiqi, F. H., Ravikumar, B., et al. (2013). IGF-1 receptor antagonism inhibits autophagy. *Hum. Mol. Genet.* 22, 4528–4544. doi: 10.1093/hmg/ddt300

Rezus, E., Burlui, A., Cardoneanu, A., Rezus, C., Codreanu, C., Parvu, M., et al. (2020). Inactivity and skeletal muscle metabolism: a vicious cycle in old age. *Int. J. Mol. Sci.* 21:592. doi: 10.3390/ijms21020592

Rion, N., Castets, P., Lin, S., Enderle, L., Reinhard, J. R., Eickhorst, C., et al. (2019a). mTOR controls embryonic and adult myogenesis via mTORC1. *Development* 146:dev172460. doi: 10.1242/dev.172460

Rion, N., Castets, P., Lin, S., Enderle, L., Reinhard, J. R., and Ruegg, M. A. (2019b). mTORC2 affects the maintenance of the muscle stem cell pool. *Skelet Muscle* 9:30.

Risson, V., Mazelin, L., Roceri, M., Sanchez, H., Moncollin, V., Corneloup, C., et al. (2009). Muscle inactivation of mTOR causes metabolic and dystrophin defects leading to severe myopathy. *J. Cell Biol.* 187, 859–874. doi: 10.1083/jcb.200903131

Robinson, S., Cooper, C., and Aihie Sayer, A. (2012). Nutrition and sarcopenia: a review of the evidence and implications for preventive strategies. *J. Aging Res.* 2012, 510801.

Rocha, M. C., Pousinha, P. A., Correia, A. M., Sebastiao, A. M., and Ribeiro, J. A. (2013). Early changes of neuromuscular transmission in the SOD1(G93A) mice model of ALS start long before motor symptoms onset. *PLoS One* 8:e73846. doi: 10.1371/journal.pone.0073846

Roux, P. P., Shahbazian, D., Vu, H., Holz, M. K., Cohen, M. S., Taunton, J., et al. (2007). RAS/ERK signaling promotes site-specific ribosomal protein S6 phosphorylation via RSK and stimulates cap-dependent translation. *J. Biol. Chem.* 282, 14056–14064. doi: 10.1074/jbc.m700906200

Rudolf, R., Bogomolovas, J., Strack, S., Choi, K. R., Khan, M. M., Wagner, A., et al. (2013). Regulation of nicotinic acetylcholine receptor turnover by MuRF1 connects muscle activity to endo/lysosomal and atrophy pathways. *Age* 35, 1663–1674. doi: 10.1007/s11357-012-9468-9

Rudolf, R., Khan, M. M., Labeit, S., and Deschenes, M. R. (2014). Degeneration of neuromuscular junction in age and dystrophy. *Front. Aging Neurosci.* 6:99. doi: 10.3389/fnagi.2014.00099

Sakuma, K., Kinoshita, M., Ito, Y., Aizawa, M., Aoi, W., and Yamaguchi, A. (2016). p62/SQSTM1 but not LC3 is accumulated in sarcopenic muscle of mice. *J. Cachexia Sarcopenia Muscle* 7, 204–212. doi: 10.1002/jcsm.12045

Sancak, Y., Bar-Peled, L., Zoncu, R., Markhard, A. L., Nada, S., and Sabatini, D. M. (2010). Ragulator-Rag complex targets mTORC1 to the lysosomal surface and is necessary for its activation by amino acids. *Cell* 141, 290–303. doi: 10.1016/j.cell.2010.02.024

Sanchez, A. M., Csibi, A., Raibon, A., Cornille, K., Gay, S., Bernardi, H., et al. (2012). AMPK promotes skeletal muscle autophagy through activation of forkhead FoxO3a and interaction with Ulk1. *J. Cell. Biochem.* 113, 695–710. doi: 10.1002/jcb.23399

Sandri, M. (2010). Autophagy in skeletal muscle. *FEBS Lett.* 584, 1411–1416. doi: 10.1016/j.febslet.2010.01.056

Santini, E., Huynh, T. N., and Klann, E. (2014). Mechanisms of translation control underlying long-lasting synaptic plasticity and the consolidation of long-term memory. *Prog. Mol. Biol. Transl. Sci.* 122, 131–167. doi: 10.1016/b978-0-12-420170-5.00005-2

Saxena, S., Roselli, F., Singh, K., Leptien, K., Julien, J. P., Gros-Louis, F., et al. (2013). Neuroprotection through excitability and mTOR required in ALS motoneurons to delay disease and extend survival. *Neuron* 80, 80–96. doi: 10.1016/j.neuron.2013.07.027

Sebastian, D., Sorianello, E., Segales, J., Irazoki, A., Ruiz-Bonilla, V., Sala, D., et al. (2016). Mfn2 deficiency links age-related sarcopenia and impaired autophagy to activation of an adaptive mitophagy pathway. *EMBO J.* 35, 1677–1693. doi: 10.15252/embj.201593084

Shahidullah, M., Le Marchand, S. J., Fei, H., Zhang, J., Pandey, U. B., Dalva, M. B., et al. (2013). Defects in synapse structure and function precede motor neuron degeneration in *Drosophila* models of FUS-related ALS. *J. Neurosci.* 33, 19590–19598. doi: 10.1523/jneurosci.3396-13.2013

Shen, W., and Ganetzky, B. (2009). Autophagy promotes synapse development in *Drosophila*. *J. Cell Biol.* 187, 71–79. doi: 10.1083/jcb.200907109

Sheth, K. A., Iyer, C. C., Wier, C. G., Crum, A. E., Bratasz, A., Kolb, S. J., et al. (2018). Muscle strength and size are associated with motor unit connectivity in aged mice. *Neurobiol. Aging* 67, 128–136. doi: 10.1016/j.neurobiolaging.2018.03.016

Sigrist, S. J., Thiel, P. R., Reiff, D. F., Lachance, P. E., Lasko, P., and Schuster, C. M. (2000). Postsynaptic translation affects the efficacy and morphology of neuromuscular junctions. *Nature* 405, 1062–1065. doi: 10.1038/35016598

Smith, D. O. (1984). Acetylcholine storage, release and leakage at the neuromuscular junction of mature adult and aged rats. *J. Physiol.* 347, 161–176. doi: 10.1113/jphysiol.1984.sp015059

Sonenberg, N., and Hinnebusch, A. G. (2009). Regulation of translation initiation in eukaryotes: mechanisms and biological targets. *Cell* 136, 731–745. doi: 10.1016/j.cell.2009.01.042

Soukup, S. F., Kuenen, S., Vanhauwaert, R., Manetsberger, J., Hernandez-Diaz, S., Swerts, J., et al. (2016). A LRRK2-Dependent EndophilinA phosphoswitch is critical for macroautophagy at presynaptic terminals. *Neuron* 92, 829–844. doi: 10.1016/j.neuron.2016.09.037

Soulard, A., Cohen, A., and Hall, M. N. (2009). TOR signaling in invertebrates. *Curr. Opin. Cell Biol.* 21, 825–836.

Strack, S., Khan, M. M., Wild, F., Rall, A., and Rudolf, R. (2015). Turnover of acetylcholine receptors at the endplate revisited: novel insights into nerve-dependent behavior. *J. Muscle Res. Cell Motil.* 36, 517–524. doi: 10.1007/s10974-015-9418-0

Strack, S., Petersen, Y., Wagner, A., Roder, I. V., Albrizio, M., Reischl, M., et al. (2011). A novel labeling approach identifies three stability levels of acetylcholine receptors in the mouse neuromuscular junction in vivo. *PLoS One* 6:e20524. doi: 10.1371/journal.pone.0020524

Tan, K. T., Ang, S. J., and Tsai, S. Y. (2019). Sarcopenia: tilting the balance of protein homeostasis. *Proteomics* 20:e1800411.

Tang, H., Inoki, K., Brooks, S. V., Okazawa, H., Lee, M., Wang, J., et al. (2019). mTORC1 underlies age-related muscle fiber damage and loss by inducing oxidative stress and catabolism. *Aging Cell* 18:e12943. doi: 10.1111/acel.12943

Tang, H., Inoki, K., Lee, M., Wright, E., Khuong, A., Sugiarto, S., et al. (2014). mTORC1 promotes denervation-induced muscle atrophy through a mechanism involving the activation of FoxO and E3 ubiquitin ligases. *Sci. Signal.* 7:ra18. doi: 10.1126/scisignal.2004809

Tang, H., Macpherson, P., Marvin, M., Meadows, E., Klein, W. H., Yang, X. J., et al. (2009). A histone deacetylase 4/myogenin positive feedback loop coordinates denervation-dependent gene induction and suppression. *Mol. Biol. Cell* 20, 1120–1131. doi: 10.1091/mbc.e08-07-0759

Tanida, I. (2011). Autophagosome formation and molecular mechanism of autophagy. *Antioxid Redox Signal.* 14, 2201–2214. doi: 10.1089/ars.2010.3482

Tee, A. R., Manning, B. D., Roux, P. P., Cantley, L. C., and Blenis, J. (2003). Tuberous sclerosis complex gene products, Tuberin and Hamartin, control mTOR signaling by acting as a GTPase-activating protein complex toward Rheb. *Curr. Biol.* 13, 1259–1268. doi: 10.1016/s0960-9822(03)00506-2

Terada, N., Patel, H. R., Takase, K., Kohno, K., Nairn, A. C., and Gelfand, E. W. (1994). Rapamycin selectively inhibits translation of mRNAs encoding elongation factors and ribosomal proteins. *Proc. Natl. Acad. Sci. U.S.A.* 91, 11477–11481. doi: 10.1073/pnas.91.24.11477

Tintignac, L. A., Brenner, H. R., and Ruegg, M. A. (2015). Mechanisms regulating neuromuscular junction development and function and causes of muscle wasting. *Physiol. Rev.* 95, 809–852. doi: 10.1152/physrev.00033.2014

Tremblay, E., Martineau, E., and Robitaille, R. (2017). Opposite synaptic alterations at the neuromuscular junction in an ALS mouse model: when motor units matter. *J. Neurosci.* 37, 8901–8918. doi: 10.1523/jneurosci.3090-16.2017

Valdez, G., Tapia, J. C., Kang, H., Clemenson, G. D. Jr., Gage, F. H., Lichtman, J. W., et al. (2010). Attenuation of age-related changes in mouse neuromuscular synapses by caloric restriction and exercise. *PNAS* 107, 14863–14868. doi: 10.1073/pnas.1002220107

Vanhauwaert, R., Kuenen, S., Masius, R., Bademosi, A., Manetsberger, J., Schoovaerts, N., et al. (2017). The SAC1 domain in synaptojanin is required for autophagosome maturation at presynaptic terminals. *EMBO J.* 36, 1392–1411. doi: 10.15252/embj.201695773

Wang, X., Blagden, C., Fan, J., Nowak, S. J., Taniuchi, I., Littman, D. R., et al. (2005). Runx1 prevents wasting, myofibrillar disorganization, and autophagy of skeletal muscle. *Genes Dev.* 19, 1715–1722. doi: 10.1101/gad.1318305

Wang, X., Li, W., Williams, M., Terada, N., Alessi, D. R., and Proud, C. G. (2001). Regulation of elongation factor 2 kinase by p90(RSK1) and p70 S6 kinase. *EMBO J.* 20, 4370–4379. doi: 10.1093/emboj/20.16.4370

White, Z., White, R. B., McMahon, C., Grounds, M. D., and Shavlakadze, T. (2016). High mTORC1 signaling is maintained, while protein degradation pathways are perturbed in old murine skeletal muscles in the fasted state. *Int. J. Biochem. Cell Biol.* 78, 10–21. doi: 10.1016/j.biocel.2016.06.012

Willadt, S., Nash, M., and Slater, C. R. (2016). Age-related fragmentation of the motor endplate is not associated with impaired neuromuscular transmission in the mouse diaphragm. *Sci. Rep.* 6:24849.

Wohlgemuth, S. E., Seo, A. Y., Marzetti, E., Lees, H. A., and Leeuwenburgh, C. (2010). Skeletal muscle autophagy and apoptosis during aging: effects of calorie restriction and life-long exercise. *Exp.Gerontol.* 45, 138–148. doi: 10.1016/j.exger.2009.11.002

Wokke, J. H., Jennekens, F. G., van den Oord, C. J., Veldman, H., Smit, L. M., and Leppink, G. J. (1990). Morphological changes in the human end plate with age. *J. Neurol. Sci.* 95, 291–310. doi: 10.1016/0022-510x(90)90076-y

Wong, C. O., Palmieri, M., Li, J., Akhmedov, D., Chao, Y., Broadhead, G. T., et al. (2015). Diminished MTORC1-Dependent JNK activation underlies the neurodevelopmental defects associated with lysosomal dysfunction. *Cell Rep.* 12, 2009–2020. doi: 10.1016/j.celrep.2015.08.047

Wong, M., and Martin, L. J. (2010). Skeletal muscle-restricted expression of human SOD1 causes motor neuron degeneration in transgenic mice. *Hum. Mol. Genet.* 19, 2284–2302. doi: 10.1093/hmg/ddq106

Yamazaki, Y., Kamei, Y., Sugita, S., Akaike, F., Kanai, S., Miura, S., et al. (2010). The cathepsin L gene is a direct target of FOXO1 in skeletal muscle. *Biochem.J.* 427, 171–178. doi: 10.1042/bj20091346

Yampolsky, P., Pacifici, P. G., and Witzemann, V. (2010). Differential muscle-driven synaptic remodeling in the neuromuscular junction after denervation. *Eur. J. Neurosci.* 31, 646–658. doi: 10.1111/j.1460-9568.2010.07096.x

Yang, G., Murashige, D. S., Humphrey, S. J., and James, D. E. (2015). A positive feedback loop between Akt and mTORC2 via SIN1 phosphorylation. *Cell Rep.* 12, 937–943. doi: 10.1016/j.celrep.2015.07.016

Yang, H. S., Jansen, A. P., Komar, A. A., Zheng, X., Merrick, W. C., Costes, S., et al. (2003). The transformation suppressor Pdcd4 is a novel eukaryotic translation initiation factor 4A binding protein that inhibits translation. *Mol. Cell Biol.* 23, 26–37. doi: 10.1128/mcb.23.1.26-37.2003

Yang, Q., Inoki, K., Kim, E., and Guan, K. L. (2006). TSC1/TSC2 and Rheb have different effects on TORC1 and TORC2 activity. *Proc. Natl. Acad. Sci. U.S.A.* 103, 6811–6816. doi: 10.1073/pnas.0602282103

Zhang, Q., Duplany, A., Moncollin, V., Mouradian, S., Goillot, E., Mazelin, L., et al. (2019). Lack of muscle mTOR kinase activity causes early onset myopathy and compromises whole-body homeostasis. *J. Cachexia Sarcopenia Muscle* 10, 35–53. doi: 10.1002/jcsm.12336

Zhang, X., Chen, S., Song, L., Tang, Y., Shen, Y., Jia, L., et al. (2014). MTOR-independent, autophagic enhancer trehalose prolongs motor neuron survival and ameliorates the autophagic flux defect in a mouse model of amyotrophic lateral sclerosis. *Autophagy* 10, 588–602. doi: 10.4161/auto.27710

Zhang, X., Li, L., Chen, S., Yang, D., Wang, Y., Zhang, X., et al. (2011). Rapamycin treatment augments motor neuron degeneration in SOD1(G93A) mouse model of amyotrophic lateral sclerosis. *Autophagy* 7, 412–425.

Zhao, J., Brault, J. J., Schild, A., Cao, P., Sandri, M., Schiaffino, S., et al. (2007). FoxO3 coordinately activates protein degradation by the autophagic/lysosomal and proteasomal pathways in atrophying muscle cells. *Cell Metab.* 6, 472–483. doi: 10.1016/j.cmet.2007.11.004

Zinzalla, V., Stracka, D., Oppliger, W., and Hall, M. N. (2011). Activation of mTORC2 by association with the ribosome. *Cell* 144, 757–768. doi: 10.1016/j.cell.2011.02.014

Zoncu, R., Bar-Peled, L., Efeyan, A., Wang, S., Sancak, Y., and Sabatini, D. M. (2011). mTORC1 senses lysosomal amino acids through an inside-out mechanism that requires the vacuolar H(+)-ATPase. *Science* 334, 678–683. doi: 10.1126/science.1207056

Conflict of Interest: The authors declare that the research was conducted in the absence of any commercial or financial relationships that could be construed as a potential conflict of interest.

The reviewer RR declared a past co-authorship with several of the authors PC, MR to the handling editor.

Copyright © 2020 Castets, Ham and Rüegg. This is an open-access article distributed under the terms of the Creative Commons Attribution License (CC BY). The use, distribution or reproduction in other forums is permitted, provided the original author(s) and the copyright owner(s) are credited and that the original publication in this journal is cited, in accordance with accepted academic practice. No use, distribution or reproduction is permitted which does not comply with these terms.

frontiers in Molecular Neuroscience

REVIEW
published: 02 September 2020
doi: 10.3389/fnmol.2020.00159

Myasthenia Gravis With Antibodies Against Muscle Specific Kinase: An Update on Clinical Features, Pathophysiology and Treatment

*Michelangelo Cao[1], Inga Koneczny[2] and Angela Vincent[1]**

[1]Nuffield Department of Clinical Neurosciences, Weatherall Institute of Molecular Medicine, University of Oxford, Oxford, United Kingdom, [2]Division of Neuropathology and Neurochemistry, Department of Neurology, Medical University of Vienna, Vienna, Austria

Muscle Specific Kinase myasthenia gravis (MuSK-MG) is an autoimmune disease that impairs neuromuscular transmission leading to generalized muscle weakness. Compared to the more common myasthenia gravis with antibodies against the acetylcholine receptor (AChR), MuSK-MG affects mainly the bulbar and respiratory muscles, with more frequent and severe myasthenic crises. Treatments are usually less effective with the need for prolonged, high doses of steroids and other immunosuppressants to control symptoms. Under physiological condition, MuSK regulates a phosphorylation cascade which is fundamental for the development and maintenance of postsynaptic AChR clusters at the neuromuscular junction (NMJ). Agrin, secreted by the motor nerve terminal into the synaptic cleft, binds to low density lipoprotein receptor-related protein 4 (LRP4) which activates MuSK. In MuSK-MG, monovalent MuSK-IgG4 autoantibodies block MuSK-LRP4 interaction preventing MuSK activation and leading to the dispersal of AChR clusters. Lower levels of divalent MuSK IgG1, 2, and 3 antibody subclasses are also present but their contribution to the pathogenesis of the disease remains controversial. This review aims to provide a detailed update on the epidemiological and clinical features of MuSK-MG, focusing on the pathophysiological mechanisms and the latest indications regarding the efficacy and safety of different treatment options.

Keywords: myasthenia gravis, MuSK, autoantibodies, neuromuscular junction, acetylcholine receptor

OPEN ACCESS

Edited by:
Robert W. Burgess,
Jackson Laboratory, United States

Reviewed by:
Kinji Ohno,
Nagoya University, Japan
Stuart E. Dryer,
University of Houston, United States

***Correspondence:**
Angela Vincent
angela.vincent@ndcn.ox.ac.uk

Received: *14 June 2020*
Accepted: *03 August 2020*
Published: *02 September 2020*

Citation:
Cao M, Koneczny I and Vincent A (2020) Myasthenia Gravis With Antibodies Against Muscle Specific Kinase: An Update on Clinical Features, Pathophysiology and Treatment. Front. Mol. Neurosci. 13:159. doi: 10.3389/fnmol.2020.00159

OVERVIEW

Myasthenia gravis with antibodies against Muscle Specific Kinase myasthenia gravis (MuSK-MG) is an autoimmune disease that impairs transmission at the neuromuscular junction (NMJ), leading to generalized weakness and fatigability of skeletal muscles. MuSK-MG represents an important subgroup of autoimmune myasthenia affecting 5–70% of patients (depending on geographical location) who are negative for the more common antibodies against the acetylcholine receptor (AChR; Hoch et al., 2001; Vincent and Leite, 2005). Compared to the form with AChR antibodies, MuSK-MG differs in terms of epidemiology, clinical features, pathogenic mechanisms, and response to treatment. Autoantibodies, which are mainly of the monovalent IgG4 subclass, target and

block the function of MuSK, a tyrosine kinase located on the muscle post-synaptic membrane, disrupting a finely tuned pathway that regulates the development and maintenance of high-density clusters of AChRs at the NMJ. IgG1, 2 and 3 MuSK antibodies are also shown *in vitro* to be potentially pathogenic but their mechanisms *in vivo* have not been identified.

The following review will describe the clinical and pathophysiological features of MuSK-MG, focusing on the effect of the autoantibodies on the AChR clustering pathway, and the main principles of diagnosis and treatment.

EPIDEMIOLOGY

Several epidemiological studies have been carried out since MuSK antibodies were discovered in 2001 (Hoch et al., 2001) and the incidence of MuSK-MG appears to vary widely across countries (Vincent et al., 2008). Therefore, the general prevalence of the disease is difficult to estimate due to this variability. Mediterranean countries, especially Italy, Turkey, and Greece, present the highest frequency of MuSK-MG (Evoli et al., 2003; Tsiamalos et al., 2009). On the other hand, prevalence appears to be lower among those populations that live at northern latitudes (Niks et al., 2007; Vincent et al., 2008) and higher in people of Afro-American origin (Oh et al., 2009). Considering this particular ethnic-geographical distribution, together with the association with HLA class II DR14 DQ5 (Niks et al., 2006; Bartoccioni et al., 2009; Alahgholi-Hajibehzad et al., 2013), genetic background is likely to play a significant role in the etiology of MuSK-MG although other—and still undetermined—environmental factors are likely to be involved.

Association with thymus pathology (either thymic hyperplasia or thymoma) has only rarely been reported and this has a direct implication on therapeutic management of patients as thymectomy is not indicated in the current clinical practice (Marx et al., 2013; Clifford et al., 2019).

MuSK-MG affects predominantly women (up to 9:1 female:male ratio), especially young females in their third decade (Evoli et al., 2003; Guptill et al., 2011) and it is reported rarely in elders and children (Pasnoor et al., 2010; Skjei et al., 2013). This is in contrast with the distribution of AChR-MG in which an increase of incidence in older males has been observed over the last few decades (Carr et al., 2010).

CLINICAL FEATURES

Like other diseases that affect neuromuscular transmission, the main clinical characteristic of MuSK-MG is the fluctuating weakness and fatigability of the skeletal muscles, which improve with rest and worsen after exercise. However, a diagnosis of MuSK-MG can be challenging as clinical signs of the disease, and pattern of muscle involvement can differ in several ways from other forms of myasthenia. In particular, symptom fluctuation may be subtle and, therefore, go unnoticed. Moreover, proximal limb involvement can be mild or even absent while respiratory distress and other bulbar symptoms, such as difficulties in swallowing, chewing, and speaking, can be severe and rapidly progressive. The misinterpretation of these symptoms, which could support a diagnosis of a primary myopathy or motor neuron disorder (Huijbers et al., 2016), may contribute to a delay in the recognition and treatment of MuSK-MG patients.

Ocular manifestations, usually consistent with mild and symmetrical ophthalmoparesis and ptosis (drooping and weakness of the eyelid), were initially thought to be less prominent in MuSK-MG as they were reported to be the only symptom at onset in 36% of MuSK-MG cases compared to 60% of AChR-MG (Guptill et al., 2011). However, a recent retrospective analysis of Italian patients showed that the involvement of extra-ocular muscles was present in more than 96% of the population studied, with a frequency comparable to AChR-MG, and represents the first manifestation of the disease in almost 60% of cases (Evoli et al., 2017). On the other hand, the purely ocular disease is considered to be particularly rare—or at least underdiagnosed—as all the patients in both those studies evolved into generalized MG over time.

A highly specific clinical feature of MuSK-MG is the involvement of bulbar and respiratory muscles, which affects most of the patients and can be particularly severe. Patients usually experience variable degrees of dysarthria (often with nasal voice), dysphagia (mainly for fluids and associated sometimes with weight loss), dysphonia, and dyspnoea (Evoli, 2006; Ohta et al., 2007; Pasnoor et al., 2010; Guptill et al., 2011). Respiratory crises are particularly frequent (up to 35% of cases) representing a serious life-threatening event and are described more commonly compared to AChR-MG (Vincent et al., 2003; Deymeer et al., 2007). The weakness of neck and axial muscles is usually associated with bulbar symptoms and, in patients with a long history of severe disease, facial and tongue atrophy represents a common finding (Evoli et al., 2003; Farrugia et al., 2006b). When muscle atrophy occurs, it is clinically associated with non-fluctuating weakness, myopathic changes in the electrophysiology recordings, and fatty tissue infiltration at the muscle MRI scans.

PATHOPHYSIOLOGY OF MuSK-MG

The AChR Clustering Pathway

To understand how autoantibodies directed against MuSK impair transmission at the NMJ, leading to the full clinical spectrum of myasthenia, it is necessary to understand the key function of MuSK in the development and maintenance of the NMJ and particularly in the clustering of AChRs (**Figure 1**). MuSK is essential during the early stages of NMJ development, mediating the signaling between the motor nerve terminal and the muscle fiber, and guiding innervation by the growing motor nerve towards areas where pre-patterned AChR clusters are expressed (DeChiara et al., 1996; Glass et al., 1996b; Flanagan-Steet et al., 2005; Panzer et al., 2006).

The signaling molecule that triggers all the downstream events of the AChR clustering pathway is a heparan-sulfate proteoglycan called agrin, which is secreted by the motor nerve terminal and binds to its receptor, low-density lipoprotein receptor-related protein 4 (LRP4), expressed on the muscular

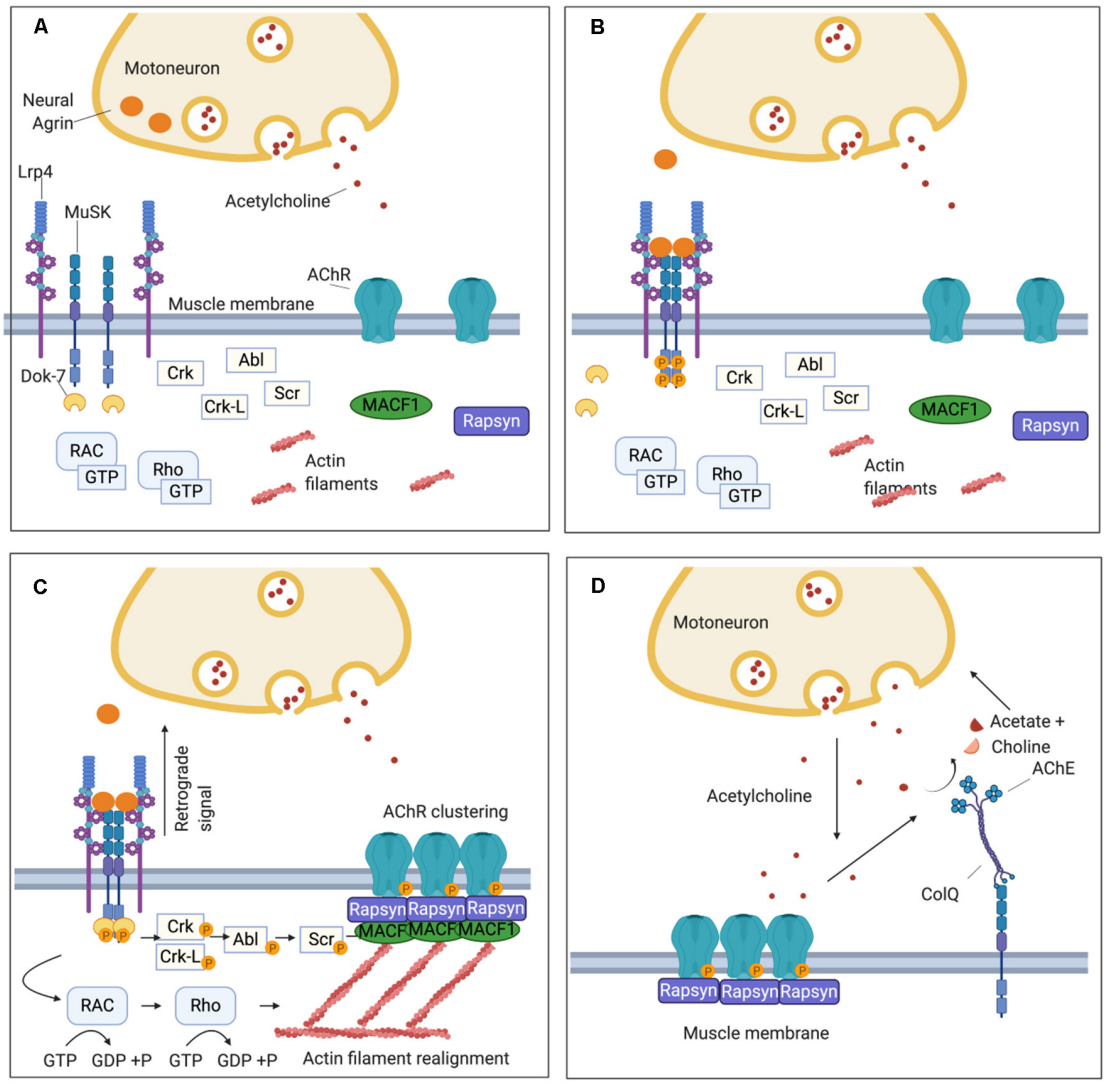

FIGURE 1 | Schematic representation of the neuromuscular junction (NMJ) and the clustering pathway of acetylcholine receptors (AChRs). **(A)** On the muscle post-synaptic membrane, low density lipoprotein receptor-related protein 4 (LRP4) and Muscle Specific Kinase (MuSK) form a loose tetramer, and, at this stage, AChRs are dispersed along the sarcolemma. **(B)** Agrin is secreted by the motor nerve terminal into the synaptic cleft and interacts with LRP4 inducing a conformational change in the LRP4-MuSK tetramer. This leads to MuSK activation through an auto-phosphorylation loop of the tyrosine residues in its intracytoplasmatic domain. **(C)** The recruitment of DOK7 amplifies MuSK phosphorylation and triggers the phosphorylation cascade downstream that involves several intermediate proteins including Crk, Ckr-l, Abl, and Scr. Concomitantly, a subsidiary pathway leads to cytoskeletal rearrangements through the activation of Rac1 and Rho GTPases. The clustering pathway culminates in the phosphorylation of the subunits of the AChR and the recruitment of rapsyn, which anchors the AChR clusters to the underlying actin filaments. Furthermore, LRP4 participates in presynaptic development through a retrograde signal which increases the clustering of ACh vesicles in the motor nerve terminal. **(D)** *Via* the extracellular matrix (ECM), MuSK interacts also with ColQ which, in turn, is attached in tetramers to the enzyme acetylcholinesterase (AChE) responsible for the hydrolysis of acetylcholine (ACh) after its binding to the AChR.

sarcolemma (Godfrey et al., 1984; McMahan, 1990; Glass et al., 1996a; Zhang et al., 2008; **Figures 1A,B**). LRP4 plays a double role in synapsis maturation: it mediates agrin-induced MuSK activation and, through a retrograde-signaling to the motor axon, it contributes to the pre-synaptic maturation increasing the clustering of acetylcholine vesicles (Wu et al., 2012; Yumoto et al., 2012; **Figure 1C**). Alongside agrin, laminin-121 and other proteins of the laminin family, which are synthesized by the muscle cell and expressed in the basal lamina, are essential in shaping the final structure of the NMJ. They contribute to the formation of the junctional folds and balance the growth of the pre-synaptic components of the NMJ such as the synaptic bouton of the nerve terminal and the Schwann cells (Noakes et al., 1995; Patton et al., 2001).

When agrin binds to the first β-propeller (BP) domain of LRP4 (Zhang et al., 2011), it strengthens a heteromeric tetramer with MuSK in a 2:2 stoichiometry. This conformational change in LRP4-MuSK interaction triggers the auto- and trans-

phosphorylation of MuSK intracytoplasmic domain and the beginning of a phosphorylation cascade that culminates with the clustering of AChRs (Zong et al., 2012; **Figure 1B**). To sustain MuSK activation and stimulate the downstream pathway, however, the recruitment of an additional intracellular adaptor, the Downstream of Kinase 7 (DOK7), is necessary. DOK7, in the form of a dimer, interacts with the intracytoplasmic domain of MuSK, enhancing the trans-phosphorylation of MuSK's tyrosine residues (Bergamin et al., 2010).

MuSK and DOK7 activate each other and this reciprocal activation triggers all the downstream events, which have been only partially defined. Following MuSK-DOK7 activation, several other adaptor proteins are phosphorylated and recruited, in particular Crk and Crk-L (Hallock et al., 2010), as well as other kinases, such as Abl (Finn et al., 2003), Scr (Mittaud et al., 2001), and the GTPases Rac1 and Rho which induce cytoskeleton modifications contributing to the maturation of AChR clusters (Weston et al., 2003; Bai et al., 2018). The whole cascade converges into the phosphorylation of the AChR subunits and rapsyn; rapsyn is a structural protein that self-aggregates providing a scaffold that anchors AChRs with the actin cytoskeleton—through the mediation of microtubule actin cross-linking factor 1 (MACF1)—to form the mature clusters (Borges and Ferns, 2001; Lee et al., 2009; Zuber and Unwin, 2013; Oury et al., 2019; Xing et al., 2019; **Figure 1C**).

To prevent the formation of AChR clusters in extrasynaptic sites, and to reduce the risk of tetanic contraction caused by an overstimulation of the muscle, several negative regulators control the clustering pathway and the expression of AChRs on the muscle membrane. One of the most important of these regulators is acetylcholine itself which downregulates the expression of AChRs. During neuromuscular transmission, ACh binds to the AChRs and subsequently is removed by acetylcholinesterase (AChE), within the extracellular matrix (ECM), that hydrolyzes acetylcholine to choline and acetate. AChE is bound to ColQ, the collagen that is arranged as trimers to form a triple helix. AChE binds to the collagen tails of ColQ in the form of tetramers (Krejci et al., 1991; Gašperši č et al., 1999). ColQ is located in the ECM, where it is anchored *via* MuSK to the synapse (Cartaud et al., 2004; **Figure 1D**).

In the absence of AChE, sustained ACh stimulation induces a prolonged Ca^{++} influx which activates calpain, a protease constitutively inhibited by rapsyn, triggering AChR cluster dispersal mediated by Cdk5 (Lin et al., 2005; Chen et al., 2007). While in AChR-MG an excess of ACh caused by treatment with AChE inhibitors does not contribute significantly to AChR loss, perhaps because it is effectively counterbalanced by the activation of a functional MuSK-DOK7 pathway, AChE inhibitors exacerbate MuSK-MG symptoms; this is likely due to a downregulation of the AChR following the ACh increase without the counterbalancing provided by the MuSK pathway (see the following section regarding treatment). Also, the prolongation of endplate currents observed in a MuSK-MG mouse model (Patel et al., 2014) suggests that MuSK antibodies that interfere with the interaction between MuSK and ColQ (Kawakami et al., 2011; to which AChE is attached) might reduce the catalytic activity of the AChE further contributing to the resistance of MuSK-MG patients to treatment with AChE inhibitor (Patel et al., 2014).

Another negative regulator of the clustering pathway is the SRC homology two domain-containing phosphotyrosine phosphatase 2 (SHP2). This phosphatase is activated by MuSK through the intermediate action of Src and SIRPα1 proteins and, in a negative feedback loop, it reduces MuSK phosphorylation (Zhao et al., 2007). SHP2 is thought to also play a role during embryonic development by preventing the formation of AChR clusters in extra-synaptic sites that are not directly in contact with the motor nerve terminal (Qian et al., 2008). From a clinical perspective, targeting this or other negative regulators of AChR clustering could represent a potential strategy to develop novel and specific therapeutic approaches.

MuSK Antibodies—Discovery and Pathogenicity Studies

The constant and finely-tuned activation of the agrin-LRP4-MuSK-DOK7 pathway maintains the AChRs in high-density clusters on the post-synaptic membrane that is vital for the correct function of the NMJ. Indeed, clustered receptors are optimal to respond to the signal transmitted by the motor nerve terminal, channeling the depolarization down into the folds where the opening of the voltage-gated sodium channels triggers the muscle action potential.

The existence of a distinct target for patients with MG who did not have AChR antibodies had been proposed as early as 1976 (Lindstrom et al., 1976) and demonstrated, in principle, in 1986 in which immunoglobulin preparations from AChR-Ab negative myasthenic patients were able to impair neuromuscular function (Mossman et al., 1986). At that time, a specific target was not identified but, retrospectively, more than half the patients used were positive for MuSK antibodies (AV unpublished data). Eventually, the existence of an IgG antibody was shown by demonstrating the binding of AChR-Ab negative patient IgG to the TE671 human immortalized muscle cells (Blaes et al., 2000; Scuderi et al., 2002). In 1996, the Yancopoulos group at Regerneron Inc USA had discovered MuSK as an essential protein in muscle development restricted to the NMJ (Glass et al., 1996a). MuSK was thus a very good candidate for the missing target and this was demonstrated by showing binding to COS cells expressing recombinant MuSK, and by binding to the recombinant extracellular domain of MuSK in an ELISA. Also, MuSK IgG antibodies inhibited agrin-induced AChR clustering on C2C12 myotubes (Hoch et al., 2001). MuSK was shown independently to be immunoprecipitated and identified by mass spectroscopy by the Evoli group (Scuderi et al., 2002) and the approach to immunoprecipitate MuSK from the TE671 cells confirmed and optimized by Littleton et al. (2009).

One of the most intriguing aspects of the pathogenicity of MuSK antibodies resides within the nature of the antibodies themselves. Compared to AChR-MG, where autoantibodies are mainly of the IgG1 and less frequently IgG3 subclasses (Vincent and Newsom-Davis, 1982), MuSK antibodies are, on the contrary, mostly IgG4s (McConville et al., 2004). Unlike IgG1-3 antibodies, IgG4s are functionally monovalent (**Figure 2**). This is because single amino acid differences between

IgG1 and IgG4 in the hinge region of the CH3 backbone allow for greater stereometric flexibility (**Figures 2A,B**). As a consequence, intrachain (instead of interchain) disulfide bridges form under reducing conditions, thereby leaving the two half-molecules of IgG4 without covalent connection (van der Neut Kolfschoten et al., 2007). Further single amino acid differences in the CH3 domain reduce noncovalent interactions between the heavy chains (**Figure 2B**). Taken together this allows the Fab-arm exchange phenomenon (reviewed in Vidarsson et al., 2014) by which each half-antibody exchanges with other half-antibodies that are randomly selected from the pool of total IgG4 half-antibodies (**Figure 2C**). As a result, most if not all IgG4 MuSK antibodies are monovalent, rather than divalent, for their antigen (Koneczny et al., 2017), which does not allow for divalent-dependent internalization of the antigen, a mechanism widely recognized in antibody-mediated diseases. Additional single amino acid differences in the CH2 domain of IgG4 render it unable to bind to C1q to activate the complement cascade or FcγR to activate immune cells. Instead, IgG4 antibodies can only block the function of a protein or inhibit its interaction with other proteins (reviewed in Koneczny, 2018).

With the discovery of MuSK as the antigen, both *in vitro* and *in vivo* models provided strong evidence of the pathogenicity of MuSK antibodies. Subsequent experiments carried out on different animal models—either passively immunized with MG patients' plasma or actively immunized with purified recombinant MuSK—showed clinical symptoms and/or impaired neuromuscular transmission consistent with the myasthenic phenotype, including muscle weakness and fatigability, reduction of endplate AChR numbers, and reduction of endplate potential (EPP) and miniature EPP amplitudes (Shigemoto et al., 2006; Cole et al., 2010; Klooster et al., 2012; Viegas et al., 2012). Notably, delayed-synapsing muscles (specifically diaphragm, sternomastoid and tibialis posterior), in which synaptogenesis requires a longer period to complete, were more severely affected in a MuSK immunized model compared to fast-synapsing muscles (intercostal, adductor longus and tibialis anterior; Xu et al., 2006). This suggests that differences in muscle development could affect susceptibility to the effects of MuSK antibodies and might partially explain the clinical pattern of weakness in MuSK-MG.

Insights regarding the pathogenic mechanism by which MuSK antibodies cause myasthenia were provided by further *in vitro* experiments performed on cultured myotubes, which are derived from the mouse C2C12 immortalized muscle cell line. In mouse myotubes incubated with plasma or purified antibodies obtained from MuSK-MG patients, MuSK phosphorylation was markedly reduced (Huijbers et al., 2013; Koneczny et al., 2013); and not restored by recombinant agrin. Moreover, AChR clustering was substantially reduced (Hoch et al., 2001; Koneczny et al., 2013; Huda et al., 2020). The inhibition of MuSK phosphorylation was shown to be dependent on IgG4 antibodies, which prevented the binding of LRP4 to MuSK (Huijbers et al., 2013; Koneczny et al., 2013).

Figure 3 shows an example of the *in vitro* effect of MuSK purified IgG4 antibodies on C2C12 myotubes for AChR clustering and MuSK phosphorylation. In this established model,

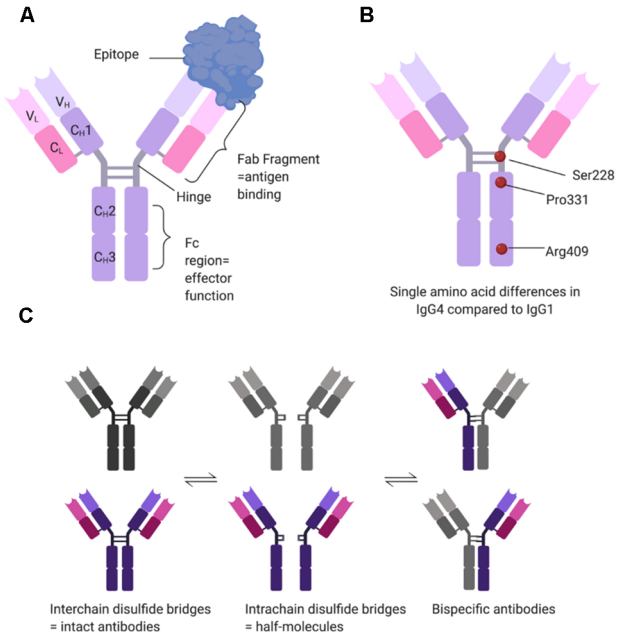

FIGURE 2 | Structural determinants of IgG4 subclass antibodies. **(A)** IgG4 consists of two heavy (H) and two light (L) chains, each with one variable (V) domain, and one (CL) or three (CH1–CH3) constant domains. In the hinge region, the two heavy chains are connected covalently by two interchain disulfide bridges. The variable domains and the first constant domain form the Fab fragment, which binds the antigen, while the hinge and the CH2–CH3 domains form the Fc region which provides effector function such as binding of C1q or Fc gamma receptors. **(B)** IgG1 and IgG4 have over 90% sequence homology, but single amino acid differences affect the structure and function of the antibody. Three relevant examples are serine at position 228 instead of a proline, allowing for structural flexibility and a switch to intrachain disulfide bridges. Proline at position 331 prevents binding of C1q, and arginine at position 409 leads to reduced non-covalent interactions between the two heavy chains. **(C)** Under reducing conditions (e.g., 1 mM glutathione), IgG4 can undergo Fab-arm exchange. The interchain disulfide bridges change to intrachain disulfide bridges, disconnecting the two half-molecules of the antibody. These then stochastically recombine with other half-molecules, forming bi-specific antibodies. Under reducing conditions, the different states of IgG4 are in equilibrium.

to study the clustering of AChRs, myotubes are exposed to the compound/sample of interest (such as recombinant agrin, patients' plasmas, or purified antibody preparations) up to 16 h to allow full cluster maturation. The AChR clusters are then labeled with fluorescent α–bungarotoxin, a toxin purified from the krait snake venom that binds specifically and irreversibly to the α subunit of the AChR (Changeux et al., 1970). The shape, size, and number of AChR clusters are then analyzed and quantified. Typically, myotubes express few spontaneous AChR clusters (**Figure 3A**—DMEM). After overnight incubation with agrin, the number of clusters dramatically increases (**Figure 3A**—agrin) but this is prevented by the presence of MuSK antibodies (**Figure 3C**—MuSK IgG4 + agrin). Alongside the analysis of AChR clustering, MuSK phosphorylation can be detected through western blotting after incubation of the cells with the antibodies and immunoprecipitation of MuSK. A representative western blot is shown in **Figure 3B**. The western blot membrane

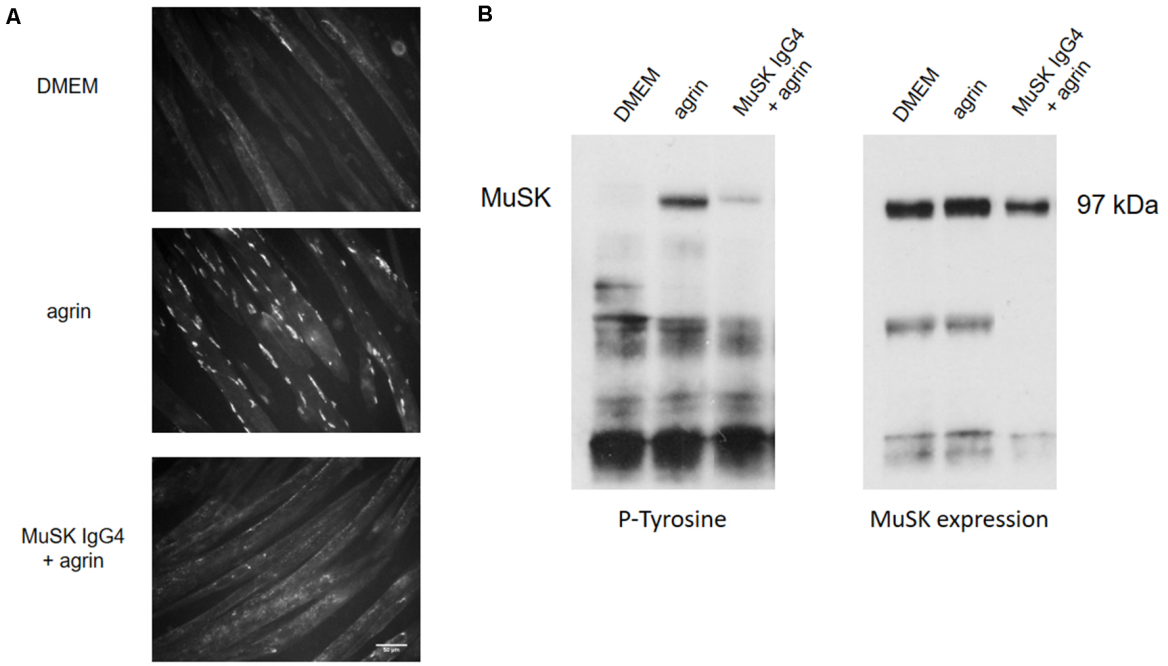

FIGURE 3 | Effects of MuSK IgG4 antibodies on AChR clustering and MuSK phosphorylation on C2C12 mouse myotubes. **(A)** Myotubes form few spontaneous AChR clusters (upper panel—DMEM) but, after physiological stimulation with agrin, their number increase markedly (middle panel—agrin). However, when the myotubes are exposed to MuSK antibodies, agrin-induced AChR clustering is severely impaired (lower panel—MuSK IgG4). Images are taken with an Olympus IX71 fluorescence microscope at 20× magnifications. Scale bar represents 50 μm. **(B)** Example of western blots to analyze MuSK phosphorylation. On the left, blot probed for phosphorylated tyrosine residues; on the right, the same blot is stripped and reprobed for MuSK expression. MuSK corresponds to a band at 97 kDa. MuSK phosphorylation is typically not detectable in the presence of medium only (first column—DMEM). After incubation with agrin for 45 min, MuSK phosphorylation increases markedly (second column—agrin) but this is prevented in the presence of MuSK IgG4s (third column—MuSK IgG4). Unpublished work, similar to Koneczny et al. (2013) and Huda et al. (2020).

is first probed with an anti-phosphotyrosine antibody and the bands corresponding to MuSK identified at 97 kDa (**Figure 3B**, left). The level of phosphorylation is then normalized to the total expression of MuSK which is detected on the same nitrocellulose membrane that has been stripped and reprobed with a specific anti-MuSK antibody (**Figure 3B**, right). Basal MuSK phosphorylation is usually barely detectable in normal myotubes but increases sharply after agrin incubation (bands shown in **Figure 3B** are after 45 min of exposure). Consistently with the inhibition of AChR clustering, MuSK-IgG4 antibodies prevent the increase of MuSK phosphorylation in the presence of normal agrin stimulation.

MuSK antibodies were demonstrated to prevent the interaction between LRP4 and MuSK (Koneczny et al., 2013; **Figure 4A**). They target mainly the first Ig-like domain of MuSK, an epitope which is located on the extracellular part of the protein and mediates LRP4-MuSK binding (McConville et al., 2004; Otsuka et al., 2015). According to this pathogenic model, the disruption of the functional tetramer formed by MuSK and LRP4 prevents MuSK from being activated following agrin-LRP4 binding (Huijbers et al., 2013; Küçükerden et al., 2016). MuSK is therefore not able to respond to agrin stimulation and, consequently, the entire AChR clustering cascade is inhibited. The on-going turnover of AChRs and dispersal by acetylcholine (see above) leads ultimately to the reduction in AChR clusters on the post-synaptic membrane of the NMJ. Moreover, *in vivo* models of MuSK-MG lack the presynaptic adaptive increase of ACh release (quantal content) observed in AChR-MG models (Mori et al., 2012; Viegas et al., 2012; Patel et al., 2014). A likely explanation is that MuSK antibodies disrupt the retrograde signaling mediated by LRP4, which increases the release of acetylcholine compensating the dispersal of AChRs (**Figure 4A**). An additional proposed mechanism of MuSK antibodies, that could be available to both IgG 1–3 and monovalent IgG4 autoantibodies, could be to block the ColQ-MuSK interaction (**Figure 4B**; Kawakami et al., 2011). This could reduce AChE at the MuSK-MG synapse and, conversely, increase the concentration of ACh within the synapse and causing dispersal of the receptors; it is proposed that this could be responsible for the hypersensitivity to treatment with AChE inhibitors in MuSK MG patients (Evoli et al., 2008; Morsch et al., 2013).

Another Player of the Game: The IgG1, 2 and 3 Subclass Antibodies

Alongside the prominent, and better-characterized, MuSK IgG4 antibody population, a variable proportion of MuSK IgG1, 2 and 3 antibodies are usually detectable in most patients. The

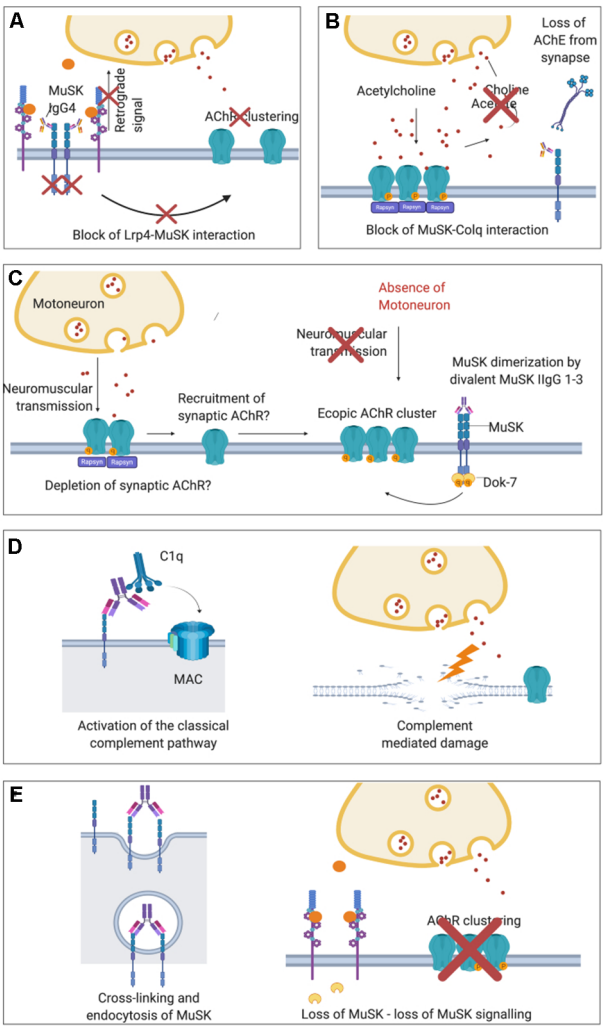

FIGURE 4 | Proposed pathological mechanisms of MuSK autoantibodies at the NMJ. **(A)** In MuSK-MG, autoantibodies of the IgG4 subclass bind to the ectodomain of MuSK preventing its interaction with LRP4 and therefore block down-stream signaling. The phosphorylation cascade is therefore inhibited causing the ultimate dispersal of AChR clusters. Loss of retrograde signaling mediated by LRP4 may also explain the absence of presynaptic adaptive increase of ACh vesicles observed in MuSK-MG animal models which are otherwise characteristic in AChR-MG. **(B)** Block of ColQ-MuSK binding by MuSK autoantibodies has been proposed to be a pathogenic mechanism that may lead to a loss of AChE from the ECM at the NMJ. **(C)** Divalent binding of commercial or cloned (monospecific) MuSK antibodies has been proposed to cause MuSK dimerization and activation, leading to ectopic, extra-synaptic AChR clusters. These would not participate in neuromuscular transmission as they would lack adjacent motoneuron terminals. For the formation of ectopic AChR clusters, AChR may also be recruited from synapses thus depleting the NMJ from AChR. **(D)** *In vivo* MuSK antibodies (IgG1–3) may recruit C1q and activate the classical complement pathway, causing complement-mediated damage at the NMJ. **(E)** MuSK antibodies could also cross-link MuSK and lead to increased internalization of MuSK, thus effectively depleting MuSK from the muscle membrane and cause a loss of agrin-LRP4-MuSK-DOK7 signal transduction.

role and importance of these antibody subclasses are still a matter of debate but there is evidence that IgG1-3s could also actively contribute to the pathogenic process of MuSK-MG. Similar to IgG4s, MuSK IgG1-3s are indeed able to disperse *in vitro* agrin-induced AChR clusters in C2C12 myotubes, even though they do not inhibit the LRP4-MuSK interaction (Koneczny et al., 2013). In the same study, IgG1-3s also prevented cluster formation in an additional *in vitro* model in which AChR clusters were constitutively induced in the myotubes by the overexpression of *DOK7* rather than by the normal stimulation with agrin. As DOK7 acts downstream of MuSK, these findings suggest that the effect of MuSK IgG1-3s may not be limited to the potential disruption of LRP4-MuSK-DOK7 interaction but could also involve other parts of the AChR clustering pathway.

In addition to these findings, *in vivo* evidence of IgG1-3 pathogenicity is provided by a model in which a mouse knockout of murine IgG1-equivalent to human IgG4-developed myasthenic features when immunized against MuSK. In this case, the immune response was sustained by the murine equivalent of human IgG1-3 antibodies (Küçükerden et al., 2016) and the authors suggested that both complement activation and direct blocking of LRP4-MuSK interaction could be the underlying mechanisms of the disease.

Initial insights on the pathogenic mechanism through which MuSK IgG1-3s might act is suggested by two recent *in vitro* studies in which monoclonal MuSK antibodies were generated from patient-derived clonal MuSK-specific B cells and plasma cells and tested on C2C12 myotubes (Huijbers et al., 2019; Takata et al., 2019). These antibodies were engineered and produced as divalent proteins irrespective of their original subclasses (either IgG1, 2 or 3 or IgG4). In the absence of physiological agrin stimulation, these monoclonal antibodies actively increased MuSK phosphorylation (likely due to their divalent binding to two MuSK molecules) and, at the same time, AChR clustering was inhibited. Interestingly, divalent MuSK antibodies were found to induce low levels of AChR clustering, which were suggested to result in extra-synaptic AChR clusters that may deplete AChR from synapses (**Figure 4C**). Nevertheless, the number of induced AChR clusters was very low. Mutations in the kinase domain of *MUSK* which increases MuSK phosphorylation while impairing the clustering of AChRs have also been reported recently (Rodríguez Cruz et al., 2020) suggesting that a non-physiological MuSK activation could be detrimental for the formation of clusters. Since gain-of-function mutations and MuSK-activating antibodies both impair AChR clustering, there are new and still unanswered questions regarding the precise mechanisms through which MuSK phosphorylation regulates the clustering pathway. Further potential mechanisms that have been suggested for MuSK IgG1-3s are activation of complement (**Figure 4D**; Tüzün et al., 2011) and cross-linking and endocytosis of MuSK (**Figure 4E**; Cole et al., 2010). These are unlikely to be mechanisms of IgG4s, as it cannot bind C1q and activate complement, and is bi-specific and unable to cross-link MuSK. The mechanisms are, however, in theory, available to MuSK IgG1-3 subclass antibodies.

DIAGNOSIS OF MuSK-MG

As for other disorders of the NMJ, the diagnosis of MuSK-MG is based on clinical symptomatology, electromyography recording,

and antibody detection. Clinical suspicion arises when the patient presents with typical myasthenic features, namely fluctuating muscle weakness and fatigability, diplopia and/or eyelid ptosis, and predominant involvement of bulbar and respiratory muscles. Additional empirical evidence that supports the diagnosis of MuSK-MG is the lack of response—or even the worsening of symptoms—following administration of AChE inhibitors (Evoli et al., 2003; Guptill et al., 2011). Although the exact mechanism that sustains this effect is not completely understood, *in vivo* studies showed that MuSK-MG models lack the presynaptic adaptive increase of ACh release observed in AChR-Ab models (Mori et al., 2012; Viegas et al., 2012; Patel et al., 2014). Furthermore, a loss of AChE from the synapse as a consequence of a block of ColQ-MuSK interaction has been proposed (Kawakami et al., 2011). Following treatment with AChE inhibitors, the higher amount of ACh released into the synaptic cleft could increase the physiological dispersal of AChRs, which in turn would not be compensated by a functional agrin-LRP4-MuSK activation, therefore worsening the condition (Morsch et al., 2013).

When performed on clinically affected muscles (usually face and neck), electrophysiological studies with decrement and/or single-fiber jitter recording represent a useful tool to support the diagnosis of myasthenia, while studies on limb muscles may be negative (Farrugia et al., 2006a). Nevertheless, particular attention must be taken in the interpretation of electrophysiology results in cases of suspected MuSK-MG as misleading signs of denervation and neuromyotonia has been reported in the presence of MuSK antibodies (Simon et al., 2013; Furuta et al., 2015; Huijbers et al., 2016). Therefore, the whole clinical picture of the patient should always be evaluated carefully.

The detection of MuSK antibodies in patients' sera represents the gold standard to confirm a clinical diagnosis of MuSK-MG. Three different laboratory techniques are available to detect MuSK antibodies: the radioimmunoprecipitation assay (RIA), ELISA, and the cell-based assay (CBA). The RIA represents the most common and specific test, reaching almost 100% of specificity (although it is difficult to estimate its sensitivity due to the variability in the proportion of MuSK-MG patients among the different populations studied). The assay involves immunoprecipitation of the extracellular domain of ^{125}I-MuSK incubated with patient sera (Matthews et al., 2004; McConville et al., 2004). MuSK ELISAs are commercially available and occasionally used in research studies, but we observed that a small fraction of MuSK antibody-positive patient sera tested by RIA was not recognized as positive in ELISA (Koneczny et al., 2017). Alternatively, a CBA can be used, avoiding the need for radioactivity and providing a more physiological environment of the antigen, as MuSK is expressed in mammalian cells, warranting appropriate glycosylation, folding and positioning at the cell surface. A typical CBA is shown in **Figure 5** in which HEK 293 cells are transfected with recombinant MuSK tagged with a fluorescent protein (in this case mCherry) and then exposed to different dilutions of serum from MuSK-MG patients and healthy individuals (used as control). MuSK antibodies attached to the cell surface are then detected with a secondary fluorescent anti-human antibody. Positivity is graded according to the degree of cell surface fluorescence and co-localization with labeled MuSK-transfected cells (Leite et al., 2008; Huda et al., 2017). The use of the CBA on patients who were seronegative by RIA—for both AChR and MuSK antibodies—slightly increased MuSK antibody detection. On those patients detected only with the MuSK CBA, it is worth noting that myasthenic symptoms were reported to be milder and their antibodies were less effective in inhibiting AChR clustering in *in vitro* assays (Huda et al., 2017).

TREATMENT OF MuSK-MG

In general terms, myasthenia gravis can be considered one of the few treatable neurological disorders in which a complete and stable remission can be achieved for a significant proportion of patients. However, the form caused by antibodies against MuSK often represents a difficult therapeutic challenge due to its severity and often poor response to treatment.

Symptomatic Drugs

As mentioned above, symptomatic therapy with acetylcholinesterase inhibitors is often ineffective and, conversely, can induce exacerbation of myasthenia (Evoli et al., 2003; Guptill et al., 2011). Another symptomatic drug, 3,4-diaminopyridine that improves neuromuscular transmission by increasing the presynaptic release of ACh vesicles, showed promising results when tested in an *in vivo* model (Morsch et al., 2013) and when administered on a few selected pediatric and adult MuSK-MG patients (Skjei et al., 2013; Evoli et al., 2016). Increasing the release of ACh vesicles without affecting the duration of ACh in the synaptic cleft could be one reason why the 3,4-diaminopyridine is more effective than ACh-esterase inhibitors. The β-adrenergic agonists salbutamol and ephedrine have been successfully used in the treatment of congenital myasthenic syndromes, specifically with mutations in *AGRN*, *DOK7, COLQ*, and *MUSK* (Lee et al., 2018; Owen et al., 2018), and also showed effectiveness when tested on a MuSK-MG patient (Haran et al., 2013). In addition to the evidence provided by empirical clinical experience, the use of sympathomimetic drugs in myasthenic syndromes is supported by evidence regarding the role of sympathetic innervation in maintaining shape, size, and function of NMJs (Khan et al., 2016). In this study, chemical sympathectomy induced a reduction in size and complexity of the NMJs, and a concomitant decrease in amplitude and time to peak of the compound muscle action potentials (CMAP) in model animals. These effects were rescued by sympathomimetics. Although this treatment approach appears to be promising, randomized clinical trials are still needed to evaluate systematically the potential efficacy, and safety, in MuSK-MG.

Finally, it is worth mentioning that counteracting the specific pathogenic effects of IgG4 antibodies on MuSK phosphorylation could represent a novel approach in the development of new symptomatic treatments for MuSK-MG. A recent *in vitro* study showed that the selective inhibition of an intracellular phosphatase, the SH2 domain-containing phosphatase 2 (SHP2), can increase MuSK phosphorylation and prevent AChR clusters from dispersal when C2C12 myotubes were exposed to MuSK

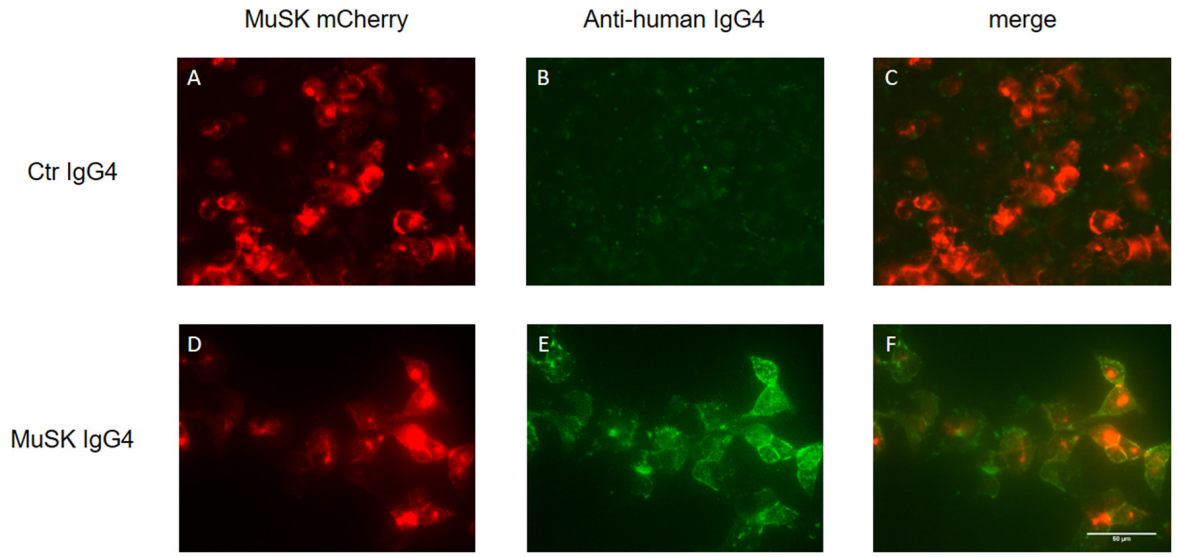

FIGURE 5 | Cell-based assay (CBA) of MuSK IgG4 antibody subclasses. HEK293 cells are transfected with MuSK-mCherry (in red; **A,D**) and exposed to MuSK-MG IgG4 antibodies (lower panels) or antibodies purified from a healthy individual as control (upper panel). MuSK antibodies attached to the cell surface are then detected with a secondary fluorescent antibody specific for the IgG subclasses of interest (in green; **B,E**). The merged image from healthy control shows the absence of co-localization between MuSK-transfected HEK cells and purified antibodies **(C)**. Conversely, MuSK IgG4 antibodies give a very strong positive signal **(E)** with full colocalization with MuSK in the merge picture **(F)**. Images are taken with an Olympus IX71 fluorescence microscope at 40× magnifications. Scale bar represents 50 μm. Unpublished work, similar to Huda et al. (2017).

IgG4 antibodies, preventing their detrimental effects (Huda et al., 2020). A similar approach to preserve the integrity of the NMJ was performed in *SOD1-G93A* mice, a model of motor neuron disease, which were treated with a monoclonal antibody to MuSK that directly increases MuSK phosphorylation (Cantor et al., 2018). In this case, boosting the activation of MuSK slowed the course of the experimental disease, preventing the progression of diaphragm denervation, and prolonged the overall lifespan of the animals. Although different models and experimental techniques were used in the two aforementioned studies, their results suggest that modulating MuSK or downstream phosphorylation could represent a promising way towards the development of new selective treatments for disorders affecting the NMJ.

Corticosteroids and Other Immunomodulatory Treatments

Overall, the general guidelines for the use of steroids and other immunosuppressants do not differ between MuSK- and AChR-MG, and treatment should be tailored according to the individual response of each patient. Steroids, in particular prednisone and prednisolone, are generally introduced early on for their effectiveness in controlling symptoms. Response to steroids is variable and, compared to AChR-MG, a higher proportion of MuSK-MG patients require high doses and prolonged treatment to achieve full control of the disease (Guptill and Sanders, 2010; Evoli et al., 2012). The major issue of long-term administration of steroids concerns the occurrence of relevant side effects such as increased blood pressure, risk of diabetes, overweight, osteoporosis, and possibly increasing a tendency to muscle atrophy already significant in MuSK-MG patients (Benveniste et al., 2005; Farrugia et al., 2006b). For these reasons, once full symptom control is reached, the steroids should be decreased progressively to achieve the lowest dose that maintains pharmacological remission. Immunosuppressive drugs, such as azathioprine and mycophenolate, are often introduced as steroid-sparing agents when it is not possible to wean the patient from a long-term high dose of steroids. However, a high proportion of MuSK-MG patients require combined therapy with immunosuppressants and steroids to achieve satisfactory symptom control, further highlighting an overall lower response to treatments compared to AChR-MG (Evoli et al., 2008, 2012; Sanders and Evoli, 2010).

The treatment of severe relapses, with mainly bulbar symptomatology, and life-threatening myasthenic crisis are similar between MuSK- and AChR-MG. Acute administration of intravenous immunoglobulins (IVIg) and plasma exchange are both usually effective (for the latter up to 96% of positive response irrespective of patients' antibody status) with rapid control of the symptoms which last for about 4–6 weeks (Usmani et al., 2019). Although considered equal in the treatment of myasthenia (Rønager et al., 2001), plasma exchange has been reported to be faster and more effective compared to IVIg in MuSK-MG patients (Guptill and Sanders, 2010; Pasnoor et al., 2010) and, therefore, should be prioritized.

Refractory MG patients, in whom at least two independent immunosuppressive treatments have been carried out at therapeutic dosage without benefit in controlling the disease, should be considered for treatment with rituximab, a monoclonal chimeric IgG1 that depletes B lymphocytes through specific binding to the CD20 transmembrane antigen (Maddison et al.,

2011; Kaegi et al., 2019; Di Stefano et al., 2020). In MuSK-MG patients, rituximab treatment appears to be particularly effective and this could be because IgG4 antibodies sustain the main pathogenic mechanism of the disease. Short-lived plasma cells producing IgG4 antibodies may be more susceptible to the drug as indicated by studies on other diseases caused by IgG4 antibodies (such as pemphigus and IgG4-related disease) in which significant clinical improvement and reduction in antibody titers were observed (Khosroshahi et al., 2010; Díaz-Manera et al., 2012; Carruthers et al., 2015; Kamisawa and Okazaki, 2017; Kurihara et al., 2019). The use of rituximab treatment in MuSK-MG is supported by several case reports, local studies, and, more recently, by bigger nation-wide group analysis (Hain et al., 2006; Khosroshahi et al., 2010; Nowak et al., 2011; Díaz-Manera et al., 2012; Keung et al., 2013; Hehir et al., 2017; Topakian et al., 2019). Currently, treatment with rituximab in MuSK-MG has a level IV evidence according to the latest multicenter prospective review conducted by Hehir et al. (2017). Although randomized clinical trials still need to be performed, all the studies conducted so far consistently indicate rituximab's long-lasting effectiveness and safety for MuSK-MG patients, and an increase of its use in current clinical practice. Considering the high rate of positive response, it would be advisable that rituximab treatment is considered also for those severe patients who require a high level of immunosuppression even if they do not meet the criteria of refractory disease.

AUTHOR CONTRIBUTIONS

MC designed, conceptualized, and drafted the review. IK contributed to editing the text and created the original images. AV conceptualized, drafted, and supervised the review.

FUNDING

IK was funded by a Hertha Firnberg project grant (project number T996-B30) by the Austrian Science Fund (FWF). Figures created with Biorender (license: IK). MC was funded by a Research Training Fellowship by the European Academy of Neurology (EAN) and by the Nuffield Department of Clinical Neurosciences.

REFERENCES

Alahgholi-Hajibehzad, M., Yilmaz, V., Gulsen-Parman, Y., Aysal, F., Oflazer, P., Deymeer, F., et al. (2013). Association of HLA-DRB1*14, -DRB1*16 and -DQB1*05 with MuSK-myasthenia gravis in patients from Turkey. *Hum. Immunol.* 74, 1633–1635. doi: 10.1016/j.humimm.2013.08.271

Bai, Y., Guo, D., Sun, X., Tang, G., Liao, T., Peng, Y., et al. (2018). Balanced Rac1 activity controls formation and maintenance of neuromuscular acetylcholine receptor clusters. *J. Cell Sci.* 131:jcs215251. doi: 10.1242/jcs.215251

Bartoccioni, E., Scuderi, F., Augugliaro, A., Chiatamone Ranieri, S., Sauchelli, D., Alboino, P., et al. (2009). HLA class II allele analysis in MuSK-positive myasthenia gravis suggests a role for DQ5. *Neurology* 72, 195–197. doi: 10.1212/01.wnl.0000339103.08830.86

Benveniste, O., Jacobson, L., Farrugia, M. E., Clover, L., and Vincent, A. (2005). MuSK antibody positive myasthenia gravis plasma modifies MURF-1 expression in C2C12 cultures and mouse muscle *in vivo*. *J. Neuroimmunol.* 170, 41–48. doi: 10.1016/j.jneuroim.2005.08.016

Bergamin, E., Hallock, P. T., Burden, S. J., and Hubbard, S. R. (2010). The cytoplasmic adaptor protein Dok7 activates the receptor tyrosine kinase MuSK *via* dimerization. *Mol. Cell* 39, 100–109. doi: 10.1016/j.molcel.2010.06.007

Blaes, F., Beeson, D., Plested, P., Lang, B., and Vincent, A. (2000). IgG from "seronegative" myasthenia gravis patients binds to a muscle cell line, TE671, but not to human acetylcholine receptor. *Ann. Neurol.* 47, 504–510. doi: 10.1002/1531-8249(200004)47:4<504::aid-ana14>3.0.co;2-q

Borges, L. S., and Ferns, M. (2001). Agrin-induced phosphorylation of the acetylcholine receptor regulates cytoskeletal anchoring and clustering. *J. Cell Biol.* 153, 1–12. doi: 10.1083/jcb.153.1.1

Cantor, S., Zhang, W., Delestree, N., Remedio, L., Mentis, G. Z., and Burden, S. J. (2018). Preserving neuromuscular synapses in ALS by stimulating MuSK with a therapeutic agonist antibody. *eLife* 7:e34375. doi: 10.7554/eLife.34375

Carr, A. S., Cardwell, C. R., McCarron, P. O., and McConville, J. (2010). A systematic review of population based epidemiological studies in Myasthenia Gravis. *BMC Neurol.* 10:46. doi: 10.1186/1471-2377-10-46

Carruthers, M. N., Topazian, M. D., Khosroshahi, A., Witzig, T. E., Wallace, Z. S., Hart, P. A., et al. (2015). Rituximab for IgG4-related disease: a prospective, open-label trial. *Ann. Rheum. Dis.* 74, 1171–1177. doi: 10.1136/annrheumdis-2014-206605

Cartaud, A., Strochlic, L., Guerra, M., Blanchard, B., Lambergeon, M., Krejci, E., et al. (2004). MuSK is required for anchoring acetylcholinesterase at the neuromuscular junction. *J. Cell Biol.* 165, 505–515. doi: 10.1083/jcb.200307164

Changeux, J. P., Kasai, M., and Lee, C. Y. (1970). Use of a snake venom toxin to characterize the cholinergic receptor protein. *Proc. Natl. Acad. Sci. U S A* 67, 1241–1247. doi: 10.1073/pnas.67.3.1241

Chen, F., Qian, L., Yang, Z. H., Huang, Y., Ngo, S. T., Ruan, N. J., et al. (2007). Rapsyn interaction with calpain stabilizes AChR clusters at the neuromuscular junction. *Neuron* 55, 247–260. doi: 10.1016/j.neuron.2007.06.031

Clifford, K. M., Hobson-Webb, L. D., Benatar, M., Burns, T. M., Barnett, C., Silvestri, N. J., et al. (2019). Thymectomy may not be associated with clinical improvement in MuSK myasthenia gravis. *Muscle Nerve* 59, 404–410. doi: 10.1002/mus.26404

Cole, R. N., Ghazanfari, N., Ngo, S. T., Gervásio, O. L., Reddel, S. W., and Phillips, W. D. (2010). Patient autoantibodies deplete postsynaptic muscle-specific kinase leading to disassembly of the ACh receptor scaffold and myasthenia gravis in mice. *J. Physiol.* 588, 3217–3229. doi: 10.1113/jphysiol.2010.190298

DeChiara, T. M., Bowen, D. C., Valenzuela, D. M., Simmons, M. V., Poueymirou, W. T., Thomas, S., et al. (1996). The receptor tyrosine kinase MuSK is required for neuromuscular junction formation *in vivo*. *Cell* 85, 501–512. doi: 10.1016/s0092-8674(00)81251-9

Deymeer, F., Gungor-Tuncer, O., Yilmaz, V., Parman, Y., Serdaroglu, P., Ozdemir, C., et al. (2007). Clinical comparison of anti-MuSK- vs. anti-AChR-positive and seronegative myasthenia gravis. *Neurology* 68, 609–611. doi: 10.1212/01.wnl.0000254620.45529.97

Di Stefano, V., Lupica, A., Rispoli, M. G., Di Muzio, A., Brighina, F., and Rodolico, C. (2020). Rituximab in AChR subtype of myasthenia gravis: systematic review. *J. Neurol. Neurosurg. Psychiatry* 91, 392–395. doi: 10.1136/jnnp-2019-322606

Díaz-Manera, J., Martínez-Hernández, E., Querol, L., Klooster, R., Rojas-García, R., Suárez-Calvet, X., et al. (2012). Long-lasting treatment effect of rituximab in MuSK myasthenia. *Neurology* 78, 189–193. doi: 10.1212/WNL.0b013e3182407982

Evoli, A. (2006). Clinical aspects of neuromuscular transmission disorders. *Acta Neurol. Scand. Suppl.* 183, 8–11. doi: 10.1111/j.1600-0404.2006.00606.x

Evoli, A., Alboini, P. E., Bisonni, A., Mastrorosa, A., and Bartoccioni, E. (2012). Management challenges in muscle-specific tyrosine kinase myasthenia gravis. *Ann. N Y Acad. Sci.* 1274, 86–91. doi: 10.1111/j.1749-6632.2012.06781.x

Evoli, A., Alboini, P. E., Damato, V., and Iorio, R. (2016). 3,4-Diaminopyridine may improve myasthenia gravis with MuSK antibodies. *Neurology* 86, 1070–1071. doi: 10.1212/wnl.0000000000002466

Evoli, A., Alboini, P. E., Iorio, R., Damato, V., and Bartoccioni, E. (2017). Pattern of ocular involvement in myasthenia gravis with MuSK antibodies. *J. Neurol. Neurosurg. Psychiatry* 88, 761–763. doi: 10.1212/WNL.0000000000002466

Evoli, A., Bianchi, M. R., Riso, R., Minicuci, G. M., Batocchi, A. P., Servidei, S., et al. (2008). Response to therapy in myasthenia gravis with anti-MuSK antibodies. *Ann. N Y Acad. Sci.* 1132, 76–83. doi: 10.1196/annals.1405.012

Evoli, A., Tonali, P. A., Padua, L., Monaco, M. L., Scuderi, F., Batocchi, A. P., et al. (2003). Clinical correlates with anti-MuSK antibodies in generalized seronegative myasthenia gravis. *Brain* 126, 2304–2311. doi: 10.1093/brain/awg223

Farrugia, M. E., Kennett, R. P., Newsom-Davis, J., Hilton-Jones, D., and Vincent, A. (2006a). Single-fiber electromyography in limb and facial muscles in muscle-specific kinase antibody and acetylcholine receptor antibody myasthenia gravis. *Muscle Nerve* 33, 568–570. doi: 10.1002/mus.20491

Farrugia, M. E., Robson, M. D., Clover, L., Anslow, P., Newsom-Davis, J., Kennett, R., et al. (2006b). MRI and clinical studies of facial and bulbar muscle involvement in MuSK antibody-associated myasthenia gravis. *Brain* 129, 1481–1492. doi: 10.1093/brain/awl095

Finn, A. J., Feng, G., and Pendergast, A. M. (2003). Postsynaptic requirement for Abl kinases in assembly of the neuromuscular junction. *Nat. Neurosci.* 6, 717–723. doi: 10.1038/nn1071

Flanagan-Steet, H., Fox, M. A., Meyer, D., and Sanes, J. R. (2005). Neuromuscular synapses can form *in vivo* by incorporation of initially aneural postsynaptic specializations. *Development.* 132, 4471–4481. doi: 10.1242/dev.02044

Furuta, N., Ishizawa, K., Shibata, M., Tsukagoshi, S., Nagamine, S., Makioka, K., et al. (2015). Anti-MuSK antibody-positive myasthenia gravis mimicking amyotrophic lateral sclerosis. *Intern Med.* 54, 2497–2501. doi: 10.2169/internalmedicine.54.4645

Gašperšič, R., Koritnik, B., Crne-Finderle, N., and Sketelj, J. (1999). Acetylcholinesterase in the neuromuscular junction. *Chem. Biol. Interact.* 119–120, 301–308. doi: 10.1016/s0009-2797(99)00040-x

Glass, D. J., Bowen, D. C., Stitt, T. N., Radziejewski, C., Bruno, J., Ryan, T. E., et al. (1996a). Agrin acts *via* a MuSK receptor complex. *Cell* 85, 513–523. doi: 10.1016/s0092-8674(00)81252-0

Glass, D. J., DeChiara, T. M., Stitt, T. N., DiStefano, P. S., Valenzuela, D. M., and Yancopoulos, G. D. (1996b). The receptor tyrosine kinase MuSK is required for neuromuscular junction formation and is a functional receptor for agrin. *Cold Spring Harb. Symp. Quant. Biol.* 61, 435–444. doi: 10.1101/SQB.1996.061.01.046

Godfrey, E. W., Nitkin, R. M., Wallace, B. G., Rubin, L. L., and McMahan, U. J. (1984). Components of Torpedo electric organ and muscle that cause aggregation of acetylcholine receptors on cultured muscle cells. *J. Cell Biol.* 99, 615–627. doi: 10.1083/jcb.99.2.615

Guptill, J. T., and Sanders, D. B. (2010). Update on muscle-specific tyrosine kinase antibody positive myasthenia gravis. *Curr. Opin. Neurol.* 23, 530–535. doi: 10.1097/WCO.0b013e32833c0982

Guptill, J. T., Sanders, D. B., and Evoli, A. (2011). Anti-MuSK antibody myasthenia gravis: clinical findings and response to treatment in two large cohorts. *Muscle Nerve* 44, 36–40. doi: 10.1002/mus.22006

Hain, B., Jordan, K., Deschauer, M., and Zierz, S. (2006). Successful treatment of MuSK antibody-positive myasthenia gravis with rituximab. *Muscle Nerve* 33, 575–580. doi: 10.1002/mus.20479

Hallock, P. T., Xu, C. F., Park, T. J., Neubert, T. A., Curran, T., and Burden, S. J. (2010). Dok-7 regulates neuromuscular synapse formation by recruiting Crk and Crk-L. *Genes Dev.* 24, 2451–2461. doi: 10.1101/gad.1977710

Haran, M., Schattner, A., Mate, A., Starobin, D., Haran, G., and Shtalrid, M. (2013). Can a rare form of myasthenia gravis shed additional light on disease mechanisms? *Clin. Neurol. Neurosurg.* 115, 562–566. doi: 10.1016/j.clineuro.2012.06.038

Hehir, M. K., Hobson-Webb, L. D., Benatar, M., Barnett, C., Silvestri, N. J., Howard, J. F., et al. (2017). Rituximab as treatment for anti-MuSK myasthenia gravis: multicenter blinded prospective review. *Neurology* 89, 1069–1077. doi: 10.1212/WNL.0000000000004341

Hoch, W., McConville, J., Helms, S., Newsom-Davis, J., Melms, A., and Vincent, A. (2001). Auto-antibodies to the receptor tyrosine kinase MuSK in patients with myasthenia gravis without acetylcholine receptor antibodies. *Nat. Med.* 7, 365–368. doi: 10.1038/85520

Huda, S., Cao, M., De Rosa, A., Woodhall, M., Rodriguez Cruz, P. M., Cossins, J., et al. (2020). SHP2 inhibitor protects AChRs from effects of myasthenia gravis MuSK antibody. *Neurol. Neuroimmunol. Neuroinflamm.* 7:e645. doi: 10.1212/nxi.0000000000000645

Huda, S., Waters, P., Woodhall, M., Leite, M. I., Jacobson, L., De Rosa, A., et al. (2017). IgG-specific cell-based assay detects potentially pathogenic MuSK-Abs in seronegative MG. *Neurol. Neuroimmunol. Neuroinflamm.* 4:e357. doi: 10.1212/nxi.0000000000000357

Huijbers, M. G., Niks, E. H., Klooster, R., de Visser, M., Kuks, J. B., Veldink, J. H., et al. (2016). Myasthenia gravis with muscle specific kinase antibodies mimicking amyotrophic lateral sclerosis. *Neuromuscul. Disord.* 26, 350–353. doi: 10.1016/j.nmd.2016.04.004

Huijbers, M. G., Vergoossen, D. L., Fillie-Grijpma, Y. E., van Es, I. E., Koning, M. T., Slot, L. M., et al. (2019). MuSK myasthenia gravis monoclonal antibodies: valency dictates pathogenicity. *Neurol. Neuroimmunol. Neuroinflamm.* 6:e547. doi: 10.1212/nxi.0000000000000547

Huijbers, M. G., Zhang, W., Klooster, R., Niks, E. H., Friese, M. B., Straasheijm, K. R., et al. (2013). MuSK IgG4 autoantibodies cause myasthenia gravis by inhibiting binding between MuSK and Lrp4. *Proc. Natl. Acad. Sci. U S A* 110, 20783–20788. doi: 10.1073/pnas.1313944110

Kaegi, C., Wuest, B., Schreiner, J., Steiner, U. C., Vultaggio, A., Matucci, A., et al. (2019). Systematic review of safety and efficacy of rituximab in treating immune-mediated disorders. *Front. Immunol.* 10:1990. doi: 10.3389/fimmu.2019.01990

Kamisawa, T., and Okazaki, K. (2017). Diagnosis and treatment of IgG4-related disease. *Curr. Top. Microbiol. Immunol.* 401, 19–33. doi: 10.1007/82_2016_36

Kawakami, Y., Ito, M., Hirayama, M., Sahashi, K., Ohkawara, B., Masuda, A., et al. (2011). Anti-MuSK autoantibodies block binding of collagen Q to MuSK. *Neurology* 77, 1819–1826. doi: 10.1212/WNL.0b013e318237f660

Keung, B., Robeson, K. R., DiCapua, D. B., Rosen, J. B., O'Connor, K. C., Goldstein, J. M., et al. (2013). Long-term benefit of rituximab in MuSK autoantibody myasthenia gravis patients. *J. Neurol. Neurosurg. Psychiatry* 84, 1407–1409. doi: 10.1136/jnnp-2012-303664

Khan, M. M., Lustrino, D., Silveira, W. A., Wild, F., Straka, T., Issop, Y., et al. (2016). Sympathetic innervation controls homeostasis of neuromuscular junctions in health and disease. *Proc. Natl. Acad. Sci. U S A* 113, 746–750. doi: 10.1073/pnas.1524272113

Khosroshahi, A., Bloch, D. B., Deshpande, V., and Stone, J. H. (2010). Rituximab therapy leads to rapid decline of serum IgG4 levels and prompt clinical improvement in IgG4-related systemic disease. *Arthritis Rheum.* 62, 1755–1762. doi: 10.1002/art.27435

Klooster, R., Plomp, J. J., Huijbers, M. G., Niks, E. H., Straasheijm, K. R., Detmers, F. J., et al. (2012). Muscle-specific kinase myasthenia gravis IgG4 autoantibodies cause severe neuromuscular junction dysfunction in mice. *Brain* 135, 1081–1101. doi: 10.1093/brain/aws025

Koneczny, I. (2018). A new classification system for IgG4 autoantibodies. *Front. Immunol.* 9:97. doi: 10.3389/fimmu.2018.00097

Koneczny, I., Cossins, J., Waters, P., Beeson, D., and Vincent, A. (2013). MuSK myasthenia gravis IgG4 disrupts the interaction of LRP4 with MuSK but both IgG4 and IgG1–3 can disperse preformed agrin-independent AChR clusters. *PLoS One* 8:e80695. doi: 10.1371/journal.pone.0080695

Koneczny, I., Stevens, J. A., De Rosa, A., Huda, S., Huijbers, M. G., Saxena, A., et al. (2017). IgG4 autoantibodies against muscle-specific kinase undergo Fab-arm exchange in myasthenia gravis patients. *J. Autoimmun.* 77, 104–115. doi: 10.1016/j.jaut.2016.11.005

Krejci, E., Coussen, F., Duval, N., Chatel, J. M., Legay, C., Puype, M., et al. (1991). Primary structure of a collagenic tail peptide of Torpedo acetylcholinesterase: co-expression with catalytic subunit induces the production of collagen-tailed forms in transfected cells. *EMBO J.* 10, 1285–1293. doi: 10.1002/j.1460-2075.1991.tb08070.x

Küçükerden, M., Huda, R., Tüzün, E., Yilmaz, A., Skriapa, L., Trakas, N., et al. (2016). MuSK induced experimental autoimmune myasthenia gravis does not require IgG1 antibody to MuSK. *J. Neuroimmunol.* 295–296, 84–92. doi: 10.1016/j.jneuroim.2016.04.003

Kurihara, Y., Yamagami, J., Funakoshi, T., Ishii, M., Miyamoto, J., Fujio, Y., et al. (2019). Rituximab therapy for refractory autoimmune bullous diseases: a multicenter, open-label, single-arm, phase 1/2 study on 10 Japanese patients. *J. Dermatol.* 46, 124–130. doi: 10.1111/1346-8138.14732

Lee, M., Beeson, D., and Palace, J. (2018). Therapeutic strategies for congenital myasthenic syndromes. *Ann. N Y Acad. Sci.* 1412, 129–136. doi: 10.1111/nyas.13538

Lee, W. Y., Free, C. R., and Sine, S. M. (2009). Binding to gating transduction in nicotinic receptors: Cys-loop energetically couples to pre-M1 and M2–M3 regions. *J. Neurosci.* 29, 3189–3199. doi: 10.1523/JNEUROSCI.6185-08.2009

Leite, M. I., Jacob, S., Viegas, S., Cossins, J., Clover, L., Morgan, B. P., et al. (2008). IgG1 antibodies to acetylcholine receptors in 'seronegative' myasthenia gravis. *Brain* 131, 1940–1952. doi: 10.1093/brain/awn092

Lin, W., Dominguez, B., Yang, J., Aryal, P., Brandon, E. P., Gage, F. H., et al. (2005). Neurotransmitter acetylcholine negatively regulates neuromuscular synapse formation by a Cdk5-dependent mechanism. *Neuron* 46, 569–579. doi: 10.1016/j.neuron.2005.04.002

Lindstrom, J. M., Seybold, M. E., Lennon, V. A., Whittingham, S., and Duane, D. D. (1976). Antibody to acetylcholine receptor in myasthenia gravis. Prevalence, clinical correlates, and diagnostic value. *Neurology* 26, 1054–1059. doi: 10.1212/wnl.26.11.1054

Littleton, E., Dreger, M., Palace, J., and Vincent, A. (2009). Immunocapture and identification of cell membrane protein antigenic targets of serum autoantibodies. *Mol. Cell. Proteomics* 8, 1688–1696. doi: 10.1074/mcp.m800563-mcp200

Maddison, P., McConville, J., Farrugia, M. E., Davies, N., Rose, M., Norwood, F., et al. (2011). The use of rituximab in myasthenia gravis and Lambert-Eaton myasthenic syndrome. *J. Neurol. Neurosurg. Psychiatry* 82, 671–677. doi: 10.1136/jnnp.2009.197632

Marx, A., Pfister, F., Schalke, B., Saruhan-Direskeneli, G., Melms, A., and Ströbel, P. (2013). The different roles of the thymus in the pathogenesis of the various myasthenia gravis subtypes. *Autoimmun. Rev.* 12, 875–884. doi: 10.1016/j.autrev.2013.03.007

Matthews, I., Chen, S., Hewer, R., McGrath, V., Furmaniak, J., and Rees Smith, B. (2004). Muscle-specific receptor tyrosine kinase autoantibodies—a new immunoprecipitation assay. *Clin. Chim. Acta* 348, 95–99. doi: 10.1016/j.cccn.2004.05.008

McConville, J., Farrugia, M. E., Beeson, D., Kishore, U., Metcalfe, R., Newsom-Davis, J., et al. (2004). Detection and characterization of MuSK antibodies in seronegative myasthenia gravis. *Ann. Neurol.* 55, 580–584. doi: 10.1002/ana.20061

McMahan, U. J. (1990). The agrin hypothesis. *Cold Spring Harb. Symp. Quant. Biol.* 55, 407–418. doi: 10.1101/sqb.1990.055.01.041

Mittaud, P., Marangi, P. A., Erb-Vogtli, S., and Fuhrer, C. (2001). Agrin-induced activation of acetylcholine receptor-bound Src family kinases requires Rapsyn and correlates with acetylcholine receptor clustering. *J. Biol. Chem.* 276, 14505–14513. doi: 10.1074/jbc.m007024200

Mori, S., Kubo, S., Akiyoshi, T., Yamada, S., Miyazaki, T., Hotta, H., et al. (2012). Antibodies against muscle-specific kinase impair both presynaptic and postsynaptic functions in a murine model of myasthenia gravis. *Am. J. Pathol.* 180, 798–810. doi: 10.1016/j.ajpath.2011.10.031

Morsch, M., Reddel, S. W., Ghazanfari, N., Toyka, K. V., and Phillips, W. D. (2013). Pyridostigmine but not 3,4-diaminopyridine exacerbates ACh receptor loss and myasthenia induced in mice by muscle-specific kinase autoantibody. *J. Physiol.* 591, 2747–2762. doi: 10.1113/jphysiol.2013.251827

Mossman, S., Vincent, A., and Newsom-Davis, J. (1986). Myasthenia gravis without acetylcholine-receptor antibody: a distinct disease entity. *Lancet* 1, 116–119. doi: 10.1016/s0140-6736(86)92259-2

Niks, E. H., Kuks, J. B., Roep, B. O., Haasnoot, G. W., Verduijn, W., Ballieux, B. E., et al. (2006). Strong association of MuSK antibody-positive myasthenia gravis and HLA-DR14-DQ5. *Neurology* 66, 1772–1774. doi: 10.1212/01.wnl.0000218159.79769.5c

Niks, E. H., Kuks, J. B., and Verschuuren, J. J. (2007). Epidemiology of myasthenia gravis with anti-muscle specific kinase antibodies in The Netherlands. *J. Neurol. Neurosurg. Psychiatry* 78, 417–418. doi: 10.1136/jnnp.2006.102517

Noakes, P. G., Gautam, M., Mudd, J., Sanes, J. R., and Merlie, J. P. (1995). Aberrant differentiation of neuromuscular junctions in mice lacking s-laminin/laminin β 2. *Nature* 374, 258–262. doi: 10.1038/374258a0

Nowak, R. J., Dicapua, D. B., Zebardast, N., and Goldstein, J. M. (2011). Response of patients with refractory myasthenia gravis to rituximab: a retrospective study. *Ther. Adv. Neurol. Disord.* 4, 259–266. doi: 10.1177/1756285611411503

Oh, S. J., Morgan, M. B., Lu, L., Hatanaka, Y., Hemmi, S., Young, A., et al. (2009). Racial differences in myasthenia gravis in Alabama. *Muscle Nerve* 39, 328–332. doi: 10.1002/mus.21191

Ohta, K., Shigemoto, K., Fujinami, A., Maruyama, N., Konishi, T., and Ohta, M. (2007). Clinical and experimental features of MuSK antibody positive MG in Japan. *Eur. J. Neurol.* 14, 1029–1034. doi: 10.1111/j.1468-1331.2007.01870.x

Otsuka, K., Ito, M., Ohkawara, B., Masuda, A., Kawakami, Y., Sahashi, K., et al. (2015). Collagen Q and anti-MuSK autoantibody competitively suppress agrin/LRP4/MuSK signaling. *Sci. Rep.* 5:13928. doi: 10.1038/srep13928

Oury, J., Liu, Y., Topf, A., Todorovic, S., Hoedt, E., Preethish-Kumar, V., et al. (2019). MACF1 links Rapsyn to microtubule- and actin-binding proteins to maintain neuromuscular synapses. *J. Cell Biol.* 218, 1686–1705. doi: 10.1083/jcb.201810023

Owen, D., Topf, A., Preethish-Kumar, V., Lorenzoni, P. J., Vroling, B., Scola, R. H., et al. (2018). Recessive variants of MuSK are associated with late onset CMS and predominant limb girdle weakness. *Am. J. Med. Genet. A* 176, 1594–1601. doi: 10.1002/ajmg.a.38707

Panzer, J. A., Song, Y., and Balice-Gordon, R. J. (2006). *In vivo* imaging of preferential motor axon outgrowth to and synaptogenesis at prepatterned acetylcholine receptor clusters in embryonic zebrafish skeletal muscle. *J. Neurosci.* 26, 934–947. doi: 10.1523/JNEUROSCI.3656-05.2006

Pasnoor, M., Wolfe, G. I., Nations, S., Trivedi, J., Barohn, R. J., Herbelin, L., et al. (2010). Clinical findings in MuSK-antibody positive myasthenia gravis: a U.S. experience. *Muscle Nerve* 41, 370–374. doi: 10.1002/mus.21533

Patel, V., Oh, A., Voit, A., Sultatos, L. G., Babu, G. J., Wilson, B. A., et al. (2014). Altered active zones, vesicle pools, nerve terminal conductivity and morphology during experimental MuSK myasthenia gravis. *PLoS One* 9:e110571. doi: 10.1371/journal.pone.0110571

Patton, B. L., Cunningham, J. M., Thyboll, J., Kortesmaa, J., Westerblad, H., Edstrom, L., et al. (2001). Properly formed but improperly localized synaptic specializations in the absence of laminin α4. *Nat. Neurosci.* 4, 597–604. doi: 10.1038/88414

Qian, Y. K., Chan, A. W., Madhavan, R., and Peng, H. B. (2008). The function of Shp2 tyrosine phosphatase in the dispersal of acetylcholine receptor clusters. *BMC Neurosci.* 9:70. doi: 10.1186/1471-2202-9-70

Rodríguez Cruz, P. M., Cossins, J., Cheung, J., Maxwell, S., Jayawant, S., Herbst, R., et al. (2020). Congenital myasthenic syndrome due to mutations in MUSK suggests that the level of MuSK phosphorylation is crucial for governing synaptic structure. *Hum. Mutat.* 41, 619–631. doi: 10.1002/humu.23949

Rønager, J., Ravnborg, M., Hermansen, I., and Vorstrup, S. (2001). Immunoglobulin treatment versus plasma exchange in patients with chronic moderate to severe myasthenia gravis. *Artif. Organs* 25, 967–973. doi: 10.1046/j.1525-1594.2001.06717.x

Sanders, D. B., and Evoli, A. (2010). Immunosuppressive therapies in myasthenia gravis. *Autoimmunity* 43, 428–435. doi: 10.3109/08916930903518107

Scuderi, F., Marino, M., Colonna, L., Mannella, F., Evoli, A., Provenzano, C., et al. (2002). Anti-p110 autoantibodies identify a subtype of "seronegative" myasthenia gravis with prominent oculobulbar involvement. *Lab. Invest.* 82, 1139–1146. doi: 10.1097/01.lab.0000028144.48023.9b

Shigemoto, K., Kubo, S., Maruyama, N., Hato, N., Yamada, H., Jie, C., et al. (2006). Induction of myasthenia by immunization against muscle-specific kinase. *J. Clin. Invest.* 116, 1016–1024. doi: 10.1172/JCI21545

Simon, N. G., Reddel, S. W., Kiernan, M. C., and Layzer, R. (2013). Muscle-specific kinase antibodies: a novel cause of peripheral nerve hyperexcitability? *Muscle Nerve* 48, 819–823. doi: 10.1002/mus.23907

Skjei, K. L., Lennon, V. A., and Kuntz, N. L. (2013). Muscle specific kinase autoimmune myasthenia gravis in children: a case series. *Neuromuscul. Disord.* 23, 874–882. doi: 10.1016/j.nmd.2013.07.010

Takata, K., Stathopoulos, P., Cao, M., Mane-Damas, M., Fichtner, M. L., Benotti, E. S., et al. (2019). Characterization of pathogenic monoclonal autoantibodies derived from muscle-specific kinase myasthenia gravis patients. *JCI Insight* 4:e127167. doi: 10.1172/jci.insight.127167

Topakian, R., Zimprich, F., Iglseder, S., Embacher, N., Guger, M., Stieglbauer, K., et al. (2019). High efficacy of rituximab for myasthenia gravis: a comprehensive nationwide study in Austria. *J. Neurol.* 266, 699–706. doi: 10.1007/s00415-019-09191-6

Tsiamalos, P., Kordas, G., Kokla, A., Poulas, K., and Tzartos, S. J. (2009). Epidemiological and immunological profile of muscle-specific kinase

myasthenia gravis in Greece. *Eur. J. Neurol.* 16, 925–930. doi: 10.1111/j.1468-1331.2009.02624.x

Tüzün, E., Yilmaz, V., Parman, Y., Oflazer, P., Deymeer, F., and Saruhan-Direskeneli, G. (2011). Increased complement consumption in MuSK-antibody-positive myasthenia gravis patients. *Med. Princ. Pract.* 20, 581–583. doi: 10.1159/000330031

Usmani, A., Kwan, L., Wahib-Khalil, D., Trivedi, J., Nations, S., and Sarode, R. (2019). Excellent response to therapeutic plasma exchange in myasthenia gravis patients irrespective of antibody status. *J. Clin. Apher.* 34, 416–422. doi: 10.1002/jca.21694

van der Neut Kolfschoten, M., Schuurman, J., Losen, M., Bleeker, W. K., Martinez-Martinez, P., Vermeulen, E., et al. (2007). Anti-inflammatory activity of human IgG4 antibodies by dynamic Fab arm exchange. *Science* 317, 1554–1557. doi: 10.1126/science.1144603

Vidarsson, G., Dekkers, G., and Rispens, T. (2014). IgG subclasses and allotypes: from structure to effector functions. *Front. Immunol.* 5:520. doi: 10.3389/fimmu.2014.00520

Viegas, S., Jacobson, L., Waters, P., Cossins, J., Jacob, S., Leite, M. I., et al. (2012). Passive and active immunization models of MuSK-Ab positive myasthenia: electrophysiological evidence for pre and postsynaptic defects. *Exp. Neurol.* 234, 506–512. doi: 10.1016/j.expneurol.2012.01.025

Vincent, A., Bowen, J., Newsom-Davis, J., and McConville, J. (2003). Seronegative generalised myasthenia gravis: clinical features, antibodies and their targets. *Lancet Neurol.* 2, 99–106. doi: 10.1016/s1474-4422(03)00306-5

Vincent, A., and Leite, M. I. (2005). Neuromuscular junction autoimmune disease: muscle specific kinase antibodies and treatments for myasthenia gravis. *Curr. Opin. Neurol.* 18, 519–525. doi: 10.1097/01.wco.0000180660.57801.3f

Vincent, A., Leite, M. I., Farrugia, M. E., Jacob, S., Viegas, S., Shiraishi, H., et al. (2008). Myasthenia gravis seronegative for acetylcholine receptor antibodies. *Ann. N Y Acad. Sci.* 1132, 84–92. doi: 10.1196/annals.1405.020

Vincent, A., and Newsom-Davis, J. (1982). Acetylcholine receptor antibody characteristics in myasthenia gravis. I. Patients with generalized myasthenia or disease restricted to ocular muscles. *Clin. Exp. Immunol.* 49, 257–265.

Weston, C., Gordon, C., Teressa, G., Hod, E., Ren, X. D., and Prives, J. (2003). Cooperative regulation by Rac and Rho of agrin-induced acetylcholine receptor clustering in muscle cells. *J. Biol. Chem.* 278, 6450–6455. doi: 10.1074/jbc.m210249200

Wu, H., Lu, Y., Shen, C., Patel, N., Gan, L., Xiong, W. C., et al. (2012). Distinct roles of muscle and motoneuron LRP4 in neuromuscular junction formation. *Neuron* 75, 94–107. doi: 10.1016/j.neuron.2012.04.033

Xing, G., Jing, H., Zhang, L., Cao, Y., Li, L., Zhao, K., et al. (2019). A mechanism in agrin signaling revealed by a prevalent Rapsyn mutation in congenital myasthenic syndrome. *eLife* 8:e49180. doi: 10.7554/elife.49180

Xu, K., Jha, S., Hoch, W., and Dryer, S. E. (2006). Delayed synapsing muscles are more severely affected in an experimental model of MuSK-induced myasthenia gravis. *Neuroscience* 143, 655–659. doi: 10.1016/j.neuroscience.2006.09.022

Yumoto, N., Kim, N., and Burden, S. J. (2012). Lrp4 is a retrograde signal for presynaptic differentiation at neuromuscular synapses. *Nature* 489, 438–442. doi: 10.1038/nature11348

Zhang, W., Coldefy, A. S., Hubbard, S. R., and Burden, S. J. (2011). Agrin binds to the N-terminal region of Lrp4 protein and stimulates association between Lrp4 and the first immunoglobulin-like domain in muscle-specific kinase (MuSK). *J. Biol. Chem.* 286, 40624–40630. doi: 10.1074/jbc.M111.279307

Zhang, B., Luo, S., Wang, Q., Suzuki, T., Xiong, W. C., and Mei, L. (2008). LRP4 serves as a coreceptor of agrin. *Neuron* 60, 285–297. doi: 10.1016/j.neuron.2008.10.006

Zhao, X. T., Qian, Y. K., Chan, A. W., Madhavan, R., and Peng, H. B. (2007). Regulation of ACh receptor clustering by the tyrosine phosphatase Shp2. *Dev. Neurobiol.* 67, 1789–1801. doi: 10.1002/dneu.20556

Zong, Y., Zhang, B., Gu, S., Lee, K., Zhou, J., Yao, G., et al. (2012). Structural basis of agrin-LRP4-MuSK signaling. *Genes Dev.* 26, 247–258. doi: 10.1101/gad.180885.111

Zuber, B., and Unwin, N. (2013). Structure and superorganization of acetylcholine receptor-rapsyn complexes. *Proc. Natl. Acad. Sci. U S A* 110, 10622–10627. doi: 10.1073/pnas.1301277110

Conflict of Interest: The University of Oxford holds a patent for use of MuSK for antibody assays, licensed to Athena Diagnostics. AV receives a proportion of royalties.

The remaining authors declare that the research was conducted in the absence of any commercial or financial relationships that could be construed as a potential conflict of interest.

Copyright © 2020 Cao, Koneczny and Vincent. This is an open-access article distributed under the terms of the Creative Commons Attribution License (CC BY). The use, distribution or reproduction in other forums is permitted, provided the original author(s) and the copyright owner(s) are credited and that the original publication in this journal is cited, in accordance with accepted academic practice. No use, distribution or reproduction is permitted which does not comply with these terms.

frontiers in Molecular Neuroscience

REVIEW
published: 08 September 2020
doi: 10.3389/fnmol.2020.581097

The Structure, Function, and Physiology of the Fetal and Adult Acetylcholine Receptor in Muscle

*Hakan Cetin[1,2], David Beeson[2], Angela Vincent[2] and Richard Webster[2]**

[1] Department of Neurology, Medical University of Vienna, Vienna, Austria, [2] Nuffield Department of Clinical Neurosciences, University of Oxford, Oxford, United Kingdom

The neuromuscular junction (NMJ) is a highly developed synapse linking motor neuron activity with muscle contraction. A complex of molecular cascades together with the specialized NMJ architecture ensures that each action potential arriving at the motor nerve terminal is translated into an action potential in the muscle fiber. The muscle-type nicotinic acetylcholine receptor (AChR) is a key molecular component located at the postsynaptic muscle membrane responsible for the generation of the endplate potential (EPP), which usually exceeds the threshold potential necessary to activate voltage-gated sodium channels and triggers a muscle action potential. Two AChR isoforms are found in mammalian muscle. The fetal isoform is present in prenatal stages and is involved in the development of the neuromuscular system whereas the adult isoform prevails thereafter, except after denervation when the fetal form is re-expressed throughout the muscle. This review will summarize the structural and functional differences between the two isoforms and outline congenital and autoimmune myasthenic syndromes that involve the isoform specific AChR subunits.

Keywords: fetal acetylcholine receptor, adult acetylcholine receptor, ion channel, myasthenia, neuromuscular junction, muscle development

OPEN ACCESS

Edited by:
Laure Strochlic, Institut National de la Santé et de la Recherche Médicale (INSERM), France

Reviewed by:
Joseph Henry Steinbach, Washington University in St. Louis, United States
James N. Sleigh, University College London, United Kingdom

***Correspondence:**
Richard Webster
richard.webster@ndcn.ox.ac.uk

***Received:** 07 July 2020*
***Accepted:** 13 August 2020*
***Published:** 08 September 2020*

Citation:
Cetin H, Beeson D, Vincent A and Webster R (2020) The Structure, Function, and Physiology of the Fetal and Adult Acetylcholine Receptor in Muscle. Front. Mol. Neurosci. 13:581097. doi: 10.3389/fnmol.2020.581097

STRUCTURAL DETERMINANTS OF FUNCTIONAL DIFFERENCES BETWEEN FETAL AND ADULT AChRS

The nicotinic AChR in muscle forms a heteropentamer consisting of two α-, one β-, and one δ-subunit with one γ-subunit in the fetal AChR isoform that is replaced by an ε-subunit in the adult AChR isoform (**Figure 1A**). All AChR subunits have a large extracellular N-terminal domain containing a signature sequence of 13 residues flanked by cysteines (C130-C144 in the human γ-subunit and C128-C142 in the human ε-subunit), four transmembrane domains (M1-M4) and a cytoplasmic loop domain of variable size and amino acid sequence between the M3 and M4 transmembrane helices (145 amino acids in the human γ-subunit and 128 amino acids in the human ε-subunit) (**Figure 1B**). Various functional differences between fetal and adult AChRs have been linked to structural differences between the γ- and ε-subunit (**Table 1**), but a generalization of the conclusions is limited by the variety of experiments performed in different species, which is important to consider especially in the context of human disease.

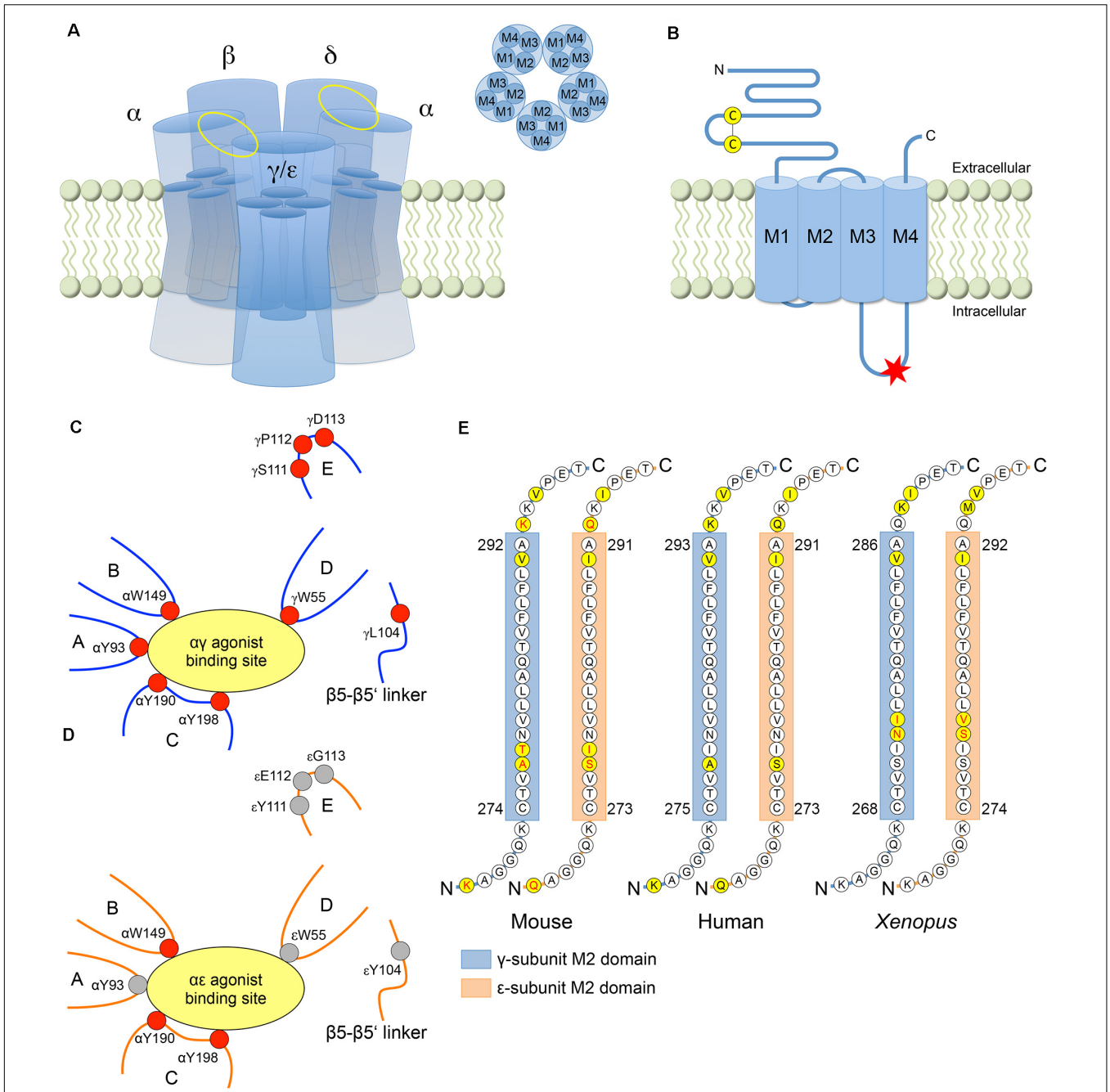

FIGURE 1 | Structural differences between the γ- and ε-subunit. **(A)** AChR consisting of five subunits with the fetal specific γ-subunit or the adult specific ε-subunit. Each subunit has four helical transmembrane domains M1-M4. The αγ/αε and αδ agonist binding sites are located between the corresponding subunits (yellow ellipses). **(B)** AChR subunit with N-terminal extracellular domain containing the Cys-loop, four transmembrane domains and a cytoplasmic loop domain between M3 and M4. In human, a consensus sequence for phosphorylation by protein kinase A (RRXSX, where X is any amino acid) is only present in the M3-M4 loop of the ε-subunit (red asterisk) without any corresponding sequence in the γ-subunit (residues 370–374 in the ε-subunit, i.e., RRASS). **(C)** At the αγ binding site, the favorable free energy resulting from the change of ACh affinities upon transformation of the AChR from the resting into the open-channel state is provided by the five aromatic core residues αY93, αW149, αY190, αY198, and γW55 from discontinuous sections of the primary sequence that rearrange close to the binding site upon agonist binding. The relative conformation of the aromatic core is stabilized by four other residues (γL104, γS111, γP112, and γD113) increasing the affinity of the αγ binding site to the agonist. **(D)** At the αε binding site, acetylcholine binding energy is provided by only three (instead of five) aromatic core residues (αW149, αY190, and αY198), resulting in a lower affinity to the agonist (with residues contributing to acetylcholine binding energy in red). **(E)** The majority of the amino acid residues of the pore forming M2 domain is highly conserved across paralogs and species. The γ- and ε-subunits differ at only three amino acid residues in mouse and *Xenopus*, and at two residues in human (yellow circles). The AChR isoform specific conductance was shown to be determined by amino acid residues within the M2 domain (in mouse and *Xenopus*) and both flanking regions (in mouse) (amino acids in red).

TABLE 1 | Functional differences between the fetal and adult AChR.

	Fetal AChR	Adult AChR	References	Species
Subunits	$\alpha_2\beta\delta\gamma$	$\alpha_2\beta\delta\varepsilon$		
Time of occurrence	Up to 2nd postnatal week	Thereafter	Sakmann and Brenner, 1978	Rat
	Up to 31st prenatal week, with low-level expression from sub- and perisynaptic nuclei thereafter in human	Thereafter	Hesselmans et al., 1993	Human
Location in adult muscle	Extrajunctional and junctional	Junctional	Berg et al., 1972	Rat
			Brenner et al., 1990	Rat
			Gu and Hall, 1988	Rat
Expression in extraocular muscles	En grappe endplates	En plaque endplates	Fraterman et al., 2006	Rat
	En grappe endplates	En plaque endplates	Missias et al., 1996	Mouse
	En grappe/en plaque endplates	En grappe/en plaque endplates	Kaminski et al., 1996	Rat
Conductance	40 pS	60 pS	Mishina et al., 1986	Calf
	53 pS	75 pS	Bouzat et al., 1994	Mouse
Open time	7.2 ms	2.3 ms	Mishina et al., 1986	Calf
	5.7 ms	1.6 ms	Kopta and Steinbach, 1994	Mouse
	7.9 ms	4.1 ms	Newland et al., 1995	Human
Ca^{2+} permeability	Lower	Higher	Villarroel and Sakmann, 1996	Rat
			Fucile et al., 2006	Human
			Ragozzino et al., 1998	Mouse
Resting affinity to ACh, k_D	0.75 nM	22.11 nM	Nayak et al., 2014)	Mouse
Resting affinity to choline k_D	1.29 μM	27.30 μM	Nayak et al., 2014	Mouse
Affinity to ^{125}I-α-bungarotoxin, k_D	0.04 nM	0.10 nM	Vincent et al., 1998	Human

AChR Affinity to Acetylcholine and Channel Open Time

Each AChR has two agonist binding sites located in the extracellular domain at the interface between the principal α-subunits and the adjacent complementary γ-/ε- or δ-subunit (**Figures 1A,C,D**). The αγ site was shown to have a ∼35–40-fold higher affinity for acetylcholine compared with the αδ and αε sites in mice (Nayak et al., 2014), resulting in a ∼3-fold longer mean open time of fetal AChRs as compared with adult AChRs (Kopta and Steinbach, 1994). Different loops from discontinuous sections of the subunit primary sequences rearrange close to the binding sites upon agonist binding (Unwin, 2005), and a core of five aromatic amino acids from different loops were shown to be required for the stabilization of the agonist (**Figures 1C,D**): αY93 (loop A), αW149 (loop B), αY190 (loop C), αY198 (loop C) and γW55 (loop D) (or εW55 and δW57, respectively) (Nayak et al., 2014, 2016). At the αδ and αε sites, the free energy corresponding to the ACh affinity change in the open-channel versus resting state is mainly provided by αW149, αY190 and αY198, which together contribute −5.1 kcal/M at the αε site and −5.3 kcal/M at the αδ site (−10.4 kcal/M for αδ and αε together). At αγ, by contrast, αY93 and (especially) γW55 additionally contribute to the favorable free energy reaching a total of −7.1 kcal/M at the αγ site and of −12.4 kcal/M at the αγ site together with the αδ site (Nayak et al., 2014). However, as the core of aromatic amino acids does not differ between the three agonist binding sites, the more favorable free energy at the αγ site as compared to the αδ and αε sites must be attributed to residues in other sections of the γ-subunit, which modify the relative conformation of the aromatic core at the αγ site. Using molecular dynamic simulations and single channel electrophysiology, three residues in loop E (S111, P112, and D113) and one residue in the β5-β5′ linker (L104) near the core of the γ-subunit (C4 group) were shown to influence affinity (**Figures 1C,D**; Nayak et al., 2016). In constructs harboring those four residues in the δ- or ε-subunit ($\alpha\delta^{C4\gamma}$ or $\alpha\varepsilon^{C4\gamma}$), the exchange of the C4 group largely swapped fetal versus adult AChR affinities and open-channel lifetimes (although not accounting completely for the differences in fetal and adult AChR affinities). Further analyses revealed that the C4 group changed the aromatic core into a more compact, organized and stable conformation, with W55 now significantly contributing to AChR affinity in the $\alpha\delta^{C4\gamma}$ and $\alpha\varepsilon^{C4\gamma}$ constructs (Nayak et al., 2016).

The difference between fetal and adult mean open times was also reported to be determined by a 30-residue segment within the M3-M4 cytoplasmic loop at its C-terminal end as part of an amphipathic helix (Bouzat et al., 1994). In addition, two residues at the N-terminal end of the M4 domain (L458 and M460) were shown to contribute to long duration openings of fetal AChRs, and increased the mean open time of adult AChRs when introduced into the ε-subunit (Bouzat et al., 1994).

AChR Conductance

Both AChR isoforms are selective for cations (Adams et al., 1980), the conductance of which is determined by the charge distribution along the ion permeation pathway formed by the second transmembrane (M2) domain of each of the AChR subunits (Unwin, 1995). Negatively charged residues adjacent to the extra- and intracellular portion of the pore together with the hydrophobic lining of the pore are major determinants of

channel conductance (Imoto et al., 1988). In the closed AChR conformation, the hydrophobic residues of the pore prevent ion permeation by restricting water occupancy (Beckstein et al., 2001; Song and Corry, 2009). Upon AChR activation, the hydrophobic gate is relieved by widening of the pore due to a displacement of the M2 domains that allows the hydration of the pore and the conduction of ions (Miyazawa et al., 2003; Unwin and Fujiyoshi, 2012).

Adult AChRs are characterized by higher conductance (60 pS) as compared to the fetal AChR (40 pS) (Mishina et al., 1986). Using rat constructs in *Xenopus* oocytes, the exchange of the four transmembrane domains M1-M4 between γ- and ε-subunits was shown to completely reverse the difference in conductance between fetal and adult AChRs (Herlitze et al., 1996). Further analyses revealed that the major determinant of the difference in conductance was located in the M2 domains (**Figure 1E**), which differ at only three residues between the γ- and ε-subunit in mouse. Two of these residues (γA277 and γT278 versus εS276 and εI277) together with residues flanking the M2 domains (γK268 and γK293 versus εQ267 and εQ292) were shown to determine key differences in AChR isoform specific conductance (Herlitze et al., 1996). The significance of the M2 domain for AChR conductance was confirmed by experiments using *Xenopus* constructs, that also differed at three residues between the γ- and ε-subunit and where the exchange of two residues (γN273 and γI274 versus εS279 and εV280) contributed to a 20% decrease of the adult AChR conductance and a 22% increase of the fetal AChR conductance (Sullivan et al., 1999). As another effect of the εS279N and εV280I mutations, the mean channel open time of adult AChRs was prolonged 3.5-fold, and the γN273S mutation was associated with a 2.5-times decreased mean channel open time of the fetal AChR (with no additional effect of the γI274V mutation) (Sullivan et al., 1999). These findings were in contrast to experiments using mouse constructs that reported no contribution of the γ- and ε-subunit M2 domains to the AChR isoform specific difference in channel open times (Bouzat et al., 1994), thus revealing significant differences between amphibian and mammalian AChRs with respect to the structural determinants of fetal and adult AChR function.

AChR Desensitization and Recovery From Desensitization

Desensitization corresponds to an accumulation of receptors in an agonist-bound but non-conducting conformational state (Sakmann et al., 1980; Colquhoun and Ogden, 1988), with a desensitization gate distinct from the activation gate (Auerbach and Akk, 1998; Wilson and Karlin, 2001) that was shown to be located at the intracellular portion of the M2 domain (Wilson and Karlin, 2001). Experiments in different models and using different applications of the patch-clamp technique revealed highly variable time constants of desensitization onset ranging from milliseconds (Paradiso and Brehm, 1998; Jahn et al., 2001; Krampfl et al., 2002) to seconds (Hopfield et al., 1988; Wagoner and Pallotta, 1988) or even minutes (Chesnut, 1983). With phosphorylation of the M3-M4 cytoplasmic AChR domains resulting in facilitation of desensitization and recovery from desensitization (Huganir et al., 1986; Hopfield et al., 1988; Hoffman et al., 1994; Paradiso and Brehm, 1998), it was possible that post-translational AChR modification together with different applications of the patch-clamp technique contributed to the varying desensitization time constants in different experimental models and between the two AChR isoforms (Auerbach and Akk, 1998; Paradiso and Brehm, 1998; Jahn et al., 2001; Krampfl et al., 2002). In a systematic analysis of desensitization and recovery from desensitization using muscle and non-muscle cell lines expressing human AChRs, recovery from desensitization was found to be faster in adult as compared to fetal human AChRs, with similar desensitization time constants between the two AChR isoforms (Cetin et al., 2019). Further analyses revealed that the M3-M4 cytoplasmic domain was a major determinant of the AChR isoform specific difference in recovery kinetics, as its exchange between the γ- and ε-subunit in chimeric constructs was sufficient to reverse recovery from desensitization between either of the AChR isoforms. Protein kinase A mediated phosphorylation of a consensus site only present in the M3-M4 cytoplasmic domain of the ε-subunit (**Figure 1B**) could have led to the observed difference in recovery kinetics between fetal and adult AChRs but this was not investigated further.

REGULATION OF FETAL AND ADULT AChR EXPRESSION

The Conversion From Fetal to Adult AChRs Is Part of the NMJ Maturation

Efficient neuromuscular transmission strongly depends on the tuned coordination of structural and molecular interactions between motor neurons and muscle fibers during neuromuscular junction (NMJ) development. Rodent NMJs have been extensively studied and helped to gain insight into some of the fundamental processes involved in NMJ maturation. Soon after myoblasts fuse to form myotubes and before innervation, fetal AChRs are evenly distributed along muscle fibers (**Figure 2A**) and, when motor nerves reach the diaphragm in mice around embryonic day 12.5 (E12.5), the AChRs start to aggregate at the myotube center to form primitive clusters (Lin et al., 2001; Yang et al., 2001). This nerve-independent prepatterning has been suggested to be involved in axon guidance activity (Lin et al., 2008), and was shown to require the expression of postsynaptic muscle-specific kinase (MuSK) (Kim and Burden, 2008) and low-density lipoprotein related protein 4 (LRP4) (Weatherbee et al., 2006). Wnt signaling was also suggested to contribute to prepatterning in myotubes (Jing et al., 2009; Zhang et al., 2012).

Muscle innervation undergoes a substantial change during NMJ development. The period between E13.5 and E18 in mice is dominated by co-innervation of NMJs by multiple axons, most of which are eliminated in the first two postnatal weeks (Tapia et al., 2012). In a single study on human muscle, by contrast, elimination of multiple innervation occurred prenatally between the sixteenth and twenty-fifth week of gestation (Hesselmans et al., 1993). Synapse elimination in mice was associated with the disappearance of temporally correlating

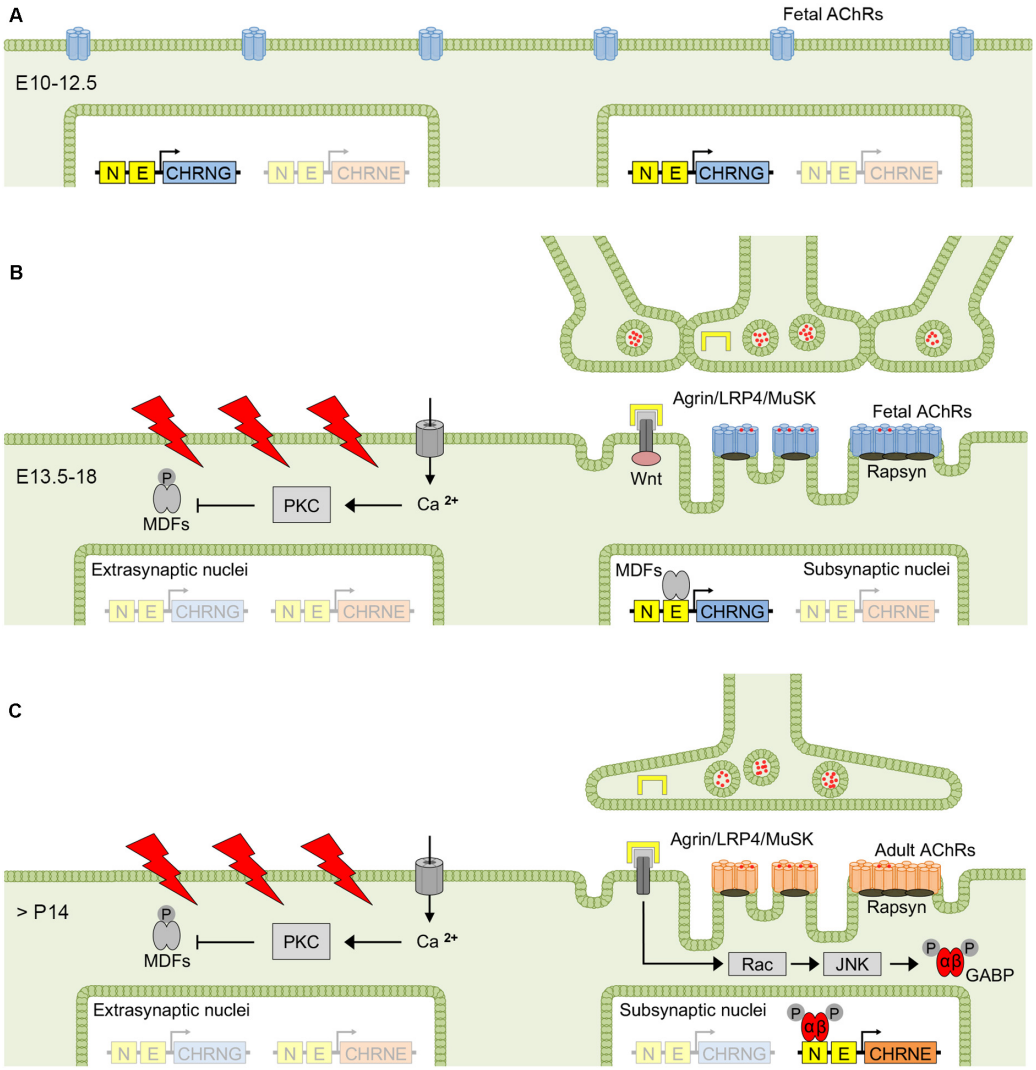

FIGURE 2 | Factors determining fetal and adult AChR expression at the NMJ. Before innervation, fetal AChRs are evenly distributed at the surface of mouse myotubes **(A)**, but aggregate to clusters at the myotube center between E13.5 and E18 (i.e., prepatterning), when myotubes start to become innervated **(B)**. The exact mechanism of prepatterning is unclear but was suggested to be nerve-independent and require MuSK, LRP4 and Wnt signaling. The first 2 weeks after birth are dominated by synapse elimination resulting in singly innervated muscle fibers, and electrical activation and nerve-released agrin determine the conversion from fetal to adult AChRs, with the latter predominantly expressed in the adult muscle **(C)**. AChR, acetylcholine receptor; GABP, GA-binding protein; JNK, c-Jun NH_2-terminal kinase; MDF, myogenic determination factor; MuSK, muscle-specific kinase; LRP4, low-density lipoprotein related protein 4; PKC, protein kinase C.

motor neuron activity based on the reduced gap junctional coupling of motor neurons (Personius and Balice-Gordon, 2001). As a result, asynchronous activation of the endplate region determines the elimination of the less active axonal input and, consecutively, gain of territory by the more active input (Personius et al., 2007). In rodents, the transition from multiple to single muscle fiber innervation coincides with the repression of γ-subunit mRNA and increasing ε-subunit mRNA levels transcribed from subjunctional myonuclei, whereas in human muscle, the conversion from fetal to adult AChR expression was shown to take place weeks after the transition from poly- to mononeuronal innervation (Hesselmans et al., 1993), and γ-subunit expression is maintained at low levels throughout life. Upon denervation and in human conditions that result in axonal damage (Gattenlohner et al., 2002) or lower motor neuron dysfunction such as amyotrophic lateral sclerosis (Tsujihata et al., 2001), there is an upregulation of γ-subunit expression (in slow-twitch fibers). Re-expression of the fetal AChR also occurs upon denervation in rat (Witzemann et al., 1989), mouse (Merlie et al., 1984; Goldman et al., 1988) and chicken muscle (Tsay and Schmidt, 1989), and was shown to correlate with increasing γ-subunit mRNA levels (Witzemann et al., 1989). In cases of denervation shortly after birth, the reciprocal change of γ- and ε-subunit mRNA levels is absent, and instead there is an increase of mRNA levels of all AChR subunits, with ε-subunit mRNA increasing postnatally in denervated muscle as it does

in normal muscle (Witzemann et al., 1989). The generation of action potentials in the muscle fiber by activation of AChRs via nerve-released acetylcholine and the endplate potential was shown to be crucial for the regulation of AChR subunit mRNA expression (Sanes and Lichtman, 1999), with disinhibition of AChR subunit mRNA transcription in extrasynaptic nuclei upon denervation (Goldman et al., 1988) or pharmacological blockade of postsynaptic AChRs by α-bungarotoxin (Asher et al., 1991).

Determinants of the Developmental AChR γ- to ε-Subunit Transition in Rodents

Most of the data on neuromuscular development derives from experiments with rodents, and partly chicken (Klarsfeld et al., 1989; Huang et al., 1992), and might not necessarily apply to the human situation. Therefore, this section focuses on the NMJ development in rodents, and human specific features will be outlined later in section "Developmental AChR γ- to ε-Subunit Transition in Human."

The AChR isoform conversion is accomplished by complementary γ- and ε-subunit mRNA expression and integrates two different mechanisms that depend on motor neuron innervation. Electrical stimulation of the muscle fiber has a repressive impact on AChR gene transcription in muscle, whereas nerve-released signals increase AChR gene transcription in subsynaptic nuclei, thereby concentrating AChR surface expression to the postsynaptic membrane (Missias et al., 1996; Sanes and Lichtman, 1999; Schaeffer et al., 2001). The γ- and ε-subunit genes respond differently to these regulatory mechanisms, leading to a distinct expression pattern in subsynaptic and extrasynaptic nuclei during NMJ development (Missias et al., 1996). The γ-subunit gene is activated in all myonuclei during the initial period of myotube formation, becomes restricted to subsynaptic nuclei around the time of innervation, and disappears almost completely after birth in mice (Sakmann and Brenner, 1978). The ε-subunit, by contrast, is expressed in the adult muscle and from subsynaptic nuclei only.

Complex molecular pathways have been reported to underlie the mechanisms that control the differential γ- and ε-subunit mRNA expression, i.e., electrical muscle fiber activity and binding of motor neuron derived factors, although the exact signal cascades have not been fully unraveled yet (Tintignac et al., 2015). Depolarization of the muscle membrane by action potentials leads to an increase of cytosolic calcium resulting in activation of protein kinase C (Klarsfeld et al., 1989; Huang et al., 1992), which in turn phosphorylates and down-regulates the activity of myogenic determination factors (MDFs) (Eftimie et al., 1991; Huang et al., 1992; **Figures 2B,C**). MDFs comprise a number of transcriptional activators that recognize a 6 bp CANNTG motif (where N can be any nucleotide) or E-box present in the promoter region of several AChR subunit genes (Liu et al., 2000). The PKC-mediated inhibition of MDFs activity thereby results in a reduction of AChR subunit mRNA transcription in extrasynaptic nuclei. In subsynaptic nuclei, by contrast, transcription is under the control of nerve-released factors such as agrin (Jones et al., 1996). Agrin is a basal lamina proteoglycan that forms tetrameric agrin-LRP4 complexes and enhances phosphorylation and activation of MuSK (Zong et al., 2012), which in turn induces AChR subunit gene transcription via Rac-GTPase and c-Jun NH_2-terminal kinase (JNK) (Lacazette et al., 2003; Escher et al., 2005) resulting in the phosphorylation of GA-binding protein GABPα/GABPβ dimers, both members of the Ets family of transcription factors (Schaeffer et al., 1998; Schaeffer et al., 2001). Phosphorylated GABPα/GABPβ dimers target the N-box containing the CCGGAA consensus sequence present in all AChR subunit gene promoters (Duclert et al., 1993; Koike et al., 1995; Fromm and Burden, 1998) and enhance AChR subunit gene transcription from subsynaptic nuclei (**Figure 2C**).

The Time Course of AChR γ- to ε-Subunit Transition Depends on the Muscle Fiber Type

Motor units in mammalian muscle differ in their contractile properties and pattern of activity. Slow-twitch muscle fibers are innervated by motor neurons that fire in long trains of lower frequencies ranging between 10 and 20 Hz. Fast-twitch muscle fibers, by contrast, are innervated by motor neurons firing at short bursts of higher frequencies around 100 Hz (Hennig and Lomo, 1985). Immunohistochemistry of mouse muscles at different developmental stages using γ- or ε-subunit specific antibodies revealed that the subunit transition was delayed by about a week in the slow-twitch soleus muscle (with fetal AChRs still present at the NMJ up to P30) as compared to the fast-twitch extensor digitorum longus muscle (Missias et al., 1996). Their level increases in conditions associated with axonal damage and denervation in both human (Gattenlohner et al., 2002) and rodents (Kues et al., 1995; Wang et al., 2006). In human, however, the increased γ-subunit transcript levels were limited to slow-twitch fibers only (corresponding to the delayed subunit transition in slow-twitch fibers), with no up-regulation in denervated fast-twitch fibers, whereas in mouse models the upregulation of γ-subunit transcription can occur in both slow- and fast-twitch muscle fibers (Seaberg et al., 2015; Wang et al., 2016). It was thus hypothesized that γ-subunit expression is controlled by a muscle fiber type-restricted transcriptional program in human (Gattenlohner et al., 2002), the underlying mechanisms of which are yet to be revealed.

Retention of Fetal AChR Expression Traits in Adult Extraocular Muscles

Extraocular muscles (EOMs) are characterized by specific functional and antigenic features (Kaminski et al., 1990; Yu Wai Man et al., 2005; Fraterman et al., 2006), but as mouse or rat tissue was used in most experimental studies, the data might not necessarily reflect human physiology.

As compared to limb muscles, EOMs are characterized by higher motor neuron firing rates, and consist of a mixture of both multiply innervated slow-twitch or tonic fibers and singly innervated fast-twitch fibers, with singly innervated fibers exhibiting the highest discharge frequencies (>600 Hz in monkeys; Robinson, 1970). In mice, around 80% of the EOM fibers are singly innervated and have an en plaque endplate in

the muscle midbelly (Khanna et al., 2003), whereas 20% of the fibers are multiply innervated and characterized by en grappe endplates scattered along the proximal and distal end of the EOM, arising from one or more motor neurons (Porter and Baker, 1996; Khanna et al., 2003). In singly innervated fibers, firing of motor neurons generate action potentials that lead to fast-twitch contractions. Multiply innervated fibers, by contrast, have a slow-twitch or tonic mode of contraction activated focally at each synapse without the generation or propagation of action potentials (Chiarandini and Stefani, 1979). The two types of endplates differ in the transcriptional expression of AChR isoform specific subunits in rats, with ε-subunit mRNA restricted to en plaque endplates and γ-subunit mRNA to en grappe endplates (Fraterman et al., 2006). The same conclusion was made before in experiments using AChR isoform specific antibodies on mouse EOMs, with adult AChR expression restricted to en plaque endplates and fetal AChR expression to en grappe endplates (Missias et al., 1996). Yet another study on the γ- and ε-subunit immunoreactivity in rat EOMs reported contrasting results with binding of fetal and adult AChR specific antibodies to both en plaque and en grappe endplates (Kaminski et al., 1996). Several explanations were discussed to potentially underlie these discrepancies including species and age differences but also differences between global and orbital portions of EOMs (Missias et al., 1996; Fraterman et al., 2006).

Total ε-subunit mRNA levels were shown to be higher in EOMs compared to limb or intercostal muscles in human (MacLennan et al., 1997), reflecting the high density of endplates and thus high density of subsynaptic nuclei synthesizing AChR mRNAs. As AChR surface expression was not examined, however, a direct correlation of γ- or ε-subunit mRNA levels with fetal or adult AChR surface expression might be limited. The subunit conversion time course in fast-twitch singly innervated EOM fibers is similar to that of fast-twitch limb muscles with no detectable γ-subunit levels after 2 weeks postnatally in rodents (Missias et al., 1996; Fraterman et al., 2006).

Developmental AChR γ- to ε-Subunit Transition in Human

Neuromuscular junction development has extensively been studied in rodents (Tintignac et al., 2015), revealing insight into general mechanisms of synaptic transmission. Human NMJs and AChRs share many common features with rodents, but there are also important differences that need to be acknowledged, especially in the context of human disease. The developmental AChR γ- to ε-subunit transition occurs in the second to third trimester in human (Hesselmans et al., 1993) and thus earlier than in mice, in which the transition takes place in the first 2 weeks after birth with no detectable fetal AChR expression thereafter (Sakmann and Brenner, 1978; Fischbach and Schuetze, 1980). In human, by contrast, γ-subunit mRNA continues to be expressed at low levels from sub- and perisynaptic nuclei (MacLennan et al., 1997; Croxen et al., 2001; Gattenlohner et al., 2002). This is relevant in a group of genetic disorders of the neuromuscular junction (i.e., congenital myasthenic syndrome, CMS) with underlying null mutations of the CHRNE gene coding for the ε-subunit (Croxen et al., 2001), as the persistent low-level fetal AChR expression is sufficient to enable neuromuscular transmission and patient survival. Mutant mice lacking the ε-subunit, by contrast, die within 14 weeks after birth (Missias et al., 1997).

SIGNIFICANCE OF FETAL AND ADULT AChR EVOLUTION FOR NMJ FUNCTION

Two whole genome duplications taking place around 500 million years ago (and before the divergence of the major vertebrate lineages) followed by gene elimination expanded a set of 10 ancestral AChR subunit genes to 16 genes in mammals including humans (Pedersen et al., 2019). As a result of the genomic duplications, a common CHRNG/CHRNE ancestor gave rise to the CHRNG and CHRNE genes in vertebrates coding for the γ- and ε-subunit, respectively. In birds, however, the CHRNE gene seems to be absent (Le Novere et al., 2002; Pedersen et al., 2019). As the CHRNB1 gene was also found to be missing in the chicken genome, it was suggested that in birds CHRNB1 and CHRNE may be located on microchromosomes that are difficult to sequence due to their GC-rich content (Pedersen et al., 2019). Alternatively, CHRNE could also have been lost in birds. This is supported by electrophysiological studies revealing that the mean AChR open time in mature chicken muscle is as long as that of fetal AChRs (Schuetze, 1980; Harvey and Van Helden, 1981) and lacks the decrease typically associated with the conversion from fetal to adult AChRs (Sakmann and Brenner, 1978). Interestingly, γ-subunit transcripts could only be detected before embryonic day 16, diminished thereafter and re-appeared only after denervation in chicken muscle tissue, suggesting the existence of another AChR subunit analogous to the ε-subunit in the adult chicken muscle (Moss et al., 1987, 1989). It was hypothesized that an AChR harboring an alternative subunit would have channel properties indistinguishable from a receptor containing the γ-subunit, or alternatively would comprise just α-, β-, and δ-subunits (Moss et al., 1987).

The γ- and ε-subunit expression in a great variety of species (Tsunoyama and Gojobori, 1998; Pedersen et al., 2019) is likely to have resulted from positive selection, as neither of the two subunits underwent gene elimination, but the physiological significance of the developmental conversion from fetal to adult AChRs remains largely unknown. Fetal AChRs are likely to be important for the prepatterning of AChR clusters in a central band during NMJ development and before innervation. In fact, using chimeric mice with a γ^{ε} -subunit (containing the C-terminal 382 amino acids of the ε-subunit) instead of the γ-subunit, prepatterning was substantially altered with formation of functional neuromuscular synapses outside the central, narrow endplate band region in the diaphragm (Koenen et al., 2005). One function of fetal AChRs could thus be to ensure a proper innervation pattern. In developing fibers, it was hypothesized that fetal AChRs may also facilitate neuromuscular transmission after innervation by allowing more charge to enter the cell during a single opening of average duration as compared to adult AChRs (Tintignac et al., 2015), which might be required

for normal neuromuscular development. This is supported by experiments in rat soleus muscle, in which miniature endplate currents (mepcs) were shown to trigger spontaneous contractions of neonatal muscle fibers (expressing fetal AChRs) but not of adult muscle fibers (Jaramillo et al., 1988). The injection of both fetal- (i.e., low-amplitude and long-duration) and adult-type (i.e., high-amplitude and short-duration) mepcs into the same embryonic muscle fiber caused miniature endplate potentials of nearly the same amplitude but only fetal-type mepcs triggered action potentials. It was therefore concluded that the longer duration of fetal-type mepcs was essential for the excitation of embryonic muscle fibers. However, the spontaneous contractions elicited by fetal-type mepcs disappeared upon muscle fiber growth, which may have resulted from decreasing muscle fiber impedance rather than from the switch to the adult AChR isoform (Jaramillo et al., 1988). In another theory it was speculated that the higher sensitivity of the fetal AChR to choline could have a synergistic effect on the endplate current in developing fibers (Nayak et al., 2014), with the background level of choline shown to be especially high in fetal serum (Zeisel and Niculescu, 2006). Adult AChRs, by contrast, are characterized by faster recovery rates from desensitization (Cetin et al., 2019), and their appearance in the adult muscle could provide an adaptation to increasing motor neuron firing rates after birth, facilitating a robust and reproducible high-frequent neuromuscular transmission by preventing adult AChRs from accumulation in desensitized states. The robust high-frequent neuromuscular transmission could further be supported by the shorter mean open-channel time of adult AChRs and the faster decay of the associated endplate currents, as the depression of macroscopic currents upon repetitive stimulation was shown to depend on the particular balance between gating, entry into desensitization and the acetylcholine dissociation rate constants; this was confirmed by a study using mouse constructs, in which adult AChRs associated with faster deactivation (corresponding to a higher acetylcholine dissociation rate constant) and slower gating kinetics were less prone to desensitization (Elenes et al., 2006). And finally, the higher Ca^{2+} permeability of adult AChRs (with a fractional Ca^{2+} current of 4.2% as compared to 2.1% in the fetal isoform) could have additional physiological relevance in the regulation of neuromuscular synapse efficacy (Ragozzino et al., 1998). Transsynaptic retrograde modulation of presynaptic secretion mechanisms by the localized Ca^{2+} influx into the postsynaptic muscle cell was reported in developing *Xenopus* neuromuscular synapses (Cash et al., 1996), and autoregulatory AChR phosphorylation induced by intracellular Ca^{2+} was shown in rat myotubes (Miles et al., 1994).

FETAL OR ADULT AChR ISOFORM RELATED MYASTHENIC SYNDROMES

Myasthenia Gravis

Myasthenia gravis (MG) is an autoimmune disorder of the neuromuscular junction and mediated by autoantibodies binding to molecular targets at the postsynaptic muscle membrane. MG is clinically characterized by muscle weakness and increased fatiguability of limb, bulbar and/or extraocular muscles (Cetin and Vincent, 2018). Autoantibodies directed against the muscle AChR (AChR-Abs) can be detected in about 80% of patients with generalized MG and 50% of patients with MG restricted to the EOMs (ocular MG) (Lindstrom et al., 1976; Vincent and Newsom-Davis, 1985). There is no clear evidence for a correlation of AChR-Ab titers with disease severity between individuals (Vincent and Newsom Davis, 1980; Roses et al., 1981), although ocular MG patients tend to have lower AChR-Ab concentrations (Vincent and Newsom Davis, 1980). Within an individual undergoing treatment, however, there is usually a good correlation between the fall in antibody levels and clinical improvement; both reversing if the treatment (e.g., plasma exchange) is stopped (Newsom-Davis et al., 1979).

The AChR-Abs appear to be polyclonal and heterogenous even in individual patients and were shown to target the extracellular domains of all five subunits including the γ- or ε-subunit (Vincent and Newsom-Davis, 1979; Vincent et al., 1987; Tzartos et al., 1998; Kostelidou et al., 2007; Zisimopoulou et al., 2008), with a relatively high but variable proportion of the antibodies binding to the main immunogenic region on the two α-subunits (Tzartos et al., 1982; Whiting et al., 1986). Antibodies with preferential binding to the γ- or the ε-subunit can more often be found in ocular MG patients (Vincent and Newsom-Davis, 1982; MacLennan et al., 1997; Shi et al., 2012). Using cell-based assays expressing fetal or adult AChRs, the proportion of MG patients with γ- or ε-subunit specific AChR-Abs was higher in ocular MG (12 and 14%, respectively) as compared to generalized MG (2 and 7%, respectively) (Shi et al., 2012). Using radioimmunoprecipitation assays, AChR-Abs from ocular MG patients were shown to react better with adult AChRs (Vincent and Newsom-Davis, 1982; MacLennan et al., 1997), in contrast to the earlier suggestion that the preferential involvement of the EOMs in ocular MG patients was a result of fetal AChR expression by these muscles (Horton et al., 1993; Oda, 1993). The higher susceptibility of EOMs in MG was instead ascribed to a lower safety factor of singly innervated fast-twitch fibers resulting from less prominent postsynaptic folds with fewer AChRs on the postsynaptic membrane (Kaminski et al., 1990; Yu Wai Man et al., 2005). Moreover, women with very high levels of antibodies that inhibit the ion channel activity of fetal AChRs, but not adult AChRs (see below), do not have predominant ocular symptoms.

Higher motor neuron firing frequencies could further contribute to a lower safety factor by increasing the release of acetylcholine from the presynaptic terminal sufficiently to overcome the catalytic activity of the acetylcholine esterase, thus leading to prolongation of the lifetime of acetylcholine in the synaptic cleft and accumulation of AChRs in desensitized states (Magleby and Pallotta, 1981; Ruzzier and Scuka, 1986; Giniatullin et al., 1993). Additionally, prolonged high frequency vesicle release can lead to depletion of presynaptic vesicles with consequent reduction of the quantal content (Kaminski et al., 1990). In multiply innervated tonic fibers, on the other hand, contraction depends directly on the depolarization of the postsynaptic membrane induced by the endplate current rather than a sodium channel-dependent action potential (Kaminski et al., 1990; Yu Wai Man et al., 2005). EOMs also

differ immunologically from limb muscles in that complement regulatory genes are expressed in lower levels that may contribute to the susceptibility of EOMs to MG (Porter et al., 2001; Kaminski et al., 2004), with preferential involvement of EOMs at lower AChR-Ab titers (Vincent and Newsom Davis, 1980).

Neonatal Myasthenic Syndromes Due to Placental Transfer of Maternal AChR-Abs

Neonates born to mothers with MG can sometimes develop transient neonatal MG (TNMG) due to placental transfer of AChR-IgG-Abs (Papazian, 1992; Vernet-Der Garabedian et al., 1994). In cases with restriction of fetal movement *in utero* during the second trimester, the clinical picture is characterized by multiple joint contractures or skeletal deformities such as scoliosis and lung hypoplasia. This condition is termed arthrogryposis multiplex congenita (AMC) and often associated with the requirement of the neonates for assisted ventilation or with prenatal or neonatal death (Vincent et al., 1995). AMC is sometimes classified as the most severe form of the fetal acetylcholine receptor inactivation syndrome (FARIS), which sometimes follows TNMG with the development of a persistent myopathy predominantly affecting facial and bulbar muscles, hearing loss, pyloric stenosis and central nervous system involvement in early childhood (Oskoui et al., 2008; Hacohen et al., 2015; Allen et al., 2016). Mothers of myasthenic neonates can have clinically manifest MG, and the treatment of those mothers after diagnosis can lead to the subsequent birth of healthy babies. In babies with AMC, however, some mothers are asymptomatic with unrecognized disease (Barnes et al., 1995; Vincent et al., 1995; Riemersma et al., 1996), suggesting that the AChR-Abs are different from those usually found in MG. In fact, AChR-Abs in AMC (and FARIS) preferably bind to fetal AChRs (Vincent et al., 1995; Hacohen et al., 2015), whereas AChR-Abs crossing the placenta in TNMG commonly bind to both fetal and adult AChRs via the shared α-subunits (Vernet-Der Garabedian et al., 1994). Fetal AChR-Abs were also more common in women who developed MG after pregnancy as compared with women who presented before pregnancy, and were therefore hypothesized to be induced by the fetus (Matthews et al., 2002). These antibodies were shown to inhibit fetal but not adult AChR function (Vincent et al., 1995), with 80% current reduction within 2 min application of serum from mothers of neonates born with AMC (Cetin et al., 2020). When injected into pregnant mice, a proportion of the mouse embryos showed fixed joint deformities, were paralyzed or stillborn (Jacobson et al., 1999), confirming the pathogenic role of the fetal AChR-Abs.

CHRNG Associated Congenital Myasthenic Syndrome

Mutations of the AChR γ-subunit gene CHRNG have been found to underlie Escobar type multiple pterygium syndrome (Hoffmann et al., 2006; Morgan et al., 2006), an autosomal recessive form of AMC characterized by webbing (pterygia), congenital fixed joint deformities and scoliosis (Escobar et al., 1978; Rajab et al., 2005). Respiratory distress, intrauterine death and stillbirths are common. The developmental abnormalities result from the truncation or low expression of the γ-subunit, with loss of fetal AChR function at sensitive times of neuromuscular development (Murray and Drachman, 1969; Hammond and Donnenfeld, 1995). The AChR subunits have to be assembled in the endoplasmic reticulum before the receptor can be inserted into the plasma membrane, starting with the formation of an αβγ trimer and sequential addition of a δ- and a second α-subunit (Green and Claudio, 1993; Wanamaker et al., 2003). If the γ-subunit is missing, the receptor cannot reach the cell surface resulting in AChR deficiency (Hoffmann et al., 2006). Patients usually show little or no progression of their condition and no myasthenic symptoms after birth, as neuromuscular transmission continues to be mediated by the adult AChR, although they may display residual developmental abnormalities such as webbing of the neck and between the fingers. The survival of some cases in which the γ-subunit is missing due to truncating mutations within the N-terminal region would indicate at least some early low-level expression of the ε-subunit (Hesselmans et al., 1993).

CHRNE Associated Congenital Myasthenic Syndrome

Mutations of the AChR ε-subunit gene CHRNE are the most frequent and depending on the ethnic population may account for over 30% of cases with congenital myasthenic syndromes (Engel et al., 2003, 2015; Finlayson et al., 2013). Mutations are found along the entire gene including the promoter region (Nichols et al., 1999; Engel et al., 2015) and result in protein truncation, missense mutation of essential residues or in reduced levels of ε-subunit mRNA expression. The defects are heterogeneous and include AChR deficiency, slow-channel, fast-channel and low-conductance syndromes (Ohno et al., 1997; Webster et al., 2012; Rodriguez Cruz et al., 2018). The high prevalence of CHRNE mutations has been attributed to the phenotypic rescue by the persistent low-level expression of the γ-subunit that is sufficient to enable patients with ε-subunit null alleles to survive (Croxen et al., 2001; Cossins et al., 2004). The phenotypic spectrum of CHRNE associated primary AChR deficiency is variable and ranges from mild to severe, but most patients are characterized by marked ophthalmoparesis (Engel et al., 1996; Burke et al., 2004; Rodriguez Cruz et al., 2015), which could be related to the exceptionally high motor neuron firing frequencies of extraocular muscles (Yu Wai Man et al., 2005), requiring fast recovery rates from AChR desensitization for efficient neuromuscular transmission. Neuromuscular transmission in patients with CHRNE null mutations, however, has to depend on the fetal AChR with slow recovery rates from desensitization. Fetal AChRs could accrue into desensitized states and might be unable to promote efficient neuromuscular transmission at high motor neuron firing frequencies (Cetin et al., 2019).

CONCLUDING REMARKS

The transition from fetal to adult AChR expression during NMJ development represents a characteristic feature in mammals with

complex regulatory mechanisms mediated by the fine-tuned electrical and molecular communication between nerve and muscle. Intensive research of the past decades produced insight into functional differences between both AChR isoforms and has helped to understand better their physiological significance and their role in different myasthenic syndromes. However, some key aspects of fetal and adult AChR function remain to be answered. Especially the elucidation of the structural determinants of desensitization and recovery from desensitization in fetal and adult AChRs and their evaluation in animal models could further help to unravel the significance of desensitization in NMJ physiology and disease.

AUTHOR CONTRIBUTIONS

HC drafted the manuscript and prepared the figures. DB, AV, and RW edited and reviewed the manuscript. All authors contributed to the article and approved the submitted version.

FUNDING

We are grateful for financial support offered by the following funding agencies: HC was funded by an Erwin Schrödinger Fellowship (J3589) by the Austrian Science Fund (FWF) and by a grant from the Nuffield Department of Clinical Neurosciences, University of Oxford. DB holds a Medical Research Council Programme Grant (MR/M006824/1), which funds RW.

ACKNOWLEDGMENTS

We thank Prof. Dan Larhammar (University of Uppsala, Uppsala, Sweden) for helpful discussion of evolutionary aspects of the AChR subunits.

REFERENCES

Adams, D. J., Dwyer, T. M., and Hille, B. (1980). The permeability of endplate channels to monovalent and divalent metal cations. *J. Gen. Physiol.* 75, 493–510. doi: 10.1085/jgp.75.5.493

Allen, N. M., Hacohen, Y., Palace, J., Beeson, D., Vincent, A., and Jungbluth, H. (2016). Salbutamol-responsive fetal acetylcholine receptor inactivation syndrome. *Neurology* 86, 692–694. doi: 10.1212/wnl.0000000000002382

Asher, O., Provenzano, C., and Fuchs, S. (1991). Regulation of acetylcholine receptor gene expression in rats treated with alpha-bungarotoxin. *FEBS Lett.* 282, 242–246. doi: 10.1016/0014-5793(91)80487-n

Auerbach, A., and Akk, G. (1998). Desensitization of mouse nicotinic acetylcholine receptor channels. A two-gate mechanism. *J. Gen. Physiol.* 112, 181–197. doi: 10.1085/jgp.112.2.181

Barnes, P. R., Kanabar, D. J., Brueton, L., Newsom-Davis, J., Huson, S. M., Mann, N. P., et al. (1995). Recurrent congenital arthrogryposis leading to a diagnosis of myasthenia gravis in an initially asymptomatic mother. *Neuromuscul. Disord.* 5, 59–65. doi: 10.1016/0960-8966(94)e0029-8

Beckstein, O., Biggin, P. C., and Sansom, M. S. P. (2001). A hydrophobic gating mechanism for nanopores. *J. Phys. Chem. B* 105, 12902–12905. doi: 10.1021/jp012233y

Berg, D. K., Kelly, R. B., Sargent, P. B., Williamson, P., and Hall, Z. W. (1972). Binding of -bungarotoxin to acetylcholine receptors in mammalian muscle (snake venom-denervated muscle-neonatal muscle-rat diaphragm-SDS-polyacrylamide gel electrophoresis). *Proc. Natl. Acad. Sci. U.S.A.* 69, 147–151.

Bouzat, C., Bren, N., and Sine, S. M. (1994). Structural basis of the different gating kinetics of fetal and adult acetylcholine receptors. *Neuron* 13, 1395–1402. doi: 10.1016/0896-6273(94)90424-3

Brenner, H. R., Witzemann, V., and Sakmann, B. (1990). Imprinting of acetylcholine receptor messenger RNA accumulation in mammalian neuromuscular synapses. *Nature* 344, 544–547. doi: 10.1038/344544a0

Burke, G., Cossins, J., Maxwell, S., Robb, S., Nicolle, M., Vincent, A., et al. (2004). Distinct phenotypes of congenital acetylcholine receptor deficiency. *Neuromuscul. Disord.* 14, 356–364. doi: 10.1016/j.nmd.2004.03.005

Cash, S., Dan, Y., Poo, M. M., and Zucker, R. (1996). Postsynaptic elevation of calcium induces persistent depression of developing neuromuscular synapses. *Neuron* 16, 745–754. doi: 10.1016/s0896-6273(00)80095-1

Cetin, H., Liu, W., Cheung, J., Cossins, J., Vanhaesebrouck, A., Maxwell, S., et al. (2019). Rapsyn facilitates recovery from desensitization in fetal and adult acetylcholine receptors expressed in a muscle cell line. *J. Physiol.* 597, 3713–3725. doi: 10.1113/jp277819

Cetin, H., and Vincent, A. (2018). Pathogenic mechanisms and clinical correlations in autoimmune myasthenic syndromes. *Semin. Neurol.* 38, 344–354. doi: 10.1055/s-0038-1660500

Cetin, H., Webster, R., Liu, W. W., Nagaishi, A., Koneczny, I., Zimprich, F., et al. (2020). Myasthenia gravis AChR antibodies inhibit function of rapsyn-clustered AChRs. *J. Neurol. Neurosurg. Psychiatry* 91, 526–532. doi: 10.1136/jnnp-2019-322640

Chesnut, T. J. (1983). Two-component desensitization at the neuromuscular junction of the frog. *J. Physiol.* 336, 229–241. doi: 10.1113/jphysiol.1983.sp014578

Chiarandini, D. J., and Stefani, E. (1979). Electrophysiological identification of two types of fibres in rat extraocular muscles. *J. Physiol.* 290, 453–465. doi: 10.1113/jphysiol.1979.sp012783

Colquhoun, D., and Ogden, D. C. (1988). Activation of ion channels in the frog end-plate by high concentrations of acetylcholine. *J. Physiol.* 395, 131–159. doi: 10.1113/jphysiol.1988.sp016912

Cossins, J., Webster, R., Maxwell, S., Burke, G., Vincent, A., and Beeson, D. (2004). A mouse model of AChR deficiency syndrome with a phenotype reflecting the human condition. *Hum. Mol. Genet.* 13, 2947–2957. doi: 10.1093/hmg/ddh320

Croxen, R., Young, C., Slater, C., Haslam, S., Brydson, M., Vincent, A., et al. (2001). End-plate gamma- and epsilon-subunit mRNA levels in AChR deficiency syndrome due to epsilon-subunit null mutations. *Brain* 124, 1362–1372. doi: 10.1093/brain/124.7.1362

Duclert, A., Savatier, N., and Changeux, J. P. (1993). An 83-nucleotide promoter of the acetylcholine receptor epsilon-subunit gene confers preferential synaptic expression in mouse muscle. *Proc. Natl. Acad. Sci. U.S.A.* 90, 3043–3047. doi: 10.1073/pnas.90.7.3043

Eftimie, R., Brenner, H. R., and Buonanno, A. (1991). Myogenin and MyoD join a family of skeletal muscle genes regulated by electrical activity. *Proc. Natl. Acad. Sci. U.S.A.* 88, 1349–1353. doi: 10.1073/pnas.88.4.1349

Elenes, S., Ni, Y., Cymes, G. D., and Grosman, C. (2006). Desensitization contributes to the synaptic response of gain-of-function mutants of the muscle nicotinic receptor. *J. Gen. Physiol.* 128, 615–627. doi: 10.1085/jgp.200609570

Engel, A. G., Ohno, K., Bouzat, C., Sine, S. M., and Griggs, R. C. (1996). End-plate acetylcholine receptor deficiency due to nonsense mutations in the epsilon subunit. *Ann. Neurol.* 40, 810–817. doi: 10.1002/ana.410400521

Engel, A. G., Ohno, K., and Sine, S. M. (2003). Sleuthing molecular targets for neurological diseases at the neuromuscular junction. *Nat. Rev. Neurosci.* 4, 339–352. doi: 10.1038/nrn1101

Engel, A. G., Shen, X. M., Selcen, D., and Sine, S. M. (2015). Congenital myasthenic syndromes: pathogenesis, diagnosis, and treatment. *Lancet Neurol.* 14:461.

Escher, P., Lacazette, E., Courtet, M., Blindenbacher, A., Landmann, L., Bezakova, G., et al. (2005). Synapses form in skeletal muscles lacking neuregulin receptors. *Science* 308, 1920–1923. doi: 10.1126/science.1108258

Escobar, V., Bixler, D., Gleiser, S., Weaver, D. D., and Gibbs, T. (1978). Multiple pterygium syndrome. *Am. J. Dis. Child.* 132, 609–611.

Finlayson, S., Beeson, D., and Palace, J. (2013). Congenital myasthenic syndromes: an update. *Pract. Neurol.* 13, 80–91. doi: 10.1136/practneurol-2012-000404

Fischbach, G. D., and Schuetze, S. M. (1980). A post-natal decrease in acetylcholine channel open time at rat end-plates. *J. Physiol.* 303, 125–137. doi: 10.1113/jphysiol.1980.sp013275

Fraterman, S., Khurana, T. S., and Rubinstein, N. A. (2006). Identification of acetylcholine receptor subunits differentially expressed in singly and multiply innervated fibers of extraocular muscles. *Invest. Ophthalmol. Vis. Sci.* 47, 3828–3834. doi: 10.1167/iovs.06-0073

Fromm, L., and Burden, S. J. (1998). Synapse-specific and neuregulin-induced transcription require an ets site that binds GABPalpha/GABPbeta. *Genes Dev.* 12, 3074–3083. doi: 10.1101/gad.12.19.3074

Fucile, S., Sucapane, A., Grassi, F., Eusebi, F., and Engel, A. G. (2006). The human adult subtype ACh receptor channel has high Ca2+ permeability and predisposes to endplate Ca2+ overloading. *J. Physiol.* 573, 35–43. doi: 10.1113/jphysiol.2006.108092

Gattenlohner, S., Schneider, C., Thamer, C., Klein, R., Roggendorf, W., Gohlke, F., et al. (2002). Expression of foetal type acetylcholine receptor is restricted to type 1 muscle fibres in human neuromuscular disorders. *Brain* 125, 1309–1319. doi: 10.1093/brain/awf136

Giniatullin, R. A., Khazipov, R. N., and Vyskocil, F. (1993). A correlation between quantal content and decay time of endplate currents in frog muscles with intact cholinesterase. *J. Physiol.* 466, 95–103.

Goldman, D., Brenner, H. R., and Heinemann, S. (1988). Acetylcholine receptor alpha-, beta-, gamma-, and delta-subunit mRNA levels are regulated by muscle activity. *Neuron* 1, 329–333.

Green, W. N., and Claudio, T. (1993). Acetylcholine receptor assembly: subunit folding and oligomerization occur sequentially. *Cell* 74, 57–69. doi: 10.1016/0092-8674(93)90294-z

Gu, Y., and Hall, Z. W. (1988). Immunological evidence for a change in subunits of the acetylcholine receptor in developing and denervated rat muscle. *Neuron* 1, 117–125. doi: 10.1016/0896-6273(88)90195-x

Hacohen, Y., Jacobson, L. W., Byrne, S., Norwood, F., Lall, A., Robb, S., et al. (2015). Fetal acetylcholine receptor inactivation syndrome: a myopathy due to maternal antibodies. *Neurol. Neuroimmunol. Neuroinflamm.* 2:e57. doi: 10.1212/nxi.0000000000000057

Hammond, E., and Donnenfeld, A. E. (1995). Fetal akinesia. *Obstet. Gynecol. Surv.* 50, 240–249.

Harvey, A. L., and Van Helden, D. (1981). Acetylcholine receptors in singly and multiply innervated skeletal muscle fibres of the chicken during development. *J. Physiol.* 317, 397–411. doi: 10.1113/jphysiol.1981.sp013832

Hennig, R., and Lomo, T. (1985). Firing patterns of motor units in normal rats. *Nature* 314, 164–166. doi: 10.1038/314164a0

Herlitze, S., Villarroel, A., Witzemann, V., Koenen, M., and Sakmann, B. (1996). Structural determinants of channel conductance in fetal and adult rat muscle acetylcholine receptors. *J. Physiol.* 492(Pt 3), 775–787. doi: 10.1113/jphysiol.1996.sp021345

Hesselmans, L. F., Jennekens, F. G., Van Den Oord, C. J., Veldman, H., and Vincent, A. (1993). Development of innervation of skeletal muscle fibers in man: relation to acetylcholine receptors. *Anat. Rec.* 236, 553–562. doi: 10.1002/ar.1092360315

Hoffman, P. W., Ravindran, A., and Huganir, R. L. (1994). Role of phosphorylation in desensitization of acetylcholine receptors expressed in *Xenopus oocytes*. *J. Neurosci.* 14, 4185–4195. doi: 10.1523/jneurosci.14-07-04185.1994

Hoffmann, K., Muller, J. S., Stricker, S., Megarbane, A., Rajab, A., Lindner, T. H., et al. (2006). Escobar syndrome is a prenatal myasthenia caused by disruption of the acetylcholine receptor fetal gamma subunit. *Am. J. Hum. Genet.* 79, 303–312. doi: 10.1086/506257

Hopfield, J. F., Tank, D. W., Greengard, P., and Huganir, R. L. (1988). Functional modulation of the nicotinic acetylcholine receptor by tyrosine phosphorylation. *Nature* 336, 677–680. doi: 10.1038/336677a0

Horton, R. M., Manfredi, A. A., and Conti-Tronconi, B. M. (1993). The 'embryonic' gamma subunit of the nicotinic acetylcholine receptor is expressed in adult extraocular muscle. *Neurology* 43, 983–986. doi: 10.1212/wnl.43.5.983

Huang, C. F., Tong, J., and Schmidt, J. (1992). Protein kinase C couples membrane excitation to acetylcholine receptor gene inactivation in chick skeletal muscle. *Neuron* 9, 671–678. doi: 10.1016/0896-6273(92)90030-h

Huganir, R. L., Delcour, A. H., Greengard, P., and Hess, G. P. (1986). Phosphorylation of the nicotinic acetylcholine receptor regulates its rate of desensitization. *Nature* 321, 774–776. doi: 10.1038/321774a0

Imoto, K., Busch, C., Sakmann, B., Mishina, M., Konno, T., Nakai, J., et al. (1988). Rings of negatively charged amino acids determine the acetylcholine receptor channel conductance. *Nature* 335, 645–648. doi: 10.1038/335645a0

Jacobson, L., Polizzi, A., Morriss-Kay, G., and Vincent, A. (1999). Plasma from human mothers of fetuses with severe arthrogryposis multiplex congenita causes deformities in mice. *J. Clin. Invest.* 103, 1031–1038. doi: 10.1172/jci5943

Jahn, K., Mohammadi, B., Krampfl, K., Abicht, A., Lochmuller, H., and Bufler, J. (2001). Deactivation and desensitization of mouse embryonic- and adult-type nicotinic receptor channel currents. *Neurosci. Lett.* 307, 89–92. doi: 10.1016/s0304-3940(01)01929-2

Jaramillo, F., Vicini, S., and Schuetze, S. M. (1988). Embryonic acetylcholine receptors guarantee spontaneous contractions in rat developing muscle. *Nature* 335, 66–68. doi: 10.1038/335066a0

Jing, L., Lefebvre, J. L., Gordon, L. R., and Granato, M. (2009). Wnt signals organize synaptic prepattern and axon guidance through the zebrafish unplugged/MuSK receptor. *Neuron* 61, 721–733. doi: 10.1016/j.neuron.2008.12.025

Jones, G., Herczeg, A., Ruegg, M. A., Lichtsteiner, M., Kroger, S., and Brenner, H. R. (1996). Substrate-bound agrin induces expression of acetylcholine receptor epsilon-subunit gene in cultured mammalian muscle cells. *Proc. Natl. Acad. Sci. U.S.A.* 93, 5985–5990. doi: 10.1073/pnas.93.12.5985

Kaminski, H. J., Kusner, L. L., and Block, C. H. (1996). Expression of acetylcholine receptor isoforms at extraocular muscle endplates. *Invest. Ophthalmol. Vis. Sci.* 37, 345–351.

Kaminski, H. J., Li, Z., Richmonds, C., Lin, F., and Medof, M. E. (2004). Complement regulators in extraocular muscle and experimental autoimmune myasthenia gravis. *Exp. Neurol.* 189, 333–342. doi: 10.1016/j.expneurol.2004.06.005

Kaminski, H. J., Maas, E., Spiegel, P., and Ruff, R. L. (1990). Why are eye muscles frequently involved in myasthenia gravis? *Neurology* 40, 1663–1669. doi: 10.1212/wnl.40.11.1663

Khanna, S., Richmonds, C. R., Kaminski, H. J., and Porter, J. D. (2003). Molecular organization of the extraocular muscle neuromuscular junction: partial conservation of and divergence from the skeletal muscle prototype. *Invest. Ophthalmol. Vis. Sci.* 44, 1918–1926. doi: 10.1167/iovs.02-0890

Kim, N., and Burden, S. J. (2008). MuSK controls where motor axons grow and form synapses. *Nat. Neurosci.* 11, 19–27. doi: 10.1038/nn2026

Klarsfeld, A., Laufer, R., Fontaine, B., Devillers-Thiery, A., Dubreuil, C., and Changeux, J. P. (1989). Regulation of muscle AChR alpha subunit gene expression by electrical activity: involvement of protein kinase C and Ca2+. *Neuron* 2, 1229–1236. doi: 10.1016/0896-6273(89)90307-3

Koenen, M., Peter, C., Villarroel, A., Witzemann, V., and Sakmann, B. (2005). Acetylcholine receptor channel subtype directs the innervation pattern of skeletal muscle. *EMBO Rep.* 6, 570–576. doi: 10.1038/sj.embor.7400429

Koike, S., Schaeffer, L., and Changeux, J. P. (1995). Identification of a DNA element determining synaptic expression of the mouse acetylcholine receptor delta-subunit gene. *Proc. Natl. Acad. Sci. U.S.A.* 92, 10624–10628. doi: 10.1073/pnas.92.23.10624

Kopta, C., and Steinbach, J. H. (1994). Comparison of mammalian adult and fetal nicotinic acetylcholine receptors stably expressed in fibroblasts. *J. Neurosci.* 14, 3922–3933. doi: 10.1523/jneurosci.14-06-03922.1994

Kostelidou, K., Trakas, N., and Tzartos, S. J. (2007). Extracellular domains of the beta, gamma and epsilon subunits of the human acetylcholine receptor as immunoadsorbents for myasthenic autoantibodies: a combination of immunoadsorbents results in increased efficiency. *J. Neuroimmunol.* 190, 44–52. doi: 10.1016/j.jneuroim.2007.07.018

Krampfl, K., Jahn, K., Cordes, A. L., Dengler, R., and Bufler, J. (2002). Analysis of a slow desensitized state of recombinant adult-type nicotinic acetylcholine receptor channels. *Eur. J. Neurosci.* 16, 652–658. doi: 10.1046/j.1460-9568.2002.02114.x

Kues, W. A., Brenner, H. R., Sakmann, B., and Witzemann, V. (1995). Local neurotrophic repression of gene transcripts encoding fetal AChRs at rat neuromuscular synapses. *J. Cell Biol.* 130, 949–957. doi: 10.1083/jcb.130.4.949

Lacazette, E., Le Calvez, S., Gajendran, N., and Brenner, H. R. (2003). A novel pathway for MuSK to induce key genes in neuromuscular synapse formation. *J. Cell Biol.* 161, 727–736. doi: 10.1083/jcb.200210156

Le Novere, N., Corringer, P. J., and Changeux, J. P. (2002). The diversity of subunit composition in nAChRs: evolutionary origins, physiologic and pharmacologic consequences. *J. Neurobiol.* 53, 447–456. doi: 10.1002/neu.10153

Lin, S., Landmann, L., Ruegg, M. A., and Brenner, H. R. (2008). The role of nerve- versus muscle-derived factors in mammalian neuromuscular junction formation. *J. Neurosci.* 28, 3333–3340. doi: 10.1523/jneurosci.5590-07.2008

Lin, W., Burgess, R. W., Dominguez, B., Pfaff, S. L., Sanes, J. R., and Lee, K. F. (2001). Distinct roles of nerve and muscle in postsynaptic differentiation of the neuromuscular synapse. *Nature* 410, 1057–1064. doi: 10.1038/35074025

Lindstrom, J. M., Seybold, M. E., Lennon, V. A., Whittingham, S., and Duane, D. D. (1976). Antibody to acetylcholine receptor in myasthenia gravis. Prevalence, clinical correlates, and diagnostic value. *Neurology* 26, 1054–1059. doi: 10.1212/wnl.26.11.1054

Liu, S., Spinner, D. S., Schmidt, M. M., Danielsson, J. A., Wang, S., and Schmidt, J. (2000). Interaction of MyoD family proteins with enhancers of acetylcholine receptor subunit genes in vivo. *J. Biol. Chem.* 275, 41364–41368. doi: 10.1074/jbc.m004172200

MacLennan, C., Beeson, D., Buijs, A. M., Vincent, A., and Newsom-Davis, J. (1997). Acetylcholine receptor expression in human extraocular muscles and their susceptibility to myasthenia gravis. *Ann. Neurol.* 41, 423–431. doi: 10.1002/ana.410410404

Magleby, K. L., and Pallotta, B. S. (1981). A study of desensitization of acetylcholine receptors using nerve-released transmitter in the frog. *J. Physiol.* 316, 225–250. doi: 10.1113/jphysiol.1981.sp013784

Matthews, I., Sims, G., Ledwidge, S., Stott, D., Beeson, D., Willcox, N., et al. (2002). Antibodies to acetylcholine receptor in parous women with myasthenia: evidence for immunization by fetal antigen. *Lab. Invest.* 82, 1407–1417. doi: 10.1097/01.lab.0000032379.63784.9c

Merlie, J. P., Isenberg, K. E., Russell, S. D., and Sanes, J. R. (1984). Denervation supersensitivity in skeletal muscle: analysis with a cloned cDNA probe. *J. Cell Biol.* 99, 332–335. doi: 10.1083/jcb.99.1.332

Miles, K., Audigier, S. S., Greengard, P., and Huganir, R. L. (1994). Autoregulation of phosphorylation of the nicotinic acetylcholine receptor. *J. Neurosci.* 14, 3271–3279. doi: 10.1523/jneurosci.14-05-03271.1994

Mishina, M., Takai, T., Imoto, K., Noda, M., Takahashi, T., Numa, S., et al. (1986). Molecular distinction between fetal and adult forms of muscle acetylcholine receptor. *Nature* 321, 406–411. doi: 10.1038/321406a0

Missias, A. C., Chu, G. C., Klocke, B. J., Sanes, J. R., and Merlie, J. P. (1996). Maturation of the acetylcholine receptor in skeletal muscle: regulation of the AChR gamma-to-epsilon switch. *Dev. Biol.* 179, 223–238. doi: 10.1006/dbio.1996.0253

Missias, A. C., Mudd, J., Cunningham, J. M., Steinbach, J. H., Merlie, J. P., and Sanes, J. R. (1997). Deficient development and maintenance of postsynaptic specializations in mutant mice lacking an 'adult' acetylcholine receptor subunit. *Development* 124, 5075–5086.

Miyazawa, A., Fujiyoshi, Y., and Unwin, N. (2003). Structure and gating mechanism of the acetylcholine receptor pore. *Nature* 423, 949–955. doi: 10.1038/nature01748

Morgan, N. V., Brueton, L. A., Cox, P., Greally, M. T., Tolmie, J., Pasha, S., et al. (2006). Mutations in the embryonal subunit of the acetylcholine receptor (CHRNG) cause lethal and Escobar variants of multiple pterygium syndrome. *Am. J. Hum. Genet.* 79, 390–395. doi: 10.1086/506256

Moss, S. J., Beeson, D. M., Jackson, J. F., Darlison, M. G., and Barnard, E. A. (1987). Differential expression of nicotinic acetylcholine receptor genes in innervated and denervated chicken muscle. *EMBO J.* 6, 3917–3921. doi: 10.1002/j.1460-2075.1987.tb02732.x

Moss, S. J., Darlison, M. G., Beeson, D. M., and Barnard, E. A. (1989). Development expression of the genes encoding the four subunits of the chicken muscle acetylcholine receptor. *J. Biol. Chem.* 264, 20199–20205.

Murray, P. D., and Drachman, D. B. (1969). The role of movement in the development of joints and related structures: the head and neck in the chick embryo. *J. Embryol. Exp. Morphol.* 22, 349–371.

Nayak, T. K., Bruhova, I., Chakraborty, S., Gupta, S., Zheng, W., and Auerbach, A. (2014). Functional differences between neurotransmitter binding sites of muscle acetylcholine receptors. *Proc. Natl. Acad. Sci. U.S.A.* 111, 17660–17665. doi: 10.1073/pnas.1414378111

Nayak, T. K., Chakraborty, S., Zheng, W., and Auerbach, A. (2016). Structural correlates of affinity in fetal versus adult endplate nicotinic receptors. *Nat. Commun.* 7:11352.

Newland, C. F., Beeson, D., Vincent, A., and Newsom-Davis, J. (1995). Functional and non-functional isoforms of the human muscle acetylcholine receptor. *J. Physiol.* 489(Pt 3), 767–778. doi: 10.1113/jphysiol.1995.sp021090

Newsom-Davis, J., Wilson, S. G., Vincent, A., and Ward, C. D. (1979). Long-term effects of repeated plasma exchange in myasthenia gravis. *Lancet* 1, 464–468. doi: 10.1016/s0140-6736(79)90823-7

Nichols, P., Croxen, R., Vincent, A., Rutter, R., Hutchinson, M., Newsom-Davis, J., et al. (1999). Mutation of the acetylcholine receptor epsilon-subunit promoter in congenital myasthenic syndrome. *Ann. Neurol.* 45, 439–443. doi: 10.1002/1531-8249(199904)45:4<439::aid-ana4>3.0.co;2-w

Oda, K. (1993). Differences in acetylcholine receptor-antibody interactions between extraocular and extremity muscle fibers. *Ann. N. Y. Acad. Sci.* 681, 238–255. doi: 10.1111/j.1749-6632.1993.tb22889.x

Ohno, K., Quiram, P. A., Milone, M., Wang, H. L., Harper, M. C., Pruitt, J. N., et al. (1997). Congenital myasthenic syndromes due to heteroallelic nonsense/missense mutations in the acetylcholine receptor epsilon subunit gene: identification and functional characterization of six new mutations. *Hum. Mol. Genet.* 6, 753–766. doi: 10.1093/hmg/6.5.753

Oskoui, M., Jacobson, L., Chung, W. K., Haddad, J., Vincent, A., Kaufmann, P., et al. (2008). Fetal acetylcholine receptor inactivation syndrome and maternal myasthenia gravis. *Neurology* 71, 2010–2012. doi: 10.1212/01.wnl.0000336929.38733.7a

Papazian, O. (1992). Transient neonatal myasthenia gravis. *J. Child Neurol.* 7, 135–141. doi: 10.1177/088307389200700202

Paradiso, K., and Brehm, P. (1998). Long-term desensitization of nicotinic acetylcholine receptors is regulated via protein kinase A-mediated phosphorylation. *J. Neurosci.* 18, 9227–9237. doi: 10.1523/jneurosci.18-22-09227.1998

Pedersen, J. E., Bergqvist, C. A., and Larhammar, D. (2019). Evolution of vertebrate nicotinic acetylcholine receptors. *BMC Evol. Biol.* 19:38. doi: 10.1186/s12862-018-1341-8

Personius, K. E., and Balice-Gordon, R. J. (2001). Loss of correlated motor neuron activity during synaptic competition at developing neuromuscular synapses. *Neuron* 31, 395–408. doi: 10.1016/s0896-6273(01)00369-5

Personius, K. E., Chang, Q., Mentis, G. Z., O'donovan, M. J., and Balice-Gordon, R. J. (2007). Reduced gap junctional coupling leads to uncorrelated motor neuron firing and precocious neuromuscular synapse elimination. *Proc. Natl. Acad. Sci. U.S.A.* 104, 11808–11813. doi: 10.1073/pnas.0703357104

Porter, J. D., and Baker, R. S. (1996). Muscles of a different 'color': the unusual properties of the extraocular muscles may predispose or protect them in neurogenic and myogenic disease. *Neurology* 46, 30–37. doi: 10.1212/wnl.46.1.30

Porter, J. D., Khanna, S., Kaminski, H. J., Rao, J. S., Merriam, A. P., Richmonds, C. R., et al. (2001). Extraocular muscle is defined by a fundamentally distinct gene expression profile. *Proc. Natl. Acad. Sci. U.S.A.* 98, 12062–12067.

Ragozzino, D., Barabino, B., Fucile, S., and Eusebi, F. (1998). Ca2+ permeability of mouse and chick nicotinic acetylcholine receptors expressed in transiently transfected human cells. *J. Physiol.* 507(Pt 3), 749–757. doi: 10.1111/j.1469-7793.1998.749bs.x

Rajab, A., Hoffmann, K., Ganesh, A., Sethu, A. U., and Mundlos, S. (2005). Escobar variant with pursed mouth, creased tongue, ophthalmologic features, and scoliosis in 6 children from Oman. *Am. J. Med. Genet. A* 134A, 151–157. doi: 10.1002/ajmg.a.30583

Riemersma, S., Vincent, A., Beeson, D., Newland, C., Hawke, S., Vernet-Der Garabedian, B., et al. (1996). Association of arthrogryposis multiplex congenita with maternal antibodies inhibiting fetal acetylcholine receptor function. *J. Clin. Invest.* 98, 2358–2363. doi: 10.1172/jci119048

Robinson, D. A. (1970). Oculomotor unit behavior in the monkey. *J. Neurophysiol.* 33, 393–403. doi: 10.1152/jn.1970.33.3.393

Rodriguez Cruz, P. M., Palace, J., and Beeson, D. (2018). The neuromuscular junction and wide heterogeneity of congenital myasthenic syndromes. *Int. J. Mol. Sci.* 19:1677. doi: 10.3390/ijms19061677

Rodriguez Cruz, P. M., Palace, J., Ramjattan, H., Jayawant, S., Robb, S. A., and Beeson, D. (2015). Salbutamol and ephedrine in the treatment of severe AChR deficiency syndromes. *Neurology* 85, 1043–1047. doi: 10.1212/wnl.0000000000001952

Roses, A. D., Olanow, C. W., Mcadams, M. W., and Lane, R. J. (1981). No direct correlation between serum antiacetylcholine receptor antibody levels and clinical state of individual patients with myasthenia gravis. *Neurology* 31, 220–224. doi: 10.1212/wnl.31.2.220

Ruzzier, F., and Scuka, M. (1986). The effect of repetitive neuromuscular activity on the sensitivity of acetylcholine receptors. *Pflugers Arch.* 406, 99–103. doi: 10.1007/bf00586669

Sakmann, B., and Brenner, H. R. (1978). Change in synaptic channel gating during neuromuscular development. *Nature* 276, 401–402. doi: 10.1038/276401a0

Sakmann, B., Patlak, J., and Neher, E. (1980). Single acetylcholine-activated channels show burst-kinetics in presence of desensitizing concentrations of agonist. *Nature* 286, 71–73. doi: 10.1038/286071a0

Sanes, J. R., and Lichtman, J. W. (1999). Development of the vertebrate neuromuscular junction. *Annu. Rev. Neurosci.* 22, 389–442. doi: 10.1146/annurev.neuro.22.1.389

Schaeffer, L., De Kerchove D'exaerde, A., and Changeux, J. P. (2001). Targeting transcription to the neuromuscular synapse. *Neuron* 31, 15–22. doi: 10.1016/s0896-6273(01)00353-1

Schaeffer, L., Duclert, N., Huchet-Dymanus, M., and Changeux, J. P. (1998). Implication of a multisubunit Ets-related transcription factor in synaptic expression of the nicotinic acetylcholine receptor. *EMBO J.* 17, 3078–3090. doi: 10.1093/emboj/17.11.3078

Schuetze, S. M. (1980). The acetylcholine channel open time in chick muscle is not decreased following innervation. *J. Physiol.* 303, 111–124. doi: 10.1113/jphysiol.1980.sp013274

Seaberg, B., Henslee, G., Wang, S., Paez-Colasante, X., Landreth, G. E., and Rimer, M. (2015). Muscle-derived extracellular signal-regulated kinases 1 and 2 are required for the maintenance of adult myofibers and their neuromuscular junctions. *Mol. Cell. Biol.* 35, 1238–1253. doi: 10.1128/mcb.01071-14

Shi, Q. G., Wang, Z. H., Ma, X. W., Zhang, D. Q., Yang, C. S., Shi, F. D., et al. (2012). Clinical significance of detection of antibodies to fetal and adult acetylcholine receptors in myasthenia gravis. *Neurosci. Bull.* 28, 469–474. doi: 10.1007/s12264-012-1256-0

Song, C., and Corry, B. (2009). Role of acetylcholine receptor domains in ion selectivity. *Biochim. Biophys. Acta* 1788, 1466–1473. doi: 10.1016/j.bbamem.2009.04.015

Sullivan, M. P., Owens, J. L., and Kullberg, R. W. (1999). Role of M2 domain residues in conductance and gating of acetylcholine receptors in developing Xenopus muscle. *J. Physiol.* 515(Pt 1), 31–39. doi: 10.1111/j.1469-7793.1999.031ad.x

Tapia, J. C., Wylie, J. D., Kasthuri, N., Hayworth, K. J., Schalek, R., Berger, D. R., et al. (2012). Pervasive synaptic branch removal in the mammalian neuromuscular system at birth. *Neuron* 74, 816–829. doi: 10.1016/j.neuron.2012.04.017

Tintignac, L. A., Brenner, H. R., and Ruegg, M. A. (2015). Mechanisms regulating neuromuscular junction development and function and causes of muscle wasting. *Physiol. Rev.* 95, 809–852.

Tsay, H. J., and Schmidt, J. (1989). Skeletal muscle denervation activates acetylcholine receptor genes. *J. Cell Biol.* 108, 1523–1526.

Tsujihata, M., Ito, H., Satoh, A., Yoshimura, T., Motomura, M., and Nakamura, T. (2001). Semiquantitative measurement of acetylcholine receptor at the motor end-plate in myasthenia gravis. *Intern. Med.* 40, 376–381.

Tsunoyama, K., and Gojobori, T. (1998). Evolution of nicotinic acetylcholine receptor subunits. *Mol. Biol. Evol.* 15, 518–527.

Tzartos, S. J., Barkas, T., Cung, M. T., Mamalaki, A., Marraud, M., Orlewski, P., et al. (1998). Anatomy of the antigenic structure of a large membrane autoantigen, the muscle-type nicotinic acetylcholine receptor. *Immunol. Rev.* 163, 89–120.

Tzartos, S. J., Seybold, M. E., and Lindstrom, J. M. (1982). Specificities of antibodies to acetylcholine receptors in sera from myasthenia gravis patients measured by monoclonal antibodies. *Proc. Natl. Acad. Sci. U.S.A.* 79, 188–192.

Unwin, N. (1995). Acetylcholine receptor channel imaged in the open state. *Nature* 373, 37–43.

Unwin, N. (2005). Refined structure of the nicotinic acetylcholine receptor at 4A resolution. *J. Mol. Biol.* 346, 967–989.

Unwin, N., and Fujiyoshi, Y. (2012). Gating movement of acetylcholine receptor caught by plunge-freezing. *J. Mol. Biol.* 422, 617–634.

Vernet-Der Garabedian, B., Lacokova, M., Eymard, B., Morel, E., Faltin, M., Zajac, J., et al. (1994). Association of neonatal myasthenia gravis with antibodies against the fetal acetylcholine receptor. *J. Clin. Invest.* 94, 555–559.

Villarroel, A., and Sakmann, B. (1996). Calcium permeability increase of endplate channels in rat muscle during postnatal development. *J. Physiol.* 496(Pt 2), 331–338.

Vincent, A., Jacobson, L., and Curran, L. (1998). Alpha-Bungarotoxin binding to human muscle acetylcholine receptor: measurement of affinity, delineation of AChR subunit residues crucial to binding, and protection of AChR function by synthetic peptides. *Neurochem. Int.* 32, 427–433.

Vincent, A., Newland, C., Brueton, L., Beeson, D., Riemersma, S., Huson, S. M., et al. (1995). Arthrogryposis multiplex congenita with maternal autoantibodies specific for a fetal antigen. *Lancet* 346, 24–25.

Vincent, A., and Newsom Davis, J. (1980). Anti-acetylcholine receptor antibodies. *J. Neurol. Neurosurg. Psychiatry* 43, 590–600.

Vincent, A., and Newsom-Davis, J. (1979). alpha-Bungarotoxin and anti-acetylcholine receptor antibody binding to the human acetylcholine receptor. *Adv Cytopharmacol.* 3, 269–278.

Vincent, A., and Newsom-Davis, J. (1982). Acetylcholine receptor antibody characteristics in myasthenia gravis. I. Patients with generalized myasthenia or disease restricted to ocular muscles. *Clin. Exp. Immunol.* 49, 257–265.

Vincent, A., and Newsom-Davis, J. (1985). Acetylcholine receptor antibody as a diagnostic test for myasthenia gravis: results in 153 validated cases and 2967 diagnostic assays. *J. Neurol. Neurosurg. Psychiatry* 48, 1246–1252.

Vincent, A., Whiting, P. J., Schluep, M., Heidenreich, F., Lang, B., Roberts, A., et al. (1987). Antibody heterogeneity and specificity in myasthenia gravis. *Ann. N. Y. Acad. Sci.* 505, 106–120.

Wagoner, P. K., and Pallotta, B. S. (1988). Modulation of acetylcholine receptor desensitization by forskolin is independent of cAMP. *Science* 240, 1655–1657.

Wanamaker, C. P., Christianson, J. C., and Green, W. N. (2003). Regulation of nicotinic acetylcholine receptor assembly. *Ann. N. Y. Acad. Sci.* 998, 66–80.

Wang, S., Seaberg, B., Paez-Colasante, X., and Rimer, M. (2016). Defective acetylcholine receptor subunit switch precedes atrophy of slow-twitch skeletal muscle fibers lacking ERK1/2 Kinases in Soleus muscle. *Sci. Rep.* 6:38745.

Wang, X., Engisch, K. L., Teichert, R. W., Olivera, B. M., Pinter, M. J., and Rich, M. M. (2006). Prolongation of evoked and spontaneous synaptic currents at the neuromuscular junction after activity blockade is caused by the upregulation of fetal acetylcholine receptors. *J. Neurosci.* 26, 8983–8987.

Weatherbee, S. D., Anderson, K. V., and Niswander, L. A. (2006). LDL-receptor-related protein 4 is crucial for formation of the neuromuscular junction. *Development* 133, 4993–5000.

Webster, R., Maxwell, S., Spearman, H., Tai, K., Beckstein, O., Sansom, M., et al. (2012). A novel congenital myasthenic syndrome due to decreased acetylcholine receptor ion-channel conductance. *Brain* 135, 1070–1080.

Whiting, P. J., Vincent, A., Schluep, M., and Newsom-Davis, J. (1986). Monoclonal antibodies that distinguish between normal and denervated human acetylcholine receptor. *J. Neuroimmunol.* 11, 223–235.

Wilson, G., and Karlin, A. (2001). Acetylcholine receptor channel structure in the resting, open, and desensitized states probed with the substituted-cysteine-accessibility method. *Proc. Natl. Acad. Sci. U.S.A.* 98, 1241–1248.

Witzemann, V., Barg, B., Criado, M., Stein, E., and Sakmann, B. (1989). Developmental regulation of five subunit specific mRNAs encoding acetylcholine receptor subtypes in rat muscle. *FEBS Lett.* 242, 419–424.

Yang, X., Arber, S., William, C., Li, L., Tanabe, Y., Jessell, T. M., et al. (2001). Patterning of muscle acetylcholine receptor gene expression in the absence of motor innervation. *Neuron* 30, 399–410.

Yu Wai Man, C. Y., Chinnery, P. F., and Griffiths, P. G. (2005). Extraocular muscles have fundamentally distinct properties that make them selectively vulnerable to certain disorders. *Neuromuscul. Disord.* 15, 17–23.

Zeisel, S. H., and Niculescu, M. D. (2006). Perinatal choline influences brain structure and function. *Nutr. Rev.* 64, 197–203.

Zhang, B., Liang, C., Bates, R., Yin, Y., Xiong, W. C., and Mei, L. (2012). Wnt proteins regulate acetylcholine receptor clustering in muscle cells. *Mol. Brain* 5:7.

Zisimopoulou, P., Lagoumintzis, G., Poulas, K., and Tzartos, S. J. (2008). Antigen-specific apheresis of human anti-acetylcholine receptor autoantibodies from myasthenia gravis patients' sera using *Escherichia coli*-expressed receptor domains. *J. Neuroimmunol.* 200, 133–141.

Zong, Y., Zhang, B., Gu, S., Lee, K., Zhou, J., Yao, G., et al. (2012). Structural basis of agrin-LRP4-MuSK signaling. *Genes Dev.* 26, 247–258.

Conflict of Interest: The authors declare that the research was conducted in the absence of any commercial or financial relationships that could be construed as a potential conflict of interest.

Copyright © 2020 Cetin, Beeson, Vincent and Webster. This is an open-access article distributed under the terms of the Creative Commons Attribution License (CC BY). The use, distribution or reproduction in other forums is permitted, provided the original author(s) and the copyright owner(s) are credited and that the original publication in this journal is cited, in accordance with accepted academic practice. No use, distribution or reproduction is permitted which does not comply with these terms.

frontiers in Molecular Neuroscience

BRIEF RESEARCH REPORT
published: 08 September 2020
doi: 10.3389/fnmol.2020.00154

Gene Expression Profile at the Motor Endplate of the Neuromuscular Junction of Fast-Twitch Muscle

*Kun Huang[1], Jin Li[1], Mikako Ito[1], Jun-Ichi Takeda[1], Bisei Ohkawara[1], Tomoo Ogi[2], Akio Masuda[1] and Kinji Ohno[1]**

[1]Division of Neurogenetics, Center for Neurological Diseases and Cancer, Nagoya University Graduate School of Medicine, Nagoya, Japan, [2]Department of Genetics, Research Institute of Environmental Medicine (RIeM), Nagoya University, Nagoya, Japan

The neuromuscular junction (NMJ) is a prototypic chemical synapse between the spinal motor neuron and the motor endplate. Gene expression profiles of the motor endplate are not fully elucidated. Collagen Q (ColQ) is a collagenic tail subunit of asymmetric forms of acetylcholinesterase and is driven by two distinct promoters. p*ColQ1* is active throughout the slow-twitch muscle, whereas p*ColQ1a* is active at the motor endplate of fast-twitch muscle. We made a transgenic mouse line that expresses nuclear localization signal (NLS)-attached Cre recombinase under the control of p*ColQ1a* (p*ColQ1a*-Cre mouse). RiboTag mouse expresses an HA-tagged ribosomal subunit, RPL22, in cells expressing Cre recombinase. We generated p*ColQ1a*-Cre:RiboTag mouse, and confirmed that HA-tagged RPL22 was enriched at the NMJ of tibialis anterior (TA) muscle. Next, we confirmed that *Chrne* and *Musk* that are specifically expressed at the NMJ were indeed enriched in HA-immunoprecipitated (IP) RNA, whereas *Sox10* and *S100b*, markers for Schwann cells, and *Icam1*, a marker for vascular endothelial cells, and *Pax3*, a marker for muscle satellite cells, were scarcely detected. Gene set enrichment analysis (GSEA) of RNA-seq data showed that "phosphatidylinositol signaling system" and "extracellular matrix receptor interaction" were enriched at the motor endplate. Subsequent analysis revealed that genes encoding diacylglycerol kinases, phosphatidylinositol kinases, phospholipases, integrins, and laminins were enriched at the motor endplate. We first characterized the gene expression profile under translation at the motor endplate of TA muscle using the RiboTag technique. We expect that our gene expression profiling will help elucidate molecular mechanisms of the development, maintenance, and pathology of the NMJ.

Keywords: neuromuscular junction, motor endplate, collagen Q, ribotag mouse, gene expression profile

OPEN ACCESS

Edited by:
Ruth Herbst,
Medical University of Vienna, Austria

Reviewed by:
Said Hashemolhosseini,
University of Erlangen Nuremberg, Germany
Karl Tsim,
Hong Kong University of Science and Technology, Hong Kong

Correspondence:
Kinji Ohno
ohnok@med.nagoya-u.ac.jp

Received: *30 May 2020*
Accepted: *27 July 2020*
Published: *08 September 2020*

Citation:
Huang K, Li J, Ito M, Takeda J-I, Ohkawara B, Ogi T, Masuda A and Ohno K (2020) Gene Expression Profile at the Motor Endplate of the Neuromuscular Junction of Fast-Twitch Muscle. Front. Mol. Neurosci. 13:154. doi: 10.3389/fnmol.2020.00154

INTRODUCTION

Neuromuscular junction (NMJ) is a prototypic synapse between the spinal motor neuron and the motor endplate (Hirsch, 2007; Ohno et al., 2017). At the NMJ, acetylcholinesterase (AChE) rapidly hydrolyzes acetylcholine (ACh) released from the nerve terminal (Ohno et al., 1998; Gaspersic et al., 1999). At the NMJ, a globular form of AChE makes a homomeric tetramer. One, two, and three tetrameric AChE are bound to triple-helical collagen Q (ColQ) to make asymmetric A_4, A_8, and A_{12} forms, and are anchored to the synaptic basal lamina (Nazim et al., 2017). Transcription of

Colq is driven by two distinct promoters of p*ColQ1* and p*ColQ1a* (**Figure 1A**; Krejci et al., 1999; Lee et al., 2004; Ting et al., 2005). p*ColQ1* is active throughout the slow-twitch muscle. p*ColQ1* starts transcription from *Colq* exon 1 to generate A_4 and A_8 forms. In contrast, p*ColQ1a* is active at the NMJ, but not at the extrajunctional regions, of the fast-twitch muscle. p*ColQ1a* starts transcription from *Colq* exon 1a to predominantly generate A_{12} form. Human p*ColQ1a* carries consensus sequences for transcriptional factors E-protein (E-box, CANNTG), NFAT (GGAAA), c-Ets transcription factor [c-Ets, (C/A)GGA(A/T)], Elk-1, N-box (CCGGAA), and MEF2 (CTAAAAATAA), which play essential roles in muscle-specific and NMJ-specific transcriptional activities (Lee et al., 2004).

Massive parallel sequencing of RNA (RNA-seq) enabled the identification of gene expression profiles in specific tissues and cells at an unprecedented level of accuracy. Also, tissue-specific and cell-type-specific transcriptomic profiling is made available by fluorescence-activated cell sorting (FACS), laser capture microdissection, and single-cell RNA-seq (scRNA-seq; Kim et al., 2015). However, gene expression profiles can be artificially changed in the course of FACS and scRNA-seq procedures. In laser capture microdissection, target cells are frequently contaminated by surrounding cells, because target cells should be free from laser burns. RiboTag mouse technique was developed to circumvent these disadvantages (Sanz et al., 2009). RiboTag mouse carries an RPL22 subunit of the ribosome with a hemagglutinin tag at the C-terminal end (RPL22-HA), and its expression is induced by Cre recombinase (Sanz et al., 2009). Cell-type-specific expression of Cre recombinase thus enables isolation of total mRNA under translation in a cell-type-specific manner.

In our study, we first generated a transgenic p*ColQ1a*-Cre mouse that specifically expresses Cre recombinase in the subsynaptic nuclei of fast-twitch muscle. As far as we know, no transgenic mouse has been generated to express Cre recombinase at the motor endplate. We confirmed that Cre recombinase is highly expressed at the NMJ of fast-twitch muscle, but not of slow-twitch muscle, in the p*ColQ1a*-Cre mouse. To characterize gene expression profiles at the motor endplate of fast-twitch muscle, we made p*ColQ1a*-Cre:RiboTag mouse that expresses RPL22-HA only at the motor endplate. Quantitative RT-PCR (qRT-PCR) showed that mRNA immunoprecipitated with the HA tag from tibialis anterior (TA) muscle of p*ColQ1a*-Cre:RiboTag mouse was enriched for motor endplate-specific genes, and mostly depleted for genes specific for Schwann cells and vascular endothelial cells. RNA-seq analysis of HA-immunoprecipitated mRNA revealed enrichment of genes encoding diacylglycerol kinases, phosphatidylinositol kinases, phospholipases, integrins, and laminins.

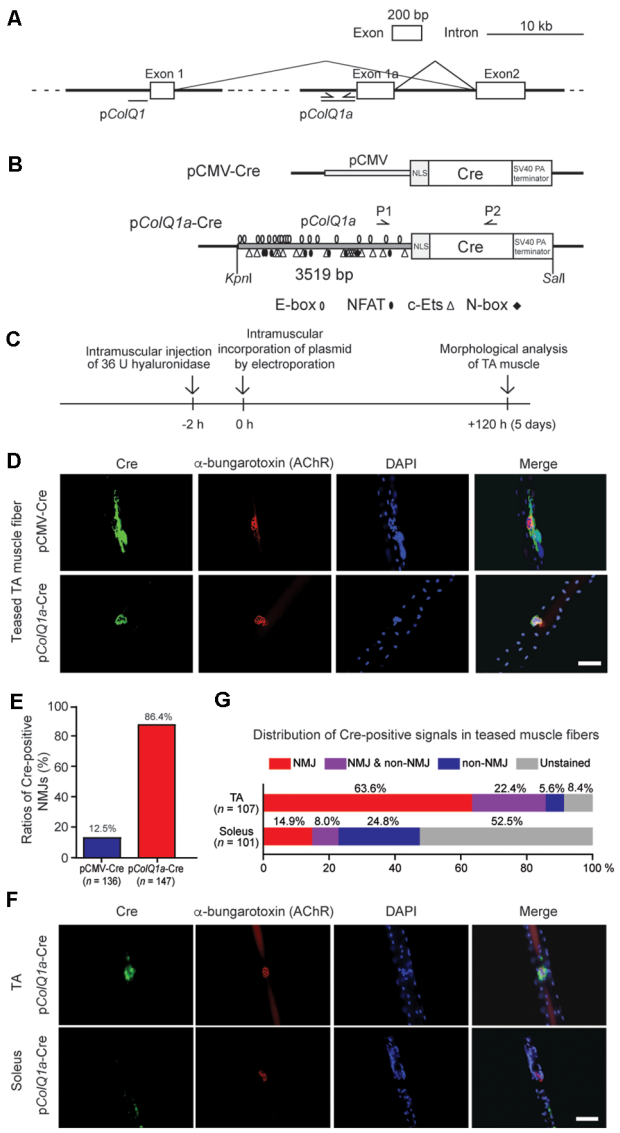

FIGURE 1 | Mouse p*ColQ1a* promoter expresses Cre at the neuromuscular junction (NMJ) of the tibialis anterior (TA) muscle. **(A)** Mouse *Colq* is driven by two distinct promoters. p*ColQ1* drives transcription from exon 1, whereas p*ColQ1a* drives transcription from exon 1a. PCR primers (**Supplementary Table S1**) to amplify a 3519-bp fragment of p*ColQ1a* are indicated by arrows. **(B)** Schematic of pCMV-Cre and p*ColQ1a*-Cre. pCMV or p*ColQ1a* was fused to the nuclear localization signal (NLS) sequence and the Cre recombinase gene. P1 and P2 arrows indicate the positions of genotyping primers. Putative binding motifs of transcription factors (E-box, NFAT, c-Ets, and N-box) are indicated (Lee et al., 2004). **(C)** The protocol of muscle electroporation. **(D)** Representative immunostaining of Cre (green) and Alexa594-conjugated α-bungarotoxin-staining for AChR (red) of teased TA muscle fibers at 5 days after electroporation of the indicated plasmids. The nuclei were stained with DAPI. Scale bar = 30 μm. **(E)** Ratios of Cre-positive NMJs in teased TA muscle fibers electroporated with pCMV-Cre and p*ColQ1a*-Cre in 4 pCMV-Cre mice (n = 136 fibers, respectively) and 5 p*ColQ1a*-Cre mice (n = 147 fibers). $P < 0.001$ by Fisher's exact test (see **Supplementary Table S3** for individual counts). **(F)** Representative images showing NMJ-specific expression of Cre in teased TA muscle fibers but not in teased soleus muscle fibers of the p*ColQ1a*-Cre mouse. Teased muscle fibers were stained with anti-Cre antibody (green) and

(*Continued*)

MATERIALS AND METHODS

Construction of Plasmids

A Cre cDNA originating from Type I topoisomerase of bacteriophage P1 fragment was amplified from a pAAV-Cre plasmid (AAV-401, Cell Biolabs). The nuclear localization signal (NLS) of the SV40 large T antigen sequence (5'-GAGCACCA

FIGURE 1 | Continued
Alexa594-conjugated α-bungarotoxin 594 (red). Nuclei were stained with DAPI. Scale bar = 30 μm. **(G)** Distribution of Cre-positive signals along teased muscle fibers of TA and soleus muscles of the p*ColQ1a*-Cre mouse. The total number of teased muscle fibers is shown in parentheses. $P < 0.001$ by Fisher's exact test (see **Supplementary Table S4** for individual counts).

TGCCAAAAAAGAAGAGAAAGGTATCCAATTTAC-3') was synthesized by Sigma–Aldrich. A 3519-bp mouse p*ColQ1a* promoter (positions 31,557,371–31,553,853 on chromosome 14 according to GRCm38/mm10) was amplified by PCR using genomic DNA of C57BL/6 mouse. We ligated p*ColQ1a*, NLS, and Cre cDNA to generate p*ColQ1a*-Cre (**Figure 1B**). As a control, we generated pCMV-Cre. Primers for PCR are shown in **Supplementary Table S1**. Plasmids were purified with the EndoFree Megaprep DNA Purification System (Qiagen). The absence of artifacts in the plasmid inserts was confirmed by Sanger sequencing.

Immunofluorescent Staining

TA and soleus muscles were harvested and fixed in 4% paraformaldehyde (PFA) for 1 h and were teased into muscle fibers in phosphate-buffered saline (PBS). The teased fibers were incubated in 100 mM glycine in PBS for 15 min at room temperature (RT). The fibers were washed in PBS three times for 15 min each and were incubated in a blocking buffer (2% bovine serum albumin, 5% goat serum, and 0.5% Triton X-100 in PBS) for 1 h at RT. After blocking, the fibers were incubated with mouse monoclonal anti-Cre recombinase antibody (1:100, MAB3120, Millipore) or anti-HA antibody (1:200, Covance) in a blocking buffer overnight at 4°C. After washed in 0.1% Triton X-100 in PBS several times, the fibers were incubated with FITC-conjugated goat anti-mouse IgG (1:100, FI2000, Vector Laboratories). AChR was stained with Alexa 594-conjugated α-bungarotoxin (1:500, B13423, Invitrogen) for 2 h at RT. Finally, the fibers were covered by a coverslip with Vectashield with 4',6-diamidino-2-phenylindole (DAPI; Vector Laboratories). Fluorescence signals were quantified by the IX71 microscope (Olympus) equipped with the MetaMorph imaging software (Molecular Devices).

Frozen sections of TA muscle at 10 μm were incubated with a primary antibody (anti-HA antibody at 1:200, Covance) overnight at 4°C. The sections were added with FITC-conjugated goat anti-mouse IgG (1:100, FI2000, Vector Laboratories) and Alexa 594-conjugated α-bungarotoxin (1:500, B13423, Invitrogen) followed by incubation for 1 h at RT. Finally, the sections were covered by a coverslip with Vectashield with DAPI, and fluorescence signals were quantified as stated above.

Electroporation of Plasmids Into Mouse TA and Soleus Muscle

All mouse experiments were approved by the Animal Care and Use Committee of the Nagoya University Graduate School of Medicine and were performed following the relevant guidelines. Under deep anesthesia of a 6-week-old C57BL/6 mouse, 36 U hyaluronidase (H4272, SIGMA) was injected into the TA muscle 2 h before injection of pCMV-Cre or p*ColQ1a*-Cre. Then, 50 μl of each plasmid (1,000 ng/μl) was injected into the TA or soleus muscle and applied electrical pulses at 50 volts. The electric pulses were delivered in parallel to the muscle fibers with forceps-shaped electrodes (CUY650P3, Nepa Gene) connected to an electric pulse generator (NEPA21, Nepa Gene). The electrical pulses were comprised of three pulses of a rectangular wave for 25 ms at a rate of 3 Hz, followed by three pulses of the opposite polarity with the same protocol. TA or soleus muscle was harvested on day 5 after electroporation.

Generation of p*ColQ1a*-Cre Mouse

A fragment of p*ColQ1a*-Cre (**Figure 1B**) was microinjected into fertilized eggs of C57BL/6 mouse. The microinjection and subsequent transfer to foster mothers were technically supported by the Division of Experimental Animals, Nagoya University Graduate School of Medicine.

Generation of p*ColQ1a*-Cre:RiboTag Mouse

RiboTag mice were kindly provided by Dr. Taiji Matsusaka at Tokai University under the permission of Dr. Paul S. Amieux at Western Washington University (Sanz et al., 2009). RiboTag mouse was mated to p*ColQ1a*-Cre mouse to obtain p*ColQ1a*-Cre:RiboTag mouse.

Immunoprecipitation Assays

Immunoprecipitation (IP) of pooled TA muscles of 6-week-old p*ColQ1a*-Cre:RiboTag mice was performed as described previously with minor modifications (Sanz et al., 2009). Briefly, TA muscle was mashed by FastPrep 24 Instrument (MBP) in an IP buffer (50 mM Tris-HCl, pH 7.5, 100 mM KCl, 12 mM $MgCl_2$, 1% Nonidet P-40, 1 mM DTT, 400 units/ml Toyobo RNase Inhibitor, 1 mg/ml heparin, 100 μg/ml cycloheximide, and the cOmplete protease inhibitor (one tablet in 25 ml, Roche). Then, anti-HA antibody (1:300, Covance) was added to 1,200 μl of cleared homogenates and incubated for 6 h at 4°C. Then protein G magnetic beads (Dynabeads, Invitrogen) in an IP buffer were added and incubated overnight at 4°C. After incubation, beads were washed four times for 5 min in a high-salt buffer (50 mM Tris-HCl, pH 7.5, 300 mM KCl, 12 mM $MgCl_2$, 1% Nonidet P-40, 1 mM DTT, and 100 μg/ml cycloheximide) in the presence of 400 units/ml RNase Inhibitor (Toyobo) and the cOmplete™ protease inhibitor (one tablet in 25 ml, Roche). RNA was eluted in an RLT buffer with β-mercaptoethanol (Qiagen) and was purified by RNeasy Micro Kit (Qiagen) with DNase treatment. Total RNA was quantified and its quality was evaluated by RNA integrity number (RIN; Schroeder et al., 2006) representing the quality and integrity of RNA using an Agilent 2100 Bioanalyzer with the RNA 6000 Pico kit (Agilent Technologies).

Gene Expression Analysis

After confirming that the RIN was higher than 7.0, total RNA was reverse-transcribed using random hexamer primers (Thermo Fisher Scientific) and ReverTra Ace (Toyobo). Quantitative RT-PCR (qRT-PCR) was performed with the LightCycler 480 (Roche Applied Science) using the TB Green Premix ExTaq II (Takara Bio). Gene expression levels were normalized to that of glyceraldehyde-3-phosphate

dehydrogenase (*Gapdh*), and also to the ratio of input RNA. For both IP RNA and input RNA, TA muscles of 10, 11, 12, and 16 p*ColQ1a*-Cre:Ribotag mice were pooled into four independent samples to be analyzed in quadruplicate. qRT-PCR primers are indicated in **Supplementary Table S2**.

High-Throughput RNA Sequencing (RNA-Seq)

In the four pooled pairs of IP RNA and input RNA samples stated above, a pair of samples arising from 11 p*ColQ1a*-Cre:Ribotag mice had the highest RIN in both IP RNA and input RNA, and was subjected to RNA-seq. Quality of the RNA samples was checked using both an Agilent TapeStation and an Agilent 2100 Bioanalyzer with the RNA 6000 Nano Kit, and the following thresholds were applied: quantity (>100 ng), concentration (>1 ng/μl), no contamination of DNA, no degradation of RNA confirmed by rRNA peaks (18S, 28S), and RIN (>7.0). RNA-seq of Input RNA and IP RNA was performed at Macrogen and BGI, respectively. At both companies, a sequencing library was prepared using the TruSeq Stranded mRNA kit (Illumina), and the library was read on Illumina NovaSeq 6000 (150 bp paired-end reads). As the amount of IP RNA remained low even after pooling TA muscles, IP RNA was linearly amplified by the Smart-seq2 protocols (Picelli et al., 2014). Raw reads were mapped to the mouse reference genome (NCBI37/mm9) using STAR version 2.5.3a (Dobin et al., 2013) with standard options for the long RNA-seq pipeline by ENCODE (Consortium, 2012). Transcripts per million (TPM) of each gene was calculated by RSEM version 1.3.1 with default parameters (Li and Dewey, 2011).

Gene Set Enrichment Analysis (GSEA)

We performed pathway analysis with Gene Set Enrichment Analysis (GSEA[1]; Vickers et al., 2008) using the following parameters: the number of permutations was 1,000; the phenotype labels were "IP vs. input;" the collapse/remap to gene symbols was "collapse;" the permutation type was configured to the "gene set" to avoid the potential problem of small sample size; and the chip platform was "Mouse Gene Symbol Remapping to Human Orthologs MSigDB.v7.1.chip." The KEGG subset of canonical pathways (186 gene sets) was used as a reference gene set. Nominal p-value <0.05 and false-discovery rate (FDR) q-value <0.25 were used as the cut-off criteria (Reimand et al., 2019).

RESULTS

Mouse p*ColQ1a* Promoter Expresses Cre at the NMJ of the TA Muscle

Transcriptions of the mouse *ColQ* gene start from exons 1 and 1a, which are driven by p*ColQ1* and p*ColQ1a* promoters, respectively (**Figure 1A**). A 3519-bp DNA fragment of mouse p*ColQ1a* was amplified by PCR and was added 5′ to the nuclear localization signal (NLS) and Cre cDNA to generate a p*ColQ1a*-Cre plasmid (**Figure 1B**). As the skeletal muscle fibers are comprised of multi-nucleated cells, NLS-mediated confinement of Cre in the nuclei was essential.

To confirm that p*ColQ1a*-Cre expresses Cre specifically in the subsynaptic nuclei of TA muscle, we introduced p*ColQ1a*-Cre in the mouse hindlimb by electroporation (**Figure 1C**; Murakami et al., 2003; Young and Dean, 2015). pCMV-Cre was used as a control. The TA and soleus muscles were teased into single fibers to visualize the NMJs. pCMV-Cre expressed Cre throughout TA muscle, and only 12.5% of Cre-positive areas were overlapped with AChR-positive areas. In contrast, p*ColQ1a*-Cre expressed Cre at the NMJ of TA muscle, and 86.4% of Cre-positive areas were overlapped with AChR-positive areas (**Figures 1D,E** and **Supplementary Table S3**). These results indicate that the p*ColQ1a* promoter drove the subsynaptic expression of Cre in the TA muscle.

Next, we generated a transgenic mouse line carrying p*ColQ1a*-Cre. The expression of Cre was again examined in teased muscle fibers of the TA and soleus muscles, which are mostly comprised of fast-twitch and slow-twitch muscle fibers, respectively (**Figure 1F**). In TA muscle, 63.6% of teased muscle fibers expressed Cre at the NMJ. In contrast, in soleus muscle, the ratio was only 14.9%. Notably, 52.5% of the soleus muscle fibers did not express Cre either at the NMJ or at the extrajunctional regions (**Figure 1G** and **Supplementary Table S4**). These results indicate that the 3519-bp fragment of the mouse p*ColQ1a* promoter region restricted the expression of Cre at the NMJs of fast-twitch muscle but not of slow-twitch muscle.

p*ColQ1a*-Cre:Ribotag Mouse Expresses HA-Tagged Ribosomal Protein RPL22 at the NMJ of TA Muscle

We next mated our p*ColQ1a*-Cre mouse with RiboTag mouse (Sanz et al., 2009). The generated p*ColQ1a*-Cre:Ribotag mouse should express HA-tagged ribosomal protein RPL22 specifically at the motor endplate of fast-twitch muscle. To verify that the HA-tagged ribosomes were expressed specifically at the NMJ in p*ColQ1a*-Cre:RiboTag mice, we immunostained the HA-tag in cross-sections of TA muscle (**Figure 2A**) and teased TA muscle fibers (**Figure 2B**). Staining for the HA-tag was mostly overlapped with α-bungarotoxin-stained AChR in cross-sections of TA muscle (**Figure 2A**) and teased TA muscle fibers (**Figure 2B**).

Enrichment of NMJ-Specific Genes and Paucity of Genes in Other Cell Types in TA Muscle of p*ColQ1a*-Cre:Ribotag Mouse

To identify gene expression profiles at the motor endplate of TA muscle, we immunoprecipitated mRNA under translation using an anti-HA antibody, which was compared with input RNA (**Figure 2C**). We obtained ∼30 ng of immunoprecipitated (IP) RNA and ∼200 ng of input RNA by pooling TA muscles of 11 p*ColQ1a*-Cre:RiboTag mice. As a control, we confirmed that only 0.67 ng RNA was immunoprecipitated by anti-HA antibody by pooling TA muscles of eight wild type mice. We confirmed that the RNA integrity numbers (RIN), representing the quality of RNA, of the IP and input RNA were more than

[1]http://software.broadinstitute.org/gsea/index.jsp

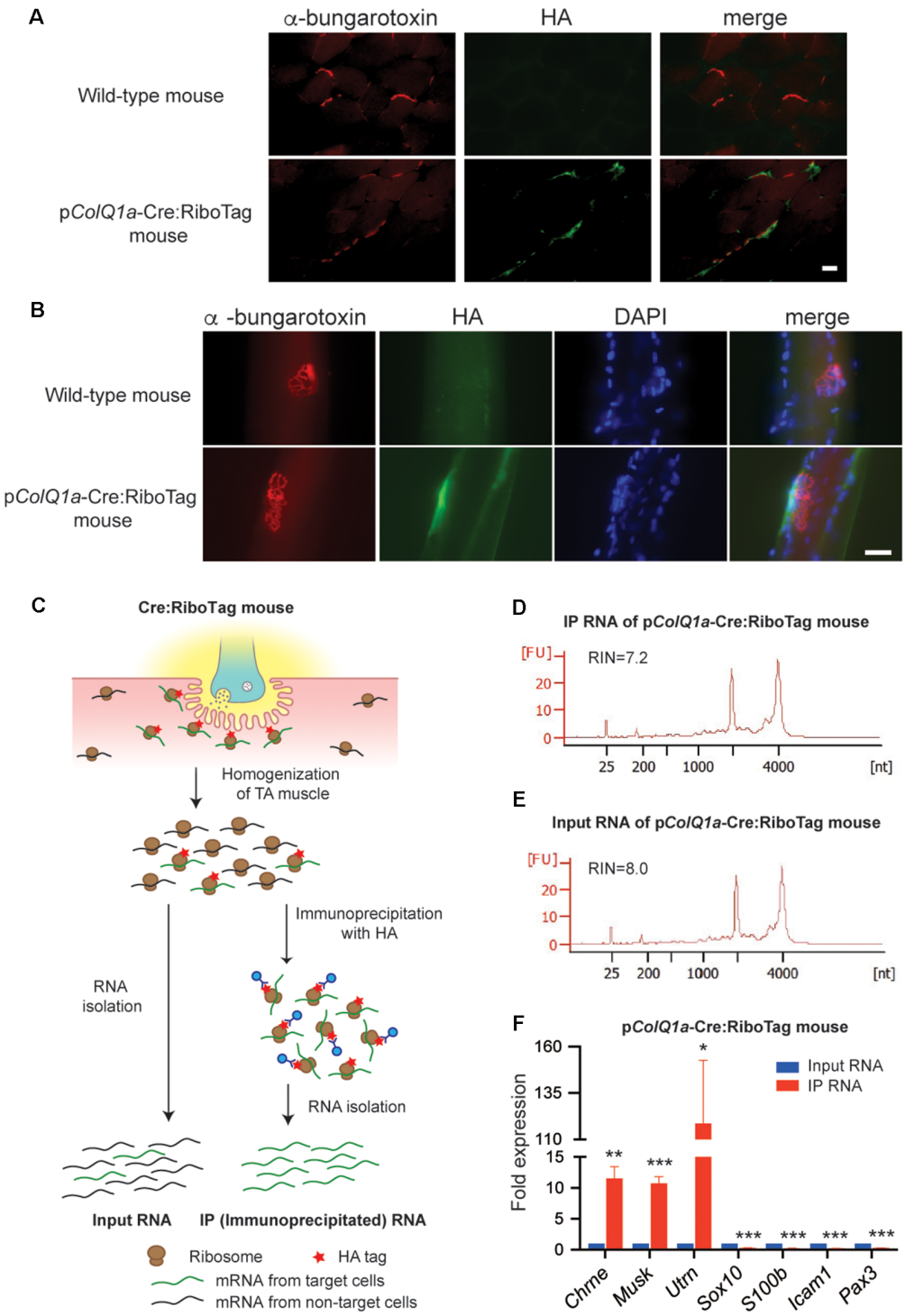

FIGURE 2 | p*ColQ1a*-Cre:Ribotag mouse to disclose a gene expression profile at the motor endplate TA muscle. **(A,B)** Immunofluorescence staining of TA muscle of wild-type and p*ColQ1a*-Cre:RiboTag mice. Muscle sections **(A)** and teased muscle fibers **(B)** are stained with anti-HA antibody (green) and Alexa594-conjugated α-bungarotoxin 594 (red). Nuclei are stained with DAPI. Scale bar = 15 μm. **(C)** Schematic of the RiboTag technique for gene expression profiling at the motor endplate of TA muscle. **(D,E)** Agilent Technologies 2100 Bioanalyzer PicoChip outputs showing the quality of immunoprecipitated (IP) RNA **(D)** and input RNA **(E)**. **(F)** qRT-PCR of NMJ-specific *Chrne*, *Musk*, and *Utrn* genes, Schwann cell-specific *Sox10* and *S100b*, vascular endothelial cell-specific *Icam1*, and muscle satellite cell-specific *Pax3*. Gene expression level in IP RNA was normalized to that of *Gapdh*, and also to the ratio in input RNA. TA muscles of 10, 11, 12, and 16 p*ColQ1a*-Cre:Ribotag mice were pooled into four independent samples, and were analyzed in quadruplicate ($n = 4$). Mean and SD is indicated. $^{*}p < 0.05$, $^{**}p < 0.01$ and $^{***}p < 0.001$ by paired Student's *t*-test.

7.0 (**Figures 2D,E**). We first verified that expressions of *Chrne*, *MuSK*, and *Utrn* that should be concentrated in the subsynaptic nuclei were enriched in IP RNA (**Figure 2F**). In contrast, markers for Schwann cells (*Sox10* and *S100b*), vascular endothelial cells (*Icam1*), and muscle satellite cells (*Pax3*) were markedly attenuated in IP RNA (**Figure 2F**). Therefore, IP RNA of TA muscles of p*ColQ1a*-Cre:RiboTag mice were highly enriched in motor endplate-specific genes with scarce contamination of genes from adjacent cells at the NMJ.

Differential Gene Expression (DGE) Analysis Reveals Genes That Are Up- or Down-Regulated at the Motor Endplate of TA Muscle

To extensively characterize a gene expression profile under translation at the motor endplate of TA muscle, we performed RNA-seq analysis of IP RNA and input RNA. A scatter plot of transcripts per million (TPM) of 22,383 protein-coding genes in IP RNA and input RNA showed that the coefficient of determination (r^2) was 0.6225 (**Figure 3A**). As have been previously applied in other studies (Srivastava et al., 2017; Wang et al., 2019), we arbitrarily filtered genes with TPM >0.5 and fold change (IP/input or input/IP) >10. Differential gene expression (DGE) analysis identified 1177 genes: 1153 genes were upregulated and 24 genes were downregulated in the subsynaptic nuclei of TA muscle. The top 20 upregulated genes and the top 20 downregulated genes are graphically shown in **Figures 3B,C**, respectively.

Gene Set Enrichment Analysis (GSEA) Reveals Key Gene Sets That Are Enriched at the Motor Endplate of TA Muscle

To further characterize gene sets that were specifically enriched at the motor endplate of TA muscle, we performed GSEA using 186 gene sets retrieved from the Kyoto Encyclopedia of Genes and Genomes (KEGG) database. We found that two gene sets of "phosphatidylinositol signaling system" and "ECM receptor interaction" were enriched at the motor endplate (nominal $p < 0.05$, FDR $q < 0.25$; **Figures 4A–C** and **Supplementary Table S5**). We also made a set of genes that are expressed at the motor endplate and are associated with myasthenia gravis and postsynaptic congenital myasthenic syndromes such as *Chrne*, *Musk*, and *Dok7*. GSEA analysis showed that these genes were enriched at the motor endplate of TA muscle but without statistical significance, which was likely due to the limited number of genes ($p = 0.070$, **Supplementary Figure S1** and **Supplementary Table S5**). The gene set "phosphatidylinositol signaling system" included genes encoding diacylglycerol kinases (*DGK**), phosphatidylinositol kinases (*PIK**), and phospholipases (*PL**). Similarly, the gene set "ECM receptor interaction" included genes encoding integrins (*ITG**) and laminins (*LAM**). We made our own gene sets for the five gene families and performed GSEA analysis, and found that these genes were indeed enriched at the motor endplate of TA muscle (**Figures 4D–I** and **Supplementary Table S5**).

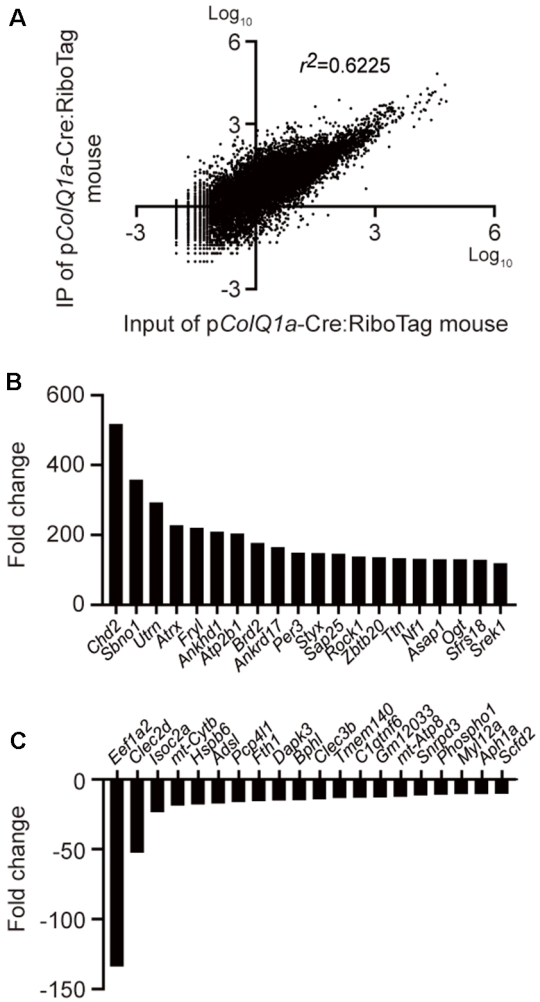

FIGURE 3 | Differentially expressed genes between IP RNA and input RNA of the TA muscle. **(A)** Scatter plot of gene expressions in transcripts per million (TPM) between IP RNA and input RNA. The coefficient of determination (r^2) is indicated. Representative upregulated **(B)** and downregulated **(C)** genes that were ranked top 20 each.

DISCUSSION

We first confirmed that p*ColQ1a* drives the expression of NLS-tagged Cre recombinase specifically at the motor endplate of TA muscle (**Figure 1**), and made a transgenic p*ColQ1a*-Cre mouse line. We then mated RiboTag mouse with the p*ColQ1a*-Cre mouse to make p*ColQ1a*-Cre:RiboTag mouse, which expressed an HA-tagged RPL22 specifically at the motor endplate of TA muscle (**Figure 2**) and enabled NMJ-specific gene expression profiling. mRNA under translation at the motor endplate was co-immunoprecipitated by an anti-HA antibody (**Figure 2C**). We confirmed that motor endplate-specific *Chrne* and *Musk* were enriched in IP RNA, whereas Schwann cell-specific *Sox10* and *S100b*, vascular endothelial cell-specific *Icam1*, and muscle satellite cell-specific *Pax3* were much reduced in IP RNA (**Figure 2F**). We then analyzed IP RNA by RNA-seq. We compared IP RNA with input RNA obtained

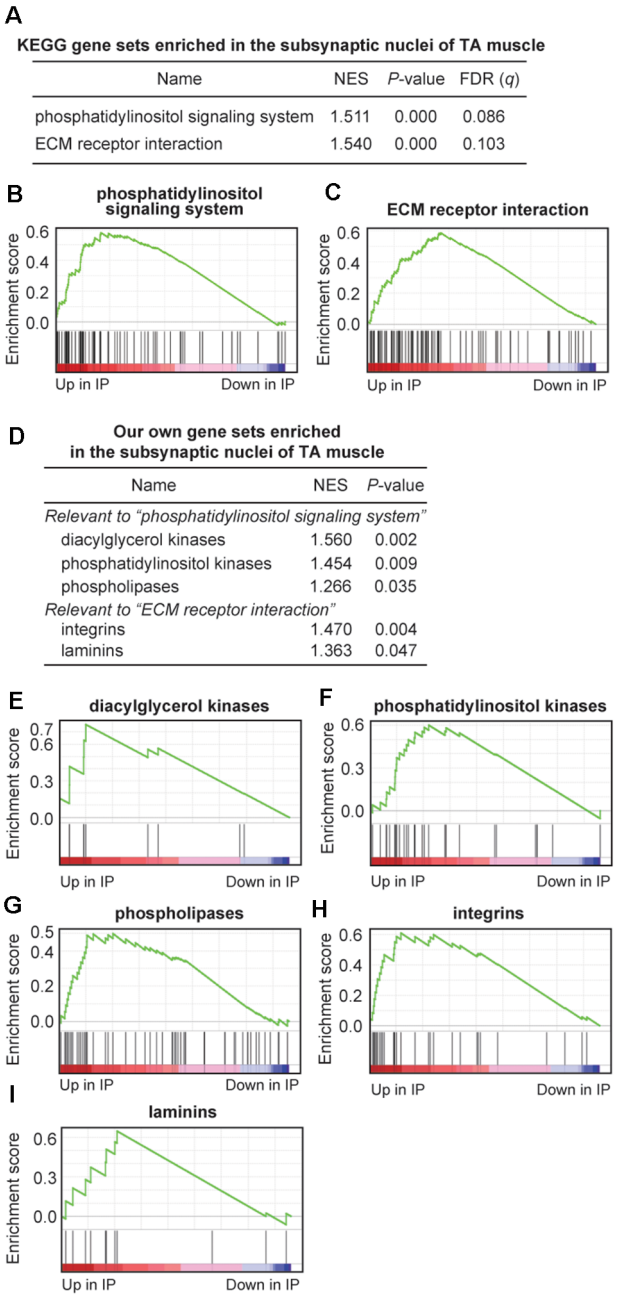

FIGURE 4 | Gene sets enriched at the motor endplate of TA muscle by Gene Set Enrichment Analysis (GSEA) analysis. **(A–C)** Two KEGG gene sets were enriched at the motor endplate of TA muscle, which exceeded the thresholds of nominal p-value < 0.05 and false-discovery rate (FDR) q-value < 0.25. NES, normalized enrichment score of GSEA. **(D–I)** Enrichment at the motor endplate of TA muscle of our gene sets inspired by the two KEGG gene sets **(A)**. Our own gene sets are not subsets of the two KEGG gene sets but include additional relevant genes. See **Supplementary Table S5** for gene names and TPM values included in each gene set.

from whole TA muscle to characterize motor endplate-specific gene expression profile of TA muscle (**Figures 3**, **4**).

The mechanisms of NMJ-specific transcriptions of *ColQ* has been previously reported. Laser capture microdissection of the mouse NMJ revealed NMJ-specific expression of *ColQ* in the extraocular muscles (Ketterer et al., 2010) and the TA muscle (Nazarian et al., 2005; Ketterer et al., 2010). The NMJ-specific expression of *ColQ* is mediated by transcriptional upregulation at the NMJ and transcriptional downregulation in the extra-junctional regions. The E-box (CANNTG) in p*ColQ1a* binds to the myogenic differentiation factors (MDFs) of the MyoD family and drives muscle-specific gene expression (Lee et al., 2004). Contrarily, muscle action potentials suppress the E-box at the extra-junctional regions to drive NMJ-specific expression of an E-box-bearing gene (Ting et al., 2005). Transcription of most muscle-specific genes, however, are not suppressed by electrical activity, and other unidentified *cis*-elements are likely to be operational to achieve electrical transcriptional suppression (Ohno et al., 1999). Transcriptional upregulation of p*ColQ1a* at the NMJ is mediated by the N-box (CCGGAA; Lee et al., 2004). The N-box (CGGAA) is also the neuregulin-response element in mouse *Chrnd* encoding the δ subunit of acetylcholine receptor (AChR; Fromm and Burden, 1998) and in rat *Chrne* encoding the AChR ε subunit (Sapru et al., 1998). Similar involvement of the neuregulin-responsive N-box in the NMJ-specific transcription of *ColQ* in mouse have also been reported (Lee et al., 2004; Ting et al., 2005). Also, specific activation of p*ColQ1* and p*ColQ1a* in slow- and fast-twitch muscles, respectively, is mediated by a slow upstream regulatory element (SURE) in p*ColQ1* and a fast intronic regulatory element (FIRE) in p*ColQ1a* (Lee et al., 2004; Ting et al., 2005).

Cell-type-specific expression analysis has gained popularity in the past decades and is of particular importance to understand the biology of certain cell types or structures. The NMJ is one such complicated example consisting of presynaptic, synaptic, and postsynaptic components within a complex tissue environment (Slater, 2017; Huang et al., 2019). As stated above, NMJ-specific gene expression profiles have been analyzed by laser capture microdissection of extraocular muscles (Ketterer et al., 2010) and TA muscle (Nazarian et al., 2005; Ketterer et al., 2010), which, however, were inevitably contaminated with vascular endothelial cells, lymphocytes, and terminal Schwann cells. p*ColQ1a*-Cre:RiboTag mouse enabled extensive profiling of gene expressions under translation at the motor endplate of TA muscle with minimal contamination of adjacent cells. Gene expression profiling with RiboTag mouse inherently relies on the tissue- or cell-type-specific expression of HA-tagged RPL22 (Sanz et al., 2009). Although p*ColQ1a* was likely to be specifically active at the motor endplate of TA muscle, the transgenic p*ColQ1a*-Cre mouse carried a 3519-bp fragment of the *ColQ1a* promoter, which should have allowed a small amount of leaky expression of Cre recombinase at extra-junctional regions. A combination of laser capture microdissection and RiboTag may elucidate more precise gene expression profiles of the NMJ.

GSEA analysis revealed that two gene sets of "phosphatidylinositol signaling system" and "ECM receptor interaction" in the KEGG database were enriched at the subsynaptic nuclei of TA muscle (**Figures 4A–C**). Inspection of the two upregulated gene sets prompted us to make our own gene sets that covered more relevant genes than the KEGG database. Being prompted by the gene set of

"phosphatidylinositol signaling system," we found that genes encoding diacylglycerol kinases, phosphatidylinositol kinases, and phospholipases were enriched at the motor endplate of TA muscle (**Figures 4D–G**). Diacylglycerol kinases (DGK) are enzymes that phosphorylate diacylglycerol to yield phosphatidic acid. In the adult mouse, DGK-ζ encoded by *DGKZ* binds to syntrophin on the sarcolemma and is concentrated at the NMJ in a dystrophin-independent manner (Abramovici et al., 2003). DGK-ζ is likely to control lipid-signaling pathways to regulate actin organization (Abramovici et al., 2003). In *C. elegans*, presynaptic diacylglycerol facilitates the release of acetylcholine at NMJ, and DGK possibly regulates the abundance of presynaptic diacylglycerol (Lackner et al., 1999). We showed that DGK-η (*DGKH*) and DGK-θ (*DGKQ*) were 140-fold and 27-fold enriched at the motor endplate, respectively, and were more enriched than DGK-ζ (*DGKZ*; **Supplementary Table S5**). These and other DGKs may have undisclosed roles at the motor endplate. Phospholipases are enzymes that hydrolyze phospholipids into inositol phosphates and diacylglycerol, which are implicated as second messengers for the subsequent cellular events (Kadamur and Ross, 2013). Phospholipase C (PLC), one of the major classes of phospholipases, evokes endplate responses to acetylcholine in rodent skeletal muscle (Harborne et al., 1987). Two other classes of phospholipases are likely to have presynaptic roles. Phospholipase D blocks acetylcholine release by reducing the number of active presynaptic-releasing sites (Humeau et al., 2001). Phospholipase A_2 regulates acetylcholine release with an inhibitory or excitatory effect in several distinct phases by controlling the Ca^{2+} or K^+ channels (Fathi et al., 2001). We showed that phospholipases D and A_2 are also enriched at the motor endplate (**Supplementary Table S5**), and these phospholipases may exert their effects by signaling through the motor endplate to the nerve terminal or by exerting undisclosed roles at the motor endplate. Similarly, by being prompted by the gene set of "ECM receptor interaction," we found that genes encoding integrins and laminins were enriched at the motor endplate of TA muscle (**Figures 4D,H,I**). Integrins are cell surface receptors that facilitate adhesion of ECM molecules. The roles of integrins at the NMJ have been analyzed for integrins α3 and α7β1. Integrin α3 regulates multiple aspects of the development, function, and maintenance of the NMJ (Ross et al., 2017). Integrin α3 is required for fully efficient neurotransmission at the NMJ and also for the connection of motor neurons to the muscle fibers (Ross et al., 2017). Integrin α7β1 is concentrated at the postsynaptic NMJ in human and mouse, and their abundance is slightly increased in *mdx* mice in response to dystrophin deficiency (Hodges et al., 1997). We showed that yet uncharacterized integrins α2b and α10 were 163-fold and 68-fold enriched at the motor endplate (**Supplementary Table S5**). These and other integrins may have essential effects on the NMJ. Some laminins are also enriched at the NMJ (Rogers and Nishimune, 2017). Laminins α5 and β2 are enriched at the synaptic basal lamina, and laminin α4 is surrounding the nerve terminal, whereas laminins α2, β1, and γ1 are ubiquitously expressed on muscle fibers (Nishimune et al., 2008; Singhal and Martin, 2011). We found that laminins α3 and γ3 were 25-fold and 6-fold enriched at the motor endplate, respectively (**Supplementary Table S5**), and these laminins may have yet undisclosed roles at the NMJ.

To summarize, we have determined a gene expression profile at the motor endplate of TA muscle, which was expected to be minimally contaminated with adjacent cells at the NMJ. We expect that our gene expression profiling will contribute to the understanding of the molecular mechanisms of development, maintenance, and pathology of the NMJ.

DATA AVAILABILITY STATEMENT

FASTQ files are available at the DNA Data Bank of Japan (DDBJ) under the accession number DRA010277 (https://www.ncbi.nlm.nih.gov/sra/?term=DRA010277).

ETHICS STATEMENT

The animal study was reviewed and approved by Animal Care and Use Committee of the Nagoya University Graduate School of Medicine.

AUTHOR CONTRIBUTIONS

KO conceived the project. KH, MI, and KO designed experiments. KH and JL performed most of the experiments with the help of MI, BO, and AM. RNA-seq analysis was performed by J-IT and TO. KH, MI, and KO wrote the article.

FUNDING

This study was supported by grants-in-aid by Japan Society for the Promotion of Science (18K14684, JP18K06058, JP18K06483, 19K22802, JP20H03561, and JP20K06925); Ministry of Health, Labour, and Welfare, Japan (20FC1036); Japan Agency for Medical Research and Development (19ek0109230, 20gm1010002, 20ek0109281, and 20bm080400); and National Center of Neurology and Psychiatry (2-5).

ACKNOWLEDGMENTS

We would like to acknowledge Dr. Taiji Matsusaka at Tokai University and Dr. Paul S. Amieux at Western Washington University for providing us with RiboTag mouse. We also acknowledge the staff at the Division of Experimental Animals, Nagoya University Graduate School of Medicine for their technical support. We would like to thank Ms. Keiko Itano at Nagoya University for creating artworks.

SUPPLEMENTARY MATERIAL

The Supplementary Material for this article can be found online at: https://www.frontiersin.org/articles/10.3389/fnmol.2020.00154/full#supplementary-material.

FIGURE S1 | GSEA analysis of a set of genes that are associated with myasthenia gravis and postsynaptic congenital myasthenic syndromes. See **Supplementary Table S5** for gene names and TPM values included in the gene set.

TABLE S1 | Primer sequences for plasmid construction and genotyping.

TABLE S2 | Primer sequences for qRT-PCR.

TABLE S3 | The Numbers of Cre-positive and Cre-negative NMJs in teased TA muscle fibers electroporated with pCMV-Cre or p*ColQ1a*-Cre.

TABLE S4 | Distribution of Cre-positive signals in teased muscle fibers of the TA and soleus muscles of the p*ColQ1a*-Cre mouse.

TABLE S5 | Detailed values of RNA-seq analysis. TPM of 22,382 genes in input RNA and IP RNA. Results of GSEA analysis of two KEGG gene sets and five our own gene sets that were enriched at the motor endplate of TA muscle.

REFERENCES

Abramovici, H., Hogan, A. B., Obagi, C., Topham, M. K., and Gee, S. H. (2003). Diacylglycerol kinase-zeta localization in skeletal muscle is regulated by phosphorylation and interaction with syntrophins. *Mol. Biol. Cell.* 14, 4499–4511. doi: 10.1091/mbc.e03-03-0190

Consortium, E. P. (2012). An integrated encyclopedia of DNA elements in the human genome. *Nature* 489, 57–74. doi: 10.1038/nature11247

Dobin, A., Davis, C. A., Schlesinger, F., Drenkow, J., Zaleski, C., Jha, S., et al. (2013). STAR: ultrafast universal RNA-seq aligner. *Bioinformatics* 29, 15–21. doi: 10.1093/bioinformatics/bts635

Fathi, H. B., Rowan, E. G., and Harvey, A. L. (2001). The facilitatory actions of snake venom phospholipase A(2) neurotoxins at the neuromuscular junction are not mediated through voltage-gated K(+) channels. *Toxicon* 39, 1871–1882. doi: 10.1016/s0041-0101(01)00170-2

Fromm, L., and Burden, S. J. (1998). Synapse-specific and neuregulin-induced transcription require an ets site that binds GABPα/GABPβ. *Genes Dev.* 12, 3074–3083. doi: 10.1101/gad.12.19.3074

Gaspersic, R., Koritnik, B., Crne-Finderle, N., and Sketelj, J. (1999). Acetylcholinesterase in the neuromuscular junction. *Chem. Biol. Interact.* 119-120, 301–308. doi: 10.1016/s0009-2797(99)00040-x

Harborne, A. J., Turner, A. W., Murphy, R. L., and Smith, M. E. (1987). Action of phospholipase C at the neuromuscular junction in rodent skeletal muscles. *Eur. J. Pharmacol.* 143, 163–170. doi: 10.1016/0014-2999(87)90529-2

Hirsch, N. P. (2007). Neuromuscular junction in health and disease. *Br. J. Anaesth.* 99, 132–138. doi: 10.1093/bja/aem144

Hodges, B. L., Hayashi, Y. K., Nonaka, I., Wang, W., Arahata, K., and Kaufman, S. J. (1997). Altered expression of the α7β1 integrin in human and murine muscular dystrophies. *J. Cell. Sci.* 110, 2873–2881.

Huang, K., Luo, Y. B., and Yang, H. (2019). Autoimmune channelopathies at neuromuscular junction. *Front. Neurol.* 10:516. doi: 10.3389/fneur.2019.00516

Humeau, Y., Vitale, N., Chasserot-Golaz, S., Dupont, J. L., Du, G., Frohman, M. A., et al. (2001). A role for phospholipase D1 in neurotransmitter release. *Proc. Natl. Acad. Sci. U S A* 98, 15300–15305. doi: 10.1073/pnas.261358698

Kadamur, G., and Ross, E. M. (2013). Mammalian phospholipase C. *Annu. Rev. Physiol.* 75, 127–154. doi: 10.1146/annurev-physiol-030212-183750

Ketterer, C., Zeiger, U., Budak, M. T., Rubinstein, N. A., and Khurana, T. S. (2010). Identification of the neuromuscular junction transcriptome of extraocular muscle by laser capture microdissection. *Invest. Ophthalmol. Vis. Sci.* 51, 4589–4599. doi: 10.1167/iovs.09-4893

Kim, T., Lim, C. S., and Kaang, B. K. (2015). Cell type-specific gene expression profiling in brain tissue: comparison between TRAP, LCM and RNA-seq. *BMB Rep.* 48, 388–394. doi: 10.5483/bmbrep.2015.48.7.218

Krejci, E., Legay, C., Thomine, S., Sketelj, J., and Massoulie, J. (1999). Differences in expression of acetylcholinesterase and collagen Q control the distribution and oligomerization of the collagen-tailed forms in fast and slow muscles. *J. Neurosci.* 19, 10672–10679. doi: 10.1523/jneurosci.19-24-10672.1999

Lackner, M. R., Nurrish, S. J., and Kaplan, J. M. (1999). Facilitation of synaptic transmission by EGL-30 Gqα and EGL-8 PLCβ: DAG binding to UNC-13 is required to stimulate acetylcholine release. *Neuron* 24, 335–346. doi: 10.1016/s0896-6273(00)80848-x

Lee, H. H., Choi, R. C., Ting, A. K., Siow, N. L., Jiang, J. X., Massoulie, J., et al. (2004). Transcriptional regulation of acetylcholinesterase-associated collagen ColQ: differential expression in fast and slow twitch muscle fibers is driven by distinct promoters. *J. Biol. Chem.* 279, 27098–27107. doi: 10.1074/jbc.m402596200

Li, B., and Dewey, C. N. (2011). RSEM: accurate transcript quantification from RNA-Seq data with or without a reference genome. *BMC Bioinformatics* 12:323. doi: 10.1186/1471-2105-12-323

Murakami, T., Nishi, T., Kimura, E., Goto, T., Maeda, Y., Ushio, Y., et al. (2003). Full-length dystrophin cDNA transfer into skeletal muscle of adult mdx mice by electroporation. *Muscle Nerve* 27, 237–241. doi: 10.1002/mus.10283

Nazarian, J., Bouri, K., and Hoffman, E. P. (2005). Intracellular expression profiling by laser capture microdissection: three novel components of the neuromuscular junction. *Physiol. Genomics* 21, 70–80. doi: 10.1152/physiolgenomics.00227.2004

Nazim, M., Masuda, A., Rahman, M. A., Nasrin, F., Takeda, J. I., Ohe, K., et al. (2017). Competitive regulation of alternative splicing and alternative polyadenylation by hnRNP H and CstF64 determines acetylcholinesterase isoforms. *Nucleic Acids Res.* 45, 1455–1468. doi: 10.1093/nar/gkw823

Nishimune, H., Valdez, G., Jarad, G., Moulson, C. L., Muller, U., Miner, J. H., et al. (2008). Laminins promote postsynaptic maturation by an autocrine mechanism at the neuromuscular junction. *J. Cell. Biol.* 182, 1201–1215. doi: 10.1083/jcb.200805095

Ohno, K., Anlar, B., and Engel, A. G. (1999). Congenital myasthenic syndrome caused by a mutation in the Ets-binding site of the promoter region of the acetylcholine receptor epsilon subunit gene. *Neuromuscul. Disord.* 9, 131–135. doi: 10.1016/s0960-8966(99)00007-3

Ohno, K., Brengman, J., Tsujino, A., and Engel, A. G. (1998). Human endplate acetylcholinesterase deficiency caused by mutations in the collagen-like tail subunit (ColQ) of the asymmetric enzyme. *Proc. Natl. Acad. Sci. U S A* 95, 9654–9659. doi: 10.1073/pnas.95.16.9654

Ohno, K., Ohkawara, B., and Ito, M. (2017). Agrin-LRP4-MuSK signaling as a therapeutic target for myasthenia gravis and other neuromuscular disorders. *Expert Opin. Ther. Targets* 21, 949–958. doi: 10.1080/14728222.2017.1369960

Picelli, S., Faridani, O. R., Bjorklund, A. K., Winberg, G., Sagasser, S., and Sandberg, R. (2014). Full-length RNA-seq from single cells using Smart-seq2. *Nat. Protoc.* 9, 171–181. doi: 10.1038/nprot.2014.006

Reimand, J., Isserlin, R., Voisin, V., Kucera, M., Tannus-Lopes, C., Rostamianfar, A., et al. (2019). Pathway enrichment analysis and visualization of omics data using g:profiler, GSEA, cytoscape and enrichmentmap. *Nat. Protoc.* 14, 482–517. doi: 10.1038/s41596-018-0103-9

Rogers, R. S., and Nishimune, H. (2017). The role of laminins in the organization and function of neuromuscular junctions. *Matrix Biol.* 57-58, 86–105. doi: 10.1016/j.matbio.2016.08.008

Ross, J. A., Webster, R. G., Lechertier, T., Reynolds, L. E., Turmaine, M., Bencze, M., et al. (2017). Multiple roles of integrin-α3 at the neuromuscular junction. *J. Cell. Sci.* 130, 1772–1784. doi: 10.1242/jcs.201103

Sanz, E., Yang, L., Su, T., Morris, D. R., Mcknight, G. S., and Amieux, P. S. (2009). Cell-type-specific isolation of ribosome-associated mRNA from complex tissues. *Proc. Natl. Acad. Sci. U S A* 106, 13939–13944. doi: 10.1073/pnas.0907143106

Sapru, M. K., Florance, S. K., Kirk, C., and Goldman, D. (1998). Identification of a neuregulin and protein-tyrosine phosphatase response element in the nicotinic acetylcholine receptor epsilon subunit gene: regulatory role of an Rts transcription factor. *Proc. Natl. Acad. Sci. U S A* 95, 1289–1294. doi: 10.1073/pnas.95.3.1289

Schroeder, A., Mueller, O., Stocker, S., Salowsky, R., Leiber, M., Gassmann, M., et al. (2006). The RIN: an RNA integrity number for assigning integrity values to RNA measurements. *BMC Mol. Biol.* 7:3. doi: 10.1186/1471-2199-7-3

Singhal, N., and Martin, P. T. (2011). Role of extracellular matrix proteins and their receptors in the development of the vertebrate neuromuscular junction. *Dev. Neurobiol.* 71, 982–1005. doi: 10.1002/dneu.20953

Slater, C. R. (2017). The structure of human neuromuscular junctions: some unanswered molecular questions. *Int. J. Mol. Sci.* 18:2183. doi: 10.3390/ijms18102183

Srivastava, R., Budak, G., Dash, S., Lachke, S. A., and Janga, S. C. (2017). Transcriptome analysis of developing lens reveals abundance of

novel transcripts and extensive splicing alterations. *Sci. Rep.* 7:11572. doi: 10.1038/s41598-017-10615-4

Ting, A. K., Siow, N. L., Kong, L. W., and Tsim, K. W. (2005). Transcriptional regulation of acetylcholinesterase-associated collagen ColQ in fast- and slow-twitch muscle fibers. *Chem. Biol. Interact.* 157-158, 63–70. doi: 10.1016/j.cbi.2005.10.009

Vickers, A. J., Cronin, A. M., Elkin, E. B., and Gonen, M. (2008). Extensions to decision curve analysis, a novel method for evaluating diagnostic tests, prediction models and molecular markers. *BMC Med. Inform. Decis. Mak.* 8:53. doi: 10.1186/1472-6947-8-53

Wang, K., Wang, D., Zheng, X., Qin, A., Zhou, J., Guo, B., et al. (2019). Multi-strategic RNA-seq analysis reveals a high-resolution transcriptional landscape in cotton. *Nat. Commun.* 10:4714. doi: 10.1038/s41467-019-12575-x

Young, J. L., and Dean, D. A. (2015). Electroporation-mediated gene delivery. *Adv. Genet.* 89, 49–88. doi: 10.1016/bs.adgen.2014.10.003

Conflict of Interest: The authors declare that the research was conducted in the absence of any commercial or financial relationships that could be construed as a potential conflict of interest.

Copyright © 2020 Huang, Li, Ito, Takeda, Ohkawara, Ogi, Masuda and Ohno. This is an open-access article distributed under the terms of the Creative Commons Attribution License (CC BY). The use, distribution or reproduction in other forums is permitted, provided the original author(s) and the copyright owner(s) are credited and that the original publication in this journal is cited, in accordance with accepted academic practice. No use, distribution or reproduction is permitted which does not comply with these terms.

frontiers in Molecular Neuroscience

BRIEF RESEARCH REPORT
published: 23 October 2020
doi: 10.3389/fnmol.2020.567676

Investigation of *MLH1, MGMT, CDKN2A*, and *RASSF1A* Gene Methylation in Thymomas From Patients With Myasthenia Gravis

Fabio Coppedè[1], Roberta Ricciardi[2,3], Angela Lopomo[1], Andrea Stoccoro[1], Anna De Rosa[2], Melania Guida[2], Loredana Petrucci[2], Michelangelo Maestri[2], Marco Lucchi[3,4] and Lucia Migliore[1]*

[1]Department of Translational Research and of New Surgical and Medical Technologies, Medical Genetics Laboratory, University of Pisa, Pisa, Italy, [2]Department of Clinical and Experimental Medicine, Neurology Unit, University of Pisa, Pisa, Italy, [3]Division of Thoracic Surgery, Cardiothoracic and Vascular Surgery Department, Pisa University Hospital, Pisa, Italy, [4]Department of Surgical, Medical and Molecular Pathology and Critical Care Medicine, University of Pisa, Pisa, Italy

A feature of thymomas is their frequent association with myasthenia gravis (MG), an autoimmune disease characterized by the production of autoantibodies directed to different targets at the neuromuscular junction. Indeed, almost 30–40% of thymomas are found in patients with a type of MG termed thymoma-associated MG (TAMG). Recent studies suggest that TAMG-associated thymomas could represent a molecularly distinct subtype of thymic epithelial tumors (TETs), but few data are still available concerning the epigenetic modifications occurring in TAMG tissues. The promoter methylation levels of DNA repair (*MLH1* and *MGMT*) and tumor suppressor genes (*CDKN2A* and *RASSF1A*) have been frequently investigated in TETs, but methylation data in TAMG tissues are scarce and controversial. To further address this issue, we investigated *MLH1*, *MGMT*, *CDKN2A*, and *RASSF1A* methylation levels in blood samples and surgically resected thymomas from 69 patients with TAMG and in the adjacent normal thymus available from 44 of them. Promoter methylation levels of *MLH1*, *MGMT*, *CDKN2A*, and *RASSF1A* genes were not increased in cancer with respect to healthy tissues and did not correlate with the histological or pathological features of the tumor or with the MG symptoms. The present study suggests that hypermethylation of these genes is not frequent in TAMG tissues.

Keywords: epigenetics, DNA methylation, CDKN2A, RASSF1A, MLH1, MGMT, thymoma, myasthenia gravis

OPEN ACCESS

Edited by:
Laure Strochlic, Institut National de la Santé et de la Recherche Médicale (INSERM), France

Reviewed by:
Alexander Marx, Heidelberg University, Germany
Linda L. Kusner, George Washington University, United States

****Correspondence:***
Fabio Coppedè
fabio.coppede@med.unipi.it

Received: *30 May 2020*
Accepted: *18 September 2020*
Published: *23 October 2020*

Citation:
Coppedè F, Ricciardi R, Lopomo A, Stoccoro A, De Rosa A, Guida M, Petrucci L, Maestri M, Lucchi M and Migliore L (2020) Investigation of MLH1, MGMT, CDKN2A, and RASSF1A Gene Methylation in Thymomas From Patients With Myasthenia Gravis. Front. Mol. Neurosci. 13:567676. doi: 10.3389/fnmol.2020.567676

INTRODUCTION

Myasthenia gravis (MG) is an autoimmune disease characterized by the production of autoantibodies directed to different targets at the neuromuscular junction, in most of the cases against the nicotinic acetylcholine receptor (AChR+ MG patients; Marx et al., 2015). Thymomas are tumors that originate from epithelial cells of the thymus and are often accompanied by non-neoplastic lymphocytic proliferation. These tumors are classified

into five subtypes (A, AB, B1, B2, and B3) according to the tumor cell morphology and to the proportion of associated immature T cells (Marx et al., 2014). The Masaoka–Koga staging system groups thymomas into four stages, namely stage I that includes encapsulated tumors, stages II and III for tumors showing direct local invasion, and stage IV for those with a metastatic spread (Ried et al., 2016). One of the unique features of thymomas is their frequent association with AChR+ MG, so that about 30–40% of thymomas are found in patients with a type of MG termed thymoma-associated MG (TAMG; Marx et al., 2015).

Epigenetic modifications, and particularly the gene silencing resulting from hypermethylation of tumor suppressor and DNA repair genes, play a pivotal role in tumor development and progression (Costa-Pinheiro et al., 2015). A recent whole-genome methylation study has suggested that TAMG-associated thymomas are epigenetically distinct from thymomas that develop in people without MG (Bi et al., 2019). However, the study compared very few samples (Bi et al., 2019), so that larger studies are required to epigenetically characterize those tumors and their different histological subtypes, as well as to understand the links between the epigenetic modifications observed in TAMG tissues and the severity of the MG symptoms.

The methylation levels of the DNA repair and tumor suppressor genes *MLH1*, *MGMT*, *CDKN2A*, and *RASSF1A* have frequently been investigated in thymic epithelial tumors (TETs), including thymomas (Hirabayashi et al., 1997; Suzuki et al., 2005; Chen et al., 2009; Hirose et al., 2009; Mokhtar et al., 2014; Kajiura et al., 2017). Collectively, those studies have shown that hypermethylation of those genes is more frequent in thymic carcinomas than in thymomas, but most of those studies did not clarify if thymoma samples were from patients with TAMG or from patients without MG, while others included very few TAMG-associated thymomas, making it not possible to correlate the observed methylation levels with tumor stage, histology, or MG symptoms; in addition, no data were often available from adjacent normal thymic tissues in order to compare the methylation levels between pathological and healthy samples. Furthermore, most of the available studies have been performed in Chinese or Japanese populations and studies in Caucasians are limited (Hirabayashi et al., 1997; Suzuki et al., 2005; Chen et al., 2009; Hirose et al., 2009; Mokhtar et al., 2014; Kajiura et al., 2017). A recent study was performed on 117 TETs using multiplatform omics analyses and including 97 white, six black, and 12 Asian samples and 32 thymomas from patients with TAMG (Radovich et al., 2018). The study revealed an increased prevalence of aneuploidy among MG+ thymomas, but the MG status was not associated with any methylation signature (Radovich et al., 2018).

The present study was performed to investigate if *MLH1*, *MGMT*, *CDKN2A*, and *RASSF1A* genes are hypermethylated in TAMG-associated thymomas with respect to the normal residual thymuses or circulating lymphocytes of the same patients, and if the methylation patterns of TAMG-associated thymomas exhibit differences in relation to age, gender, and TAMG clinical features.

METHODS

Study Population

The study was performed on available DNA samples from a previously described dataset composed by 69 patients with AChR+ TAMG of Caucasian origin, collected at the Myasthenia Clinic of the Pisa University Hospital (Lopomo et al., 2016). DNA samples were collected from both blood and surgically resected tumor tissues of the 69 patients and from the adjacent normal tissue, available from 44 of them. Trained neurologists evaluated each patient, and the diagnosis of MG was made based on the clinical symptoms together with positivity to AChR antibodies. All the patients had computed tomography (CT) scans of the chest followed by thymectomy. The medical personnel of the Division of Thoracic Surgery of the Pisa University Hospital assessed thymoma staging and histology. MG symptoms of thymectomy were assessed according to the MG Foundation of America (MGFA) classification (Jaretzki et al., 2000). Ninety-seven percent of the patients were taking steroids at the time of surgical specimen collection. In addition, 10% of them were following immunosuppressant and/or immunomodulatory therapy, 6% followed a cisplatin-based chemotherapy prior to surgery, and 4% underwent radiotherapy. None of the patients included in the study was treated with demethylating agents such as DNA methyltransferase inhibitors (DNMTi). Each patient gave an informed written consent for inclusion in the study that was conducted in accordance with the Declaration of Helsinki and approved by the Ethics Committee of the Pisa University Hospital (Protocol number 21302/2015). Demographic and clinical characteristics of the study population are shown (**Table 1**).

Assessment of *MLH1*, *MGMT*, *CDKN2A*, and *RASSF1A* Promoter Methylation

An aliquot of 1 ml of peripheral blood in EDTA tubes, obtained by venipuncture, and about 40 mg of tumor tissue and of the adjacent normal tissue, which were clearly distinguishable, obtained during thymectomy, were collected and stored at −20°C until DNA extraction. The adjacent normal tissue was separated from the thymoma by macrodissection and histologically controlled for absence of tumor contamination. Genomic DNA was extracted using the QIAmp DNA Mini Kit (Qiagen, Milan, Italy, Catalog N° 51304) following the manufacturer's protocol, from 200 μl of whole blood and from about 20 mg of tissue. A Nano Drop ND 2000c spectrophotometer (NanoDrop Thermo Fisher Scientific) was used to quantify the extracted DNA. Two hundred nanograms of DNA from each sample was treated with sodium bisulfite in order to convert all unmethylated cytosines into uracil using the EpiTect Bisulfite Kit (Qiagen, Catalog N° 59104). A sample of completely unmethylated genomic DNA (amplified human genomic DNA, completely unmethylated, Qiagen, Catalog N° 59568) was used as control assay to check the bisulfite conversion efficiency that resulted to be of 99% in average. Promoter methylation was evaluated with methylation sensitive-high

TABLE 1 | Demographic and clinicopathological characteristics of the studied population (adapted from Lopomo et al., 2016).

TAMG patients	Age ± SD (years)	Gender *N* (%)	MG onset *N* (%)	Thymoma histology *N* (%)	Masaoka-Koga stage *N* (%)	MGFA classification *N* (%)	Therapy* *N* (%)
N = 69	55.5 ± 13.2	F: 37 (54) M: 32 (46)	<50 years: 26 (38) ≥50 years: 43 (62)	A: 13 (18.8) AB: 13 (18.8) B1: 5 (7.2) B2: 23 (33.4) B3: 8 (11.6) B2–B3: 5 (7.2) NS: 2 (3.0)	I: 7 (10) IIa: 15 (22) IIb: 29 (42) III: 7 (10) IVa: 9 (13) NS: 2 (3)	No symptoms 10 (14) Class I: 18 (26) Class IIa: 4 (6) Class IIb: 12 (17.5) Class IIIb: 17 (24.5) Class IVa: 0 (0) Class IVb: 4 (6) Class V. 0 (0) NS: 4 (6)	Steroids: 67 (97) Immune: 7 (10) Chemo: 4 (6) Radio: 3 (4)

*TAMG, thymoma-associated myasthenia gravis; MG, myasthenia gravis; F, females; M, males; N, number; NS, not specified; MGFA, MG Foundation of America, classification at thymectomy; Immuno, immunomodulatory/immunosuppressant drugs (azathioprine, methotrexate, intravenous immunoglobulins, cyclosporine); Chemo, cisplatin-based chemotherapy; Radio, radiotherapy. *Almost all the patients (97%) were taking steroids prior to and/or at the time of surgical specimen collection.*

resolution melting (MS-HRM) analysis, using primers and protocols previously developed and validated in our laboratory and largely applied by our group for the analysis of gene-specific methylation in human cancers (Migheli et al., 2013; Coppedè et al., 2014). Primer sequences and annealing temperatures (T_a) used during MS-HRM analysis, number of investigated CpG sites, and length of the analyzed amplicons are reported in **Table 2**. All the methodological details of the MS-HRM analyses can be found elsewhere (Coppedè et al., 2014), and we previously validated the MS-HRM protocols used in this study with pyrosequencing, which is considered the gold standard technique for DNA methylation investigations (Failli et al., 2013; Migheli et al., 2013). Briefly, the MS-HRM analyses were performed using a CFX96 Real-Time PCR detection system (Bio-Rad, Milan) with the following protocol: 1 cycle of 95°C for 12 min, 50 cycles of 95°C for 30 s, gene-specific annealing temperature (**Table 2**) for 45 s and 72°C for 30 s, followed by an HRM step of 95°C for 10 s and 50°C for 1 min, 65°C for 15 s, and continuous acquisition to 95°C at one acquisition per 0.2°C. PCR was performed in a final volume of 10 μl, containing 5 μl of master mix (Qiagen, Catalog N° 59445), 10 pmol of each primer, and 10 ng of bisulfite-modified DNA template. Each reaction was performed in duplicate, and we analyzed 10% of the samples independently on separate occasions to verify the interassay variability. We mixed fully methylated and unmethylated DNA samples (EpiTect methylated and unmethylated human control DNA, bisulfite converted, Qiagen, Milan, Italy, Catalog N° 59695) to generate standard curves (**Figure 1**), and the methylation level of each sample was quantified using an interpolation method developed and described in our laboratory (Migheli et al., 2013). Three positive and three negative controls were included in the analyses. Positive controls are DNA samples from patients with colorectal cancer that showed hypermethylation (promoter methylation levels ranging from 70–100%) of the investigated genes in the cancer but not in the adjacent healthy mucosa. Negative controls are DNA samples from patients with colorectal cancer that showed hypomethylation (promoter methylation levels ranging from 1–5%) of the investigated genes in both cancer and adjacent healthy mucosa (**Supplementary Figure 1**). Both positive and negative controls were selected among DNA samples whose methylation levels have previously been assessed and validated in our laboratory (Coppedè et al., 2014).

Statistical Analyses

Differences in mean methylation levels among tissues (thymomas, normal thymuses, and blood) were evaluated with analysis of variance (ANOVA). ANOVA was also used to evaluate the effect of clinical, demographic, and pathological features, such as thymoma histology, tumor staging, gender, MG onset, and symptoms, on the mean methylation levels of the studied genes. Linear regression analysis was performed to search for correlation between age and methylation levels. Analyses were performed with the MedCalc statistical software v. 12.5. We used the *post hoc* Bonferroni's correction tool in MedCalc to correct the *p* values for the multiple comparisons among groups. The statistical power of the study was evaluated with the clinical tool and

TABLE 2 | Primer sequences and annealing temperatures (T_a) used during MS-HRM analysis, amplicon length, and number of CpG sites for each gene.

Gene	Primer sequences	T_a	Amplicon length (bp)	CpG sites
MGMT	F 5′-GCGTTTCGGATATGTTGGGATAAGT-3′ R 5′-AACGACCCAAACACTCACCAAA-3′	58°	110	12
MLH1	F 5′-AGTTTTAAAAACTGAATTAATAGGAAGAG-3′ R 5′-ACTACCCGCTACCTAAAAAAATATAC-3′	56°	81	5
CDKN2A	F 5′-CGGAGGAAGAAAGAGGAGGGGT-3′ R 5′-CGCTACCTACTCTCCCCCTCT-3′	62°	93	7
RASSF1A	F 5′-TCGGGTTTTATAGTTTTTGTATTTAGGTTTT-3′ R 5′-CCTCCCCCAAAATCCAAACTAA-3′	60°	87	7

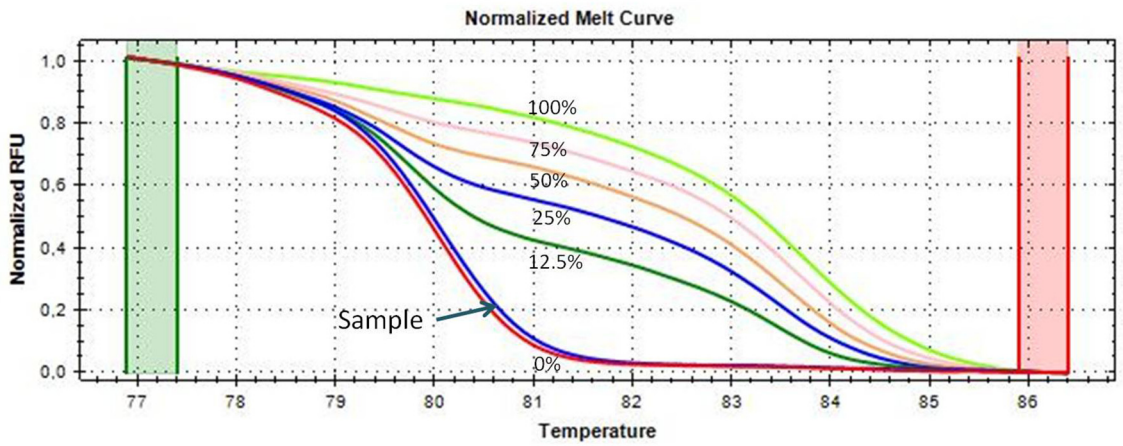

FIGURE 1 | Melting curves of the *CDKN2A* gene generated by samples with known methylation levels (0, 12.5, 25, 50, 75, and 100% methylation, respectively), obtained by mixing the fully methylated and unmethylated standard DNA samples. A thymoma sample showing almost 0% promoter methylation is shown and indicated with an arrow; its melting curve is very similar and partially juxtaposed to that of the completely unmethylated standard DNA (red curve).

calculators for medical professionals: ClinCalc[1]. The sample size was chosen to have an *a priori* power of >80% to detect mean methylation differences of 5% or higher among groups. A *post hoc* analysis based on the distribution of methylation data observed in our samples revealed that five samples per group were enough to have 90% power to detect mean DNA methylation differences of 5% or higher among groups, and that including 40 samples per group allowed to have more than 80% power to detect mean DNA methylation differences of 2% or higher among groups.

RESULTS

Figure 2 shows the mean methylation levels of the studied regions in blood, tumor tissue, and adjacent healthy thymic tissue of the whole study cohort. MS-HRM analyses showed that *MLH1* methylation levels were very low in peripheral blood (0.64 ± 0.13%), adjacent tumor tissue (0.40 ± 0.19%), and in thymomas (0.19 ± 0.14%), and no overall difference among the three tissues was observed ($p = 0.08$; **Figure 2A**). Particularly, no differences in *MLH1* mean methylation levels between peripheral blood and adjacent healthy tissue ($p = 0.68$), between peripheral blood and thymomas ($p = 0.07$) and between adjacent tumor tissue and thymomas ($p = 0.86$) were detected. **Figure 2B** shows the mean methylation levels of *MGMT* in peripheral blood (0.30 ± 0.04%), adjacent healthy tissue (0.32 ± 0.05%), and tumor tissue (0.16 ± 0.05%). Overall, there was no difference among the three tissues ($p = 0.07$), and no differences in *MGMT* mean methylation levels between peripheral blood and adjacent tumor tissue ($p = 1.00$), between peripheral blood and thymomas ($p = 0.15$), and between adjacent tumor tissue and thymomas ($p = 0.07$) were detected. **Figure 2C** shows the mean methylation levels of *CDKN2A* in peripheral blood (0.57 ± 0.10%), in healthy adjacent tissue (0.42 ± 0.11), and in thymoma tissue (0.47 ± 0.10%). There was no overall difference among the three tissues ($p = 0.64$). No differences in *CDKN2A* mean methylation levels between peripheral blood and adjacent tumor tissue ($p = 1.00$), between peripheral blood and thymomas ($p = 1.00$), and between adjacent tumor tissue and thymomas ($p = 1.00$) were detected. **Figure 2D** shows the mean methylation levels of *RASSF1A* in peripheral blood (0.84 ± 0.30%), in healthy adjacent tissue (1.32 ± 0.30), and in thymoma tissue (1.41 ± 0.30%). Overall, no significant difference was observed among the three investigated tissues ($p = 0.36$). No differences in *RASSF1A* mean methylation levels between peripheral blood and adjacent tumor tissue ($p = 0.80$), between peripheral blood and thymomas ($p = 0.56$), and between adjacent tumor tissue and thymomas ($p = 1.00$) were detected. In addition, the comparison of the methylation levels observed in the thymoma and in the normal thymus, for each of the 44 patients with available healthy thymus, is shown (**Supplementary Figures 2–5**). All the investigated genes were largely demethylated in thymomas, and no correlation with the demographic (age and gender) or clinical data (tumor histology and grade) was observed (**Supplementary Table 1**).

DISCUSSION

In the present study, we investigated the promoter methylation levels of *MLH1*, *MGMT*, *CDKN2A*, and *RASSF1A* in blood and tumor tissue DNA from 69 patients with TAMG, as well as in the healthy thymic epithelial tissue adjacent to the tumor available from 44 of them. The promoters of *MLH1*, *MGMT*, *CDKN2A*, and *RASSF1A* genes resulted completely demethylated in the studied samples, and no difference in average promoter methylation levels was observed in the comparison of cancerous and healthy thymic tissue. Similarly, no correlation with

[1]http://clincalc.com/Stats/Power.aspx

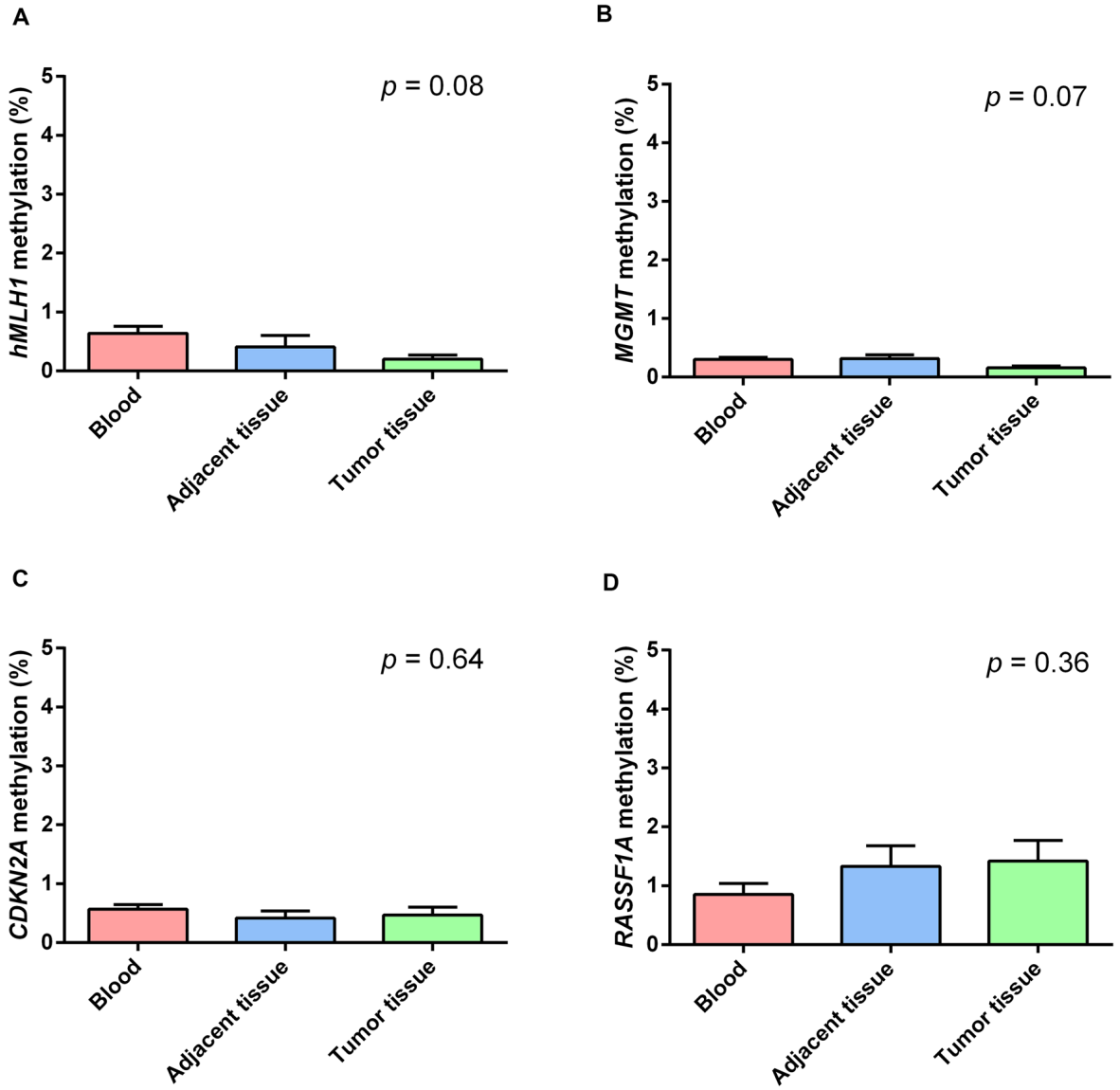

FIGURE 2 | Methylation levels of the studied genes in blood (red), healthy thymic tissue (blue), and tumor tissue (green). **(A)** *MLH1*. **(B)** *MGMT*. **(C)** *CDKN2A*. **(D)** *RASSF1A*. All the investigated genes resulted largely hypomethylated in the studied tissues, and no significant difference among them was observed. Data are shown as means ± SEM (mean standard error), and for each gene, we compared 69 blood samples, 69 thymomas, and 44 healthy thymuses. The *p* value reflects the Bonferroni's corrected *p* value of the comparison of mean methylation levels among the three groups.

demographic data of the patients or clinical characteristics of the tumors was found.

We decided to investigate these four genes because their methylation levels have frequently been investigated in TETs, but their methylation levels in TAMG-associated thymomas are still scarce. Collectively, previous studies in TETs have shown that these genes are frequently hypermethylated in thymic carcinomas, but studies investigating their methylation levels in thymomas have provided conflicting and inconclusive results. Moreover, those studies included very few TAMG-associated thymomas (Hirabayashi et al., 1997; Suzuki et al., 2005; Chen et al., 2009; Mokhtar et al., 2014; Kajiura et al., 2017). Also genome-wide methylation data in TAMG are conflicting. Indeed, the comparison of two TAMG-associated thymomas and four thymomas from people without MG revealed that the DNA methylation profiling of MG-associated thymomas was significantly distinguished from that of non-MG thymomas (Bi et al., 2019). However, a larger study on 117 TET samples, that included 32 thymomas from patients with TAMG, showed that the MG status was not associated with any methylation signature (Radovich et al., 2018). These genome-wide studies, however, do not show details on the methylation levels of the four genes investigated in the present study, namely *MGMT*, *MLH1*, *CDKN2A*, and *RASSF1A*.

For all these reasons, we designed the present study to deeply investigate *MGMT*, *MLH1*, *CDKN2A*, and *RASSF1A* methylation levels in a cohort of Caucasian TAMG samples large enough to evaluate the contribution of tumor stage and histology, as well as those of the MG clinical subtypes, to the observed findings. Our investigation revealed that all of *MLH1*, *MGMT*, *CDKN2A*, and *RASSF1A* gene promoters were completely demethylated in TAMG samples, with average methylation levels of about 1–2%. At best of our knowledge, no previous study compared *MLH1*, *MGMT*, *CDKN2A*, and *RASSF1A* gene methylation levels among thymoma samples, healthy thymic samples, and circulating blood DNA from the same patients, and the present study revealed that *MLH1*, *MGMT*, *CDKN2A*, and *RASSF1A* genes showed similar and very low methylation patterns in the three investigated tissues, and no difference was observed between pathological and healthy thymus. Similarly, no correlation was found between gene methylation levels and the histological or clinical characteristics of the tumors. Unfortunately, we could not collect RNA samples from our patients in order to perform gene expression analysis. However, we used quantitative MS-HRM protocols previously validated with pyrosequencing (Migheli et al., 2013; Coppedè et al., 2014) and/or with DNA methylation arrays (Coppedè et al., 2017). These protocols were able to quantify from very low methylation levels of about 0–1% up to 80–100% promoter methylation (Coppedè et al., 2014, 2017), and we previously demonstrated that very low methylation levels of these genes (1–2% in average) are found in healthy tissues, including blood DNA from healthy people or the healthy colonic mucosa (Coppedè et al., 2014, 2017). By contrast, methylation levels of 80% or higher were frequently observed in colorectal cancer specimens, resulting in loss of protein expression (Coppedè et al., 2014). Collectively, the present study suggests that the promoter methylation levels of *MLH1*, *MGMT*, *CDKN2A*, and *RASSF1A* genes are very low in TAMG samples and are comparable with those observed in healthy tissues. A previous study performed by us in the same cohort revealed no difference in the methylation levels of DNA methyltransferase genes (*DNMT1*, *DNMT3A*, and *DNMT3B*) between thymomas and healthy thymus (Lopomo et al., 2016). A more recent investigation in the same cohort revealed that the *GHSR* gene was modestly hypermethylated only in less than 30% of the samples (Coppedè et al., 2020), while it resulted strongly hypermethylated in thymic carcinomas (Kishibuchi et al., 2020).

One of the limits of the present study is the unavailability of thymoma samples from individuals without MG to make comparisons, so that we cannot understand whether the almost-complete absence of methylation of the investigated genes is a unique feature of TAMG-associated thymomas or not. Larger studies are therefore needed, investigating all in one point mutations, chromosome rearrangements, and epigenetic signatures of the different TET subtypes. Another limitation of the study is that all but two patients were taking corticosteroids at the time of sample collection or before. The methylation levels observed in these two patients are not dissimilar from those observed in individuals taking corticosteroids (**Supplementary Figures 2–5**), and all the investigated genes were demethylated in their tissues. Further studies are however required to clarify if corticosteroid treatment could impair the methylation levels of the studied genes. Previous studies in Asian samples have shown that *MLH1*, *MGMT*, *CDKN2A*, and *RASSF1A* genes are hypomethylated in thymomas as compared with thymic carcinomas or neuroendocrine tumors (Hirabayashi et al., 1997; Suzuki et al., 2005; Chen et al., 2009; Mokhtar et al., 2014; Kajiura et al., 2017). We have not included thymic carcinomas or neuroendocrine tumors in the present investigation to make comparisons, but all the four genes were scarcely methylated in the thymoma samples from Caucasian patients with TAMG included in the present study.

In summary, the present study reveals that the promoter methylation levels of *MLH1*, *MGMT*, *CDKN2A*, and *RASSF1A* genes are not increased in thymomas with respect to the healthy tissues of patients with MG and do not correlate with histological or pathological features.

DATA AVAILABILITY STATEMENT

The raw data supporting the conclusions of this article will be made available by the authors, without undue reservation.

ETHICS STATEMENT

The studies involving human participants were reviewed and approved by Pisa University Hospital Ethics Committee. The patients/participants provided their written informed consent to participate in this study.

AUTHOR CONTRIBUTIONS

FC conceived and designed the study, provided reagents and funds, and wrote the article. LM critically reviewed the manuscript. AL performed methylation experiments. AS supervised methylation experiments and performed the statistical analysis. RR, AD, LP, MG, and MM performed neurological examinations of the patients and disease diagnosis. ML evaluated thymic pathology. All authors contributed to the article and approved the submitted version.

FUNDING

The study was supported by researcher's intramural funds (COPPEDE-ATENEO funds). Additional support was provided by "Associazione MIA Onlus (Associazione Italiana Miastenia Onlus)."

SUPPLEMENTARY MATERIAL

The Supplementary Material for this article can be found online at: https://www.frontiersin.org/articles/10.3389/fnmol.2020.567676/full#supplementary-material.

REFERENCES

Bi, Y., Meng, Y., Niu, Y., Li, S., Liu, H., He, J., et al. (2019). Genome-wide DNA methylation profile of thymomas and potential epigenetic regulation of thymoma subtypes. *Oncol. Rep.* 41, 2762–2774. doi: 10.3892/or.2019.7035

Chen, C., Yin, B., Wei, Q., Li, D., Hu, J., Yu, F., et al. (2009). Aberrant DNA methylation in thymic epithelial tumors. *Cancer Invest.* 27, 582–591. doi: 10.1080/07357900802620869

Coppedè, F., Migheli, F., Lopomo, A., Failli, A., Legitimo, A., Consolini, R., et al. (2014). Gene promoter methylation in colorectal cancer and healthy adjacent mucosa specimens: correlation with physiological and pathological characteristics and with biomarkers of one-carbon metabolism. *Epigenetics* 9, 621–633. doi: 10.1007/s004649900410

Coppedè, F., Stoccoro, A., Nicolì, V., Gallo, R., De Rosa, A., Guida, M., et al. (2020). Investigation of GHSR methylation levels in thymomas from patients with Myasthenia Gravis. *Gene* 752:144774. doi: 10.1007/s004649900410

Coppedè, F., Tannorella, P., Stoccoro, A., Chico, L., Siciliano, G., Bonuccelli, U., et al. (2017). Methylation analysis of DNA repair genes in Alzheimer's disease. *Mech. Ageing Dev.* 161, 105–111. doi: 10.1007/s004649900410

Costa-Pinheiro, P., Montezuma, D., Henrique, R., and Jeronimo, C. (2015). Diagnostic and prognostic epigenetic biomarkers in cancer. *Epigenomics* 7, 1003–1015. doi: 10.2217/epi.15.56

Failli, A., Legitimo, A., Migheli, F., Coppedè, F., Mathers, J. C., Spisni, R., et al. (2013). Efficacy and feasibility of the epithelial cell adhesion molecule (EpCAM) immunomagnetic cell sorter for studies of DNA methylation in colorectal cancer. *Int. J. Mol. Sci.* 15, 44–57. doi: 10.3390/ijms15010044

Hirabayashi, H., Fujii, Y., Sakaguchi, M., Tanaka, H., Yoon, H. E., Komoto, Y., et al. (1997). p16INK4, pRB, p53 and cyclin D1 expression and hypermethylation of CDKN2 gene in thymoma and thymic carcinoma. *Int. J. Cancer* 73, 639–644. doi: 10.1002/(sici)1097-0215(19971127)73:5<639::aid-ijc5>3.0.co;2-y

Hirose, Y., Kondo, K., Takizawa, H., Nagao, T., Nakagawa, Y., Fujino, H., et al. (2009). Aberrant methylation of tumour-related genes in thymic epithelial tumours. *Lung Cancer* 64, 155–159. doi: 10.1016/j.lungcan.2008.07.015

Jaretzki, A. 3rd., Barohn, R. J., Ernstoff, R. M., Kaminski, H. J., Keesey, J. C., Penn, A. S., et al. (2000). Myasthenia gravis: recommendations for clinical research standards. Task force of the medical scientific advisory board of the myasthenia gravis foundation of America. *Ann. Thorac. Surg.* 70, 327–334. doi: 10.1016/s0003-4975(00)01595-2

Kajiura, K., Takizawa, H., Morimoto, Y., Masuda, K., Tsuboi, M., Kishibuchi, R., et al. (2017). Frequent silencing of RASSF1A by DNA methylation in thymic neuroendocrine tumours. *Lung Cancer* 111, 116–123. doi: 10.1016/j.lungcan.2017.05.019

Kishibuchi, R., Kondo, K., Soejima, S., Tsuboi, M., Kajiura, K., Kawakami, Y., et al. (2020). DNA methylation of GHSR, GNG4, HOXD9 and SALL3 is a common epigenetic alteration in thymic carcinoma. *Int. J. Oncol.* 56, 315–326. doi: 10.3892/ijo.2019.4915

Lopomo, A., Ricciardi, R., Maestri, M., De Rosa, A., Melfi, F., Lucchi, M., et al. (2016). Gene-specific methylation analysis in thymomas of patients with myasthenia gravis. *Int. J. Mol. Sci.* 17:2121. doi: 10.3390/ijms17122121

Marx, A., Porubsky, S., Belharazem, D., Saruhan-Direskeneli, G., Schalke, B., Ströbel, P., et al. (2015). Thymoma related myasthenia gravis in humans and potential animal models. *Exp. Neurol.* 270, 55–65. doi: 10.1016/j.expneurol.2015.02.010

Marx, A., Ströbel, P., Badve, S. S., Chalabreysse, L., Chan, J. K., Chen, G., et al. (2014). ITMIG consensus statement on the use of the WHO histological classification of thymoma and thymic carcinoma: refined definitions, histological criteria and reporting. *J. Thorac. Oncol.* 9, 596–611. doi: 10.1097/JTO.0000000000000154

Migheli, F., Stoccoro, A., Coppedè, F., Wan Omar, W. A., Failli, A., Consolini, R., et al. (2013). Comparison study of MS-HRM and pyrosequencing techniques for quantification of APC and CDKN2A gene methylation. *PLoS One* 8:e52501. doi: 10.1371/journal.pone.0052501

Mokhtar, M., Kondo, K., Namura, T., Ali, A. H., Fujita, Y., Takai, C., et al. (2014). Methylation and expression profiles of MGMT gene in thymic epithelial tumors. *Lung Cancer* 83, 279–287. doi: 10.1016/j.lungcan.2013.12.004

Radovich, M., Pickering, C. R., Felau, I., Ha, G., Zhang, H., Jo, H., et al. (2018). The integrated genomic landscape of thymic epithelial tumors. *Cancer Cell.* 33, 244.e10–258.e10. doi: 10.1016/j.ccell.2018.01.003

Ried, M., Marx, A., Götz, A., Hamer, O., Schalke, B., Hofmann, H. S., et al. (2016). State of the art: diagnostic tools and innovative therapies for treatment of advanced thymoma and thymic carcinoma. *Eur. J. Cardiothorac. Surg.* 49, 1545–1552. doi: 10.1093/ejcts/ezv426

Suzuki, M., Chen, H., Shigematsu, H., Ando, S., Iida, T., Nakajima, T., et al. (2005). Aberrant methylation: common in thymic carcinomas, rare in thymomas. *Oncol. Rep.* 14, 1621–1624. doi: 10.3892/or.14.6.1621

Conflict of Interest: The authors declare that the research was conducted in the absence of any commercial or financial relationships that could be construed as a potential conflict of interest.

Copyright © 2020 Coppedè, Ricciardi, Lopomo, Stoccoro, De Rosa, Guida, Petrucci, Maestri, Lucchi and Migliore. This is an open-access article distributed under the terms of the Creative Commons Attribution License (CC BY). The use, distribution or reproduction in other forums is permitted, provided the original author(s) and the copyright owner(s) are credited and that the original publication in this journal is cited, in accordance with accepted academic practice. No use, distribution or reproduction is permitted which does not comply with these terms.

frontiers in Molecular Neuroscience

ORIGINAL RESEARCH
published: 26 October 2020
doi: 10.3389/fnmol.2020.567084

Lack of Desmin in Mice Causes Structural and Functional Disorders of Neuromuscular Junctions

*Nane Eiber[1], Franziska Fröb[1], Mirjam Schowalter[2], Christian Thiel[3,4], Christoph S. Clemen[2,5,6], Rolf Schröder[2,4] and Said Hashemolhosseini[1,4]**

[1]Institute of Biochemistry, Friedrich-Alexander-University of Erlangen-Nürnberg, Erlangen, Germany, [2]Institute of Neuropathology, University Hospital Erlangen, Friedrich-Alexander-University of Erlangen-Nürnberg, Erlangen, Germany, [3]Medical Faculty, Institute of Human Genetics, Friedrich-Alexander-University of Erlangen-Nürnberg, Erlangen, Germany, [4]Muscle Research Center Erlangen (MURCE), Friedrich-Alexander-University of Erlangen-Nürnberg, Erlangen, Germany, [5]Institute of Aerospace Medicine, German Aerospace Center (DLR), Cologne, Germany, [6]Medical Faculty, Center for Physiology and Pathophysiology, Institute of Vegetative Physiology, University of Cologne, Cologne, Germany

Desmin, the major intermediate filament (IF) protein in muscle cells, interlinks neighboring myofibrils and connects the whole myofibrillar apparatus to myonuclei, mitochondria, and the sarcolemma. However, desmin is also known to be enriched at postsynaptic membranes of neuromuscular junctions (NMJs). The pivotal role of the desmin IF cytoskeletal network is underscored by the fact that over 120 mutations of the human *DES* gene cause hereditary and sporadic myopathies and cardiomyopathies. A subgroup of human desminopathies comprises autosomal recessive cases resulting in the complete abolition of desmin protein. In these patients, who display a more severe phenotype than the autosomal dominant cases, it has been reported that some individuals also suffer from a myasthenic syndrome in addition to the classical occurrence of myopathy and cardiomyopathy. Since further studies on the NMJ pathology are hampered by the lack of available human striated muscle biopsy specimens, we exploited homozygous desmin knock-out mice which closely mirror the striated muscle pathology of human patients lacking desmin protein. Here, we report on the impact of the lack of desmin on the structure and function of NMJs and the transcription of genes coding for postsynaptic proteins. Desmin knock-out mice display a fragmentation of NMJs in soleus, but not in the extensor digitorum longus muscle. Moreover, soleus muscle fibers show larger NMJs. Further, transcription levels of acetylcholine receptor (AChR) genes are increased in muscles from desmin knock-out mice, especially of the AChRγ subunit, which is known as a marker of muscle fiber regeneration. Electrophysiological recordings depicted a pathological decrement of nerve-dependent endplate potentials and an increased rise time of the nerve-independent miniature endplate potentials. The latter appears related to the fragmentation of NMJs in desmin knockout mice. Our study highlights the essential role of desmin for the structural and functional integrity of mammalian NMJs.

Keywords: desminopathy, skeletal muscle, neuromuscular junction, desmin, nicotinic acetylcholine receptor, postsynaptic gene, myasthenic syndrome

OPEN ACCESS

Edited by:
Ruth Herbst,
Medical University of Vienna, Austria

Reviewed by:
Maria Jolanta Redowicz,
Nencki Institute of Experimental Biology (PAS), Poland
Xin-Ming Shen,
Mayo Clinic, United States

****Correspondence:***
Said Hashemolhosseini
said.hashemolhosseini@fau.de

Received: *29 May 2020*
Accepted: *22 September 2020*
Published: *26 October 2020*

Citation:
Eiber N, Fröb F, Schowalter M, Thiel C, Clemen CS, Schröder R and Hashemolhosseini S (2020) Lack of Desmin in Mice Causes Structural and Functional Disorders of Neuromuscular Junctions. Front. Mol. Neurosci. 13:567084. doi: 10.3389/fnmol.2020.567084

INTRODUCTION

Mutations of the human desmin gene on chromosome 2q35 cause a wide variety of hereditary and sporadic myopathies and cardiomyopathies (Clemen et al., 2013). Desminopathies exist in autosomal-dominant and -recessive subforms. While the latter usually display a childhood-onset and a more severe cardiac and skeletal muscle phenotype, the autosomal-dominant forms are typically characterized by an adult-onset between the third and the fourth decade of life (Clemen et al., 2013). Desmin, the major intermediate filament (IF) protein of muscle cells, serves to maintain myofibrillar cytoarchitecture and distributes externally applied mechanical stress intracellularly (Paulin and Li, 2004). Desmin and associated IFs form a 3-dimensional scaffold around Z-disks whilst linking myofibrils and mechanically and functionally connecting them to nuclei, mitochondria, and sarcolemma (Schröder and Schoser, 2009). Over the last two decades, more than 120 disease-causing desmin mutations have been described; with the human R350P desmin mutation being the most frequently reported gene defect in desminopathies (Clemen et al., 2015[1]).

The recessive desminopathies can further be divided into subgroups. In one group mutant desmin protein is expressed, whereas. in the other, desmin protein expression is completely abolished (Carmignac et al., 2009; Henderson et al., 2013). Desmin knock-out mice (Milner et al., 1996; Li et al., 1997), which were published long before the first report on a human patient lacking desmin are disease models for the second group (Li et al., 1996). Notably, one study already demonstrated that ablation of desmin protein expression in mice leads to a disorganization of the Neuromuscular junctions (NMJs; Agbulut et al., 2001).

Recently, two cousins with severe, infantile-onset and generalized muscle weakness and fatigability were reported in whom a homozygous DES truncating mutation leads to the complete lack of desmin protein (Durmus et al., 2016). In addition to myopathy and cardiomyopathy, these patients developed a myasthenic syndrome, which was partially improved in response to salbutamol treatment. Electrophysiological analyses of the above-mentioned cousins revealed a decremental response over 10% on repetitive nerve stimulation, indicated a clinically relevant neuromuscular NMJ transmission defect (Durmus et al., 2016).

Since appropriate human skeletal muscle biopsies from intercostal muscles are not available from desmin knock-out patients, we studied the structural and functional NMJ pathology in desmin knock-out mice.

MATERIALS AND METHODS

Mice Strains

Homozygous desmin knock-out mice (B6J.129Sv-*Des*^{tm1Cba}/Cscl[2]; breeding pairs were received by courtesy from Denise Paulin, Université Pierre et Marie Curie, Paris, France; Li et al., 1996) and wild-type littermates aged 3 to 4, as well as 7 to 8 months of age, were used. Mouse experiments were performed following animal welfare laws and approved by the responsible local committee [animal protection officer, Sachgebiet Tierschutzangelegenheiten, FAU Erlangen-Nürnberg, AZ: I/39/EE006, TS-07/11). Mice were housed in cages that were maintained in a room with temperature $22 \pm 1°C$ and relative humidity 50–60% on a 12 h light/dark cycle. Water and food were provided *ad libitum*.

Newton Meter

Muscle force was measured with all four limbs by Grip Strength Test Meter (Bioseb, Chaville, France).

Electrophysiology

Nerve-Muscle Preparations and Extracellular Recording

Electrophysiological recordings were essentially done as previously described (Kravic et al., 2016, 2018). Isolated diaphragm-phrenic nerve preparations were maintained in Liley's solution gassed with 95% O_2 and 5% CO_2 at room temperature (Liley, 1956). The recording chamber had a volume of ca. 1 ml and was perfused at a rate of 1 ml/min. The nerve was drawn up into a suction electrode for stimulation with pulses of 0.1 ms duration. The preparation was placed on the stage of a Zeiss Axio Examiner Z1 microscope fitted with incident light fluorescence illumination with filters for red (Zeiss filter set 20) fluorescing fluorophore (Carl Zeiss MicroImaging, Göttingen). At the beginning of the experiment, the compound muscle action potential (cMAP) was recorded using a micropipette with a tip diameter of ca. 10 μm, filled with a bathing solution. The electrode was positioned so that the latency of the major negative peak was minimized. The electrode was then positioned 100 μm above the surface of the muscle and cMAP was recorded.

Intracellular Recording and Data Analysis

To block muscle action potentials, so that endplate potentials (EPPs) and endplate currents (EPCs) could be recorded (Plomp et al., 1992; Rogozhin et al., 2008) μ-conotoxin GIIIB (μ-CTX, 2 μM; Peptide Institute, Osaka) was added to Liley's solution. At the same time, AChRs were labeled by adding 0.5×10^{-8} M of rhodamine-α-bungarotoxin (BTX; Life Technologies, Darmstadt) to the same solution. In some experiments, the effect of the toxin wore off after 1–2 h and contractions resumed in response to nerve stimulation. These preparations were then exposed a second time to the toxin. Two intracellular electrodes (resistance 10–15 MΩ) were inserted within 50 μm of the NMJs under visual inspection (Rogozhin et al., 2008). The current was passed through one electrode to maintain the membrane potential within 2 mV of −75 mV while voltage transients were recorded with the other. Signals were amplified by an Axoclamp 900A and digitized at 40 kHz by a Digidata 1440A under the control of pCLAMP 10 (Molecular Devices, Sunny Vale). Voltage records were filtered at 3 kHz and current records at 1 kHz (8-pole Bessel filter). Current transients were recorded using the two-electrode voltage-clamp facility of the Axoclamp 900A. Clamp gains were usually 300–1,000, reducing the voltage

[1]http://www.interfil.org/
[2]http://www.informatics.jax.org/allele/MGI:2159584

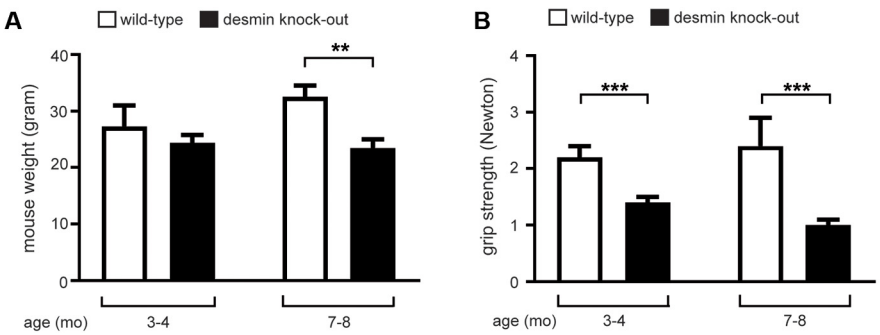

FIGURE 1 | Desmin knock-out mice show reduced muscle strength and have a lower body weight with advancing age. **(A)** For 3–4 months old desmin knock-out mice, a total of three wild-types and four mutant mice were measured. For 7–8 months old desmin knock-out mice, a total of four wild-types and five mutant mice were measured. Statistical significance was determined by unpaired two-tailed *t*-test (**$P < 0.01$). **(B)** Newton meter measurements of muscle force of desmin mutant mice showed significant muscle weakness. For 3–4 months old desmin knock-out mice, a total of three wild-types and four mutant mice were measured. For 7–8 months old desmin knock-out mice, a total of four wild-types and five mutant mice were measured. Statistical significance was determined by unpaired two-tailed *t*-test (***$P < 0.001$).

transients to <3% of their unclamped amplitudes. At most NMJs, 50–100 spontaneous quantal events were recorded for 1 min. Records were analyzed using pCLAMP 10. Spontaneous events were extracted using the "template search" facility and edited by the eye to remove obvious artifacts. Events recorded from each NMJ were averaged and the amplitude, rise time, and single exponential decay time were determined.

3D Imaging and Analysis

3D Imaging was essentially performed as previously described (Durmus et al., 2016; Kravic et al., 2016). Mice were killed by CO_2 affixation. Mouse soleus and extensor digitorum longus muscles were dissected and fixed in 2% PFA for 2 h at 4°C. Muscle bundles containing 5–10 fibers were prepared and stained with BTX 1:2,500 (Invitrogen) for 1 h at room temperature. Stained bundles were washed three times 5 min in PBS and embedded in Mowiol.

3D images of NMJs were taken with a 40× oil objective (Zeiss Examiner E1). Images were deconvolved and analyzed using different modules in AxioVision Software. The following parameters were determined for each NMJ: volume, surface, gray sum, gray mean, and the number of fragments. More than 100 NMJs were analyzed.

GO and Gene Set Enrichment Analysis

RNA sequencing was performed on RNA extracted from the gastrocnemius muscle of 3-month-old wild-type and desmin knock-out mice and is available by GEO accession number GSE154573[3]. RNA was extracted from five gastrocnemius muscle per genotype and pooled to reduce variability. Raw data files (fastq) were used to generate Bam files. Bam files of wild-type and desmin knock-out samples were uploaded to the Galaxy Server[4] and gene expression was measured using the tool "feature counts" (Galaxy Version 1.6.4 + galaxy1) and an annotation file of mouse genes (mm10). Feature counts were further used to determine differentially expressed genes by "DESeq2" (Galaxy Version 2.11.40.5). Significantly regulated genes were ranked according to their log2 fold change. Genes with a log2 fold change "≥1" or "≤−1" were submitted to the Gene Ontology enRIchment anaLysis and visuaLizAtion tool (GOrilla[5]) and subsequently analyzed using REVIGO[6]. For GSEA, the list of ranked genes was submitted to the Gene Set Enrichment Analysis tool (GSEA[7], Mootha et al., 2003; Subramanian et al., 2005) using a gene-set list of genes specific for the GO term "NMJ" obtained from AMIGO[8]).

Statistical Analysis

Data are presented as the mean values, and the error bars indicate ± SEM. The significance is calculated by unpaired, two-tailed *t*-test, or as indicated by the figure legends, and provided as real *P*-values that are believed to be categorized for different significance levels, like, ***$P < 0.001$, **$P < 0.01$, or *$P < 0.05$.

RESULTS

Desmin Knock-Out Mice Show Reduced Muscle Strength and Have a Lower Body Weight With Advancing Age

First, we asked for phenotypical changes of desmin knock-out mice in comparison with controls. Based on patient data, we expect a loss of muscle grip strength in the desmin knock-out mice. This might be accompanied by an impact on the bodyweight of the mice. Moreover, since pathological disorders of the skeletal muscles are often observed being age-dependent, two age stages of the mice were examined, i.e., 3–4 and 7–8-month-old mice. The weight of the mice turned out to be reduced at both stages of age (**Figure 1**). The decrease in body

[3]www.ncbi.nlm.nih.gov/geo/query/acc.cgi?acc=GSE154573
[4]https://usegalaxy.eu/
[5]http://cbl-gorilla.cs.technion.ac.il/
[6]http://revigo.irb.hr/
[7]https://www.gsea-msigdb.org/gsea/index.jsp
[8]http://amigo.geneontology.org/amigo

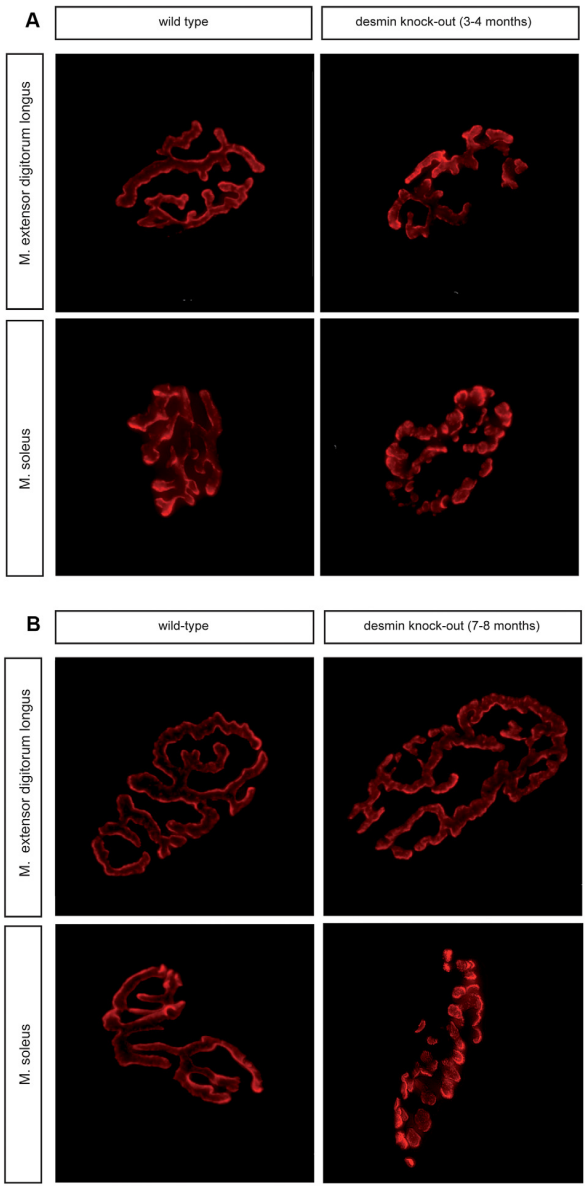

FIGURE 2 | Soleus muscle of desmin knock-out mice show a higher degree of fragmentation of their neuromuscular junctions (NMJs). **(A)** Representative images of BTX wild-type and desmin knock-out homozygous NMJs of oxidative soleus and glycolytic extensor digitorum longus muscles are shown. Note, NMJs of oxidative soleus muscle are fragmented in the absence of desmin. 3–4 months old mice were used. **(B)** Representative images of BTX wild-type and desmin knock-out homozygous NMJs of oxidative soleus and glycolytic extensor digitorum longus muscles are shown. Note, NMJs of oxidative soleus muscle are fragmented in the absence of desmin. 7–8 months old mice were used.

weight in 3–4-month-old mice was indicated, but not statistically significant (**Figure 1A**). In 7–8-month-old mice, the bodyweight of the mutant mice dropped by more than 25% compared to the controls (**Figure 1A**). This observed decrease in weight of the desmin knock-out mice correlated with a decrease in muscle strength (**Figure 1B**). At the age of 3–4 months, a significant decrease of muscle grip strength was measured in desmin knock-out mice in comparison with controls, and this decrease was even more prominent at the age of 7–8 months with approx. 30% (**Figure 1B**).

The NMJs of Desmin Knock-Out Mice Show a Higher Degree of Fragmentation

Many perturbations of NMJs lead to structural disorders and are often represented by fragmentation of NMJs (Li et al., 2018). Here, NMJs of soleus and extensor digitorum longus muscles were analyzed in 3–4 and 7–8 month old desmin knock-out mice. Immunofluorescence stains of muscle fiber bundles with BTX (rhodamine-α-bungarotoxin) revealed NMJs of extensor digitorum longus muscles being non-fragmented in comparison with controls regardless of the age (**Figures 2A,B**). Similar treatment and analysis of muscle fiber bundles of soleus muscles, however, showed a prominent and significant fragmentation at both investigated age stages (**Figures 2A,B**). Quantitative analysis of numbers of fragments per NMJ confirmed the non-fragmented status of extensor digitorum longus NMJs (**Figures 3A,C**). For the NMJs in soleus, it turned out that NMJs with low fragmentation grade (1–5 fragments) are reduced by more than 50% in desmin knock-out mice in comparison with controls (**Figures 3B,D**). The number of fragmented NMJs was increased by more than 10×-fold in both, NMJs composed of 6–10 and those with more than 10 fragments (**Figures 3B,C**).

Desmin Knock-Out Mice Display Enlarged NMJs

To explore the *in vivo* role of desmin for the structural integrity of NMJs, we used the whole-mount BTX stains of desmin knock-out and control mouse muscle fibers for quantitative 3D morphometrical analysis. Notably, the total volume of NMJs appeared significantly enlarged in desmin knock-out mice when compared to controls. This phenomenon was observed in soleus in an age-independent fashion (**Figures 4A,E**), but not extensor digitorum longus muscles. This change in volume was also expected and reflected by a similar change in their "sum fluorescence intensity" (**Figures 4C,G**). An increase in surface area would also be expected from larger and at the same time fragmented NMJs, and could be confirmed regardless of age (**Figures 4B,F**). Further, we asked whether the ablation of desmin protein impaired the intensity of BTX-labeled NMJs, which was analyzed by measuring the "mean fluorescence intensity." A change of the "mean fluorescence intensity" might reflect a different number of AChRα subunits per NMJ in the absence of desmin. Regardless of the fragmentation status and investigated muscle type, no significant change of the "mean fluorescence intensity" was found in desmin knock-out in comparison with control muscles (**Figures 4D,H**).

Gene Set Enrichment Analysis of Transcriptome Data Discloses a Dysregulation of Synaptic Gene Expression

We asked for the reasons for NMJ fragmentation in the desmin knock-out soleus. One of them might be a differentially regulated synaptic gene expression in those muscle fibers. We

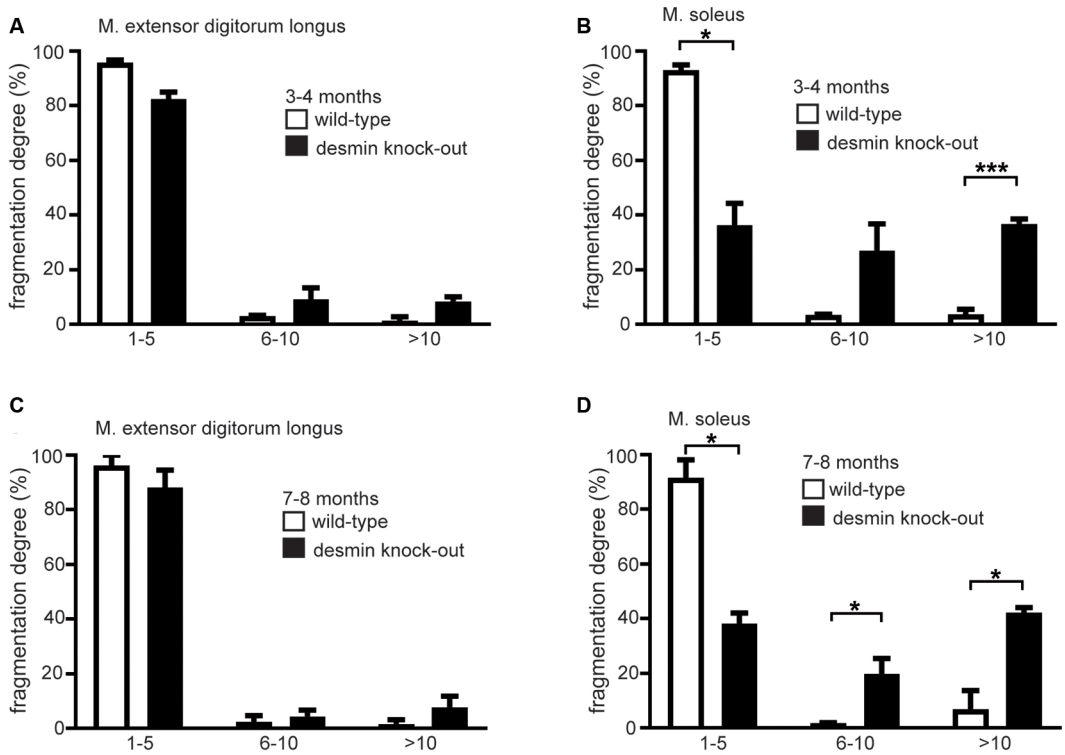

FIGURE 3 | The soleus muscle of desmin knock-out mice shows a higher degree of fragmentation of their NMJs. **(A,B)** The extensor digitorum longus or soleus muscle NMJs were categorized in groups according to their number of fragments. The number of NMJs in each group is given as the percentage of the total NMJ number for each genotype. For extensor digitorum longus a total of 96 wild-types and 89 homozygous, for soleus muscle 90 wild-type and 103 homozygous NMJs were counted (n = 3 mouse pairs). Mice were 3–4 months old. Statistical significance was determined by unpaired two-tailed t-test (*$P < 0.05$, ***$P < 0.001$). **(C,D)** The extensor digitorum longus or soleus muscle NMJs were categorized in groups according to their number of fragments. The number of NMJs in each group is given as the percentage of the total NMJ number for each genotype. For extensor digitorum longus a total of 102 wild-types and 95 homozygous, for soleus muscle 99 wild-type and 102 homozygous NMJs were counted (n = 3 mouse pairs). Mice were 7–8 months old. Statistical significance was determined by unpaired two-tailed t-test (*$P < 0.05$).

elucidated the muscle transcriptome of desmin knock-out mice in comparison with the wild-type littermate controls by comparative RNA-Seq experiments. Employing GO term analyses revealed mostly genes belonging to the "regulation of multicellular organismal process" being upregulated and "negative regulation of CD8-positive, alpha-beta T cell differentiation" being downregulated (**Figures 5A,B**). These topics do not necessarily reflect changes in NMJ biology. Since synaptic gene expression is under-represented in total RNA of muscles due to a very low number of synaptic nuclei in comparison with extrasynaptic nuclei in muscle fibers, a closer look at the synaptic genes and their log2fc was required and indicated that NMJ-specific genes were differentially regulated in the absence of desmin in comparison with controls (**Figure 5C**). Therefore, Gene Set Enrichment Analysis (GSEA) with an NMJ-specific gene list was carried out (**Figure 5D**).

Some usual suspects, which control the formation and maintenance of the postsynaptic apparatus at NMJs, are the different subunits of the AChRs, the scaffold protein Rapsyn, the nerve-derived heparan sulfate proteoglycan Agrin, and its receptors, co-receptors, and signaling pathway adaptors, Lrp4, the muscle-specific receptor tyrosine kinase MuSK, and Dok7 (Herrmann et al., 2015). As proof, the desmin mRNA was down-regulated in desmin knock-out muscles in comparison to control; in principle means that it is absent as expected in desmin knock-out mice. Notably, the expression of several synaptic genes, like different Acetylcholine receptor (AChR) subunits is statistically significantly up-regulated in desmin knock-out fibers in comparison with controls (**Figure 5C**). In contrast, the transcript amounts of the other synaptic candidate genes, like Dok7, Rapsyn, and MuSK, were only slightly down-regulated (**Figure 5C**).

Electrophysiological Recordings of Desmin Knock-Out Mice Muscle Fibers Highlight a Higher Decrement After Repetitive Stimulation and Increased Rise Times of mEPPs

To better understand the physiological consequences regarding neuromuscular transmission in desmin knock-out mice, like the potential occurrence of muscle fatigability, we next assessed

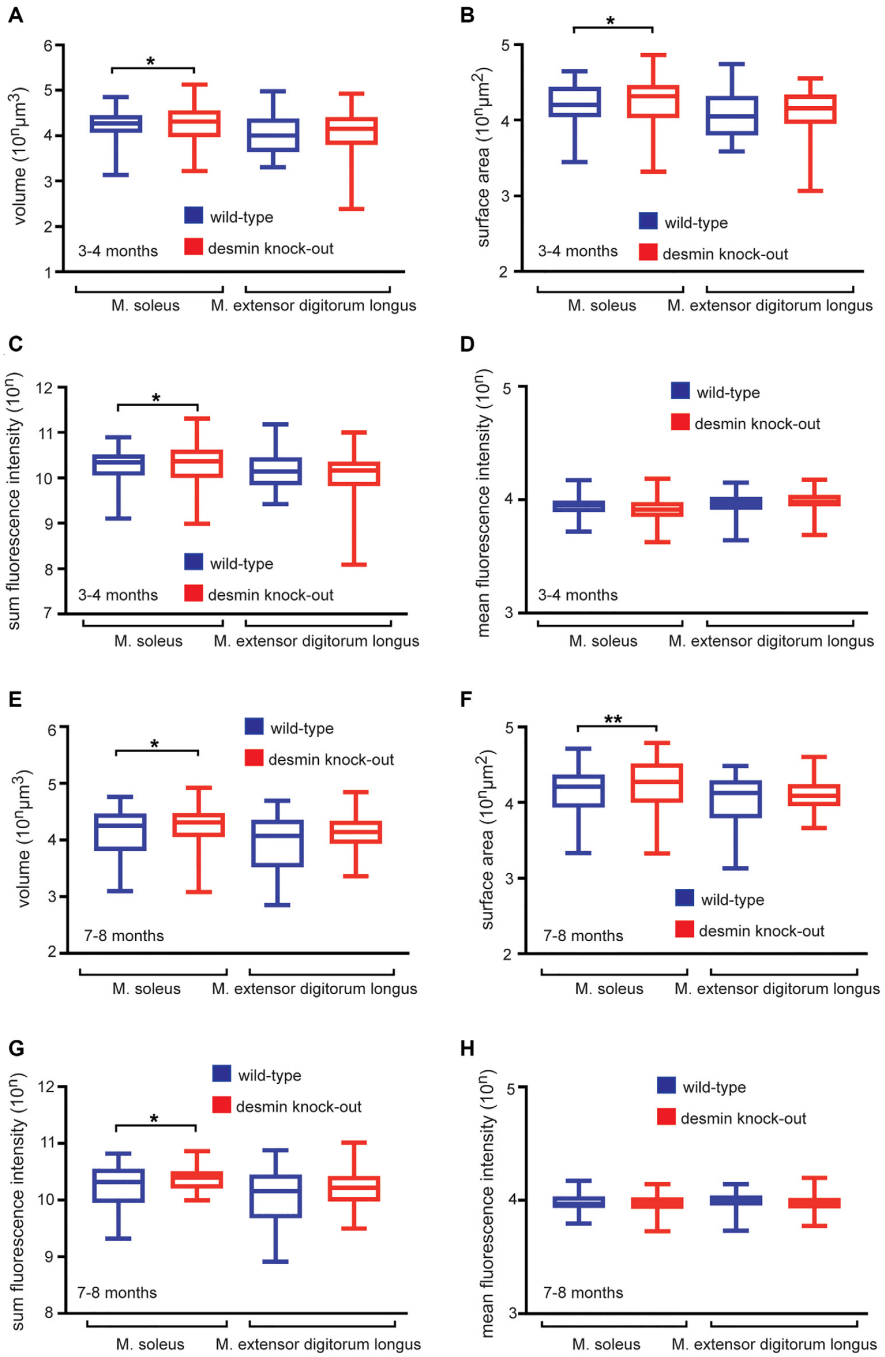

FIGURE 4 | Desmin knock-out mice display enlarged NMJs in soleus muscle. **(A–D)** Hindlimb muscles of 3–4 months old wild-type and homozygous desmin knock-out mice were dissected to stain fiber bundles with BTX. Imaging was done with a fluorescence microscope, and z-stacks were acquired for quantitative 3D morphometry. **(A–D)** Box and Whisker plots depict the recorded average volume, surface, and sum fluorescence intensity per NMJ of indicated genotypes and muscles. Note, surface, volume, and sum fluorescence intensity of NMJs are significantly higher in homozygous desmin knock-out mice in soleus muscle in comparison to wild-type littermates. For extensor digitorum longus muscle a total of 96 wild-types and 89 homozygous NMJs, for soleus muscle 90 wild-type and 103 homozygous NMJs were counted ($n = 3$ mouse pairs). Statistical significance was determined by unpaired two-tailed t-test ($^*P < 0.05$). **(E–H)** Hindlimb muscles of 7–8 months old wild-type and homozygous desmin knock-out mice were dissected to stain fiber bundles with BTX. Imaging was done with a fluorescence microscope, and z-stacks were acquired for quantitative 3D morphometry. **(E–H)** Box and Whisker plots depict the recorded average volume, surface, and sum fluorescence intensity per NMJ of indicated genotypes and muscles. Note, surface, volume, and sum fluorescence intensity of NMJs are significantly higher in homozygous desmin knock-out mice in soleus muscle in comparison to the controls. For extensor digitorum longus muscle a total of 102 wild-types and 95 homozygous NMJs, for soleus muscle 99 wild-type and 102 homozygous NMJs were counted ($n = 3$ mouse pairs). Statistical significance was determined by unpaired two-tailed t-test ($^*P < 0.05$, $^{**}P < 0.01$).

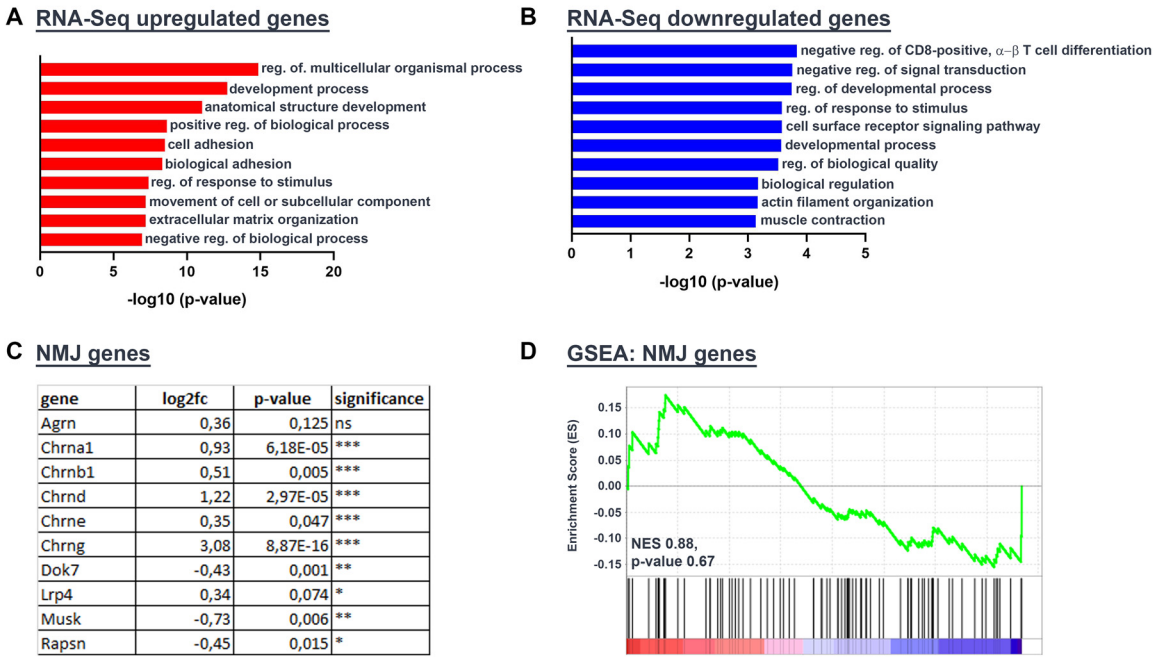

gene	log2fc	p-value	significance
Agrn	0,36	0,125	ns
Chrna1	0,93	6,18E-05	***
Chrnb1	0,51	0,005	***
Chrnd	1,22	2,97E-05	***
Chrne	0,35	0,047	***
Chrng	3,08	8,87E-16	***
Dok7	-0,43	0,001	**
Lrp4	0,34	0,074	*
Musk	-0,73	0,006	**
Rapsn	-0,45	0,015	*

FIGURE 5 | Gene Set Enrichment Analysis of Transcriptome Data discloses a dysregulation of synaptic gene expression. RNA-Seq of five wild-types and five desmin knock-out mouse tissue specimens derived from gastrocnemius/plantaris muscles revealed several differentially regulated genes. **(A,B)** GO Analysis was performed with genes that were up- or downregulated at least 2-fold in desmin knock-out mice (up log2fc $\geq$1, down log2fc ≤ -1). **(C)** The table depicts a set of NMJ-specific genes with their RNA-Seq expression results in the desmin knock-out genotype as compared to wild-type controls [log2fc, *p*-value: *p* (*$P \leq 0.05$; **$P \leq 0.01$; ***$P \leq 0.001$)]. **(D)** Gene set enrichment blot from GSEA analysis of RNA-Seq data with the NMJ gene set. Normalized enrichment score (NES) and *p*-value are listed at the bottom of the blot.

neuromuscular transmission by repetitive stimulation of the phrenic nerve with 20 Hz trains for 10 s and calculated the decrement of EPP amplitude (**Figure 6A**). We measured a significant decremental response in both 3–4 and 7–8 months-old desmin knock-out mice in comparison with controls (**Figure 6A**).

We also asked whether the absence of desmin impinges functional channel characteristics of the AChRs. By monitoring nerve-independently appearing miniature endplate potentials, we neither detected a change in their frequency, amplitude nor decay time constant (**Figures 6B–D**), but observed a significant increase of the rise times of the miniature EPP (mEPP) in desmin knock-out diaphragms in comparison with controls (**Figure 6E**). This change was also visible by analyzing the rise time of the mEPC (**Figure 6F**). Neither input resistance (data not shown) nor EPP or EPC amplitudes were different comparing desmin knock-out with control mice (**Figures 6G,H**). Quantal content remained also unchanged in the comparison between desmin knock-out and control mice (data not shown).

DISCUSSION

An extension of our previous work in human patients lacking desmin (Durmus et al., 2016), we here analyzed the structure and function of NMJ in patient-mimicking desmin knock-out mice. For this purpose, two age bins (3–4 and 7–8 month old homozygous desmin knock-out mice) were investigated to elucidate age-dependent effects. In keeping with the myasthenic phenotype in the reported desmin knock-out patients, our analysis depicted NMJ pathology on various levels. Our morphological analysis denoted a fragmentation of NMJs in soleus but not extensor digitorum longus muscle, thus mirroring our previous findings in homozygous desmin R349P knock-in mice, which only express R349P mutant desmin protein (Durmus et al., 2016).

For elucidating structural characteristics of the NMJs in desmin knock-out mice, we applied a 3D quantitative morphology analysis, a methodology which was previously successfully employed (Durmus et al., 2016; Kravic et al., 2016; Giacomazzi et al., 2017; Cescon et al., 2018; Eiber et al., 2019). Here, we found that the increase of NMJ fragmentation not only correlated with an increase of surface area like expected (**Figures 4B,F**), but there was also an increase of the dimensions of NMJs detectable in desmin knock-out mice in comparison with control mice, reflected by an increase in volume and sum fluorescence intensity (**Figures 4A,C,E,G**). This observation was also present, though to a lower extent, in the desmin R349P knock-in mice (Durmus et al., 2016).

In this study, we went further and asked for the reason of NMJ fragmentation in the absence of desmin. A possible cause might be different gene expression profiles of synaptic genes. Total RNA sequencing was employed to enlighten the transcriptome

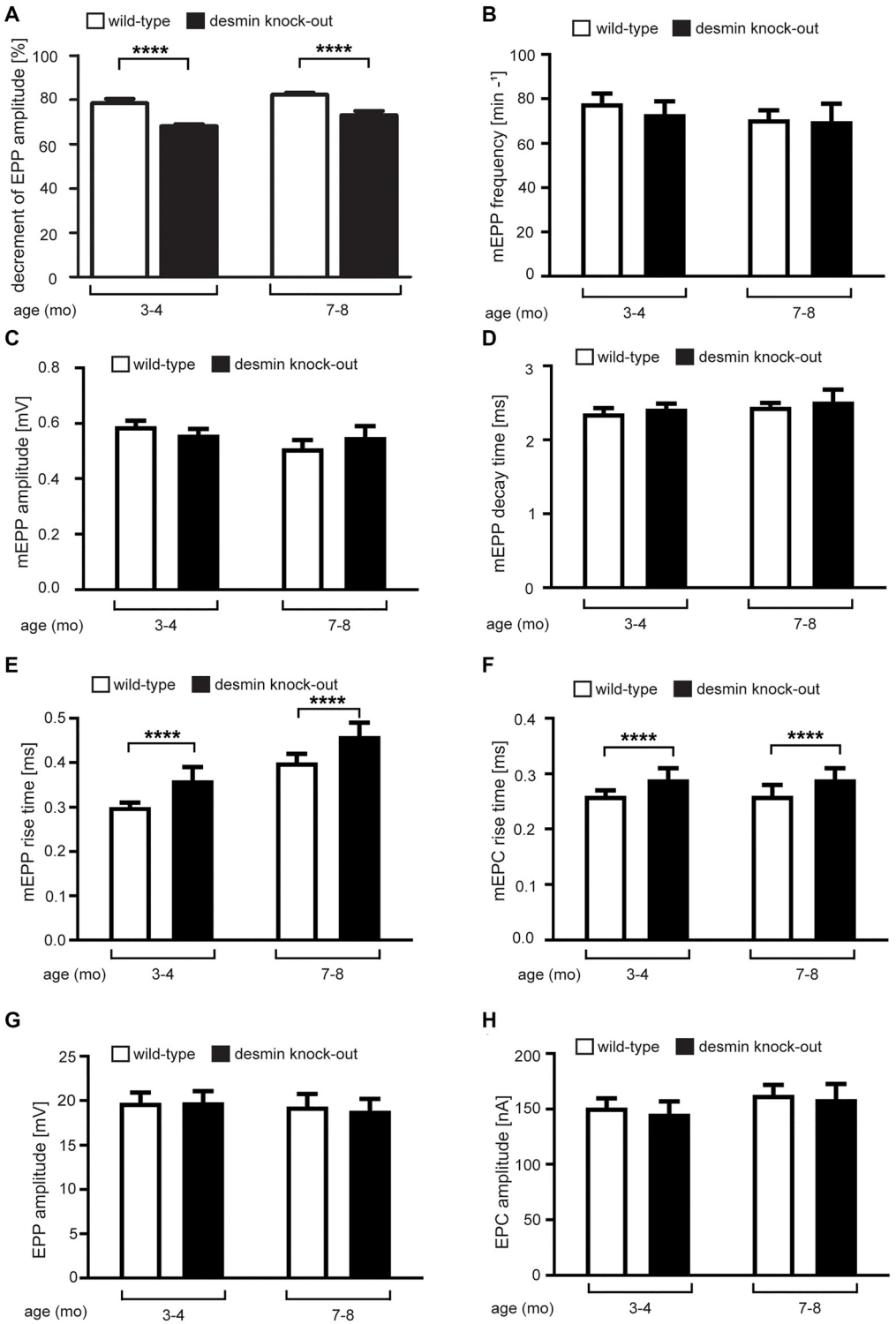

FIGURE 6 | Electrophysiological recordings of desmin knock-out mice muscle fibers reveal a higher decrement after repetitive stimulation and increased rise times of mEPPs. Recordings were done with wild-type and desmin knock-out soleus muscles in 3–4 months-old and 7–8 months-old mice. The graphs show these data as follows: **(A)** Decrement of the endplate potential amplitude, **(B)** mEPP frequency, **(C)** mEPP amplitude, **(D)** mEPP decay time constant, **(E)** mEPP rise time, **(F)** mEPC rise time, **(G)** EPP amplitude, and **(H)** EPC amplitude. Statistical significance was in all cases determined by unpaired two-tailed *t*-test (****$P < 0.0001$). Note, in desmin knock-out mice the decrement of EPP amplitude was reduced and mEPP/mEPC rise times increased. All other parameters recorded were not changed between wild-type and desmin knock-out genotypes.

profile of desmin knock-out muscles. For technical reasons, the total RNA of the gastrocnemius and plantaris muscles were used for this study. Although it might have been more adequate to use total RNA from soleus, we do not consider that a problem because of the detected changes (see below) and being aware that also the plantaris muscle contains a decent amount of slow fiber types (Huraskin et al., 2016). Almost all AChR subunit genes were upregulated in desmin knock-out mice in comparison to the wild-type littermate controls (**Figure 5**). This upregulation of AChR subunit genes might indicate a high turnover dynamics of the clustered AChRs, like being reported previously in another context (Eiber et al., 2019). Even the transcription of the AChRγ subunit was up-regulated (**Figure 5**), like it was shown for R349P desmin knock-in mice, pointing to potential degenerative events ongoing in the absence of desmin. The transcription of other players at NMJs, like MuSK, Dok7, and Rapsyn, was not much affected (**Figure 5**).

Finally, electrophysiological recordings were used to look for physiological impairments of neuromuscular transmission in desmin knock-out mice, which was not previously studied using desmin R349P knock-in mice (Durmus et al., 2016). For these recordings, soleus muscles of desmin knock-out mice and controls were used. The decrement of endplate potential amplitudes was reduced in desmin knock-out mice in an age-independent manner (**Figure 6A**), and accompanied by a surprising increase of rising times of mEPPs and mEPCs in desmin knock-out mice (**Figures 6E,F**). The increased rise times of mEPPs and mEPCs in knock-out mice shown in **Figures 6E,F** might reflect the observed fragmentation of NMJs, which also accounts for the greater decrement of EPP amplitude with 20 Hz stimulation for 10 s than that in the control. An increase of the rise time might also be the consequence of myofibrillar changes or in a more direct fashion by the specific interaction of desmin with synaptic proteins. We are aware that our data does not clarify all questions. Of course, it is obvious and tempting to assume that only NMJs of the soleus muscle is fragmented, because this muscle is also composed of fast type I fibers compared to the extensor digitorum longus muscle being composed solely of type II fibers. However, our preliminary studies point to an even distribution of fragmented NMJs in the soleus muscle between type I and type II fibers (unpublished data). It remains to understand why then NMJs of soleus are fragmented, but not of extensor digitorum longus muscle. Another question which should be addressed in the future is whether the observed changes between NMJs from soleus and extensor digitorum longus muscle are associated with the changes in the myofiber morphology; in other words, whether the NMJ aberrations could be a result of changes in the fiber structure to understand whether NMJ fragmentation is a primary or secondary effect. To our knowledge, desmin knock-out mice were not analyzed regarding changes in the fiber structure in a muscle-specific manner previously. However, imaging studies did not reveal obvious changes in sarcomere misalignment at the NMJs in flexor digitorum brevis muscles of desmin knock-out mice (Goodall et al., 2012). Our preliminary data (unpublished) do not correlate with severe fiber structure changes being present differently in soleus in comparison to extensor digitorum longus muscle.

In summary, our data highlight the essential role of desmin for the structural and functional integrity of NMJs in man and mice.

DATA AVAILABILITY STATEMENT

The datasets generated for this study are available by GEO accession number GSE154573 (www.ncbi.nlm.nih.gov/geo/query/acc.cgi?acc=GSE154573).

ETHICS STATEMENT

The animal study was reviewed and approved by Animal protection officer, Sachgebiet Tierschutzangelegenheiten, FAU Erlangen-Nürnberg, AZ: I/39/EE006, TS-07/11.

AUTHOR CONTRIBUTIONS

NE, FF, MS, CT, CC, RS, and SH designed and performed the experiments. NE, FF, CC, RS, and SH prepared figures and wrote the original draft. All authors performed review and editing of the manuscript. All authors contributed to the article and approved the submitted version.

FUNDING

The work in the labs of SH and RS was supported by the German Research Council DFG (HA3309/3-1, HA3309/6-1, HA3309/7-1, and SCHR562/16-1). The doctoral thesis work of MS was supported by a medical student grant of the Interdisciplinary Center for Clinical Research (IZKF), Medical Faculty, Friedrich-Alexander University Erlangen-Nürnberg, Erlangen.

REFERENCES

Agbulut, O., Li, Z., Perie, S., Ludosky, M. A., Paulin, D., Cartaud, J., et al. (2001). Lack of desmin results in abortive muscle regeneration and modifications in synaptic structure. *Cell Motil. Cytoskeleton* 49, 51–66. doi: 10.1002/cm.1020

Carmignac, V., Sharma, S., Arbogast, S., Fischer, D., Serreri, C., Serria, M., et al. (2009). A homozygous desmin deletion causes an Emery-Dreifuss like recessive myopathy with desmin depletion. *Neuromus. Disord.* 19, 600–600. doi: 10.1016/j.nmd.2009.06.179

Cescon, M., Gregorio, I., Eiber, N., Borgia, D., Fusto, A., Sabatelli, P., et al. (2018). Collagen VI is required for the structural and functional integrity of the neuromuscular junction. *Acta Neuropathol.* 136, 483–499. doi: 10.1007/s00401-018-1860-9

Clemen, C. S., Herrmann, H., Strelkov, S. V., and Schroder, R. (2013). Desminopathies: pathology and mechanisms. *Acta Neuropathol.* 125, 47–75. doi: 10.1007/s00401-012-1057-6

Clemen, C. S., Stockigt, F., Strucksberg, K. H., Chevessier, F., Winter, L., Schutz, J., et al. (2015). The toxic effect of R350P mutant desmin in striated muscle of man and mouse. *Acta Neuropathol.* 129, 297–315. doi: 10.1007/s00401-014-1363-2

Durmus, H., Ayhan, O., Cirak, S., Deymeer, F., Parman, Y., Franke, A., et al. (2016). Neuromuscular endplate pathology in recessive desminopathies:

lessons from man and mice. *Neurology* 87, 799–805. doi: 10.1212/WNL.0000000000003004

Eiber, N., Rehman, M., Kravic, B., Rudolf, R., Sandri, M., and Hashemolhosseini, S. (2019). Loss of protein kinase Csnk2b/CK2β at neuromuscular junctions affects morphology and dynamics of aggregated nicotinic acetylcholine receptors, neuromuscular transmission and synaptic gene expression. *Cells* 8:940. doi: 10.3390/cells8080940

Giacomazzi, G., Holvoet, B., Trenson, S., Caluwe, E., Kravic, B., Grosemans, H., et al. (2017). MicroRNAs promote skeletal muscle differentiation of mesodermal iPSC-derived progenitors. *Nat. Commun.* 8:1249. doi: 10.1038/s41467-017-01359-w

Goodall, M. H., Ward, C. W., Pratt, S. J. P., Bloch, R. J., and Lovering, R. M. (2012). Structural and functional evaluation of branched myofibers lacking intermediate filaments. *Am. J. Physiol. Cell Physiol.* 303, C224–232. doi: 10.1152/ajpcell.00136.2012

Henderson, M., De Waele, L., Hudson, J., Eagle, M., Sewry, C., Marsh, J., et al. (2013). Recessive desmin-null muscular dystrophy with central nuclei and mitochondrial abnormalities. *Acta Neuropathol.* 125, 917–919. doi: 10.1007/s00401-013-1113-x

Herrmann, D., Straubinger, M., and Hashemolhosseini, S. (2015). Protein kinase CK2 interacts at the neuromuscular synapse with Rapsyn, Rac1, 14–3-3γ, and Dok-7 proteins and phosphorylates the latter two. *J. Biol. Chem.* 290, 22370–22384. doi: 10.1074/jbc.M115.647610

Huraskin, D., Eiber, N., Reichel, M., Zidek, L. M., Kravic, B., Bernkopf, D., et al. (2016). Wnt/β-catenin signaling *via* Axin2 is required for myogenesis and, together with YAP/Taz and Tead1, active in IIa/IIx muscle fibers. *Development* 143, 3128–3142. doi: 10.1242/dev.139907

Kravic, B., Harbauer, A. B., Romanello, V., Simeone, L., Vogtle, F. N., Kaiser, T., et al. (2018). In mammalian skeletal muscle, phosphorylation of TOMM22 by protein kinase CSNK2/CK2 controls mitophagy. *Autophagy* 14, 311–335. doi: 10.1080/15548627.2017.1403716

Kravic, B., Huraskin, D., Frick, A. D., Jung, J., Redai, V., Palmisano, R., et al. (2016). LAP proteins are localized at the post-synaptic membrane of neuromuscular junctions and appear to modulate synaptic morphology and transmission. *J. Neurochem.* 139, 381–395. doi: 10.1111/jnc.13710

Li, Z., Colucci-Guyon, E., Pinçon-Raymond, M., Mericskay, M., Pournin, S., Paulin, D., et al. (1996). Cardiovascular lesions and skeletal myopathy in mice lacking desmin. *Dev. Biol.* 175, 362–366. doi: 10.1006/dbio.1996.0122

Li, Z., Mericskay, M., Agbulut, O., Butler-Browne, G., Carlsson, L., Thornell, L. E., et al. (1997). Desmin is essential for the tensile strength and integrity of myofibrils but not for myogenic commitment, differentiation, and fusion of skeletal muscle. *J. Cell Biol.* 139, 129–144. doi: 10.1083/jcb.139.1.129

Li, L., Xiong, W. C., and Mei, L. (2018). Neuromuscular junction formation, aging, and disorders. *Annu. Rev. Physiol.* 80, 159–188. doi: 10.1146/annurev-physiol-022516-034255

Liley, A. W. (1956). An investigation of spontaneous activity at the neuromuscular junction of the rat. *J. Physiol.* 132, 650–666. doi: 10.1113/jphysiol.1956.sp005555

Milner, D. J., Weitzer, G., Tran, D., Bradley, A., and Capetanaki, Y. (1996). Disruption of muscle architecture and myocardial degeneration in mice lacking desmin. *J. Cell Biol.* 134, 1255–1270. doi: 10.1083/jcb.134.5.1255

Mootha, V. K., Lindgren, C. M., Eriksson, K. F., Subramanian, A., Sihag, S., Lehar, J., et al. (2003). PGC-1α-responsive genes involved in oxidative phosphorylation are coordinately downregulated in human diabetes. *Nat. Genet.* 34, 267–273. doi: 10.1038/ng1180

Paulin, D., and Li, Z. (2004). Desmin: a major intermediate filament protein essential for the structural integrity and function of muscle. *Exp. Cell Res.* 301, 1–7. doi: 10.1016/j.yexcr.2004.08.004

Plomp, J. J., van Kempen, G. T., and Molenaar, P. C. (1992). Adaptation of quantal content to decreased postsynaptic sensitivity at single endplates in α-bungarotoxin-treated rats. *J. Physiol.* 458, 487–499. doi: 10.1113/jphysiol.1992.sp019429

Rogozhin, A. A., Pang, K. K., Bukharaeva, E., Young, C., and Slater, C. R. (2008). Recovery of mouse neuromuscular junctions from single and repeated injections of botulinum neurotoxin A. *J. Physiol.* 586, 3163–3182. doi: 10.1113/jphysiol.2008.153569

Schröder, R., and Schoser, B. (2009). Myofibrillar myopathies: a clinical and myopathological guide. *Brain Pathol.* 19, 483–492. doi: 10.1111/j.1750-3639.2009.00289.x

Subramanian, A., Tamayo, P., Mootha, V. K., Mukherjee, S., Ebert, B. L., Gillette, M. A., et al. (2005). Gene set enrichment analysis: a knowledge-based approach for interpreting genome-wide expression profiles. *Proc. Natl. Acad. Sci. U S A* 102, 15545–15550. doi: 10.1073/pnas.0506580102

Conflict of Interest: The authors declare that the research was conducted in the absence of any commercial or financial relationships that could be construed as a potential conflict of interest.

Copyright © 2020 Eiber, Fröb, Schowalter, Thiel, Clemen, Schröder and Hashemolhosseini. This is an open-access article distributed under the terms of the Creative Commons Attribution License (CC BY). The use, distribution or reproduction in other forums is permitted, provided the original author(s) and the copyright owner(s) are credited and that the original publication in this journal is cited, in accordance with accepted academic practice. No use, distribution or reproduction is permitted which does not comply with these terms.

frontiers in Molecular Neuroscience

REVIEW
published: 16 November 2020
doi: 10.3389/fnmol.2020.568426

Impairment Mechanisms and Intervention Approaches for Aged Human Neuromuscular Junctions

Yomna Badawi[1] *and Hiroshi Nishimune*[1,2]*

[1] *Department of Anatomy and Cell Biology, University of Kansas School of Medicine, Kansas City, KS, United States,*
[2] *Neurobiology of Aging, Tokyo Metropolitan Institute of Gerontology, Itabashi, Japan*

The neuromuscular junction (NMJ) is a chemical synapse formed between a presynaptic motor neuron and a postsynaptic muscle cell. NMJs in most vertebrate species share many essential features; however, some differences distinguish human NMJs from others. This review will describe the pre- and postsynaptic structures of human NMJs and compare them to NMJs of laboratory animals. We will focus on age-dependent declines in function and changes in the structure of human NMJs. Furthermore, we will describe insights into the aging process revealed from mouse models of accelerated aging. In addition, we will compare aging phenotypes to other human pathologies that cause impairments of pre- and postsynaptic structures at NMJs. Finally, we will discuss potential intervention approaches for attenuating age-related NMJ dysfunction and sarcopenia in humans.

Keywords: active zone (AZ), aging, caloric restriction, exercise, laminin, neuromuscular disease, progeria, synapse

OPEN ACCESS

Edited by:
Hanns Lochmuller,
University of Ottawa, Canada

Reviewed by:
Clarke Slater,
Retired, Newcastle upon Tyne, United Kingdom
Robert W. Burgess,
Jackson Laboratory, United States
Rüdiger Rudolf,
Mannheim University of Applied Sciences, Germany

***Correspondence:**
Hiroshi Nishimune
nishimun@tmig.or.jp

Received: *01 June 2020*
Accepted: *16 October 2020*
Published: *16 November 2020*

Citation:
Badawi Y and Nishimune H (2020) Impairment Mechanisms and Intervention Approaches for Aged Human Neuromuscular Junctions. Front. Mol. Neurosci. 13:568426. doi: 10.3389/fnmol.2020.568426

INTRODUCTION

Synapses are required to maintain the proper function of the nervous system both in health and during disease. The neuromuscular junction (NMJ) is a synapse critical for the transfer of information between a presynaptic motor neuron and a postsynaptic muscle fiber at specialized sites on the muscle plasma membrane called endplates. During development, motor neurons seek out and find nascent endplates on the sarcolemmal surface (skeletal muscle fiber plasma membrane) (Frank and Fischbach, 1979; Sanes and Lichtman, 2001). Innervation of muscle fibers by motor neurons ensures proper control of skeletal muscle contraction through the regulated release of neurotransmitters. Among vertebrate NMJs, the neurotransmitter acetylcholine (ACh) is released from highly specialized sites at the presynaptic membrane called active zones. By electron microscopy analysis, active zones appear as electron-dense projections on the presynaptic membrane where synaptic vesicles fuse for subsequent exocytosis (Couteaux and Pecot-Dechavassine, 1970; Tsuji, 2006). In human NMJs, freeze-fracture electron microscopy shows

Abbreviations: ACh, acetylcholine; AChR, acetylcholine receptors; ALS, amyotrophic lateral sclerosis; CMS, congenital myasthenic syndromes; dSTORM, direct stochastic optical reconstruction microscopy; ERCC1, excision repair cross-complementing group 1; LEMS, Lambert-Eaton myasthenia syndrome; LRP4, low-density lipoprotein receptor-related protein 4; MuSK, muscle-specific kinase; MG, myasthenia gravis; MHC, myosin heavy chain isoform; mTOR, mammalian/mechanistic Target of Rapamycin; NMJ, neuromuscular junction; SOD1, superoxide dismutase 1; STED, stimulated emission depletion; SNAP25, synaptosomal associated protein-25; SNARE, soluble *N*-ethylmaleimide-sensitive factor activating protein receptor; VGCC, voltage-gated calcium channels.

double parallel rows of about 20 large particles in the p-face of the presynaptic membrane, which was interpreted as an active zone unit structure (Fukunaga et al., 1982). The macromolecules in the active zones interact with docked synaptic vesicles, which has been revealed in frog and mouse NMJs by electron microscopy tomography (Harlow et al., 2001; Nagwaney et al., 2009; Szule et al., 2012; Harlow et al., 2013; Jung et al., 2018). These docked synaptic vesicle fuse with the plasma membrane following calcium influx into the presynaptic terminals with the help of SNARE (Soluble *N*-ethylmaleimide-sensitive factor activating protein receptor) proteins including SNAP-25, synaptobrevin/VAMP, and syntaxin 1 (Jahn and Scheller, 2006; Sudhof and Rothman, 2009). The calcium influx required for neuromuscular transmission at adult mammalian NMJs is primarily mediated by P/Q-type voltage-gated calcium channels (VGCC) (Uchitel et al., 1992; Rosato Siri and Uchitel, 1999). Electron microscopy studies have shown that presynaptic active zones are positioned apposed to the openings of post-synaptic junctional folds (Couteaux and Pecot-Dechavassine, 1970; Patton et al., 2001). Junctional folds are small invaginations of the postsynaptic membrane that increases the area of acetylcholine receptors (AChRs) accumulation to efficiently receive ACh released from motor nerve terminals following depolarization by the action potential (Fertuck and Salpeter, 1974, 1976; Anderson and Cohen, 1977; Frank and Fischbach, 1979). Voltage-gated sodium channels are located in the troughs of post-synaptic junctional folds to generate action potentials (Caldwell, 2000). The activation of voltage-gated sodium channels in mice is responsible for 15–20% of the endplate potential (Hong and Chang, 1989). The high density of voltage-gated sodium channels and the increased local input resistance due to the narrow structure at the junctional folds are expected to amplify the neurotransmission for more efficient muscle depolarization (Wood and Slater, 2001). For the organization of postsynaptic specialization, agrin (a proteoglycan) is released from nerve terminals and binds to the low-density lipoprotein receptor (LDLR)-related protein 4 (LRP4) localized in the postsynaptic membrane (DeChiara et al., 1996; Kim et al., 2008). The interaction of agrin and LRP4 activates the protein tyrosine kinase function of the co-receptor muscle-specific kinase (MuSK), which localize together with AChR (Valenzuela et al., 1995). The activation of MuSK is essential for the clustering of AChRs through the AChR-associated protein Rapsyn (Apel et al., 1997; Lee et al., 2009) and the organizer protein Dok-7 (Beeson et al., 2006; Okada et al., 2006; Hallock et al., 2010).

Impairments of active zones are seen in pathological conditions, including the autoimmune disease, Lambert–Eaton myasthenia syndrome (LEMS), and Pierson's syndrome. LEMS is caused by autoantibodies including ones against P/Q-type VGCCs, and Pierson syndrome occurs due to mutation in *lamb2* gene (Takamori et al., 2000; Zenker et al., 2004). Active zone loss may occur in these diseases due to a disruption in the interaction between muscle-derived laminin β2 (Sanes and Hall, 1979; Hunter et al., 1989) and P/Q-type VGCC, which is necessary for the active zone organization (**Figure 1**) (Nishimune et al., 2004).

Although NMJs in most vertebrate species share many essential features, there are also significant differences (**Figure 1**), which will be described in this review. Human NMJs, are among the smallest and release the smallest number of ACh containing synaptic vesicles at the presynaptic terminal (Oda, 1984; Slater et al., 1992; Slater, 2015, 2017). However, they have very extensive postsynaptic junctional folds, which may amplify transmitter action (Wokke et al., 1990; Slater et al., 1992). Human NMJs are also susceptible to pathological processes and are targets in several neurodegenerative conditions, including aging. This review will focus on recent findings regarding human NMJs and a comparison of what is known about other mammalian NMJs. We will describe age-related changes at human NMJs and insights about potential mechanisms of aging obtained from animal models of accelerated aging. Furthermore, we will compare aging to other human neurological diseases that cause impairments of pre- and post-synaptic structures at NMJs.

STRUCTURE OF THE HUMAN NEUROMUSCULAR JUNCTION

Human NMJs analyzed by freeze-fracture electron microscopy show double parallel rows of large intramembranous particles on the cytosolic half of a plasma membrane (the P-face), containing 3–15 particles per row spaced 20 nm apart (Fukunaga et al., 1982). This structure is considered to represent an active zone unit. Similar structures are identified in rodent and lizard NMJs, which appear as double parallel rows of large intramembranous particles on the P-face (Ellisman et al., 1976; Walrond and Reese, 1985; Fukuoka et al., 1987). In humans, these active zone units are distributed at a density of 2.6 active zones per μm^2 (Fukunaga et al., 1982). Similarly, active zone units in adult mouse NMJs appear in discrete locations within one presynaptic terminal of NMJs at a density of about 2.3–2.7 active zones per μm^2 (Fukunaga et al., 1983; Fukuoka et al., 1987; Chen et al., 2012) (**Table 1**).

The application of super-resolution microscopy has revealed distribution patterns of synaptic proteins across different species at unprecedented details (Kittel et al., 2006; Willig et al., 2006; Dani et al., 2010; Ehmann et al., 2014; Nishimune et al., 2016; Jones et al., 2017). The molecular architecture of the human NMJ has been recently investigated using confocal and super-resolution microscopy (Jones et al., 2017). Confocal microscopy of motor nerve terminals at human NMJs showed distinctive "hotspots" of fluorescence of the synaptic vesicle protein SV2. This distribution pattern was qualitatively different from mouse nerve terminals, which showed homogeneity of SV2 labeling (Jones et al., 2017). Additionally, direct Stochastic Optical Reconstruction Microscopy (dSTORM) microscopy has been used to assess the nanoscale distribution of synaptosomal associated protein-25 (SNAP25), a SNARE protein in human NMJs. Parallel imaging of human and mouse NMJs using dSTORM revealed several differences between the two species. The intensity of SNAP25 labeling, the density of SNAP25 puncta within each bouton, the average area of SNAP25 puncta, and the area of SNAP25 puncta as a percentage of the total synaptic

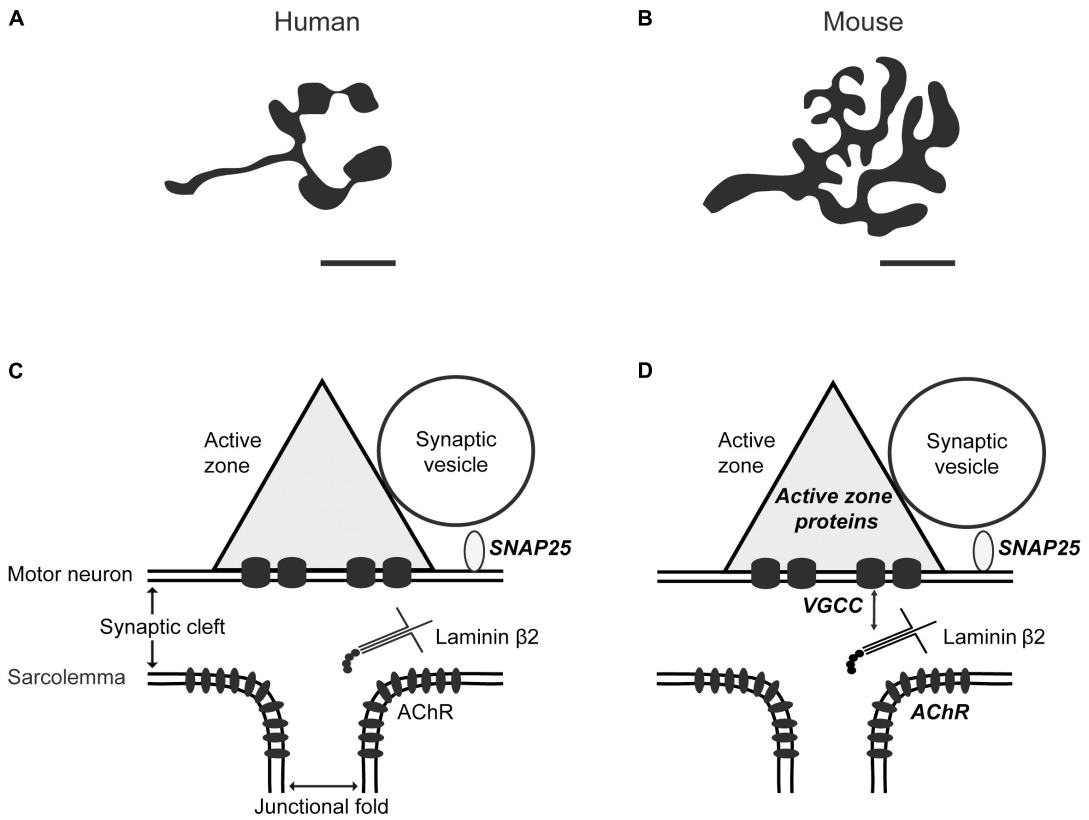

FIGURE 1 | Comparison between human and mouse neuromuscular junctions. Schematic diagrams show **(A)** human versus **(B)** mouse NMJs based on nerve-specific stains (adapted from Jones et al., 2017). The NMJ size and axon diameter are significantly smaller in humans compared to mice. Scale bar, 10 μm. A diagram depicting an active zone at the **(C)** human and **(D)** mouse NMJs. In mice, muscle-derived synapse organizer laminin β2 interacts with presynaptic voltage-gated calcium channels (VGCC) to organize active zones (Nishimune et al., 2004). Super-resolution microscopy revealed the nanoscale localization of the SNARE protein synaptosomal associated protein-25 (SNAP25) in human and mouse NMJs (Jones et al., 2017), active zone-specific proteins, and acetylcholine receptors (AChR) in mice (Nishimune et al., 2016; York and Zheng, 2017), which are described in bold italic characters. The nanoscale localization of active zone-specific proteins and acetylcholine receptors in human NMJs has not been revealed yet.

bouton area were all significantly greater in human NMJs compared to mouse NMJs (Jones et al., 2017). The total area of SNAP25 labeling per NMJ is similar in both humans and mice at approximately 15 μm^2 per NMJ (**Table 1**).

Interestingly, this SNAP25 puncta density (approximately 15 puncta per μm^2) is very similar to the density of other active zone proteins Bassoon, Piccolo and P/Q-type VGCC (approximately 10 puncta per μm^2) as revealed in mouse NMJs by Stimulated Emission Depletion (STED) super-resolution microscopy (Nishimune et al., 2016). Jones et al. (2017) reported that they were unable to label human NMJs with antibodies against Bassoon or Piccolo, suggesting possible species-specific differences in these antigens (Jones et al., 2017). Although the distribution pattern of these active zone-specific proteins is unknown in human NMJs (**Figure 1**), analysis of mouse NMJs revealed punctate and overlapping patterns of active zone proteins Bassoon and P/Q-type VGCCs (Nishimune et al., 2016). Interestingly, active zone protein Piccolo does not co-localize with Bassoon. Instead, Piccolo puncta sandwiched a Bassoon punctum in a side-by-side pattern (Nishimune et al., 2016). Current progress in the understanding of active zone nanoarchitecture and mechanisms underlying active zone organization in mammalian NMJs has been reviewed previously (Badawi and Nishimune, 2018). Future studies using super-resolution microscopy will reveal a more detailed subcellular localization of active zone proteins and address species-specific differences that may exist.

The NMJ size relative to muscle fiber diameter is smaller in humans compared to lower vertebrates (frogs and mice), as revealed by electron microscopy (Slater et al., 1992) (**Table 1**). Confocal microscopy also revealed that human NMJs have a unique morphology, being significantly smaller and more fragmented compared to mice and rats. The axon diameter is 3.69 fold smaller, and the average area of AChR clusters is 3.33 fold smaller in humans compared to mice (Jones et al., 2017). The average number of AChRs in human vastus lateralis muscle is 2.6×10^7, as determined by bungarotoxin binding sites (Slater et al., 1992). In mice, the average number of AChRs is 8.7×10^7 in the sternomastoid muscle and 3.1×10^7 in the diaphragm, also determined by bungarotoxin binding sites (Albuquerque et al., 1974). In general, AChRs in mice cluster at a concentration of approximately 10,000 per μm^2 in the

TABLE 1 | Comparison between human and mouse NMJs.

	Human	Mouse
Pre-synaptic		
Active zone size	153 × 96 nm (Fukunaga et al., 1982)	80 × 73 nm (Fukuoka et al., 1987)
Active zone density	2.6 per μm^2 (Fukunaga et al., 1982)	2.3–2.7 per μm^2 (Fukunaga et al., 1983; Fukuoka et al., 1987; Chen et al., 2012)
Bassoon and PQ-VGCC puncta density per NMJ	Not reported	5–6 puncta per μm^2 (Nishimune et al., 2016)
SNAP25 puncta density per NMJ	∼15 puncta per μm^2 (Jones et al., 2017)	∼15 puncta per μm^2 (Jones et al., 2017)
Quantal content	20–30 (Slater, 2017)	50–100 (Slater, 2017)
Nerve terminal area	122.7 μm^2 (Boehm et al., 2020)	304.0 μm^2 (Boehm et al., 2020)
Post-synaptic		
Endplate area	351.5 μm^2 (Boehm et al., 2020)	678.2 μm^2 (Boehm et al., 2020)
AChR number per NMJ	1.3–3.4 × 10^7 (Pestronk et al., 1985; Slater et al., 1992)	3.1–8.7 × 10^7 (Albuquerque et al., 1974)
Area of AChR clusters	71.7 μm^2 (Boehm et al., 2020)	238.5 μm^2 (Boehm et al., 2020)

postsynaptic membrane (Fertuck and Salpeter, 1976; Salpeter and Loring, 1985). The degree of overlap between the presynaptic motor nerve terminal and the post-synaptic component is similar between humans and mice (Slater et al., 1992; Jones et al., 2017). Although human NMJs are smaller than mouse NMJs, human motor nerves innervate muscle fibers up to twice the diameter of those in mice. The smaller size of human NMJs is not due to increased body size and mass because the NMJ size of mice and rats is similar, although rats are approximately 10-fold larger than mice (Jones et al., 2017). Furthermore, human NMJs have extensive folding of post-synaptic junctional folds, which increases the local area of membrane about eight-fold while the increase is about six-fold for mouse NMJs (Slater et al., 1992; Slater, 2017), possibly resulting in post-synaptic amplification of neurotransmitter action through the presence of voltage-gated sodium channels in high density and the increased local input resistance (Slater, 2017). On the postsynaptic side of the mouse NMJ, dSTORM revealed the nanoscale distribution of AChRs (York and Zheng, 2017). AChRs are concentrated at the mouth of postsynaptic junctional folds directly apposed to active zones of presynaptic terminals. The accumulation of AChRs under presynaptic neurotransmitter release sites may allow effective synaptic transmission (York and Zheng, 2017). The AChRs of human NMJs have only been investigated at confocal-level resolution and has not yet been analyzed using super-resolution microscopy (Jones et al., 2017).

AGE-RELATED CHANGES IN THE NEUROMUSCULAR JUNCTION

The elderly, those over 65 years, suffer from a progressive loss of muscle mass (sarcopenia), strength, and function (for review see Roubenoff, 2000; Manini et al., 2013; Gonzalez-Freire et al., 2014; Willadt et al., 2018; Clark, 2019). These losses contribute to decreased mobility, increased frailty, and risk for mortality (Fried et al., 2001). Aging in humans results in a one to 1.5% loss of strength per year after the 6th decade of life (Frontera et al., 2000). In humans, approximately 10–20% of skeletal muscle mass is lost by the 7th decade of life compared to young adults (between 8 and 45 years) (Janssen et al., 2000; Vandervoort, 2002; Mitchell et al., 2012). This loss in muscle mass is likely due to motor unit loss (Lexell et al., 1988; Lexell, 1995) and subsequent atrophy of muscle fibers (Lexell et al., 1988). The loss of muscle fibers by apoptosis seems to be at an equal level between fast (Type II) and slow (Type I) muscle fiber types in humans (Lexell et al., 1983). However, there is preferential atrophy of fast fiber type compared with slow fiber type (Lexell et al., 1988; Klein et al., 2003). In mice, one study looking at muscle fiber type susceptibility in 29-month old mice demonstrated that denervation was greater in the fast extensor digitorum longus (EDL) muscle compared to the slow soleus muscle (Chai et al., 2011). However, another study using 24-month old mice showed no differences in denervation between muscle fiber types (Valdez et al., 2012). Human autopsy studies have shown that aging is associated with a gradual loss of lumbar and cervical motor neurons (Kawamura et al., 1977; Tomlinson and Irving, 1977; Mittal and Logmani, 1987; Zhang et al., 1996). Mechanisms that lead to neuronal loss with aging in humans may involve impaired trophic signaling from the nervous system, local degeneration, increased oxidative stress in motor neurons, and feedback from dysfunctional muscle (Gonzalez-Freire et al., 2014).

Early studies have demonstrated age-related changes of NMJ innervation and AChR distribution using silver and cholinesterase staining in longitudinal sections of intercostal muscles obtained from human cadavers (between 32 and 76 years old) (Oda, 1984). Another study on autopsied subjects showed a significant decrease in presynaptic membrane length and a significant increase of postsynaptic membrane length of NMJs with aging (Arizono et al., 1984). Electron microscopy showed pre- and postsynaptic changes at the ultrastructural level (Wokke et al., 1990). Aging was associated with irregularly shaped presynaptic nerve terminals and the presence of junctional folds without an opposing nerve terminal in longitudinal sections of external intercostal muscles. Postsynaptically, electron microscopy revealed increased length and branching of the postsynaptic membrane, enlarged postsynaptic area, and degeneration of junctional folds (Wokke et al., 1990). Transverse-sections prepared from autopsied or biopsied vastus lateralis muscle provided strong evidence for repeated cycles of denervation-reinnervation, in which motor unit remodeling and fiber type grouping occurred (Lindboe and Torvik, 1982; Lexell and Downham, 1991; Mosole et al., 2014; Zampieri et al., 2016). Histological analysis of aged human muscles also showed a significant accumulation of severely atrophic, smaller sized, and angulated fibers, which suggested reinnervation failure in advanced age (Mosole et al., 2014). In aged rodent muscles, rearrangement, clustering, and angulation of muscle fibers in a motor unit have also been observed (Larsson, 1995; Rowan et al., 2011).

In contrast to previous studies, a study by Jones and colleagues reported confocal micrographs of human NMJs in skeletal muscle obtained from amputation surgery and suggested conservation of synaptic structure across the lifespan (4th to 10th decades of life) (Jones et al., 2017). They observed a mild increase in axon diameter with increasing age. However, there were no age-associated changes in the innervation or fragmentation of NMJs in longitudinal sections of leg muscles, contradicting the earlier studies demonstrating age-related changes of NMJ innervation. They also report no significant change in the endplate area or muscle fiber diameter with age in the peroneus longus muscle (Jones et al., 2017). This finding is consistent with light microscopy analysis of human external intercostal muscles in which endplate size remained stable among ages (between 4 and 77 years old), and there was no sprouting of terminal axons (Wokke et al., 1990). A study by Gambino et al. (1990) in human posterior cricoarytenoid muscles (between 4 and 95 years old) demonstrated that there is no significant increase in NMJ length and the number of axonal terminal branches during adult life. It has also been reported that measures of presynaptic and postsynaptic structural relationships were maintained in the soleus muscle of the 24-month old rats despite aging-related changes (Deschenes et al., 2013). Differences between the human studies may be attributed to methodological disparities, which include (1) amputated versus post-mortem autopsied material, (2) light microscopy versus electron microscopy, (3) longitudinal-sections versus transverse-sections, and (4) different muscle types with potentially different susceptibility. **Table 2** summarizes the age-dependent changes of human NMJs and how they compare to rodent NMJs.

Studies in mice have shown that aging leads to AChR cluster fragmentation and progressive denervation of NMJs (Andonian and Fahim, 1988; Valdez et al., 2010; Li et al., 2011; Willadt et al., 2016, 2018). NMJ denervation precedes the degradation of spinal motor neurons, suggesting a "dying back" neuropathy or distal axonopathy during the aging of mice (Valdez et al., 2010; Chai et al., 2011). We have observed that aging in mice results in a reduced number and protein levels of presynaptic active zones in innervated NMJs (Chen et al., 2012; Nishimune et al., 2016). More specifically, there is selective degeneration of active zone proteins, P/Q-type VGCC and Bassoon, at aged NMJs of 29-month-old mice compared to that of 8-month-old mice (Nishimune et al., 2016). However, Piccolo protein level at these aged NMJs remained similar to that of adult NMJs, suggesting that NMJ active zone proteins decrease selectively prior to NMJ denervation during aging in mice. Our electrophysiology study showed that the lack of Bassoon impairs P/Q-type VGCC function (Nishimune et al., 2012). Thus, the loss of active zone proteins in aged NMJs reduces synaptic vesicle release sites and calcium influx, which may lead to denervation and a loss of muscle strength. The effect of aging on presynaptic active zone proteins in humans is unknown.

Age-related functional changes of human NMJs have been analyzed using electromyography (EMG) to evaluate compound muscle action potential (CMAP) and motor unit number estimation (MUNE). Additionally, single-fiber EMG (SFEMG) has been used to analyze action potentials from individual muscle fibers and the variation in time of two action potentials of the same motor unit (jitter). The MUNE values of limb muscles decrease in older humans compared to that of the young (Galea, 1996; McNeil et al., 2005; Power et al., 2010; Hourigan et al., 2015; Piasecki et al., 2016). This decrease in MUNE values is consistent with the gradual loss of motor neurons (Kawamura et al., 1977; Tomlinson and Irving, 1977; Mittal and Logmani, 1987). In addition, MUNE values decrease in the skeletal muscles of aged mice (Sheth et al., 2018; Chugh et al., 2020). In accordance with the decrease of MUNE values and motor neuron number, the CMAP decreases in old humans compared to that of the young (Piasecki et al., 2016), and in aged mice compared to young mice (Sheth et al., 2018). SFEMG studies have found mild increases in jitter in some muscles suggesting a mild change in neurotransmission efficiency in humans between 10 and 90 years old (Bromberg and Scott, 1994).

TABLE 2 | Age-dependent changes in human and rodent NMJs.

	Human	Rodent
Presynaptic changes		
Active zone density	Unknown	Decreases (Chen et al., 2012)
Active zone-specific proteins	Unknown	Selective degeneration of bassoon, piccolo and P/Q type VGCC protein level and density per synapse (Chen et al., 2012; Nishimune et al., 2012; Nishimune et al., 2016)
Synaptic vesicle density	Unknown	Decreases (Fahim and Robbins, 1982; Banker et al., 1983)
Nerve terminal branching	Increases (Oda, 1984), no change (Gambino et al., 1990)	Increases (Fahim et al., 1983; Li et al., 2011; Valdez et al., 2012)
Denervation	Increases in intercoastal (Oda, 1984) and VL muscles (Lexell and Downham, 1991; Mosole et al., 2014; Zampieri et al., 2016), no change in the peroneus longus muscle (Jones et al., 2017)	Increases in TA, plantaris, and EDL muscle (Fahim and Robbins, 1982; Deschenes et al., 2010; Valdez et al., 2010; Chai et al., 2011)
Postsynaptic changes		
NMJ fragmentation	No change in the peroneus longus muscle (Jones et al., 2017)	Increases in the EDL, diaphragm, soleus, sternomastoid, and TA muscles (Andonian and Fahim, 1988; Valdez et al., 2010; Li et al., 2011; Willadt et al., 2016)
Endplate area	Increases (Oda, 1984) and no change (Wokke et al., 1990) in intercostal muscles. No change in the peroneus longus muscle (Jones et al., 2017)	No change in the EDC, EDL, GM, and soleus muscles (Banker et al., 1983)
Postsynaptic folds number and regularity	Decreases (Arizono et al., 1984; Wokke et al., 1990)	Decreases (Fahim and Robbins, 1982)

The age range for human studies is 4–95 years, and the age range for rodent studies is 21 days to 33 months (mice) and 56 days to 24 months (rats). EDC, extensor digitorum communis; EDL, extensor digitorum longus; GM, gluteus maximus; NMJ, neuromuscular junction; TA, tibialis anterior; VGCC, voltage-gated calcium channel; VL, vastus lateralis.

Age-related functional changes of rodent NMJs have been studied using dissected nerve-muscle preparations, direct stimulation of motor nerves, and intracellular recordings from the muscle, which has not been done for human studies (Willadt et al., 2018). Aged mice show decreased MUNE values, as mentioned previously (Sheth et al., 2018; Chugh et al., 2020), and age-related increase of the blockade of synaptic transmission (Chugh et al., 2020). These findings seem consistent with the NMJ denervation observed in old mice. However, many studies of aged mice and rats revealed increases or no change of miniature endplate potential (mEPP) amplitude, endplate potential, and quantal content (Banker et al., 1983; Kelly and Robbins, 1983; Smith, 1988; Fahim, 1997; Willadt et al., 2016). Some of these changes may relate to the reduced Ca^{2+} clearance rates in presynaptic terminals (Smith, 1988) or increased input resistance postsynaptic membrane in some aged NMJs (Banker et al., 1983; Fahim, 1997). These age-related changes may be compensatory mechanisms for the reduced MUNE; however, they do not seem to be in accordance with the age-related increase of the blockade of synaptic transmission (Chugh et al., 2020) or the NMJ denervation observed in old mice. Furthermore, the increase of NMJ fragmentation observed in aged mice was not associated with functional impairment (Willadt et al., 2016).

Taken together, these results suggest that age-dependent changes in structure and motor unit number (denervation) occur in human NMJs, but further studies are needed to reveal the relationship between functional and structural changes related to the aging of NMJs. The sections below will discuss mouse models that reproduce key phenotypes of neuromuscular and cellular impairment seen during aging. We will also discuss potential similarities in molecular pathways between aging and neuromuscular disease because the phenotypes of human aging, and that of neuromuscular disease model mice share defects in pre- and postsynaptic NMJ structures.

INSIGHTS FROM ANIMAL MODELS OF ACCELERATED AGING

Human progeroid syndromes are genetic disorders characterized by a shortened lifespan and the premature development of phenotypes, which are normally associated with advanced age (Martin, 1978). Progeroid syndromes can occur as a result of a single gene mutation (Martin, 1978; Warner and Sierra, 2003). Therefore, mouse models of progeroid syndromes have been developed to study the mechanisms and pathways involved in aging. Mouse models of accelerated aging are useful because of their short lifespan, the specific targeting of a single gene, and the phenotypic similarities with physiological aging (Harkema et al., 2016). Obtaining insights into the aging process can lead to the identification of possible targets for sarcopenia prevention. In the section below, we will discuss observations made in few mouse models of accelerated aging and compare them to neuromuscular aging phenotypes described in aged mice and elderly humans. The following mouse models were selected based on the association between the gene modifications and neuromuscular dysfunction phenotypes. The selection is not ment to cover all animal models of accelerated aging. Many reviews provide a more extensive list of progeroid mouse models associated with gene modifications resulting in additional pathologic phenotypes implicated in physiological aging, for example in the central nervous system, cardiovascular system, bones, and joints (Carrero et al., 2016; Harkema et al., 2016; Folgueras et al., 2018).

Zmpste24$^{-/-}$ Mice

Accelerated aging was observed in a mouse model with a deletion of zinc metalloproteinase (Zmpste24) required for processing of prelamin A to lamin A (Leung et al., 2001; Bergo et al., 2002). Lamin A is a component of the nuclear envelope and interacts with membrane-associated proteins to form the nuclear lamina (Aebi et al., 1986). Lamin A has been suggested to play a role in physiological aging (Scaffidi and Misteli, 2006) because a gene mutation in Lamin A (*Lmna*) causes incomplete processing of prelamin A protein and the affected children show symptoms of premature aging (De Sandre-Giovannoli et al., 2003; Eriksson et al., 2003). The *Zmpste24*$^{-/-}$ model has a defect in prelamin A processing and is similar to the Hutchinson–Gilford progeria syndrome (Bergo et al., 2002). Muscles of *Zmpste24*$^{-/-}$ mice exhibit characteristics of sarcopenia, including both muscle atrophy and weakness (Bergo et al., 2002; Greising et al., 2012). More specifically, the contractile capacity of muscles of the anterior leg (extensor hallucis longus, EDL and tibialis anterior) were 30–90% weaker than those of control mice (Greising et al., 2012). Consistently, hindlimb muscles (EDL, tibialis anterior, soleus, and gastrocnemius) were 32–47% smaller in the *Zmpste24*$^{-/-}$ mice and contained significantly more collagen compared to control littermates (Greising et al., 2012). Additionally, the ankle range of motion was 70% lower in *Zmpste24*$^{-/-}$ than control mice. Combined together, muscle atrophy, collagen accumulation, and abnormal joint mechanics contribute to poor neuromuscular performance and muscle weakness shown by *Zmpste24*$^{-/-}$ mice (Greising et al., 2012). These phenotypes caused by decreased Zmpste24 activity are similar to those seen in aged mice and elderly humans, suggesting that defective lamin A processing plays a role in the aging process. These observations are consistent with the recent demonstration of age-related decline in the expression of lamin A/C in the synaptic region of muscles and a role of lamin A/C in preventing NMJ degeneration (Gao et al., 2020).

Bub1b$^{H/H}$ and *Bub1b*$^{+/GTTA}$ Mice

Accelerated sarcopenia and a shortened lifespan were observed in mice with low levels of the spindle assembly checkpoint protein BubR1, including *Bub1b*$^{H/H}$ mice with two hypomorphic alleles and *Bub1b*$^{+/GTTA}$ mice with the human nonsense mutation 2211insGTTA (Baker et al., 2004; Wijshake et al., 2012). These mice show a decrease in muscle fiber diameter in gastrocnemius, paraspinal, and abdominal muscles, with increased intermuscular fibrosis, and impaired regenerative capacity (Baker et al., 2008; Wijshake et al., 2012). The effect of BubR1 deficiency on NMJ structure and the innervation rate remain unknown. However, BubR1 deficiency in *Bub1b*$^{H/H}$ mice is a trigger for *Cdkn2a*

locus activation, which encodes the tumor suppressors $p16^{Ink4a}$ and $p19^{ARF}$ (Baker et al., 2008). Both $p16^{Ink4a}$ and $p19^{ARF}$ are effectors of cellular senescence (Baker et al., 2008) or a state of irreversible growth arrest (Collado et al., 2007). The levels of the senescence markers, $p16^{Ink4a}$ and $p19^{ARF}$, were also found to be elevated in the skeletal muscle of *Bub1b*$^{+/GTTA}$ mice (Wijshake et al., 2012). The inducible clearance of $p16^{Ink4a}$ positive senescent cells upon administration of a drug in *Bub1b*$^{H/H}$ mice results in attenuation of sarcopenia and premature aging (Baker et al., 2011). Furthermore, breeding *Bub1b*$^{H/H}$ mutant mice on a $p16^{Ink4a}$ homozygous-null background attenuated cellular senescence and premature aging in skeletal tissues, and a 25% extension in lifespan compared to *Bub1b*$^{H/H}$ mice (Baker et al., 2008). These results, combined with the decline of BubR1 expression in aged wild-type mice (Baker et al., 2004), suggest that BubR1 may play a role in physiological aging.

Ercc1$^{\Delta/-}$ Mice

Genotoxic stress as a result of cumulative damage to DNA is considered a dominant mechanism underlying aging (Hoeijmakers, 2009). The excision repair cross-complementing group 1 (ERCC1) gene functions in the nucleotide excision repair pathway (Westerveld et al., 1984). Previous studies of *ERCC1* deficient patients (Jaspers et al., 2007; Ahmad et al., 2010) and *ERCC1*$^{-/-}$ mice (Weeda et al., 1997) have indicated that a loss of *ERCC1* nuclease function causes a premature aging degenerative phenotype in several organ systems and juvenile death. The very short lifespan of *ERCC1*$^{-/-}$ mice (which is less than 38 days) hinders the investigation of age-dependent neurodegeneration. Therefore, Weeda et al. (1997) also examined *ERCC1*$^{\Delta/-}$ mice lacking one allele and having reduced activity in the other allele due to a seven amino-acid carboxy-terminal truncation. *ERCC1*$^{\Delta/-}$ mice have a shortened life span of 6–7 months, severe locomotor deficits, and reduced ability to maintain balance (de Waard et al., 2010). Grip strength and accelerating rotarod test performances are reduced in *ERCC1*$^{\Delta/-}$ mice at 16 weeks of age. Full and partial denervation of NMJs occurs in the lumbrical muscles of *ERCC1*$^{\Delta/-}$ mice at 8 and 16 weeks. There is also a significant increase in the number of motor endplates that are innervated by more than one incoming axon collateral in *ERCC*$^{\Delta/-}$ mice (de Waard et al., 2010). This sprouting of new collateral axonal branches occurs as a compensatory mechanism to reinnervate denervated muscle fibers. These results suggest that the accumulation of DNA damage may play a role in neuronal aging and motor neuron vulnerability in aging.

Sod1$^{-/-}$ Mice

Oxidative stress is one of the leading theories on mechanisms underlying age-related muscle denervation (Fulle et al., 2004; Salmon et al., 2010). Reactive oxygen species-mediated oxidative damage to proteins, lipids, and DNA are kept in check by antioxidants under normal physiological conditions. However, excessive reactive oxygen species production can overwhelm the antioxidant defense, leading to increased oxidative damage of cellular machinery (Park, 2015). Studies on the genetic ablation of superoxide dismutase 1 (SOD1), a free radical scavenging enzyme, have shown that superoxide (O_2^-/HO_2) can be toxic, and the lack of Cu/Zn SOD contributes to a deleterious phenotype in various model systems (Phillips et al., 1989; Ho et al., 1998; McFadden et al., 1999; Sanchez et al., 2005; Muller et al., 2006). Mice lacking Cu/Zn SOD1 (*Sod1*$^{-/-}$) show phenotypes that resemble an acceleration of normal age-related sarcopenia (Muller et al., 2006) and exhibit a 30% reduction in lifespan (Elchuri et al., 2005). Hindlimb muscle mass in *Sod1*$^{-/-}$ mice is approximately 50% lower than in age-matched wild-type mice. Skeletal muscle tissue from *Sod1*$^{-/-}$ mice show increased oxidative damage of proteins, lipids, and DNA compared to control mice. These differences are accompanied by a 40% decrease in voluntary wheel running at 6 months of age, and about 50% worse Rotarod performance in *Sod1*$^{-/-}$ mice compared to wildtype littermates (Muller et al., 2006). Interestingly, depletion of Cu/Zn SOD1 in either the motor neuron or muscle alone is not sufficient to reproduce a sarcopenic phenotype and that a loss of Cu/Zn SOD1 in both neurons and muscle is required to generate atrophy (Zhang et al., 2013; Sataranatarajan et al., 2015). Furthermore, *Sod1*$^{-/-}$ mice display progressive NMJ denervation despite the absence of losses of spinal cord motor neurons and ventral root axons (Flood et al., 1999; Shefner et al., 1999; Jang et al., 2010; Fischer et al., 2011, 2012). Denervation and sprouting occur in these mice at 1–4 months of age, preceding muscle fiber loss that occurs between 3 and 4 months of age (Muller et al., 2006; Fischer et al., 2011, 2012). Muscle denervation and abnormalities in motor axon morphology of *Sod1*$^{-/-}$ mice are greater in the gastrocnemius and tibialis anterior muscles compared to the soleus muscle (Muller et al., 2006; Fischer et al., 2011, 2012). The gastrocnemius and tibialis anterior muscles have a higher proportion of fast muscle fibers, and the soleus muscle has a higher proportion of slow muscle fibers. Therefore, fast muscles are more vulnerable to NMJ denervation and muscle fiber loss in *Sod1*$^{-/-}$ mice, similar to what occurs in humans aging studies (Lexell et al., 1988; Lexell, 1995). Myosin heavy chain isoform (MHC) type II (fast) muscle fibers in elderly humans are more affected than MHC isoform type I (slow) fibers during age-related NMJ denervation (Lexell et al., 1988; Lexell, 1995). Overall, these results demonstrate that Cu/Zn SOD1 is necessary for normal neuromuscular functions and suppression of age-dependent neuromuscular degeneration.

These animal models show accelerated aging with defects of the neuromuscular system including sarcopenia, axonal sprouting, and denervation like physiological aging. These mice provides opportunities to study NMJ changes, understand pathological mechanisms, and identify therapeutic targets to delay or prevent the onset of age-related neuromuscular impairments.

COMPARISON WITH OTHER DISEASES THAT AFFECT THE NMJ

The mechanisms that form NMJs during development or degenerate NMJs in neuromuscular diseases may underlie the mechanisms of physiological aging in humans. For example, a loss in presynaptic active zones has been observed in NMJs of

aged mice (Chen et al., 2012). Similarly, active zone structure is impaired in human neurological diseases, including LEMS and Pierson syndrome. LEMS patients develop autoantibodies against P/Q-type VGCCs, which is thought to cause internalization of P/Q-type VGCCs into nerve terminals (Lambert and Elmqvist, 1971; Fukunaga et al., 1982; Flink and Atchison, 2003). LEMS patients exhibit a reduced number of NMJ active zones, reduced synaptic transmission, weakened muscles, and fatigue (Lambert and Elmqvist, 1971; Fukunaga et al., 1982) similar to what is observed in aging. Interestingly, some LEMS patients develop autoantibodies specifically against the domain of P/Q-type VGCCs, where laminin β2 binds to (Takamori et al., 2000; Nishimune et al., 2004). These autoantibodies may cause a loss of interaction between the synapse organizer laminin β2 and VGCCs, which may inhibit the organization of active zones. Consistently, mice immunized with LEMS patient IgGs also show a reduced number of active zones (Fukunaga et al., 1983). Thus, the interaction between P/Q-type VGCCs and laminin β2 is essential for organizing the presynaptic active zones. Meanwhile, Pierson syndrome patients lack functional laminin β2 due to a genetic mutation and show a reduction in active zones at the NMJ, impairments in synaptic transmission including reduced mEPP frequency and amplitude, and denervation (Zenker et al., 2004; Maselli et al., 2009). These clinical characteristics of Pierson syndrome are consistent with the phenotypes of laminin β2 knockout mice (Noakes et al., 1995). Together, these observations suggest that laminin β2 plays an important role in active zone organization in humans and a potential role in the maintenance of active zones in aged NMJs.

Myasthenia gravis (MG), the most common disorder of NMJs, is caused by autoantibodies against postsynaptic membrane proteins (Conti-Fine et al., 2006; Vincent et al., 2006; Shigemoto et al., 2010). The characteristic clinical features of MG include fatigue, muscular atrophy, weakness, and ptosis (Slater et al., 2006; Phillips and Vincent, 2016). Analyses of patient sera showed that the majority of MG patients produce autoantibodies against AChRs (∼85%). Autoantibodies against muscle-specific kinase (MuSK) makeup ∼8% of MG patients and were found in 70% of MG patients who lacked autoantibodies against AChRs (Gilhus and Verschuuren, 2015; Binks et al., 2016). Furthermore, autoantibodies against LRP4 were found in 2–54% of MG patients who were negative for anti-AChR and anti-MuSK antibodies (Higuchi et al., 2011; Zhang et al., 2012; Zisimopoulou et al., 2014). Various studies using animal models that received injections of MG patient IgG have shown that these antibodies are pathogenic. AChR antibodies increase the rate of AChR internalization, and a loss of AChRs at the NMJ impairs neuromuscular transmission (Engel et al., 1977; Phillips and Vincent, 2016). The postsynaptic membrane shows a diminished response to ACh and a reduction in EPPs and mEPPs amplitudes (Loutrari et al., 1992; Ruff and Lennon, 2008). MG patients' MuSK antibodies prevent the assembly and activation of the agrin-LRP4-MuSK complex necessary for NMJ maintenance (Huijbers et al., 2013; Otsuka et al., 2015). MuSK and LRP4-immunized mice also show impairments of neuromuscular transmission as well as a reduction in the size of motor terminals apposing AChR clusters at NMJs (Mori et al., 2012; Zhang et al., 2012; Mori et al., 2017). Transverse-sections of muscles from MuSK-immunized rabbits showed angular muscle fibers (Shigemoto et al., 2006) similar to what is seen in transverse-sections of aged muscle fibers (Larsson, 1995; Zampieri et al., 2016). LRP4-immunized mice showed significantly decreased staining areas of the presynaptic proteins, synaptophysin and bassoon, at NMJs compared to controls (Mori et al., 2017). However, the normalized bassoon staining area was unchanged compared to control mice because the synapse area is also reduced in these mice (Mori et al., 2017). It is worth noting that gene mutations in the agrin-LRP4-MuSK-Dok7-rapsyn-AChR pathway, including the genes *AGRN, MUSK, DOK7, RAPSN*, cause congenital myasthenic syndromes (CMSs). CMSs are characterized by weakness and fatigue, similar to MG (Rothbart, 1937). However, CMS is not a degenerative disorder like aging but a developmental disorder, which has been reviewed previously (Engel et al., 2010, 2015; Webster, 2018). In aged mice, the agrin-LRP4-MuSK-AChR signaling pathway is implicated in aging-associated NMJ deficits (Zhao et al., 2018). LRP4 protein levels are decreased in aged muscles and restoring the levels of LRP4 by transgenic expression or stabilization with sarcoglycan alpha maintained NMJ innervation, alleviated AChR fragmentation, and improved synaptic transmission (Zhao et al., 2018). Furthermore, viral-mediated upregulation of *DOK7* in aged mouse muscle significantly enhanced motor function, muscle strength, NMJ innervation, and compound muscle action potential amplitudes (Ueta et al., 2020). Thus, studying the role of the agrin-LRP4-MuSK-Dok7-rapsyn-AChR signaling pathway in aging has identified a potential therapeutic target for alleviating NMJ decline in aging. This elucidation was helped by the prior knowledge demonstrating the importance of this signaling pathway for NMJ development, maintenance, and degeneration in MG (Li et al., 2018).

Amyotrophic lateral sclerosis (ALS) is a neurodegenerative disorder characterized by a gradual loss of motor neurons that leads to paralysis and death (Brown, 1995). The first gene mutations associated with familial ALS were identified in the *SOD1* gene (Rosen et al., 1993). These findings led to the development of the transgenic mouse model for ALS expressing the human SOD1 gene with glycine 93 to alanine (G93A) mutation identified in patients ($SOD1^{G93A}$ mice) (Gurney et al., 1994). $SOD1^{G93A}$ mice exhibit progressive denervation, motor neuron loss, muscle weakness, and paralysis similar to ALS patients (Gurney et al., 1994; Chiu et al., 1995; Tu et al., 1996; Wong and Martin, 2010; Rocha et al., 2013; Dobrowolny et al., 2018). NMJ denervation is observed as early as 47 days of age in these mice (Kennel et al., 1996; Fischer et al., 2004) and precedes both motor neuron loss (Gurney et al., 1994; Dadon-Nachum et al., 2011) and muscle atrophy (Brooks et al., 2004; Marcuzzo et al., 2011). These characteristics are similar to those observed in the rodent models of aging (Chai et al., 2011; Valdez et al., 2012) as well as in $SOD1^{-/-}$ mouse models of accelerated aging (Shi et al., 2014). In addition, $SOD1^{G93A}$ mice display preferential denervation of fast-twitch muscles (Atkin et al., 2005; Hegedus et al., 2007, 2008). It has been suggested that both fast type muscle and motor units are preferentially vulnerable to the disease process in ALS patients (Dengler et al., 1990; Sanjak et al., 2001).

This increased susceptibility to NMJ denervation in fast type muscles has also been demonstrated in aged mice (Chai et al., 2011; Valdez et al., 2012) and *SOD1*$^{-/-}$ mouse models of accelerated aging (Fischer et al., 2011, 2012).

Identifying similarities between aging and phenotypes of neurodegenerative diseases may suggest common molecular pathways that underlie aging-related degeneration of NMJs. Furthermore, understanding the molecular basis of NMJ dysfunction in animal models is essential for translating research to study aging in humans and search for candidate targets for therapeutic intervention of sarcopenia and frailty. For example, a mechanism of peripheral neuropathy elucidated from aged mice may provide a novel therapeutic approach for age-related degeneration observed in the elderly (Yuan et al., 2018). The previous reviews have discussed the possible functional significance associated with age-related changes in NMJ structure, which include denervation, fragmentation, axonal branching, decreased synaptic vesicles, and altered postsynaptic folding (Willadt et al., 2016; Li et al., 2018). Importantly, studying NMJ dysfunction is essential for understanding musculoskeletal impairment during aging.

INTERVENTIONS TO IMPROVE AGE-RELATED NMJ DYSFUNCTION IN HUMANS

Exercise and caloric restriction attenuate age-related declines in the mammalian neuromuscular system and are potential interventions to delay the onset of age-related NMJ dysfunction and sarcopenia (Cadore et al., 2014; Most et al., 2017; Lopez et al., 2018; Lavin et al., 2019). Aging leads to a loss of motor units, as described in the previous section titled "age-related changes in the NMJ." In humans, a study on master athletes indicates that high levels of life-long physical activity may ameliorate this loss of functional motor units in the tibialis anterior muscle into the 7th decade of life compared to age-matched controls (Power et al., 2010). Unlike the tibialis anterior leg muscle, the estimated number of functional motor units in the biceps brachii arm muscle of masters runners was lower in old age compared with young adults (Power et al., 2012). These findings indicate that high levels of chronic activation is necessary for delaying the age-related loss of motor units, and the beneficial effect is specific to the muscle exposed to the long term high levels of physical activity (Power et al., 2012). The number of functional motor units in a human muscle group can be estimated using a minimally invasive electrophysiological technique (decomposition-enhanced spike-triggered averaging) (McComas et al., 1971). This technique can also provide indirect evidence of collateral reinnervation using the peak amplitude of the mean surface-detected motor unit potential (Power et al., 2016). World champion master runners in their ninth decade of life had a greater number of remaining motor units and reduced collateral reinnervation compared to age-matched non-athletes (Power et al., 2016). Furthermore, master athletes had a 14% greater amount of excitable muscle mass and better neuromuscular transmission stability or preterminal axon stability, as indicated by lower jitter values, compared with age-matched non-athletes (Power et al., 2016). Additionally, biopsies from seniors physically active at high-level (65–79 years old) revealed a significantly higher percentage of slow-type myofibers and increased muscle fiber-type groupings, suggesting that long-term cycles of denervation/reinnervation have occurred (Mosole et al., 2014). People aged 70 years or older who reported walking 4–7 days per week showed a reduced risk of lower-body mobility impairments compared to elderly who reported walking fewer days per week (Clark, 1996). Moderate to high levels of physical activity in aged adults was associated with a significant increase in life expectancy and disability-free years before death compared to aged adults who reported low physical activity (Ferrucci et al., 1999). Starting exercise training in old age can also lead to significant health improvements. Nine weeks of training improved muscle strength and recovered myofiber atrophy in 70-year-old subjects compared to pre-training (Zampieri et al., 2016). Together, these results demonstrate that exercise maintains neuromuscular stability and ameliorates the loss of motor units associated with aging well into the later decades of human life.

In rodents, endurance exercise has a beneficial effect on NMJs in the aging muscle. Running wheel and treadmill running has been shown to reduce post-synaptic AChR fragmentation related to rodent aging, and help maintain NMJ innervation and endplate area (Andonian and Fahim, 1988; Fahim, 1997; Valdez et al., 2010; Deschenes et al., 2011; Cheng et al., 2013). Presynaptically, exercise has been shown to maintain active zone protein content. Active zone protein levels in NMJs are reduced during aging, but resistance training ameliorated the loss of Bassoon at NMJs of 24-month-old aged rats to young adult levels (Nishimune et al., 2012). This finding is consistent with endurance training improving NMJ function in aged mice, which was revealed using electrophysiology (Fahim, 1997). To our knowledge, no other studies investigated active zone proteins at NMJs combined with exercise training. More work is needed to understand the molecular mechanisms by which exercise modulates active zones and active zone proteins during aging.

Caloric restriction is a long-term dietary intervention in which caloric intake is reduced, but malnutrition is avoided (Anderson and Weindruch, 2012). The first description of the possible benefits and mechanisms of caloric restriction in aging has been demonstrated through the studies of rodent and invertebrate species (Fontana et al., 2010; Anderson and Weindruch, 2012). The caloric restriction prolonged the lifespan of rodents in an inverse linear manner when caloric intake is reduced at 10–30% compared to *ad libitum* intake of a standard diet (Weindruch et al., 1986; Anderson and Weindruch, 2010). Furthermore, a 40% reduction in caloric intake in mice from 4 to 24 months of age led to the maintenance of NMJs in the tibialis anterior muscle compared to control mice fed a standard diet *ad libitum* (Valdez et al., 2010). The frequencies of AChR fragmentation and NMJ denervation were significantly lower in these calorically restricted mice than in control aged mice indicating an attenuation of the age-related changes in the NMJ structure (Valdez et al., 2010). The use of the caloric restriction mimetic, resveratrol had a beneficial effect on NMJs and preserving muscle

fiber morphology in the EDL muscle of 2-year-old mice (Stockinger et al., 2017). The beneficial effect of caloric restriction on health has also been reported in non-human primates (Roth et al., 2000). In rhesus monkeys, caloric restriction of 30% reduced intake improves survival and delays the onset of sarcopenia and age-associated diseases (McKiernan et al., 2011). Analysis of vastus lateralis muscle biopsies showed that caloric restriction attenuated age-related changes in the proportion of Type II muscle fibers and fiber transverse-sectional area (McKiernan et al., 2011). Epidemiological studies show evidence that caloric restriction without malnutrition may also have health-promoting effects in humans. A large population of centenarians is found on the island of Okinawa, where individuals reportedly eat fewer calories on average than people in mainland Japan (Chan et al., 1997). Randomized controlled trials of caloric restriction in the United States show a decline in markers of oxidative stress and DNA-damage after 6 months compared to controls on a weight-maintenance diet (Heilbronn et al., 2006; Civitarese et al., 2007). Skeletal muscle biopsies collected from the trial participants showed that caloric restriction induces mitochondrial biogenesis and decreases superoxide dismutase activity, which in turn lowers oxidative stress (Civitarese et al., 2007). A caloric restriction trial in healthy, adult humans demonstrated that a 15% caloric restriction over 2-years resulted in beneficial metabolic adaption and a reduction in biomarkers associated with aging compared to an *ad libitum* control group (Redman et al., 2018). Studies in *Caenorhabditis elegans*, *Drosophila,* and yeast suggest a possible link between the TOR (Target of Rapamycin) pathway and caloric restriction (Kapahi et al., 2004; Kaeberlein et al., 2005; Hansen et al., 2007). The potential role of mTOR signaling in the aging process of these model organisms in addition to mammals has been reviewed previously (Saxton and Sabatini, 2017; Papadopoli et al., 2019). In mice, a sirtuin, Sirt1 has been shown to regulate aging and longevity. Brain specific overexpression of *Sirt1* in mice protected against the age-related decline in skeletal muscle and resulted in more youthful-appearing NMJs (Ghosh and Zhou, 2015; Snyder-Warwick et al., 2018). The mechanisms linking Sirt1 from the hypothalamus to skeletal muscle in mice and the involvement of SIRT1 in humans remains to be elucidated. Aside from caloric restriction, there is evidence for a beneficial effect of specific nutrients and dietary supplements on the aged neuromuscular system in humans. A recent review discussed potential mechanisms of promoting healthy neuromuscular aging by β-hydroxy-β-methylbutyrate, creatine, dietary phospholipids, omega-3 fatty acids, and vitamin D (Kougias et al., 2018). Additional clinical research investigating optimal dosages and durations of caloric restriction and nutritional intervention is needed to determine whether these effects can attenuate the aging process.

Examining the pathological mechanisms of neurodegenerative diseases with phenotypes similar to aging will help evaluate the molecular changes that underlie the structural and functional changes seen during aging. These include changes in active zone number and composition, NMJ innervation, and muscle mass. Also, mouse models of accelerated aging add value by identifying new pathways involved in aging. Importantly, the conserved beneficial effect in rodents, non-human primates, and humans supports the importance of caloric restriction and exercise for improving physical function in the elderly. Taken together, these strategies are likely to contribute to the development of interventions for preventing age-related neuromuscular dysfunction, sarcopenia, and frailty.

AUTHOR CONTRIBUTIONS

YB and HN contributed to the conception and writing of this review manuscript. Both authors contributed to the article and approved the submitted version.

FUNDING

This work was supported by the National Institute of Health (1R01AG051470 for HN) and Japan Society for the Promotion of Science (19K24690 for HN).

ACKNOWLEDGMENTS

We thank the topic editors for the invitation to this manuscript.

REFERENCES

Aebi, U., Cohn, J., Buhle, L., and Gerace, L. (1986). The nuclear lamina is a meshwork of intermediate-type filaments. *Nature* 323, 560–564. doi: 10.1038/323560a0

Ahmad, A., Enzlin, J. H., Bhagwat, N. R., Wijgers, N., Raams, A., Appledoorn, E., et al. (2010). Mislocalization of XPF-ERCC1 nuclease contributes to reduced DNA repair in XP-F patients. *PLoS Genet.* 6:e1000871. doi: 10.1371/journal.pgen.1000871

Albuquerque, E. X., Barnard, E. A., Porter, C. W., and Warnick, J. E. (1974). The density of acetylcholine receptors and their sensitivity in the postsynaptic membrane of muscle endplates. *Proc. Natl. Acad. Sci. U.S.A.* 71, 2818–2822. doi: 10.1073/pnas.71.7.2818

Anderson, M. J., and Cohen, M. W. (1977). Nerve-induced and spontaneous redistribution of acetylcholine receptors on cultured muscle cells. *J. Physiol.* 268, 757–773. doi: 10.1113/jphysiol.1977.sp011880

Anderson, R. M., and Weindruch, R. (2010). Metabolic reprogramming, caloric restriction and aging. *Trends Endocrinol. Metab.* 21, 134–141. doi: 10.1016/j.tem.2009.11.005

Anderson, R. M., and Weindruch, R. (2012). The caloric restriction paradigm: implications for healthy human aging. *Am. J. Hum. Biol.* 24, 101–106. doi: 10.1002/ajhb.22243

Andonian, M. H., and Fahim, M. A. (1988). Endurance exercise alters the morphology of fast- and slow-twitch rat neuromuscular junctions. *Int. J. Sports Med.* 9, 218–223. doi: 10.1055/s-2007-1025009

Apel, E. D., Glass, D. J., Moscoso, L. M., Yancopoulos, G. D., and Sanes, J. R. (1997). Rapsyn is required for MuSK signaling and recruits synaptic components to a MuSK-containing scaffold. *Neuron* 18, 623–635. doi: 10.1016/s0896-6273(00)80303-7

Arizono, N., Koreto, O., Iwai, Y., Hidaka, T., and Takeoka, O. (1984). Morphometric analysis of human neuromuscular junction in different ages. *Acta Pathol. Jpn.* 34, 1243–1249. doi: 10.1111/j.1440-1827.1984.tb00551.x

Atkin, J. D., Scott, R. L., West, J. M., Lopes, E., Quah, A. K., and Cheema, S. S. (2005). Properties of slow- and fast-twitch muscle fibres in a mouse model of amyotrophic lateral sclerosis. *Neuromuscul. Disord.* 15, 377–388. doi: 10.1016/j.nmd.2005.02.005

Badawi, Y., and Nishimune, H. (2018). Presynaptic active zones of mammalian neuromuscular junctions: nanoarchitecture and selective impairments in aging. *Neurosci. Res.* 127, 78–88. doi: 10.1016/j.neures.2017.11.014

Baker, D. J., Jeganathan, K. B., Cameron, J. D., Thompson, M., Juneja, S., Kopecka, A., et al. (2004). BubR1 insufficiency causes early onset of aging-associated phenotypes and infertility in mice. *Nat. Genet.* 36, 744–749. doi: 10.1038/ng1382

Baker, D. J., Perez-Terzic, C., Jin, F., Pitel, K. S., Niederlander, N. J., Jeganathan, K., et al. (2008). Opposing roles for p16Ink4a and p19Arf in senescence and ageing caused by BubR1 insufficiency. *Nat. Cell Biol.* 10, 825–836. doi: 10.1038/ncb1744

Baker, D. J., Wijshake, T., Tchkonia, T., LeBrasseur, N. K., Childs, B. G., van de Sluis, B., et al. (2011). Clearance of p16Ink4a-positive senescent cells delays ageing-associated disorders. *Nature* 479, 232–236. doi: 10.1038/nature10600

Banker, B. Q., Kelly, S. S., and Robbins, N. (1983). Neuromuscular transmission and correlative morphology in young and old mice. *J. Physiol.* 339, 355–377. doi: 10.1113/jphysiol.1983.sp014721

Beeson, D., Higuchi, O., Palace, J., Cossins, J., Spearman, H., Maxwell, S., et al. (2006). Dok-7 mutations underlie a neuromuscular junction synaptopathy. *Science* 313, 1975–1978. doi: 10.1126/science.1130837

Bergo, M. O., Gavino, B., Ross, J., Schmidt, W. K., Hong, C., Kendall, L. V., et al. (2002). Zmpste24 deficiency in mice causes spontaneous bone fractures, muscle weakness, and a prelamin A processing defect. *Proc. Natl. Acad. Sci. U.S.A.* 99, 13049–13054. doi: 10.1073/pnas.192460799

Binks, S., Vincent, A., and Palace, J. (2016). Myasthenia gravis: a clinical-immunological update. *J. Neurol.* 263, 826–834. doi: 10.1007/s00415-015-7963-5

Boehm, I., Alhindi, A., Leite, A. S., Logie, C., Gibbs, A., Murray, O., et al. (2020). Comparative anatomy of the mammalian neuromuscular junction. *J. Anat.* 237, 827–836. doi: 10.1111/joa.13260

Bromberg, M. B., and Scott, D. M. (1994). Single fiber EMG reference values: reformatted in tabular form. AD HOC Committee of the AAEM single fiber special interest group. *Muscle Nerve* 17, 820–821. doi: 10.1002/mus.880170720

Brooks, K. J., Hill, M. D., Hockings, P. D., and Reid, D. G. (2004). MRI detects early hindlimb muscle atrophy in Gly93Ala superoxide dismutase-1 (G93A SOD1) transgenic mice, an animal model of familial amyotrophic lateral sclerosis. *NMR Biomed.* 17, 28–32. doi: 10.1002/nbm.861

Brown, R. H. (1995). Amyotrophic lateral sclerosis: recent insights from genetics and transgenic mice. *Cell* 80, 687–692. doi: 10.1016/0092-8674(95)90346-1

Cadore, E. L., Pinto, R. S., Bottaro, M., and Izquierdo, M. (2014). Strength and endurance training prescription in healthy and frail elderly. *Aging Dis.* 5, 183–195. doi: 10.14336/ad.2014.0500183

Caldwell, J. H. (2000). Clustering of sodium channels at the neuromuscular junction. *Microsc. Res. Tech.* 49, 84–89. doi: 10.1002/(SICI)1097-0029(20000401)49:1<84::AID-JEMT9<3.0.CO;2-E

Carrero, D., Soria-Valles, C., and Lopez-Otin, C. (2016). Hallmarks of progeroid syndromes: lessons from mice and reprogrammed cells. *Dis. Model. Mech.* 9, 719–735. doi: 10.1242/dmm.024711

Chai, R. J., Vukovic, J., Dunlop, S., Grounds, M. D., and Shavlakadze, T. (2011). Striking denervation of neuromuscular junctions without lumbar motoneuron loss in geriatric mouse muscle. *PLoS One* 6:e28090. doi: 10.1371/journal.pone.0028090

Chan, Y. C., Suzuki, M., and Yamamoto, S. (1997). Dietary, anthropometric, hematological and biochemical assessment of the nutritional status of centenarians and elderly people in Okinawa, Japan. *J. Am. Coll. Nutr.* 16, 229–235. doi: 10.1080/07315724.1997.10718679

Chen, J., Mizushige, T., and Nishimune, H. (2012). Active zone density is conserved during synaptic growth but impaired in aged mice. *J. Comp. Neurol.* 520, 434–452. doi: 10.1002/cne.22764

Cheng, A., Morsch, M., Murata, Y., Ghazanfari, N., Reddel, S. W., and Phillips, W. D. (2013). Sequence of age-associated changes to the mouse neuromuscular junction and the protective effects of voluntary exercise. *PLoS One* 8:e67970. doi: 10.1371/journal.pone.0067970

Chiu, A. Y., Zhai, P., Dal Canto, M. C., Peters, T. M., Kwon, Y. W., Prattis, S. M., et al. (1995). Age-dependent penetrance of disease in a transgenic mouse model of familial amyotrophic lateral sclerosis. *Mol. Cell Neurosci.* 6, 349–362. doi: 10.1006/mcne.1995.1027

Chugh, D., Iyer, C. C., Wang, X., Bobbili, P., Rich, M. M., and Arnold, W. D. (2020). Neuromuscular junction transmission failure is a late phenotype in aging mice. *Neurobiol. Aging* 86, 182–190. doi: 10.1016/j.neurobiolaging.2019.10.022

Civitarese, A. E., Carling, S., Heilbronn, L. K., Hulver, M. H., Ukropcova, B., Deutsch, W. A., et al. (2007). Calorie restriction increases muscle mitochondrial biogenesis in healthy humans. *PLoS Med.* 4:e76. doi: 10.1371/journal.pmed.0040076

Clark, B. C. (2019). Neuromuscular changes with aging and sarcopenia. *J. Frailty Aging* 8, 7–9. doi: 10.14283/jfa.2018.35

Clark, D. O. (1996). The effect of walking on lower body disability among older blacks and whites. *Am. J. Public Health* 86, 57–61. doi: 10.2105/ajph.86.1.57

Collado, M., Blasco, M. A., and Serrano, M. (2007). Cellular senescence in cancer and aging. *Cell* 130, 223–233. doi: 10.1016/j.cell.2007.07.003

Conti-Fine, B. M., Milani, M., and Kaminski, H. J. (2006). Myasthenia gravis: past, present, and future. *J. Clin. Invest.* 116, 2843–2854. doi: 10.1172/JCI29894

Couteaux, R., and Pecot-Dechavassine, M. (1970). Synaptic vesicles and pouches at the level of" active zones" of the neuromuscular junction. *C. R. Acad. Hebd. Seances Acad. Sci. D* 271, 2346–2349.

Dadon-Nachum, M., Melamed, E., and Offen, D. (2011). The "dying-back" phenomenon of motor neurons in ALS. *J. Mol. Neurosci.* 43, 470–477. doi: 10.1007/s12031-010-9467-1

Dani, A., Huang, B., Bergan, J., Dulac, C., and Zhuang, X. (2010). Superresolution imaging of chemical synapses in the brain. *Neuron* 68, 843–856. doi: 10.1016/j.neuron.2010.11.021

De Sandre-Giovannoli, A., Bernard, R., Cau, P., Navarro, C., Amiel, J., Boccaccio, I., et al. (2003). Lamin a truncation in Hutchinson-Gilford progeria. *Science* 300:2055. doi: 10.1126/science.1084125

de Waard, M. C., van der Pluijm, I., Zuiderveen Borgesius, N., Comley, L. H., Haasdijk, E. D., Rijksen, Y., et al. (2010). Age-related motor neuron degeneration in DNA repair-deficient Ercc1 mice. *Acta Neuropathol.* 120, 461–475. doi: 10.1007/s00401-010-0715-9

DeChiara, T. M., Bowen, D. C., Valenzuela, D. M., Simmons, M. V., Poueymirou, W. T., Thomas, S., et al. (1996). The receptor tyrosine kinase MuSK is required for neuromuscular junction formation in vivo. *Cell* 85, 501–512. doi: 10.1016/s0092-8674(00)81251-9

Dengler, R., Konstanzer, A., Kuther, G., Hesse, S., Wolf, W., and Struppler, A. (1990). Amyotrophic lateral sclerosis: macro-EMG and twitch forces of single motor units. *Muscle Nerve* 13, 545–550. doi: 10.1002/mus.880130612

Deschenes, M. R., Hurst, T. E., Ramser, A. E., and Sherman, E. G. (2013). Presynaptic to postsynaptic relationships of the neuromuscular junction are held constant across age and muscle fiber type. *Dev. Neurobiol.* 73, 744–753. doi: 10.1002/dneu.22095

Deschenes, M. R., Roby, M. A., Eason, M. K., and Harris, M. B. (2010). Remodeling of the neuromuscular junction precedes sarcopenia related alterations in myofibers. *Exp. Gerontol.* 45, 389–393. doi: 10.1016/j.exger.2010.03.007

Deschenes, M. R., Roby, M. A., and Glass, E. K. (2011). Aging influences adaptations of the neuromuscular junction to endurance training. *Neuroscience* 190, 56–66. doi: 10.1016/j.neuroscience.2011.05.070

Dobrowolny, G., Martini, M., Scicchitano, B. M., Romanello, V., Boncompagni, S., Nicoletti, C., et al. (2018). Muscle expression of SOD1(G93A) triggers the dismantlement of neuromuscular junction via PKC-Theta. *Antioxid Redox Signal.* 28, 1105–1119. doi: 10.1089/ars.2017.7054

Ehmann, N., Van De Linde, S., Alon, A., Ljaschenko, D., Keung, X. Z., Holm, T., et al. (2014). Quantitative super-resolution imaging of Bruchpilot distinguishes active zone states. *Nat. Commun.* 5:4650. doi: 10.1038/ncomms5650

Elchuri, S., Oberley, T. D., Qi, W., Eisenstein, R. S., Jackson Roberts, L., Van Remmen, H., et al. (2005). CuZnSOD deficiency leads to persistent and widespread oxidative damage and hepatocarcinogenesis later in life. *Oncogene* 24, 367–380. doi: 10.1038/sj.onc.1208207

Ellisman, M. H., Rash, J. E., Staehelin, L. A., and Porter, K. R. (1976). Studies of excitable membranes. II. A comparison of specializations at neuromuscular junctions and nonjunctional sarcolemmas of mammalian fast and slow twitch muscle fibers. *J. Cell Biol.* 68, 752–774. doi: 10.1083/jcb.68.3.752

Engel, A. G., Lambert, E. H., and Gomez, M. R. (1977). A new myasthenic syndrome with end-plate acetylcholinesterase deficiency, small nerve terminals, and reduced acetylcholine release. *Ann. Neurol.* 1, 315–330. doi: 10.1002/ana.410010403

Engel, A. G., Shen, X. M., Selcen, D., and Sine, S. M. (2010). What have we learned from the congenital myasthenic syndromes. *J. Mol. Neurosci.* 40, 143–153. doi: 10.1007/s12031-009-9229-0

Engel, A. G., Shen, X. M., Selcen, D., and Sine, S. M. (2015). Congenital myasthenic syndromes: pathogenesis, diagnosis, and treatment. *Lancet Neurol.* 14:461. doi: 10.1016/S1474-4422(15)00010-1

Eriksson, M., Brown, W. T., Gordon, L. B., Glynn, M. W., Singer, J., Scott, L., et al. (2003). Recurrent de novo point mutations in lamin A cause Hutchinson-Gilford progeria syndrome. *Nature* 423, 293–298. doi: 10.1038/nature01629

Fahim, M. A. (1997). Endurance exercise modulates neuromuscular junction of C57BL/6NNia aging mice. *J. Appl. Physiol. (1985)* 83, 59–66. doi: 10.1152/jappl.1997.83.1.59

Fahim, M. A., Holley, J. A., and Robbins, N. (1983). Scanning and light microscopic study of age changes at a neuromuscular junction in the mouse. *J. Neurocytol.* 12, 13–25. doi: 10.1007/Bf01148085

Fahim, M. A., and Robbins, N. (1982). Ultrastructural studies of young and old mouse neuromuscular junctions. *J. Neurocytol.* 11, 641–656. doi: 10.1007/bf01262429

Ferrucci, L., Izmirlian, G., Leveille, S., Phillips, C. L., Corti, M. C., Brock, D. B., et al. (1999). Smoking, physical activity, and active life expectancy. *Am. J. Epidemiol.* 149, 645–653. doi: 10.1093/oxfordjournals.aje.a009865

Fertuck, H. C., and Salpeter, M. M. (1974). Localization of acetylcholine receptor by 125I-labeled alpha-bungarotoxin binding at mouse motor endplates. *Proc. Natl. Acad. Sci. U.S.A.* 71, 1376–1378. doi: 10.1073/pnas.71.4.1376

Fertuck, H. C., and Salpeter, M. M. (1976). Quantitation of junctional and extrajunctional acetylcholine receptors by electron microscope autoradiography after 125I-alpha-bungarotoxin binding at mouse neuromuscular junctions. *J. Cell Biol.* 69, 144–158. doi: 10.1083/jcb.69.1.144

Fischer, L. R., Culver, D. G., Tennant, P., Davis, A. A., Wang, M., Castellano-Sanchez, A., et al. (2004). Amyotrophic lateral sclerosis is a distal axonopathy: evidence in mice and man. *Exp. Neurol.* 185, 232–240. doi: 10.1016/j.expneurol.2003.10.004

Fischer, L. R., Igoudjil, A., Magrane, J., Li, Y., Hansen, J. M., Manfredi, G., et al. (2011). SOD1 targeted to the mitochondrial intermembrane space prevents motor neuropathy in the Sod1 knockout mouse. *Brain* 134(Pt 1), 196–209. doi: 10.1093/brain/awq314

Fischer, L. R., Li, Y., Asress, S. A., Jones, D. P., and Glass, J. D. (2012). Absence of SOD1 leads to oxidative stress in peripheral nerve and causes a progressive distal motor axonopathy. *Exp. Neurol.* 233, 163–171. doi: 10.1016/j.expneurol.2011.09.020

Flink, M. T., and Atchison, W. D. (2003). Ca2+ channels as targets of neurological disease: Lambert-Eaton Syndrome and other Ca2+ channelopathies. *J. Bioenerg. Biomembr.* 35, 697–718. doi: 10.1023/b:jobb.0000008033.02320.10

Flood, D. G., Reaume, A. G., Gruner, J. A., Hoffman, E. K., Hirsch, J. D., Lin, Y. G., et al. (1999). Hindlimb motor neurons require Cu/Zn superoxide dismutase for maintenance of neuromuscular junctions. *Am. J. Pathol.* 155, 663–672. doi: 10.1016/S0002-9440(10)65162-0

Folgueras, A. R., Freitas-Rodriguez, S., Velasco, G., and Lopez-Otin, C. (2018). Mouse models to disentangle the hallmarks of human aging. *Circ. Res.* 123, 905–924. doi: 10.1161/CIRCRESAHA.118.312204

Fontana, L., Partridge, L., and Longo, V. D. (2010). Extending healthy life span–from yeast to humans. *Science* 328, 321–326. doi: 10.1126/science.1172539

Frank, E., and Fischbach, G. D. (1979). Early events in neuromuscular junction formation in vitro: induction of acetylcholine receptor clusters in the postsynaptic membrane and morphology of newly formed synapses. *J. Cell Biol.* 83, 143–158. doi: 10.1083/jcb.83.1.143

Fried, L. P., Tangen, C. M., Walston, J., Newman, A. B., Hirsch, C., Gottdiener, J., et al. (2001). Frailty in older adults: evidence for a phenotype. *J. Gerontol. A Biol. Sci. Med. Sci.* 56, M146–M156. doi: 10.1093/gerona/56.3.m146

Frontera, W. R., Hughes, V. A., Fielding, R. A., Fiatarone, M. A., Evans, W. J., and Roubenoff, R. (2000). Aging of skeletal muscle: a 12-yr longitudinal study. *J. Appl. Physiol. (1985)* 88, 1321–1326. doi: 10.1152/jappl.2000.88.4.1321

Fukunaga, H., Engel, A. G., Lang, B., Newsom-Davis, J., and Vincent, A. (1983). Passive transfer of Lambert-Eaton myasthenic syndrome with IgG from man to mouse depletes the presynaptic membrane active zones. *Proc. Natl. Acad. Sci. U.S.A.* 80, 7636–7640.

Fukunaga, H., Engel, A. G., Osame, M., and Lambert, E. H. (1982). Paucity and disorganization of presynaptic membrane active zones in the lambert-eaton myasthenic syndrome. *Muscle Nerve* 5, 686–697. doi: 10.1002/mus.880050905

Fukuoka, T., Engel, A. G., Lang, B., Newsom-Davis, J., Prior, C., and Wray, D. W. (1987). Lambert-Eaton myasthenic syndrome: I. Early morphological effects of IgG on the presynaptic membrane active zones. *Ann. Neurol.* 22, 193–199. doi: 10.1002/ana.410220203

Fulle, S., Protasi, F., Di Tano, G., Pietrangelo, T., Beltramin, A., Boncompagni, S., et al. (2004). The contribution of reactive oxygen species to sarcopenia and muscle ageing. *Exp. Gerontol.* 39, 17–24. doi: 10.1016/j.exger.2003.09.012

Galea, V. (1996). Changes in motor unit estimates with aging. *J. Clin. Neurophysiol.* 13, 253–260. doi: 10.1097/00004691-199605000-00010

Gambino, D. R., Malmgren, L. T., and Gacek, R. R. (1990). Age-related changes in the neuromuscular junctions in the human posterior cricoarytenoid muscles: a quantitative study. *Laryngoscope* 100, 262–268. doi: 10.1288/00005537-199003000-00010

Gao, N., Zhao, K., Cao, Y., Ren, X., Jing, H., Xing, G., et al. (2020). A role of lamin A/C in preventing neuromuscular junction decline in mice. *J. Neurosci.* 40, 7203–7203. doi: 10.1523/JNEUROSCI.0443-20.2020

Ghosh, S., and Zhou, Z. (2015). SIRTain regulators of premature senescence and accelerated aging. *Protein Cell* 6, 322–333. doi: 10.1007/s13238-015-0149-1

Gilhus, N. E., and Verschuuren, J. J. (2015). Myasthenia gravis: subgroup classification and therapeutic strategies. *Lancet Neurol.* 14, 1023–1036. doi: 10.1016/S1474-4422(15)00145-3

Gonzalez-Freire, M., de Cabo, R., Studenski, S. A., and Ferrucci, L. (2014). The neuromuscular junction: aging at the crossroad between nerves and muscle. *Front. Aging Neurosci.* 6:208. doi: 10.3389/fnagi.2014.00208

Greising, S. M., Call, J. A., Lund, T. C., Blazar, B. R., Tolar, J., and Lowe, D. A. (2012). Skeletal muscle contractile function and neuromuscular performance in Zmpste24 -/- mice, a murine model of human progeria. *Age (Dordr)* 34, 805–819. doi: 10.1007/s11357-011-9281-x

Gurney, M. E., Pu, H., Chiu, A. Y., Dal Canto, M. C., Polchow, C. Y., Alexander, D. D., et al. (1994). Motor neuron degeneration in mice that express a human Cu,Zn superoxide dismutase mutation. *Science* 264, 1772–1775. doi: 10.1126/science.8209258

Hallock, P. T., Xu, C. F., Park, T. J., Neubert, T. A., Curran, T., and Burden, S. J. (2010). Dok-7 regulates neuromuscular synapse formation by recruiting Crk and Crk-L. *Genes Dev.* 24, 2451–2461. doi: 10.1101/gad.1977710

Hansen, M., Taubert, S., Crawford, D., Libina, N., Lee, S. J., and Kenyon, C. (2007). Lifespan extension by conditions that inhibit translation in Caenorhabditis elegans. *Aging Cell* 6, 95–110. doi: 10.1111/j.1474-9726.2006.00267.x

Harkema, L., Youssef, S. A., and de Bruin, A. (2016). Pathology of mouse models of accelerated aging. *Vet. Pathol.* 53, 366–389. doi: 10.1177/0300985815625169

Harlow, M. L., Ress, D., Stoschek, A., Marshall, R. M., and McMahan, U. J. (2001). The architecture of active zone material at the frog's neuromuscular junction. *Nature* 409, 479–484. doi: 10.1038/35054000

Harlow, M. L., Szule, J. A., Xu, J., Jung, J. H., Marshall, R. M., and McMahan, U. J. (2013). Alignment of synaptic vesicle macromolecules with the macromolecules in active zone material that direct vesicle docking. *PLoS One* 8:e69410. doi: 10.1371/journal.pone.0069410

Hegedus, J., Putman, C. T., and Gordon, T. (2007). Time course of preferential motor unit loss in the SOD1 G93A mouse model of amyotrophic lateral sclerosis. *Neurobiol. Dis.* 28, 154–164. doi: 10.1016/j.nbd.2007.07.003

Hegedus, J., Putman, C. T., Tyreman, N., and Gordon, T. (2008). Preferential motor unit loss in the SOD1 G93A transgenic mouse model of amyotrophic lateral sclerosis. *J. Physiol.* 586, 3337–3351. doi: 10.1113/jphysiol.2007.149286

Heilbronn, L. K., de Jonge, L., Frisard, M. I., DeLany, J. P., Larson-Meyer, D. E., Rood, J., et al. (2006). Effect of 6-month calorie restriction on biomarkers of longevity, metabolic adaptation, and oxidative stress in overweight individuals: a randomized controlled trial. *JAMA* 295, 1539–1548. doi: 10.1001/jama.295.13.1539

Higuchi, O., Hamuro, J., Motomura, M., and Yamanashi, Y. (2011). Autoantibodies to low-density lipoprotein receptor-related protein 4 in myasthenia gravis. *Ann. Neurol.* 69, 418–422. doi: 10.1002/ana.22312

Ho, Y. S., Gargano, M., Cao, J., Bronson, R. T., Heimler, I., and Hutz, R. J. (1998). Reduced fertility in female mice lacking copper-zinc superoxide dismutase. *J. Biol. Chem.* 273, 7765–7769. doi: 10.1074/jbc.273.13.7765

Hoeijmakers, J. H. (2009). DNA damage, aging, and cancer. *N. Engl. J. Med.* 361, 1475–1485. doi: 10.1056/NEJMra0804615

Hong, S. J., and Chang, C. C. (1989). Use of geographutoxin II (mu-conotoxin) for the study of neuromuscular transmission in mouse. *Br. J. Pharmacol.* 97, 934–940. doi: 10.1111/j.1476-5381.1989.tb12034.x

Hourigan, M. L., McKinnon, N. B., Johnson, M., Rice, C. L., Stashuk, D. W., and Doherty, T. J. (2015). Increased motor unit potential shape variability across consecutive motor unit discharges in the tibialis anterior and vastus medialis muscles of healthy older subjects. *Clin. Neurophysiol.* 126, 2381–2389. doi: 10.1016/j.clinph.2015.02.002

Huijbers, M. G., Zhang, W., Klooster, R., Niks, E. H., Friese, M. B., Straasheijm, K. R., et al. (2013). MuSK IgG4 autoantibodies cause myasthenia gravis by inhibiting binding between MuSK and Lrp4. *Proc. Natl. Acad. Sci. U.S.A.* 110, 20783–20788. doi: 10.1073/pnas.1313944110

Hunter, D. D., Shah, V., Merlie, J. P., and Sanes, J. R. (1989). A laminin-like adhesive protein concentrated in the synaptic cleft of the neuromuscular junction. *Nature* 338, 229–234. doi: 10.1038/338229a0

Jahn, R., and Scheller, R. H. (2006). SNAREs–engines for membrane fusion. *Nat. Rev. Mol. Cell Biol.* 7, 631–643. doi: 10.1038/nrm2002

Jang, Y. C., Lustgarten, M. S., Liu, Y., Muller, F. L., Bhattacharya, A., Liang, H., et al. (2010). Increased superoxide in vivo accelerates age-associated muscle atrophy through mitochondrial dysfunction and neuromuscular junction degeneration. *FASEB J.* 24, 1376–1390. doi: 10.1096/fj.09-146308

Janssen, I., Heymsfield, S. B., Wang, Z. M., and Ross, R. (2000). Skeletal muscle mass and distribution in 468 men and women aged 18-88 yr. *J. Appl. Physiol. (1985)* 89, 81–88. doi: 10.1152/jappl.2000.89.1.81

Jaspers, N. G., Raams, A., Silengo, M. C., Wijgers, N., Niedernhofer, L. J., Robinson, A. R., et al. (2007). First reported patient with human ERCC1 deficiency has cerebro-oculo-facio-skeletal syndrome with a mild defect in nucleotide excision repair and severe developmental failure. *Am. J. Hum. Genet.* 80, 457–466. doi: 10.1086/512486

Jones, R. A., Harrison, C., Eaton, S. L., Llavero Hurtado, M., Graham, L. C., Alkhammash, L., et al. (2017). Cellular and molecular anatomy of the human neuromuscular junction. *Cell Rep.* 21, 2348–2356. doi: 10.1016/j.celrep.2017.11.008

Jung, J. H., Szule, J. A., Stouder, K., Marshall, R. M., and McMahan, U. J. (2018). Active zone material-directed orientation, docking, and fusion of dense core vesicles alongside synaptic vesicles at neuromuscular junctions. *Front. Neuroanat.* 12:72. doi: 10.3389/fnana.2018.00072

Kaeberlein, M., Powers, R. W. III, Steffen, K. K., Westman, E. A., Hu, D., Dang, N., et al. (2005). Regulation of yeast replicative life span by TOR and Sch9 in response to nutrients. *Science* 310, 1193–1196. doi: 10.1126/science.1115535

Kapahi, P., Zid, B. M., Harper, T., Koslover, D., Sapin, V., and Benzer, S. (2004). Regulation of lifespan in Drosophila by modulation of genes in the TOR signaling pathway. *Curr. Biol.* 14, 885–890. doi: 10.1016/j.cub.2004.03.059

Kawamura, Y., O'Brien, P., Okazaki, H., and Dyck, P. J. (1977). Lumbar motoneurons of man II: the number and diameter distribution of large- and intermediate-diameter cytons in "motoneuron columns" of spinal cord of man. *J. Neuropathol. Exp. Neurol.* 36, 861–870. doi: 10.1097/00005072-197709000-00010

Kelly, S. S., and Robbins, N. (1983). Progression of age changes in synaptic transmission at mouse neuromuscular junctions. *J. Physiol.* 343, 375–383. doi: 10.1113/jphysiol.1983.sp014898

Kennel, P. F., Finiels, F., Revah, F., and Mallet, J. (1996). Neuromuscular function impairment is not caused by motor neurone loss in FALS mice: an electromyographic study. *Neuroreport* 7, 1427–1431. doi: 10.1097/00001756-199605310-00021

Kim, N., Stiegler, A. L., Cameron, T. O., Hallock, P. T., Gomez, A. M., Huang, J. H., et al. (2008). Lrp4 is a receptor for Agrin and forms a complex with MuSK. *Cell* 135, 334–342. doi: 10.1016/j.cell.2008.10.002

Kittel, R. J., Wichmann, C., Rasse, T. M., Fouquet, W., Schmidt, M., Schmid, A., et al. (2006). Bruchpilot promotes active zone assembly, Ca2+ channel clustering, and vesicle release. *Science* 312, 1051–1054. doi: 10.1126/science.1126308

Klein, C. S., Marsh, G. D., Petrella, R. J., and Rice, C. L. (2003). Muscle fiber number in the biceps brachii muscle of young and old men. *Muscle Nerve* 28, 62–68. doi: 10.1002/mus.10386

Kougias, D. G., Das, T., Perez, A. B., and Pereira, S. L. (2018). A role for nutritional intervention in addressing the aging neuromuscular junction. *Nutr. Res.* 53, 1–14. doi: 10.1016/j.nutres.2018.02.006

Lambert, E. H., and Elmqvist, D. (1971). Quantal components of end-plate potentials in the myasthenic syndrome. *Ann. N. Y. Acad. Sci.* 183, 183–199. doi: 10.1111/j.1749-6632.1971.tb30750.x

Larsson, L. (1995). Motor units: remodeling in aged animals. *J. Gerontol. A Biol. Sci. Med. Sci.* 50, 91–95. doi: 10.1093/gerona/50a.special_issue.91

Lavin, K. M., Roberts, B. M., Fry, C. S., Moro, T., Rasmussen, B. B., and Bamman, M. M. (2019). The importance of resistance exercise training to combat neuromuscular aging. *Physiology (Bethesda)* 34, 112–122. doi: 10.1152/physiol.00044.2018

Lee, Y., Rudell, J., and Ferns, M. (2009). Rapsyn interacts with the muscle acetylcholine receptor via alpha-helical domains in the alpha, beta, and epsilon subunit intracellular loops. *Neuroscience* 163, 222–232. doi: 10.1016/j.neuroscience.2009.05.057

Leung, G. K., Schmidt, W. K., Bergo, M. O., Gavino, B., Wong, D. H., Tam, A., et al. (2001). Biochemical studies of Zmpste24-deficient mice. *J. Biol. Chem.* 276, 29051–29058. doi: 10.1074/jbc.M102908200

Lexell, J. (1995). Human aging, muscle mass, and fiber type composition. *J. Gerontol. A Biol. Sci. Med. Sci.* 50, 11–16. doi: 10.1093/gerona/50a.special_issue.11

Lexell, J., and Downham, D. Y. (1991). The occurrence of fibre-type grouping in healthy human muscle: a quantitative study of cross-sections of whole vastus lateralis from men between 15 and 83 years. *Acta Neuropathol.* 81, 377–381. doi: 10.1007/bf00293457

Lexell, J., Henriksson-Larsen, K., Winblad, B., and Sjostrom, M. (1983). Distribution of different fiber types in human skeletal muscles: effects of aging studied in whole muscle cross sections. *Muscle Nerve* 6, 588–595. doi: 10.1002/mus.880060809

Lexell, J., Taylor, C. C., and Sjostrom, M. (1988). What is the cause of the ageing atrophy? Total number, size and proportion of different fiber types studied in whole vastus lateralis muscle from 15- to 83-year-old men. *J. Neurol. Sci.* 84, 275–294.

Li, L., Xiong, W. C., and Mei, L. (2018). Neuromuscular junction formation, aging, and disorders. *Annu. Rev. Physiol.* 80, 159–188. doi: 10.1146/annurev-physiol-022516-034255

Li, Y., Lee, Y., and Thompson, W. J. (2011). Changes in aging mouse neuromuscular junctions are explained by degeneration and regeneration of muscle fiber segments at the synapse. *J. Neurosci.* 31, 14910–14919. doi: 10.1523/JNEUROSCI.3590-11.2011

Lindboe, C. F., and Torvik, A. (1982). The effects of ageing, cachexia and neoplasms on striated muscle. Quantitative histological and histochemical observations on an autopsy material. *Acta Neuropathol.* 57, 85–92. doi: 10.1007/bf00685374

Lopez, P., Pinto, R. S., Radaelli, R., Rech, A., Grazioli, R., Izquierdo, M., et al. (2018). Benefits of resistance training in physically frail elderly: a systematic review. *Aging Clin. Exp. Res.* 30, 889–899. doi: 10.1007/s40520-017-0863-z

Loutrari, H., Kokla, A., and Tzartos, S. J. (1992). Passive transfer of experimental myasthenia gravis via antigenic modulation of acetylcholine receptor. *Eur. J. Immunol.* 22, 2449–2452. doi: 10.1002/eji.1830220939

Manini, T. M., Hong, S. L., and Clark, B. C. (2013). Aging and muscle: a neuron's perspective. *Curr. Opin. Clin. Nutr. Metab. Care* 16, 21–26. doi: 10.1097/MCO.0b013e32835b5880

Marcuzzo, S., Zucca, I., Mastropietro, A., de Rosbo, N. K., Cavalcante, P., Tartari, S., et al. (2011). Hind limb muscle atrophy precedes cerebral neuronal degeneration in G93A-SOD1 mouse model of amyotrophic lateral sclerosis: a longitudinal MRI study. *Exp. Neurol.* 231, 30–37. doi: 10.1016/j.expneurol.2011.05.007

Martin, G. M. (1978). Genetic syndromes in man with potential relevance to the pathobiology of aging. *Birth Defects Orig. Artic Ser.* 14, 5–39.

Maselli, R. A., Ng, J. J., Anderson, J. A., Cagney, O., Arredondo, J., Williams, C., et al. (2009). Mutations in LAMB2 causing a severe form of synaptic congenital myasthenic syndrome. *J. Med. Genet.* 46, 203–208. doi: 10.1136/jmg.2008.063693

McComas, A. J., Fawcett, P. R., Campbell, M. J., and Sica, R. E. (1971). Electrophysiological estimation of the number of motor units within a human muscle. *J. Neurol. Neurosurg. Psychiatry* 34, 121–131. doi: 10.1136/jnnp.34.2.121

McFadden, S. L., Ding, D., Reaume, A. G., Flood, D. G., and Salvi, R. J. (1999). Age-related cochlear hair cell loss is enhanced in mice lacking copper/zinc superoxide dismutase. *Neurobiol. Aging* 20, 1–8. doi: 10.1016/s0197-4580(99)00018-4

McKiernan, S. H., Colman, R. J., Lopez, M., Beasley, T. M., Aiken, J. M., Anderson, R. M., et al. (2011). Caloric restriction delays aging-induced cellular phenotypes in rhesus monkey skeletal muscle. *Exp. Gerontol.* 46, 23–29. doi: 10.1016/j.exger.2010.09.011

McNeil, C. J., Doherty, T. J., Stashuk, D. W., and Rice, C. L. (2005). Motor unit number estimates in the tibialis anterior muscle of young, old, and very old men. *Muscle Nerve* 31, 461–467. doi: 10.1002/mus.20276

Mitchell, W. K., Williams, J., Atherton, P., Larvin, M., Lund, J., and Narici, M. (2012). Sarcopenia, dynapenia, and the impact of advancing age on human skeletal muscle size and strength; a quantitative review. *Front. Physiol.* 3:260. doi: 10.3389/fphys.2012.00260

Mittal, K. R., and Logmani, F. H. (1987). Age-related reduction in 8th cervical ventral nerve root myelinated fiber diameters and numbers in man. *J. Gerontol.* 42, 8–10. doi: 10.1093/geronj/42.1.8

Mori, S., Kubo, S., Akiyoshi, T., Yamada, S., Miyazaki, T., Hotta, H., et al. (2012). Antibodies against muscle-specific kinase impair both presynaptic and postsynaptic functions in a murine model of myasthenia gravis. *Am. J. Pathol.* 180, 798–810. doi: 10.1016/j.ajpath.2011.10.031

Mori, S., Motohashi, N., Takashima, R., Kishi, M., Nishimune, H., and Shigemoto, K. (2017). Immunization of mice with LRP4 induces myasthenia similar to MuSK-associated myasthenia gravis. *Exp. Neurol.* 297, 158–167. doi: 10.1016/j.expneurol.2017.08.006

Mosole, S., Carraro, U., Kern, H., Loefler, S., Fruhmann, H., Vogelauer, M., et al. (2014). Long-term high-level exercise promotes muscle reinnervation with age. *J. Neuropathol. Exp. Neurol.* 73, 284–294. doi: 10.1097/nen.0000000000000032

Most, J., Tosti, V., Redman, L. M., and Fontana, L. (2017). Calorie restriction in humans: an update. *Ageing Res. Rev.* 39, 36–45. doi: 10.1016/j.arr.2016.08.005

Muller, F. L., Song, W., Liu, Y., Chaudhuri, A., Pieke-Dahl, S., Strong, R., et al. (2006). Absence of CuZn superoxide dismutase leads to elevated oxidative stress and acceleration of age-dependent skeletal muscle atrophy. *Free Radic. Biol. Med.* 40, 1993–2004. doi: 10.1016/j.freeradbiomed.2006.01.036

Nagwaney, S., Harlow, M. L., Jung, J. H., Szule, J. A., Ress, D., Xu, J., et al. (2009). Macromolecular connections of active zone material to docked synaptic vesicles and presynaptic membrane at neuromuscular junctions of mouse. *J. Comp. Neurol.* 513, 457–468. doi: 10.1002/cne.21975

Nishimune, H., Badawi, Y., Mori, S., and Shigemoto, K. (2016). Dual-color STED microscopy reveals a sandwich structure of Bassoon and Piccolo in active zones of adult and aged mice. *Sci. Rep.* 6:27935. doi: 10.1038/srep27935

Nishimune, H., Numata, T., Chen, J., Aoki, Y., Wang, Y., Starr, M. P., et al. (2012). Active zone protein Bassoon co-localizes with presynaptic calcium channel, modifies channel function, and recovers from aging related loss by exercise. *PLoS One* 7:e38029. doi: 10.1371/journal.pone.0038029

Nishimune, H., Sanes, J. R., and Carlson, S. S. (2004). A synaptic laminin-calcium channel interaction organizes active zones in motor nerve terminals. *Nature* 432, 580–587. doi: 10.1038/nature03112

Noakes, P. G., Gautam, M., Mudd, J., Sanes, J. R., and Merlie, J. P. (1995). Aberrant differentiation of neuromuscular junctions in mice lacking s-laminin/laminin beta2. *Nature* 374:258. doi: 10.1038/374258a0

Oda, K. (1984). Age changes of motor innervation and acetylcholine receptor distribution on human skeletal muscle fibres. *J. Neurol. Sci.* 66, 327–338. doi: 10.1016/0022-510x(84)90021-2

Okada, K., Inoue, A., Okada, M., Murata, Y., Kakuta, S., Jigami, T., et al. (2006). The muscle protein Dok-7 is essential for neuromuscular synaptogenesis. *Science* 312, 1802–1805. doi: 10.1126/science.1127142

Otsuka, K., Ito, M., Ohkawara, B., Masuda, A., Kawakami, Y., Sahashi, K., et al. (2015). Collagen Q and anti-MuSK autoantibody competitively suppress agrin/LRP4/MuSK signaling. *Sci. Rep.* 5:13928. doi: 10.1038/srep13928

Papadopoli, D., Boulay, K., Kazak, L., Pollak, M., Mallette, F., Topisirovic, I., et al. (2019). mTOR as a central regulator of lifespan and aging. *F1000Res* 8:998. doi: 10.12688/f1000research.17196.1

Park, K. H. (2015). Mechanisms of muscle denervation in aging: insights from a mouse model of amyotrophic lateral sclerosis. *Aging Dis.* 6, 380–389. doi: 10.14336/AD.2015.0506

Patton, B. L., Cunningham, J. M., Thyboll, J., Kortesmaa, J., Westerblad, H., Edstrom, L., et al. (2001). Properly formed but improperly localized synaptic specializations in the absence of laminin alpha4. *Nat. Neurosci.* 4, 597–604. doi: 10.1038/88414

Pestronk, A., Drachman, D. B., and Self, S. G. (1985). Measurement of junctional acetylcholine receptors in myasthenia gravis: clinical correlates. *Muscle Nerve* 8, 245–251. doi: 10.1002/mus.880080311

Phillips, J. P., Campbell, S. D., Michaud, D., Charbonneau, M., and Hilliker, A. J. (1989). Null mutation of copper/zinc superoxide dismutase in Drosophila confers hypersensitivity to paraquat and reduced longevity. *Proc. Natl. Acad. Sci. U.S.A.* 86, 2761–2765. doi: 10.1073/pnas.86.8.2761

Phillips, W. D., and Vincent, A. (2016). Pathogenesis of myasthenia gravis: update on disease types, models, and mechanisms. *F1000Res* 5:1513. doi: 10.12688/f1000research.8206.1

Piasecki, M., Ireland, A., Stashuk, D., Hamilton-Wright, A., Jones, D. A., and McPhee, J. S. (2016). Age-related neuromuscular changes affecting human vastus lateralis. *J. Physiol.* 594, 4525–4536. doi: 10.1113/JP271087

Power, G. A., Allen, M. D., Gilmore, K. J., Stashuk, D. W., Doherty, T. J., Hepple, R. T., et al. (2016). Motor unit number and transmission stability in octogenarian world class athletes: can age-related deficits be outrun? *J. Appl. Physiol.* 121, 1013–1020. doi: 10.1152/japplphysiol.00149.2016

Power, G. A., Dalton, B. H., Behm, D. G., Doherty, T. J., Vandervoort, A. A., and Rice, C. L. (2012). Motor unit survival in lifelong runners is muscle dependent. *Med. Sci. Sports Exerc.* 44, 1235–1242. doi: 10.1249/MSS.0b013e318249953c

Power, G. A., Dalton, B. H., Behm, D. G., Vandervoort, A. A., Doherty, T. J., and Rice, C. L. (2010). Motor unit number estimates in masters runners: use it or lose it? *Med. Sci. Sports Exerc.* 42, 1644–1650. doi: 10.1249/MSS.0b013e3181d6f9e9

Redman, L. M., Smith, S. R., Burton, J. H., Martin, C. K., Il'yasova, D., and Ravussin, E. (2018). Metabolic slowing and reduced oxidative damage with sustained caloric restriction support the rate of living and oxidative damage theories of aging. *Cell Metab.* 27, 805–815.e4. doi: 10.1016/j.cmet.2018.02.019

Rocha, M. C., Pousinha, P. A., Correia, A. M., Sebastiao, A. M., and Ribeiro, J. A. (2013). Early changes of neuromuscular transmission in the SOD1(G93A) mice model of ALS start long before motor symptoms onset. *PLoS One* 8:e73846. doi: 10.1371/journal.pone.0073846

Rosato Siri, M. D., and Uchitel, O. D. (1999). Calcium channels coupled to neurotransmitter release at neonatal rat neuromuscular junctions. *J Physiol* 514(Pt 2), 533–540. doi: 10.1111/j.1469-7793.1999.533ae.x

Rosen, D. R., Siddique, T., Patterson, D., Figlewicz, D. A., Sapp, P., Hentati, A., et al. (1993). Mutations in Cu/Zn superoxide dismutase gene are associated with familial amyotrophic lateral sclerosis. *Nature* 362, 59–62. doi: 10.1038/362059a0

Roth, G. S., Ingram, D. K., Black, A., and Lane, M. A. (2000). Effects of reduced energy intake on the biology of aging: the primate model. *Eur. J. Clin. Nutr.* 54(Suppl. 3), S15–S20.

Rothbart, H. B. (1937). Myasthenia gravis in children: its familial incidence. *J. Am. Med. Assoc.* 108, 715–717. doi: 10.1001/jama.1937.02780090027008

Roubenoff, R. (2000). Sarcopenia and its implications for the elderly. *Eur. J. Clin. Nutr.* 54(Suppl. 3), S40–S47.

Rowan, S. L., Purves-Smith, F. M., Solbak, N. M., and Hepple, R. T. (2011). Accumulation of severely atrophic myofibers marks the acceleration of sarcopenia in slow and fast twitch muscles. *Exp. Gerontol.* 46, 660–669. doi: 10.1016/j.exger.2011.03.005

Ruff, R. L., and Lennon, V. A. (2008). How myasthenia gravis alters the safety factor for neuromuscular transmission. *J. Neuroimmunol.* 201-202, 13–20. doi: 10.1016/j.jneuroim.2008.04.038

Salmon, A. B., Richardson, A., and Perez, V. I. (2010). Update on the oxidative stress theory of aging: does oxidative stress play a role in aging or healthy aging? *Free Radic. Biol. Med.* 48, 642–655. doi: 10.1016/j.freeradbiomed.2009.12.015

Salpeter, M. M., and Loring, R. H. (1985). Nicotinic acetylcholine receptors in vertebrate muscle: properties, distribution and neural control. *Prog. Neurobiol.* 25, 297–325. doi: 10.1016/0301-0082(85)90018-8

Sanchez, R. J., Srinivasan, C., Munroe, W. H., Wallace, M. A., Martins, J., Kao, T. Y., et al. (2005). Exogenous manganous ion at millimolar levels rescues all known

dioxygen-sensitive phenotypes of yeast lacking CuZnSOD. *J. Biol. Inorg. Chem.* 10, 913–923. doi: 10.1007/s00775-005-0044-y

Sanes, J. R., and Hall, Z. W. (1979). Antibodies that bind specifically to synaptic sites on muscle fiber basal lamina. *J. Cell Biol.* 83(Pt 1), 357–370. doi: 10.1083/jcb.83.2.357

Sanes, J. R., and Lichtman, J. W. (2001). Induction, assembly, maturation and maintenance of a postsynaptic apparatus. *Nat. Rev. Neurosci.* 2, 791–805. doi: 10.1038/35097557

Sanjak, M., Brinkmann, J., Belden, D. S., Roelke, K., Waclawik, A., Neville, H. E., et al. (2001). Quantitative assessment of motor fatigue in amyotrophic lateral sclerosis. *J. Neurol. Sci.* 191, 55–59.

Sataranatarajan, K., Qaisar, R., Davis, C., Sakellariou, G. K., Vasilaki, A., Zhang, Y., et al. (2015). Neuron specific reduction in CuZnSOD is not sufficient to initiate a full sarcopenia phenotype. *Redox Biol.* 5, 140–148. doi: 10.1016/j.redox.2015.04.005

Saxton, R. A., and Sabatini, D. M. (2017). mTOR Signaling in Growth, Metabolism, and Disease. *Cell* 168, 960–976. doi: 10.1016/j.cell.2017.02.004

Scaffidi, P., and Misteli, T. (2006). Lamin A-dependent nuclear defects in human aging. *Science* 312, 1059–1063. doi: 10.1126/science.1127168

Shefner, J. M., Reaume, A. G., Flood, D. G., Scott, R. W., Kowall, N. W., Ferrante, R. J., et al. (1999). Mice lacking cytosolic copper/zinc superoxide dismutase display a distinctive motor axonopathy. *Neurology* 53, 1239–1246. doi: 10.1212/wnl.53.6.1239

Sheth, K. A., Iyer, C. C., Wier, C. G., Crum, A. E., Bratasz, A., Kolb, S. J., et al. (2018). Muscle strength and size are associated with motor unit connectivity in aged mice. *Neurobiol. Aging* 67, 128–136. doi: 10.1016/j.neurobiolaging.2018.03.016

Shi, Y., Ivannikov, M. V., Walsh, M. E., Liu, Y., Zhang, Y., Jaramillo, C. A., et al. (2014). The lack of CuZnSOD leads to impaired neurotransmitter release, neuromuscular junction destabilization and reduced muscle strength in mice. *PLoS One* 9:e100834. doi: 10.1371/journal.pone.0100834

Shigemoto, K., Kubo, S., Maruyama, N., Hato, N., Yamada, H., Jie, C., et al. (2006). Induction of myasthenia by immunization against muscle-specific kinase. *J. Clin. Invest.* 116, 1016–1024. doi: 10.1172/jci21545

Shigemoto, K., Kubo, S., Mori, S., Yamada, S., Akiyoshi, T., and Miyazaki, T. (2010). Muscle weakness and neuromuscular junctions in aging and disease. *Geriatr. Gerontol. Int.* 10(Suppl. 1), S137–S147. doi: 10.1111/j.1447-0594.2010.00608.x

Slater, C. R. (2015). The functional organization of motor nerve terminals. *Prog. Neurobiol.* 134, 55–103. doi: 10.1016/j.pneurobio.2015.09.004

Slater, C. R. (2017). The structure of human neuromuscular junctions: some unanswered molecular questions. *Int. J. Mol. Sci.* 18:2183. doi: 10.3390/ijms18102183

Slater, C. R., Fawcett, P. R., Walls, T. J., Lyons, P. R., Bailey, S. J., Beeson, D., et al. (2006). Pre- and post-synaptic abnormalities associated with impaired neuromuscular transmission in a group of patients with 'limb-girdle myasthenia'. *Brain* 129(Pt 8), 2061–2076. doi: 10.1093/brain/awl200

Slater, C. R., Lyons, P. R., Walls, T. J., Fawcett, P. R., and Young, C. (1992). Structure and function of neuromuscular junctions in the vastus lateralis of man. A motor point biopsy study of two groups of patients. *Brain* 115(Pt 2), 451–478. doi: 10.1093/brain/115.2.451

Smith, D. O. (1988). Muscle-specific decrease in presynaptic calcium dependence and clearance during neuromuscular transmission in aged rats. *J. Neurophysiol.* 59, 1069–1082. doi: 10.1152/jn.1988.59.4.1069

Snyder-Warwick, A. K., Satoh, A., Santosa, K. B., Imai, S. I., and Jablonka-Shariff, A. (2018). Hypothalamic Sirt1 protects terminal Schwann cells and neuromuscular junctions from age-related morphological changes. *Aging Cell* 17:e12776. doi: 10.1111/acel.12776

Stockinger, J., Maxwell, N., Shapiro, D., deCabo, R., and Valdez, G. (2017). Caloric restriction mimetics slow aging of neuromuscular synapses and muscle fibers. *J. Gerontol. A Biol. Sci. Med. Sci.* 73, 21–28. doi: 10.1093/gerona/glx023

Sudhof, T. C., and Rothman, J. E. (2009). Membrane fusion: grappling with SNARE and SM proteins. *Science* 323, 474–477. doi: 10.1126/science.1161748

Szule, J. A., Harlow, M. L., Jung, J. H., De-Miguel, F. F., Marshall, R. M., and McMahan, U. J. (2012). Regulation of synaptic vesicle docking by different classes of macromolecules in active zone material. *PLoS One* 7:e33333. doi: 10.1371/journal.pone.0033333

Takamori, M., Maruta, T., and Komai, K. (2000). Lambert-Eaton myasthenic syndrome as an autoimmune calcium-channelopathy. *Neurosci. Res.* 36, 183–191. doi: 10.1016/s0168-0102(99)00135-2

Tomlinson, B. E., and Irving, D. (1977). The numbers of limb motor neurons in the human lumbosacral cord throughout life. *J. Neurol. Sci.* 34, 213–219. doi: 10.1016/0022-510x(77)90069-7

Tsuji, S. (2006). Rene Couteaux (1909-1999) and the morphological identification of synapses. *Biol. Cell* 98, 503–509. doi: 10.1042/BC20050036

Tu, P. H., Raju, P., Robinson, K. A., Gurney, M. E., Trojanowski, J. Q., and Lee, V. M. (1996). Transgenic mice carrying a human mutant superoxide dismutase transgene develop neuronal cytoskeletal pathology resembling human amyotrophic lateral sclerosis lesions. *Proc. Natl. Acad. Sci. U.S.A.* 93, 3155–3160. doi: 10.1073/pnas.93.7.3155

Uchitel, O. D., Protti, D. A., Sanchez, V., Cherksey, B. D., Sugimori, M., and Llinas, R. (1992). P-type voltage-dependent calcium channel mediates presynaptic calcium influx and transmitter release in mammalian synapses. *Proc. Natl. Acad. Sci. U.S.A.* 89, 3330–3333. doi: 10.1073/pnas.89.8.3330

Ueta, R., Sugita, S., Minegishi, Y., Shimotoyodome, A., Ota, N., Ogiso, N., et al. (2020). DOK7 gene therapy enhances neuromuscular junction innervation and motor function in aged mice. *iScience* 23:101385. doi: 10.1016/j.isci.2020.101385

Valdez, G., Tapia, J. C., Kang, H., Clemenson, G. D. Jr., Gage, F. H., Lichtman, J. W., et al. (2010). Attenuation of age-related changes in mouse neuromuscular synapses by caloric restriction and exercise. *Proc. Natl. Acad. Sci. U.S.A.* 107, 14863–14868. doi: 10.1073/pnas.1002220107

Valdez, G., Tapia, J. C., Lichtman, J. W., Fox, M. A., and Sanes, J. R. (2012). Shared resistance to aging and ALS in neuromuscular junctions of specific muscles. *PLoS One* 7:e34640. doi: 10.1371/journal.pone.0034640

Valenzuela, D. M., Stitt, T. N., DiStefano, P. S., Rojas, E., Mattsson, K., Compton, D. L., et al. (1995). Receptor tyrosine kinase specific for the skeletal muscle lineage: expression in embryonic muscle, at the neuromuscular junction, and after injury. *Neuron* 15, 573–584. doi: 10.1016/0896-6273(95)90146-9

Vandervoort, A. A. (2002). Aging of the human neuromuscular system. *Muscle Nerve* 25, 17–25. doi: 10.1002/mus.1215

Vincent, A., Lang, B., and Kleopa, K. A. (2006). Autoimmune channelopathies and related neurological disorders. *Neuron* 52, 123–138. doi: 10.1016/j.neuron.2006.09.024

Walrond, J. P., and Reese, T. S. (1985). Structure of axon terminals and active zones at synapses on lizard twitch and tonic muscle fibers. *J. Neurosci.* 5, 1118–1131. doi: 10.1523/jneurosci.05-05-01118.1985

Warner, H. R., and Sierra, F. (2003). Models of accelerated ageing can be informative about the molecular mechanisms of ageing and/or age-related pathology. *Mech. Ageing Dev.* 124, 581–587. doi: 10.1016/s0047-6374(03)00008-3

Webster, R. G. (2018). Animal models of the neuromuscular junction, vitally informative for understanding function and the molecular mechanisms of congenital myasthenic syndromes. *Int. J. Mol. Sci.* 19:1326. doi: 10.3390/ijms19051326

Weeda, G., Donker, I., de Wit, J., Morreau, H., Janssens, R., Vissers, C. J., et al. (1997). Disruption of mouse ERCC1 results in a novel repair syndrome with growth failure, nuclear abnormalities and senescence. *Curr. Biol.* 7, 427–439. doi: 10.1016/s0960-9822(06)00190-4

Weindruch, R., Walford, R. L., Fligiel, S., and Guthrie, D. (1986). The retardation of aging in mice by dietary restriction: longevity, cancer, immunity and lifetime energy intake. *J. Nutr.* 116, 641–654. doi: 10.1093/jn/116.4.641

Westerveld, A., Hoeijmakers, J. H., van Duin, M., de Wit, J., Odijk, H., Pastink, A., et al. (1984). Molecular cloning of a human DNA repair gene. *Nature* 310, 425–429. doi: 10.1038/310425a0

Wijshake, T., Malureanu, L. A., Baker, D. J., Jeganathan, K. B., van de Sluis, B., and van Deursen, J. M. (2012). Reduced life- and healthspan in mice carrying a mono-allelic BubR1 MVA mutation. *PLoS Genet.* 8:e1003138. doi: 10.1371/journal.pgen.1003138

Willadt, S., Nash, M., and Slater, C. (2018). Age-related changes in the structure and function of mammalian neuromuscular junctions. *Ann. N. Y. Acad. Sci.* 1412, 41–53. doi: 10.1111/nyas.13521

Willadt, S., Nash, M., and Slater, C. R. (2016). Age-related fragmentation of the motor endplate is not associated with impaired neuromuscular transmission in the mouse diaphragm. *Sci. Rep.* 6:24849. doi: 10.1038/srep24849

Willig, K. I., Rizzoli, S. O., Westphal, V., Jahn, R., and Hell, S. W. (2006). STED microscopy reveals that synaptotagmin remains clustered after synaptic vesicle exocytosis. *Nature* 440, 935–939. doi: 10.1038/nature04592

Wokke, J. H., Jennekens, F. G., van den Oord, C. J., Veldman, H., Smit, L. M., and Leppink, G. J. (1990). Morphological changes in the human end plate with age. *J. Neurol. Sci.* 95, 291–310. doi: 10.1016/0022-510x(90)90076-y

Wong, M., and Martin, L. J. (2010). Skeletal muscle-restricted expression of human SOD1 causes motor neuron degeneration in transgenic mice. *Hum. Mol. Genet.* 19, 2284–2302. doi: 10.1093/hmg/ddq106

Wood, S. J., and Slater, C. R. (2001). Safety factor at the neuromuscular junction. *Prog. Neurobiol.* 64, 393–429. doi: 10.1016/s0301-0082(00)00055-1

York, A. L., and Zheng, J. Q. (2017). Super-resolution microscopy reveals a nanoscale organization of acetylcholine receptors for trans-synaptic alignment at neuromuscular synapses. *eNeuro* 4. doi: 10.1523/ENEURO.0232-17.2017

Yuan, X., Klein, D., Kerscher, S., West, B. L., Weis, J., Katona, I., et al. (2018). Macrophage depletion ameliorates peripheral neuropathy in aging mice. *J. Neurosci.* 38, 4610–4620. doi: 10.1523/JNEUROSCI.3030-17.2018

Zampieri, S., Mammucari, C., Romanello, V., Barberi, L., Pietrangelo, L., Fusella, A., et al. (2016). Physical exercise in aging human skeletal muscle increases mitochondrial calcium uniporter expression levels and affects mitochondria dynamics. *Physiol. Rep.* 4:e13005. doi: 10.14814/phy2.13005

Zenker, M., Aigner, T., Wendler, O., Tralau, T., Muntefering, H., Fenski, R., et al. (2004). Human laminin beta2 deficiency causes congenital nephrosis with mesangial sclerosis and distinct eye abnormalities. *Hum. Mol. Genet.* 13, 2625–2632. doi: 10.1093/hmg/ddh284

Zhang, B., Tzartos, J. S., Belimezi, M., Ragheb, S., Bealmear, B., Lewis, R. A., et al. (2012). Autoantibodies to lipoprotein-related protein 4 in patients with double-seronegative myasthenia gravis. *Arch. Neurol.* 69, 445–451. doi: 10.1001/archneurol.2011.2393

Zhang, C., Goto, N., Suzuki, M., and Ke, M. (1996). Age-related reductions in number and size of anterior horn cells at C6 level of the human spinal cord. *Okajimas Folia Anat. Jpn.* 73, 171–177. doi: 10.2535/ofaj1936.73.4_171

Zhang, Y., Davis, C., Sakellariou, G. K., Shi, Y., Kayani, A. C., Pulliam, D., et al. (2013). CuZnSOD gene deletion targeted to skeletal muscle leads to loss of contractile force but does not cause muscle atrophy in adult mice. *FASEB J.* 27, 3536–3548. doi: 10.1096/fj.13-228130

Zhao, K., Shen, C., Li, L., Wu, H., Xing, G., Dong, Z., et al. (2018). Sarcoglycan alpha mitigates neuromuscular junction decline in aged mice by stabilizing LRP4. *J. Neurosci.* 38, 8860–8873. doi: 10.1523/JNEUROSCI.0860-18.2018

Zisimopoulou, P., Evangelakou, P., Tzartos, J., Lazaridis, K., Zouvelou, V., Mantegazza, R., et al. (2014). A comprehensive analysis of the epidemiology and clinical characteristics of anti-LRP4 in myasthenia gravis. *J. Autoimmun.* 52, 139–145. doi: 10.1016/j.jaut.2013.12.004

Conflict of Interest: The authors declare that the research was conducted in the absence of any commercial or financial relationships that could be construed as a potential conflict of interest.

Copyright © 2020 Badawi and Nishimune. This is an open-access article distributed under the terms of the Creative Commons Attribution License (CC BY). The use, distribution or reproduction in other forums is permitted, provided the original author(s) and the copyright owner(s) are credited and that the original publication in this journal is cited, in accordance with accepted academic practice. No use, distribution or reproduction is permitted which does not comply with these terms.

frontiers in Molecular Neuroscience

REVIEW
published: 03 December 2020
doi: 10.3389/fnmol.2020.610964

The Neuromuscular Junction in Health and Disease: Molecular Mechanisms Governing Synaptic Formation and Homeostasis

Pedro M. Rodríguez Cruz[1,2], Judith Cossins[1,2], David Beeson[1,2] and Angela Vincent[1,2]*

[1] Nuffield Department of Clinical Neurosciences, University of Oxford, Oxford, United Kingdom, [2] Neurosciences Group, Weatherall Institute of Molecular Medicine, University of Oxford, The John Radcliffe Hospital, Oxford, United Kingdom

The neuromuscular junction (NMJ) is a highly specialized synapse between a motor neuron nerve terminal and its muscle fiber that are responsible for converting electrical impulses generated by the motor neuron into electrical activity in the muscle fibers. On arrival of the motor nerve action potential, calcium enters the presynaptic terminal, which leads to the release of the neurotransmitter acetylcholine (ACh). ACh crosses the synaptic gap and binds to ACh receptors (AChRs) tightly clustered on the surface of the muscle fiber; this leads to the endplate potential which initiates the muscle action potential that results in muscle contraction. This is a simplified version of the events in neuromuscular transmission that take place within milliseconds, and are dependent on a tiny but highly structured NMJ. Much of this review is devoted to describing in more detail the development, maturation, maintenance and regeneration of the NMJ, but first we describe briefly the most important molecules involved and the conditions that affect their numbers and function. Most important clinically worldwide, are myasthenia gravis (MG), the Lambert-Eaton myasthenic syndrome (LEMS) and congenital myasthenic syndromes (CMS), each of which causes specific molecular defects. In addition, we mention the neurotoxins from bacteria, snakes and many other species that interfere with neuromuscular transmission and cause potentially fatal diseases, but have also provided useful probes for investigating neuromuscular transmission. There are also changes in NMJ structure and function in motor neuron disease, spinal muscle atrophy and sarcopenia that are likely to be secondary but might provide treatment targets. The NMJ is one of the best studied and most disease-prone synapses in the nervous system and it is amenable to *in vivo* and *ex vivo* investigation and to systemic therapies that can help restore normal function.

Keywords: neuromuscular junction, myasthenia gravis, congenital myasthenic syndromes, spinal muscular atrophy, sarcopenia, MuSK, DOK7, Agrin

OPEN ACCESS

Edited by:
Laure Strochlic, Institut National de la Santé et de la Recherche Médicale (INSERM), France

Reviewed by:
Nils Erik Gilhus, University of Bergen, Norway
Mohammed Akaaboune, University of Michigan, United States

****Correspondence:***
Pedro M. Rodríguez Cruz
pedro.rodriguezcruz@ndcn.ox.ac.uk

Received: *28 September 2020*
Accepted: *30 October 2020*
Published: *03 December 2020*

Citation:
Rodríguez Cruz PM, Cossins J, Beeson D and Vincent A (2020) The Neuromuscular Junction in Health and Disease: Molecular Mechanisms Governing Synaptic Formation and Homeostasis. Front. Mol. Neurosci. 13:610964. doi: 10.3389/fnmol.2020.610964

INTRODUCTION

The neuromuscular junction (NMJ) is a simple synapse between the motor nerve terminal and the surface of a muscle fiber sarcolemma, but is nevertheless complex in its structure and function. Most of what we know about development of the NMJ comes from work in rodents, particularly mice and evidence from work on human muscle is sparse. During development, nascent skeletal

muscle fibers express AChRs on their surface and the axons of motor neurons are guided to innervate the fibers, leading to the clustering of AChRs at high density underneath the motor nerve terminals. Despite being functionally active in the embryonic stage, NMJs undergo complex postnatal maturation during the first weeks of life that consist of an increase in size, morphological changes and the development of invaginations in the subsynaptic sarcolemma. The apparent macroscopic stability of the NMJ during adulthood hides numerous mechanisms that allow the homeostasis of the neuromuscular synapse in health and disease. This review covers the molecular mechanisms underlying the development and homeostasis of the NMJ and their contribution to health and disease.

THE ORGANIZATION OF THE NMJ

The NMJs are very small structures (∼30 μm long) compared to the length of the muscle fibers they innervate which can be anything from less than a cm (e.g., intercostal muscle) to more than 20 cm (e.g., sartorius, the long muscle of the thigh). Typically, each skeletal muscle fibers has a single NMJ where the motor axon joins the muscle fiber. The most common classification divides the NMJ into a presynaptic terminal, a postsynaptic muscle membrane and the space that lies between called the synaptic cleft. The classic morphology of the NMJ in murine animal models is described as a pretzel-shaped structure (**Figure 1**). The human NMJs are typically smaller, less complex, and more fragmented than those widely studied in murine animal models (Jones et al., 2017), although they exhibit a higher degree of postsynaptic membrane folding than any other species (Slater, 2017).

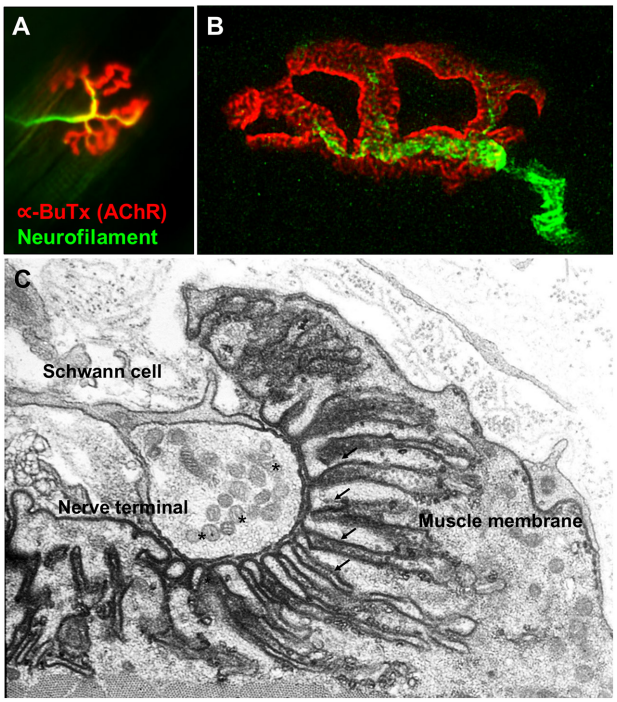

FIGURE 1 | Fluorescence and electron microscopy images of the NMJ. **(A)** Fluorescence microscopy image of the NMJ showing the nerve terminal (green) innervating the muscle endplate (red) stained with fluorescently conjugated α-bungarotoxin that binds to the AChRs. **(B)** Super-resolution confocal microscopy image of the NMJ showing the postsynaptic muscle membrane and the junctional folds at the top of which AChRs are concentrated (image provided by Dr. J. Cheung). **(C)** Electron microscopy image of the NMJ. The presynaptic nerve terminal is filled with synaptic vesicles containing acetylcholine (*). The postsynaptic muscle membrane exhibits a high degree of folding which extends into the muscle sarcoplasm (arrows) in order to increase the total endplate surface. The NMJ is covered by terminal Schwann cells. Used with permission from Slater (2017).

Presynaptic Terminal

Motor nerves travel from the spinal cord to skeletal muscles where they divide into terminal branches and subsequently form synaptic boutons that contact the muscle surface (Desaki and Uehara, 1981). Synaptic boutons are small protuberances found at the terminal end of motor axons. They are filled with synaptic vesicles containing the neurotransmitter ACh ready for vesicle exocytosis. The nerve terminal has complex machinery in place to allow the synthesis, exocytosis and recycling of these synaptic vesicles (Lai et al., 2017). Non-myelinating Schwann cells called perisynaptic or terminal Schwann cells (tSCs) cover the NMJ, and there is increasing evidence that they contribute to synapse formation, maintenance and repair (Feng and Ko, 2008).

Synaptic Cleft

The synaptic cleft is the gap between the presynaptic terminal and the postsynaptic muscle membrane, which is filled with a specialized form of extracellular matrix called synaptic basal lamina (Sanes, 2003). This matrix is crucial for the alignment, organization and structural integrity of the NMJ. The main components of the basal lamina include laminins and different types of collagens (Shi et al., 2012). In particular, it is of relevance that the enzyme acetylcholinesterase (AChE), which terminates synaptic transmission by breaking down acetylcholine, is attached to the basal lamina thanks to ColQ, an NMJ-specific collagen-like tail (Ohno et al., 1998).

Postsynaptic Muscle Membrane

The postsynaptic membrane is a specialized structure with a high degree of folding, as shown by electron microscopy studies (De Harven and Coers, 1959). Motor nerve terminals are embedded in the muscle in a gutter or primary cleft. Furthermore, there are a series of invaginations of the muscle membrane that extend into the sarcoplasm called secondary junctional folds. They increase the overall surface of the postsynaptic membrane, and the AChRs clustered at high density on the crest of these folds, juxtaposed to the presynaptic active zones. At the bottoms of the folds, voltage-gated Na+ channels are concentrated to facilitate the excitability of the postsynaptic membrane.

NEUROMUSCULAR TRANSMISSION

The enzyme choline acetyltransferase (ChAT) synthesizes acetylcholine (ACh) from acetyl coenzyme A (AcCoA) and

choline (Nachmansohn and Machado, 1943). Subsequently, acetylcholine is packed into synaptic vesicles thanks to the vesicular acetylcholine transporter (VAChT) (Roghani et al., 1994). Pools of synaptic vesicles accumulate in the presynaptic terminal near release sites termed active zones (Sudhof, 2012). Upon arrival of an action potential, voltage-gated calcium channels (VGCCs) open and Ca^{2+} inflow triggers vesicle fusion to the plasma membrane and exocytosis through the Soluble N-ethylmaleimide-sensitive factor Attachment protein Receptor (SNARE) complex (Baker and Hughson, 2016). ACh released by the presynaptic terminal binds to the ACh binding site located at the α and either δ or ε-subunits interfaces of the AChR. Upon ACh binding, the AChR subunits undergo a conformational change to open the channel creating a pore (Miyazawa et al., 2003). This event allows the influx of positively charged ions to move across the channel generating a change in the membrane potential that triggers an endplate potential (EPP). In a healthy individual, the depolarization of the postsynaptic membrane generated by the EPP is greater than the threshold needed to activate the $Na_v1.4$ voltage-gated sodium channels and generate an action potential. The action potential spreads from the motor endplate to the rest of the sarcolemma, resulting in contraction of the muscle (Engel et al., 2015).

Importantly the NMJ is an all-or-none synapse. If the endplate potential does not reach the threshold for opening of sodium channels, or if there are insufficient sodium channels in the postsynaptic folds to generate an action potential, muscle contraction does not occur. In health, the EPP is more than sufficient to reach threshold, and the sodium channels are concentrated at the depths of the postsynaptic folds where they can be efficiently opened by the voltage change. This is the *margin of safety, or safety factor of neuromuscular transmission*, which allows the NMJ to continue to function under various physiological conditions and stresses. In disease, this margin of safety can be reduced at individual endplates, or many of them, leading to reduced neuromuscular transmission and muscle weakness (Wood and Slater, 2001). These concepts are crucial in understanding the diseases that cause muscle weakness (**Table 1**). Much of what is summarized below is covered in detail by other authors in this Special Issue (Cao et al., 2020; Takamori, 2020).

DISORDERS OF THE NMJ

Venoms and Neurotoxins

Much of what we first learnt regarding the molecules at NMJ that are essential for its function, and also targets in disease came from the study of specific neurotoxins, particularly those from snake venoms on transmission at the NMJ (Vincent, 2020). Envenomation by snake bite is a very important disease globally and leads to a variety of symptoms of which, since the NMJ is accessible to the systemic circulation, defects in transmission are often early with respiratory failure (Warrell, 2010, 2019).

Botulism is an important presynaptic disorder, which is caused by a toxin produced by the anaerobic bacterium, *Clostridium botulinum*. The botulinum toxin (Botox) is a proteolytic enzyme that gets transported into the motor nerve and other nerve terminals, cleaves SNARE proteins, preventing vesicle fusion and ACh release (Schiavo et al., 2000). Tetanus toxin produced by *Clostridium tetani* is also taken up by presynaptic motor nerve terminals but travels retrogradely, via the motor neuron cell body, to the inhibitor nerve terminals of the spinal cord where it prevents the release of GABA and glycine leading to painful muscle spasms. Each of these conditions can be life-threatening due to muscle paralysis or, in the case of tetanus toxin, uncontrolled muscle contractions.

Myasthenia Gravis

Autoantibodies against the muscle acetylcholine nicotinic receptor (AChR) cause myasthenia gravis (MG), the most common disorder of neuromuscular transmission, which is characterized by fatigable muscle weakness (Lindstrom et al., 1976; Vincent and Newsom-Davis, 1985). The AChR antibodies are predominantly IgG1 and IgG3 subclasses and lead to loss of AChRs by two main mechanisms; mainly complement activation, cross-linking and internalization of AChRs (Le Panse and Berrih-Aknin, 2013). Classic treatment is with immunosuppressive drugs and cholinesterase inhibitors to prevent the breakdown of ACh by AChE; this leads to longer duration of ACh in the synapse leading to larger and slightly prolonged EPPs.

Interestingly, there are patients in rare occasions with autoantibodies against the fetal γ-subunit of the AChR, which is present prenatally but largely replaced by the ε-subunit before birth at approximately 33 weeks (AChR γ-to-ε switch) (Missias et al., 1996). As a result, these antibodies have little effect in adults but they can cause neonatal myasthenia (Vernet-Der Garabedian et al., 1994) or arthrogryposis multiplex congenita (Oskoui et al., 2008) via maternal transfer to the fetus.

Around 10–20% of MG patients are seronegative for AChR antibodies but a variable proportion (0–70%) have antibodies to the Muscle-Specific Kinase (MuSK) (Hoch et al., 2001). MuSK autoantibodies are predominantly of the IgG4 subtype and impair agrin signaling by disrupting the interaction of MuSK with the low density lipoprotein receptor-related protein-4 (LRP4) (Koneczny et al., 2013). MuSK-MG has distinct clinical features and response to treatment, including the worsening of symptoms with anticholinesterase therapy (Evoli et al., 2003). The clinical features of this form of MG and the mechanisms by which the antibodies act can be found in *Cao et al.*, this volume (Cao et al., 2020). MG patients seronegative for MuSK and AChR antibodies by radioimmunoprecipitation assay (RIA) may have antibodies to clustered AChRs by cell-based assay (CBA) (Leite et al., 2008). These antibodies have similar pathogenic mechanisms to AChR antibodies detected by RIA (Jacob et al., 2012). They can be useful in clinical practice, especially in children, for planning treatment and to distinguish from congenital myasthenic syndromes (CMS) (Rodríguez Cruz et al., 2015). LRP4 antibodies have also been reported in seronegative MG (Zhang et al., 2012), but the detection rates are highly variable between studies, and some cases are also positive for AChR and MuSK antibodies (Higuchi et al., 2011). A further uncertainty comes from studies showing LRP4 antibodies in some patients with amyotrophic lateral sclerosis (Tzartos et al., 2014). Finally, autoantibodies to other immunogenic targets such

TABLE 1 | Disorders of neuromuscular transmission.

Venoms and Neurotoxins		
Snake bite		
Botulism		
Tetanus		
Myasthenia gravis		
AChR antibodies		
MuSK antibodies		
Antibodies to clustered AChRs		
LRP4 antibodies		
Lambert-Eaton Myasthenic Syndrome		
VGCC antibodies		
CMS subtype	**Gene**	**Inheritance**
Proteins with defined NMJ function		
Presynaptic		
Choline O-Acetyltransferase	*CHAT*	AR
Unconventional myosin 9	*MYO9*	AR
PREPL	*PREPL*	AR
Vesicular ACh transporter (VAChT)	*SLC18A3*	AR
High-affinity choline transporter 1 (ChT)	*SLC5A7*	AR
Synaptosome Associated Protein 25	*SNAP25B*	AD
Synaptotagmin 2	*SYT2*	AD
Munc13-1	*UNC13-1*	AR
Rabphilin 3A	*RPH3A*	AR
Synaptobrevin 1	*VAMP1*	AR
Synaptic		
Collagen Type XIII Alpha 1 Chain	*COL13A1*	AR
Endplate AChE deficiency	*COLQ*	AR
Laminin α5 deficiency	*LAMA5*	AR
Laminin ß2 deficiency	*LAMB2*	AR
Postsynaptic		
Agrin (neuronal)	*AGRN*	AR
Primary AChR deficiency	*CHRNA, CHRNB, CHRND, CHRNE*	AR
Slow channel syndrome	*CHRNA, CHRNB, CHRND, CHRNE*	AD
Fast channel syndrome	*CHRNA, CHRNB, CHRND, CHRNE*	AR
Low conductance syndrome	*CHRNE*	AR
Escobar syndrome	*CHRNG*	AR
DOK7	*DOK7*	AR
LRP4	*LRP4*	AR
MACF1	*MACF1*	AR
MuSK	*MUSK*	AR
Plectin deficiency	*PLEC1*	AR
Rapsyn	*RAPSN*	AR
Na^+ channel myasthenia	*SCN4A*	AR
Ubiquitously expressed proteins		
ALG2	*ALG2*	AR
ALG14	*ALG14*	AR
DPAGT1	*DPAGT1*	AR
GFPT1	*GFPT1*	AR
GMPPB	*GMPPB*	AR
SLC25A1	*SLC25A1*	AR

ALG2, Alpha-1,3/1,6-Mannosyltransferase; ALG14, UDP-N Acetylglucosaminyltransferase Subunit; DOK7, Docking protein 7; DPAGT1, Dolichyl-Phosphate N-Acetylglucosaminephosphotransferase 1; GFPT1, Glutamine-Fructose-6-Phosphate Transaminase 1; GMPPB, GDP-Mannose Pyrophosphorylase B; LRP4, LDL Receptor Related Protein 4; MACF1, microtubule actin cross linking factor 1; MuSK, Muscle specific kinase; PREPL, Prolyl Endopeptidase-Like gene.

as agrin (Gasperi et al., 2014), COLQ (Zoltowska Katarzyna et al., 2014) and cortactin (Gallardo et al., 2014) have been described. However, their pathogenic contribution and overall importance in clinical diagnosis require further study.

Lambert-Eaton Myasthenic Syndrome (LEMS)

This disease is rarer than MG and is caused by autoantibodies against P/Q type VGCCs on the presynaptic terminal at the NMJ (Eaton and Lambert, 1957; Lennon et al., 1995). Half of LEMS patients have an associated tumor, typically small-cell lung carcinoma (SCLC), which also expresses functional VGCC. The pathogenic mechanism is from cross-linking and internalization of the VGCCs by antibodies leading to reduced expression on the presynaptic nerve terminal (Nagel et al., 1988). This results in the functional loss of VGCC in active zones, reduced Ca^{2+} entry during depolarization and a subsequent decrease in quantal content and ACh release. Complement-dependent mechanisms don't appear to be relevant, though it is not clear why not.

CMS

Congenital myasthenic syndromes are a group of inherited disorders caused by mutations in genes encoding for proteins that are essential for the integrity of neuromuscular transmission (Rodríguez Cruz et al., 2018). Over the years, deciphering the underlying pathogenic mechanism of CMS has helped to improve our understanding of the NMJ and refine therapeutic strategies with other drugs like 3,4-Diaminopyridine, β2−adrenergic agonists, and open-channel blockers fluoxetine and quinidine (Harper et al., 2003; Lashley et al., 2010). At present, mutations in more than 30 different genes are known to cause CMS. Most common classification is based on the location of the mutated protein (presynaptic, synaptic and postsynaptic). All CMSs present with fatigable muscle weakness, but age at onset, symptoms, distribution of weakness, and response to treatment vary, depending on the molecular mechanism resulting from the genetic defect. Future therapies may include the use of novel and more specific β2−adrenergic agonists, modulation of the Agrin-LRP4-MusK-DOK7 pathway and gene replacement therapy (Arimura et al., 2014).

Other Neuromuscular Disorders Where the NMJ Is Involved

There is increasing evidence that muscle endplates may also be affected in motor unit disorders that are not believed to primarily affect the NMJ, including spinal muscular atrophy (SMA) and amyotrophic lateral sclerosis (ALS). SMA is an autosomal recessive disease caused by insufficient levels of survival motor neuron (SMN) protein that results in progressive loss of lower motor neurons, denervation and muscle atrophy (Ahmad et al., 2016). Studies in animal models of SMA have shown that earliest structural defects appear distally at the NMJ during postnatal maturation, even in the absence neuromuscular transmission failure or motor neuron loss (Kariya et al., 2008; Lee et al., 2011). Furthermore, patients with types 2 and 3 SMA suffer from objective motor fatigue (Wolfe et al., 2016) and 3Hz repetitive nerve stimulation shows pathological decrement in half of them (Wadman et al., 2012). Open pilot studies have reported the benefit of salbutamol in SMA patients (Pane et al., 2008). It is thought that salbutamol increases *SMN* mRNA and protein levels in SMA fibroblasts (Angelozzi et al., 2008) and patients (Tiziano et al., 2019) by promoting exon 7 inclusion in *SMN2* transcripts. However, given the remarkable effect of β2−adrenergic agonists in CMS (Lashley et al., 2010; Rodríguez Cruz et al., 2015), the effect seen in SMA patients could be at least partly related to an improvement in the NMJ function and structure.

There are several studies suggesting that ALS is a distal axonopathy where pathological changes start preclinically with denervation of the muscle endplates and then proceed in a "dying back" pattern that results in motor neuron loss (Fischer et al., 2004; Gould, 2006). While evidence supporting this hypothesis comes mainly from *SOD1*-ALS mouse models, a recent investigation suggests a direct link between NMJ signaling pathways and *FUS* (Picchiarelli et al., 2019), an ALS-associated gene whose dominant mutations cause aggressive forms of the disease. Recent studies have shown that modulation of agrin signaling by AAV-DOK7 gene therapy (Miyoshi et al., 2017) and MuSK stimulation (Cantor et al., 2018) can increase motor activity and lifespan of the *SOD1-G93A* ALS mouse model by slowing muscle denervation. Other disorders where NMJ structural defects could play a role comprise autosomal dominant Emery-Dreifuss muscular dystrophy (AD-EDMD) (Méjat et al., 2009) and some forms of Charcot-Marie-Tooth disease (CMT) (Sleigh et al., 2014). Finally there are some congenital myopathies with secondary neuromuscular transmission abnormalities (Rodríguez Cruz et al., 2014) where achieving a precise diagnosis is important as patients could benefit from symptomatic treatment with anticholinesterases.

Ageing and Sarcopenia

The progressive decline in muscle mass and function related to ageing is known as sarcopenia. The mouse NMJ undergo dramatic structural changes with ageing in the form of increased fragmentation of endplates (Valdez et al., 2010). It is thought that this could be secondary to degeneration and regeneration of muscle fibers at the neuromuscular synapse (Li et al., 2011). Interestingly, overexpression of neurotrypsin in motoneurons destabilizes NMJs by increasing the proteolytic cleavage of agrin (Bolliger et al., 2010) and installs a phenotype compatible with sarcopenia in young adult mice (Bütikofer et al., 2011). Stabilization of the NMJs could represent a potential therapy for sarcopenia as shown by the injection of a soluble fragment of neuronal agrin (NT- 1654) in neurotrypsin overexpressing mice (Hettwer et al., 2014). Another study showed that sarcoglycan alpha reduces NMJ decline in aged mice by stabilizing LRP4 (Zhao et al., 2018). Remarkably, caloric restriction and exercise was shown to mitigate age-related changes in mouse NMJs, which opens the door to non-pharmacological interventions (Valdez et al., 2010). These observations have linked sarcopenia with the deterioration of the NMJ structure. However, a recent study showed that human NMJs, in contrast to mice, are remarkably stable throughout adult life with lack of age-related remodeling signs in the muscles tested (Jones et al., 2017). Therefore,

there may be significant variability in age-related events among muscles. Furthermore, a key question that remains unanswered is whether the age-related NMJ decline contributes to or results from sarcopenia.

MOLECULAR MECHANISMS INVOLVED IN SYNAPSE FORMATION AND MAINTENANCE

Multiple mechanisms govern the assembly and homeostasis of the neuromuscular synapse as described earlier. This section will cover in greater detail the best-defined pathways and the clinical impact when perturbed. First, it is worth visualizing the NMJ in relation to the muscles that it regulates to understand that this tiny synapse has to function correctly to control the timing and efficiency of that muscle (**Figure 1**).

The Agrin-LRP4-MuSK Signaling Pathway

The agrin signaling pathway is essential for both NMJ formation (DeChiara et al., 1996; Gautam et al., 1996; Okada et al., 2006; Weatherbee et al., 2006) and maintenance (Kong et al., 2004; Barik et al., 2014; Tezuka et al., 2014; Eguchi et al., 2016; **Figure 2**). Several genetic and autoimmune disorders affecting this pathway are known to cause disease (Liyanage et al., 2002). Agrin is a large proteoglycan (>200 KDa) with multiple domains that binds to laminins through the N-terminal domain, and to LRP4 and α-dystroglycan via its C-terminus (**Figure 3A**). A neuronal isoform of agrin, generated by alternative splicing to introduce eight additional amino acids at the Z site, is secreted from the presynaptic terminal into the basal lamina as the first step in the AChR clustering pathway (Ferns et al., 1993). Following its release, agrin binds to LRP4 on the postsynaptic muscle membrane, and this, in turn, activates MuSK (Zhang et al., 2008). LRP4 is able to self-associate and interact with MuSK independently of agrin (inactive state) but is not capable of activating MuSK (Kim et al., 2008).

MuSK is made up of three IgG-like domains, a frizzled domain (FzD), a short transmembrane (TM) and a juxtamembrane (JMR) region, a kinase domain (KD), and a short C-terminal tail (Hubbard and Gnanasambandan, 2013; **Figure 3B**). MuSK kinase activity is strictly regulated to limit ligand-independent activation primarily through the juxtamembrane region and the activation loop (Till et al., 2002). The interaction between the juxtamembrane region and the kinase core inhibits kinase activity. The activation loop adopts a pseudo-substrate conformation that occupies the active site cleft of the kinase domain and impedes ATP binding thus blocking kinase activation (Till et al., 2002). Also, MuSK activation is regulated by the muscle tyrosine phosphatase Shp2 (Madhavan et al., 2005). All of these regulatory mechanisms seem critical for the control of postsynaptic differentiation at the NMJ (Madhavan and Peng, 2005), but they are by no means the only molecules involved, and more could be identified in the future.

The formation of a tetrameric complex between agrin and LRP4 increases the binding of LRP4 to the first IgG-like domain of MuSK (Zong et al., 2012), leading to MuSK activation via dimerization and trans-autophosphorylation of specific tyrosine residues within the cytoplasmic region (Schlessinger, 2000). Phosphorylation of Tyr553 destabilizes the juxtamembrane conformation that prevents the phosphorylation of the activation loop and the creation of an active binding site for downstream of kinase-7 (DOK7), a cytoplasmic adaptor of MuSK with a phosphotyrosine binding domain (PTB). The subsequent transphosphorylation (Tyr750, Tyr754, and Tyr755) of the activation loop results in full kinase activation.

Intracellular Pathways Downstream of MuSK

The agrin-LRP4-MuSK signal is propagated downstream leading to the clustering of AChRs by the scaffold protein rapsyn. However, how the signal is transduced from MuSK to rapsyn is not understood, with the exception of the key adapter protein DOK7, which is required for full MuSK activation (Inoue et al., 2009). DOK7 is composed of an N-terminal pleckstrin homology (PH) domain, a phosphotyrosine-binding (PTB) domain and a C-terminal domain (Cossins et al., 2012; **Figure 3C**). Mutations in *DOK7* underlie a NMJ synaptopathy and comprise a major form of CMS (Beeson et al., 2006).

Structural studies have shown that the PH/PTB domains also mediate DOK7 dimerization, which is necessary to activate MuSK *in vivo* (Bergamin et al., 2010). Interestingly, over-expression of DOK7 in cultured myotubes in the absence of agrin results in full MuSK activation and clustering of AChRs (Inoue et al., 2009), which suggests that DOK7 regulates synapse formation and maintenance by controlling MuSK activity. The C-terminal region of DOK7 has two tyrosine residues, Y396 and Y406, which are phosphorylated by agrin stimulation (Hallock et al., 2010). These residues and their surrounding sequences form Src homology2 (SH2) target motifs that recruit adaptor proteins Crk and Crk-L via their SH2 domains. More recently, adaptor proteins Sorbs1 and -2 have been found to interact with Crk-L and be necessary for AChR cluster formation (Hallock et al., 2016). *In vitro* phosphorylation assays and murine studies have shown that DOK7 C-terminal domain plays a key, but not essential, role in MuSK activation and NMJ development (Ueta et al., 2017). Similarly, patients with DOK7-CMS homozygous for c.1124_1127dupTGCC, which results in a truncated form of DOK7 lacking the SH2 target motifs, have impaired yet active NMJs. However, the selective inactivation of Crk and Crk-L in skeletal muscle causes severe NMJ defects in mice, which suggests that DOK7 could act by two distinct pathways mediated by the N-terminal and C-terminal domains, respectively (Hallock et al., 2010).

Additional players identified in myotubes include Dishevelled-1 (Dvl1) and Tid1, two non-catalytic adapter proteins binding MuSK and contributing in a poorly understood way to AChR clustering. Dvl1 was found to interact with MuSK and regulate AChR clustering through its interaction with downstream kinase PAK1 (Luo et al., 2002) suggesting that agrin

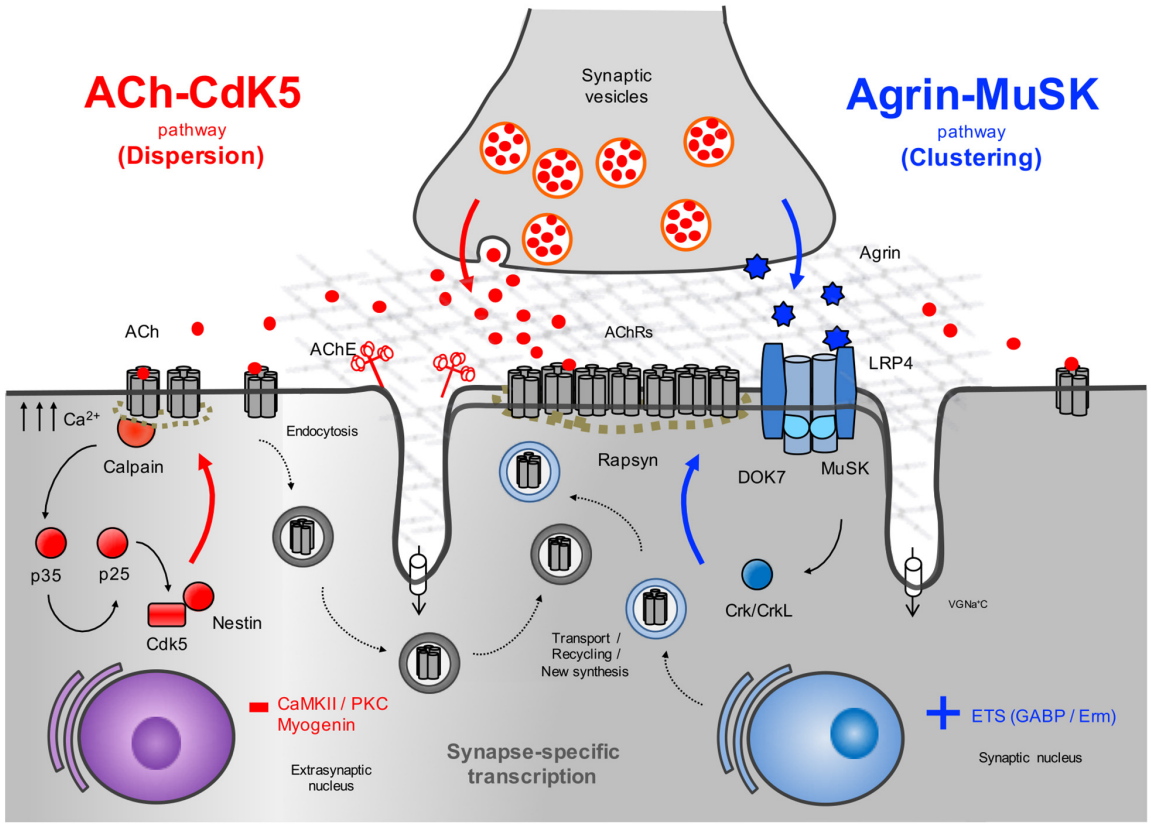

FIGURE 2 | Schematic representation of the AChR clustering and dispersal pathways. Upon the release of agrin by the nerve terminal, agrin binds to LRP4 resulting in MuSK activation (Kim et al., 2008) and recruitment of DOK7 and Crk/CrkL (Okada et al., 2006) that further stimulates MuSK activation. The signal is propagated downstream, which results in the clustering of the AChRs by the cytoplasmic anchoring protein rapsyn. By contrast, ACh disperses AChR clusters not stabilized by agrin signaling. A cyclin-dependent kinase (CdK5) mechanism is thought to drive this pathway through the interaction of rapsyn and the calcium-dependent protease calpain (Chen et al., 2007). Calpain activity promotes the cleavage of p35 to p25 (Patrick et al., 1999), an activator of CdK5. On the other hand, rapsyn behaves as a calpain suppressor, thus stabilizing AChR clusters. It is thought that on synaptogenic induction, new synthesized AChRs may be transported and delivered to the nascent postsynaptic sites for insertion, together with AChRs endocytosed from the spontaneous AChR clusters. Synapse specific transcription in subsynaptic nuclei by different transcription factors and specific promoter elements in synaptic genes such as GABP (Schaeffer et al., 1998) and Erm (Hippenmeyer et al., 2007) is also key to achieve a high concentration of AChRs in synaptic sites. VGNa+C, volgated-gated Na+ channel.

may share the signaling pathways of Wnt, which are critical for diverse developmental processes (Komiya and Habas, 2008). However, Dvl1-deficient mice did not show apparent NMJ abnormalities (Lijam et al., 1997) although this could be due to functional redundancy among different Dvl genes. Rac and Rho are monomeric G proteins that link extracellular signals to dynamic changes in the organization of the actin cytoskeleton (Hall, 1998). Rac and Rho play a role in the coupling of agrin signaling to AChR clustering, and in addition, co-expression of constitutively active forms of Rac and Rho can induce the formation of mature AChR clusters when agrin is not present (Weston et al., 2003).

Rapsyn and Other AchR-Related Proteins

RAPSN encodes the 43 kDa receptor-associated scaffold protein of the synapse or rapsyn, which is essential for the postsynaptic specialization of the NMJ (Gautam et al., 1995). Rapsyn is enriched at the postsynaptic membrane, acting as a linker between the AChRs and the cytoskeleton via the dystrophin-associated glycoprotein complex (Apel et al., 1995; Moransard et al., 2003). Early cross-linking studies showed that rapsyn is located in close proximity to the AChR-β subunit (Burden et al., 1983). Subsequently, other AChR subunits have been found to interact with rapsyn in heterologous cell systems (Lee et al., 2010). However, the lack of a crystallographic structure means that the detailed composition of the AChRs-rapsyn network is not well understood (Zuber and Unwin, 2013). Rapsyn is composed of an N-terminal myristoylation moiety (N-Myr) necessary for submembrane localization; seven tetratricopeptide (TRP) domains responsible for rapsyn self-association (Ramarao et al., 2001; Lee et al., 2008); a coiled-coil domain that binds to the cytoplasmic loops of AChRs (Lee et al., 2008), and a RING-H2 domain that links rapsyn to the cytoskeleton through its interaction with the dystroglycan complex (**Figure 3D**; Apel et al., 1995). *RAPSN* mutations identified in humans are found along the length of the gene and the common p.N88K is located within the TRP domains (Cossins et al., 2006).

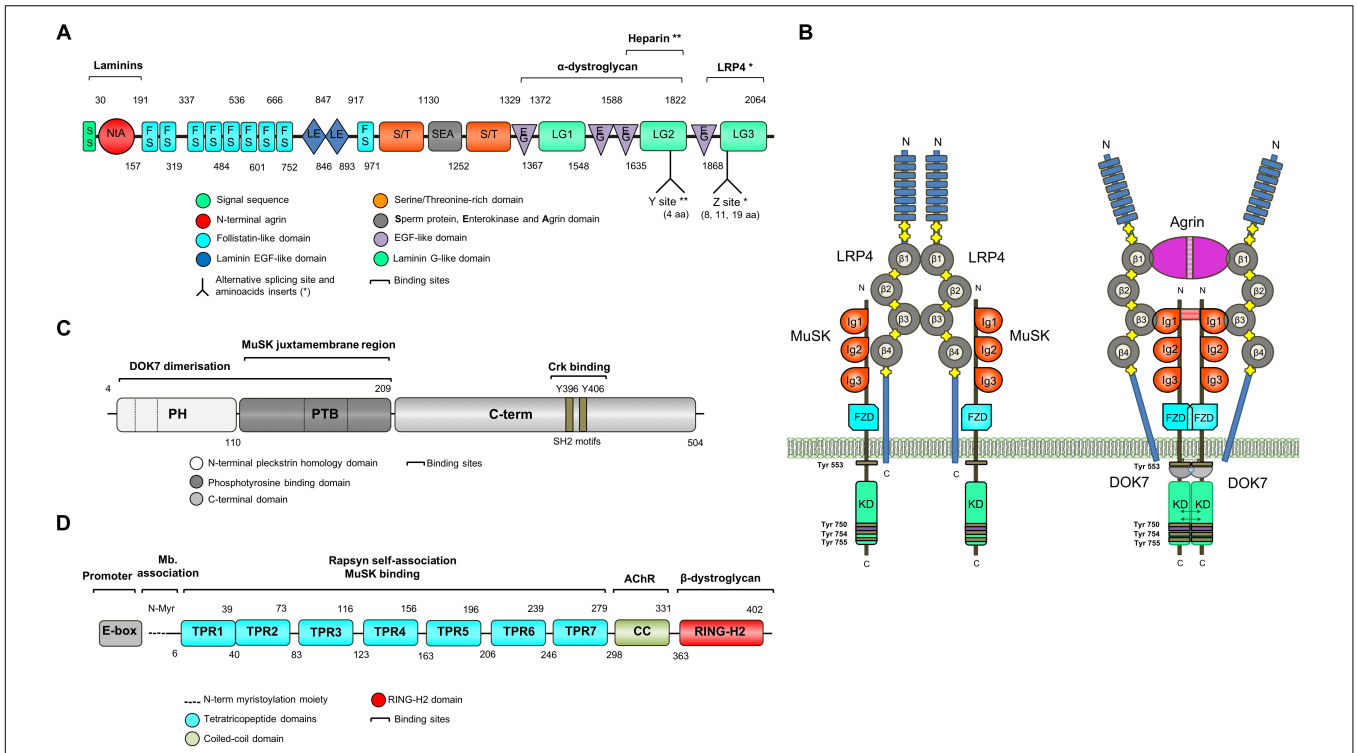

FIGURE 3 | Schematic representation of key NMJ proteins. **(A)** Agrin (RefSeq NP_001292204.1) is a large proteoglycan (>200 KDa) with multiple domains that binds to laminins through the N-terminal domain, and to LRP4 and α-dystroglycan via C-terminus. Two of the three laminin G-like domains are required for binding to α-dystroglycan. Agrin mRNA undergoes cell-specific alternative splicing at different sites (Ferns et al., 1993). When agrin is produced by motor neurons, the Z site contain amino acid inserts specifically required for MuSK activation. **(B)** The binding of agrin to the N-terminal region of LRP4 induces a conformational change (active state) promoting the binding between LRP4 and the first IgG-like domain of MuSK and the formation of a tetrameric complex (Zhang et al., 2011). This results in MuSK activation via dimerization and trans-autophosphorylation of tyrosine residues within the cytoplasmic region (Schlessinger, 2000). The increase in the catalytic activity creates active binding sites for other proteins such as DOK7, leading to in full kinase activation and amplification of the signal downstream. The composition of LRP4 includes 8 Low density lipoprotein Class A (LDLa) domains (blue) at the N terminus, followed by 4 YWTD ß-propeller domains (gray) bounded by epidermal growth factor-like modules (yellow) and a short C-terminal domain (Springer, 1998). LRP4 self-associates and interacts with MuSK in the absence of agrin (inactive state), but is not capable of activating MuSK (Kim et al., 2008). **(C)** DOK7 (RefSeq NM_173660.4) is composed of an N-terminal pleckstrin homology (PH) domain, a phosphotyrosine-binding (PTB) domain and a C-terminus. Dashes are used to mark the different exons. **(D)** Rapsyn (RefSeq NP_005046.2) is composed of a N-terminal myristoylation moiety (N-Myr) necessary for submembrane localization; seven tetratricopeptide (TRP) domains responsible for rapsyn self-association and MuSK binding (Ramarao et al., 2001; Lee et al., 2008); a coiled-coil domain that binds to the cytoplasmic loops of AChRs (Lee et al., 2008), and a RING-H2 domain that interacts with the dystroglycan complex and links with the cytoskeleton (Apel et al., 1995).

Studies in the past have shown that the phosphorylation of the AChR-β subunit mediated by agrin helps to cluster AChRs and anchor them at high density in the postsynaptic membrane, by increasing the stoichiometry of rapsyn/AChR complexes (Borges and Ferns, 2001; Borges et al., 2008). In line with this, mice lacking AChR β-subunit tyrosine phosphorylation develop simplified synapses, although NMJ formation is not compromised (Friese et al., 2007). A recent investigation proposed that the RING-H2 domain of rapsyn contains E3 ligase activity (Li et al., 2016). Another AChR-binding protein recently identified is Vezatin, which is not essential for NMJ formation but may play a role in the formation of postjunctional folds (Koppel et al., 2019).

A dense network of microtubules (MTs) and actin filaments (Dai et al., 2000; Schmidt et al., 2012) interact with the subsynaptic muscle membrane. However, the downstream signals that capture and stabilize microtubules at synaptic AChR clusters are poorly understood. Microtubule actin cross-linking factor 1 (MACF1) has been recently shown to concentrate at the NMJ, where it binds to rapsyn and could serve as an organizer for both actin and microtubule networks (Oury et al., 2019). The study showed that expression at the postsynaptic membrane of microtubule-associated proteins MAP1b, β-TUB, EB1, and Vinculin is MACF1-dependent. MACF1 is not essential for the NMJ formation but postnatal maturation is impaired in *Macf1* mutant mice. Furthermore, two patients from different kinships with CMS have been identified to carry missense variants in *MACF1* (Oury et al., 2019). A second pathway for agrin-induced recruitment of MTs to the postsynaptic membrane is via binding of MTs to CLASP2/CLIP170 (Schmidt et al., 2012).

ACh-CDK5-Calpain Dispersal Pathway

Muscle depolarization induced by ACh is a negative signal that decreases extrasynaptic AChR concentration by altering the location and stability of AChRs and also by inhibiting their transcription along the muscle fiber (An et al., 2010). This is supported by the findings of increased endplate bandwidth and excessive nerve branching in mice lacking choline

acetyltransferase (ChAT), an enzyme required for ACh synthesis (Misgeld et al., 2002). Thus, ACh disperses aneural clusters of AChRs that are not stabilized by agrin signaling. A cyclin-dependent kinase 5 (Cdk5) mechanism (Lin et al., 2005) is thought to drive this pathway through to the interaction of rapsyn and the calcium-dependent protease calpain (Chen et al., 2007; **Figure 2**). Cdk5 null mice display an abnormally wide central band of AChRs and agrin-induced AChR clustering is markedly increased when Cdk5 activity is suppressed (Fu et al., 2005). The binding of ACh to the AChRs results in increased calcium influx into the postsynaptic membrane that activates calpain activity. Calpain stimulates the cleavage of p35 to p25, a potent co-activator of Cdk5 (Patrick et al., 1999). The ACh-mediated increase in calpain/Cdk5 activity permits cytoskeletal remodeling resulting in the dispersal of AChR clusters (Xie et al., 2006). One study has implicated the intermediate filament protein Nestin in the regulation of Cdk5 activity (Yang et al., 2011). By contrast, agrin is thought to stabilize AChR clusters by promoting the recruitment of calpain to rapsyn and inhibiting calpain activity (Chen et al., 2007). In keeping with the key role of calcium in the dispersion of AChRs, another study showed that blocking dihydropyridine receptors (voltage-gated L-type Ca^{2+} channels) at the muscle membrane resulted in increased MuSK expression, leading to a broad distribution of AChRs and aberrant development of the neuromuscular synapse (Chen et al., 2011). Finally, the suppression of AChR transcription in extrasynaptic regions driven by ACh is thought to be mediated by protein kinase C (PKC) and Ca2+/calmodulin-dependent kinase II (CaMKII) signals resulting in myogenin downregulation (Li et al., 1992; Macpherson et al., 2002). As a helix-loop myogenic transcription factor, myogenin regulates expression of AChRs and other muscle genes by binding the E-boxes located in their promoter and enhancer regions (Eftimie et al., 1991).

The N-Linked Glycosylation Pathway

The *N*-linked glycosylation pathway of proteins is a ubiquitous process in eukaryote cells characterized by the sequential attachment of sugar moieties to the lipid dolichol, which is then transferred onto an asparagine residue in a nascent protein (**Figure 4**). Next-generation sequencing has aided the discovery of an unexpected relationship between myasthenic disorders and defects in the early stages of the *N*-glycosylation pathway (Senderek et al., 2011; Belaya et al., 2012; Belaya, 2015). This highlights that genes with no defined role in neuromuscular transmission can also impair the NMJ structure and function. However, the reasons why defects in a ubiquitous process may result in dysfunction largely restricted to the NMJ are not clear. Glycosylation of AChR subunits is required for the correct assembly of AChR pentamers and efficient export to the cell surface (Gehle et al., 1997). Therefore, abnormal glycosylation results in reduced numbers of AChRs at the muscle endplates, which is most likely the primary mechanism causing impaired neuromuscular transmission (Zoltowska et al., 2013). Other key proteins in NMJ formation and maintenance are also glycosylated, including agrin, dystroglycan, LRP4, MuSK, NCAM and perlecan (Martin et al., 1999). Ultrastructural studies in patients with CMS due to glycosylation defects have shown small sized endplates with simplified postsynaptic regions and poorly developed junctional folds (Belaya et al., 2012; Selcen et al., 2013). In conclusion, while the role of these proteins in the NMJ formation and maintenance is well established, the specific function of adequate glycosylation of NMJ constituents awaits further investigation.

EXTRACELLULAR ORGANIZERS

The synaptic basal lamina is a specialized form of extracellular matrix containing numerous proteins that are essential for the alignment, organization and maintenance of presynaptic and postsynaptic structures (Sanes, 2003). One of the main components are heterotrimeric proteins of high molecular weight called laminins, which are formed by the incorporation of α, β and γ chains into a cruciform structure and typically self-assemble (Mouw et al., 2014). Of relevance, it was found that soluble laminin can stimulate AChR clustering via dystroglycan independently of MuSK in cultured myotubes (Sugiyama et al., 1997; Montanaro et al., 1998). Furthermore, myotubes cultured on laminin-coated plates (in the absence of agrin) form complex branched AChR clusters similar to those seen *in vivo* following postnatal maturation. Conversely, this process is dependent on MuSK activation (Kummer et al., 2004). Synaptic laminins are also important for presynaptic differentiation as shown in mice lacking laminin β2 (Noakes et al., 1995). Furthermore, laminin α4 has been implicated in the maintenance of the NMJ (Samuel et al., 2012). Overall these studies support the role of laminin as extracellular organizers of the NMJ. Collagen IV is the most abundant protein at the basal lamina. It self-assembles into dimers and hexamers thanks to its globular domains (Mouw et al., 2014). Laminin and collagen networks are connected by Nidogen-2 (Fox et al., 2008; Mokkapati et al., 2008), a non-collagenous glycoprotein, but also anchored to the cytoskeleton by binding to laminin receptors integrin and dystroglycan (Martin et al., 1996). The dystroglycan complex is necessary for the organization and stabilization of the NMJ as shown by the presence of disrupted NMJs in chimeric mice lacking dystroglycan (Côté et al., 1999). Myotubes deficient in dystroglycan are responsive to agrin, but AChR clusters are significantly less stable (Jacobson et al., 2001). By contrast, laminin-induced AChR clusters fail to form in the absence of dystroglycan. Muscle agrin binds to the basal lamina via laminin (Denzer et al., 1997) and α-dystroglycan (Sugiyama et al., 1994), and this is important for the maintenance of the NMJ (Samuel et al., 2012). It is important to highlight that this differs from the role of neuronal agrin in AChR clustering (Ferns et al., 1996). Perlecan, another synaptic heparan sulfate proteoglycan, is linked to both α-dystroglycan and ColQ (Peng et al., 1998). Perlecan-null mice lack AChE at the NMJ confirming its role as an acceptor for collagen-tailed AChE (Arikawa-hirasawa et al., 2002). In addition, muscle-derived COL13A1, which is thought to regulate the maturation of the NMJ (Latvanlehto et al., 2010), has been identified as a CMS-causative gene (Rodríguez Cruz et al., 2019).

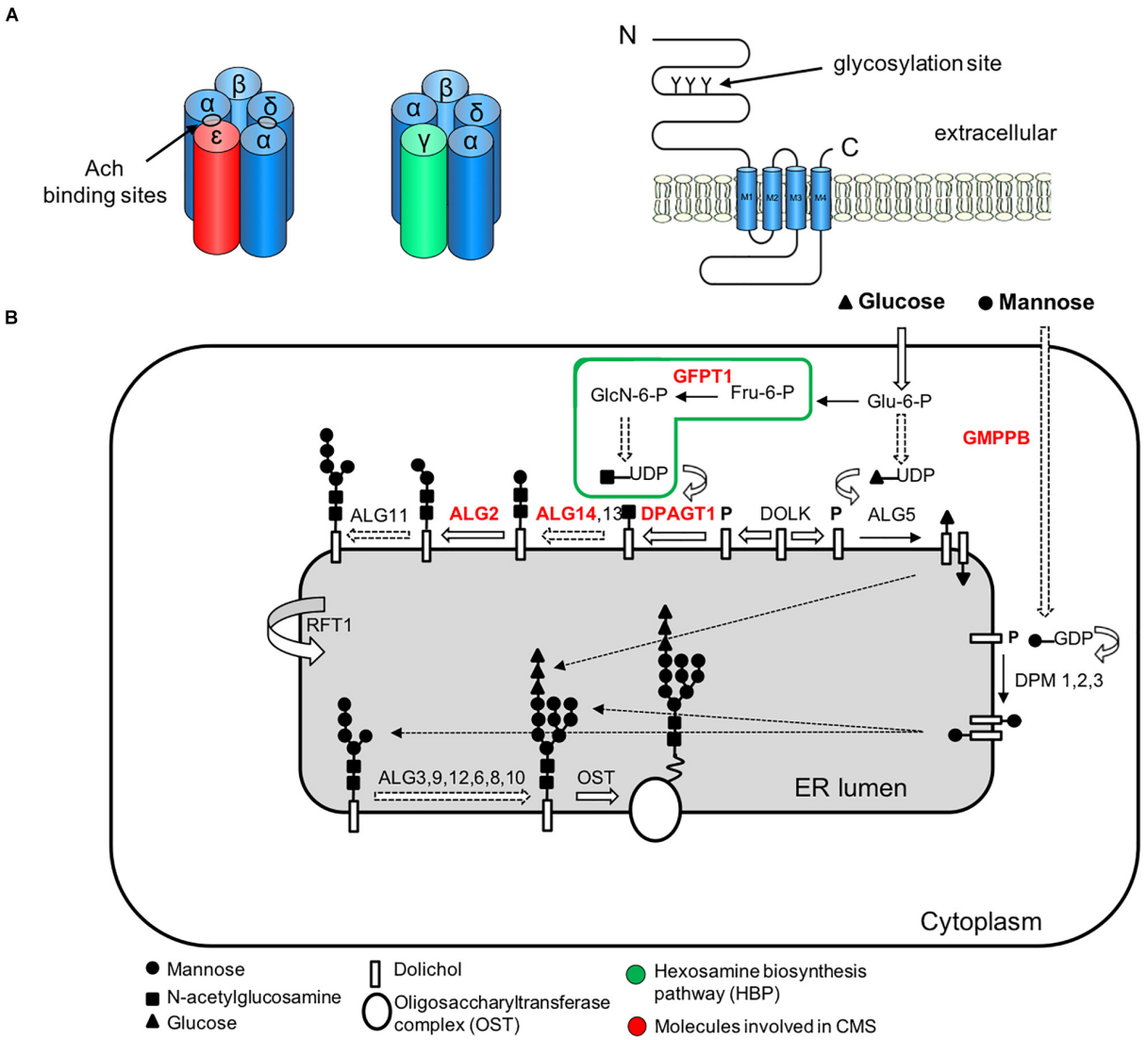

FIGURE 4 | Simplified representation of the AChR pentamer and the *N*-glycosylation pathway of proteins and CMS-related genes (red color). **(A)** Adult (red) and fetal (green) acetylcholine receptors and glycosylation sites. The AChR is made up of five subunits arranged around a central pore. Each subunit is composed of an extracellular domain, four transmembrane domains (M1–M4) and a large cytoplasmic loop linking M3 and M4. Each subunit also contains a conserved N-glycosylation consensus sequence (Asn-X-Ser/Thr) located at the N-terminal region (Gehle et al., 1997), which is necessary for the correct assembly of AChR pentamers and efficient export to the cell surface. **(B)** The *N*-linked glycosylation pathway takes place in the endoplasmic reticulum (ER). The first step is the assembly of the core glycan (*N*-acetylglucosamine, glucose and mannose) on the lipid dolichol. Next, a number of cytosolic glycosyltransferases proceed to dolichol glycosylation on the cytoplasmic face of the ER: GFPT1 synthesizes UDP-GlcNAc (Uridine diphosphate *N*-acetylglucosamine); DPAGT1 and the ALG13/14 complex add the first and second *N*-acetylglucosamine to dolichol. Additional sugar residues are incorporated by ALG2 and other enzymes. Then RFT1 flips the resulting product is flipped into the ER lumen where further sugar moieties are included until the glycan is transferred to asparagine residues of nascent proteins by the multimeric oligosaccharyl transferase complex (OST). DOLK, dolichol kinase; DPM, dolichol-phosphate mannose synthase; Fru-6-P, fructose-6-phosphate; GlcN-6-P, glucosamine-6-phosphate; Glu-6-P, glucose-6-phosphate; GMPPB, GDP-mannose pyrophosphrylase B.

ASSEMBLY AND FORMATION OF THE NMJ

Given that the NMJ is clearly a target for a number of different diseases, the majority of which involve changes in the number or function of specific molecules, it is important to understand fully the way in which this remarkable synapse develops and is maintained. However, it is important to make clear that nearly all current experimental data comes from the study of mice and that observations cannot always be translated to the human NMJ or indeed to other species and mammals (**Table 2**).

During development, the axons of motor neurons are guided to innervate skeletal muscles (Wu et al., 2010) but it is unclear whether motor neurons or muscles fibers determine the exact location of the endplate band (**Figure 5**). *In vivo* studies in mice have shown that small AChR clusters are

TABLE 2 | Molecules identified in NMJ formation, maturation and maintenance and levels of evidence.

	Molecule	Cellular level	Animal level	Human disease
NMJ formation	* Agrin	Ferns et al., 1993	Bogdanik et al., 2011	Huzé et al., 2009; Gasperi et al., 2014
	ß-catenin (muscle)	Zhang et al., 2007	Li et al., 2008	N/A
	Calpain	Chen et al., 2007	N/A	N/A
	CaMKII/PKC	Macpherson et al., 2002	N/A	N/A
	Cdk5	Fu et al., 2005	Fu et al., 2005	N/A
	Crk/CrkL	Hallock et al., 2010	Hallock et al., 2010	N/A
	Dihydropyridine-R	N/A	Chen et al., 2011	N/A
	* DOK7	Okada et al., 2006; Cossins et al., 2012	Okada et al., 2006; Arimura et al., 2014	Beeson et al., 2006
	Dvl1	Luo et al., 2002	Lijam et al., 1997	N/A
	* α-dystroglycan	Jacobson et al., 2001	Côté et al., 1999	Belaya, 2015
	Erm	N/A	Hippenmeyer et al., 2007	N/A
	FGF 7/10/22	Fox et al., 2007	Ohno et al., 1999	N/A
	GABP	Schaeffer et al., 1998	Schaeffer et al., 1998	N/A
	* Laminin ß2	Nishimune et al., 2004	Noakes et al., 1995	Matejas et al., 2010
	* LRP4	Zhang et al., 2008	Weatherbee et al., 2006; Yumoto et al., 2012	Higuchi et al., 2011; Ohkawara et al., 2013
	* MuSK	Koneczny et al., 2013	Chevessier et al., 2008; Cole et al., 2008	Hoch et al., 2001; Chevessier et al., 2004
	Myogenin	Eftimie et al., 1991	Arnold and Braun, 1996	N/A
	* N-glycosylation	Belaya et al., 2012; Zoltowska et al., 2013	Issop et al., 2018	Senderek et al., 2011; Belaya et al., 2012; Cossins et al., 2013; Belaya, 2015
	Nestin	Yang et al., 2011	Yang et al., 2011	N/A
	PAK1	Luo et al., 2002	N/A	N/A
	Perlecan	Peng et al., 1998	Arikawa-hirasawa et al., 2002	N/A
	Pro-BDNF	Yang et al., 2009	N/A	N/A
	Rac and Rho	Weston et al., 2003	N/A	N/A
	* Rapsyn	Cossins et al., 2006	Xing et al., 2019	Ohno et al., 2002
	SIRP-α	Umemori and Sanes, 2008	N/A	N/A
	Sorbs1 and Sorbs2	Hallock et al., 2016	N/A	N/A
	Tid1	Linnoila et al., 2008	N/A	N/A
NMJ maturation	* COL13A1	Latvanlehto et al., 2010	Latvanlehto et al., 2010	Logan et al., 2015
	CLASP2/CLIP170	Schmidt et al., 2012	Schmidt et al., 2012	N/A
	Ephexin1	Shi et al., 2010	Shi et al., 2010	N/A
	FGFBP1	N/A	Taetzsch et al., 2017	N/A
	GDNF	N/A	Nguyen et al., 1998	N/A
	Neurofascin 155	N/A	Roche et al., 2014	N/A
	Laminin α4	N/A	Nishimune et al., 2008	N/A
	* Laminin α5	N/A	Nishimune et al., 2008	Maselli et al., 2017
	* MACF1	Oury et al., 2019	Oury et al., 2019	Oury et al., 2019
	MHC1-I	N/A	Tetruashvily et al., 2016	N/A
	NRG1-III	N/A	Lee et al., 2016	N/A
	Vezatin	Koppel et al., 2019	Koppel et al., 2019	N/A
NMJ maintenance	* Agrin	Huzé et al., 2009	Samuel et al., 2012; Tezuka et al., 2014	Huzé et al., 2009
	α-dystrobrevin	Grady et al., 2000	Grady et al., 2000	N/A
	α-syntrophin	N/A	Adams et al., 2000	N/A
	CaMKII	N/A	Martinez-Pena et al., 2010	N/A

(Continued)

TABLE 2 | Continued

Molecule	Cellular level	Animal level	Human disease
* DOK7	Cossins et al., 2012	Eguchi et al., 2016	Beeson et al., 2006
Laminin α4	N/A	Samuel et al., 2012	N/A
* LRP4	Shen et al., 2013	Barik et al., 2014	Ohkawara et al., 2013
* MuSK	Koneczny et al., 2013	Kong et al., 2004	Hoch et al., 2001
* N-glycosylation	Belaya et al., 2012; Zoltowska et al., 2013	Issop et al., 2018	Senderek et al., 2011; Belaya et al., 2012; Cossins et al., 2013; Belaya, 2015
NCAM	N/A	Rafuse et al., 2000	N/A
Neuregulin/ErbB	N/A	Lin et al., 2000; Fu et al., 2005	N/A
Neurotrypsin	N/A	Bolliger et al., 2010	N/A
PKA/PKC	N/A	Martinez-Pena et al., 2013	N/A
Sarcoglycan-alpha	N/A	Zhao et al., 2018	N/A
Shp2	Madhavan et al., 2005	Dong et al., 2006	N/A
Src-family kinases	Smith et al., 2001	N/A	N/A

Molecules with the strongest evidence are marked with an asterisk; N/A, not available.

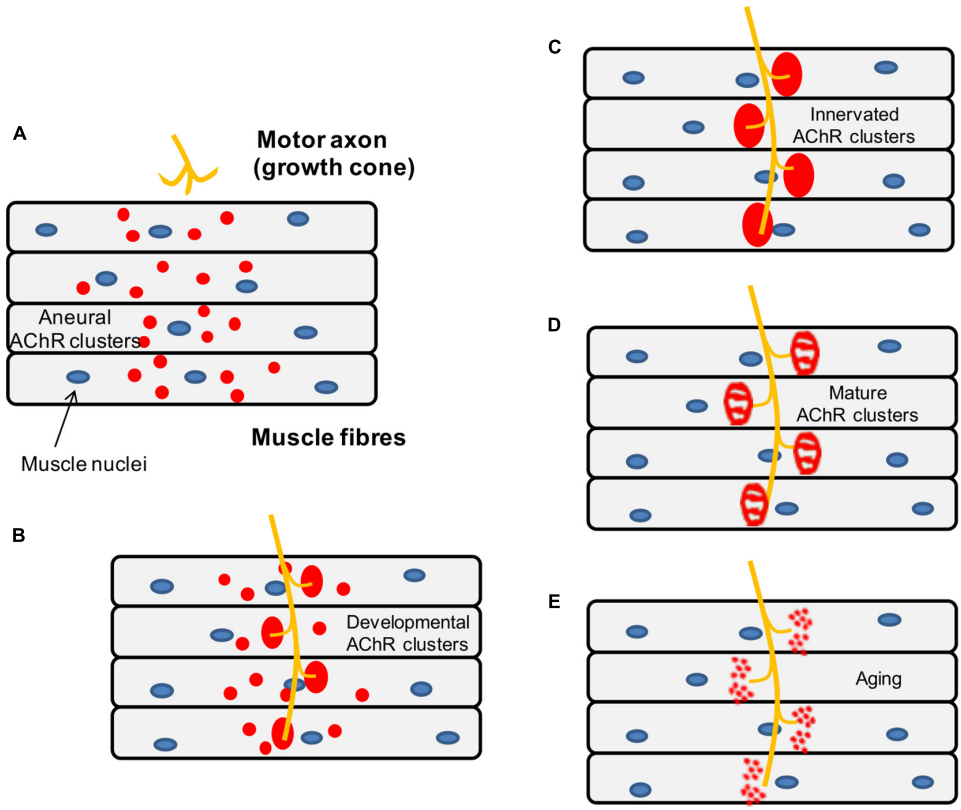

FIGURE 5 | Schematic representation of the mouse NMJ development. **(A)** Aneural AChR clusters are pre-patterned in the midbelly of the muscle fibers prior to the arrival of the nerve terminal. **(B)** Upon innervation of the pre-patterned clusters in the synaptic region, they become enlarged while aneural clusters located in the extrasynaptic region disappear. **(C)** As a result, AChR clusters are concentrated at a high density in the area underneath the nerve terminal maximizing the efficiency of neuromuscular transmission. **(D)** Postnatal maturation of AChR clusters and plaque to pretzel transformation. **(E)** Fragmentation of AChR clusters with aging.

prepatterned in the middle region of the muscle prior to the arrival of the motor axon via a process that requires MuSK and rapsyn but is not dependent on agrin (Lin et al., 2001). Furthermore, it has been shown that this phenomenon also occurs in mutant animals lacking motor nerves, which suggests that pre-patterning is nerve-independent and driven by a muscle-intrinsic program dependent on MuSK (Yang X. et al., 2001).

Subsequently, when the motor neurons innervate some of the prepatterned AChR clusters, these become enlarged and stable while aneural AChR clusters tend to disappear, so that the NMJs are eventually formed in the central region of muscle fibers. As mentioned above, neuronal agrin (McMahan, 1990) drives the process by activating the LRP4-MuSK-Dok7 pathway, which is crucial for the clustering of AChRs underneath the nerve terminal. By contrast, aneural clusters not stabilized by agrin signaling are dispersed by a negative signal, believed to be driven by the release of ACh from the presynaptic terminal (Lin et al., 2005).

Genes coding for components of the neuromuscular synapse become increasingly expressed in subsynaptic nuclei, resulting in the concentration of proteins required locally at the NMJ (Schaeffer et al., 2001), whereas expression of these specific genes is repressed at nuclei elsewhere along the muscle fiber. Even before innervation, AChR gene expression is enriched in the central region of embryonic skeletal muscles (Lin et al., 2001; Yang X. et al., 2001), which suggests that neuronal agrin is dispensable for early transcriptional compartmentalization. However, the area of AChR gene expression in muscles lacking motor axons is wider than usual, pointing that neural signals refine muscle-autonomous prepatterning (Yang X. et al., 2001). One of these signals is likely to be agrin, since compartmentalized expression in subsynaptic nuclei is severely affected in agrin and MuSK deficient mice as shown by *in situ* hybridization experiments to explore the distribution of AChR subunit mRNAs (DeChiara et al., 1996; Gautam et al., 1996). This does not occur in rapsyn deficient mice where AChR genes are selectively expressed by synaptic nuclei in the absence of AChR clusters (Gautam et al., 1995).

The communication between synaptic signals and targeted transcription is thought to be mediated by specific promoter elements in synaptic genes and E-twenty six (ETS) transcription factors. In particular, the N-box, a six-base pair element, was identified as a critical element in targeting the transcription of AChR delta (Koike et al., 1995) and epsilon subunits (Duclert et al., 1996). Disruption of this element in mouse models results in widespread expression of the reporter gene throughout the entire muscle fiber. This was further confirmed following the report of CMS patients underlying mutations in a conserved ETS binding site (N-box) in the promoter region of *CHRNE* encoding the AChR epsilon subunit (Ohno et al., 1999; Abicht et al., 2002). N-box motifs have also been reported to drive synapse-specific expression of utrophin (Gramolini et al., 1999) and AChE (Chan et al., 1999). ETS transcription factors identified in subsynaptic gene expression include GABP (GA-binding protein) α-subunit (Schaeffer et al., 1998) and Erm (Hippenmeyer et al., 2007).

Presynaptic differentiation begins after axon formation and culminates with the assembly of the neuromuscular synapse and the differentiation of a functional nerve terminal opposite the specialized postsynaptic membrane, where presynaptic proteins become concentrated. A relatively recent finding is that LRP4 works as a muscle-derived retrograde signal that controls the early steps of presynaptic differentiation by binding to motor axons and inducing clustering of synaptic vesicles and active zone proteins (Yumoto et al., 2012). Interestingly, although MuSK overexpression in *Lrp4* mutant mice restored AChR clustering, it failed to rescue presynaptic differentiation as motor axons kept growing along the muscle and rarely contacted AChR clusters (Yumoto et al., 2012). This finding suggests that, in addition to its function as a co-receptor for agrin, LRP4 has additional roles in NMJ formation that are independent of MuSK.

Other molecules identified as synaptic organizers of the presynaptic terminal include β-catenin (Li et al., 2008), laminin β2 (Nishimune et al., 2004), fibroblast growth factors (FGF) of the 7/10/22 subfamily (Fox et al., 2007), collagen IV (Fox et al., 2007) and signal regulatory protein α (SIRP-α) (Umemori and Sanes, 2008). However, in the absence of these molecules, motor axons manage to contact AChR clusters and differentiate considerably, which suggests that they act at a later stage in presynaptic differentiation compare to LRP4. Muscle-derived β-catenin, a signaling protein involved in the canonical Wnt pathway, has also been found to regulate motoneuron differentiation as mice lacking muscle β-catenin exhibit AChR clusters distributed throughout a wider region, mislocation of nerve branches and neurophysiological abnormalities (Li et al., 2008). By contrast, there are no obvious NMJ defects in motoneuron-specific β-catenin–deficient mice. Laminin β2, a component of the basal lamina, organizes active zones in motor nerve terminals by binding directly to voltage-gated calcium channels (VGCC) that are required for AChR release (Nishimune et al., 2004). It is thought that this association leads to clustering of VGCC into arrays, which in turn recruit and stabilize other constituents of the presynaptic apparatus. In agreement with this, mice lacking laminin β2 display structural abnormalities at the NMJ, namely a decreased number of active zones (Noakes et al., 1995). Furthermore, mutations in *LAMB2* encoding laminin β2 cause a severe form of synaptic CMS in humans (Maselli et al., 2009).

MATURATION OF THE NMJ

Neuromuscular junctions are functionally active in the embryonic stage, but they undergo complex postnatal maturation during the first weeks of life including synaptic elimination, endplate remodeling, and the AChR gamma-to-epsilon switch. During this period, the NMJ increases in size and the sarcolemma develops invaginations called postjunctional folds that increase total surface area. The morphology of the NMJ is changed from oval to a more complex perforated plaque, which in mice is described as pretzel-shaped, with a nearly contiguous arrangement of AChRs.

During synapse elimination, all but one axon are gradually withdrawn from multiply innervated muscle fibers, leaving a single innervating axon at each NMJ (Lichtman and Colman, 2000). This is a competitive and asynchronous process taking place at each endplate where more active synaptic sites destabilize neighboring inactive synapses (Balice-Gordon and Lichtman, 1994; Keller-Peck et al., 2001). Although synaptic activity and in particular spike timing seem to drive synaptic elimination (Favero et al., 2012), it is now believed that all three components of the NMJ contribute to this process (Lee, 2020). In particular, tSCs have been found to participate in the pruning of developing

synapses through the phagocytosis of immature axons and the displacement of nerve terminals from each other and the postsynaptic membrane (Smith et al., 2013).

A study has identified axon-tethered Neuregulin1 (NRG1-III) as a molecular determinant for tSC-driven synaptic plasticity (Lee et al., 2016). NRG1-III expression coincides temporally with synapse pruning and transgenic manipulation of NRG1-III levels in mice altered the motor input loss rate at NMJs during synapse elimination. However, it is still not clear how this relates to motor neuron activity. Another study showed that loss of glial Neurofascin155 in mice delays developmental synapse elimination by disrupting neuronal cytoskeletal organization and trafficking pathways in motor axons (Roche et al., 2014). On the muscle side, overexpression of glial cell line–derived neurotrophic factor (GDNF) causes hyperinnervation of NMJs in neonatal mice (Nguyen et al., 1998). Other candidates thought to participate in the refining of the neuromuscular circuitry include the major histocompatibility complex, class I (MHC-I) (Tetruashvily et al., 2016), pro-brain-derived neurotrophic factor (pro-BDNF) (Yang et al., 2009) and fibroblast growth factor binding protein 1 (FGFBP1) (Williams et al., 2009).

The remodeling of the murine endplates during early postnatal life results in a plaque-to-pretzel transition where the NMJs become perforated and increasingly complex with multiple branches innervated by a single axon (Slater, 1982). Using cultured aneural myotubes on laminin-coated plates that mimic the *in vivo* transformation, it was shown that perforations in the AChR aggregates bear structures resembling podosomes whose location and dynamics are spatiotemporally correlated with changes in the topology of AChR clusters (Proszynski et al., 2009). Podosomes are adhesive dynamic actin-rich matrix remodeling organelles described in numerous cell types. However, evidence for the relevance of podosomes *in vivo* is scarce and specifically, there is no definitive proof of the existence of synaptic podosomes at the NMJ in living organisms (Bernadzki et al., 2014). Other actors thought to be involved in the plaque-to-pretzel transition are synaptic laminins α4 and α5 (Nishimune et al., 2008) and ephexin1 (Shi et al., 2010). The latter is a rho guanine nucleotide exchange factor (GEF) involved in actin cytoskeletal dynamics. Adult ephexin1$^{-/-}$ mice present with severe muscle weakness, impaired neuromuscular transmission and abnormal maturation of the NMJ into the pretzel-like shape (Shi et al., 2010). Finally, being significantly smaller and more fragmented than murine NMJs (Jones et al., 2017), human neuromuscular synapses may undergo a different process of postnatal maturation.

The adult nicotinic AChR is a pentameric complex composed of four different transmembrane subunits (α-, ß-, δ-, and ε/γ-subunits) (Karlin, 2002; **Figure 4**). During early postnatal life, the fetal form of the AChR, containing a gamma subunit (2α:ß:δ:γ) is gradually replaced by an epsilon subunit-containing adult form (2α:ß:δ:ε), leading to increased calcium conductance of the receptor (Missias et al., 1996). The half-life of synaptic AChRs also increases during maturation as insertion of new AChRs and the recycling of internalized AChRs maintain the high density of AChRs at the crests of postsynaptic junctional folds (Bruneau et al., 2005; Bruneau and Akaaboune, 2006).

MAINTENANCE OF THE NMJ

The apparent macroscopic stability of the NMJ conceals a remarkable molecular dynamism where AChRs are continually exchanged between synaptic and extrasynaptic regions to maintain the high density of AChRs at the postsynaptic membrane (Akaaboune et al., 2002). The homeostasis of the neuromuscular synapse throughout life is essential for the NMJ function, as inactivation of the underlying molecular mechanisms results in synaptic disassembly (Tezuka et al., 2014).

It has been shown using postnatal knockdown experiments that most molecules involved in synaptic formation such as Agrin, MuSK and DOK7 are later required for NMJ maintenance (Kong et al., 2004; Barik et al., 2014; Tezuka et al., 2014; Eguchi et al., 2016). They may also have distinct roles in synapse formation and maintenance: for instance, the forced expression of DOK7 in agrin deficient mice restores synapse formation but NMJs disappear rapidly after birth, which points to an additional role of agrin distinct from MuSK activation in postnatal maintenance (Tezuka et al., 2014). By contrast, other molecules playing an important role in NMJ stabilization and maintenance are dispensable during synapse formation: some components of the dystrophin-glycoprotein complex (DGC) (Ibraghimov-Beskrovnaya et al., 1992), src-family kinases (Smith et al., 2001), NCAM (Rafuse et al., 2000), neuregulin (Schmidt et al., 2011), and more recently, MACF1 (Oury et al., 2019). There is also increasing evidence from clinical (Lashley et al., 2010; Rodríguez Cruz et al., 2015) and experimental studies (McMacken et al., 2019; Vanhaesebrouck et al., 2019) that β2-adrenergic signaling could play a role in NMJ homeostasis. Furthermore, one study in mice proposed that sympathetic neurons make close contact with NMJs (Khan et al., 2016).

The DGC complex links the cytoskeleton of muscle fibers to the extracellular matrix (Ibraghimov-Beskrovnaya et al., 1992). Mice lacking α-dystrobrevin, a cytoplasmic component of DGC, show no abnormalities in NMJ morphology at postnatal day 7. However, by 1 month of age and independently of muscle changes, AChRs became abnormally distributed with irregular branch borders while the size, number and arrangement of branches remained unaltered (Grady et al., 2000). Another study showed that rates of AChR turnover were significantly increased in mice lacking α-dystrobrevin compared to WT and mdx mice (Akaaboune et al., 2002). *In vitro*, α-dystrobrevin is dispensable for agrin-induced cluster formation but required for maintenance of clusters following agrin withdrawal (Grady et al., 2000). A similar phenotype was reported in α-syntrophin null mice in the absence of myopathy (Adams et al., 2000). The structural abnormalities seen in the mdx mouse model of Duchenne muscular dystrophy (Sicinski et al., 1989) are more profound with severe endplate fragmentation (Torres and Duchen, 1987). However, these are found exclusively at NMJs on regenerated muscle fibers, which indicates that endplate remodeling is related to muscle damage rather than dystrophin deficiency (Lyons and Slater, 1991).

Src family kinases (src, fyn, and yes) have been implicated in signaling pathways downstream of MuSK (Fuhrer and Hall, 1996). Studies in *src*$^{-/-}$;*fin*$^{-/-}$ and *src*$^{-/-}$;*yes*$^{-/-}$ mutant

mice showed normal NMJ development and agrin-induced phosphorylation of the AChR-ß subunit but AChR clusters in mutant cell lines were significantly less stable following agrin withdrawal (Smith et al., 2001). The neuronal cell adhesion molecule (NCAM) is thought to participate in the maturation of the presynaptic terminal as NCAM null mice present delayed presynaptic structural maturation and smaller endplates (Rafuse et al., 2000). Two serine/threonine kinases, PKC and PKA, have been implicated in the regulation of AChR dynamics at the adult NMJ of living mice by possibly acting on different receptor subunits and/or substrates involved in the anchoring of AChRs (Martinez-Pena et al., 2013). In addition, Ca^{2+}/calmodulin-dependent kinase II (CaMKII) is thought to participate in the recycling of AChRs necessary to maintain postsynaptic AChR density (Ibraghimov-Beskrovnaya et al., 1992).

Finally, it is increasingly more evident that glial cells have an important role in NMJ maintenance. Characterization of NMJs after genetic ablation of tSCs in adult mice shows NMJ fragmentation and neuromuscular transmission defects (Barik et al., 2016). In adult frogs, selective ablation of tSCs results in widespread retraction of existing synapses (Reddy et al., 2003). One possible mechanism is through neuregulin/ErbB signaling as *ErbB2*$^{-/-}$ mice lack tSCs and postjunctional folds and although they retain the ability to form neuromuscular synapses, these fail to be maintained (Riethmacher et al., 1997; Lin et al., 2000). Other study in frogs suggested that tSCs express active agrin and enhance aggregation of AChRs on muscle fibers (Yang J.F. et al., 2001).

REGENERATION OF THE NMJ

Injury to the nerve or muscle, lack of physical activity and ageing can alter synaptic organization resulting in endplate fragmentation, partial denervation and reduction in active zones and AChR density (Stanley and Drachman, 1981; Lyons and Slater, 1991; Valdez et al., 2010).

It is well known that mouse muscle endplates lose the normal pretzel shape and become fragmented with multiple spot contacts following muscle fiber damage (Lyons and Slater, 1991). One of the best examples is the *mdx* mouse model of Duchenne muscular dystrophy (Sicinski et al., 1989). In 8-week old *mdx* mice, muscle endplates from regenerating fibers appear dramatically fragmented over an enlarged postsynaptic area and nerve terminals display abnormally complex features, with a significant increase in the number of fine terminal arborizations, many bearing bouton-like swellings (Lyons and Slater, 1991). The alterations seen in the *mdx* mouse increase with ageing, probably as a consequence of recurrent muscle damage (Torres and Duchen, 1987). Interestingly, the structural changes do not alter the safety margin of neuromuscular transmission (Nagel et al., 1990). Therefore, the significance of this process is not fully understood as this could be the outcome of a physiological mechanism of NMJ maintenance rather than synapse degeneration (Slater, 2019).

Endplate reinnervation following nerve injury results in degradation of junctional AChRs, increase of their turnover rates and structural changes to the NMJ (Stanley and Drachman, 1981; Rich and Lichtman, 1989; Akaaboune et al., 1999). Upon denervation, it is thought that the upregulation of chromatin acetylation and AChR expression is mediated by signal-responsive transcriptional regulators histone deacetylase 9 (HDAC9) and 4 (HDAC4) that allow the induction of the transcription factor Myogenin (Méjat et al., 2005; Cohen et al., 2007). Protein kinase B (PKB/Akt) and mTORC1 (mammalian Target of Rapamycin Complex 1) have been implicated in regulating muscle homeostasis and maintaining NMJs after nerve injury in mice (Castets et al., 2019). Other key elements of synapse development such as Col13a1 (Zainul et al., 2018) and LRP4 (Gribble et al., 2018) have also been involved in promoting peripheral nerve regeneration. Finally, tSCs play a key role in reinnervation by guiding axons through the extension of their processes (Son and Thompson, 1995) and retracting processes from territory they previously occupied within the endplate (Kang et al., 2014).

AUTHOR CONTRIBUTIONS

PR reviewed the literature and drafted the manuscript. JC and DB contributed to critical revision of the manuscript for important intellectual content. AV contributed to critical revision of the manuscript for important intellectual content and senior authorship. All authors contributed to the article and approved the submitted version.

REFERENCES

Abicht, A., Stucka, R., Schmidt, C., Briguet, A., Höpfner, S., Song, I.-H., et al. (2002). A newly identified chromosomal microdeletion and an N-box mutation of the AChR epsilon gene cause a congenital myasthenic syndrome. *Brain* 125, 1005–1013. doi: 10.1093/brain/awf095

Adams, M. E., Kramarcy, N., Krall, S. P., Rossi, S. G., Rotundo, R. L., Sealock, R., et al. (2000). Absence of α-syntrophin leads to structurally aberrant neuromuscular synapses deficient in utrophin. *J. Cell Biol.* 150, 1385–1397. doi: 10.1083/jcb.150.6.1385

Ahmad, S., Bhatia, K., Kannan, A., and Gangwani, L. (2016). Molecular mechanisms of neurodegeneration in spinal muscular atrophy. *J. Exp. Neurosci.* 10, 39–49. doi: 10.4137/JEn.s33122

Akaaboune, M., Culican, S. M., Turney, S. G., Jeff, W., Akaaboune, M., Culican, S. M., et al. (1999). Rapid and reversible effects of activity on acetylcholine receptor density at the neuromuscular junction in vivo. *Science* 286, 503–507.

Akaaboune, M., Grady, R. M., Turney, S., Sanes, J. R., Lichtman, J. W., and Louis, S. (2002). Neurotechnique dynamics studied in vivo by reversible photo-unbinding of fluorescent ligands. *Neuron* 34, 865–876.

An, M. C., Lin, W., Yang, J., Dominguez, B., Padgett, D., Sugiura, Y., et al. (2010). Acetylcholine negatively regulates development of the neuromuscular

junction through distinct cellular mechanisms. *Proc. Natl. Acad. Sci. U.S.A.* 107, 10702–10707. doi: 10.1073/pnas.1004956107

Angelozzi, C., Borgo, F., Tiziano, F. D., Martella, A., Neri, G., and Brahe, C. (2008). Salbutamol increases SMN mRNA and protein levels in spinal muscular atrophy cells. *J. Med. Genet.* 45, 29–31. doi: 10.1136/jmg.2007.051177

Apel, E. D., Roberds, S. L., Campbell, K. P., and Merlie, J. P. (1995). Rapsyn may function as a link between the acetylcholine receptor and the agrin-binding glycoprotein complex. *Neuron* 15, 115–126.

Arikawa-hirasawa, E., Rossi, S. G., Rotundo, R. L., and Yamada, Y. (2002). Absence of acetylcholinesterase at the neuromuscular junctions of perlecan-null mice. *Nat. Neurosci.* 5, 119–123. doi: 10.1038/nn801

Arimura, S., Okada, T., Tezuka, T., Chiyo, T., Kasahara, Y., Yoshimura, T., et al. (2014). DOK7 gene therapy benefitsmouse models of diseases characterized by defects in the neuromuscular junction. *Science* 345, 1505–1508. doi: 10.5281/zenodo.11300

Arnold, H. H., and Braun, T. (1996). Targeted inactivation of myogenic factor genes reveals their role during mouse myogenesis: a review. *Int. J. Dev. Biol.* 40, 345–353.

Baker, R. W., and Hughson, F. M. (2016). Chaperoning SNARE assembly and disassembly. *Nat. Rev. Mol. Cell Biol.* 17, 1465–1487. doi: 10.1007/128

Balice-Gordon, R. J., and Lichtman, J. W. (1994). Long-term synapse loss induced by focal blockade of postsynaptlc receptors. *Nature* 372, 519–524. doi: 10.1038/372519a0

Barik, A., Li, L., Sathyamurthy, A., Xiong, W. C., and Mei, L. (2016). Schwann cells in neuromuscular junction formation and maintenance. *J. Neurosci.* 36, 9770–9781. doi: 10.1523/JNEUROSCI.0174-16.2016

Barik, A., Lu, Y., Sathyamurthy, A., Bowman, A., Shen, C., Li, L., et al. (2014). LRP4 is critical for neuromuscular junction maintenance. *J. Neurosci.* 34, 13892–13905. doi: 10.1523/JNEUROSCI.1733-14.2014

Beeson, D., Higuchi, O., Palace, J., Cossins, J., Spearman, H., Maxwell, S., et al. (2006). Dok-7 mutations underlie a neuromuscular junction synaptopathy. *Science* 313, 1975–1978. doi: 10.1126/science.1130837

Belaya, K. (2015). Mutations in GMPPB cause congenital myasthenic syndrome and bridge myasthenic disorders with dystroglycanopathies. *Brain* 138(Pt 9), 2493–2504.

Belaya, K., Finlayson, S., Slater, C. R., Cossins, J., Liu, W. W., Maxwell, S., et al. (2012). Mutations in DPAGT1 cause a limb-girdle congenital myasthenic syndrome with tubular aggregates. *Am. J. Hum. Genet.* 91, 193–201. doi: 10.1016/j.ajhg.2012.05.022

Bergamin, E., Hallock, P. T., Burden, S. J., and Hubbard, S. R. (2010). The cytoplasmic adaptor protein Dok7 activates the receptor tyrosine kinase MuSK via dimerization. *Mol. Cell* 39, 100–109. doi: 10.1016/j.molcel.2010.06.007

Bernadzki, K. M., Rojek, K. O., and Prószyński, T. J. (2014). Podosomes in muscle cells and their role in the remodeling of neuromuscular postsynaptic machinery. *Eur. J. Cell Biol.* 93, 478–485. doi: 10.1016/j.ejcb.2014.06.002

Bogdanik, L. P., Burgess, R. W., and Harbor, B. (2011). A valid mouse model of AGRIN -associated congenital myasthenic syndrome. *Hum. Mol. Genet.* 20, 4617–4633. doi: 10.1093/hmg/ddr396

Bolliger, M. F., Zurlinden, A., Lüscher, D., Bütikofer, L., Shakhova, O., Francolini, M., et al. (2010). Specific proteolytic cleavage of agrin regulates maturation of the neuromuscular junction. *J. Cell Sci.* 123, 3944–3955. doi: 10.1242/jcs.072090

Borges, L. S., and Ferns, M. (2001). Agrin-induced phosphorylation of the acetylcholine receptor regulates cytoskeletal anchoring and clustering. *J. Cell Biol.* 153, 1–11. doi: 10.1083/jcb.153.1.1

Borges, L. S., Yechikhov, S., Lee, Y. I., Rudell, J. B., Friese, M. B., Burden, S. J., et al. (2008). Identification of a motif in the acetylcholine receptor β subunit whose phosphorylation regulates rapsyn association and postsynaptic receptor localization. *J. Neurosci.* 28, 11468–11476. doi: 10.1523/JNEUROSCI.2508-08.2008

Bruneau, E. G., and Akaaboune, M. (2006). The dynamics of recycled acetylcholine receptors at the neuromuscular junction in vivo. *Development* 133, 4485–4493. doi: 10.1242/dev.02619

Bruneau, E., Sutter, D., Hume, R. I., and Akaaboune, M. (2005). Identification of nicotinic acetylcholine receptor recycling and its role in maintaining receptor density at the neuromuscular junction in vivo. *J. Neurosci.* 25, 9949–9959. doi: 10.1523/JNEUROSCI.3169-05.2005

Burden, S. J., DePalma, R. L., and Gottesman, G. S. (1983). Crosslinking of proteins in acetylcholine receptor-rich membranes: association between the beta-subunit and the 43 kd subsynaptic protein. *Cell* 35, 687–692. doi: 10.1016/0092-8674(83)90101-0

Bütikofer, L., Zurlinden, A., Bolliger, M. F., Kunz, B., and Sonderegger, P. (2011). Destabilization of the neuromuscular junction by proteolytic cleavage of agrin results in precocious sarcopenia. *FASEB J.* 25, 4378–4393. doi: 10.1096/fj.11-191262

Cantor, S., Zhang, W., Delestrée, N., Remédio, L., Mentis, G. Z., and Burden, S. J. (2018). Preserving neuromuscular synapses in ALS by stimulating MuSK with a therapeutic agonist antibody. *eLife* 7, 1–19. doi: 10.7554/eLife.34375

Cao, M., Koneczny, I., and Vincent, A. (2020). Myasthenia gravis with antibodies against muscle specific kinase: an update on clinical features, pathophysiology and treatment. *Front. Mol. Neurosci.* 13:159. doi: 10.3389/fnmol.2020.00159

Castets, P., Rion, N., Théodore, M., Falcetta, D., Lin, S., Reischl, M., et al. (2019). mTORC1 and PKB/Akt control the muscle response to denervation by regulating autophagy and HDAC4. *Nat. Commun.* 10, 1–16. doi: 10.1038/s41467-019-11227-4

Chan, R. Y. Y., Boudreau-Larivière, C., Angus, L. M., Mankal, F. A., and Jasmin, B. J. (1999). An intronic enhancer containing an N-box motif is required for synapse- and tissue-specific expression of the acetylcholinesterase gene in skeletal muscle fibers. *Proc. Natl. Acad. Sci. U.S.A.* 96, 4627–4632. doi: 10.1073/pnas.96.8.4627

Chen, F., Liu, Y., Sugiura, Y., Allen, P. D., Gregg, R. G., and Lin, W. (2011). Neuromuscular synaptic patterning requires the function of skeletal muscle dihydropyridine receptors. *Nat. Neurosci.* 14, 570–577. doi: 10.1038/nn.2792

Chen, F., Qian, L., Yang, Z., Huang, Y., Ngo, S. T., Ruan, N., et al. (2007). Rapsyn interaction with calpain stabilizes AChR clusters at the neuromuscular junction. *Neuron* 55, 247–260. doi: 10.1016/j.neuron.2007.06.031

Chevessier, F., Faraut, B., Ravel-Chapuis, A., Richard, P., Gaudon, K., Bauché, S., et al. (2004). MUSK, a new target for mutations causing congenital myasthenic syndrome. *Hum. Mol. Genet.* 13, 3229–3240. doi: 10.1093/hmg/ddh333

Chevessier, F., Girard, E., Molgó, J., Bartling, S., Koenig, J., Hantaï, D., et al. (2008). A mouse model for congenital myasthenic syndrome due to MuSK mutations reveals defects in structure and function of neuromuscular junctions. *Hum. Mol. Genet.* 17, 3577–3595. doi: 10.1093/hmg/ddn251

Cohen, T. J., Waddell, D. S., Barrientos, T., Lu, Z., Feng, G., Cox, G. A., et al. (2007). The histone deacetylase HDAC4 connects neural activity to muscle transcriptional reprogramming. *J. Biol. Chem.* 282, 33752–33759. doi: 10.1074/jbc.M706268200

Cole, R. N., Reddel, S. W., Gervásio, O. L., and Phillips, W. D. (2008). Anti-MuSK patient antibodies disrupt the mouse neuromuscular junction. *Ann. Neurol.* 63, 782–789. doi: 10.1002/ana.21371

Cossins, J., Belaya, K., Hicks, D., Salih, M. A., Finlayson, S., Carboni, N., et al. (2013). Congenital myasthenic syndromes due to mutations in ALG2 and ALG14. *Brain* 136, 944–956. doi: 10.1093/brain/awt010

Cossins, J., Burke, G., Maxwell, S., Spearman, H., Man, S., Kuks, J., et al. (2006). Diverse molecular mechanisms involved in AChR deficiency due to rapsyn mutations. *Brain* 129, 2773–2783. doi: 10.1093/brain/awl219

Cossins, J., Liu, W. W., Belaya, K., Maxwell, S., Oldridge, M., Lester, T., et al. (2012). The spectrum of mutations that underlie the neuromuscular junction synaptopathy in DOK7 congenital myasthenic syndrome. *Hum. Mol. Genet.* 21, 3765–3775. doi: 10.1093/hmg/dds198

Côté, P. D., Moukhles, H., Lindenbaum, M., and Carbonetto, S. (1999). Chimaeric mice deficient in dystroglycans develop muscular dystrophy and have disrupted myoneural synapses. *Nat. Genet.* 23, 338–342. doi: 10.1038/15519

Dai, Z., Luo, X., Xie, H., Peng, H. B., Hill, C., and Carolina, N. (2000). The actin-driven movement and formation of acetylcholine receptor clusters. *J. Cell Biol.* 150, 1321–1334.

De Harven, E., and Coers, C. (1959). Electron microscope study of the human endometrium. *J. Biophys. Biochem. Cytol.* 6, 7–10.

DeChiara, T. M., Bowen, D. C., Valenzuela, D. M., Simmons, M. V., Poueymirou, W. T., Thomas, S., et al. (1996). The receptor tyrosine kinase MuSK is required for neuromuscular junction formation in vivo. *Cell* 85, 501–512.

Denzer, A. J., Brandenberger, R., Gesemann, M., Chiquet, M., and Ruegg, M. A. (1997). Agrin binds to the nerve–muscle basal lamina via laminin. *J. Cell Biol.* 137, 671–683.

Desaki, J., and Uehara, Y. (1981). The overall morphology of neuromuscular junctions as revealed by scanning electron microscopy. *J. Neurocytol.* 10, 101–110. doi: 10.1007/BF01181747

Dong, X. P., Li, X. M., Gao, T. M., Zhang, E. E., Feng, G. S., Xiong, W. C., et al. (2006). Shp2 is dispensable in the formation and maintenance of the neuromuscular junction. *NeuroSignals* 15, 53–63. doi: 10.1159/000094484

Duclert, A., Savatier, N., Schaeffer, L., and Changeux, J. P. (1996). Identification of an element crucial for the sub-synaptic expression of the acetylcholine receptor ε-subunit gene. *J. Biol. Chem.* 271, 17433–17438. doi: 10.1074/jbc.271.29.17433

Eaton, L. M., and Lambert, E. H. (1957). Electromyography and electric stimulation of nerves in diseases of motor unit; observations on myasthenic syndrome associated with malignant tumors. *J. Am. Med. Assoc.* 163, 1117–1124.

Eftimie, R., Brenner, H. R., and Buonanno, A. (1991). Myogenin and MyoD join a family of skeletal muscle genes regulated by electrical activity. *Proc. Natl. Acad. Sci. U.S.A.* 88, 1349–1353. doi: 10.1073/pnas.88.4.1349

Eguchi, T., Tezuka, T., Miyoshi, S., and Yamanashi, Y. (2016). Postnatal knockdown of dok-7 gene expression in mice causes structural defects in neuromuscular synapses and myasthenic pathology. *Genes Cells* 21, 670–676. doi: 10.1111/gtc.12370

Engel, A. G., Shen, X., Selcen, D., and Sine, S. M. (2015). Congenital myasthenic syndromes: pathogenesis, diagnosis, and treatment. *Lancet Neurol.* 14, 420–434. doi: 10.1016/S1474-4422(14)70201-7

Evoli, A., Tonali, P. A., Padua, L., Lo Monaco, M., Scuderi, F., Batocchi, A. P., et al. (2003). Clinical correlates with anti-MuSK antibodies in generalized seronegative myasthenia gravis. *Brain* 126, 2304–2311. doi: 10.1093/brain/awg223

Favero, M., Busetto, G., and Cangiano, A. (2012). Spike timing plays a key role in synapse elimination at the neuromuscular junction. *Proc. Natl. Acad. Sci. U.S.A.* 109, E1667–E1675. doi: 10.1073/pnas.1201147109

Feng, Z., and Ko, C.-P. (2008). The role of glial cells in the formation and maintenance of the neuromuscular junction. *Ann. N. Y. Acad. Sci.* 1132, 19–28. doi: 10.1196/annals.1405.016

Ferns, M. J., Campanelli, J. T., Scheller, R. H., and Hall, Z. (1993). The ability of agrin to cluster AChRs depends on alternative splicing and on cell surface proteoglycans. *Neuron* 11, 491–502.

Ferns, M., Deiner, M., and Hall, Z. (1996). Agrin-induced acetylcholine receptor clustering in mammalian muscle rexluires tyrosine phosphorylation. *J. Cell Biol.* 132, 937–944.

Fischer, L. R., Culver, D. G., Tennant, P., Davis, A. A., Wang, M., Castellano-Sanchez, A., et al. (2004). Amyotrophic lateral sclerosis is a distal axonopathy: evidence in mice and man. *Exp. Neurol.* 185, 232–240. doi: 10.1016/j.expneurol.2003.10.004

Fox, M. A., Ho, M. S. P., Smyth, N., and Sanes, J. R. (2008). A synaptic nidogen: Developmental regulation and role of nidogen-2 at the neuromuscular junction. *Neural Dev.* 17:24. doi: 10.1186/1749-8104-3-24

Fox, M. A., Sanes, J. R., Borza, D. B., Eswarakumar, V. P., Fässler, R., Hudson, B. G., et al. (2007). Distinct target-derived signals organize formation, maturation, and maintenance of motor nerve terminals. *Cell* 129, 179–193. doi: 10.1016/j.cell.2007.02.035

Friese, M. B., Blagden, C. S., and Burden, S. J. (2007). Synaptic differentiation is defective in mice lacking acetylcholine receptor β-subunit tyrosine phosphorylation. *Development* 134, 4167–4176. doi: 10.1242/dev.010702

Fu, A. K. Y., Ip, F. C. F., Fu, W. Y., Cheung, J., Wang, J. H., Yung, W. H., et al. (2005). Aberrant motor axon projection, acetylcholine receptor clustering, and neurotransmission in cyclin-dependent kinase 5 null mice. *Proc. Natl. Acad. Sci. U.S.A.* 102, 15224–15229. doi: 10.1073/pnas.0507678102

Fuhrer, C., and Hall, Z. W. (1996). Functional interaction of Src family kinases with the acetylcholine receptor in C2 myotubes. *J. Biol. Chem.* 271, 32474–32481. doi: 10.1074/jbc.271.50.32474

Gallardo, E., Martínez-Hernández, E., Titulaer, M. J., Huijbers, M. G., Martínez, M. A., Ramos, A., et al. (2014). Cortactin autoantibodies in myasthenia gravis. *Autoimmun. Rev.* 13, 1003–1007. doi: 10.1016/j.autrev.2014.08.039

Gasperi, C., Melms, A., Schoser, B., Zhang, Y., Meltoranta, J., Risson, V., et al. (2014). Anti-agrin autoantibodies in myasthenia gravis. *Neurology* 82, 1976–1983. doi: 10.1212/WNL.0000000000000478

Gautam, M., Noakes, P. G., Moscoso, L., Rupp, F., Scheller, R. H., Merlie, J. P., et al. (1996). Defective neuromuscular synaptogenesis in agrin-deficient mutant mice. *Cell* 85, 525–535. doi: 10.1016/S0092-8674(00)81253-2

Gautam, M., Noakes, P. G., Mudd, J., Nichol, M., Chu, G. C., Sanes, J. R., et al. (1995). Failure of postsynaptic specialization to develop at neuromuscular junctions of rapsyn-deficient mice. *Nature* 377, 232–236.

Gehle, V. M., Walcott, E. C., Nishizaki, T., and Sumikawa, K. (1997). N-glycosylation at the conserved sites ensures the expression of properly folded functional ACh receptors. *Brain Res. Mol. Brain Res.* 45, 219–229.

Gould, T. W. (2006). Complete dissociation of motor neuron death from motor dysfunction by bax deletion in a mouse model of ALS. *J. Neurosci.* 26, 8774–8786. doi: 10.1523/JNEUROSCI.2315-06.2006

Grady, R. M., Zhou, H., Cunningham, J. M., Henry, M. D., Campbell, K. P., and Sanes, J. R. (2000). Maturation and maintenance of the neuromuscular synapse: genetic evidence for roles of the dystrophin–glycoprotein complex. *Neuron* 25, 279–293.

Gramolini, A. O., Angus, L. M., Schaeffer, L., Burton, E. A., Tinsley, J. M., Davies, K. E., et al. (1999). Induction of utrophin gene expression by heregulin in skeletal muscle cells: role of the N-box motif and GA binding protein. *Proc. Natl. Acad. Sci. U.S.A.* 96, 3223–3227. doi: 10.1073/pnas.96.6.3223

Gribble, K. D., Walker, L. J., Saint-Amant, L., Kuwada, J. Y., and Granato, M. (2018). The synaptic receptor Lrp4 promotes peripheral nerve regeneration. *Nat. Commun.* 9, 1–12. doi: 10.1038/s41467-018-04806-4

Hall, A. (1998). Rho GTPases and the actin cytoskeleton. *Science* 279, 509–514. doi: 10.1126/science.279.5350.509

Hallock, P. T., Chin, S., Blais, S., Neubert, T. A., and Glass, D. J. (2016). Sorbs1 and -2 Interact with CrkL and are required for acetylcholine receptor cluster formation. *Mol. Cell Biol.* 36, 262–270. doi: 10.1128/MCB.00775-15.Address

Hallock, P. T., Xu, C. F., Park, T. J., Neubert, T. A., and Burden, T. C. S. J. (2010). Dok-7 regulates neuromuscular synapse formation by recruiting Crk and Crk-L. *Genes Dev.* 24, 2451–2461. doi: 10.1101/gad.1977710

Harper, C. M., Fukodome, T., and Engel, A. G. (2003). Treatment of slow-channel congenital myasthenic syndrome with fluoxetine. *Neurology* 60, 1710–1713. doi: 10.1212/01.WNL.0000061483.11417.1B

Hettwer, S., Lin, S., Kucsera, S., Haubitz, M., Oliveri, F., Fariello, R. G., et al. (2014). Injection of a soluble fragment of neural agrin (NT-1654) considerably improves the muscle pathology caused by the disassembly of the neuromuscular junction. *PLoS One* 9:e88739. doi: 10.1371/journal.pone.0088739

Higuchi, O., Hamuro, J., Motomura, M., and Yamanashi, Y. (2011). Autoantibodies to low-density lipoprotein receptor-related protein 4 in myasthenia gravis. *Ann. Neurol.* 69, 418–422. doi: 10.1002/ana.22312

Hippenmeyer, S., Huber, R. M., Ladle, D. R., Murphy, K., and Arber, S. E. T. S. (2007). Transcription factor Erm controls subsynaptic gene expression in skeletal muscles. *Neuron* 55, 726–740. doi: 10.1016/j.neuron.2007.07.028

Hoch, W., McConville, J., Helms, S., Newsom-Davis, J., Melms, A., and Vincent, A. (2001). Auto-antibodies to the receptor tyrosine kinase MuSK in patients with myasthenia gravis without acetylcholine receptor antibodies. *Nat. Med.* 7, 365–368. doi: 10.1038/85520

Hubbard, S. R., and Gnanasambandan, K. (2013). Structure and activation of MuSK, a receptor tyrosine kinase central to neuromuscular junction formation. *Biochim. Biophys. Acta* 1834, 2166–2169. doi: 10.1016/j.bbapap.2013.02.034. Structure

Huzé, C., Bauché, S., Richard, P., Chevessier, F., Goillot, E., Gaudon, K., et al. (2009). Identification of an agrin mutation that causes congenital myasthenia and affects synapse function. *Am. J. Hum. Genet.* 85, 155–167. doi: 10.1016/j.ajhg.2009.06.015

Ibraghimov-Beskrovnaya, O., Ervasti, J. M., Leveille, C. J., Slaughter, C. A., Sernett, S. W., and Campbell, K. P. (1992). Primary structure of dystrophin-associated glycoproteins linking dystrophin to the extracellular matrix. *Nature* 355, 696–702. doi: 10.1038/355696a0

Inoue, A., Setoguchi, K., Matsubara, Y., Okada, K., Sato, N., Iwakura, Y., et al. (2009). Dok-7 activates the muscle receptor kinase MuSK and shapes synapse formation. *Sci. Signal.* 2, 1–9. doi: 10.1126/scisignal.2000113

Issop, Y., Hathazi, D., Khan, M. M., Rudolf, R., Weis, J., Spendiff, S., et al. (2018). GFPT1 deficiency in muscle leads to myasthenia and myopathy in mice. *Hum. Mol. Genet.* 27, 3218–3232. doi: 10.1093/hmg/ddy225

Jacob, S., Viegas, S., Leite, M. I., Webster, R., Cossins, J., Kennett, R., et al. (2012). Presence and pathogenic relevance of antibodies to clustered acetylcholine receptor in ocular and generalized myasthenia gravis. *Arch. Neurol.* 69, 994–1001. doi: 10.1001/archneurol.2012.437

Jacobson, C., Côté, P. D., Rossi, S. G., Rotundo, R. L., and Carbonetto, S. (2001). The dystroglycan complex is necessary for stabilization of acetylcholine receptor clusters at neuromuscular junctions and formation of the synaptic basement membrane. *J. Cell Biol.* 152, 435–450.

Jones, R. A., Harrison, C., Eaton, S. L., Llavero Hurtado, M., Graham, L. C., Alkhammash, L., et al. (2017). Cellular and molecular anatomy of the human neuromuscular junction. *Cell Rep.* 21, 2348–2356. doi: 10.1016/j.celrep.2017.11.008

Kang, H., Tian, L., Mikesh, M., Lichtman, J. W., and Thompson, W. J. (2014). Terminal schwann cells participate in neuromuscular synapse remodeling during reinnervation following nerve injury. *J. Neurosci.* 34, 6323–6333. doi: 10.1523/JNEUROSCI.4673-13.2014

Kariya, S., Park, G. H., Maeno-Hikichi, Y., Leykekhman, O., Lutz, C., Arkovitz, M. S., et al. (2008). Reduced SMN protein impairs maturation of the neuromuscular junctions in mouse models of spinal muscular atrophy. *Hum. Mol. Genet.* 17, 2552–2569. doi: 10.1093/hmg/ddn156

Karlin, A. (2002). Ion channel structureemerging structure of the nicotinic acetylcholine receptors. *Nat. Rev. Neurosci.* 3, 102–114. doi: 10.1038/nrn731

Keller-Peck, C. R., Walsh, M. K., Gan, W. B., Feng, G., Sanes, J. R., and Lichtman, J. W. (2001). Asynchronous synapse elimination in neonatal motor units: Studies using GFP transgenic mice. *Neuron* 31, 381–394. doi: 10.1016/S0896-6273(01)00383-X

Khan, M. M., Lustrino, D., Silveira, W. A., Wild, F., Straka, T., Issop, Y., et al. (2016). Sympathetic innervation controls homeostasis of neuromuscular junctions in health and disease. *Proc. Natl. Acad. Sci. U.S.A.* 113, 746–750. doi: 10.1073/pnas.1524272113

Kim, N., Stiegler, A. L., Cameron, T. O., Hallock, P. T., Gomez, A. M., Huang, J. H., et al. (2008). Lrp4 is a receptor for agrin and forms a complex with MuSK. *Cell* 135, 334–342. doi: 10.1016/j.cell.2008.10.002

Koike, S., Schaeffer, L., and Changeux, J. P. (1995). Identification of a DNA element determining synaptic expression of the mouse acetylcholine receptor δ-subunit gene. *Proc. Natl. Acad. Sci. U.S.A.* 92, 10624–10628. doi: 10.1073/pnas.92.23.10624

Komiya, Y., and Habas, R. (2008). Wnt signal transduction pathways. *Organogenesis* 4, 68–75. doi: 10.4161/org.4.2.5851

Koneczny, I., Cossins, J., Waters, P., Beeson, D., and Vincent, A. (2013). MuSK myasthenia gravis IgG4 disrupts the interaction of LRP4 with MuSK but both IgG4 and IgG1-3 can disperse preformed agrin-independent AChR clusters. *PLoS One* 8:e80695. doi: 10.1371/journal.pone.0080695

Kong, X. C., Barzaghi, P., and Ruegg, M. A. (2004). Inhibition of synapse assembly in mammalian muscle in vivo by RNA interference. *EMBO Rep.* 5, 183–188. doi: 10.1038/sj.embor.7400065

Koppel, N., Friese, M. B., Cardasis, H. L., Neubert, T. A., and Burden, S. J. (2019). Vezatin is required for the maturation of the neuromuscular synapse. *Mol. Biol. Cell* 30, 2571–2583. doi: 10.1091/mbc.E19-06-0313

Kummer, T. T., Misgeld, T., Lichtman, J. W., and Sanes, J. R. (2004). Nerve-independent formation of a topologically complex postsynaptic apparatus. *J. Cell Biol.* 164, 1077–1087. doi: 10.1083/jcb.200401115

Lai, Y., Choi, U. B., Leitz, J., Brose, N., Rhee, J., Brunger, A. T., et al. (2017). Molecular mechanisms of synaptic vesicle priming article molecular mechanisms of synaptic vesicle priming by Munc13 and Munc18. *Neuron* 95, 591–607.e10. doi: 10.1016/j.neuron.2017.07.004

Lashley, D., Palace, J., Jayawant, S., Robb, S., and Beeson, D. (2010). Ephedrine treatment in congenital myasthenic syndrome due to mutations in DOK7. *Neurology* 74, 1517–1523. doi: 10.1212/WNL.0b013e3181dd43bf

Latvanlehto, A., Fox, M. A., Sormunen, R., Tu, H., Oikarainen, T., Koski, A., et al. (2010). Muscle-derived collagen XIII regulates maturation of the skeletal neuromuscular junction. *J. Neurosci.* 30, 12230–12241. doi: 10.1523/JNEUROSCI.5518-09.2010

Le Panse, R., and Berrih-Aknin, S. (2013). Autoimmune myasthenia gravis: autoantibody mechanisms and new developments on immune regulation. *Curr. Opin. Neurol.* 26, 569–576. doi: 10.1097/WCO.0b013e328364d6cd

Lee, Y. I. (2020). Developmental neuromuscular synapse elimination: activity-dependence and potential downstream effector mechanisms. *Neurosci. Lett.* 718:134724. doi: 10.1016/j.neulet.2019.134724

Lee, Y. I., Li, Y., Mikesh, M., Smith, I., Nave, K. A., Schwab, M. H., et al. (2016). Neuregulin1 displayed on motor axons regulates terminal Schwann cell-mediated synapse elimination at developing neuromuscular junctions. *Proc. Natl. Acad. Sci. U.S.A.* 113, E479–E487. doi: 10.1073/pnas.1519156113

Lee, Y. I., Mikesh, M., Smith, I., Rimer, M., and Thompson, W. (2011). Muscles in a mouse model of spinal muscular atrophy show profound defects in neuromuscular development even in the absence of failure in neuromuscular transmission or loss of motor neurons. *Dev. Biol.* 356, 432–444. doi: 10.1016/j.ydbio.2011.05.667

Lee, Y., Rudell, J., and Ferns, M. (2010). Rapsyn interacts with the muscle acetylcholine receptor via α- helical domains in the α, β, and ε subunit intracellular loops. *Neuroscience* 163, 222–232. doi: 10.1016/j.neuroscience.2009.05.057.Rapsyn

Lee, Y., Rudell, J., Yechikhov, S., Taylor, R., Swope, S., and Ferns, M. (2008). Rapsyn carboxyl terminal domains mediate muscle specific kinase-induced phosphorylation of the muscle acetylcholine receptor. *Neuroscience* 153, 997–1007. doi: 10.1016/j.neuroscience.2008.03.009

Leite, M. I., Jacob, S., Viegas, S., Cossins, J., Clover, L., Morgan, B. P., et al. (2008). IgG1 antibodies to acetylcholine receptors in ' seronegative ' myasthenia gravis. *Brain* 131, 1940–1952. doi: 10.1093/brain/awn092

Lennon, V. A., Kryzer, T. J., Griesmann, G. E., O'suilleabhain, P. E., Windebank, A. J., Woppmann, A., et al. (1995). Calcium-channel antibodies in the lambert—eaton syndrome and other paraneoplastic syndromes. *N. Engl. J. Med.* 332, 1467–1475. doi: 10.1056/NEJM199506013322203

Li, L., Cao, Y., Wu, H., Ye, X., Zhu, Z., Xing, G., et al. (2016). Enzymatic activity of the scaffold protein rapsyn for synapse formation. *Neuron* 92, 1007–1019. doi: 10.1016/j.neuron.2016.10.023

Li, L., Zhou, J., James, G., Heller-Harrison, R., Czech, M. P., and Olson, E. N. (1992). FGF inactivates myogenic helix-loop-helix proteins through phosphorylation of a conserved protein kinase C site in their DNA-binding domains. *Cell* 71, 1181–1194. doi: 10.1016/S0092-8674(05)80066-2

Li, X. M., Dong, X. P., Luo, S. W., Zhang, B., Lee, D. H., Ting, A. K. L., et al. (2008). Retrograde regulation of motoneuron differentiation by muscle β-catenin. *Nat. Neurosci.* 11, 262–268. doi: 10.1038/nn2053

Li, Y., Lee, Y. I, and Thompson, W. J. (2011). Changes in aging mouse neuromuscular junctions are explained by degeneration and regeneration of muscle fiber segments at the synapse. *J. Neurosci.* 31, 14910–14919. doi: 10.1523/JNEUROSCI.3590-11.2011

Lichtman, J. W., and Colman, H. (2000). Synapse elimination and indelible memory. *Neuron* 25, 269–278. doi: 10.1016/S0896-6273(00)80893-4

Lijam, N., Paylor, R., McDonald, M. P., Crawley, J. N., Deng, C. X., Herrup, K., et al. (1997). Social interaction and sensorimotor gating abnormalities in mice lacking Dvl1. *Cell* 90, 895–905. doi: 10.1016/s0092-8674(00)80354-2

Lin, W., Burgess, R. W., Dominguez, B., Pfaff, S. L., Sanes, J. R., and Lee, K. F. (2001). Distinct roles of nerve and muscle in postsynaptic differentiation of the neuromuscular synapse. *Nature* 410, 1057–1064. doi: 10.1038/35074025

Lin, W., Dominguez, B., Yang, J., Aryal, P., Brandon, E. P., Gage, F. H., et al. (2005). Neurotransmitter acetylcholine negatively regulates neuromuscular synapse formation by a Cdk5-dependent mechanism. *Neuron* 46, 569–579. doi: 10.1016/j.neuron.2005.04.002

Lin, W., Sanchez, H. B., Deerinck, T., Morris, J. K., Ellisman, M., and Kuo-Fen, L. (2000). Aberrant development of motor axons and neuromuscular synapses in erbB2-deficient mice. *Proc. Natl. Acad. Sci. U.S.A.* 97, 1299–1304. doi: 10.1523/JNEUROSCI.23-12-05161.2003

Lindstrom, J. M., Seybold, M. E., Lennon, V. A., Whittingham, S., and Duane, D. D. (1976). Antibody to acetylcholine receptor in myasthenia gravis. Prevalence, clinical correlates, and diagnostic value. *Neurology* 26, 1054–1059.

Linnoila, J., Wang, Y., Yao, Y., and Wang, Z. Z. A. (2008). Mammalian homolog of *Drosophila* tumorous imaginal discs, Tid1, mediates agrin signaling at the neuromuscular junction. *Neuron* 60, 625–641. doi: 10.1016/j.neuron.2008.09.025

Liyanage, Y., Hoch, W., Beeson, D., and Vincent, A. (2002). The agrin/muscle-specific kinase pathway: new targets for autoimmune and genetic disorders at the neuromuscular junction. *Muscle Nerve* 25, 4–16. doi: 10.1002/mus.1218

Logan, C. V., Cossins, J., Rodríguez Cruz, P. M., Parry, D. A., Maxwell, S., Martínez-Martínez, P., et al. (2015). Congenital myasthenic syndrome Type 19 is caused by mutations in COL13A1, encoding the atypical non-fibrillar collagen type XIII α1 Chain. *Am. J. Hum. Genet.* 97, 878–885. doi: 10.1016/j.ajhg.2015.10.017

Luo, Z. G., Wang, Q., Zhou, J. Z., Wang, J., Luo, Z., Liu, M., et al. (2002). Regulation of AChR clustering by dishevelled interacting with MuSK and PAK1. *Neuron* 35, 489–505.

Lyons, P. R., and Slater, C. R. (1991). Structure and function of the neuromuscular junction in young adult mdx mice. *J. Neurocytol.* 20, 969–981.

Macpherson, P., Kostrominova, T., Tang, H., and Goldman, D. (2002). Protein kinase C and calcium/calmodulin-activated protein kinase II (CaMK II) suppress nicotinic acetylcholine receptor gene expression in mammalian muscle. A specific role for CaMK II in activity-dependent gene expression. *J. Biol. Chem.* 277, 15638–15646. doi: 10.1074/jbc.M109864200

Madhavan, R., and Peng, H. B. (2005). Critical review molecular regulation of postsynaptic differentiation at the neuromuscular junction. *IUBMB Life* 57, 719–730. doi: 10.1080/15216540500338739

Madhavan, R., Zhao, X. T., Ruegg, M. A., and Peng, H. B. (2005). Tyrosine phosphatase regulation of MuSK-dependent acetylcholine receptor clustering. *Mol. Cell Neurosci.* 28, 403–416. doi: 10.1016/j.mcn.2004.10.005

Martin, P. T., Kaufman, S. J., Kramer, R. H., and Sanes, J. R. (1996). Synaptic integrins in developing, adult, and mutant muscle: selective association of α1, α7A, and α7B integrins with the neuromuscular junction. *Dev. Biol.* 174, 125–139. doi: 10.1006/dbio.1996.0057

Martin, P. T., Scott, L. J. C., Porter, B. E., and Sanes, J. R. (1999). Distinct structures and functions of related pre- and postsynaptic carbohydrates at the mammalian neuromuscular junction. *Mol. Cell Neurosci.* 13, 105–118. doi: 10.1006/mcne.1999.0737

Martinez-Pena, Y., Valenzuela, I., Mouslim, C., and Akaaboune, M. (2010). Calcium/calmodulin kinase II-dependent acetylcholine receptor cycling at the mammalian neuromuscular junction in vivo. *J. Neurosci.* 30, 12455–12465. doi: 10.1523/JNEUROSCI.3309-10.2010

Martinez-Pena, Y., Valenzuela, I., Pires-Oliveira, M., and Akaaboune, M. (2013). PKC and PKA regulate AChR dynamics at the neuromuscular junction of living mice. *PLoS One* 8:e81311. doi: 10.1371/journal.pone.0081311

Maselli, R. A., Chong, J. X., Arredondo, J., Vázquez, J., Bamshad, M. J., Nickerson, D. A., et al. (2017). Presynaptic congenital myasthenic syndrome with a homozygous sequence variant in LAMA5 combines myopia, facial tics, and failure of neuromuscular transmission. *Am. J. Med. Genet. Part A* 173, 2240–2245. doi: 10.1002/ajmg.a.38291

Maselli, R. A., Ng, J. J., Anderson, J. A., Cagney, O., Arredondo, J., Williams, C., et al. (2009). Mutations in LAMB2 causing a severe form of synaptic congenital myasthenic syndrome. *J. Med. Genet.* 46, 203–208. doi: 10.1136/jmg.2008.063693

Matejas, V., Hinkes, B., Alkandari, F., Al-Gazali, L., Annexstad, E., Aytac, M. B., et al. (2010). Mutations in the human laminin beta2 (LAMB2) gene and the associated phenotypic spectrum. *Hum. Mutat.* 31, 992–1002. doi: 10.1002/humu.21304

McMacken, G. M., Spendiff, S., Whittaker, R. G., O'Connor, E., Howarth, R. M., Boczonadi, V., et al. (2019). Salbutamol modifies the neuromuscular junction in a mouse model of ColQ myasthenic syndrome. *Hum. Mol. Genet.* 28, 2339–2351. doi: 10.1093/hmg/ddz059

McMahan, U. J. (1990). The agrin hypothesis. *Cold Spring Harb. Symp. Quant. Biol.* 55, 407–418.

Méjat, A., Decostre, V., Li, J., Renou, L., Kesari, A., Hantaï, D., et al. (2009). Lamin A/C – mediated neuromuscular junction defects in Emery-Dreifuss muscular dystrophy. *J. Cell Biol.* 184, 31–44. doi: 10.1083/jcb.200811035

Méjat, A., Ramond, F., Bassel-Duby, R., Khochbin, S., Olson, E. N., and Schaeffer, L. (2005). Histone deacetylase 9 couples neuronal activity to muscle chromatin acetylation and gene expression. *Nat. Neurosci.* 8, 313–321. doi: 10.1038/nn1408

Misgeld, T., Burgess, R. W., Lewis, R. M., Cunningham, J. M., Lichtman, J. W., and Sanes, J. R. (2002). Roles of neurotransmitter in synapse formation: development of neuromuscular junctions lacking choline acetyltransferase. *Neuron* 36, 635–648. doi: 10.1016/S0896-6273(02)01020-6

Missias, A. C., Chu, G. C., Klocke, B. J., Sanes, J. R., and Merlie, J. P. (1996). Maturation of the acetylcholine receptor in skeletal muscle: regulation of the AChR g -to- e Switch. *Dev. Biol.* 238, 223–238.

Miyazawa, A., Fujiyoshi, Y., and Unwin, N. (2003). Structure and gating mechanism of the acetylcholein receptor pore. *Nature* 424, 949–955.

Miyoshi, S., Tezuka, T., Arimura, S., Tomono, T., Okada, T., and Yamanashi, Y. (2017). DOK7 gene therapy enhances motor activity and life span in ALS model mice. *EMBO Mol. Med.* 9, 880–889. doi: 10.15252/emmm.201607298

Mokkapati, S., Nischt, R., Smyth, N., Ho, M. S. P., and Bo, K. (2008). Nidogens – extracellular matrix linker molecules. *Microsc. Res. Tech.* 395, 387–395. doi: 10.1002/jemt.20567

Montanaro, F., Gee, S. H., Jacobson, C., Lindenbaum, M. H., Froehner, S. C., and Carbonetto, S. (1998). Laminin and alpha-dystroglycan mediate acetylcholine receptor aggregation via a MuSK-independent pathway. *J. Neurosci.* 18, 1250–1260.

Moransard, M., Borges, L. S., Willmann, R., Marangi, P. A., Brenner, H. R., Ferns, M. J., et al. (2003). Agrin regulates rapsyn interaction with surface acetylcholine receptors, and this underlies cytoskeletal anchoring and clustering *. *J. Biol. Chem.* 278, 7350–7359. doi: 10.1074/jbc.M210865200

Mouw, J. K., Ou, G., Weaver, V. M., Regeneration, T., Francisco, S., Francisco, S., et al. (2014). Extracellular matrix assembly: a multiscale deconstruction. *Nat. Rev. Mol. Cell Biol.* 15, 771–785. doi: 10.1038/nrm3902.Extracellular

Nachmansohn, D., and Machado, A. (1943). The formation of acetylcholine. A new enzyme: "choline acetylase. *J. Neurophysiol.* 6.5, 397–403.

Nagel, A., Engel, A. G., Lang, B., Newsom-Davis, J., and Fukuoka, T. (1988). Lambert-Eaton myasthenic syndrome IgG depletes presynaptic membrane active zone particles by antigenic modulation. *Ann. Neurol.* 24, 552–558. doi: 10.1002/ana.410240412

Nagel, A., Lehmann-Horn, F., and Engel, A. G. (1990). Neuromuscular transmission in the mdx mouse. *Muscle Nerve* 13, 742–749. doi: 10.1002/mus.880130813

Nguyen, Q. T., Parsadanian, A. S., Snider, W. D., and Lichtman, J. W. (1998). Hyperinnervation of neuromuscular junctions caused by GDNF overexpression in muscle. *Science* 279, 1725–1729. doi: 10.1126/science.279.5357.1725

Nishimune, H., Sanes, J. R., and Carlson, S. S. (2004). A synaptic laminin-calcium channel interaction organizes active zones in motor nerve terminals. *Nature* 432, 580–587. doi: 10.1038/nature03112

Nishimune, H., Valdez, G., Jarad, G., Moulson, C. L., Müller, U., Miner, J. H., et al. (2008). Laminins promote postsynaptic maturation by an autocrine mechanism at the neuromuscular junction. *J. Cell Biol.* 182, 1201–1215. doi: 10.1083/jcb.200805095

Noakes, P. G., Gautam, M., Mudd, J., Sanes, J. R., and Merlie, J. P. (1995). Aberrant differentiation of neuromuscular junctions in mice lacking s-laminin/laminin β2. *Nature* 374, 258–262. doi: 10.1038/374258a0

Ohkawara, B., Cabrera-Serrano, M., Nakata, T., Milone, M., Asai, N., Ito, K., et al. (2013). LRP4 third β-propeller domain mutations cause novel congenital myasthenia by compromising agrin-mediated musk signaling in a position-specific manner. *Hum. Mol. Genet.* 23, 1856–1868. doi: 10.1093/hmg/ddt578

Ohno, K., Anlar, B., and Engel, A. G. (1999). Congenital myasthenic syndrome caused by a mutation in the Ets-binding site of the promoter region of the acetylcholine receptor ϵ subunit gene. *Neuromuscul. Disord.* 9, 131–135. doi: 10.1016/S0960-8966(99)00007-3

Ohno, K., Brengman, J., Tsujino, A., and Engel, A. G. (1998). Human endplate acetylcholinesterase deficiency caused by mutations in the collagen-like tail subunit (ColQ) of the asymmetric enzyme. *Proc. Natl. Acad. Sci. U.S.A.* 95, 9654–9659.

Ohno, K., Engel, A. G., Shen, X.-M., Selcen, D., Brengman, J., Harper, C. M., et al. (2002). Rapsyn mutations in humans cause endplate acetylcholine-receptor deficiency and myasthenic syndrome. *Am. J. Hum. Genet.* 70, 875–885. doi: 10.1086/339465

Okada, K., Inoue, A., Okada, M., Murata, Y., Katuta, S., Jigami, T., et al. (2006). The muscle protein Dok-7 is essential for neuromuscular synaptogenesis. *Science* 312, 1802–1806.

Oskoui, M., Jacobson, L., Chung, W., Haddad, J., Vincent, A., Kaufmann, P., et al. (2008). Fetal acetylcholine receptor inacti-vation syndrome and maternal myas-thenia gravis. *Neurology* 71, 2008–2014.

Oury, J., Liu, Y., Töpf, A., Todorovic, S., Hoedt, E., Preethish-Kumar, V., et al. (2019). MACF1 links Rapsyn to microtubule- and actin-binding proteins to maintain neuromuscular synapses. *J. Cell Biol.* 218, 1686–1705. doi: 10.1083/jcb.201810023

Pane, M., Staccioli, S., Messina, S., D'Amico, A., Pelliccioni, M., Mazzone, E. S., et al. (2008). Daily salbutamol in young patients with SMA type II. *Neuromuscul. Disord.* 18, 536–540. doi: 10.1016/j.nmd.2008.05.004

Patrick, G. N., Zukerberg, L., Nikolic, M., de la Monte, S., Dikkes, P., and Tsai, L.-H. (1999). Conversion of p35 to p25 deregulates Cdk5 activity and promotes neurodegeneration. *Nature* 402, 615–622.

Peng, H. B., Ali, A., Dagget, D., Rauvala, H., Hassell, J., and Smalheiser, N. (1998). The relationship between perlecan and dystroglycan and its implication in the formation of the neuromuscular junction. *Cell Adhes Commun.* 5, 475–489.

Picchiarelli, G., Demestre, M., Zuko, A., Been, M., Higelin, J., Dieterlé, S., et al. (2019). FUS-mediated regulation of acetylcholine receptor transcription at neuromuscular junctions is compromised in amyotrophic lateral sclerosis. *Nat. Neurosci.* 22, 1793–1805. doi: 10.1038/s41593-019-0498-9

Proszynski, T. J., Gingras, J., Valdez, G., Krzewski, K., and Sanes, J. R. (2009). Podosomes are present in a postsynaptic apparatus and participate in its maturation. *Proc. Natl. Acad. Sci. U.S.A.* 106, 18373–18378.

Rafuse, V. F., Polo-Parada, L., and Landmesser, L. T. (2000). Structural and functional alterations of neuromuscular junctions in NCAM-deficient mice. *J. Neurosci.* 20, 6529–6539. doi: 10.1523/jneurosci.20-17-06529.2000

Ramarao, M. K., Bianchetta, M. J., Lanken, J., and Cohen, J. B. (2001). Role of rapsyn tetratricopeptide repeat and coiled-coil domains in self-association and nicotinic acetylcholine receptor clustering *. *J. Nurse Pract.* 276, 7475–7483. doi: 10.1074/jbc.M009888200

Reddy, L. V., Koirala, S., Sugiura, Y., Herrera, A. A., and Ko, C. (2003). Glial cells maintain synpatic structure and function and promote development of the neuromuscular junction in vivo. *Neuron* 40, 563–580.

Rich, M. M., and Lichtman, J. W. (1989). In vivo visualization of pre- and postsynaptic changes during synapse elimination in reinnervated mouse muscle. *J. Neurosci.* 9, 1781–1805. doi: 10.1523/jneurosci.09-05-01781.1989

Riethmacher, D., Sonnenberg-riethmacher, E., Brinkmann, V., Yamaai, T., and Lewin, G. R. (1997). Severe neuropathies in mice with targeted mutations in the ErbB3 receptor. *Nature* 389, 2–5.

Roche, S. L., Sherman, D. L., Dissanayake, K., Soucy, G., Desmazieres, A., Lamont, D. J., et al. (2014). Loss of glial Neurofascin155 delays developmental synapse elimination at the neuromuscular junction. *J. Neurosci.* 34, 12904–12918. doi: 10.1523/JNEUROSCI.1725-14.2014

Rodríguez Cruz, P. M., Al-Hajjar, M., Huda, S., Jacobson, L., Woodhall, M., Jayawant, S., et al. (2015). Clinical features and diagnostic usefulness of antibodies to clustered acetylcholine receptors in the diagnosis of seronegative myasthenia gravis. *JAMA Neurol.* 72, 642–649. doi: 10.1001/jamaneurol.2015.0203

Rodríguez Cruz, P. M., Cossins, J., De Paula Estephan, E., Munell, F., Selby, K., Hirano, M., et al. (2019). The clinical spectrum of the congenital myasthenic syndrome resulting from COL13A1 mutations. *Brain* 142, 1547–1560. doi: 10.1093/brain/awz107

Rodríguez Cruz, P. M., Sewry, C., Beeson, D., Jayawant, S., Squier, W., McWilliam, R., et al. (2014). Congenital myopathies with secondary neuromuscular transmission defects; a case report and review of the literature. *Neuromuscul. Disord.* 24, 1103–1110. doi: 10.1016/j.nmd.2014.07.005

Rodríguez Cruz, P., Palace, J., and Beeson, D. (2018). The neuromuscular junction and wide heterogeneity of congenital myasthenic syndromes. *Int. J. Mol. Sci.* 19:1677. doi: 10.3390/ijms19061677

Roghani, A., Feldman, J., Kohan, S. A., Shirzadi, A., Gundersen, C. B., Brecha, N., et al. (1994). Molecular cloning of a putative vesicular transporter for acetylcholine. *Proc. Natl. Acad. Sci. U.S.A.* 91, 10620–10624. doi: 10.1073/pnas.91.22.10620

Samuel, M. A., Valdez, G., Tapia, J. C., Lichtman, J. W., and Sanes, J. R. (2012). Agrin and synaptic laminin are required to maintain adult neuromuscular junctions. *PLoS One* 7:e46663. doi: 10.1371/journal.pone.0046663

Sanes, J. R. (2003). The basement membrane / basal lamina of skeletal muscle *. *J. Biol. Chem.* 287, 12601–12604. doi: 10.1074/jbc.R200027200

Schaeffer, L., De Kerchove d'Exaerde, A., and Changeux, J. P. (2001). Targeting transcription to the neuromuscular synapse. *Neuron* 31, 15–22. doi: 10.1016/S0896-6273(01)00353-1

Schaeffer, L., Duclert, N., Huchet-Dymanus, M., and Changeux, J. P. (1998). Implication of a multisubunit Ets-related transcription factor in synaptic expression of the nicotinic acetylcholine receptor. *EMBO J.* 17, 3078–3090. doi: 10.1093/emboj/17.11.3078

Schiavo, G., Matteoli, M., and Montecucco, C. (2000). Neurotoxins affecting neuroexocytosis. *Physiol. Rev.* 80, 717–766. doi: 10.1152/physrev.2000.80.2.717

Schlessinger, J. (2000). Cell signaling by receptor tyrosine kinases. *October* 103, 211–225. doi: 10.1016/j.cell.2010.06.011

Schmidt, N., Akaaboune, M., Gajendran, N., Martinez-Pena y Valenzuela, I., Wakefield, S., Thurnheer, R., et al. (2011). Neuregulin/ErbB regulate neuromuscular junction development by phosphorylation of α-dystrobrevin. *J. Cell Biol.* 195, 1171–1184. doi: 10.1083/jcb.201107083

Schmidt, N., Basu, S., Sladecek, S., Gatti, S., van Haren, J., Treves, S., et al. (2012). Agrin regulates CLASP2-mediated capture of microtubules at the neuromuscular junction synaptic membrane. *J. Cell Biol.* 198, 421–437. doi: 10.1083/jcb.201111130

Selcen, D., Shen, X.-M., Milone, M., Brengman, J., Ohno, K., Deymeer, F., et al. (2013). GFPT1-myasthenia: clinical, structural, and electrophysiologic heterogeneity. *Neurology* 81, 370–378. doi: 10.1212/WNL.0b013e31829c5e9c

Senderek, J., Müller, J. S., Dusl, M., Strom, T. M., Guergueltcheva, V., Diepolder, I., et al. (2011). Hexosamine biosynthetic pathway mutations cause neuromuscular transmission defect. *Am. J. Hum. Genet.* 88, 162–172. doi: 10.1016/j.ajhg.2011.01.008

Shen, C., Lu, Y., Zhang, B., Figueiredo, D., Bean, J., Jung, J., et al. (2013). Antibodies against low-density lipoprotein receptor-related protein 4 induce myasthenia gravis. *J. Clin. Invest.* 123, 5190–5202. doi: 10.1172/JCI66039

Shi, L., Butt, B., Ip, F. C. F., Dai, Y., Jiang, L., Yung, W. H., et al. (2010). Ephexin1 is required for structural maturation and neurotransmission at the neuromuscular junction. *Neuron* 65, 204–216. doi: 10.1016/j.neuron.2010.01.012

Shi, L., Fu, A. K. Y., and Ip, N. Y. (2012). Molecular mechanisms underlying maturation and maintenance of the vertebrate neuromuscular junction. *Trends Neurosci.* 35, 441–453. doi: 10.1016/j.tins.2012.04.005

Sicinski, P., Geng, Y., Ryder-cook, A. S., Barnard, E. A., Mark, G., Sicinski, P., et al. (1989). The molecular basis of muscular dystrophy in the mdx mouse: a point mutation Darlison and Pene J . Barnard published by: American Association for the advancement of science stable URL: http://www.jstor.org/stable/1704127 REFERENCES Linked references ar. *Science* 244, 1578–1580.

Slater, C. R. (1982). Postnatal maturation of nerve-muscle junctions in hindlimb muscles of the mouse. *Dev. Biol.* 94, 11–22. doi: 10.1016/0012-1606(82)90063-X

Slater, C. R. (2017). The structure of human neuromuscular junctions: some unanswered molecular questions. *Int. J. Mol. Sci.* 18:2183. doi: 10.3390/ijms18102183

Slater, C. R. (2019). 'Fragmentation' of NMJs: a sign of degeneration or regeneration? A long journey with many junctions. *Neuroscience* 439, 28–40. doi: 10.1016/j.neuroscience.2019.05.017

Sleigh, J. N., Grice, S. J., Burgess, R. W., Talbot, K., and Cader, M. Z. (2014). Neuromuscular junction maturation defects precede impaired lower motor neuron connectivity in Charcot-Marie-Tooth Type 2D mice. *Hum. Mol. Genet.* 23, 2639–2650. doi: 10.1093/hmg/ddt659

Smith, C. L., Mittaud, P., Prescott, E. D., Fuhrer, C., and Burden, S. J. (2001). Src, fyn, and yes are not required for neuromuscular synapse formation but are necessary for stabilization of agrin-induced clusters of acetylcholine receptors. *J. Neurosci.* 21, 3151–3160. doi: 10.1523/JNEUROSCI.21-09-03151.2001

Smith, I. W., Mikesh, M., Lee, Y. I., and Thompson, W. J. (2013). Terminal Schwann cells participate in the competition underlying neuromuscular synapse elimination. *J. Neurosci.* 33, 17724–17736. doi: 10.1523/JNEUROSCI.3339-13.2013

Son, Y. J., and Thompson, W. J. (1995). Nerve sprouting in muscle is induced and guided by processes extended by schwann cells. *Neuron* 14, 133–141. doi: 10.1016/0896-6273(95)90247-3

Springer, T. A. (1998). An Extracellular b -Propeller Module Predicted in Lipoprotein and Scavenger Receptors, Tyrosine Kinases, Epidermal Growth Factor Precursor, and Extracellular Matrix Components. *J. Mol. Biol.* 283, 837–862. doi: 10.1006/jmbi.1998.2115

Stanley, E. F., and Drachman, D. B. (1981). Denervation accelerates the degradation of junctional acetylcholine receptors. *Exp. Neurol.* 73, 390–396. doi: 10.1016/0014-4886(81)90274-0

Sudhof, T. C. (2012). The presynaptic active zone. *Neuron* 75, 11–25. doi: 10.1016/j.neuron.2012.06.012.The

Sugiyama, J. E., Glass, D. J., Yancopoulos, G. D., and Hall, Z. W. (1997). Laminin-induced acetylcholine receptor clustering: an alternative pathway. *J. Cell Biol.* 139, 181–191. doi: 10.1083/jcb.139.1.181

Sugiyama, J., Bowen, D. C., and Hall, Z. W. (1994). Dystroglycan binds nerve and muscle agrin. *Neuron* 13, 103–115.

Taetzsch, T., Tenga, M. J., and Valdez, G. (2017). Muscle fibers secrete FGFBP1 to slow degeneration of neuromuscular synapses during aging and progression of ALS. *J. Neurosci.* 37, 70–82. doi: 10.1523/JNEUROSCI.2992-16.2016

Takamori, M. (2020). Myasthenia gravis: from the viewpoint of pathogenicity focusing on acetylcholine receptor clustering, trans-synaptic homeostasis and synaptic stability. *Front. Mol. Neurosci.* 13:86. doi: 10.3389/fnmol.2020.00086

Tetruashvily, M. M., McDonald, M. A., Frietze, K. K., and Boulanger, L. M. (2016). MHCI promotes developmental synapse elimination and aging-related synapse loss at the vertebrate neuromuscular junction. *Brain Behav. Immun.* 56, 197–208. doi: 10.1016/j.bbi.2016.01.008

Tezuka, T., Inoue, A., Hoshi, T., Weatherbee, S. D., Burgess, R. W., Ueta, R., et al. (2014). The MuSK activator agrin has a separate role essential for postnatal maintenance of neuromuscular synapses. *Proc. Natl. Acad. Sci. U.S.A.* 111, 16556–16561. doi: 10.1073/pnas.1408409111

Till, J. H., Becerra, M., Watty, A., Lu, Y., Ma, Y., Neubert, T. A., et al. (2002). Crystal structure of the MuSK tyrosine kinase: Insights into receptor autoregulation. *Structure* 10, 1187–1196. doi: 10.1016/S0969-2126(02)00814-6

Tiziano, F. D., Lomastro, R., Abiusi, E., Pasanisi, M. B., Di Pietro, L., Fiori, S., et al. (2019). Longitudinal evaluation of SMN levels as biomarker for spinal muscular atrophy: results of a phase IIb double-blind study of salbutamol. *J. Med. Genet.* 56, 293–300. doi: 10.1136/jmedgenet-2018-105482

Torres, L. F. B., and Duchen, L. W. (1987). The mutant mdx: inherited myopathy in the mouse: morphological studies of nerves, muscles and end-plates. *Brain* 110, 269–299. doi: 10.1093/brain/110.2.269

Tzartos, J. S., Zisimopoulou, P., Rentzos, M., Karandreas, N., Zouvelou, V., Evangelakou, P., et al. (2014). LRP4 antibodies in serum and CSF from amyotrophic lateral sclerosis patients. *Ann. Clin. Transl. Neurol.* 1, 80–87. doi: 10.1002/acn3.26

Ueta, R., Tezuka, T., Izawa, Y., Miyoshi, S., Nagatoishi, S., Tsumoto, K., et al. (2017). The carboxyl-terminal region of Dok-7 plays a key, but not essential, role in activation of muscle-specific receptor kinase MuSK and neuromuscular synapse formation. *J. Biochem.* 161, 269–277. doi: 10.1093/jb/mvw073

Umemori, H., and Sanes, J. R. (2008). Signal regulatory proteins (SIRPS) are secreted presynaptic organizing molecules. *J. Biol. Chem.* 283, 34053–34061. doi: 10.1074/jbc.M805729200

Valdez, G., Tapia, J. C., Kang, H., Clemenson, G. D., Gage, F. H., Lichtman, J. W., et al. (2010). Attenuation of age-related changes in mouse neuromuscular synapses by caloric restriction and exercise. *Proc. Natl. Acad. Sci. U.S.A.* 107, 14863–14868. doi: 10.1073/pnas.1002220107

Vanhaesebrouck, A., Webster, R., Maxwell, S., Rodríguez Cruz, P., Cossins, J., Wickens, J., et al. (2019). β2-adrenergic agonists ameliorate the adverse effect of long-term pyridostigmine on neuromuscular junction structure. *Brain* 142, 3713–3727.

Vernet-Der Garabedian, B., Lacokova, M., Eymard, B., Morel, E., Faltin, M., Zajac, J., et al. (1994). Association of neonatal myasthenia gravis with antibodies against the fetal acetylcholine receptor. *J. Clin. Invest.* 94, 555–559. doi: 10.1172/JCI117369

Vincent, A. (2020). Antibodies and receptors: from neuromuscular junction to central nervous system. *Neuroscience* 439, 48–61. doi: 10.1016/j.neuroscience.2020.03.009

Vincent, A., and Newsom-Davis, J. (1985). Acetylcholine receptor antibody as a diagnostic test for myasthenia gravis: results in 153 validated cases and 2967 diagnostic assays. *J. Neurol. Neurosurg. Psychiatry* 48, 1246–1252.

Wadman, R. I., Vrancken, A. F. J. E., Van Den Berg, L. H., and Van Der Pol, W. L. (2012). Dysfunction of the neuromuscular junction in spinal muscular atrophy types 2 and 3. *Neurology* 79, 2050–2055. doi: 10.1212/WNL.0b013e3182749eca

Warrell, D. A. (2010). Snake bite. *Lancet* 375, 77–88. doi: 10.1016/S0140-6736(09)61754-2

Warrell, D. A. (2019). Venomous bites, stings, and poisoning: an update. *Infect. Dis. Clin. North Am.* 33, 17–38. doi: 10.1016/j.idc.2018.10.001

Weatherbee, S. D., Anderson, K. V., and Niswander, L. A. (2006). LDL-receptor-related protein 4 is crucial for formation of the neuromuscular junction. *Development* 133, 4993–5000. doi: 10.1242/dev.02696

Weston, C., Gordon, C., Teressa, G., Hod, E., Ren, X. D., and Prives, J. (2003). Cooperative regulation by Rac and Rho of agrin-induced acetylcholine receptor clustering in muscle cells. *J. Biol. Chem.* 278, 6450–6455. doi: 10.1074/jbc.M210249200

Williams, A. H., Valdez, G., Moresi, V., Qi, X., McAnally, J., Elliott, J. L., et al. (2009). MicroRNA-206 delays ALS progression and promotes regeneration of neuromuscular synapses in mice. *Science* 326, 1549–1554. doi: 10.1126/science.1181046

Wolfe, G. I., Kaminski, H. J., Aban, I. B., Minisman, G., Kuo, H.-C., Marx, A., et al. (2016). Randomized trial of thymectomy in myasthenia gravis. *N. Engl. J. Med.* 375, 511–522. doi: 10.1056/NEJMoa1602489

Wood, S. J., and Slater, C. R. (2001). Safety factor at the neuromuscular junction. *Prog. Neurobiol.* 64, 393–429.

Wu, H., Xiong, W. C., and Mei, L. (2010). To build a synapse: signaling pathways in neuromuscular junction assembly. *Development* 137, 1017–1033. doi: 10.1242/dev.038711

Xie, Z., Samuels, B. A., and Tsai, L. H. (2006). Cyclin-dependent kinase 5 permits efficient cytoskeletal remodeling – a hypothesis on neuronal migration. *Cereb. Cortex* 16, i64–i68. doi: 10.1093/cercor/bhj170

Xing, G., Jing, H., Zhang, L., Cao, Y., Li, L., Zhao, K., et al. (2019). A mechanism in agrin signaling revealed by a prevalent Rapsyn mutation in congenital myasthenic syndrome. *eLife* 8:e49180. doi: 10.7554/eLife.49180

Yang, F., Je, H. S., Ji, Y., Nagappan, G., Hempstead, B., and Lu, B. (2009). Pro-BDNF-induced synaptic depression and retraction at developing neuromuscular synapses. *J. Cell Biol.* 185, 727–741. doi: 10.1083/jcb.200811147

Yang, J. F., Cao, G., Koirala, S., Reddy, L. V., and Ko, C. P. (2001). Schwann cells express active agrin and enhance aggregation of acetylcholine receptors on muscle fibers. *J. Neurosci.* 21, 9572–9584. doi: 10.1523/jneurosci.21-24-09572.2001

Yang, J., Dominguez, B., De Winter, F., Gould, T. W., Eriksson, J. E., and Lee, K. F. (2011). Nestin negatively regulates postsynaptic differentiation of the neuromuscular synapse. *Nat. Neurosci.* 14, 324–330. doi: 10.1038/nn.2747

Yang, X., Arber, S., William, C., Li, L., Tanabe, Y., Jessell, T. M., et al. (2001). Patterning of muscle acetylcholine receptor gene expression in the absence of motor innervation. *Neuron* 30, 399–410. doi: 10.1016/S0896-6273(01)00287-2

Yumoto, N., Kim, N., and Burden, S. J. (2012). Lrp4 is a retrograde signal for presynaptic differentiation at neuromuscular synapses. *Nature* 489, 438–442. doi: 10.1038/nature11348

Zainul, Z., Heikkinen, A., Koivisto, H., Rautalahti, I., Kallio, M., Lin, S., et al. (2018). Collagen XIII is required for neuromuscular synapse regeneration and functional recovery after peripheral nerve injury. *J. Neurosci.* 38, 4243–4258. doi: 10.1523/JNEUROSCI.3119-17.2018

Zhang, B., Luo, S., Dong, X-P., Zhang, X., Liu, C., Luo, Z., et al. (2007). β-catenin regulates acetylcholine receptor clustering in muscle cells through interaction with rapsyn. *J. Neurosci.* 27, 3968–3973. doi: 10.1523/JNEUROSCI.4691-06.2007

Zhang, B., Luo, S., Wang, Q., Suzuki, T., Xiong, W. C., and Mei, L. (2008). LRP4 serves as a coreceptor of agrin NIH public access. *Neuron* 23, 285–297. doi: 10.1016/j.neuron.2008.10.006

Zhang, B., Tzartos, J. S., Belimezi, M., Ragheb, S., Bealmear, B., Lewis, R. A., et al. (2012). Autoantibodies to lipoprotein-related protein 4 in patients with double-seronegative myasthenia gravis. *Arch. Neurol.* 69, 445–451. doi: 10.1001/archneurol.2011.2393

Zhang, W., Coldefy, A.-S., Hubbard, S. R., and Burden, S. J. (2011). Agrin binds to the N-terminal region of Lrp4 protein and stimulates association between Lrp4 and the first immunoglobulin-like domain in muscle-specific kinase (MuSK). *J. Biol. Chem.* 286, 40624–40630. doi: 10.1074/jbc.M111.279307

Zhao, K., Shen, C., Li, L., Wu, H., Xing, G., Dong, Z., et al. (2018). Sarcoglycan alpha mitigates neuromuscular junction decline in aged mice by stabilizing LRP4. *J. Neurosci.* 38, 8860–8873. doi: 10.1523/JNEUROSCI.0860-18.2018

Zoltowska Katarzyna, M., Belaya, K., Leite, M., Patrick, W., Vincent, A., and Beeson, D. (2014). Collagen Q – A potential target for autoantibodies in myasthenia gravis. *J. Neurol. Sci.* 348, 241–244. doi: 10.1016/j.jns.2014.12.015

Zoltowska, K., Webster, R., Finlayson, S., Maxwell, S., Cossins, J., Müller, J., et al. (2013). Mutations in GFPT1 that underlie limb-girdle congenital myasthenic syndrome result in reduced cell-surface expression of muscle AChR. *Hum. Mol. Genet.* 22, 2905–2913. doi: 10.1093/hmg/ddt145

Zong, Y., Zhang, B., Gu, S., Lee, K., Zhou, J., Yao, G., et al. (2012). Structural basis of agrin – LRP4 – MuSK signaling. *Genes Dev.* 4, 247–258. doi: 10.1101/gad.180885.111.synapse

Zuber, B., and Unwin, N. (2013). Structure and superorganization of acetylcholine receptor – rapsyn complexes. *Proc. Natl. Acad. Sci. U.S.A.* 110, 10622–10627. doi: 10.1073/pnas.1301277110

Conflict of Interest: University of Oxford and AV hold patents and receive royalties for antibody assays from Euroimmun AG and Athena Diagnostics.

The remaining authors declare that the literature review was conducted in the absence of any commercial or financial relationships that could be construed as a potential conflict of interest.

Copyright © 2020 Rodríguez Cruz, Cossins, Beeson and Vincent. This is an open-access article distributed under the terms of the Creative Commons Attribution License (CC BY). The use, distribution or reproduction in other forums is permitted, provided the original author(s) and the copyright owner(s) are credited and that the original publication in this journal is cited, in accordance with accepted academic practice. No use, distribution or reproduction is permitted which does not comply with these terms.

frontiers in Human Neuroscience

ORIGINAL RESEARCH
published: 07 December 2020
doi: 10.3389/fnhum.2020.560860

Long Term Follow-Up on Pediatric Cases With Congenital Myasthenic Syndromes—A Retrospective Single Centre Cohort Study

Adela Della Marina[1], Eva Wibbeler[2], Angela Abicht[3,4], Heike Kölbel[1], Hanns Lochmüller[5,6,7], Andreas Roos[1] and Ulrike Schara[1]*

[1]Department of Neuropediatrics, Developmental Neurology and Social Pediatrics, University Children's Hospital Essen, University Duisburg-Essen, Essen, Germany, [2]Children's Hospital, University Medical Center Hamburg Eppendorf, Hamburg, Germany, [3]Medical Genetic Center Munich, Munich, Germany, [4]Friedrich-Baur Institute, Ludwig Maximilian University, Munich, Germany, [5]Children's Hospital of Eastern Ontario Research Institute, Division of Neurology, Department of Medicine, The Ottawa Hospital, Brain and Mind Research Institute, University of Ottawa, Ottawa, ON, Canada, [6]Department of Neuropediatrics and Muscle Disorders, Faculty of Medicine, Medical Center-University of Freiburg, Freiburg, Germany, [7]Centro Nacional de Análisis Genómico (CNAG-CRG), Center for Genomic Regulation, Barcelona Institute of Science and Technology (BIST), Barcelona, Spain

OPEN ACCESS

Edited by:
Filippo Brighina,
University of Palermo, Italy

Reviewed by:
Carmelo Rodolico,
University of Messina, Italy
Teerin Liewluck,
Mayo Clinic, United States
Vincenzo Di Stefano,
University of Palermo, Italy

***Correspondence:**
Adela Della Marina
adela.dellamarina@uk-essen.de

Specialty section:
This article was submitted to Motor Neuroscience, a section of the journal Frontiers in Human Neuroscience

Received: 10 May 2020
Accepted: 16 November 2020
Published: 07 December 2020

Citation:
Della Marina A, Wibbeler E, Abicht A, Kölbel H, Lochmüller H, Roos A and Schara U (2020) Long Term Follow-Up on Pediatric Cases With Congenital Myasthenic Syndromes—A Retrospective Single Centre Cohort Study. Front. Hum. Neurosci. 14:560860. doi: 10.3389/fnhum.2020.560860

Introduction: Congenital myasthenic syndromes (CMS) refer to a heterogenic group of neuromuscular transmission disorders. CMS-subtypes are diverse regarding exercise intolerance and muscular weakness, varying from mild symptoms to life-limiting forms with neonatal onset. Long-term follow-up studies on disease progression and treatment-response in pediatric patients are rare.

Patients and Methods: We analyzed retrospective clinical and medication data in a cohort of 32 CMS-patients including the application of a standardized, not yet validated test (CMS-ST) to examine muscular strength and endurance in 21 patients at the last follow-up. Findings obtained in our cohort were compared with long-term follow-up studies of (adult) CMS-cohorts from the literature by considering the underlying molecular mechanisms. Outcomes of CMS-ST were compared to results of normal clinical assessment.

Results: Thirty-two pediatric patients with defects in eight different CMS-genes were followed by a median time of 12.8 years. Fifty-nine percentage of patients manifested with first symptoms as neonates, 35% as infants. While 53% of patients presented a reduced walking distance, 34% were wheelchair-bound. Even under adequate therapy with pyridostigmine (PS) and 3,4-diaminopyridine, *CHAT*-mutations led to the progression of muscular weakness partly in combination with persistent respiratory and bulbar symptoms. *RAPSN, CHRND*, and *CHRNB1* patients with neonatal manifestation, early respiratory problems, and bulbar symptoms showed a good and maintained treatment response. *CHAT* and *CHRNE* patients required higher PS dosages, whereas *RAPSN* patients needed a lower mean dosage at the last follow-up. The benefits of short-term

Abbreviations: AChR, acetylcholine receptor; bw, body weight; ChAT, choline acetyltransferase; CMS, congenital myasthenic syndrome; CMS-ST, CMS standardized test; COLQ, endplate acetylcholinesterase deficiency; FVC, forced vital capacity; MG, Myasthenia gravis; NMJ, the neuromuscular junction; PS, Pyridostigmine; 3,4 DAP, 3,4 Diaminopyridine.

medication and long-term progression of symptoms were highly dependent on the specific genetic defect. CMS-ST was carried out in 17/21 patients, determined affected muscle groups including bulbar and ocular symptoms, some of which were not reported by the patients.

Conclusions: Our findings and comparison with the literature- suggest a better treatment-response and less severe progression of symptoms present in patients suffering from mutations in CMS-genes directly associated with receptor deficiency, while patients with defects leading to synaptopathy and presynaptic defects tend to have worse outcomes. Assessment of affected muscular groups and clinical symptoms by CMS-ST may be a useful tool for optimal therapeutic management of the patients, especially for future clinical studies.

Keywords: congenital myasthenic syndrome, neuromuscular transmission, therapy, long-term outcome, standardized testing

INTRODUCTION

Congenital myasthenic syndromes (CMS) are a phenotypic heterogeneous group of hereditary diseases caused by disturbed or impaired neuromuscular transmission, resulting in clinical symptoms such as muscle weakness and increased muscle fatigue.

Clinical presentation and severity may vary enormously and depend on the underlying genetic mutation and the regular localization of the responding protein. Abnormal muscle fatigue can affect various muscle groups: limb-girdle, distal, proximal, cervical (axial), respiratory, eye, facial, and bulbar muscles. Notably, smooth and heart muscles are generally not affected (Abicht et al., 2017). The patients present their first symptoms usually at birth or in the first 2 years of life. Nevertheless, initial manifestations are known, albeit much less frequently, up to advanced age and then are frequently misdiagnosed as seronegative MG (especially mutations in the *RAPSN, DOK7*, and slow-channel syndrome; Croxen et al., 1997; Burke et al., 2003; Durmus et al., 2018; Kao et al., 2018).

In the recent decade, the genetic background of the CMS expanded, and currently, more than 35 causative genes have been published (Engel, 2018; Thompson et al., 2018; Vanhaesebrouck and Beeson, 2019). Remarkably, synaptic (*COLQ*) and postsynaptic mutations in acetylcholine receptor *(AChR), RAPSN*, and *DOK7* are more common than mutations in genes encoding for presynaptic localized proteins as exemplified on the cohort of the Mayo clinic where synaptic/postsynaptic defects account for 87% of the diagnosed cases (Engel, 2018).

The CMS subtypes are predominantly inherited in an autosomal recessive fashion, with exception of the slow-channel syndromes and the mutations in *SNAP25* and *SYT2*, which have an autosomal dominant inheritance (Engel et al., 2015; Abicht et al., 2017; Engel, 2018; Vanhaesebrouck and Beeson, 2019).

Long term follow-up studies in pediatric patients with CMS are rare and urgently needed for the counseling of the patients and their families. Up to now, there are no standardized tests in use in children for objective measurement of muscle strength and to assess the limits of the therapy.

To overcome both limitations, we retrospectively studied the clinical characteristics and medication data of 32 children with genetically proven forms of CMS. At their last follow-up visit, 21 patients had undergone a standardized, previously not validated test (CMS-ST) to examine their muscular strength and endurance. Patients were sub-grouped according to their genetic defect and associated pathomechanism and the main focus was spent on long-term problems and the limits of the drug therapy.

MATERIALS AND METHODS

At the University Hospital of Essen (Department for Neuropediatrics), a retrospective chart review was performed for all patients diagnosed with CMS who were at regular follow up between January 2010 and December 2015. Doing so, the medical records of 32 patients from 27 families were reviewed. The prerequisite for inclusion in this study was the genetically confirmed diagnosis of a CMS. The retrospective data were collected from the patient records. Written informed consent was obtained from the participants (or rather their legal guardians) for participation in the subsequent research as well as for the publication of the findings (including any potentially-identifying information). Ethical approval for this study was obtained from the University Essen clinical ethics committee (10-4543).

For this study, a questionnaire was used and completed together with the patients and their families, and a standardized clinical examination was carried out. The following data were obtained: sex, age, identification of a causative mutation, family history, course of birth and pregnancy, early childhood development, course of the disease, initial and current symptoms, age at the diagnosis, demographic background, and applied drug and supportive therapies. Treatment modalities, time, and duration of therapy were also recorded in all patients. For patients for whom either only retrospective data could be collected or for whom there were gaps during the survey, missing clinical data were extracted from the medical records.

To evaluate the current clinical status, in 18 patients older than 3 years willing to participate, the modified quantitative

myasthenia gravis score (QMG) score was performed. The QMG score has been modified by us to allow assessments in children and infants with CMS and was applied at the last clinic visit (Chaouch et al., 2012). It is a standardized test (CMS-ST) procedure using two different forms depending on age. One is for infants and young children up to the age of three, the other for children from the age of three, adolescents, and adults (**Supplementary Figures 1A,B**).

The patients were categorized based on their genetic background in presynaptic, synaptic, and postsynaptic (with kinetic defects) sub-groups. Additionally, we compared our long-term data with clinical observations obtained in three independent long-term studies focusing on adult and mixed adult-pediatric CMS-cohorts (Natera-de Benito et al., 2017; Durmus et al., 2018; Kao et al., 2018).

Statistical Analysis

Continuous variables (age, duration of medical treatment, length of the follow-up period) are reported as mean, minimum, and maximum values. Categorical variables (disease classification) are reported as frequencies and percentages based on the total sample.

RESULTS

Patients and Demographics

The gender distribution in the present patient population was male to female 16:16.

Of 27 families, five families (19%) had two affected siblings, respectively. A total of 4 out of 27 families (15%) had one sibling who died in infancy or childhood. In 9/27 families (33%), the mother had at least one miscarriage. 6/27 families (22%) were consanguineous. For 12/27 families (44%) both parents came from Germany, for the remaining 15 families (56%) at least one parent was of non-German origin (**Supplementary Table 1**).

Genetic Background and Patient Categorization

Given that a detailed classification of CMS disease entities is suitable for use in clinical and genetic databases and decision support systems (Thompson et al., 2018), our 32 patients were assigned to eight different genetic CMS sub-forms and further sub-categorized according to the location of the loss of the functional protein (based on the underlying genetic defect) at the NMJ (**Supplementary Table 1**): "Presynaptic mutations" (*CHAT*, OMIM: 254210) were found in five patients (16%), "synaptic mutations" (*COLQ*, OMIM: 603034) in three patients (9%) and "postsynaptic mutations" in a total of 24 patients (75%). Out of these 24 patients, 8 (25%) presented with pathogenic *RAPSN*-variants (OMIM: 616326), seven patients (22%) with *CHRNE* mutations (OMIM: 608931), three patients (9%) with *DOK7* mutations (OMIM: 254300), two patients (6%) with slow-channel *CHRNE* variants (OMIM: 605809), and each one patient (3%) with mutations in *MUSK* (OMIM: 616325), *CHRND* (OMIM: 616323), *CHRNB1* (OMIM: 616314), fast-channel *CHRNE* (OMIM: 616324), respectively.

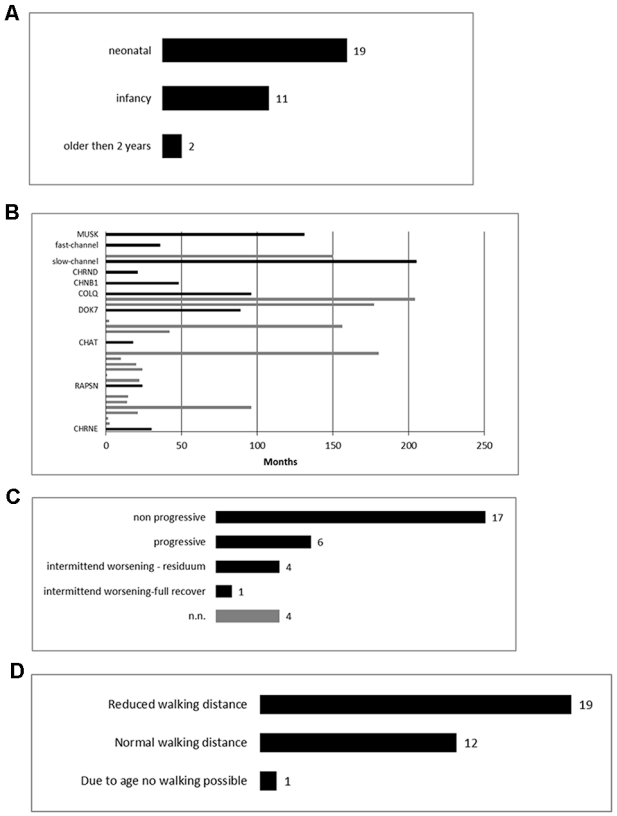

FIGURE 1 | Clinical findings of our overall congenital myasthenic syndromes (CMS) cohort. **(A)** Age of clinical manifestation of the symptoms (n = 32). **(B)** Time from onset of the first symptoms to diagnosis (n = 29). **(C)** The clinical course of the patients (n = 32). **(D)** Walking distance at the point of clinical evaluation (n = 32).

Age of Onset and Point of Diagnosis

Apart from categorization according to the underlying genetic defect and vulnerability at the NMJ, the patients were further classified according to the age of onset of their symptoms in three sub-groups: neonatal period, infancy, and older than 2 years.

The age onset varied from neonatal (59%) to 96 months (mean: 9.1 months; **Figure 1A**).

In 29 patients the exact age of diagnosis was stated with a mean of 69 months (range: 0–216 months). The mean duration between the onset of symptoms and diagnosis was 63.3 months (range 0–205 months; **Figure 1B**).

Clinical Outcome

The mean follow-up period was 144, median 153 months (range 6–346 months) and although all patients improved during the pharmacological therapy for at least some of their symptoms, several still showed disease progression over time (**Figure 1C**).

Motor Development and Endurance

Motor development in infancy was delayed in 19/32 patients (58%) and appeared to be regular in 13/32 patients (42%).

In 29/32 patients (90%), intermittent worsening (respiratory worsening or/and increased muscular weakness) occurred during the disease.

The walking distance was limited in 18/32 patients (56%), in one patient (3%) walking was not yet possible due to her age (6 months, **Figure 1D**).

Clinical Findings CMS-Patients Stratified by the Genetic Cause

Presynaptic Mutations

Choline Acetyltransferase (ChAT) Deficiency

The presynaptic sub-cohort is defined by five patients with pathogenic *CHAT* mutations (**Supplementary Table 1**). Consanguinity of the parents was present in 3/4 families (two patients were siblings).

In 2/5 patients intrauterine reduced fetal movements were noticed and 3/5 patients showed first symptoms in the neonatal period. The mean time between the onset of symptoms and diagnosis was 3 years and 8 months (range: 0 months to 13 years), with one sibling being diagnosed directly neonatal. Motor development was normal in 3/5 patients. Clinical symptoms at onset are summarized in **Table 1**.

Notably, symptoms improved in all patients under therapy with pyridostigmine (PS), with a mean dosage of 5.0 mg/kg/day (range: 3.3–8.5 mg/kg/day). 2/5 patients were additionally treated with 3,4-diaminopyridine (3,4 DAP; mean dosage 1.1 mg/kg/day (range: 0.9–1.2 mg/kg/day) showing a further improvement in symptoms. Further 2/5 patients were treated with 3,4-DAP in the past without a notable effect. At their last follow-up, all patients had generalized muscular weakness and were wheelchair depended for longer distances. Moreover, 3/5 patients presented with intellectual disability (two of them had cerebral palsy as well as severe mental impairment as residuum due to hypoxic episodes during respiratory crises).

Clinical aspects of 2/5 patients were already published (Schmidt et al., 2003; Schara et al., 2010).

Based on the CMS-ST performed, in two patients, lateral diplopia could be provoked, muscular strength was severely reduced in proximal as well in distal muscles. Although respiratory insufficiency during infections was reported from both patients, FVC was normal (**Supplementary Tables 2, 3**).

Synaptic Mutations

Endplate Acetylcholinesterase Deficiency (COLQ)

In three patients (from three independent families, consanguinity between the parents existed in 1/3 families, with one clinically affected father rejecting genetic testing) pathogenic mutations in the *COLQ* were identified (**Supplementary Table 1**).

In 2/3 patients, clinical onset was noticed in the neonatal period and in 1/3 patients during the first year of life. Only for one of these patients, the exact data concerning the diagnosis was available (at the age of 9).

The clinical symptoms at onset are summarized in **Table 1**.

The course of the disease was non-progressive in 2/3 of patients (one patient even had a normal walking distance). Two patients developed scoliosis and one was treated surgically.

All three patients experienced a worsening of their clinical symptoms under the therapy with PS. The therapy for all three was started before the genetic diagnosis was confirmed. Two patients were treated with ephedrine during the period of data collection and an improvement of their symptoms was noticed. The mean dosage was 4.4 mg/kg/day. In the case of one patient, the parents initially refused to administer ephedrine; thus she received the therapy later on and as a result, improved her walking distance. One patient showed an abnormal pupillary reflex.

Here, in only one patient the CMS-ST was performed. Her muscular strength in the upper extremities was poorer compared to lower extremities (**Supplementary Table 2**).

Postsynaptic Mutations

CHRNE

Seven patients with pathogenic mutations in the *CHRNE* came from six independent families, three of them were consanguineous. For one patient, reduced fetal movements during pregnancy were reported. Ptosis and ophthalmoparesis were present and persisted in all patients (**Table 1**).

All patients were under therapy with PS. The mean dosage was 5.1-mg/kg/day (range: 1.3–11.9 mg/kg/day). Initially, clinical improvement was noticed in all of them, however, in 2/7 patients muscle weakness increased in the disease course despite medication. Furthermore, 3/7 patients additionally received 3,4-DAP at the time of their last follow-up visit (mean dosage was 1.4-mg/kg/day; range: 0.3–2.6 mg/kg/day).

6/7 patients experienced acute worsening of their symptoms partly triggered by infections.

At last follow-up, the walking distance was limited in 4/7 patients.

Based on the CMS-ST performed, in five patients a discrepancy between the possibility to step-up (possible in 5/5) and to perform the squats (possible in 3/5) was noticed. Muscular strength was more reduced in cervical muscles than in proximal and distal muscles (**Supplementary Tables 2, 3**).

RAPSN

In eight patients from six independent, non-consanguineous families pathogenic *RAPSN* mutations were identified; in 2/6 families, two children were affected in each case.

At neonatal presentation, 7/8 patients had a facial and generalized muscular weakness, and poor abilities to cry and suck, further complicated by respiratory problems (3/8 needed ventilatory support). All patients experienced intermittent episodes with worsening of their symptoms (in 4/8 muscular weakness and respiratory insufficiency), usually triggered by infections (**Table 1**). At the last follow-up, 3/8 patients reported chewing difficulties and in 2/8 joint contractions were noticed. One patient had moderate scoliosis which developed before PS therapy was initiated. Notably, 7/8 patients had normal walking distance. All patients improved under therapy with PS (mean dosage 3.3 mg/kg/day) and the course of the disease was non-progressive. Some of the clinical symptoms in two patients from this group have been already published (Schara et al., 2012).

TABLE 1 | Response to therapy, symptoms at onset, and long term course in patients according to the NMJ-localization of the protein affected by the respective mutation.

Classification	Gene	Symptom onset (number of pat)	Response to treatment (number of pat)	Clinical symptoms at onset	Long term course/problems
Presynaptic	*CHAT*	Neonatal (3/5) Infancy (2/5)	PS: improvement (5/5) DAP: additional improvement (2/5), no improvement (2/5)	Ptosis Facial and generalized muscular weakness Bulbar symptoms Intermittent worsening with respiratory insufficiency	Progressive muscular weakness Limited walking distance Scoliosis Bulbar symptoms Respiratory insufficiency with NIV Residual symptoms due to hypoxic injury
Synaptic	*COLQ*	Neonatal (2/3) Infancy (1/3)	PS: worsening (3/3) EPH: improvement (2/3)	Ptosis, ophthalmoparesis, Facial and generalized muscular weakness High arched palate Bulbar symptoms Intermittent worsening of symptoms with respiratory insufficiency Delayed motor development	Stabilization of respiratory problems Scoliosis Respiratory insufficiency Non-progressive course Limited walking distance
Postsynaptic	*CHRNE*	Neonatal (3/7) Infancy (4/7)	PS: improvement (7/7) DAP: additional improvement (3/7)	Ptosis, ophthalmoparesis Facial and proximal muscular weakness Delayed motor development	Stabilization of respiratory symptoms Limited walking distance No effect of therapy on ophthalmoparesis
	CHRND	Neonatal (1/1)	PS: improvement (1/1)	Ptosis, ophthalmoparesis Facial and generalized muscular weakness Bulbar symptoms Intermittent worsening of symptoms with respiratory insufficiency during infections Delayed motor development	Stabilization of respiratory symptoms Non-progressive course Joint contractures
	CHRNB1	Neonatal (1/1)	PS: improvement (1/1) DAP: additional improvement	Ptosis, ophthalmoparesis Facial and generalized muscular weakness Bulbar and respiratory symptoms Intermittent worsening with respiratory insufficiency	Stabilization of respiratory symptoms Ophthalmoparesis, facial muscular weakness Limited walking distance
Postsynaptic	*MUSK*	Neonatal (1/1)	PS: partial improvement (1/1) DAP: no effect (1/1) EPH: improvement (1/1)	Ptosis, ophthalmoparesis Facial and generalized muscular weakness, axial muscular weakness Bulbar and respiratory symptoms Intermittent worsening with respiratory insufficiency Delayed motor development	Stabilization of respiratory problems Persistent axial muscular weakness Limited walking distance Scoliosis Atrophic tongue
	DOK7	Infancy (2/3) Childhood (1/3)	PS: worsening (2/3), no effect (1/3) EPH: improvement (3/3)	Reduced fetal movements during pregnancy Ptosis, facial muscular weakness Intermittent worsening of symptoms with respiratory insufficiency Limb-girdle muscular weakness Delayed motor development	Intermittent worsening with partial improvement Improvement of respiratory symptoms Nasal speech Scoliosis Limited walking distance Muscular atrophy

(Continued)

TABLE 1 | Continued

Classification	Gene	Symptom onset (number of pat)	Response to treatment (number of pat)	Clinical symptoms at onset	Long term course/problems
	RAPSN	Neonatal (7/8) Infancy (1/8)	PS: improvement (8/8)	Reduced fetal movements during pregnancy Arthrogryposis multiplex congenita Ptosis, bulbar symptoms Respiratory insufficiency during infection Delayed motor development	Improvement of symptoms, non-progressive course Stabilization of respiratory symptoms Strabismus Scoliosis Joint contractures
Postsynaptic-kinetic	*CHRNE fast*	Neonatal (1/1)	PS: improvement (1/1) DAP: additional improvement (1/1)	Ptosis, ophthalmoparesis Facial and generalized muscle weakness Bulbar and respiratory symptoms Intermittent worsening of symptoms with respiratory insufficiency	Improvement of symptoms Limited walking distance
	CHRNE slow	Infancy (2/2)	PS: no effect (2/2) CHI: improvement (2/2)	Ptosis, ophthalmoparesis Muscular hypotonia in infancy Normal motor development Distal muscular weakness	Intermittent worsening with persistent weakness Limited walking distance

Nr., number; pat, patients; PS, Pyridostigmine; DAP, 3,4 Diaminopyridine, EPH, Ephedrine, CHS, Chinidine sulfate; NIV, non-invasive ventilation.

Results of the standardized test applied in this group, showed in 2/6 patients reduced muscle endurance and in 3/6 reduced strength in neck flexors—both symptoms were not assessed through normal clinical assessment (**Supplementary Tables 2, 3**).

MUSK

A male patient from a non-consanguineous family with a pathogenic compound heterozygous *MUSK* mutation (**Supplementary Table 1**) was identified. The onset of the first symptoms was noticed in the neonatal period. He was tracheotomized from the age of 8 months to 8 years; due to respiratory insufficiency, he needed non-invasive ventilation during the night and partially during the day. He was able to walk at the age of 2 years and showed impaired mental development. His walking distance was limited due to proximal and axial muscular weakness (dropped head) and his muscular strength worsened during infections. Therapy with PS and 3,4-DAP was only partially effective as respiratory problems continued. After the confirmation of molecular genetic diagnosis at the age of 10 years, he received ephedrine and his respiratory situation, bulbar symptoms, and muscular strength improved.

CHRNB1

One female patient from a non-consanguineous family with CMS-causative mutations in the *CHRNB1* had the first onset of symptoms during the neonatal period. She experienced repeated episodes with worsening of her respiratory symptoms and muscular weakness up to the age of 2 years. She improved under therapy with PS (dosage 5.88 mg/kg/day), started at the age of 4 years. In addition, the patient received 3.4-DAP (0.44 mg/kg/day). Despite therapy, she experienced progression of her muscular endurance and at her last visit in our clinic (age 14 years and 6 months) presented with ptosis, ophthalmoparesis, facial and generalized muscular weakness accompanied by reduced walking distance.

CHRND

In one male patient from a non-consanguineous German family, compound heterozygous CMS-causative mutations in the *CHRND* were identified (**Supplementary Table 1**). His symptom onset was neonatal with a combination of facial, ocular, bulbar, and muscular symptoms. The patient improved under therapy with PS at the age of 21 months and had at last visit (age 13 years and 6 months) normal walking distance but distal finger joint contractures. The PS dosage was 5.2 mg/kg/day.

In CMS-ST, he had only mild reduced muscle endurance in his extremities, which was also reported during the normal clinical assessment (**Supplementary Tables 2, 3**).

DOK7

Two male and one female patient derived from three non-consanguineous families (all of German origin) with pathogenic *DOK7* mutations were identified in our CMS cohort (**Supplementary Table 1**). Clinical data of two patients have already been published (Schara et al., 2012; Shieh and Oh, 2018).

In two patients, the onset of symptoms (proximal weakness with reduced walking distance) was observed in infancy (12 months) and in one patient at the age of 6 years. The mean time between the onset of symptoms and diagnosis was 10 years 3 months (range: 7 years 5 months to 18). In one patient, the creatine kinase (CK) value was mildly increased (298 U/l).

Motor development in infancy was delayed in 2/3 of patients (axial weakness, in one generalized muscle weakness, and respiratory insufficiency with tracheostomy). All patients had

ptosis and muscular hypotonia (limb-girdle muscle affected; in two patients generalized muscular atrophy was noticed).

Because of some clinical features suggestive of CMS, therapy with PS was given before the genetic diagnosis. A significant worsening of the condition was noticed in two patients; in one patient there was no effect upon therapeutic intervention. Although the diagnosis and therapy were considerably delayed, all three patients had marked improvement in their muscular endurance and better walking distance under therapy with ephedrine (average dose: 1.9-mg/kg/day; range: 0.8–3.6 mg/kg/day). One patient was even symptom-free. However, the patients also reported side effects under this therapy, including palpitations, dry mouth with a sore throat, increased perspiration, light intolerance due to mydriasis, and tremor.

One patient performed CMS-ST and showed extremely weak neck flexors in combination with proximal muscle weakness (no squats possible; **Supplementary Table 2**).

Kinetic Defects of the Acetylcholine Receptor (AChR)

Slow-Channel CMS

In two female patients (siblings) of a non-consanguineous family (German origin; father also affected) pathogenic mutations leading to "slow-channel-CMS" were identified (**Supplementary Table 1**).

Muscular hypotonia as the first clinical symptom manifested at the age of 6 and 10 months but with normal further motor development. The course of the disease was progressive with episodes of muscular weakness; the younger sister had reduced walking distance. On clinical examination (aged 17 years and 11 months and 13 years and 15 months), both sisters had ptosis, ophthalmoparesis, and proximal and distal muscular weakness (especially hands and fingers).

Treatment with PS was discontinued in both due to lack of effect. The patients were under therapy with quinidine sulfate by mean dosage 6.6 mg/kg/day (range 6.1–7.2 mg/kg/day) at last follow-up. The older sister didn't indicate any subjective improvement, the younger sister showed a clear improvement of her muscular endurance.

Fast-Channel CMS

In one male patient from a non-consanguineous family, a compound heterozygous mutation causative for the manifestation of "fast-channel-CMS" was identified (**Supplementary Table 1**). The onset of the symptoms was neonatal. His motor milestones were delayed, and he had respiratory crises during infancy.

At the age of 3 years and 9 months, therapy with PS was started leading to a partial improvement of the symptoms. Therefore, 3.4 DAP was added (PS 7.0 mg/kg/day and 3.4-DAP 1.1 mg/kg/day) with further benefit. Although under this therapy, there was no further progression of his weakness, muscular hypotonia, ptosis, and ophthalmoparesis persisted. His walking distance was moderately reduced.

In CMS-ST, he had reduced muscle endurance in his extremities, which was also reported during the normal clinical assessment. Due to his age, he was not able to perform all tasks (**Supplementary Tables 2, 3**).

Standardized Testing (CMS-ST)

In three patients younger than 3 years, the standardized questionnaire was used (see **Supplementary Figure 1A**). Due to age, no standardized clinical endurance test was possible here. However, 18 patients were examined with the questionnaire for children from the age of 3 years, adolescents, and adults (**Supplementary Figure 1B**). Because of mental and motor impairment in one older patient (*CHAT* mutation, **Supplementary Table 1**, patient 1), no standardized clinical testing was possible.

A total of 14 out of the 17 patients underwent lung function testing (forced vital capacity; FVC): eight patients (*CHRNE*, *RAPSN*, and *CHRND*) presented with normal findings, whereas two (*CHRNE* and *RAPSN*) had mild and two (*RAPSN* and *COLQ*) had a moderate restrictive function, respectively. One *DOK7* patient even showed a severe restrictive ventilation disorder. There was no evidence of diaphragm weakness in lung function testing. Electrocardiogram (ECG) data were available for 15/18 patients and findings were all normal in all 15 cases. In patients between the age of 4 and 8 years, we observed only partial compliance in test performance (**Supplementary Table 2**). In **Table 2**, the results of testing in comparison to clinical assessments are presented showing more respiratory and bulbar symptoms identified by the test than reported by the patients themselves during the clinical assessment. Interestingly, in the testing of endurance, better performance was achieved by following the standardized investigation compared to the performance reported by the patients themselves (**Table 2**).

TABLE 2 | Results of standardized test (CMS-ST) in 17/21 patients compared to neurological assessment and reported symptoms by patients and their parents.

Clinical symptom	CMS-ST (*n* = 17)	Clinical assessment and self-reported (*n* = 17)
Ocular symptoms	Ptosis: 15/17 patients, Double vision: 13/17 patients	Ptosis: 13/17 patients9/17 double vision reported
Bulbar symptoms	10/17 patients	6/17 patients reported chewing problems
Respiratory function	6/14 abnormal	5/17 patients reported respiratory problems
Cervical weakness	15/17 patients	Not stated
Proximal weakness	10/17 patients	5/17 patients
Distal weakness	11/17 patients	Not stated
Impaired muscular endurance	8/17 Patienten	13/17 impaired muscular endurance reported

Pulmonary function was performed in 14/17 patients; one patient was intellectually impaired and not capable to perform the test (total: n = 17).

DISCUSSION

Here, we present a cohort of pediatric patients with genetically proven CMS-causing mutations (**Supplementary Table 1**). Pathogenic variants affecting postsynaptic proteins were more prevalent (69% of patients), especially occurring in the *RAPSN* and *CHRNE* genes—known as frequent CMS-causative genes in Middle and Eastern European and North American cohorts as well as from single-center cohort from India (Abicht et al., 2012; Natera-de Benito et al., 2017; Engel, 2018; Selvam et al., 2018). Based on a relatively large proportion of patients with Turkish and Arabian background at our muscular center, *CHAT* mutations were more frequent compared to adult cohorts from Turkey and a reported mixed adult-pediatric cohort from Spain (**Table 3A**). In all patients, the phenotype at onset was identical with descriptions from the literature and may be used as a "clinical clue" toward starting of therapeutic intervention as long as the genetic testing is still pending (Abicht et al., 2012; Durmus et al., 2018; Engel, 2018). In the context of a comparison of our cohort with adult cohorts, it is important to note that for that purpose only patients with defects in genes also identified to be mutated in our cohort have been extracted from the different studies (**Table 3A**).

Interestingly, long term symptoms and problems show mostly similar findings with only some differences compared to the observations in two adult CMS- and one adult-pediatric cohort (**Table 3A**): in comparison to adults (34%), in our group, only 6% of patients had onset of symptoms after infancy. This discrepancy implies that our patients had an earlier onset and a more severe phenotype resulting in higher severity of symptoms in the long term. This observation might accord with the fact that for some of the CMS-subtypes discrepancy for clinical manifestation was reported, even in families with the same haplotypes (*CHAT*, *CHRNE*, *RAPSN*) (Burke et al., 2003; Schara et al., 2010; Natera-de Benito et al., 2016b). However, a bias can also be caused by retrospective memorizing of disease history when personal anamnesis is made in adult patients or based on a late consultation in adulthood although the disease showed first symptoms or even full clinical manifestation in childhood.

Nonetheless, an overall finding is that disease progression and response to therapies is highly gene- and pathomechanism specific in CMS as previously reported (Thompson et al., 2019).

Presynaptic Mutations

Our data confirm the observation being made by Schara and colleagues (Schara et al., 2010) reporting that patients with presynaptic mutations in *CHAT* show progression in their muscular symptoms with persistent bulbar symptoms despite the application of standard therapy defining the need for targeted therapeutic strategies as recently described by Thompson and co-workers (Thompson et al., 2019). Worth noting, our findings support the concept of a beneficial effect of 3,4-DAP on muscular endurance as observed in the patients with *CHAT* mutations (see "Results" section), a therapeutic observation that was previously reported in only one child and one adult (Schara et al., 2010; Natera-de Benito et al., 2017).

Three patients developed scoliosis, for which no comparative data are available. Two out of three patients with scoliosis had residuum due to hypoxic episodes during infancy and are also mentally impaired. We postulate that the manifestation of scoliosis in these two patients occurred as the consequence of wheelchair dependency long-term in combination with severe axial and proximal weakness; one patient with preserved ambulation showed only mild scoliosis without the need for operative correction.

Although ocular symptoms are not known in *CHAT* patients, in ocular testing double vision could be provoked during longer glance to side as a symptom of ocular muscle weakness (**Table 2**, **Supplementary Table 2**). Cognitive impairment as a possible associated symptom have already been reported with partial association with hypoxic episodes during respiratory crises (Schara et al., 2010; McMacken et al., 2018). Based on an ubiquitous expression of ChAT, one might speculate that cognitive impairment observed in some patients might result from tissue-specific functions of the proteins which can (in some cases) only partially be compensated upon loss of the functional protein. However, compared to three adult patients described in adult cohorts (Natera-de Benito et al., 2017; Durmus et al., 2018), no information about their mental status was available.

Synaptic Mutations

In the synaptic group, the symptoms can improve even after the late start of the therapy (patient 6) and most patients seem to have a non-progressive course of the disease. Still, the walking distance can be limited with wheelchair dependence for longer distances. Persistence of the symptoms in follow up is comparable with that found in adults (Durmus et al., 2018). Also similar as in adult cohorts, scoliosis can be one of the clinical symptoms specific to AChE deficiency, as already postulated (Mihaylova et al., 2008; Wargon et al., 2012; Duran et al., 2013; Durmus et al., 2018). A very specific indicator for this mutation is worsening of symptoms under therapy with AChE inhibitors (Wargon et al., 2012; Durmus et al., 2018), a clinical observation which could be confirmed in our sub-cohort. We could observe an abnormal pupillary reflex in only one patient-supporting previous reports describing the clinical observation as a less frequent feature (Mihaylova et al., 2008). Given that the presence of abnormal pupillary reflex is often considered as a "clinical clue" for AChE-deficiency patients, the absence of this finding does not exclude *COLQ* mutations as the causative genetic variant (Wargon et al., 2012). The patient of the synaptic sub-cohort show a combination of proximal and cervical muscular weakness whereas distal muscular weakness was not present in these patients (**Table 3A**) but reported in 8/15 patients of the Spanish adult cohort (Wargon et al., 2012).

Postsynaptic Mutations

Compared to adults, long-term problems in pediatric cases of the postsynaptic group are similar and already present

TABLE 3A | Comparison of findings in different CMS cohorts. Only patients with defects in genes also identified to be mutated in our cohort have been extracted from the different studies. Comparison of adult and mixed cohort patients and our cohort including follow-up time, point of symptom onset, time of diagnosis, and clinical symptoms depending on underlying mutation and characterization depending on the functional position on NMJ.

Study	Affected genes (Nr. of pat.)	Follow-up time (range)	Symptom onset (Nr. of pat.)	Onset to diagnosis	Long term problems in different CMS subtypes	Long term problems in pre-synaptic, synaptic, and post-synaptic forms
Natera-de Benito et al. (2017)	*CHAT* (2/64) *COLQ* (9/64) *CHRNE* (15/64) *DOK7* (7/64) *RAPSN* (11/64) Slow-channel (4/64)	Mean age at last follow up 27 years (range 0.5–80)	Neonatal (17/48) Infancy (20/48) Later (11/48)	Median time from onset to diagnosis: 7 years (range 0–47.5)	Ptosis: *CHAT, COLQ, CHRNE, RAPSN, DOK7*, slow-channel Ophthalmoparesis: *CHRNE*, slow-channel Bulbar symptoms: *CHAT, COLQ, CHRNE, RAPSN, DOK7*, slow-channel Proximal muscle weakness: *COLQ, CHRNE, RAPSN, DOK7*, slow-channel Distal muscular weakness: *CHAT*, slow-channel Cervical muscular weakness: *CHAT, COLQ, RAPSN, DOK7*, slow-channel Scoliosis: *COLQ, CHRNE, DOK7*, slow-channel Wheelchair dependence: *COLQ, CHRNE, DOK7*	Presynaptic: Ptosis, bulbar symptoms, distal and cervical muscle weakness Synaptic: Ptosis, bulbar symptoms, proximal and cervical muscular weakness, scoliosis, wheelchair dependence Postsynaptic: Ptosis, ophthalmoparesis, bulbar symptoms, proximal, distal, and cervical muscle weakness, scoliosis, wheelchair dependence
Durmus et al. (2018)	*CHAT* (1/69) *COLQ* (5/69) *CHRNE* (46/69) *DOK7* (3/69) Slow-channel (3/69) Fast-channel (3/69)	Median time: 9.8 years (1–22 years)	Neonatal (26/61) Infancy (13/61) Later: (15/61) (exact information was not provided for all patients)	Mean time from onset to diagnosis: 12.9 years	Ptosis: *CHAT, CHRNE*, slow-channel Ophthalmoparesis: *CHRNE*, slow-channel Bulbar symptoms: *COLQ* Proximal muscle weakness: *CHAT, COLQ, CHRNE, DOK7* Distal muscle weakness: COLQ, slow-channel Cervical muscle weakness: slow-channel Scoliosis: *COLQ* Wheelchair dependence: *CHAT* Ventilatory supp.: *CHAT, COLQ*, slow-channel	Presynaptic: Ptosis, proximal muscle weakness, ventilatory support Synaptic: Bulbar symptoms, scoliosis, ventilator support, proximal and distal muscular weakness Postsynaptic: Ptosis, ophthalmoparesis, proximal, distal, and cervical muscle weakness, ventilatory support
Kao et al. (2018)	*COLQ* (2/34) *CHRNE* (1/34) *DOK7* (14/34) *RAPSN* (6/34) slow channel (2/34)	Not stated	Neonatal and Infancy (11/34) Before 5 years of age (17/34) Later: (6/34)	Median time from symptom onset to diagnosis: 26.0 (4–56.5) years	Ptosis: *DOK7, RAPSN* Proximal muscle weakness: *COLQ, DOK7, RAPSN* Wheelchair dependence: *DOK7, COLQ* Ventilatory supp.: *RAPSN, COLQ*	Presynaptic: No patients Synaptic: Proximal muscle weakness, wheelchair dependence, ventilatory support Postsynaptic: Ptosis, proximal muscle weakness, wheelchair dependence, ventilatory supp.

(Continued)

TABLE 3A | Continued

Study	Affected genes (Nr. of pat.)	Follow-up time (range)	Symptom onset (Nr. of pat.)	Onset to diagnosis	Long term problems in different CMS subtypes	Long term problems in pre-synaptic, synaptic, and post-synaptic forms
Our cohort	*CHAT* (5/32) *COLQ* (3/32) *CHRNE* (7/32) *DOK7* (3/32) *RAPSN* (8/32) *MUSK* (1/32) Slow channel (2/32) Fast channel (1/32)	Mean time: 12 years (range 0.5–28 years)	Neonatal (19/32) Infancy (11/32) Older than 2 years (2/32)	Mean time from symptom onset to diagnosis: 5.3 years (range 0–17 years)	Ptosis: *CHAT, COLQ, CHRNE, DOK7, RAPSN*, MUSK, slow-channel Ophthalmoparesis: *COLQ, CHRNE, DOK7, MUSK*, slow-channel Bulbar symptoms: *CHAT, COLQ, CHRNE, RAPSN*, MUSK, fast channel Proximal muscle weakness: *CHAT, COLQ, RAPSN* Distal muscle weakness: *CHAT, COLQ, RAPSN* Cervical muscle weakness: *CHAT, COLQ, RAPSN* Scoliosis: *CHAT, COLQ, CHRNE, DOK7, RAPSN, MUSK* Wheelchair dependence: *CHAT, COLQ, CHRNE, DOK7* Ventilatory supp.: *CHAT, COLQ, DOK7, MUSK* Feeding tube: *CHAT, MUSK*	Presynaptic: Ptosis, bulbar symptoms (feeding tube), proximal, distal, and cervical muscular weakness, scoliosis, wheelchair dependence, ventilatory support Synaptic: Ptosis, ophthalmoparesis, bulbar symptoms, proximal, distal, and cervical muscular weakness, scoliosis, wheelchair dependence, ventilatory support Postsynaptic: Ptosis, ophthalmoparesis, bulbar symptoms, proximal, distal, and cervical muscular weakness, scoliosis, wheelchair dependence, ventilatory supp.

TABLE 3B | Response to applied therapy in two adult/one mixed and in our cohort.

Study	Pyridostigmine	3,4 Diaminopyridine	Acetazolamide	Albuterol/Salbutamole	Ephedrine	Fluoxetine	Chinidine
Natera-de Benito et al. (2017)	↑*CHRNE, RAPSN*	↑*CHRNE, RAPSN, DOK7*	-	↑*CHAT, COLQ, DOK7*, slow channel	↑*CHAT, COLQ, DOK7*, slow channel	slow channel	-
Durmus et al. (2018)	↑*CHAT, CHRNE*, slow channel(short), fast channel ↓ *DOK7*	-	-	↑*CHAT, DOK7*, slow channel	-	↑slow channel	-
Kao et al. (2018)	↑*CHRNE, DOK7, RAPSN* ↓*DOK7*, slow channel	↑*CHRNE, DOK7, RAPSN* ↓*DOK7*	↑ *RAPSN*	↑*COLQ, CHRNE, DOK7, RAPSN*	↑*DOK7, RAPSN*	↑slow channel	-
Our cohort	↑*CHAT, CHRNE, RAPSN*, fast channel ↓*COLQ, DOK7*	↑*CHAT, CHRNE*, fast channel	-	-	↑*COLQ, DOK7*	-	↑slow channel

Nr., number; pat., patients; supp., support; ↑, improvement;↓, worsening.

at the younger age, but improve over disease course: in case of *RAPSN* and *CHRNE* mutations, an improvement of neonatal symptoms such as bulbar problems or intermittent worsening as well in muscular endurance was observed and accord with known clinical observations described previously (McMacken et al., 2018). In our post-synaptic CMS cohort, a progression of muscular weakness under therapy could only be observed in singular cases suffering from *CHRNE* mutations. Although adult patients regularly improve under therapy, also here singular cases without optimal therapy response were reported in case of *CHRNE and DOK7* mutations (Natera-de Benito et al., 2016b; Durmus et al., 2018; Kao et al., 2018; **Table 3B**).

Persistent respiratory problems were present only in one *DOK7* and one *MUSK* patients, respectively. In this context, it is important to note that for both patients the start of an appropriate therapy was delayed (*DOK7* patient 18 years, *MUSK* patient 10 years) and both were already on ventilation before the ephedrine-therapy was started.

General Therapy Response

Throughout the cohort presented here, drug therapy was started between the age of 3 weeks and 18 years. Whereas for pediatric cases no comparable long-term data are available from the present literature, those are reported for adults (Durmus et al., 2018 and **Table 3A**). Contrary to adults reporting the good effect of salbutamol/albuterol in patients with *CHAT, DOK7, COLQ, CHRNE, or RAPSN* mutations, we used ephedrine as monotherapy in case of *COLQ* and *DOK7* with good clinical response (**Table 3B**).

Although the cohort presented here is too small for an interpretation of the individual subgroups regarding the therapeutic effect, a progression of muscular weakness in a *CHAT* (five patients) group was observed despite therapy, indicating a less effective response to therapeutic intervention in this subgroup. If started administrated early, 3,4-DAP as we observed here, as well as of ephedrine/salbutamol already investigated in adult cohorts (**Table 3B**), might have an additional positive effect on long term outcome.

However, in siblings from the postsynaptic group (*RAPSN, CHRNE*) being treated very early, no severe worsening of the respiratory symptoms during the infections was observed. Thus, one might speculate that early therapeutic intervention in the postsynaptic group might prevent patients from worsening during infection triggered crises.

To our knowledge, this is the first CMS-cohort of children with mutations in genes encoding for different proteins localized to the NMJ where the dosage of therapy at the last follow-up visit has been calculated. Interestingly, only patients with *RAPSN* mutations need a low mean dosage of AChE inhibitors, at last follow up, to have a stable/static disease condition compared to patients with mutations in other CMS-causative genes. This not only has advantages based on a lower potential to suffer from side effects but also can be an indicator for stabilization of the symptoms in the course of the disease (Natera-de Benito et al., 2016a; Estephan et al., 2018). Interestingly, with 7.6 mg/kg/day the mean dosage administered to patients from a Spanish cohort (total of 10 patients, partially adults) was higher than in our patients (Natera-de Benito et al., 2016a). In our cohort the mean age at diagnosis and treatment start (3.4 years) was lower compared to the Spanish cohort (8.9 years)—so we postulate that early treatment in this group will reduce the need for medication later on.

In line with the known side effects of the drug at higher dosages, patients mentioned increased secretion production, diarrhea, and abdominal pain under the therapy with AChE inhibitors (Schara and Lochmüller, 2008).

As already described for adult CMS patients, in the case of the pediatric *DOK7*, *COLQ*, and "slow channel" patients included in this study, no beneficial changes occurred during the administration of AChE inhibitors or disease conditions even worsened significantly.

This therapy was started before the genetic diagnosis was confirmed due to some suggestive clinical features. In the case of *DOK7* patients, the weekly worsening of the muscular strength in combination with limb-girdle muscular weakness in the absence of ophthalmoplegia is the specific clinical clue. In the absence of abnormal pupillary reflexes, the phenotype of *COLQ* patients can overlap with other CMS with apnea (*CHRNE, CHRND, CHRNB1*) making the phenotypical differentiation difficult. Consequently, a very careful initiation of the therapy in case of negative genetic (or pending) findings is needed and the requirement of individual treatment strategies is suggested (Thompson et al., 2019).

Standardized Test

Although our cohort was too small for standardized evaluation of the applied test, we could observe that younger patients (under the age of 10) have problems with the implementation especially due to lack of concentration, motivation, and compliance. Therefore, we conclude that ST-CMS (**Supplementary Figure 1B**) is not suitable for standard testing in patients under the age of 10 years, whereby normal cognitive development is also crucial, especially in the testing of the endurance of each muscle group (arm or leg holding).

Interestingly, performing CMS-ST disclosed more clinical symptoms than reported by the patients themselves (**Table 2**) and can differentiate the distribution of muscular weakness. Hence, this testing protocol may be one of the possible tools for a more precise assessment of the effect of therapeutic intervention in the case of prospective studies. Due to the differences in the phenotypical presentation in dependence of the underlying mutations in different CMS-causative genes, we would propose the use of the test as a tool for assessment of intra-individual effect of therapy.

DATA AVAILABILITY STATEMENT

The original contributions presented in the study are included in the article/**Supplementary Materials**, further inquiries can be directed to the corresponding author.

ETHICS STATEMENT

The studies involving human participants were reviewed and approved by University Essen clinical ethics committee, 10-4543. Written informed consent to participate in this study was provided by the participants and their legal guardian/next of kin.

AUTHOR CONTRIBUTIONS

ADM designed the study and performed clinical follow up and study supervision as well as analysis and interpretation of data. ADM and AR designed the structure of the manuscript and wrote the first draft. EW performed clinical follow up studies, standardized testing and analysis and interpretation of data. HL provided the clinical questionnaire. AA provided the molecular genetic information. US designed the study and performed study supervision and critically revised the manuscript. EW, HK, HL and AA critically revised the manuscript and provided important intellectual content.

FUNDING

HL receives support from the Canadian Institutes of Health Research (Foundation Grant FDN-167281), the Canadian Institutes of Health Research and Muscular Dystrophy Canada (Network Catalyst Grant for NMD4C), the Canada Foundation for Innovation (CFI-JELF 38412), and the Canada Research Chairs program (Canada Research Chair in Neuromuscular Genomics and Health, 950-232279).

ACKNOWLEDGMENTS

We thank the patients and their families who agreed to take part in this study. A part of the data presented here was collected in the contest of the MD project (Dr. med.) of EW.

SUPPLEMENTARY MATERIAL

The Supplementary Material for this article can be found online at: https://www.frontiersin.org/articles/10.3389/fnhum.2020.560860/full#supplementary-material.

REFERENCES

Abicht, A., Dusl, M., Gallenmüller, C., Guergueltcheva, V., Schara, U., Della Marina, A., et al. (2012). Congenital myasthenic syndromes: achievements and limitations of phenotype-guided gene-after-gene sequencing in diagnostic practice: a study of 680 patients. *Hum. Mutat.* 33, 1474–1484. doi: 10.1002/humu.22130

Abicht, A., Muller, J. J., and Lochmüller, H. (2017). Congenital myasthenic syndromes—genereviews®—NCBI bookshelf. Available online at: https://www.ncbi.nlm.nih.gov/books/NBK1168/. Accessed December 23, 2019.

Burke, G., Cossins, J., Maxwell, S., Owens, G., Vincent, A., Robb, S., et al. (2003). Rapsyn mutations in hereditary myasthenia: distinct early- and late-onset phenotypes. *Neurology* 61, 826–828. doi: 10.1212/01.WNL.0000085865.55513.AE

Chaouch, A., Beeson, D., Hantaï, D., and Lochmüller, H. (2012). 186th ENMC international workshop: congenital myasthenic syndromes 24-26 June 2011, Naarden, The Netherlands. *Neuromuscul. Disord.* 22, 566–576. doi: 10.1016/j.nmd.2011.12.004

Croxen, R., Newland, C., Beeson, D., Oosterhuis, H., Chauplannaz, G., Vincent, A., et al. (1997). Mutations in different functional domains of the human muscle acetylcholine receptor α subunit in patients with the slow-channel congenital myasthenic syndrome. *Hum. Mol. Genet.* 6, 767–774. doi: 10.1093/hmg/6.5.767

Duran, G. S., Uzunhan, T. A., Ekici, B., Çitak, A., Aydinli, N., and Çaliş kan, M. (2013). Severe scoliosis in a patient with COLQ mutation and congenital myasthenic syndrome: a clue for diagnosis. *Acta Neurol. Belg.* 113, 531–532. doi: 10.1007/s13760-013-0179-5

Durmus, H., Shen, X. M., Serdaroglu-Oflazer, P., Kara, B., Parman-Gulsen, Y., Ozdemir, C., et al. (2018). Congenital myasthenic syndromes in Turkey: clinical clues and prognosis with long term follow-up. *Neuromuscul. Disord.* 28, 315–322. doi: 10.1016/j.nmd.2017.11.013

Engel, A. G. (2018). Congenital myasthenic syndromes in 2018. *Curr. Neurol. Neurosci. Rep.* 18:46. doi: 10.1007/s11910-018-0852-4

Engel, A. G., Shen, X. M., Selcen, D., and Sine, S. M. (2015). Congenital myasthenic syndromes: pathogenesis, diagnosis and treatment. *Lancet Neurol.* 14, 420–434. doi: 10.1016/S1474-4422(14)70201-7

Estephan, E. P., Zambon, A. A., Marchiori, P. E., da Silva, A. M. S., Caldas, V. M., Moreno, C. A. M., et al. (2018). Clinical variability of early-onset congenital myasthenic syndrome due to biallelic RAPSN mutations in Brazil. *Neuromuscul. Disord.* 28, 961–964. doi: 10.1016/j.nmd.2018.08.007

Kao, J. C., Milone, M., Selcen, D., Shen, X. M., Engel, A. G., and Liewluck, T. (2018). Congenital myasthenic syndromes in adult neurology clinic: a long road to diagnosis and therapy. *Neurology* 91, E1770–E1777. doi: 10.1212/WNL.0000000000006478

McMacken, G., Whittaker, R. G., Evangelista, T., Abicht, A., Dusl, M., and Lochmüller, H. (2018). Congenital myasthenic syndrome with episodic apnoea: clinical, neurophysiological and genetic features in the long-term follow-up of 19 patients. *J. Neurol.* 265, 194–203. doi: 10.1007/s00415-017-8689-3

Mihaylova, V., Müller, J. S., Vilchez, J. J., Salih, M. A., Kabiraj, M. M., D'Amico, A., et al. (2008). Clinical and molecular genetic findings in COLQ-mutant congenital myasthenic syndromes. *Brain* 131, 747–759. doi: 10.1093/brain/awm325

Natera-de Benito, D., Bestué, M., Vilchez, J. J., Evangelista, T., Töpf, A., García-Ribes, A., et al. (2016a). Long-term follow-up in patients with congenital myasthenic syndrome due to RAPSN mutations. *Neuromuscul. Disord.* 26, 153–159. doi: 10.1016/j.nmd.2015.10.013

Natera-de Benito, D., Domínguez-Carral, J., Muelas, N., Nascimento, A., Ortez, C., Jaijo, T., et al. (2016b). Phenotypic heterogeneity in two large roma families with a congenital myasthenic syndrome due to CHRNE 1267delG mutation. A long-term follow-up. *Neuromuscul. Disord.* 26, 789–795. doi: 10.1016/j.nmd.2016.08.005

Natera-de Benito, D., Töpf, A., Vilchez, J. J., González-Quereda, L., Domínguez-Carral, J., Díaz-Manera, J., et al. (2017). Molecular characterization of congenital myasthenic syndromes in Spain. *Neuromuscul. Disord.* 27, 1087–1098. doi: 10.1016/j.nmd.2017.08.003

Schara, U., Christen, H.-J., Durmus, H., Hietala, M., Krabetz, K., Rodolico, C., et al. (2010). Long-term follow-up in patients with congenital myasthenic syndrome due to CHAT mutations. *Eur. J. Paediatr. Neurol.* 14, 326–333. doi: 10.1016/j.ejpn.2009.09.009

Schara, U., Della Marina, A., and Abicht, A. (2012). Congenital myasthenic syndromes: current diagnostic and therapeutic approaches. *Neuropediatrics* 43, 184–193. doi: 10.1055/s-0032-1323850

Schara, U., and Lochmüller, H. (2008). Therapeutic strategies in congenital myasthenic syndromes. *Neurotherapeutics* 5, 542–547. doi: 10.1016/j.nurt.2008.07.003

Schmidt, C., Abicht, A., Krampfl, K., Voss, W., Stucka, R., Mildner, G., et al. (2003). Congenital myasthenic syndrome due to a novel missense mutation in the gene encoding choline acetyltransferase. *Neuromuscul. Disord.* 13, 245–251. doi: 10.1016/s0960-8966(02)00273-0

Selvam, P., Arunachal, G., Danda, S., Chapla, A., Sivadasan, A., Alexander, M., et al. (2018). Congenital myasthenic syndrome: spectrum of mutations in an Indian cohort. *J. Clin. Neuromuscul. Dis.* 20, 14–27. doi: 10.1097/CND.0000000000000222

Shieh, P. B., and Oh, S. J. (2018). Congenital myasthenic syndromes. *Neurol. Clin.* 36, 367–378. doi: 10.1016/j.ncl.2018.01.007

Thompson, R., Abicht, A., Beeson, D., Engel, A. G., Eymard, B., Maxime, E., et al. (2018). A nomenclature and classification for the congenital myasthenic syndromes: preparing for FAIR data in the genomic era. *Orphanet J. Rare Dis.* 13:211. doi: 10.1186/s13023-018-0955-7

Thompson, R., Bonne, G., Missier, P., and Lochmüller, H. (2019). Targeted therapies for congenital myasthenic syndromes: systematic review and steps towards a treatabolome. *Emerg. Top. Life Sci.* 3, 19–37. doi: 10.1042/etls20180100

Vanhaesebrouck, A. E., and Beeson, D. (2019). The congenital myasthenic syndromes: expanding genetic and phenotypic spectrums and refining treatment strategies. *Curr. Opin. Neurol.* 32, 696–703. doi: 10.1097/WCO.0000000000000736

Wargon, I., Richard, P., Kuntzer, T., Sternberg, D., Nafissi, S., Gaudon, K., et al. (2012). Long-term follow-up of patients with congenital myasthenic syndrome caused by COLQ mutations. *Neuromuscul. Disord.* 22, 318–324. doi: 10.1016/j.nmd.2011.09.002

Conflict of Interest: The authors declare that the research was conducted in the absence of any commercial or financial relationships that could be construed as a potential conflict of interest.

The reviewer CR declared a past co-authorship with one of the authors HL to the handling Editor.

Copyright © 2020 Della Marina, Wibbeler, Abicht, Kölbel, Lochmüller, Roos and Schara. This is an open-access article distributed under the terms of the Creative Commons Attribution License (CC BY). The use, distribution or reproduction in other forums is permitted, provided the original author(s) and the copyright owner(s) are credited and that the original publication in this journal is cited, in accordance with accepted academic practice. No use, distribution or reproduction is permitted which does not comply with these terms.

frontiers in Molecular Neuroscience

ORIGINAL RESEARCH
published: 09 December 2020
doi: 10.3389/fnmol.2020.568171

AChR β-Subunit mRNAs Are Stabilized by HuR in a Mouse Model of Congenital Myasthenic Syndrome With Acetylcholinesterase Deficiency

*Jennifer Karmouch[1†], Perrine Delers[1†], Fannie Semprez[1], Nouha Soyed[1], Julie Areias[1†], Guy Bélanger[2], Aymeric Ravel-Chapuis[2], Alexandre Dobbertin[1], Bernard J. Jasmin[2] and Claire Legay[1]**

[1] CNRS UMR 8003, Université de Paris, Sorbonne Paris Cité, Paris, France, [2] Department of Cellular and Molecular Medicine, Faculty of Medicine, University of Ottawa, Ottawa, ON, Canada

Collagen Q (COLQ) is a specific collagen that anchors acetylcholinesterase (AChE) in the synaptic cleft of the neuromuscular junction. So far, no mutation has been identified in the *ACHE* human gene but over 50 different mutations in the *COLQ* gene are causative for a congenital myasthenic syndrome (CMS) with AChE deficiency. Mice deficient for COLQ mimic most of the functional deficit observed in CMS patients. At the molecular level, a striking consequence of the absence of COLQ is an increase in the levels of acetylcholine receptor (AChR) mRNAs and proteins *in vivo* and *in vitro* in murine skeletal muscle cells. Here, we decipher the mechanisms that drive AChR mRNA upregulation in cultured muscle cells deficient for COLQ. We show that the levels of AChR β-subunit mRNAs are post-transcriptionally regulated by an increase in their stability. We demonstrate that this process results from an activation of p38 MAPK and the cytoplasmic translocation of the nuclear RNA-binding protein human antigen R (HuR) that interacts with the AU-rich element located within AChR β-subunit transcripts. This HuR/AChR transcript interaction induces AChR β-subunit mRNA stabilization and occurs at a specific stage of myogenic differentiation. In addition, pharmacological drugs that modulate p38 activity cause parallel modifications of HuR protein and AChR β-subunit levels. Thus, our study provides new insights into the signaling pathways that are regulated by ColQ-deficiency and highlights for the first time a role for HuR and p38 in mRNA stability in a model of congenital myasthenic syndrome.

Keywords: neuromuscular junction, congenital myasthenic syndromes, p38 MAPK, HuR, acetylcholine receptor mRNA, ColQ

OPEN ACCESS

Edited by:
Ruth Herbst,
Medical University of Vienna, Austria

Reviewed by:
Kinji Ohno,
Nagoya University, Japan
Tomasz Proszynski,
Łukasiewicz Research Network – PORT The Polish Center for Technology Development, Poland

***Correspondence:**
Claire Legay
Claire.legay@parisdescartes.fr;
claire.legay@univ-paris5.fr

†Present address:
Jennifer Karmouch,
Department of Genomic Medicine, The University of Texas MD Anderson Cancer Center, Houston, TX, United States
Perrine Delers,
INSERM UMR 1124, Université de Paris, Sorbonne Paris Cité, Paris, France
Julie Areias,
INSERM UMR 1051, Institute for Neurosciences of Montpellier, Université de Montpellier, Montpellier, France

Received: 31 May 2020
Accepted: 13 August 2020
Published: 09 December 2020

Citation:
Karmouch J, Delers P, Semprez F, Soyed N, Areias J, Bélanger G, Ravel-Chapuis A, Dobbertin A, Jasmin BJ and Legay C (2020) AChR β-Subunit mRNAs Are Stabilized by HuR in a Mouse Model of Congenital Myasthenic Syndrome With Acetylcholinesterase Deficiency. Front. Mol. Neurosci. 13:568171. doi: 10.3389/fnmol.2020.568171

Abbreviations: ACh, acetylcholine; AChR, acetylcholine receptor; ARE, AU-rich element; BTX, α-bungarotoxin; COLQ, collagen Q; Dok7, docking protein a; Elavl1, embryonic lethal abnormal vision like 1; ECM, extracellular matrix; GABP, GA-binding protein; GAPDH, glyceraldehyde 3-phosphate dehydrogenase; HuR, human antigen R (synonym of Elavl1); JNK, c-jun NH2-terminal kinase; LRP4, low-density lipoprotein receptor-related protein 4; MAPK, mitogen-activated protein kinase; MyoD, myoblast determination protein; MuSK, muscle specific kinase; NF-κB, nuclear factor kappa-light-chain-enhancer of activated B cells; NMJ, neuromuscular junction; SMN, survival motor neuron; UTR, untranslated region.

INTRODUCTION

The collagen Q (COLQ) plays a critical role at the mammalian neuromuscular junction (NMJ) through the anchoring and accumulation of acetylcholinesterase (AChE) in the synaptic basal lamina (Legay, 2018). It allows AChE to control acetylcholine level in the synaptic space thereby limiting the duration of synaptic transmission. To date, over 50 mutations have been identified in the human *COLQ* gene, all of which leading to a congenital myasthenic syndrome (CMS) with endplate AChE deficiency (Mihaylova et al., 2008; Vanhaesebrouck and Beeson, 2019). Congenital myasthenic syndrome with AChE deficiency is first detected in childhood and is characterized by muscle weakness, muscle atrophy, and slow pupillary response to light stimulation. As the disease progresses, skeletal deformities (e.g., lordosis or kyphoscoliosis), ptosis, ophthalmoplegia, and difficulty breathing can occur with a high risk of lethality (Mihaylova et al., 2008). A mouse model of CMS with AChE deficiency has been generated by the knock-out of the *ColQ* gene portraying the main characteristic features observed in patients suffering from CMS with muscle weakness and NMJ disorganization (Feng et al., 1999; McMacken et al., 2019). Furthermore, reintroduction of *COLQ* in these mutant mice has been shown to restore a normal phenotype in motor functions, synaptic transmission and structure of the NMJ (Ito et al., 2012).

Collagen Q contains a proline-rich attachment domain (PRAD) in the N-terminus that binds to a tryptophan amphiphilic tetramerization (WAT) sequence at the C-terminus of the AChE splice variant AChE$_T$ (Massoulié and Bon, 2006). Two clusters of basic residues are found in the central collagenous domain and bind the proteoglycan perlecan (Deprez and Inestrosa, 1995; Peng et al., 1999; Arikawa-Hirasawa et al., 2002), which in turn binds to the transmembrane protein dystroglycan (Jacobson et al., 2001). This collagenous domain is followed by a trimerization domain that allows the formation of the triple helix of COLQ (Bon et al., 2003). COLQ is synthetized by skeletal muscle cells and *ColQ* mRNAs and protein accumulate at the NMJ. However, depending on the type of muscle, COLQ is also present in extrajunctionnal regions although at reduced levels (Krejci et al., 1999). COLQ/AChE accumulation at the synapse is dictated by the interaction between COLQ C-terminus and the muscle specific kinase (MuSK), a postsynaptic signaling hub which is clustered at the NMJ (Cartaud et al., 2004). Together with its co-receptor LRP4 (low-density lipoprotein receptor-related protein 4), MuSK is responsible for acetylcholine receptor (AChR) aggregation and is indispensable for the formation of the NMJ (Li et al., 2018). In COLQ-deficient muscle cells, the number of AChR clusters is upregulated as a result of an increase in AChR mRNA levels (Sigoillot et al., 2010, 2016).

One of the mechanisms regulating mRNA levels occurs through the regulation of their stability by trans-acting factors such as RNA-binding proteins (RBPs), non-coding RNAs and microRNAs. Previous studies have reported that human antigen R (HuR), a member of the ELAVL1/Hu family of RBPs, is critical during skeletal myogenesis for the fusion of myoblasts into myotubes (Van der Giessen et al., 2003; Von Roretz et al., 2011). Human antigen R is known to coordinate the expression of muscle early genes such as *Myod1*, *Myog*, and *p21* (Figueroa et al., 2003) but also to control later expressed genes by targeting synaptic mRNAs such as *Utrn* and *Ache* (Deschenes-Furry et al., 2005; Chakkalakal et al., 2008). In addition to these mRNAs, we have shown that HuR increases the stability of AChR β-subunit transcripts following skeletal muscle denervation (Joassard et al., 2015). Since COLQ-deficient mice also exhibits an increase in the levels of AChR β-subunit mRNAs as well as a number of other synaptic mRNAs (Sigoillot et al., 2016), we explore in the present study, the possibility that COLQ controls β-subunit mRNA stabilization through a mechanism mediated by HuR in a model for CMS with AChE deficiency due to the loss of COLQ.

Here, we provide novel insights into the mechanism that regulates COLQ-mediated AChR β-subunit expression. We found that: (i) in the absence of COLQ, AChR β-subunit mRNA stability and HuR levels are increased, and HuR is translocated to the cytoplasm; (ii) HuR interacts specifically with the ARE (AU-rich elements, AREs) in the 3′UTR of AChR β-subunit transcripts to positively regulate their steady-state levels; (iii) COLQ controls HuR levels through p38 activation specifically in myotubes; and (iv) modulating p38 activity induces parallel variations in HuR proteins and AChR mRNA levels. Collectively, these findings highlight a new pathway in the CMS with AChE deficiency.

RESULTS

The Lack of COLQ Induces an Increase in AChR β-Subunit mRNA Stability

To explore the mechanisms of AChR mRNA upregulation in absence of COLQ, we decided to focus on AChR β-subunit mRNAs. The choice of this subunit mRNA was dictated by its constant expression during life and the crucial physiological role of the encoded subunit. Indeed this transcript encodes a key subunit of the AChR pentamer that interacts with rapsyn, a peripheral membrane protein (Wu et al., 2010). This interaction is responsible for AChR clustering at the NMJ, a process which is regulated by the phosphorylation of the AChR β-subunit (Wu et al., 2010), and is rate-limiting in dictating the amount and concentration of AChR pentamers at post-synaptic sites. In addition, we have shown previously, in another pathological context that AChR β-subunit mRNAs are post-transcriptionally regulated (Joassard et al., 2015). We thus first tested the influence of COLQ deficiency on the stability of this specific transcript (Karmouch, 2014).

To investigate this mechanism, we used the WT and the COLQ-deficient polyclonal mMLCL muscle cell lines (see section "Materials and Methods" for the cell lines). Acetylcholinesterase clusters are observed in the WT cell line but not in the COLQ-deficient cell line in agreement with the role of COLQ. Two days after myotube formation, cultures were treated with 4 μg/ml of the transcriptional inhibitor actinomycin D and total RNA was extracted at different time points (0, 2, 4, and 6 h post treatment). mRNAs were isolated, reverse-transcribed (RT) and quantified by Q-PCR. Quantification at the different time points showed that AChR β-subunit mRNA levels remaining in WT and COLQ-deficient cells were significantly different after 4

and 6 h of treatment. AChR β-subunit transcripts decayed at a significantly higher rate in WT cells compared to COLQ-deficient cells indicating that AChR β-subunit mRNAs are stabilized in absence of COLQ (**Figure 1A**). The half life of the AChR β-subunit mRNAs in wt cells was 5.6 h whereas the half life of the AChR β-subunit mRNAs in ColQ-deficient cells was 19.2 h. Thus, increased AChR mRNA stability correlates with the previously observed increase in AChR mRNA levels in COLQ-deficient cells.

HuR Is a Candidate Protein for AChR Transcript Stability in Absence of COLQ

The next question raised by these findings concerned the identity of the trans-acting factors that could influence the stability of AChR β-subunit mRNA. The group of Jasmin in collaboration with our group has previously shown that HUR (ELAVL1), the ubiquitously expressed RBP stabilizes AChR β-subunit mRNA in response to musle denervation by interacting with the ARE contained in its 3′UTR (Joassard et al., 2015). To explore a similar process in absence of COLQ, we initially compared the levels of HuR mRNA in WT and COLQ-deficient muscle cells. Data were obtained from a microarray previously performed at various stages of WT and COLQ-deficient myotube differentiation (time-points defined as T1, T2, and T3) (Cartaud et al., 2004; Sigoillot et al., 2016). At T1 (newly formed myotubes), myotubes are observed without yet detectable AChR clusters. T2 corresponds to further differentiated myotubes (2 days older than T1) and is characterized by the presence of AChR clusters. Three days after T2, T3 is marked by clusters of AChE-COLQ in WT cells but not in COLQ-deficient cells and appearance of the first spontaneous muscle contractions in both cell lines. In the absence of COLQ, an increase in HuR mRNA compared to WT muscle cells was observed at all time points (T1, + 1.85; T2, + 1.70; T3, + 1.63), and was significant at T1 (**Figure 1B**). HuR protein quantification from western blots showed a similar result in the absence of COLQ with a significant increase in HuR in two of the three stages of myotube differentiation with a 40% increase at T1 ($p < 0.05$) and a 60% increase at T2 ($p < 0.01$) (**Figures 1C,D**).

In response to stimuli such as stress or in pathological conditions, HuR is known to translocate from the nucleus to the cytoplasm where it binds HuR mRNA targets as to increase their stability. We therefore quantified the levels of cytoplasmic (c) and nuclear (n) HuR at T2 in WT and COLQ-deficient muscle cells using cell fractionation. As expected, 2 forms of HuR protein are visualized in the western blot showing the cytoplasmic fraction (**Figure 2A**). These forms correspond to HuR full-length and a

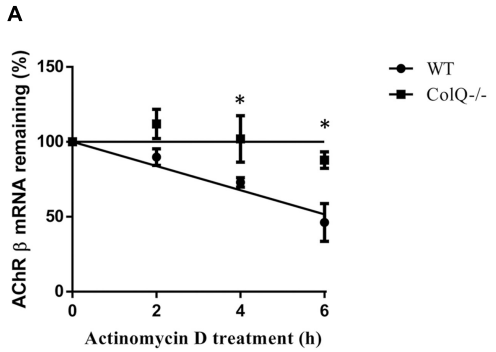

B

Gene(symbol)	Accession Number RefSeq	Fold change and significance T1	T2	T3
Elavl1 (embryonic lethal, abnormal vision, Drosophila)-like 1 (Hu antigen R)	NM_010485	+1.85**	+1.70	+1.63

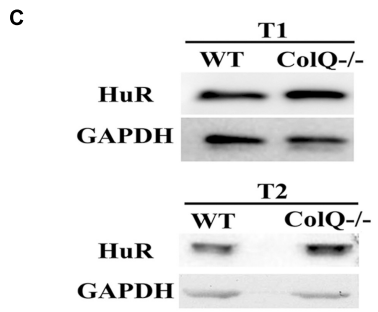

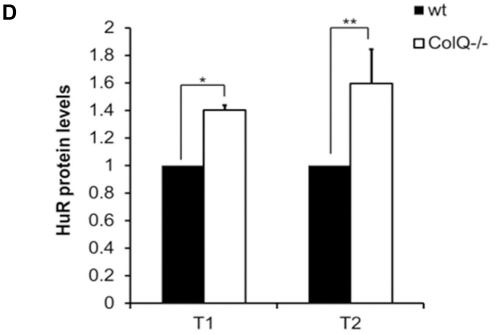

FIGURE 1 | AChR β-subunit mRNA stability, HuR mRNA and protein levels are increased in COLQ-deficient myotubes compared to WT myotubes. **(A)** 4 day differentiated myotubes were treated with the transcriptional inhibitor Actinomycin D (4 μg/ml) for 2, 4, and 6 h and mRNAs were quantified by RT-QPCR relative to 18S. AChR β-subunit mRNA decay curves are shown with all values standardized to 100% RNA at time 0. Values were plotted on a semi-log scale as percentage of mRNA quantified at time 0. Values are expressed as means ± SEM ($n = 3$). *$p < 0.05$; **$p < 0.01$. **(B)** Fold changes in HuR/Elavl1 mRNAs purified from COLQ-deficient myotubes and compared to WT myotubes ($n = 3$). **(C)** Representative western blot and **(D)** Quantification of HuR in WT and COLQ-deficient myotubes at T1 and T2 time-points normalized to GAPDH. T1, T2, and T3 represent different stages of myotubes formation (T1) and further differentiation (T2 and T3). Data are the mean values of four independent experiments ± SEMs. *$p < 0.05$; **$p < 0.01$.

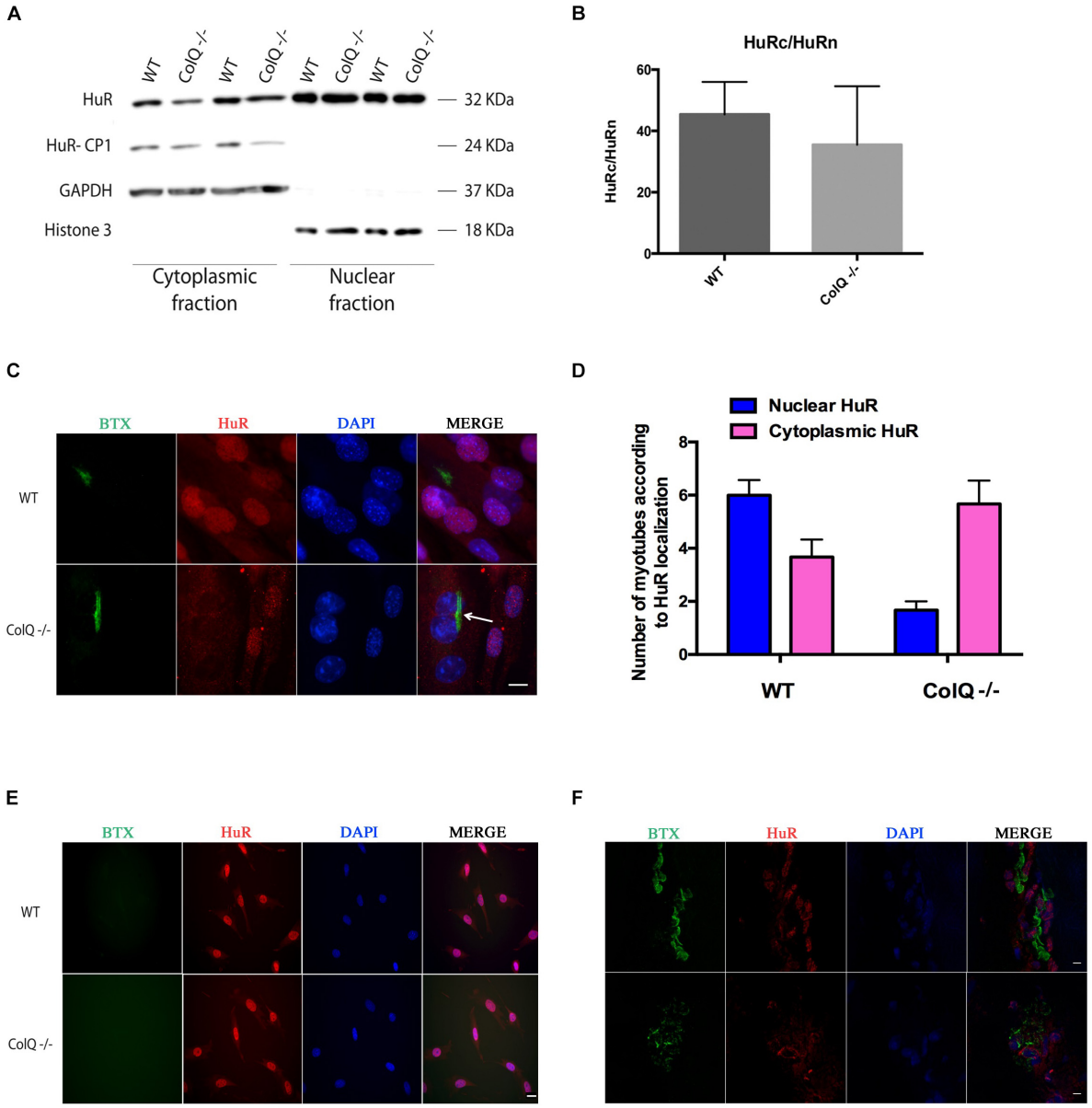

FIGURE 2 | Immunostaining of HuR but not cell fractionation reveals its translocation to the cytoplasm in COLQ-deficient myotubes *in vitro* and *in vivo* **(A–E)**. **(A)** Representative western blot of myotube cell fractionation. GADPH was used as a cytoplasmic marker, histone 3 was used as a nuclear marker. **(B)** Quantification of the ratio between cytoplasmic HuR (HuRc) and nuclear HuR (HuRn) in WT and COLQ-deficient muscle cells. Mean values (n = 4 independent experiments) ± SEMs are shown. $p < 0.05$. **(C)** Immunostaining of HuR in WT and *ColQ* -/- myotubes. AChR clusters and HuR are visualized respectively with α-bungarotoxin (BTX) and HuR antibodies. Nuclei were stained with DAPI. **(D)** Quantification of AChR positive wt and ColQ-deficient myotubes with nuclear and cytoplasmic localization of HuR. Quantification was done in three independent experiments on a total of 29 wt myotubes and 22 ColQ-deficient myotubes. **(E)** Immunostaining of HuR in WT and *ColQ* -/- myoblasts performed as in panel **(C)**. **(F)** AChR, HuR and nuclei revealed as in panel **(C)** in adult mice muscle sections. Scale bar is 20 μm in panel **(C)**, 10 μm in panel **(E)** and 5 μm inpanel **(F)**.

cleavage product of HuR termed HuR-CP1 that appears when HuR translocates to the cytoplasm. As shown in **Figures 2A,B**, HuR levels were rather variable in both cytoplasmic and nuclear fractions and no significant difference was observed for the HuRc/HuRn ratio between the 2 muscle cell lines (**Figure 2B**).

We performed immunofluorescence to visualize HuR in the 2 muscle cell lines at the same time point of cell differentiation, i.e., T2. HuR was observed in the nuclei of all WT and *ColQ* -/- myotubes without AChR clusters (pink nuclei in **Figure 2C**), whereas it was mostly located in the cytoplasm in *ColQ* -/- myotubes bearing AChR clusters (blue nuclei in **Figure 2C**, arrow) indicating that in *ColQ* -/- myotubes, HuR is translocated into the cytoplasm. Quantification of AChR positive myotubes performed on blue (cytoplasmic HuR) and pink (nuclear HuR)

nuclei reveals that in wt myotubes, HuR is observed more often in nuclei than cytoplasm whereas in ColQ-deficient myotubes, HuR is predominantly present in the cytoplasm. The nucleo-cytoplasmic ratio was 1.63 in AChR positive wt myotubes and 0.29 in AChR positive ColQ-deficient myotubes. In these assays, myotubes labeled with AChR clusters represent a minor fraction of all the myotubes in both cell lines (around 1/12). This observation explains therefore the absence of a HuR difference between WT and COLQ-deficient muscle cells in the fractionation assay shown in **Figures 2A,B**, which was performed on total myotube lysates.

In myoblasts, where AChR clusters are not yet present in both cell lines, no difference was observed between WT and COLQ-deficient muscle cells in the localization of HuR which was predominantly nuclear (**Figure 2D**). Since all AChR transcripts (except AChR β-subunit mRNAs) are also upregulated *in vivo*, we hypothesized that similarly to cultured muscle cells, HuR localization could be affected by the absence of COLQ in mouse skeletal muscles. We thus visualized HuR in muscle sections of WT and COLQ-deficient adult mice. As shown on **Figure 2E**, HuR is mostly present in the nuclei of WT muscle fibers. Conversely, HuR accumulates in the cytoplasm of COLQ-deficient fibers suggesting that similar mechanisms of AChR subunit mRNA stabilization by HuR occur *in vivo* in absence of COLQ.

HuR Mimics the AChR ß-Subunit mRNA Regulatory Effect Observed in Absence of ColQ

To examine the potential link between the presence of HuR in the cytoplasm and the increased stability of AChR β-subunit transcripts in muscle cells, we tested a direct interaction between HuR and AChR β-subunit transcripts. We performed RNA immunoprecipitation (RIP) experiments in WT differentiated myotubes (at stage T2) grown in culture. After formaldehyde cross-linking and HuR or IgG (negative control) immunoprecipitation, co-immunoprecipitated mRNAs were analyzed by quantitative RT-QPCR (**Figure 3A**). Our results show that in myogenic cells, HuR interacts with AChR β-subunit mRNAs containing an ARE site and not with the glyceraldehyde 3-phosphate dehydrogenase (GAPDH) mRNAs that do not contain ARE sites.

In order to evaluate the contribution of the 3′UTR ARE in the AChR mRNA/HuR interaction, we used constructs previously described (Joassard et al., 2015). In these constructs, both a WT and an ARE mutated form of the full-length 3′UTR of the mouse AChR β-subunit transcript are inserted downstream of the luciferase reporter gene (3′UTR WT ARE and 3′UTR ΔARE, respectively) driven by a constitutive promoter. The mutated clone contains 3 point mutations in the ARE which prevents it from recruiting HuR. If the loss of COLQ is indeed regulating AChR β-subunit mRNA through HuR, overexpression of HuR should mimic the increased AChR mRNA stability observed in the absence of COLQ.

First, to test the role of HuR binding sites contained in the 3′UTR of AChR β-subunit, COS cells were transfected with 3′UTR WT ARE or 3′UTR ΔARE constructs. Cells were harvested 48 h after transfection and the Luciferase reporter transcript levels were measured by RT-QPCR (**Figure 3B**). The mutation in the ARE motif led to a significant 37% decrease in reporter transcript levels compared to the WT construct suggesting that endogenous HuR present in COS cells is not able to stabilize mutated transcripts containing a mutated ARE. Then, to show that HuR directly controls the levels of Luciferase transcripts through ARE, we transfected the ARE WT and ARE mutated Luciferase constructs into COS cells and performed a RIP assay using HuR antibodies. The RIP analysis, completed 48 h after transfection, showed a significant interaction of the 3′UTR WT construct with HuR when compared to that of the empty vector (**Figure 3C**, top panel for the western blot, bottom panel for the quantification of luciferase mRNA). Mutation of the conserved ARE (3′UTR ΔARE) resulted in a significant 13-fold decrease in the binding of HuR to the AChR β-subunit full-length 3′UTR, with measured abundance of mutant reporter mRNA in the immunoprecipitates being similar to that of the empty vector. These results confirmed that HuR interacts with the conserved ARE element in the 3′UTR of AChR β -subunit mRNA.

To further examine the impact of HuR on AChR β-subunit mRNA levels, we overexpressed HuR in COS cells using a HuR-Flag construct co-transfected with the 3′UTR WT ARE construct. As shown on the western blot on **Figure 3D**, the HuR-Flag construct was indeed overexpressed in addition to endogenous HuR, In these conditions, Luciferase mRNA levels were increased by 100% when compared to pcDNA3 empty vector (**Figure 3E**). The ARE mutant reporter construct, on the other hand presented no alteration in its mRNA levels even in conditions where HuR was overexpressed (**Figure 3E**).

To complement these experiments, we also compared the mRNA stability of the two constructs transfected into COS cells. To this end, 48 h post-transfection, we inhibited transcription by adding actinomycin D and then measured the relative abundance of luciferase mRNAs at 0, 2, 4, and 6 h thereafter (**Figure 3F**). As shown in **Figure 3F**, the degradation rate of the mutant ARE luciferase mRNA was significantly higher when compared to that of the control. Indeed, the half life of the mutant ARE luciferase mRNA calculated from the linear regression was 4.9 h whereas the half life of the wt ARE luciferase mRNA was 22.5 h. Taken together these results indicate that HuR binds the ARE element located within the 3′UTR of AChR β, stabilizes the transcript and, as a result, increases AChR β mRNA levels as found in ColQ-deficient cells.

COLQ Regulates AChR β-Subunit mRNA Levels Through p38 MAPK Activity

The p38 MAPK pathway is known to play an important role in post-transcriptional regulation observed in ARE-containing mRNAs, by specifically regulating the abundance and/or activity of HuR (Srikantan and Gorospe, 2012). Furthermore, p38 activation has been shown to regulate AChR β-subunit mRNA stability in the mouse C2C12 muscle cell line (Joassard et al., 2015). Thus, to determine whether the absence of COLQ correlates with the activation of p38 signaling and HuR levels

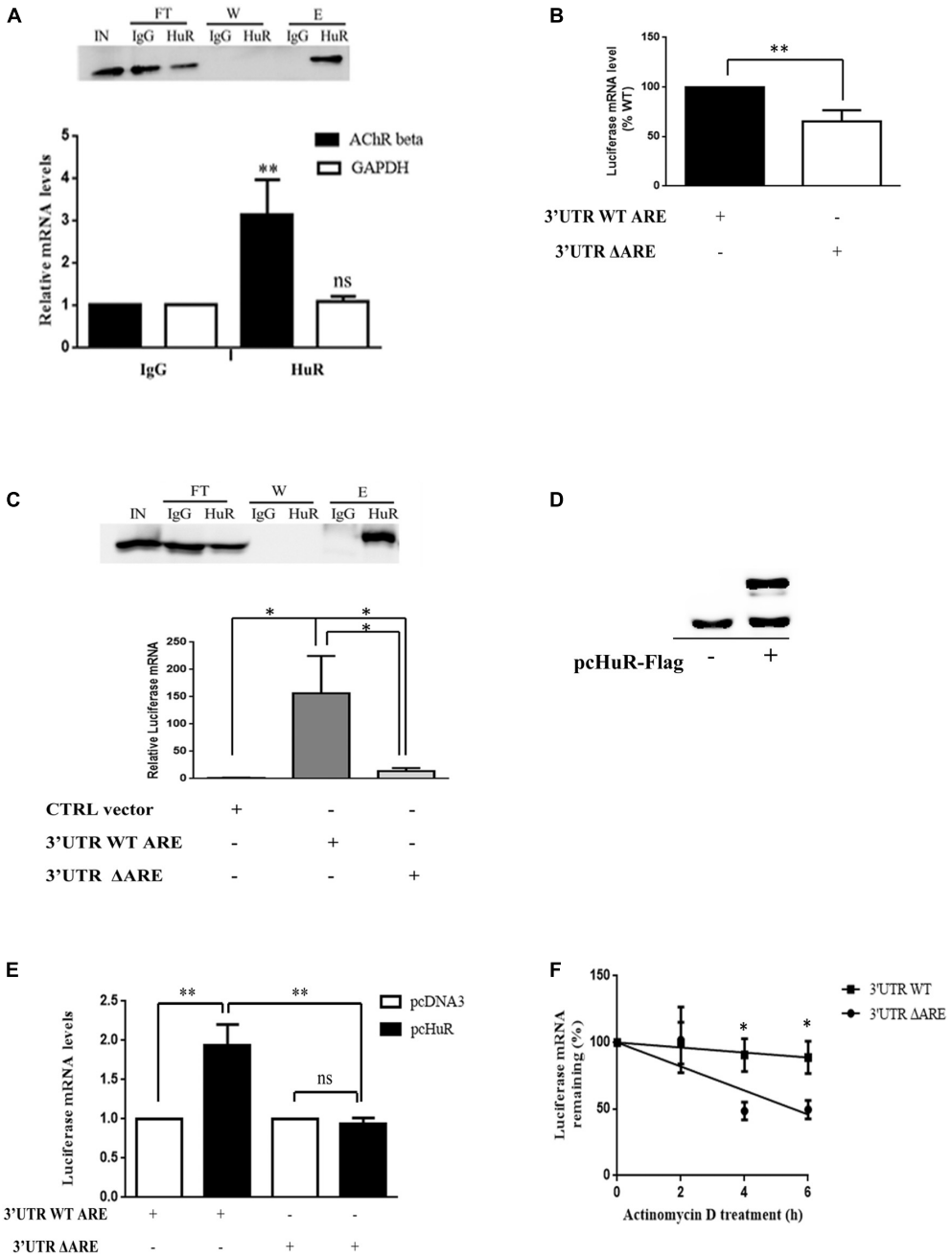

FIGURE 3 | HuR binds endogenous AChR β subunit mRNA within the 3′UTR in myotubes. **(A)** Endogenous HuR interacts with AChR β-subunit mRNA *in vitro*. RNA–protein complexes were crosslinked with formaldehyde in WT differentiated myotubes and proteins immunoprecipitated with antibodies against HuR or IgG. A representative western blot in the top panel shows these proteins in the different fractions (IN, input: FT, flow through; W, wash; E, elution). Quantification of AChR β-subunit mRNA levels is shown below. Data are presented as mean percentages of 4 independent experiments. $^{**}p < 0.01$; ns, not significant **(B)** Luciferase mRNA levels are decreased when 3′UTR ARE is mutated. Luciferase mRNA levels were quantified upon transfection of luciferase constructs containing the WT or mutated AChR β 3′UTR in COS cells ($n = 4$ independent experiments; $^{**}p < 0.01$). **(C)** HuR regulates Luciferase mRNA stability via the ARE located in the AChR β 3′UTR. RIP assays were performed in COS cells transfected with WT-Luciferase or mutated 3′UTR Luciferase constructs (3′UTR WT ARE and 3′UTR ΔARE respectively) or the empty vector containing the Luciferase coding sequence without the AChR 3′UTR insert (CTRL vector) as a control. Top panel: representative western blot showing immunoprecipitated HuR (IN, input; FT, flow through; W, wash; E, Elution). Bottom panel: quantification of Luciferase mRNA levels ($n = 4$ independent experiments; $^{*}p < 0.05$). **(D)** Western blot shows the expression of endogenous HuR and HuR-flag in transfected COS cells. **(E)** COS cells were co-transfected with Luciferase constructs containing the WT or mutated 3′UTR together with pcDNA3, or pcHuR-FLAG. Luciferase mRNAs were quantified by RT-QPCR and normalized to 18S ($n = 4$ independent experiments; $^{**}p < 0.01$) **(F)** Luciferase mRNA stability assay in COS cells transfected with WT or mutated 3′UTR constructs. Luciferase mRNAs were quantified at each time point of actinomycin treatment and were normalized to 18S mRNAs. Values were expressed as a percentage of mRNA levels relative to time 0 (as in **Figure 1A**) and these values were plotted in a semi-log scale as in **Figure 1A**. $n = 5$ independent experiments. $^{*}p < 0.05$; $^{**}p < 0.01$.

in differentiating muscle cells, we compared the phosphorylation levels of p38 in WT and COLQ-deficient cells at different stages of myotubes differentiation using western blots (**Figure 4A**). We quantified in parallel the ratios of phospho-p38/p38 and the levels of HuR in myotubes at T1, T2 and T3 (**Figures 4B,C**). The ratio of phospho-p38/p38 and the levels of HuR were both significantly higher in myotubes at T1 and T2 in absence of COLQ (**Figures 4A–C**) as well as the levels of HuR but not the ratio phospho-p38/p38 in these conditions at T3. It should be noted that although the levels of p38 seemed lower at the 3 time points in COLQ-deficient muscle cells compared to WT muscle cells, it remains that the levels of phosphorylated p38 were always higher in these cells. Thus, in myotubes, a concomitant upregulation of p38 phosphorylation and HuR levels occurs during muscle cell differentiation.

To further explore the relationship between p38, HuR and AChR β mRNA, we manipulated p38 activity by treating WT and COLQ-deficient myotubes at T2 with drugs that stimulate (anisomycin) or inhibit (SB203580) p38 activity, and quantified simultaneously the levels of phospho-p38/p38, HuR and AChR β-subunit mRNA. Analyses of western blots revealed that anisomycin-treated myotubes were responsive in both cell lines. At this stage, anisomycin treatment induced an increase in the ratio phospho-p38/total p38, HuR and AChR β-subunit mRNA in WT (**Figures 5A,B,C,G**) and *ColQ*-/- cells (**Figures 5D,E,F,H**). The 3 parameters were also affected by the p38α/β inhibitor SB203580 in WT cells (**Figure 6**). Western blot showed that inhibition of p38 activity resulted in a decrease in phospho-p38/total p38, in HuR protein levels and in AChR β-subunit mRNA levels in WT muscle cells (**Figures 6A,B,C,G**) as well as in ColQ-/- cells (**Figures 6D,E,F,H**). Altogether, in differentiated myotubes, HuR and AChR β mRNA levels are responsive to p38 activity.

DISCUSSION

The absence of COLQ or its low expression in the synaptic space at the NMJ is causative for a myasthenic syndrome with AChE deficiency. This neuromuscular disorder is mostly a consequence of high levels of ACh in the synaptic cleft due to the lack of AChE. As shown previously by our group, a striking effect of the absence of COLQ is an upregulation of all AChR subunit mRNAs correlated with an increase in the corresponding protein levels and the number of AChR clusters *in vivo* and *in vitro* (Sigoillot et al., 2010, 2016). Interestingly, other synaptic mRNAs and proteins in AChR clustering pathway such as MuSK and Rapsyn are also upregulated in the same condition (Sigoillot et al., 2016). This process is interpreted as an adaptation of the muscle cells to the overload of ACh in the synaptic cleft in an attempt to rescue the NMJ structure and function. Here, we show that a post-transcriptional mechanism of AChR mRNA stabilization is responsible for the increased levels of AChR β-subunit mRNAs observed in differentiated myotubes in response to COLQ deficiency. This mRNA stabilization is correlated with an increase in mRNA and protein levels of HuR and a cytoplasmic HuR enrichment in COLQ-deficient muscle cells. In addition, we provide evidence that ColQ deficiency stimulates p38 phosphorylation which in turn controls the levels of HuR and AChR β-subunit mRNA levels, a process that is specific of differentiated myotubes.

Until recently, the transcriptional regulation of AChR mRNAs induced by neurotrophic factors such as agrin and neuregulin, was described as the major mechanism responsible for the steady-state levels of these transcripts in skeletal muscle cells. These synaptic molecules induce the MAPK kinase (ERK), the PI3K and the JNK signaling pathways (Tansey et al., 1996; Lacazette et al., 2003; Burden et al., 2018), which converge on the activation of the Ets transcription factor, GABP (Schaeffer et al., 2001). Another member of the Ets family Erm has also been involved in the regulation of subsynaptic gene expression *in vivo* (Hippenmeyer et al., 2007) but only GABP has been shown to bind an N-box in the AChR subunit promoters inducing their transcription in synaptic nuclei (Schaeffer et al., 1998). Here, and in a previous study (Joassard et al., 2015), we found that the ARE present in the 3′UTR of AChR β-subunit transcript is a target of the RNA-stabilizing protein HuR. AREs are found in 4 of the 5 transcripts encoding AChR subunits, i.e., the α, β, δ, and γ transcripts[1] and indeed we also found a strong interaction between HuR and the 3′UTR of AChR γ and α mRNA (data not shown). No canonical ARE could be detected in AChR ε transcripts but aside from the ARE described as the traditional HuR binding site motif, other U-rich or undetermined elements have been shown to bind this protein (Lopez de Silanes et al., 2004; Lebedeva et al., 2011) and could be responsible for the interaction between HuR and this AChR transcript.

Human antigen R is predominantly nuclear and translocate to the cytoplasm in response to stimuli to stabilize ARE- containing mRNAs. This is what occurs in COLQ-deficient myotubes where HuR is translocated to the cytoplasm in differentiated myotubes, a process that correlates with AChR β-subunit transcript increased stability. Interestingly, HuR's cytoplasmic localization is only observed in COLQ-deficient myotubes bearing AChR clusters. We previously showed that the same percentage of myotubes showing AChR clusters is found in both WT and COlQ-deficient cell lines and that COLQ-deficient myotubes show a greater number of AChR clusters per myotube than WT myotubes (Sigoillot et al., 2010). This suggests that HuR could contribute to regulate AChR clustering through the stabilization of AChR mRNAs in COlQ deficient differentiated myotubes.

Our data indicate that COLQ-deficiency affects not only HuR localization but also HuR levels. This last process seems to be correlated to the level of p38 MAPK activity since activation or inhibition of this pathway correlates with increases or decreases of HuR levels, respectively. The level of HuR is known to be controlled by the transcription factor NF-κB that binds directly to the HuR promoter and by the TGFβ/Smad pathway (Kang et al., 2008; Jeyaraj et al., 2010). Post-transcriptional mechanisms also account for the regulation of HuR mRNA and protein levels since HuR itself contains ARE (Al-Ahmadi et al., 2009). Direct phosphorylation of HuR by p38α has been involved in HuR shuttling (Lafarga et al., 2009), but there is no evidence that p38

[1]http://brp.kfshrc.edu.sa/ared

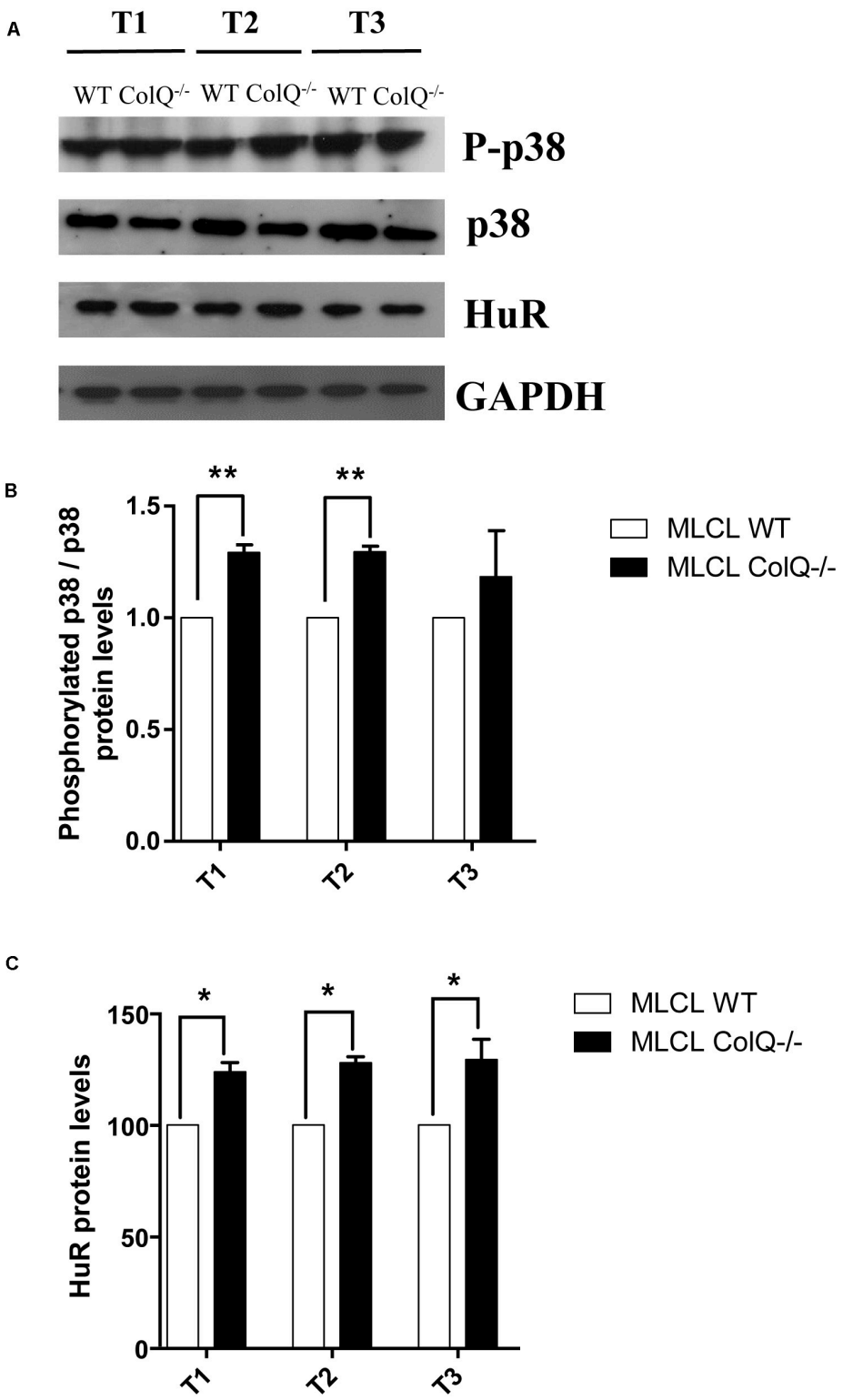

FIGURE 4 | COLQ deficiency regulates p38 phosphorylation and HuR protein levels in myotubes. **(A)** Representative western blot showing the levels of phosphorylated p38 (P-p38), p38, HuR and GADPH in WT and *ColQ* -/- myotubes at different stages of differentiation from T1 to T3. **(B)** Quantification of the ratio phosphorylated-p38/p38. **(C)** quantification of HuR protein levels. P-p38, p38 and HuR levels were normalized to GADPH. $n = 5$ independent experiments. $^{*}p < 0.05$; $^{**}p < 0.01$.

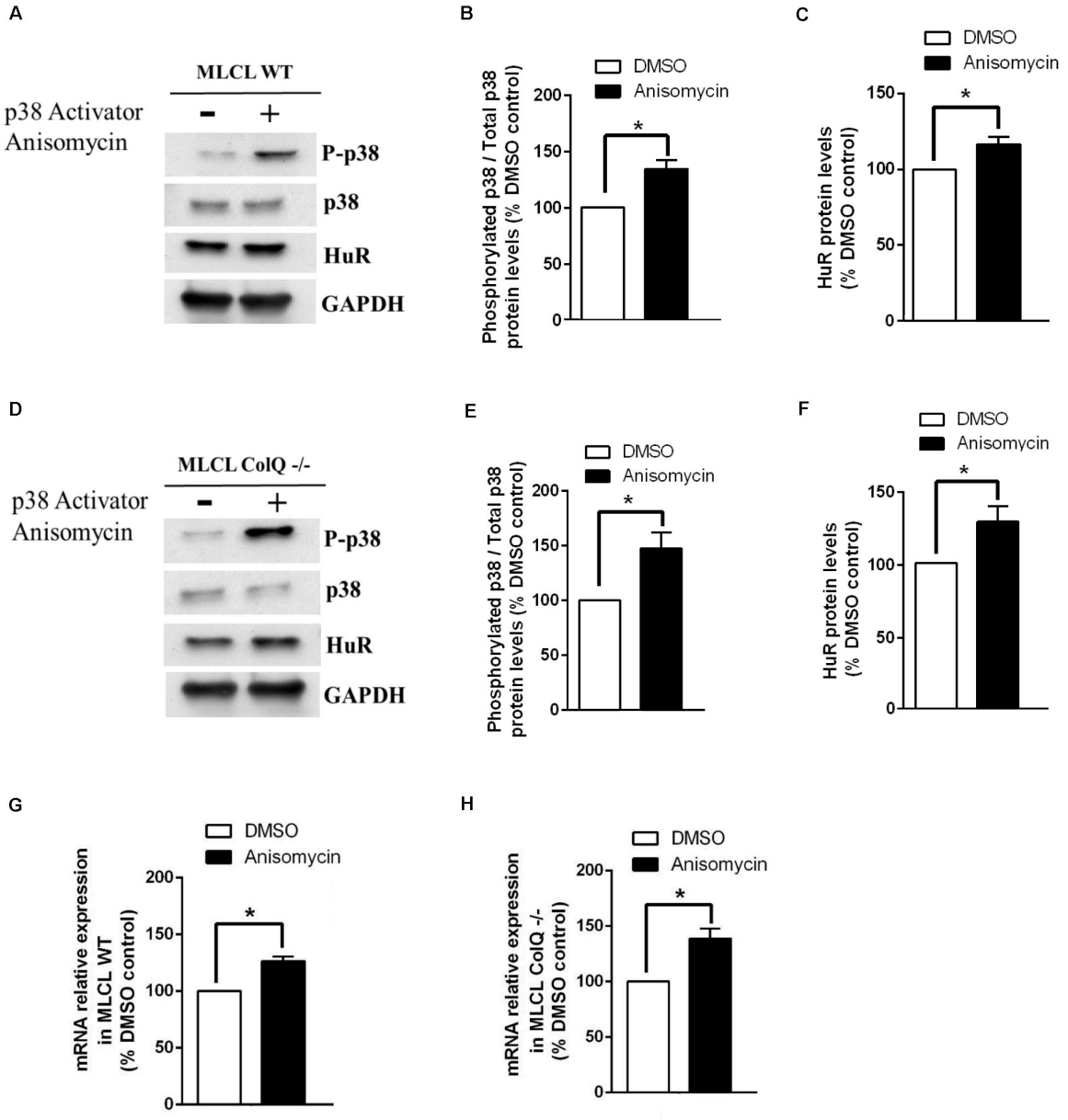

FIGURE 5 | The treatment of WT or ColQ-deficient muscle cells with an activator of p38 induces parallel increases in p38 phosphorylation, HuR protein and AChR β-subunit mRNA levels **(A–H)**. **(A,D)** Representative western blots showing phosphorylated p38, p38, HuR, and GADPH in WT and *ColQ* -/- cells. **(B,C,E,F)** Quantification of these proteins in WT **(B,C)** and *ColQ* -/- cells **(E,F)**. **(G,H)** Quantification of AChR β-subunit mRNA levels. Quantitative data correspond to the means ± SEMs (n = 5 independent experiments). *$p < 0.05$; **$p < 0.01$.

directly regulates HuR levels. However, p38α isoform has been found to activate NF-κB (Olson et al., 2007) which could in turn stimulate HuR expression. Thus the mechanisms by which p38 activation control HuR levels remains to be elucidated.

One key issue would be to identify the signaling pathway upstream of p38 activation. MAPK kinases including MKK3/6 are known to phosphorylate p38 MAPK. After skeletal muscle denervation, we previously showed that the activity of these 2 MKKs is stimulated which could be correlated to the enhanced activity of p38 in the same conditions (Joassard et al., 2015). Moreover, in our earlier study, we demonstrated that constitutively active mutant MKK6 transfected in C2C12 cells induces an increase in p38 activity and a parallel increase in AChR β-subunit mRNA levels and stability. It is thus probable that the same pathway is activated in our CMS model.

Since COLQ binds MuSK and its absence induces p38-HuR-mediated stabilization of AChR β mRNAs, one could hypothetize that MuSK is involved in p38 activation. A number of kinases

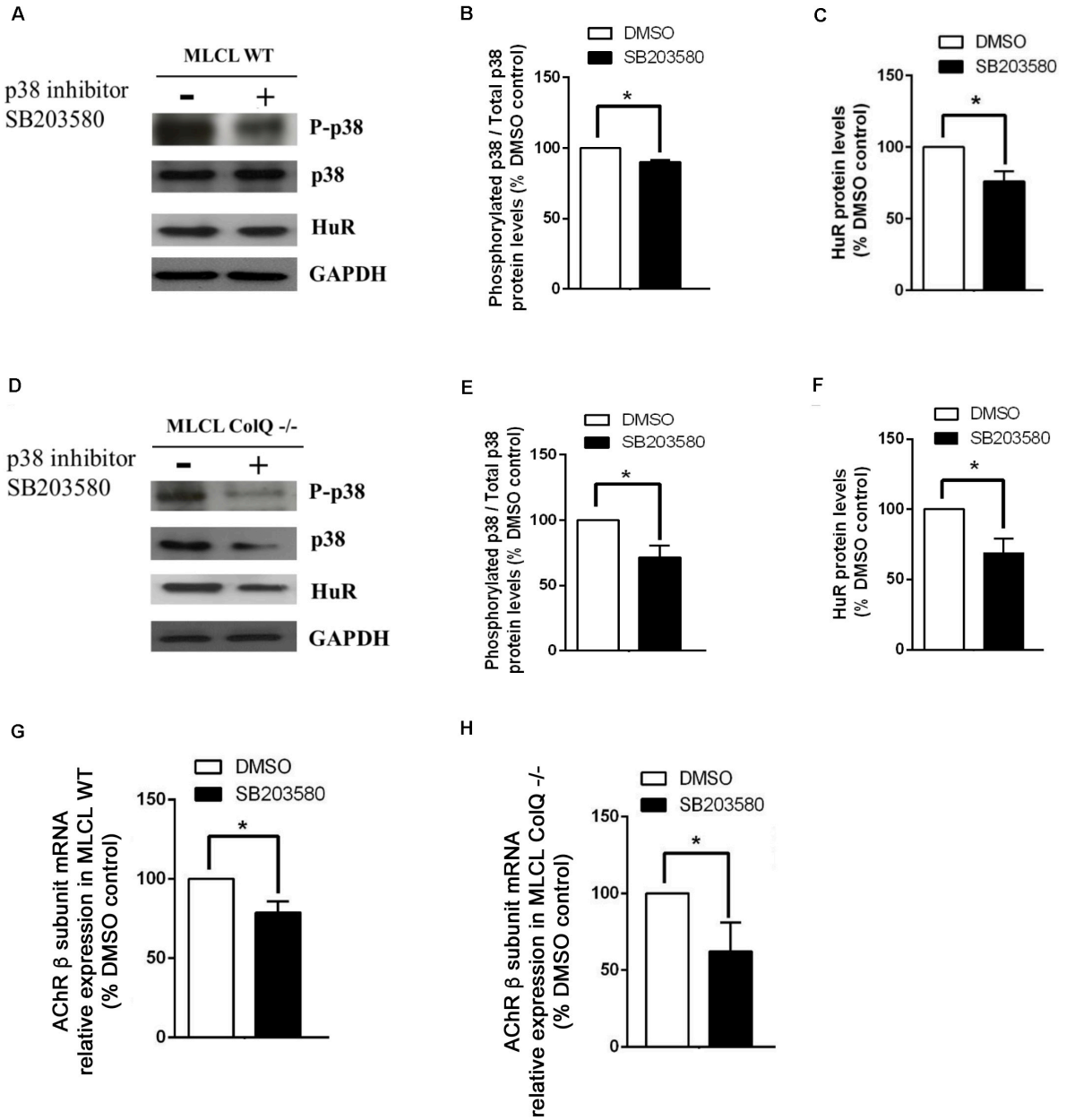

FIGURE 6 | Inhibiting p38 phosphorylation with SB203580 induces parallel decreases in p38 phosphorylation, HuR protein and AChR β mRNA levels in WT muscle cell line **(A–H)**. Legends of the different panels are as in **Figure 5**. For quantifications, the means ± SEMs are shown (n = 5 independent experiments). *$p < 0.05$; **$p < 0.01$.

have been shown to be activated by MuSK (Wu et al., 2010) but so far, there is no evidence that p38 can be recruited and activated by MuSK. In this context, the impact of COLQ on MuSK activity remains to be established. An alternative hypothesis is that p38 is activated by a COLQ-dependent indirect mechanism. In this last hypothesis, it should be reminded that one of the hallmarks of COLQ-deficient NMJ is the perturbation of the extracellular matrix organization that is illustrated by the presence of Schwann cells processes intruding into the synaptic cleft (Feng et al., 1999). This modification may induce a cellular stress and p38 has been reported as a major stress response-induced signaling pathway. The stress response could be mediated by postsynaptic transmembrane receptors such as integrins, which link the extracellular matrix to the cytoskeleton and are major sensor of mechanical forces in muscle. In this context, it will be interesting to explore the activity of the p38-HuR pathway in other myasthenic syndromes where the extracellular matrix (ECM) is affected, with particular focus on the synaptic class of these

diseases such as the laminin β2-induced myasthenic syndrome. Indeed, similar morphological defects have been observed in laminin β2-mutants (Patton et al., 1998). Here, it should point out that several other components of the ECM such as perlecan and biglycan bind indirectly or directly to MuSK (Peng et al., 1999; Amenta et al., 2012) and thus MuSK could also act as a "sensor" of ECM integrity. Interestingly, in mice deficient for collagen VI that present NMJ defects, AChR mRNAs are also upregulated raising the question in this model of the mechanism used to regulate these transcripts (Cescon et al., 2018).

A similar scenario where HuR and p38 pathway are involved in mRNA stabilization in the context of neuromuscular disease is found in spinal muscle atrophy (SMA; Farooq et al., 2009, 2013). This disease is characterized by the progressive loss of motor neurons and consequently muscle atrophy. An early hallmark in this disease is the disruption of the NMJ (Kariya et al., 2008). The causative gene for the disease, survival motor neuron (SMN), has been identified (Lefebvre et al., 1995). In human, there are two similar genes coding for *SMN, SMN1*, and *SMN2.* Most of the patients lack SMN1 gene whereas SMN2 gene is expressed at low levels. Celecoxib, an activator of p38, has been proved to increase the levels of SMN proteins by activating the p38-HuR pathway in human and mouse neuronal cells (Farooq et al., 2013). The same p38-HuR pathway has been shown to stabilize AChR β transcripts in skeletal muscle denervation and we now demonstrate that this pathway is also activated in a model of myasthenic syndrome with AChE deficiency. In conclusion, our study extends the list of neuromuscular pathological situations where the p38-HuR pathway is activated to partially compensate for synaptic defects.

MATERIALS AND METHODS

RNA Extraction and RT-PCR

Total RNA was extracted from COS-7 and muscle cells using TRIzol reagent (Invitrogen) as recommended by the manufacturer. TRIzol extracted RNAs were treated for 30 min at 37°C with DNAse followed by 10 min at 65°C with DNAse STOP (Promega kit) to eliminate possible DNA contamination. cDNAs were synthesized from DNase-treated RNAs using the reverse transcriptase (MuLV; Life technology). Real-time quantitative PCR was performed in triplicates on a 384-well plate with the ABI Prism 7900HT Sequence Detection System (Applied Biosystems). Using a QuantiTect SYBR Green PCR kit (QIAGEN, Valencia, CA, United States) according to the manufactures instructions, amplifications were performed with the following primer sequences: AChR β forward, 5'-CCTGAGGCCGCTATCCGGAC-3' reverse, 5'-TTGGCCTTCGGCTTCCGACC-3'; Luciferase forward, 5'-AAACCATGACCGAGAAGGAG-3' reverse, 5'-GTCCACGAACACAACACCAC-3' GAPDH QuantiTect primer was purchased (Qiagen).

RNA Immunoprecipitation

Muscle cells or COS-7 cells were cross-linked with 1% formaldehyde in PBS for 10 min at room temperature. The reaction was stopped with a wash in ice-cold PBS and resuspended in RIPA buffer. Cross-linked complexes were solubilized in a sonicator bath by six 30-s sonication pulses, and cellular debris were removed by centrifugation (14,000 *g* for 10 min at 4°C). Equal amounts of whole cell extracts were precleared with a Protein A/G plus beads (Santa Cruz) previously blocked with 200 μg/ml of competitor tRNA, and 40 μg/ml of salmon sperm DNA. Complexes were immunoprecipitated using 3 μg of of HuR (Santa Cruz 3A2; 1:500) or IgG antibodies (Sigma M5284; DIL?) and protein A/G plus beads overnight at 4°C. After three washes with RIPA buffer and two washes with TE buffer (10 mM Tris–HCl, pH 8.0, and 1 mM EDTA), beads containing the immunoprecipitated samples were resuspended in 100 μl of elution buffer (50 mM Tris-HCl, pH 7.0, 5 mM EDTA, 10 mM DTT, and 1% SDS). Cross-linking was reversed at 70°C for 5 h. Samples were taken throughout the protocol for RNA extraction and further RT-QPCR and western blotting to confirm the efficiency of immunoprecipitation.

Mice, Muscle Cell Lines, Culture, Treatments, Transfection, Immunohistochemistry and Cell Fractionation

Experiments using ColQ-deficient mice were performed in compliance with the European Community guidelines (N°A-75-1970). The generation of the wild type (WT), ColQ-deficient (ColQ-/-) muscle mMLCL cell lines has been previously described in Sigoillot et al. (2010). In the abbreviation mMLCL, "m" stands for mouse and "MLCL" are the initials of the researchers who made the cell lines. Myoblasts were maintained in growth medium supplemented with 10% fetal bovine serum, 20% horse serum, 2 mM glutamine, 2% penicillin/streptomycin (5000 U) and 20 U/ml γ-interferon (Roche Diagnostics) at 33°C in 8% CO_2. Myoblasts were induced to differentiate into myotubes on collagen type I coated plates in medium supplemented with 5% horse serum, 2 mM glutamine, and 2% penicillin/streptomycin (5000 U). WT and ColQ-deficient cells were treated with a p38 activator anisomycine (100 nM, 1h; Sigma-Aldrich) or a p38 inhibitor SB203580 (10 μM, 1h; Sigma-Aldrich). SB203580 inhibits p38α and p38ß but not p38γ. COS cells were transfected using Fugene HD (Promega), according to the manufacturer's instructions and resulted in <70% of cells expressing the transfected cDNAs. AChR clusters and HuR were visualized respectively with α-bungarotoxin alexa fluor 488 conjugate (1:500; Fisher) and a monoclonal antibody against HuR (1:100, 3A2; Santa Cruz) revealed with a goat anti-mouse alexa fluor 594 (1:500; Thermo Fisher Scientific). The same toxin and antibodies were used to stain AChR and HuR on sections of muscles from adult wt and ColQ-deficient mice. Cell fractionation was performed using the nuclear/cytosol fractionation kit (BioVision) and according to the protocol provided by the manufacturer.

Western Blot Analysis

Proteins were extracted from cell lines using a lysis buffer containing: TrisHCl 50 mM, NaCl 150 mM, EDTA 2mM,

Sodium orthovanadate 2 mM and TritonX100 1%. Total proteins were isolated from cell debris by centrifugation. Equal amounts of total protein (30 μg/sample) were separated on a 12% SDS-PAGE Gel and transferred onto nitrocellulose membranes. Non-specific binding was blocked with PBS and 0.1% Tween containing 5% skim milk for non-phosphorylated proteins and TBS 0.1% Tween containing 3-5% BSA when analyzing phorsphorylation state. Membranes were then incubated with primary antibodies for 1 h at RT or overnight at 4°C. After washing with PBS and 0.1% Tween or TBS 0.1% Tween (phosphorylated proteins), membranes were incubated with HRP-conjugated secondary antibodies. Repated washing was followed by revelation using ECL detection reagents (GE Healthcare) and visualized using hyperfilm ECL or ImageQuant LAS 4000. Quantifications were performed with ImageJ software. The antibodies were the following: a mouse monoclonal anti-GAPDH clone 6C5 (1: 10000; Abcam), a mouse monoclonal anti-HuR 3A2 (1:500; Santa Cruz), an anti-mouse IgG HRP (1:10000; Sigma), an anti-rabbit IgG HRP (1:10000; Sigma), an anti-histone 3 (1:1000; Cell Signaling Technologies), a mouse monoclonal anti-phosphorylated p38 (1:2000, clone 28B10; Cell Signaling Technology) and a rabbit polyclonal anti-p38 (1:1000; Cell Signaling Technology).

Statistical Analysis

Unpaired Mann–Whitney's *U* tests were used to determine the significativity between different groups of data. All quantifications are expressed as means ± SEM.

DATA AVAILABILITY STATEMENT

The raw data supporting the conclusions of this article will be made available by the authors, without undue reservation.

ETHICS STATEMENT

Ethical review and approval was not required for the animal study because cell culture.

AUTHOR CONTRIBUTIONS

JK, PD, FS, NS, JA, GB, AR-C, and AD did the experiments. BJ and CL designated the experiments. CL coordinated and supervised the experiments. All authors contributed to the article and approved the submitted version.

FUNDING

This work was supported by the Association Française contre les Myopathies (grant number 15300 to CL and BJ, 15334 to JK), the Centre National de la Recherche Scientifique, the Canadian Institutes of Health Research and the Muscular Dystrophy Association (United States). Part of the results appeared on-line in JK Ph.D.'s thesis, University of Paris Descartes in accordance with University policy.

REFERENCES

Al-Ahmadi, W., Al-Ghamdi, M., Al-Haj, L., Al-Saif, M., and Khabar, K. S. (2009). Alternative polyadenylation variants of the RNA binding protein, HuR: abundance, role of AU-rich elements and auto-regulation. *Nucleic Acids Res.* 37, 3612–3624. doi: 10.1093/nar/gkp223

Amenta, A. R., Creely, H. E., Mercado, M. L., Hagiwara, H., McKechnie, B. A., Lechner, B. E., et al. (2012). Biglycan is an extracellular MuSK binding protein important for synapse stability. *J. Neurosci.* 32, 2324–2334. doi: 10.1523/jneurosci.4610-11.2012

Arikawa-Hirasawa, E., Rossi, S. G., Rotundo, R. L., and Yamada, Y. (2002). Absence of acetylcholinesterase at the neuromuscular junctions of perlecan-null mice. *Nat. Neurosci.* 5, 119–123. doi: 10.1038/nn801

Bon, S., Ayon, A., Leroy, J., and Massoulié, J. (2003). Trimerization domain of the collagen tail of acetylcholinesterase. *Neurochem. Res.* 28, 523–535.

Burden, S. J., Huijbers, M. G., and Remedio, L. (2018). Fundamental molecules and mechanisms for forming and maintaining neuromuscular synapses. *Int. J. Mol.* 19:490. doi: 10.3390/ijms19020490

Cartaud, A., Strochlic, L., Guerra, M., Blanchard, B., Lambergeon, M., Krejci, E., et al. (2004). MuSK is required for anchoring acetylcholinesterase at the neuromuscular junction. *J. Cell Biol.* 165, 505–515. doi: 10.1083/jcb.200307164

Cescon, M., Gregorio, I., Eiber, N., Borgia, D., Fusto, A., Sabatelli, P., et al. (2018). Collagen VI is required for the structural and functional integrity of the neuromuscular junction. *Acta Neuropathol.* 136, 483–499. doi: 10.1007/s00401-018-1860-9

Chakkalakal, J. V., Miura, P., Bélanger, G., Michel, R. N., and Jasmin, B. J. (2008). Modulation of utrophin A mRNA stability in fast versus slow muscles via an AU-rich element and calcineurin signaling. *Nucleic Acids Res.* 36, 826–838. doi: 10.1093/nar/gkm1107

Deprez, P. N., and Inestrosa, N. C. (1995). Two heparin-binding domains are present on the collagenic tail of asymmetric acetylcholinesterase. *J. Biol. Chem.* 270, 11043–11046. doi: 10.1074/jbc.270.19.11043

Deschenes-Furry, J., Belanger, G., Mwanjewe, J., Lunde, J. A., Parks, R. J., Perrone-Bizzozero, N., et al. (2005). The RNA-binding protein HuR binds to acetylcholinesterase transcripts and regulates their expression in differentiating skeletal muscle cells. *J. Biol. Chem.* 280, 25361–25368. doi: 10.1074/jbc.m410929200

Farooq, F., Abadia-Molina, F., MacKenzie, D., Hadwen, J., Shamim, F., O'Reilly, S., et al. (2013). Celecoxib increases SMN and survival in a severe spinal muscular atrophy mouse model via p38 pathway activation. *Hum. Mol. Genet.* 22, 3415–3424. doi: 10.1093/hmg/ddt191

Farooq, F., Balabanian, S., Liu, X., Holcik, M., and MacKenzie, A. (2009). p38 Mitogen-activated protein kinase stabilizes SMN mRNA through RNA binding protein HuR. *Hum. Mol. Genet.* 18, 4035–4045. doi: 10.1093/hmg/ddp352

Feng, G., Krejci, E., Molgo, J., Cunningham, J. M., Massoulié, J., and Sanes, J. R. (1999). Genetic analysis of collagen Q: roles in acetylcholinesterase and butyrylcholinesterase assembly and in synaptic structure and function. *J. Cell Biol.* 144, 1349–1360. doi: 10.1083/jcb.144.6.1349

Figueroa, A., Cuadrado, A., Fan, J., Atasoy, U., Muscat, G. E., Muñoz-Canoves, P., et al. (2003). Role of HuR in skeletal myogenesis through coordinate regulation of muscle differentiation genes. *Mol. Cell. Biol.* 23, 4991–5004. doi: 10.1128/mcb.23.14.4991-5004.2003

Hippenmeyer, S., Huber, R. M., Ladle, D. R., Murphy, K., and Arber, S. (2007). ETS transcription factor Erm controls subsynaptic gene expression in skeletal muscles. *Neuron* 55, 726–740. doi: 10.1016/j.neuron.2007.07.028

Ito, M., Suzuki, Y., Okada, T., Fukudome, T., Yoshimura, T., Masuda, A., et al. (2012). Protein-anchoring strategy for delivering acetylcholinesterase to the neuromuscular junction. *Mol. Ther.* 20, 1384–1392. doi: 10.1038/mt.2012.34

Jacobson, C., Cote, P. D., Rossi, S. G., Rotundo, R. L., and Carbonetto, S. (2001). The dystroglycan complex is necessary for stabilization of acetylcholine receptor clusters at neuromuscular junctions and formation of the synaptic basement membrane. *J. Cell Biol.* 152, 435–450. doi: 10.1083/jcb.152.3.435

Jeyaraj, S. C., Singh, M., Ayupova, D. A., Govindaraju, S., and Lee, B. S. (2010). Transcriptional control of human antigen R by bone morphogenetic protein. *J. Biol. Chem.* 285, 4432–4440. doi: 10.1074/jbc.m109.062216

Joassard, O. R., Bélanger, G., Karmouch, J., Lunde, J. A., Shukla, A. H., Chopard, A., et al. (2015). HuR mediates changes in the stability of AChR β-subunit mRNAs after skeletal muscle denervation. *J. Neurosci.* 35, 10949–10962. doi: 10.1523/jneurosci.1043-15.2015

Kang, M. J., Ryu, B. K., Lee, M. G., Han, J., Lee, J. H., Ha, T. K., et al. (2008). NF-kappaB activates transcription of the RNA-binding factor HuR, via PI3K-AKT signaling, to promote gastric tumorigenesis. *Gastroenterology* 135, 2030–2042. doi: 10.1053/j.gastro.2008.08.009

Kariya, S., Park, G. H., Maeno-Hikichi, Y., Leykekhman, O., Lutz, C., Arkovitz, M. S., et al. (2008). Reduced SMN protein impairs maturation of the neuromuscular junctions in mouse models of spinal muscular atrophy. *Hum. Mol. Genet.* 17, 2552–2569. doi: 10.1093/hmg/ddn156

Karmouch, J. (2014). *Deciphering ColQ Induced Mechanisms in the Control of AChR mRNA Levels*. Ph.D. Thesis, University Paris Descartes, Paris.

Krejci, E., Legay, C., Thomine, S., Sketelj, J., and Massoulié, J. (1999). Differences in expression of acetylcholinesterase and collagen Q control the distribution and oligomerization of the collagen-tailed forms in fast and slow muscles. *J. Neurosci.* 19, 10672–10679. doi: 10.1523/jneurosci.19-24-10672.1999

Lacazette, E., Le Calvez, S., Gajendran, N., and Brenner, H. R. (2003). A novel pathway for MuSK to induce key genes in neuromuscular synapse formation. *J. Cell Biol.* 161, 727–736. doi: 10.1083/jcb.200210156

Lafarga, V., Cuadrado, A., Lopez de Silanes, I., Bengoechea, R., Fernandez-Capetillo, O., and Nebreda, A. R. (2009). p38 Mitogen-activated protein kinase- and HuR-dependent stabilization of p21(Cip1) mRNA mediates the G(1)/S checkpoint. *Mol. Cell. Biol.* 29, 4341–4351. doi: 10.1128/mcb.00210-09

Lebedeva, S., Jens, M., Theil, K., Schwanhäusser, B., Selbach, M., Landthaler, M., et al. (2011). Transcriptome-wide analysis of regulatory interactions of the RNA-binding protein HuR. *Mol. Cell.* 43, 340–352. doi: 10.1016/j.molcel.2011.06.008

Lefebvre, S., Burglen, L., Reboullet, S., Clermont, O., Burlet, P., Viollet, L., et al. (1995). Identification and characterization of a spinal muscular atrophy-determining gene. *Cell* 80, 155–165.

Legay, C. (2018). Congenital myasthenic syndromes with acetylcholinesterase deficiency, the pathophysiological mechanisms. *Ann. N. Y. Acad. Sci.* 1413, 104–110. doi: 10.1111/nyas.13595

Li, L., Xiong, W. C., and Mei, L. (2018). Neuromuscular junction formation, aging, and disorders. *Annu. Rev. Physiol.* 80, 159–188.

Lopez de Silanes, I., Zhan, M., Lal, A., Yang, X., and Gorospe, M. (2004). Identification of a target RNA motif for RNA-binding protein HuR. *Proc. Natl. Acad. Sci. U.S.A.* 101, 2987–2992. doi: 10.1073/pnas.0306453101

Massoulié, J., and Bon, S. (2006). The C-terminal T peptide of cholinesterases: structure, interactions, and influence on protein folding and secretion. *J. Mol. Neurosci.* 30, 233–236. doi: 10.1385/jmn:30:1:233

McMacken, G. M., Spendiff, S., Whittaker, R. G., O'Connor, E., Howarth, R. M., Boczonadi, V., et al. (2019). Salbutamol modifies the neuromuscular junction in a mouse model of ColQ myasthenic syndrome. *Hum. Mol. Genet.* 28, 2339–2351. doi: 10.1093/hmg/ddz059

Mihaylova, V., Muller, J. S., Vilchez, J. J., Salih, M. A., Kabiraj, M. M., D'Amico, A., et al. (2008). Clinical and molecular genetic findings in COLQ-mutant congenital myasthenic syndromes. *Brain* 131, 747–759. doi: 10.1093/brain/awm325

Olson, C. M., Hedrick, M. N., Izadi, H., Bates, T. C., Olivera, E. R., and Anguita, J. (2007). p38 mitogen-activated protein kinase controls NF-kappaB transcriptional activation and tumor necrosis factor alpha production through RelA phosphorylation mediated by mitogen- and stress-activated protein kinase 1 in response to Borrelia burgdorferi antigens. *Infect. Immun.* 75, 270–277. doi: 10.1128/iai.01412-06

Patton, B. L., Chiu, A. Y., and Sanes, J. R. (1998). Synaptic laminin prevents glial entry into the synaptic cleft. *Nature* 393, 698–701. doi: 10.1038/31502

Peng, H. B., Xie, H., Rossi, S. G., and Rotundo, R. L. (1999). Acetylcholinesterase clustering at the neuromuscular junction involves perlecan and dystroglycan. *J. Cell Biol.* 145, 911–921. doi: 10.1083/jcb.145.4.911

Schaeffer, L., de Kerchove d'Exaerde, A., and Changeux, J. P. (2001). Targeting transcription to the neuromuscular synapse. *Neuron* 31, 15–22. doi: 10.1016/s0896-6273(01)00353-1

Schaeffer, L., Duclert, N., Huchet-Dymanus, M., and Changeux, J. P. (1998). Implication of a multisubunit Ets-related transcription factor in synaptic expression of the nicotinic acetylcholine receptor. *EMBO J.* 17, 3078–3090. doi: 10.1093/emboj/17.11.3078

Sigoillot, S. M., Bourgeois, F., Karmouch, J., Molgó, J., Dobbertin, A., Chevalier, C., et al. (2016). Neuromuscular junction immaturity and muscle atrophy are hallmarks of the ColQ-deficient mouse, a model of congenital myasthenic syndrome with acetylcholinesterase deficiency. *FASEB J.* 30, 2382–2399. doi: 10.1096/fj.201500162

Sigoillot, S. M., Bourgeois, F., Lambergeon, M., Strochlic, L., and Legay, C. (2010). ColQ controls postsynaptic differentiation at the neuromuscular junction. *J. Neurosci.* 30, 13–23. doi: 10.1523/jneurosci.4374-09.2010

Srikantan, S., and Gorospe, M. (2012). HuR function in disease. *Front. Biosci.* 17, 189–205. doi: 10.2741/3921

Tansey, M. G., Chu, G. C., and Merlie, J. P. (1996). ARIA/HRG regulates AChR epsilon subunit gene expression at the neuromuscular synapse via activation of phosphatidylinositol 3-kinase and Ras/MAPK pathway. *J. Cell Biol.* 134, 465–476. doi: 10.1083/jcb.134.2.465

Van der Giessen, K., Di-Marco, S., Clair, E., and Gallouzi, I. E. (2003). RNAi-mediated HuR depletion leads to the inhibition of muscle cell differentiation. *J. Biol. Chem.* 278, 47119–47128. doi: 10.1074/jbc.m308889200

Vanhaesebrouck, A. E., and Beeson, D. (2019). The congenital myasthenic syndromes: expanding genetic and phenotypic spectrums and refining treatment strategies. *Curr. Opin. Neurol* 32, 696–703. doi: 10.1097/wco.0000000000000736

Von Roretz, C., Beauchamp, P., Di Marco, S., and Gallouzi, I. E. (2011). HuR and myogenesis: being in the right place at the right time. *Biochim. Biophys. Acta* 1813, 1663–1667. doi: 10.1016/j.bbamcr.2011.01.036

Wu, H., Xiong, W. C., and Mei, L. (2010). To build a synapse: signaling pathways in neuromuscular junction assembly. *Development* 137, 117–1033.

Conflict of Interest: The authors declare that the research was conducted in the absence of any commercial or financial relationships that could be construed as a potential conflict of interest.

Copyright © 2020 Karmouch, Delers, Semprez, Soyed, Areias, Bélanger, Ravel-Chapuis, Dobbertin, Jasmin and Legay. This is an open-access article distributed under the terms of the Creative Commons Attribution License (CC BY). The use, distribution or reproduction in other forums is permitted, provided the original author(s) and the copyright owner(s) are credited and that the original publication in this journal is cited, in accordance with accepted academic practice. No use, distribution or reproduction is permitted which does not comply with these terms.

frontiers in Molecular Neuroscience

ORIGINAL RESEARCH
published: 17 December 2020
doi: 10.3389/fnmol.2020.594220

Modulation of the Acetylcholine Receptor Clustering Pathway Improves Neuromuscular Junction Structure and Muscle Strength in a Mouse Model of Congenital Myasthenic Syndrome

Sally Spendiff[1], Rachel Howarth[2], Grace McMacken[3], Tracey Davey[2], Kaitlyn Quinlan[1], Emily O'Connor[1,4], Clarke Slater[2], Stefan Hettwer[5], Armin Mäder[5], Andreas Roos[1,6], Rita Horvath[7] and Hanns Lochmüller[1,4,8,9]*

[1] Children's Hospital of Eastern Ontario Research Institute, Ottawa, ON, Canada, [2] Institute of Neuroscience, Newcastle University, Newcastle upon Tyne, United Kingdom, [3] Department of Neurosciences, Royal Victoria Hospital, Belfast, United Kingdom, [4] Brain and Mind Research Institute, University of Ottawa, Ottawa, ON, Canada, [5] Neurotune AG, Schlieren, Zurich, [6] Department of Paediatric Neurology, University Hospital Essen, University of Duisburg-Essen, Essen, Germany, [7] Department of Clinical Neurosciences, University of Cambridge, Cambridge, United Kingdom, [8] Department of Neuropediatrics and Muscle Disorders, Medical Center – University of Freiburg, Freiburg, Germany, [9] Centro Nacional de Análisis Genómico (CNAG-CRG), Center for Genomic Regulation, Barcelona Institute of Science and Technology (BIST), Barcelona, Spain

OPEN ACCESS

Edited by:
Fiorenzo Conti,
Marche Polytechnic University, Italy

Reviewed by:
Sophie Nicole,
Institut National de la Santé et de la Recherche Médicale (INSERM), France
Francesca Grassi,
Sapienza University of Rome, Italy

***Correspondence:**
Sally Spendiff
sspendiff@cheo.on.ca

Received: 12 August 2020
Accepted: 24 November 2020
Published: 17 December 2020

Citation:
Spendiff S, Howarth R, McMacken G, Davey T, Quinlan K, O'Connor E, Slater C, Hettwer S, Mäder A, Roos A, Horvath R and Lochmüller H (2020) Modulation of the Acetylcholine Receptor Clustering Pathway Improves Neuromuscular Junction Structure and Muscle Strength in a Mouse Model of Congenital Myasthenic Syndrome. Front. Mol. Neurosci. 13:594220. doi: 10.3389/fnmol.2020.594220

Introduction: Congenital myasthenic syndromes (CMS) are a diverse group of inherited neuromuscular disorders characterized by a failure of synaptic transmission at the neuromuscular junction (NMJ). CMS often present early with fatigable weakness and can be fatal through respiratory complications. The *AGRN* gene is one of over 30 genes known to harbor mutations causative for CMS. In this study, we aimed to determine if a compound (NT1654), developed to stimulate the acetylcholine receptor (AChR) clustering pathway, would benefit a mouse model of CMS caused by a loss-of-function mutation in *Agrn* (*Agrn*^{nmf380} mouse).

Methods: *Agrn*^{nmf380} mice received an injection of either NT1654 or vehicle compound daily, with wild-type litter mates used for comparison. Animals were weighed daily and underwent grip strength assessments. After 30 days of treatment animals were sacrificed, and muscles collected. Investigations into NMJ and muscle morphology were performed on collected tissue.

Results: While minimal improvements in NMJ ultrastructure were observed with electron microscopy, gross NMJ structure analysis using fluorescent labelling and confocal microscopy revealed extensive postsynaptic improvements in *Agrn*^{nmf380} mice with NT1654 administration, with variables frequently returning to wild type levels. An improvement in muscle weight and myofiber characteristics helped increase forelimb grip strength and body weight.

Conclusions: We conclude that NT1654 restores NMJ postsynaptic structure and improves muscle strength through normalization of muscle fiber composition and the

prevention of atrophy. We hypothesize this occurs through the AChR clustering pathway in *Agrn*^{nmf380} mice. Future studies should investigate if this may represent a viable treatment option for patients with CMS, especially those with mutations in proteins of the AChR clustering pathway.

Keywords: neuromuscular junction, congenital myasthenia syndromes (CMS), therapies, neuromuscular disease (NMD), preclinical "*in vivo*" study, animal model, neuromuscular disorders

INTRODUCTION

Proper functioning of the neuromuscular junction (NMJ) relies on efficient signaling to the muscle. This requires structural integrity of the NMJ which is mediated by a process that involves clustering of acetylcholine receptors (AChRs) at the postsynaptic membrane. This is achieved in part through the AGRIN/LRP4/MuSK pathway (**Supplementary Figure 1**). AGRIN is synthesized by motor neurons, muscle cells, and other non-neuronal cells, but it is only that transported from the motor neurons to the axon terminals that is comprised of the domains needed for AChR clustering (Bezakova et al., 2001). Neural AGRIN (z type generated by alternative splicing) released by motor nerves, binds to low-density lipoprotein receptor-related protein 4 (LRP4) which causes phosphorylation of muscle specific kinase (MuSK) (Kim et al., 2008). Once phosphorylated, MuSK recruits downstream of tyrosine kinase 7 (DOK7), which stimulates further MuSK phosphorylation (Burden et al., 2013). This causes receptor associated-protein of the synapse (RAPSYN) to form complexes with AChRs and help with their insertion into the postsynaptic membrane and anchoring to the cytoskeleton (Gervásio and Phillips, 2005). This pathway is important in both NMJ development and maintenance (Bezakova et al., 2001; Tezuka et al., 2014).

The congenital myasthenic syndromes (CMS) are caused by mutations in genes important for neuromuscular transmission. These mutations can be presynaptic, postsynaptic, in the synaptic cleft, or even in ubiquitously expressed proteins. CMS lead to disabling fatigable muscle weakness and can be fatal due to respiratory muscle weakness. Mutations in over 30 genes are known to be causative for CMS, and at least 16 have been identified in the *AGRN* gene (Finsterer, 2019; Ohkawara et al., 2020). *AGRN* mutations can impact AChR clustering by decreasing the phosphorylation of MuSK, degrading secreted neural AGRIN, and impairing the anchoring of AGRIN to the sarcolemma (Ohkawara et al., 2020). Patients with *AGRN* mutations present with exercise-induced proximal or distal muscle weakness, and varying degrees of ptosis, ophthalmoplegia, facial weakness, and respiratory muscle weakness. Neurophysiological tests typically reveal a decrement in compound muscle action potential on repetitive nerve stimulation, and muscle biopsies may show a myofibre Type I (TI) predominance, atrophy of Type II myofibers, an increase in small angular myofibers, and abnormal NMJ morphology (Huze et al., 2009; Maselli et al., 2012; Nicole et al., 2014).

Since the AGRIN protein is a key component of the AChR clustering pathway, it is possible that its manipulation could ameliorate the CMS phenotype. NT1654 is a 44 KDa C-Terminal neurotrypsin resistant fragment of mouse AGRIN (Hettwer et al., 2014) (**Supplementary Figure 1**). It has previously been used to ameliorate the NMJ pathology in rodent models of spinal muscular atrophy (Boido et al., 2018) and myasthenia gravis (Li et al., 2018), and in a zebrafish model of presynaptic CMS caused by mutations in *MYO9A* (O'Connor et al., 2018).

The aim of this study was to determine if NT1654 would benefit a mouse model of CMS caused by *Agrn* gene mutations. To answer this question, we used the *Agrn*^{nmf380} mouse generated through N-ethyl N-nitrosourea (ENU) chemical mutagenesis that induced a mutation in *Agrn* (nmf380-F1061S), resulting in a partial loss of function of the protein. Mice homozygous for the mutation are smaller than littermates, display poor hindlimb motor control and atrophy, and typically die within a few weeks to months of birth. They also have an increase in TI myofibers and abnormal NMJ morphology, closely recapitulating the human form of the disease (Bogdanik and Burgess, 2011).

MATERIALS AND METHODS

Animal Husbandry

The *Agrn*^{nmf380} mouse with a point mutation in the *Agrn* gene on the C57BL/6J background was obtained from the Burgess lab (Bogdanik and Burgess, 2011). All animal procedures were performed in accordance with the Animals Scientific Procedures Act of 1986 under project license 70/8538. Animals were housed under 12 h light/dark cycles in the Functional Genomics Unit, at Newcastle University, and had access to standard chow and water *ad libitum*. Since *Agrn*^{nmf380} mice had hindlimb wasting, soaked diet was always available on the cage floor. Animals were weighed and monitored daily and any animal found to have lost >17% of body weight or showing a severe phenotype was humanely culled.

Treatment Protocol and Tissue Collection

Animals were assigned at postnatal day 5 (P5) to either a drug treatment (NT) or vehicle control (Veh) group, with wild type (WT) litter mates being used for comparison. *Agrn*^{nmf380} mice assigned to the NT group received a daily sub-cutaneous injection (scruff of the neck) of NT1654 (Neurotune AG), a modified form of AGRIN, at 10 mg/kg. The drug was carried in phosphate-buffered saline (PBS) so *Agrn*^{nmf380} mice assigned to the Veh group received a daily injection of PBS at a corresponding volume. Animals were injected for 30 days and culled at the end of the study by cervical dislocation and tissues harvested and weighed. A pilot study previously examined the effects of administering 2, 5, and 10 mg/kg of NT1654 to

WT and *Agrn*^{nmf380} animals. No deleterious effects in terms of body weight, liver enzymes, or liver and kidney histology were observed at any drug concentration (data not shown), so the highest concentration (10 mg/kg) of the drug was used. This was also consistent with previous rodent trials of this compound that produced positive results (Hettwer et al., 2014; Boido et al., 2018).

Muscle Strength Assessments

Animals underwent three strength assessments. The first was a hindlimb suspension test designed for neonates at P7. Following this at P22-24 and P33-35 grip strength was assessed using a Grip Strength meter with grid attachment (Bioseb), both according to established protocols (Willmann et al., 2011). Both tests were performed in a room separate to the holding room with only the tester present to minimize disturbance for the animals. For the hindlimb suspension test, neonates were suspended face down by their hindlimbs inside a 50 ml falcon tube containing bedding packed into the bottom of the tube. Measurements of hanging time prior to falling, number of pulls, and a hindlimb suspension score (HLS) based on the evaluation of hindlimb spread, were recorded. The average of three attempts was taken. For grip strength assessment the mouse was held firmly by the tail and allowed to grab the grid with either its front or all four paws and then pulled back in the horizontal plane until the animal released its grip. Animals were tested six times (3 × forelimb, 3 × fore and hindlimb) in a session with a break of at least 1 min between tests. No decrease in grip strength was noted across the six tests performed during the testing session. The force recorded on the meter was noted and the mouse returned to its home cage. Experiments were conducted in a blinded fashion.

Myofiber Characteristics

Labelling of myosin heavy chains (myofiber type) and laminin was performed as previously described (Aare et al., 2016). Muscles for labelling were mounted on cork discs using optimal cutting temperature compound and then frozen in liquid nitrogen pre-cooled isopentane before being stored at −80°C. Transverse 10 μm sections of the soleus muscle were cut using a Microm HM 500 cryostat and labelled for myosin heavy Chains (MHC) and laminin. Muscle was first washed 1 × 5 min in PBS, then blocked in 10% normal goat serum (NGS) for 1 h at room temperature (RT). Primary antibodies were purchased from Developmental Studies Hybridoma Bank; BA-F8 (mouse anti-MHC1 IgG2b, 1:25), Sc-71 (mouse anti-MHC2a IgG1, 1:200), and BF-F3 (mouse anti-MHC2b 1:200) were applied to one section, and on a second serial section 6H1 (mouse anti-MHC2× IgGM, 1:25) was labelled. Both sections were also reacted against rabbit anti-laminin IgG (1:750, Millipore-Sigma). Muscles were incubated for 1 h (RT) and then washed 3 × 5 min in PBS. Secondary antibodies (ThermoFisher Scientific): Alexa Fluor 350 IgG2b (y2b) goat anti-mouse (A-21140, 1:500), Alexa Fluor 594 IgG1 (y1) goat anti-mouse (A-21125, 1:100), Alexa Fluor 488 IgM goat anti-mouse (A-21042, 1:500), and Alexa Fluor 488 IgG goat anti-rabbit (A-11008, 1:500) were applied for 1 h (RT). Following this, sections were given a final wash of 3 × 5 min and mounted using Vectashield hardset mounting medium (Vector Laboratories). Tiled images of the whole muscle were captured on a Zeiss Axio Imager microscope with Zen software and analyzed using FIJI (Schindelin et al., 2012) by an investigator blinded to the experimental group. Transverse myofibers were traced, and the MHC type noted. The percentage of each MHC type was noted for each animal and then these data used for statistics. Fiber type grouping was recorded through the identification of 'enclosed myofibers', i. e., those that were completely surrounded by myofibers of the same MHC type. The number of enclosed fibers was then expressed as a percentage of the total fibers recorded for that animal.

Hematoxylin and Eosin (H & E) staining was performed on transverse sections from the soleus muscle. Sections were initially rinsed in tap water, then placed in Myer's Hematoxylin (Millipore-Sigma) for 1 min. They were then rinsed in tap water until the water ran clear and placed in eosin (Millipore-Sigma) for 30 s. They were again rinsed in tap water, dehydrated through a graded ethanol series (75, 95, 100% ×2), cleared with two changes of xylene and mounted using DPX Mountant for Histology (Millipore-Sigma). Images were captured using a Mbf Biosciences Tissue Scope.

NMJ Labelling, Capturing, and Analysis

NMJ labelling was performed on soleus muscle using previously published protocols (Cipriani et al., 2018). Muscles were washed in ice–cold PBS for 2 × 10 min and then separated out into small bundles of about five fibres using tweezers under a stereo-microscope. They were fixed overnight at 4°C in 2% paraformaldehyde (PFA). The following morning, they were washed 2 × 1 h with ice–cold PBS to remove the PFA. They were treated for 10 min with Analar Ethanol followed by 10 min with Analar Methanol, both at −20°C. Tissues were then incubated with blocking/permeabilization solution (5% horse serum, 5% BSA, 2% Triton X-100 in PBS) for 4 h at RT with gentle agitation. Muscle bundles were incubated with antibodies, diluted in blocking buffer without triton, against neurofilament (mouse monoclonal IgG1, Cell Signalling, 1:100) and synaptophysin (rabbit polyclonal, ThermoFisherScientific, 1:100), overnight at 4°C with agitation and then for a further 2 h at RT the next morning. Muscles were then washed in blocking buffer 4 × 1 h at RT. They were incubated with Alexa 488-Conjugated α-Bungarotoxin (ThermoFisherScientific 1:250), Alexa Fluor 594 goat anti-rabbit IgG, and Alexa Fluor 594 goat anti-mouse IgG1 (ThermoFisher 1:200) for 4 h at RT. Samples were washed 4 × 1 h in PBS and then mounted using Vectashield hardset mounting medium. Images were captured using a Nikon A1R laser scanning confocal microscope using NIS-elements AR 4.20.02 software. Parameters were kept constant for all samples and Z-stack images were acquired with a ×63 oil immersion objective at 2 μm intervals.

Analysis was performed blinded according to the NMJ_Morph protocol (Jones et al., 2016) developed using FIJI (Schindelin et al., 2012). To set the threshold, a maximum intensity projection was used as a reference while adjusting the threshold for the image so that it best matched the maximum intensity projection. In addition to the 19 variables calculated as part of the NMJ_Morph package, we also quantified the NMJs that completely lacked either synaptophysin or α-bungarotoxin

staining. All variables were calculated from each NMJ with the ranges of NMJs studied were 16 to 44 for WT, 2 to 17 for PBS and 13 to 43 for NT animals. While this was below the recommended number of 30 suggested in the protocol, the investigator endeavored to capture all NMJs in each muscle preparation.

Electron Microscopy

Electron microscopy (EM) of the intercostal muscles from male mice was performed by the Electron Microscopy Research Services at Newcastle University. Tissues were fixed in 2% buffered glutaraldehyde, osmicated in 1% phosphate-buffered osmium tetroxyde, then dehydrated and embedded in epoxy resin. One micro meter semi-thin sections were stained with toluidine blue and then ultrathin sections were contrasted with uranyl acetate and lead citrate. EM images were captured using a CM10 transmission electron microscopy (Philips, Amsterdam, The Netherlands). Images were analysed using FIJI (Schindelin et al., 2012) with the observer blinded to the experimental group. Measurements were made of a number of variables according to previously published protocols (Slater et al., 1992; Wood and Slater, 1997), along with measurements of the number of secondary synaptic folds, their length, and number of branches, width of synaptic cleft, Schwann cell infiltration into the cleft, and the number of folds with clusters of synaptic vesicles opposite (**Supplementary Figure 2**).

Statistics

Data were initially recorded using Microsoft Excel and then analysed using GraphPad Prism v 8.4.0. Data were checked for normality using the D'Agostino-Pearson test and the appropriate statistical analysis applied as described in the figure legend. Outliers were identified using the ROUT (Q = 1%) method. Data points that were found to be outliers were left in place but their presence in the data set highlighted in the figure legends. Normally distributed data are expressed as mean ± standard deviation (SD), while data not normally distributed are presented as median (25th, 75th percentile) number of NMJs analyzed. A P value of <0.05 was considered significant and values are given in the figure legend.

RESULTS

Agrn^{nmf380} animals were given daily injections from postnatal day 5 (P5) for 30 days with either 10 mg/kg of NT1654 (NT) or PBS (Veh), with a WT group also included for comparison. Data were collected from 9 WT (4M and 5F), 7 Veh (3M and 4F), and 7 NT (2M and 5F) animals. Seven animals (4 Veh and 3 NT) had to be humanely culled during the study due to weight loss of more than 17%, as per our animal welfare guidelines. This resulted in the average ages of the Veh and the NT animals being younger that WT at tissue harvest (WT 36.13 ± 0.83 days, Veh 24.57 ± 8.63 days, NT 27.29 ± 10.66 days) which may have influenced comparisons between WT and *Agrn*^{nmf380} animals for some variables. While experimental animals were obtained through Het × Het crosses, only 12.4% of homozygous animals were obtained, with the remaining 51.3% being heterozygous and 36.3% WT animals. As a result, we were unable to have equal numbers of males and females in each group and for some variables sex specific differences were noted, for example body weight and NMJ morphology. In these cases, the results from just a single sex have been presented (that for which a greater number were present) and this has been indicated in the figure legend.

Body Weight

Animals were weighed daily to determine the amount of drug to administer, as a health monitoring tool, and as an experimental variable. As previously noted (Bogdanik and Burgess, 2011), Veh animals were considerably smaller with hindlimb muscle wasting (**Figure 1A**) and spinal curvature. Their body weight was considerably reduced in comparison to WT littermates (**Figure 1B** and **Supplemental Figure 3**). Administration of NT1654 improved body weight though not back to WT levels. Interestingly, the body weight of the NT and Veh animals diverged around day P16-17, which is consistent with the previously observed complete breakdown in NMJ morphology by P18 in these animals (Bogdanik and Burgess, 2011). We did not observe any improvement in the spinal curvature.

Muscle Strength

Muscle strength was measured using a hindlimb suspension test (tube test) at P7 and by a grip strength assessment using a grip strength meter at P24 and at P34. At P7 there was no significant difference in hang time between WT, Veh, or NT animals (**Figure 2A**). The number of pulls the mice attempted was also recorded (**Figure 2B**). WT animals pulled up more than either the Veh or NT animals, but again there was no significant difference between groups. The hind limb suspension (HLS) score is denoted by the position of the legs on the tube with a four denoting a raised tail and legs spread wide on the tube and a one being given for legs completely together and a lowered tail (Willmann et al., 2011). There were no significant differences between groups in HLS scores (**Figure 2C**). This was consistent with NMJs in the limbs of the *Agrn*^{nmf380} mice having a 'normal' innervation and size at day P9 (Bogdanik and Burgess, 2011).

Around P24, differences between WT and Veh animals in terms of forelimb grip strength became apparent. WT animals were more than twice as strong as Veh animals, with no significant differences between Veh and NT animals. By P34 WT animals remained significantly stronger than Veh animals, and interestingly treatment with NT1654 made NT animals over twice as strong as Veh animals. While NT animals were never quite as strong as WT animals, there was never any significant difference noted between them at either time point (**Figure 2D**). In addition to forelimb grip strength we also measured combined fore- and hindlimb grip strength by holding the mouse in such a way to allow it to grip the grid with all four paws. At P24 there was no significant difference in grip strength between the three animal groups (**Figure 2E**). By P34 of the study WT animals were significantly stronger than both Veh and NT animals. Unlike forelimb grip strength, NT animals were not significantly stronger than Veh animals following 30 days of treatment. *Agrn*^{nmf380} mice display extensive hindlimb wasting (**Figure 1A**) and it is possible that this was not rescuable by the NT1654 treatment. By dividing the force generated in

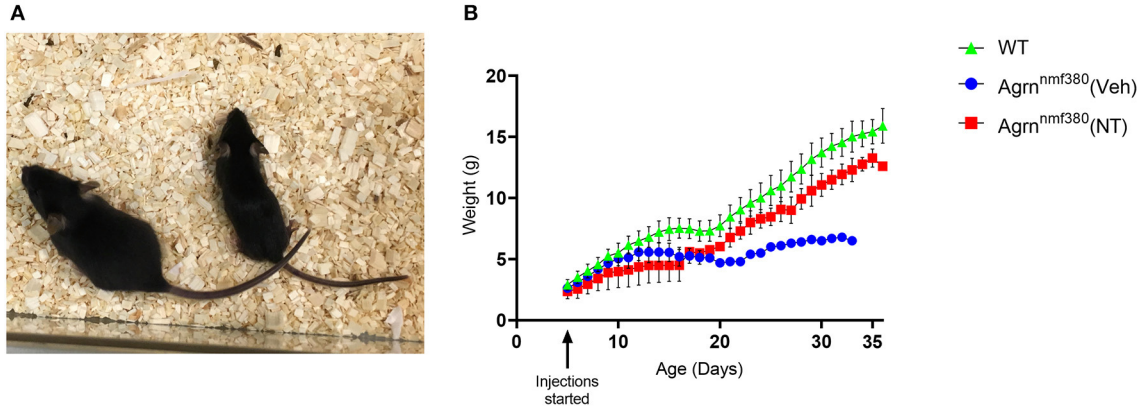

FIGURE 1 | Body weight of female *Agrn*^{nmf380} animals treated with NT1654. Veh animals displayed hindlimb wasting, a slight curvature of the spine and were considerably smaller than their WT littermates at 31 days **(A)**. Administration of NT1654 partially rescued body weight in *Agrn*^{nmf380} animals **(B)**. Graph shows mean ± S.D, $N = 5$ WT, 4 Veh, 5 NT. 1 WT, 3 Veh, and 2 NT animals were culled due to weight loss before the end of the study, which will have impacted the mean and SD values in this graph.

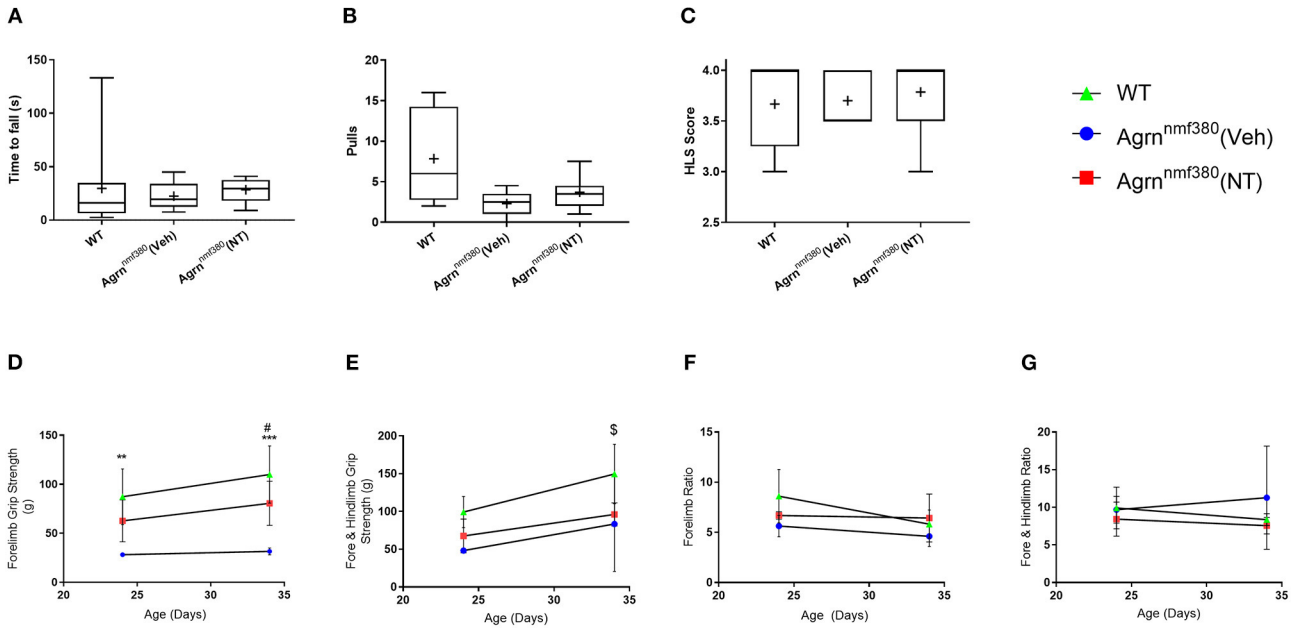

FIGURE 2 | Strength assessment in WT, Veh, and NT male and female animals. **(A)** At P7 no significant difference was observed in seconds to fall (Kruskal–Wallis test followed by Dunn's multiple comparisons test). The value at 133 s was identified as an outlier but had no effect on the significance level of the data. **(B)** The number of pulls also did not vary considerably between groups (Kruskal–Wallis test followed by Dunn's multiple comparisons test). **(C)** There were no differences in the HLS scores between WT, Veh, and NT animals. While the NT scores of 3 and 3.5 were identified as data outliers they did not influence the significance of the test (Kruskal–Wallis test followed by Dunn's multiple comparisons test). Box and whiskers plots show 5–95 percentile, with + indicating the mean. $N = 9$ WT, 5 Veh, 7 NT. **(D)** WT animals had significantly stronger forelimb grip strength than Veh animals during at P24 and P34. Treatment with NT1654 significantly improved forelimb grip strength over Veh animals at P34 (Mixed effect model followed by Sidak's multiple comparisons tests). **(E)** WT animals were significantly stronger than both Veh and NT animals following 30 days of treatment in terms of combined fore- and hindlimb grip strength (Mixed effect model followed by Sidak's multiple comparisons tests). Normalizing grip strength to body weight revealed that grip strength was dependent on mass for both fore **(F)** and combined fore and hindlimb strength **(G)** (Mixed effect model followed by Sidak's multiple comparisons tests). Graphs show mean ± SD. $N = 9$ WT, 3 Veh, 4 NT *Denotes significant difference between WT and Veh, $^{*}P < 0.05$ $^{**}P < 0.005$ $^{***}P < 0.0005$, $^{\#}$Denotes significant difference between NT and Veh $^{\#}P < 0.05$, $^{\$}$denotes significant difference between WT and NT $^{\$}P < 0.05$.

grams (g) by the body weight of the animals it is possible to determine the force ratio. For both fore- and combined fore-/hindlimb grip strength, there were no differences at any time point in force generated (**Figures 2F,G**). This could suggest that differences in force were attributable to an increase in muscle mass.

Muscle Weights

As we hypothesized that the changes in absolute grip strength were attributable to an increase in muscle mass, we weighed the muscles during harvest (**Supplementary Table 1 and Figure 3**). WT animals had significantly heavier absolute muscle weight than Veh animals ($P < 0.0001$). The reduction of muscle mass in Veh animals was partially prevented by drug administration in NT animals (**Figure 3A**). While NT animals had significantly heavier muscles than Veh animals ($P = 0.0193$) they did not fully recover and remained significantly lighter than WT animals ($P < 0.0001$). When expressed as a percentage of body weight (**Figure 3B**) WT animals continued to have significantly heavier muscles than Veh and NT animals ($P < 0.0001$). However, NT animals no longer had a heavier muscle weight than Veh.

Myofibre Morphology, Myosin Heavy Chain (MHC) Type, and Myofiber Type Grouping

Images were labelled for MHCs (**Figure 4A**) and analyzed using Fiji with the observer blinded to the experimental group. As expected following the muscle weight data, WT animals had a significantly larger (42%) myofiber area than Veh, which was then increased in NT animals so that there only remained a 7% difference in myofiber size between WT and NT animals. This increase came from a rescue of very small fibers and a hypertrophy of other fibers (**Figures 4A,B**). As previously reported in both patients (Huze et al., 2009; Maselli et al., 2012; Nicole et al., 2014) and *Agrn*^{nmf380} mice (Bogdanik and Burgess, 2011), Veh animals had a significantly higher percentage of TI myofibers than WT (**Figure 4C**). This increase in TI myofibres is coupled with a reduction in the percentage of TIIa and TIIx myofibers. This could be attributable to atrophy of TIIa and TIIx fibers or a fiber type shifting to an increasingly slow phenotype. Interestingly, treatment with NT1654 restored myofiber type proportions to WT levels, with NT mice demonstrating a similar TI myofiber percentage to WT animals, and an increase in TIIa myofibres when compared to Veh mice (**Figure 4C**).

To investigate the fiber type changes further, we analyzed myofiber size by type. TI myofibers of Veh animals were 81% the size of those from WT animals, however their TIIa and TIIx myofibers were only 58 and 19%, the size of WT animals respectively, suggesting a greater atrophy of TII myofibers over TI (**Figures 4D–F**, **Supplementary Table 2**). Treatment with NT1654 had no significant effect on TI myofiber size, although there did appear to be a small accumulation of fibers with a much larger cross-sectional area and slightly fewer with a very small cross-sectional area. Treatment partially rescued TIIa and TIIx myofiber size suggesting that NT1654 treatment reduced the TII myofiber atrophy seen in Veh animals, accounting for the normalization of the fiber type. MHC co-expressing myofibers, those displaying more than one MHC, are often used as an indicator of myofiber denervation (Aare et al., 2016). While Veh animals had higher levels of co-expressing myofibers than both WT and NT mice, this difference was not significant (**Figure 4C**). Another marker of denervation often observed in the muscle is that of myofiber type grouping, where a myofiber is entirely enclosed by myofibers of the same MHC. This is an indicator of myofiber reinnervation by a neighboring nerve following myofiber denervation. However, there was no significant difference in the number of enclosed myofibers between groups (**Figure 4G**).

A test for outliers suggested a number of values for the NT animals (71) were outliers, while the number of outliers in WT (1) and Veh (3) was considerably lower. A Barlett's test demonstrated that these groups had significantly different standard deviations ($P < 0.0001$), which is clearly visible in the long 'tail' of higher values for the NT animals (**Figure 4B**). These large myofibers could represent a response to the NT1654 treatment rather than being 'true outliers', especially as they were mostly accounted for by TIIa myofibers (53).

H & E staining in the Veh animals revealed a very non-uniform muscle pattern (**Figure 4H**) characterized by uneven fiber size including very small fibers, internalized nuclei, and fibrotic tissue. Fiber morphology appeared more uniform in the NT animals, although the fibers still appeared smaller.

NMJ Structure

Abnormal NMJ morphology has been noted in both humans and mice with mutations in the *AGRN* gene (Bogdanik and Burgess, 2011; Nicole et al., 2014), this was evident in the current study (**Figure 5A** and **Supplementary Table 3**). We measured NMJ structure in the soleus muscle using antibodies against neurofilament and synaptophysin and using α-Bungarotoxin to label AChRs (**Figure 5A**) and then in the intercostal muscles with EM (**Supplementary Figure 4**).

In the soleus muscle postsynaptic and some presynaptic variables were impacted by the *Agrn* mutation (**Supplementary Table 3**), with Veh animals having a reduced AChR and endplate area (**Figures 5B,C**) as determined with α-Bungarotoxin staining. Treatment with NT1654 prevented these decreases to the point that NT animals were no longer significantly lower than WT animals. A number of NMJs in the Veh mice did not have any α-bungarotoxin labelling, indicating a lack of AChRs, this was never observed in the WT or NT animals (**Supplementary Table 3**). Unlike other studies that have investigated NMJ pathology, we did not observe any change in the degree of fragmentation in our mouse model of NMJ dysfunction (**Supplementary Table 3**). We also observed a number of changes in presynaptic measurements, despite the presynapse not being the primary target of the mutation or the treatment. The number of terminal branches was decreased in Veh animals compared to WT, but this did not occur in NT mice (**Figure 5D**). The nerve terminal area was significantly bigger in NT mice when compared to WT (**Figure 5E**), despite this not being an impacted variable in the Veh animals, demonstrating the remarkable plasticity of the NMJ.

As with myofiber area, the variance of morphological parameters in NT animals was considerably greater than in either the WT or Veh models (**Figures 5B–E** and **Supplementary Table 3**). Similar to **Figures 4B,D,E**, key NMJ variables had a long tail of large values. AChR area (**Figure 5B**) and nerve terminal area (**Figure 5E**) both had unequal variances in their distributions (Bartletts test, $P < 0.0005$), with NT animals showing an elongated tail towards the

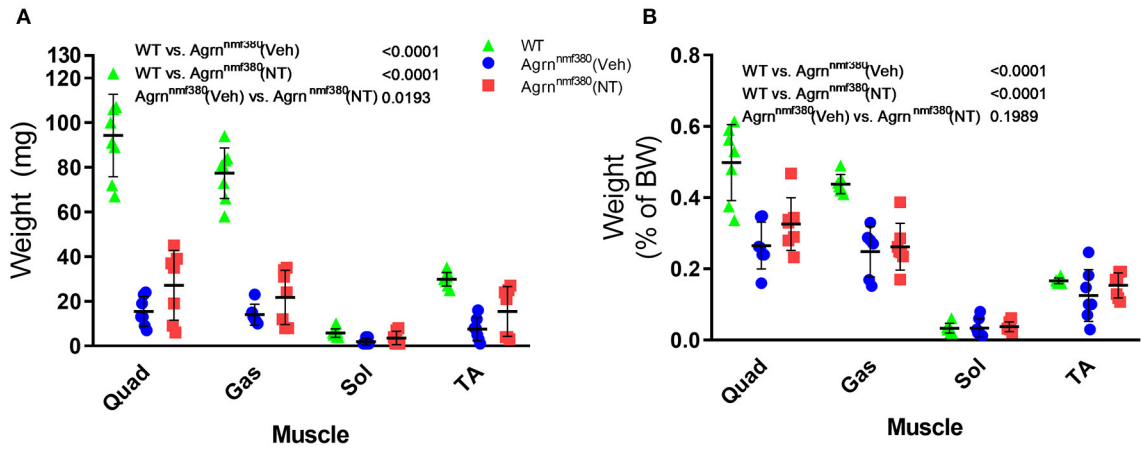

FIGURE 3 | Muscle harvest weight in male and female animals. Hindlimb muscles were blotted dry and weighed following excision. Treatment with NT1654 partially rescued muscle weight although not back to WT levels (2-way ANOVA followed by Tukey's multiple comparison tests) **(A)**. Following normalization to body weight NT animals no longer demonstrated a heavier muscle weight over Veh animals **(B)**. (2-way ANOVA followed by Tukey's multiple comparison tests) $N = 8$ WT, 7 Veh, 7 NT, Quad, quadriceps; Gas, gastrocnemius; Sol, Soleus; TA, Tibialis anterior.

larger areas. Unfortunately, we were unable to measure the size of the myofibers on which we measured these NMJ morphological parameters, so we are unable to determine if these larger NMJs were present on the larger myofibers.

In the intercostal muscles of male mice, a visual inspection of electron-micrographs appeared to show disruption at the NMJ (**Supplementary Figure 4**), this was not reflected in the measurements recorded. The only difference between groups was an increase in the length of the postsynaptic folds (CFL) in the Veh animals which returned to WT levels in NT animals (**Supplementary Table 4**). An increase in fold length was also observed in a previous study of *Agrn*^{nmf380} animals (Bogdanik and Burgess, 2011). No differences were noted in the length of the presynaptic terminal in contact with the myofiber (PreL), the total length of the postsynaptic membrane (FoldL), the number of folds (NF), or in derived variables like the branching index (number of branches divided by NF), or the occupancy, which is a measure of the amount of the postsynaptic apparatus in contact with the axon terminal. However, the limited size of our samples of NMJs may have reduced the accuracy of these results.

DISCUSSION

In this study we tested the hypothesis that a systemically delivered protein that retains the signaling function of neural AGRIN would improve the phenotype and NMJ structure in CMS through increasing the numbers of AChR. We found that treatment of mice with mutations in the *Agrn* gene with a modified AGRIN compound (NT1654) restored many aspects of NMJ postsynaptic structure, myofiber morphology and type, and improved muscle strength and body weight. This is the first time that NT1654, a compound that specifically targets the NMJ through protein replacement, has been shown to be effective in a mouse model of CMS. This combined with its potential IV or subcutaneous administration route raises the possibility that NT1654 could be helpful for patients with CMS in the future.

NT1654 is a modified form of mouse AGRIN composed of the c-terminal fragment. We are aware that agrin has a number of binding sites to components of the extracellular matrix such as laminin or heparan sulfate. When engineering NT-1654, solubility of the fragment was one of the key criteria besides resistance to neurotrypsin cleavage. Hence, the portion of the protein that interacts with the matrix was eliminated (y0) and the z8 insert binds to LRP4 only (Hettwer et al., 2014). In addition, the neurotrypsin cleavage β-site has been modified, neurotrypsin being the protease that usually breaks down AGRIN (Stephan et al., 2008). This compound has been shown to cluster AChRs in differentiated C_2C_{12} cells and *in vivo* in a surgically denervated WT mouse (Hettwer et al., 2014). The authors also tested their compound in a mouse model (SARCO mouse) in which NMJs were denervated through the overexpression of neurotrypsin (Bolliger et al., 2010; Hettwer et al., 2014). Similar to the *Agrn*^{nmf380} mouse, the SARCO mouse had a reduction in body weight and grip strength along with a breakdown in postsynaptic structures. This started to occur around P8 in SARCO mice and a little later in our *Agrn*^{nmf380} mice around P14-18. Like the current study, Hettwer and colleagues also found that NT1654 improved grip strength, recovered postsynaptic structures, and normalized myofiber type in the SARCO mouse (Hettwer et al., 2014). As neurotrypsin cleaves AGRIN it is perhaps not surprising that the two models share similar phenotypes and exhibit similar responses to NT1654.

NT1654 has also been tested in a mouse model of spinal muscular atrophy, where it increased life span, body weight, hindlimb suspension test scores, myofiber size, innervated endplates, and also rescued myofiber type distribution, although without significant increase in spinal motor neurons (Boido et al., 2018). In a rat model of myasthenia gravis, NT1654 improved weight gain, reduced the decrement seen with repetitive nerve

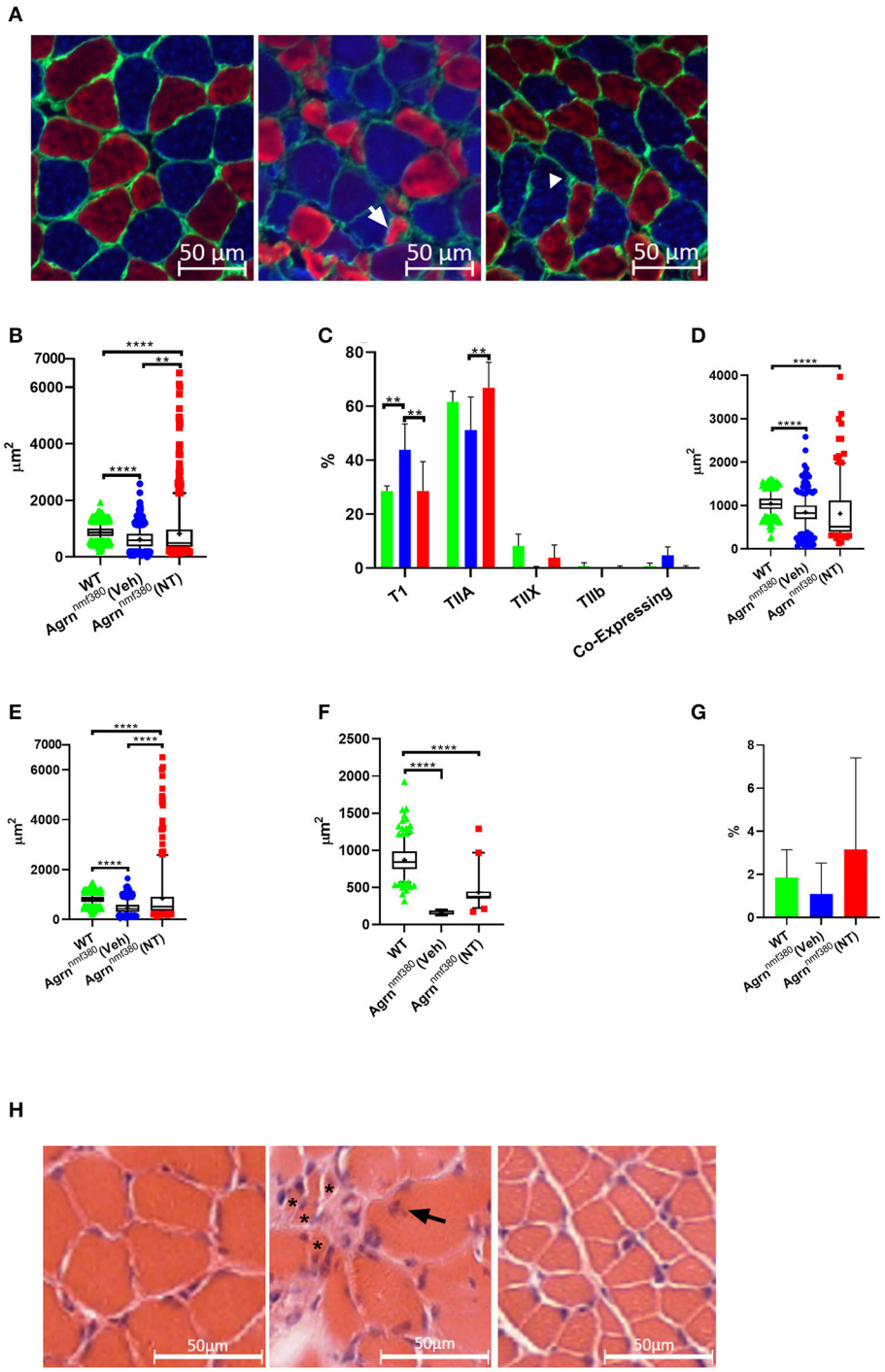

FIGURE 4 | Myofiber morphology and type in WT, Veh, and NT female animals. **(A)** Soleus muscle was labelled for MHC in WT (left), Veh (middle), and NT (right) animals, so that Type I myofibers = blue, Type IIa myofibers = red, Type IIb and Laminin = green. Type IIx myofibers were labelled on a serial section. Arrow indicates an atrophic TIIa fiber and the arrowhead indicates a hypotrophic TI fiber. **(B)** While Veh animals had significantly smaller myofibers than WT animals the fiber size was increased with NT1654 administration through a combination of a reduction in very small fibers and hypertrophy of other fibers (Kruskal–Wallis test followed by Dunn's multiple comparisons test). **(C)** Veh animals had an increased percentage of TI myofibers coupled with a decrease in TIIa/x myofibers, this was prevented with NT treatment (2-way ANOVA followed by Tukey's multiple comparison tests). Veh animals had smaller TI **(D)**, TIIa **(E)** and TIIx **(F)** myofibers than WT animals. TII myofiber atrophy was partially prevented with drug treatment in the NT animals (Kruskal–Wallis test followed by Dunn's multiple comparisons test). **(G)** There were no significant differences in the percentage of enclosed myofibres between groups. Box and whiskers plots show 5-95 percentile, with + indicating the mean, bar charts show mean + SD. ($N = 4$ WT, 3 Veh, 4 NT, $^{**}P < 0.005$ $^{****}P < 0.0001$). **(H)** Transvers soleus muscle from WT (Left), Veh (middle), and NT (right) animals were imaged following H and E staining. In the Veh animals multiple very small atrophic myofibers (*) were visible, along with internalized nuclei (arrow).

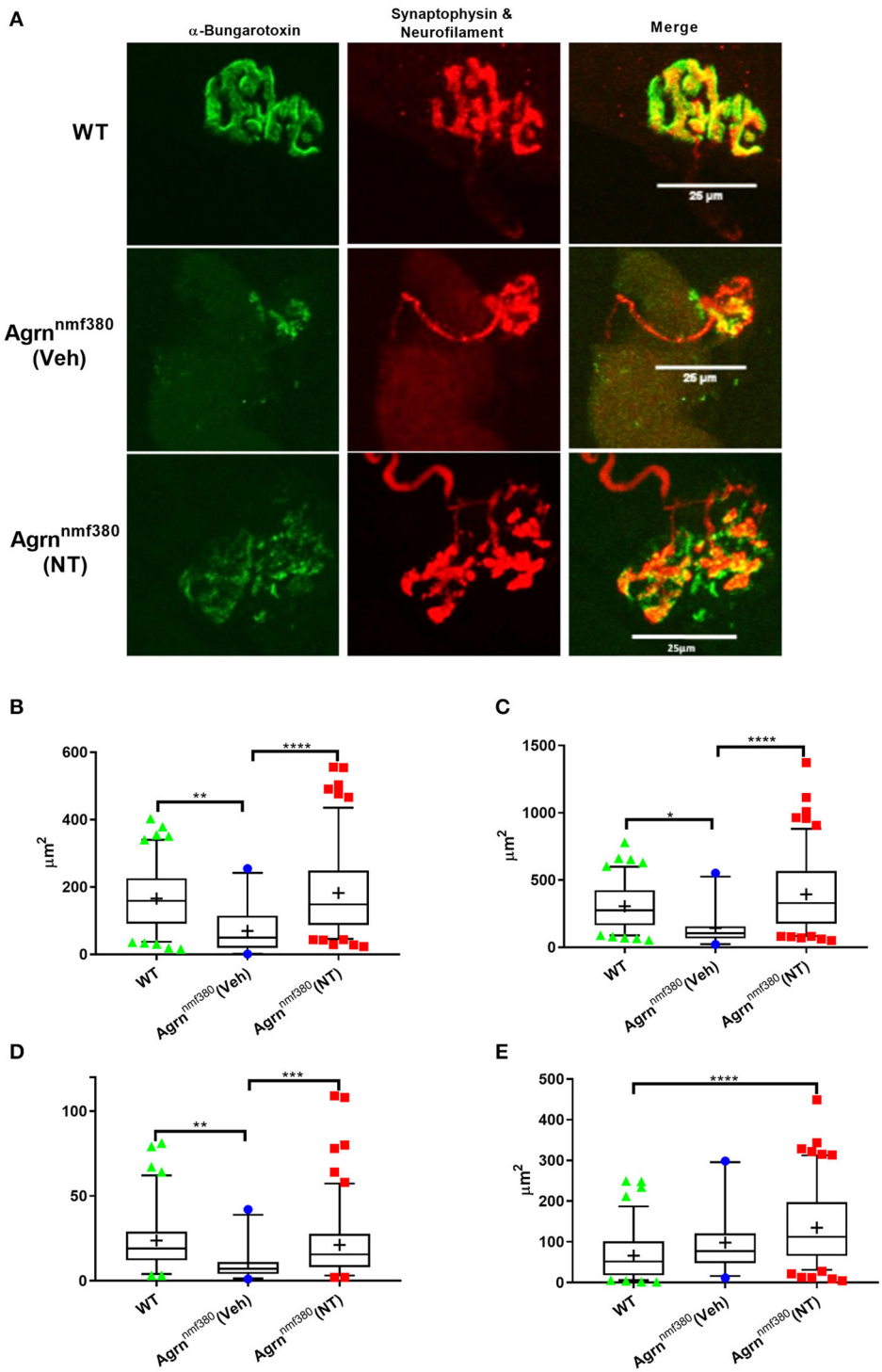

FIGURE 5 | NMJ structure in WT, Veh, and NT female animals. **(A)** Whole muscle mounts of the soleus were labelled with α-bungarotoxin (green), neurofilament (red), and synaptophysin (red). Analysis was performed on maximum intensity projections as stipulated in the analysis protocol. Images shown have been adjusted for brightness and contrast to better demonstrate the image features, scale bar is 25µm. WT animals had larger AChR area **(B)**, endplate area **(C)**, and number of terminal branches **(D)** than Veh animals, which returned to WT levels in NT animals. The nerve terminal area was significantly larger in NT animals compared to WT **(E)**, despite this not being an impacted variable. Kruskal–Wallis test followed by Dunn's multiple comparisons test, Box and whiskers plots show 5–95 percentile, with + indicating the mean, $N = 4$ WT, 3 Veh, and 5 NT, $^{**}P < 0.005$, $^{***}P < 0.0005$, $^{****}P < 0.0001$.

stimuli, increased AChRs and their overlap with nerve terminals, and reversed the reduction in myofiber size. The authors suggested that it may be useful as an adjunctive therapy with current treatments for autoimmune myasthenia gravis (Li et al., 2018). In a zebrafish model of presynaptic CMS, the compound was also found to increase spontaneous chorion movements, swimming speed and distance, and AChR cluster intensity (O'Connor et al., 2018).

We started treatment in the first week of life of these animals. This is a time when the axon terminal is very small with an irregular structure and the postsynaptic apparatus is oval with uniform α-bungarotoxin staining, indicating an immature AChR pattern (Slater, 1982). During this time we did not observe any functional differences in body weight or strength between our animals. It was during the initial stages of NMJ maturation that we started to note a difference in body weight and grip strength between WT and Veh animals. It is during this intermediate stage that the NMJs start to show small areas where α-bungarotoxin labelling is not as intense suggesting a more complex pattern, before fully maturing between days P17-21 (Slater, 1982). While the Veh animals did harbor some NMJs that reached maturity, as evidenced by the presence of postsynaptic folds in EM images, it would appear that it is this maturation stage, heavily disrupted in Veh animals, that is impacted with NT1654 administration.

Treatment with NT1654 improved many aspects of NMJ morphology that were disrupted in Veh animals. We observed improvements in both AChR and endplate area in NT animals, as well as an increase in the nerve terminal area—despite this not being found as impacted in Veh animals. Many aspects of structure are associated with function, variation in the frequency of miniature endplate potentials and quantal content has previously been associated with structural size changes in the endplate and nerve terminal in rodents and humans (Hutchinson et al., 1993; Slater et al., 2006; Jones et al., 2016). While it is likely that the structural changes we observed in the current study influenced the function of the NMJ, we would need to perform detailed electrophysiological investigations to confirm this, for example electromyographs or *ex vivo* muscle force experiments. Interestingly we did not observe any changes in the degree of fragmentation in our Veh animals, a phenomenon often observed in animal models of NMJ dysfunction (Hettwer et al., 2014) and aging (Willadt et al., 2016). Although the functional relevance of these fragmented junctions is under debate (Willadt et al., 2016) and their absence in our model does not preclude a functional impairment.

We observed a significant growth in myofibers in the mice treated with NT1654 which we hypothesize is attributable to the normalization of the NMJs. However, AGRIN has been shown to fulfil roles outside of AChR clustering, for example it is involved in skeletal muscle differentiation through its action on excitation-contraction coupling and the development of the membrane resting potential (Jurdana et al., 2009). We cannot, therefore, rule out the possibility that NT1654 caused the hypertrophy of muscle fibers through an additional pathway. Some of these hypertrophic fibers were larger than those observed in WT animals. Occasionally, large fibers are found in neuropathies. However, for denervation to play a role in our study, we would have expected increased numbers of MHC co-expressing and rounded fibers in NT animals. It was previously shown that NT1654 also increases the number of myofibers (Hettwer et al., 2014; Boido et al., 2018), however we did not measure this parameter. In CMS (Huze et al., 2009) and many other neuromuscular disorders (Ciciliot et al., 2013) a fast-to-slow myofiber type change has been noted. In this case the prevention of the TII myofiber atrophy prevented the fast-to-slow myofiber percentage changes observed in *Agrn*^{nmf380} animals (Bogdanik and Burgess, 2011). We hypothesize that these improvements in muscle fiber size and MHC normalization resulted in an increase in muscle and body weight and accounted for the increase in grip strength.

There has been a consistent improvement in NMJ characteristics across species and diseases with the administration of NT1654. The common improvement in AChR clustering would appear to support the theory that NT1654 targets the NMJ through the stimulation of the AGRIN/LRP4/MuSK pathway. As NT1654 primarily targets a postsynaptic pathway, its effects on the presynaptic NMJ structure in this study may initially be surprising with NT1654 increasing the nerve terminal area and complexity of the presynaptic structures. However, the involvement of the AGRIN/LRP4/MuSK pathway in controlling presynaptic differentiation is well known. The *Agrn*^{nmf380} mouse demonstrates abnormal presynaptic sprouting (Bogdanik and Burgess, 2011), and expression of a mini-agrin compound in skeletal muscle can restore presynaptic terminals in AGRIN deficient mice (Lin et al., 2008). Molecules downstream of AGRIN also impact the presynaptic terminal, with presynaptic NMJ functional and structural abnormalities being noted in mice with antibodies against LRP4 (Shen et al., 2013) and MuSK (Viegas et al., 2012). This strongly supports the presence of bi-directional signaling between the pre and postsynapse and could explain the benefits on presynaptic structures that we observed with NT1654 administration. It will be interesting to assess if NT1654 is effective in CMS subtypes caused by presynaptic (Herrmann et al., 2014; O'Connor et al., 2016) or even glycosylation related mutations (Senderek et al., 2011; Cossins et al., 2013). A number of neuropathies have also been demonstrated to have NMJ involvement (Sleigh et al., 2014; Cipriani et al., 2018), for which NT1654 may offer a therapeutic potential.

These findings are promising as currently treatment options for patients with CMS are limited and very much depend on the nature of the gene mutation (McMacken et al., 2017). Acetylcholinesterase (AChE) inhibitors, for example pyridostigmine, work by blocking the enzyme that breaks down the acetylcholine bound to the AChR on the postsynaptic membrane, thereby prolonging the open state of the receptors. However, in patients who have mutations resulting in AChE deficit (COLQ) and with mutations in DOK7 this treatment is detrimental and should be avoided. Some patients respond to 3,4-Diaminopyridine which blocks presynaptic potassium channels, thus prolonging the release of ACh into the synaptic cleft. However, this can be accompanied by dose-related side effects. Sympathomimetics, for example salbutamol and ephedrine,

have been successfully used to treat certain CMS. Their exact mechanism of action is currently unknown, but they have been shown to act postsynaptically (Clausen et al., 2018; McMacken et al., 2018, 2019; Webster et al., 2020). However, they can take a while to provide clinical improvement and again can have side effects, including cardiac complications. For these reasons it is important to find other therapeutics that can replace or even work in conjunction with already established treatments.

In this study, animals were treated daily for 30 days, starting at P5 with a subcutaneous injection of the compound. Previous investigations have shown these mice to start developing NMJ dysfunction between P9 and P13 (Bogdanik and Burgess, 2011). While we would have preferred to begin treatment of the *Agrn*^{nmf380} mice after the onset of NMJ pathology and carry it on for longer than 30 days to test if the drug could reverse rather than prevent the pathology, the severe phenotype of the animals limited the duration of experiments. Despite this limitation we were still able to detect changes with this shortened protocol. In addition, we originally aimed to examine both male and female mice, however, *Agrn*^{nmf380} mice were not born in sufficient numbers to provide adequate numbers of animals in each group. This was made more difficult by sex-related differences, for example male WT animals consistently had larger values than females in aspects of NMJ morphology like AChR area endplate perimeter. It would be interesting to see if these sex-related differences influenced how males and females responded to treatment. This study examined functionally very different muscles during testing. Our *in vitro* investigations focused on hindlimb muscles, however, given the differences noted between WT and Veh animals in forelimb grip strength and the improvements noted following drug treatment, it would be interesting to perform *in vitro* investigations on selected muscles of the forelimb in future. The underlying structural differences and responses to pathology in NMJs of different regions in the mouse (Sleigh et al., 2014; Jones et al., 2016) could have influenced the responses to NT1654.

In conclusion, treatment of *Agrn*^{nmf380} mice with the modified AGRIN compound (NT1654) resulted in the prevention of pre- and post-synaptic NMJ morphology breakdown, which we hypothesize contributed to myofiber hypertrophy in both TI and TII myofibers, and importantly prevented the atrophy of TII myofibers. In turn this caused an increase in muscle and animal weight and an increase in forelimb strength. This study adds to the evidence of the efficacy of NT1654 in conditions where the NMJ is compromised and strongly suggests that patients with CMS attributable to mutations in *AGRN* could benefit from this treatment.

DATA AVAILABILITY STATEMENT

The raw data supporting the conclusions of this article will be made available by the authors, without undue reservation.

ETHICS STATEMENT

The animal study was reviewed and approved by Newcastle University Animal Welfare and Ethical Review Body (AWERB).

AUTHOR CONTRIBUTIONS

HL, RH, SH, AM, and GM developed the project concept. SS, RH, GM, TD, and KQ performed the experiments and data analysis. HL, RH, AR, CS, and EO provided ongoing supervision for the project. SS wrote the manuscript with input from HL and CS. All authors edited and approved of the submitted version.

FUNDING

This research was funded by the Wellcome Trust (Pathfinder Award, 201064/Z/16/Z) and the Medical Research Council (Confidence in Concept Fund). HL receives support from the Canadian Institutes of Health Research (Foundation Grant FDN-167281), the Canadian Institutes of Health Research and Muscular Dystrophy Canada (Network Catalyst Grant for NMD4C), the Canada Foundation for Innovation (CFI-JELF 38412), and the Canada Research Chairs program (Canada Research Chair in Neuromuscular Genomics and Health, 950-232279). RH received funding from the Newton Fund UK/Turkey (MR/N027302/1), the Medical Research Council (UK) (MR/N025431/1), the Wellcome Investigator fund (109915/Z/15/Z), the Lily Foundation UK, and the Evelyn Trust (19/14). EO was supported by a postdoctoral fellowship from AFM-Téléthon (22569). GM was supported by a Guarantors of Brain/Association of British Neurologists Clinical Research Training Fellowship.

ACKNOWLEDGMENTS

We would like to thank Robert Burgess for supplying the *Agrn*^{nmf380} mouse and Neurotune AG for supplying the NT1654 compound. The BA-F8, SC-71, and BF-F3 monoclonal antibodies deposited by Schiaffino, S., and the 6H1 monoclonal antibody deposited by Lucas, C., were obtained from the Developmental Studies Hybridoma Bank, created by the NICHD of the NIH and maintained at The University of Iowa, Department of Biology, Iowa City, IA 52242. We are extremely grateful to the staff of The Ottawa Hospital General Campus 6East.

SUPPLEMENTARY MATERIAL

The Supplementary Material for this article can be found online at: https://www.frontiersin.org/articles/10.3389/fnmol.2020.594220/full#supplementary-material

REFERENCES

Aare, S., Spendiff, S., Vuda, M., Elkrief, D., Perez, A., Wu, Q., et al. (2016). Failed reinnervation in aging skeletal muscle. *Skelet. Muscle* 6, 29. doi: 10.1186/s13395-016-0101-y

Bezakova, G., Helm, J. P., Francolini, M., and Lømo, T. (2001). Effects of purified recombinant neural and muscle agrin on skeletal muscle fibers *in vivo*. *J. Cell Biol.* 153, 1441–1452. doi: 10.1083/jcb.153.7.1441

Bogdanik, L. P., and Burgess, R. W. (2011). A valid mouse model of AGRIN-associated congenital myasthenic syndrome. *Hum. Mol. Genet.* 20, 4617–4633. doi: 10.1093/hmg/ddr396

Boido, M., De Amicis, E., Valsecchi, V., Trevisan, M., Ala, U., Ruegg, M. A., et al. (2018). Increasing agrin function antagonizes muscle atrophy and motor impairment in spinal muscular atrophy. *Front. Cell Neurosci.* 12:17. doi: 10.3389/fncel.2018.00017

Bolliger, M. F., Zurlinden, A., Lüscher, D., Bütikofer, L., Shakhova, O., Francolini, M., et al. (2010). Specific proteolytic cleavage of agrin regulates maturation of the neuromuscular junction. *J. Cell Sci.* 123, 3944–3955. doi: 10.1242/jcs.072090

Burden, S. J., Yumoto, N., and Zhang, W. (2013). The role of MuSK in synapse formation and neuromuscular disease. *Cold Spring Harb. Perspect. Biol.* 5:a009167. doi: 10.1101/cshperspect.a009167

Ciciliot, S., Rossi, A. C., Dyar, K. A., Blaauw, B., and Schiaffino, S. (2013). Muscle type and fiber type specificity in muscle wasting. *Int. J. Biochem. Cell Biol.* 45, 2191–2199. doi: 10.1016/j.biocel.2013.05.016

Cipriani, S., Phan, V., Medard, J. J., Horvath, R., Lochmuller, H., Chrast, R., et al. (2018). Neuromuscular junction changes in a mouse model of Charcot-Marie-Tooth Disease Type 4C. *Int. J. Mol. Sci.* 19:4072. doi: 10.3390/ijms19124072

Clausen, L., Cossins, J., and Beeson, D. (2018). Beta-2 adrenergic receptor agonists enhance AChR clustering in C2C12 myotubes: implications for therapy of myasthenic disorders. *J. Neuromuscul. Dis.* 5, 231–240. doi: 10.3233/jnd-170293

Cossins, J., Belaya, K., Hicks, D., Salih, M. A., Finlayson, S., Carboni, N., et al. (2013). Congenital myasthenic syndromes due to mutations in ALG2 and ALG14. *Brain* 136, 944–956. doi: 10.1093/brain/awt010

Finsterer, J. (2019). Congenital myasthenic syndromes. *Orphanet. J. Rare Dis.* 14:57. doi: 10.1186/s13023-019-1025-5

Gervásio, O. L., and Phillips, W. D. (2005). Increased ratio of rapsyn to ACh receptor stabilizes postsynaptic receptors at the mouse neuromuscular synapse. *J. Physiol.* 562, 673–685. doi: 10.1113/jphysiol.2004.077685

Herrmann, D. N., Horvath, R., Sowden, J. E., Gonzalez, M., Sanchez-Mejias, A., Guan, Z., et al. (2014). Synaptotagmin 2 mutations cause an autosomal-dominant form of lambert-eaton myasthenic syndrome and nonprogressive motor neuropathy. *Am. J. Hum. Genet.* 95, 332–339. doi: 10.1016/j.ajhg.2014.08.007

Hettwer, S., Lin, S., Kucsera, S., Haubitz, M., Oliveri, F., Fariello, R. G., et al. (2014). Injection of a soluble fragment of neural agrin (NT-1654) considerably improves the muscle pathology caused by the disassembly of the neuromuscular junction. *PLoS One* 9:e88739. doi: 10.1371/journal.pone.0088739

Hutchinson, D. O., Walls, T. J., Nakano, S., Camp, S., Taylor, P., Harper, C. M., et al. (1993). Congenital endplate acetylcholinesterase deficiency. *Brain* 116, 633–653. doi: 10.1093/brain/116.3.633

Huze, C., Bauche, S., Richard, P., Chevessier, F., Goillot, E., Gaudon, K., et al. (2009). Identification of an agrin mutation that causes congenital myasthenia and affects synapse function. *Am. J. Hum. Genet.* 85, 155–167. doi: 10.1016/j.ajhg.2009.06.015

Jones, R. A., Reich, C. D., Dissanayake, K. N., Kristmundsdottir, F., Findlater, G. S., Ribchester, R. R., et al. (2016). NMJ-morph reveals principal components of synaptic morphology influencing structure-function relationships at the neuromuscular junction. *Open Biol.* 6:160240. doi: 10.1098/rsob.160240

Jurdana, M., Fumagalli, G., Grubic, Z., Lorenzon, P., Mars, T., and Sciancalepore, M. (2009). Neural agrin changes the electrical properties of developing human skeletal muscle cells. *Cell Mol. Neurobiol.* 29, 123–131. doi: 10.1007/s10571-008-9304-z

Kim, N., Stiegler, A. L., Cameron, T. O., Hallock, P. T., Gomez, A. M., Huang, J. H., et al. (2008). Lrp4 is a receptor for agrin and forms a complex with MuSK. *Cell* 135, 334–342. doi: 10.1016/j.cell.2008.10.002

Li, Z., Li, M., Wood, K., Hettwer, S., Muley, S. A., Shi, F. D., et al. (2018). Engineered agrin attenuates the severity of experimental autoimmune myasthenia gravis. *Muscle Nerve.* 57, 814–820. doi: 10.1002/mus.26025

Lin, S., Maj, M., Bezakova, G., Magyar, J. P., Brenner, H. R., and Ruegg, M. A. (2008). Muscle-wide secretion of a miniaturized form of neural agrin rescues focal neuromuscular innervation in agrin mutant mice. *Proc. Natl. Acad. Sci. U.S.A.* 105, 11406–11411. doi: 10.1073/pnas.0801683105

Maselli, R. A., Fernandez, J. M., Arredondo, J., Navarro, C., Ngo, M., Beeson, D., et al. (2012). LG2 agrin mutation causing severe congenital myasthenic syndrome mimics functional characteristics of non-neural (z-) agrin. *Hum. Genet.* 131, 1123–1135. doi: 10.1007/s00439-011-1132-4

McMacken, G., Abicht, A., Evangelista, T., Spendiff, S., and Lochmüller, H. (2017). The increasing genetic and phenotypical diversity of congenital myasthenic syndromes. *Neuropediatrics* 48, 294–308. doi: 10.1055/s-0037-1602832

McMacken, G., Cox, D., Roos, A., Muller, J., Whittaker, R., and Lochmuller, H. (2018). The beta-adrenergic agonist salbutamol modulates neuromuscular junction formation in zebrafish models of human myasthenic syndromes. *Hum. Mol. Genet.* 27, 1556–1564. doi: 10.1093/hmg/ddy062

McMacken, G. M., Spendiff, S., Whittaker, R. G., O'Connor, E., Howarth, R. M., Boczonadi, V., et al. (2019). Salbutamol modifies the neuromuscular junction in a mouse model of ColQ myasthenic syndrome. *Hum. Mol. Genet.* 28, 2339–2351. doi: 10.1093/hmg/ddz059

Nicole, S., Chaouch, A., Torbergsen, T., Bauche, S., de Bruyckere, E., Fontenille, M. J., et al. (2014). Agrin mutations lead to a congenital myasthenic syndrome with distal muscle weakness and atrophy. *Brain* 137, 2429–2443. doi: 10.1093/brain/awu160

O'Connor, E., Phan, V., Cordts, I., Cairns, G., Hettwer, S., Cox, D., et al. (2018). MYO9A deficiency in motor neurons is associated with reduced neuromuscular agrin secretion. *Hum. Mol. Genet.* 27, 1434–1446. doi: 10.1093/hmg/ddy054

O'Connor, E., Topf, A., Muller, J. S., Cox, D., Evangelista, T., Colomer, J., et al. (2016). Identification of mutations in the MYO9A gene in patients with congenital myasthenic syndrome. *Brain* 139, 2143–2153. doi: 10.1093/brain/aww130

Ohkawara, B., Shen, X., Selcen, D., Nazim, M., Bril, V., Tarnopolsky, M. A., et al. (2020). Congenital myasthenic syndrome-associated agrin variants affect clustering of acetylcholine receptors in a domain-specific manner. *JCI Insight* 5:e132023. doi: 10.1172/jci.insight.132023

Schindelin, J., Arganda-Carreras, I., Frise, E., Kaynig, V., Longair, M., Pietzsch, T., et al. (2012). Fiji: an open-source platform for biological-image analysis. *Nat. Methods* 9, 676–682. doi: 10.1038/nmeth.2019

Senderek, J., Muller, J. S., Dusl, M., Strom, T. M., Guergueltcheva, V., Diepolder, I., et al. (2011). Hexosamine biosynthetic pathway mutations cause neuromuscular transmission defect. *Am. J. Hum. Genet.* 88, 162–172. doi: 10.1016/j.ajhg.2011.01.008

Shen, C., Lu, Y., Zhang, B., Figueiredo, D., Bean, J., Jung, J., et al. (2013). Antibodies against low-density lipoprotein receptor-related protein 4 induce myasthenia gravis. *J. Clin. Invest.* 123, 5190–5202. doi: 10.1172/jci66039

Slater, C. R. (1982). Postnatal maturation of nerve-muscle junctions in hindlimb muscles of the mouse. *Dev. Biol.* 94, 11–22. doi: 10.1016/0012-1606(82)90063-x

Slater, C. R., Fawcett, P. R., Walls, T. J., Lyons, P. R., Bailey, S. J., Beeson, D., et al. (2006). Pre- and post-synaptic abnormalities associated with impaired neuromuscular transmission in a group of patients with 'limb-girdle myasthenia'. *Brain* 129, 2061–2076. doi: 10.1093/brain/awl200

Slater, C. R., Lyons, P. R., Walls, T. J., Fawcett, P. R., and Young, C. (1992). Structure and function of neuromuscular junctions in the vastus lateralis of man. A motor point biopsy study of two groups of patients. *Brain* 115, 451–478.

Sleigh, J. N., Grice, S. J., Burgess, R. W., Talbot, K., and Cader, M. Z. (2014). Neuromuscular junction maturation defects precede impaired lower motor neuron connectivity in Charcot-Marie-Tooth type 2D mice. *Hum. Mol. Genet.* 23, 2639–2650. doi: 10.1093/hmg/ddt659

Stephan, A., Mateos, J. M., Kozlov, S. V., Cinelli, P., Kistler, A. D., Hettwer, S., et al. (2008). Neurotrypsin cleaves agrin locally at the synapse. *Faseb. J.* 22, 1861–1873. doi: 10.1096/fj.07-100008

Tezuka, T., Inoue, A., Hoshi, T., Weatherbee, S. D., Burgess, R. W., Ueta, R., et al. (2014). The MuSK activator agrin has a separate role essential for postnatal maintenance of neuromuscular synapses. *Proc. Natl. Acad. Sci. U.S.A.* 111, 16556–16561. doi: 10.1073/pnas.1408409111

Viegas, S., Jacobson, L., Waters, P., Cossins, J., Jacob, S., Leite, M. I., et al. (2012). Passive and active immunization models of MuSK-Ab positive myasthenia: electrophysiological evidence for pre and postsynaptic defects. *Exp. Neurol.* 234, 506–512. doi: 10.1016/j.expneurol.2012.01.025

Webster, R. G., Vanhaesebrouck, A. E., Maxwell, S. E., Cossins, J. A., Liu, W., Ueta, R., et al. (2020). Effect of salbutamol on neuromuscular junction function and structure in a mouse model of DOK7 congenital myasthenia. *Hum. Mol. Genet.* 29, 2325–2336. doi: 10.1093/hmg/ddaa116

Willadt, S., Nash, M., and Slater, C. R. (2016). Age-related fragmentation of the motor endplate is not associated with impaired neuromuscular transmission in the mouse diaphragm. *Sci. Rep.* 6:24849. doi: 10.1038/srep24849

Willmann, R., Dubach, J., and Chen, K. (2011). Developing standard procedures for pre-clinical efficacy studies in mouse models of spinal muscular atrophy: report of the expert workshop "Pre-clinical testing for SMA", Zurich, March 29-30th 2010. *Neuromuscul. Disord.* 21, 74–77. doi: 10.1016/j.nmd.2010.09.014

Wood, S. J., and Slater, C. R. (1997). The contribution of postsynaptic folds to the safety factor for neuromuscular transmission in rat fast- and slow-twitch muscles. *J. Physiol.* 500, 165–176. doi: 10.1113/jphysiol.1997.sp022007

Conflict of Interest: SH and AM are employed by Neurotune AG. Remaining authors declare that the research was conducted in the absence of any commercial or financial relationships that could be construed as a potential conflict of interest

Copyright © 2020 Spendiff, Howarth, McMacken, Davey, Quinlan, O'Connor, Slater, Hettwer, Mäder, Roos, Horvath and Lochmüller. This is an open-access article distributed under the terms of the Creative Commons Attribution License (CC BY). The use, distribution or reproduction in other forums is permitted, provided the original author(s) and the copyright owner(s) are credited and that the original publication in this journal is cited, in accordance with accepted academic practice. No use, distribution or reproduction is permitted which does not comply with these terms.

Advantages of publishing in Frontiers

OPEN ACCESS
Articles are free to read for greatest visibility and readership

FAST PUBLICATION
Around 90 days from submission to decision

HIGH QUALITY PEER-REVIEW
Rigorous, collaborative, and constructive peer-review

TRANSPARENT PEER-REVIEW
Editors and reviewers acknowledged by name on published articles

Frontiers
Avenue du Tribunal-Fédéral 34
1005 Lausanne | Switzerland

Visit us: www.frontiersin.org
Contact us: frontiersin.org/about/contact

REPRODUCIBILITY OF RESEARCH
Support open data and methods to enhance research reproducibility

DIGITAL PUBLISHING
Articles designed for optimal readership across devices

FOLLOW US
@frontiersin

IMPACT METRICS
Advanced article metrics track visibility across digital media

EXTENSIVE PROMOTION
Marketing and promotion of impactful research

LOOP RESEARCH NETWORK
Our network increases your article's readership